

Acta Physiologica Scandinavica

Published monthly for the
Scandinavian Physiological Society

Vol 107 No 1 September 1979

Editorial Board

P Kruheffer
København

M R Bergström
Turku

J Jansen
Oslo

Y Zotterman
Stockholm

U S. von Euler
(Editor) Stockholm

Editorial office

Acta Physiologica Scandinavica
Karolinska Institutet
S-104 01 Stockholm

The "Acta physiologica scandinavica" are published for the Scandinavian Society for Physiology and contain contributions to Physiology, Medical Chemistry or Pharmacology by Scandinavian authors or from Scandinavian laboratories. The articles are published in English, French or German. Each number consists of about 8 printed sheets, 4 numbers forming a volume. Not more than 3 volumes will appear each year. Subscriptions should be mailed to Acta Physiologica Scandinavica, Karolinska Institutet, S 104 01 Stockholm, Sweden. Price per volume 140 Sw. Cr.

Manuscripts from Denmark should be sent to Professor P. Kruheffer
Med. Fysiologiske Inst., B Universitetet, Juliane Mariesvej 30 DK 2100 København O

Manuscripts from Finland should be sent to Professor M. R. Bergström,
Fysiologiska Institutionen, Siltavuorenpenger 20, SF-00170 Helsinki

Manuscripts from Norway should be sent to Dr. med. Jan Jansen,
Fysiologisk Institutt, Universitetet, Karl Johans Gate 47 N Oslo and

Manuscripts from Sweden should be sent to Professor Y. Zotterman,
Wenner Gren Center Konferenssekretariatet, 23 tr Sveavägen 166, S-113 46 Stockholm.

Contents

- 1 NORESSON, E., RICKSTEN, S.-E., HALLBÄCK, MORLANDER, M. & THORÉN, P. Performance of the hypertrophied left ventricle in spontaneously hypertensive rat. Effects of changes in preload and afterload
- 9 NORESSON, E., RICKSTEN, S. E. & THORÉN, P. Left atrial pressure in normotensive and spontaneously hypertensive rats
- 13 THORÉN, P., NORESSON, E. & RICKSTEN, S.-E. Reexciting of cardiac C-fiber endings in the spontaneously hypertensive rat
- 19 GALBO, H., HOLST, J. J. & CHRISTENSEN, N. J. The effect of different diets and of insulin on the hormonal response to prolonged exercise
- 23 BERGH, U. & EKBLOM, B. Influence of muscle temperature on maximal muscle strength and power output in human skeletal muscles
- 29 ÖRLANDER, J., KIERSLING, K. H. & LARSSON, L. Skeletal muscle metabolism, morphology and function in sedentary smokers and nonsmokers
- 47 FUGL-MEYER, A. R., SJÖSTRÖM, M. & WÄHLBY, L. Human plantar flexion strength and structure
- 57 MÆLLUND, G., LINDQVIST, L., RÖNQVIST, G. & NILSSON, B. O. The effect of α -aminobutyric acid and 2,4-diaminobutyric acid on mouse blastocyst outgrowth in vitro
- 63 CLAUSEN, G., HOPE, A. & AUKLAND, K. Partition of 125 I-iodoantipyrine among erythrocytes, plasma, and renal cortex in the dog
- 69 CLAUSEN, G., HOPE, A., KIRKEBO, A., TYSSE, BOTH, I. & AUKLAND, K. Distribution of blood flow in the dog kidney. I. Saturation rates for inert diffusible tracers, 125 I-iodoantipyrine and tritiated water versus uptake of microspheres under control conditions
- 83 PETERSSON, G., AHLMAN, H., DAHLSTRÖM, A., KEWENTER, J., LARSSON, I. & LARSSON, P. A. The effect of transmural field stimulation on the serotonin content in rat duodenal enterochromaffin cells—in vitro
- 89 HALLBÄCK, D. A., JODAL, M. & LUNDGREN, O. Importance of sodium and glucose for the establishment of a vitreous tissue hyperosmolality by the intestinal countercurrent multiplier

Appended Supplements

- Supplementum 468. ÅKERSTEDT, T. Altered sleep/wake patterns and circadian rhythms.
- Supplementum 470. PETERSSON, G. The neural control of the serotonin content in mammalian enterochromaffin cells.

Instructions to authors

Manuscripts (2 copies) should be sent to the National Editor in double spacing on one side of paper of size 21 × 30 cm (A 4) with 4 cm margin. A short title (max. 40 letters) may be suggested. An abstract, not exceeding 200 words should be submitted.

In general, a succinct style and restriction to the necessary of documentation and discussion effectively aids in reducing publication time.

References should be given with full title and name of journals, abbreviated in accordance with 4th Ed. of *World List of Scientific Periodicals*, with volume number and first and last page numbers.

Figures should not be larger than manuscript pages and sent in as glossy prints in a size larger than that required for reproduction. Lettering should be large enough to permit suitable reduction and preferably of uniform size. Photomicrographs should be calibrated on the print (not as enlargement factor in figure text). Figure texts should be assembled on separate sheets.

Tables should be kept at minimum, both in number and size, with text above the table (not on separate sheets). Single numbers in a series should be replaced by mean and S.D. or mean and S.E., in the latter case with number of observations.

Key words (5–10) are recommended in order to facilitate indexing.

For abbreviations, units, and symbols see special list in the Journal and recent articles.

More detailed instructions to authors are found in *NORDIC BIOMEDICAL MANUSCRIPTS. Instructions & guidelines*, published by the Nordic Publication Committee for Medicine, Ed. G. Svartz, Malmberg & R. Goldmann, Universitetsforlaget, Oslo 1978.

The international system of units (SI)

The following symbols and units, recommended by the SI, are being used in *Acta Physiologica Scandinavica*. Certain units, not included in SI, will still be permitted.

SI units with recommended symbols

Units	Symbols
kilogramme	kg
second, millisecond	s ms
mole, millimole, micro- mole, nanomole, picomole	mol mmol μ mol nmol pmol
meter millimeter micrometer nanometer	m mm μ m nm
candela	cd
steradian	sr
hertz (frequency)	Hz (s^{-1})
newton (force)	N (kg m/s ²)
pascal (pressure)	Pa (N/m ²)
joule (energy)	J (N m)
watt (effect)	W (J/s)
lumen (lightflow)	lm (cd sr)
lux (illumination)	lx (lm/m ²)

Permitted non SI units

Unit	Symbols
gramme	g
minute	min
hour	h
molarity (mol/liter) (calorie) (kilopond) (millimeters of mer- cury) (millibar)	M cal (4.184 J) kp (9.81 N) [*] mmHg (1.333 mbar) mbar (100 Pa) Ci
curie	
liter milliliter micro- liter	l ml μ l
degree Celsius	°C

Conversion factors to be given in Methods.

Contents

- 87 WISBERG, T. VAAGE, J. & SCOTT, E. Release of prostaglandin-like substances during elevations of left atrial pressure in the cat
 - 105 MÄRKSTÖ, P. T. KOKKONEN, J. & RANTA, T. Effects of acute hypotension and hypertension on serum TSH concentrations in male rats
 - 109 KAMULAINEN, H., MÄLSTRÖM, L. & VEHKO, V. Morphometry of myocardial apex in endurance-trained mice of different ages
 - 115 HALLBÄCK, D.-Å., JÖDAL, M., BJÖRGVIST, A. & LUNDGREN, D. Viscous tissue osmolarity and intestinal transport of water and electrolytes
 - 127 HAKUMÄKI, M. O. K. Influence of intravenous infusion on heart rate, sympathetic and vagal activity of termination and left atrial and aortic baroreceptor activity in dogs
 - 135 ABRAHAMSSON, T. HOLMGREN, S., NILSSON, S. & PETERSSON, K. On the chromaffin system of the African lungfish, *Protopterus aethiopicus*
 - 141 ABRAHAMSSON, T. HOLMGREN, S., NILSSON, S. & PETERSSON, K. Adrenergic and cholinergic effects on the heart, the lung and the spleen of the African lungfish, *Protopterus aethiopicus*
 - 148 ABRAHAMSSON, T. JÖNSSON, A.-C. & NILSSON, S. Catecholamine synthesis in the chromaffin tissue of the African lungfish, *Protopterus aethiopicus*
 - 153 HARDEBO, J. E. & NILSSON, B. Estimation of cerebral extraction of circulating compounds by the brain uptake index method: Influence of circulation time, volume injection, and cerebral blood flow
 - 161 HARDEBO, J. E., FALCK, B. & ÖWMAN, CH. A comparative study on the uptake and subsequent decarboxylation of monoamine precursors in cerebral microvessels
 - 169 EDIN, R., AHLMAN, H. & KEWENTER, J. The vagal control of the feline pyloric sphincter
- Short Communications*
- 175 SEJRSEN, P. A note on the bolus injection, residue detection method for measurement of capillary permeability
 - 177 FUXE, K., JONSSON, G., BOLME, P. ANDERSSON, K., AGNATI, L. F. GOLDSTEIN, M. & HÖK FELT T. Reduction of adrenaline turnover in carotid vascular areas of rat medulla oblongata by clonidine
 - 181 TONPE, N. & UNDBLOM, B. The influence of prostaglandin synthetase inhibition on the spontaneous contractile activity and induced responses of the hamster oviduct
 - 185 EDIN, R., LUNDBERG, J. M., AHLMAN, H., DAHLSTRÖM, A., FAHRENKRUG, J., HÖKFELT T. & KEWENTER, J. On the VIP-ergic innervation of the feline pylorus
 - 189 NIELSEN, PL. A 3 to 2 coupling of the Na-K pump responsible for the transepithelial Na transport in frog skin disclosed by the effect of Ba
- Appended Supplements*
- Supplementum 471. WALLEVIG, K. In vivo structure and stability of serum albumin in relation to its normal catabolism
- Supplementum 472. DAHLBERG, B. Transcapillary solute exchange in skeletal muscle after injury and during shock

Instructions to authors

Manuscripts (2 copies) should be sent to the National Editor in double spacing on one side of paper of size 21 x 30 cm (A 4) with 4 cm margin. A short title (max. 40 letters) may be suggested. An abstract, not exceeding 200 words should be submitted.

In general, a succinct style and restriction to the necessary of documentation and discussion effectively aids in reducing publication time.

References should be given with full title and name of journals, abbreviated in accordance with 4th Ed. of *World List of Scientific Periodicals*, with volume number and first and last page numbers.

Figures should not be larger than manuscript pages and sent in as glossy prints in a size larger than that required for reproduction. Lettering should be large enough to permit suitable reduction and preferably of uniform size. Photomicrographs should be calibrated on the print (not as enlargement factor in figure text). Figure texts should be assembled on separate sheets.

Tables should be kept at minimum, both in number and size, with text above the table (not on separate sheets). Single numbers in a series should be replaced by mean and S.D. or mean and S.E., in the latter case with number of observations.

Key words (5-10) are recommended in order to facilitate indexing.

For abbreviations, units, and symbols see special list in the Journal and recent articles.

More detailed instructions to authors are found in *NORDIC BIOMEDICAL MANUSCRIPTS, Instructions & guidelines*, published by the Nordic Publication Committee for Medicine, Ed. G. Svartz Malmberg & R. Goldmann, Universitetsforlaget, Oslo 1978.

The International system of units (SI)

The following symbols and units, recommended by the SI, are being used in *Acta Physiologica Scandinavica*. Certain units, not included in SI, will still be permitted.

SI units with recommended symbols

Units	Symbols
kilogramme	kg
second, millisecond	s ms
mole, millimole, micro- mole, nanomole, picomole	mol mmol μ mol nmol pmol
meter millimeter	m mm μ m nm
micrometer	μ m
nanometer	nm
candela	cd
steradian	sr
hertz (frequency)	Hz (s^{-1})
newton (force)	N ($kg \cdot m/s^2$)
pascal (pressure)	Pa (N/m^2)
joule (energy)	J ($N \cdot m$)
watt (effect)	W (J/s)
lumen (lightflow)	lm (cd sr)
lux (illumination)	lx (lm/m^2)

Permitted non SI units

Unit	Symbols
gramme	g
minute	min
hour	h
molarity (mol/liter)	M
(calorie)	cal (4.184 J)
(kilopond)	kp (9.81 N)
(millimeters of mer- cury)	mmHg (1.333 mbar)
(millibar)	mbar (100 Pa)
curie	Cl
liter milliliter micro- liter	l ml μ l
degree Celsius	C

Conversion factors to be given in Methods.

Contents

- 183 CASS, A. & DALMARK, M. Chloride transport by self-exchange and by KCl salt diffusion in gramicidin-treated human red blood cells
 - 208 JANSSON, S. E., HÄRKÖNEN, M. H. & HELVE, H. Metabolic properties of nerve endings isolated from rat brain
 - 213 PARTANEN, S., KAAKKOLA, S. & KÄÄRIÄINEN, I. Tryptophylglycine dipeptide in ACTH/MSH cells of the bovine hypothalamus: its identification and studies on its endonocleptive effects in mice
 - 218 HYVÄRINEN, J., LAAKSO, M., ROINE, R. & LEI, K. Comparison of effects of pentobarbital and ethanol on the neuronal activity in the posterior periaqueductal nucleus
 - 227 ABDUL-RAHMAN, A., DAHLGREN, N., JOHANSSON, B. B. & SIESJÖ, B. K. Increase in local cerebral blood flow induced by circulating adrenaline: involvement of blood-brain barrier dysfunction
 - 233 EDSTRÖM, A., HANSON, M., WALLIN, M. & CEDERHOLM, B. Inhibition of fast axonal transport and microtubule polymerization in vitro by colchicine and colchicine
 - 238 HALLBÄCK, D.-A., JODAL, M. & LUNDGREN, O. Effects of cholera toxin on viscous tissue osmolality and fluid and electrolyte transport in the small intestine of the cat
 - 251 BING, J. & POULSEN, K. Aggression-provoked resin release from extramedullary and extracerebral sources in mice
 - 257 LITHELL, H., ÖRLANDER, J., SCHÉLE, R., SJÖDIN, B. & KARLSSON, J. Changes in lipoprotein-lipase activity and lipid stores in human skeletal muscle with prolonged heavy exercise
 - 263 ROSELL, S. & RÖKAEUS, Å. The effect of ingestion of amino acids, glucose and fat on circulating neurotensin-like immunoreactivity (NTLI) in man
 - 269 GALBO, H., SAUGMANN, P. & RICHTER, E. A. Increased hepatic glycogen synthetase and decreased phosphorylase in trained rats
 - 273 GABRIELSEN, G. & STEEN, J. B. Tachycardia during egg hypothermia in incubating ptarmigan (*Lagopus lagopus*)
- Short Communications*
- 279 LUNDBERG, J. M., HÖKFELT, T., FAHRENKRUG, J., NILSSON, G. & TERENTUS, L. Peptides in the cat carotid body (glomus caroticum): VIP, enkephalin- and substance P-like immunoreactivity
 - 283 SAKABE, T. & SIESJÖ, B. K. The effect of indomethacin on the blood flow-metabolism couple in the brain under normal, hypercapnic and hypoxic conditions
 - 285 OTTESSEN, B., ULRICHSEN, H., WAGNER, G. & FAHRENKRUG, J. Vasoreactive intestinal polypeptide (VIP) inhibits oxytocin induced activity of the rabbit myocardium
- Appendix Supplement*
Supplementum 473. XVI Scandinavian Congress of Physiology and Pharmacology Oslo 1979

Instructions to authors

Manuscripts (2 copies) should be sent to the National Editor in double spacing on one side of paper of size 21 × 30 cm (A 4) with 4 cm margin. A short title (max. 40 letters) may be suggested. An abstract, not exceeding 200 words should be submitted.

In general, a succinct style and restriction to the necessary of documentation and discussion effectively aids in reducing publication time.

References should be given with full title and name of journals, abbreviated in accordance with 4th Ed. of *World List of Scientific Periodicals*, with volume number and first and last page numbers.

Figures should not be larger than manuscript pages and sent in as glossy prints in a size larger than that required for reproduction. Lettering should be large enough to permit suitable reduction and preferably of uniform size. Photomicrographs should be calibrated on the print (not as enlargement factor in figure text). Figure texts should be assembled on separate sheets.

Tables should be kept at minimum, both in number and size, with text above the table (not on separate sheets). Single numbers in a series should be replaced by mean and S.D. or mean and S.E., in the latter case with number of observations.

Key words (5–10) are recommended in order to facilitate indexing.

For abbreviations, units, and symbols see special list in the Journal and recent articles.

More detailed instructions to authors are found in *NORDIC BIOMEDICAL MANUSCRIPTS*. Instructions & guidelines, published by the Nordic Publication Committee for Medicine, Ed. G. Svartz, Malmberg & R. Goldmann, Universitetsforlaget, Oslo 1978.

The international system of units (SI)

The following symbols and units, recommended by the SI, are being used in *Acta Physiologica Scandinavica*. Certain units, not included in SI, will still be permitted.

SI units with recommended symbols

Units	Symbols
kilogramme	kg
second, millisecond	s ms
mole, millimole, micro-mole, nanomole, picomole	mol mmol μ mol nmol pmol
meter millimeter micrometer nanometer	m mm μ m nm
candela	cd
steradian	sr
hertz (frequency)	Hz (s^{-1})
newton (force)	N ($kg\ m/s^2$)
pascal (pressure)	Pa (N/m^2)
joule (energy)	J ($N\ m$)
watt (effect)	W (J/s)
lumen (lightflow)	lm ($cd\ sr$)
lux (illumination)	lx (lm/m^2)

Permitted non SI units

Unit	Symbols
gramme	g
minute	min
hour	h
molarity (mol/liter) (calorie) (kilopond) (millimeters of mercury) (millibar) (curie)	M cal (4 184 J) kp (9.81 N) mmHg (1,333 mbar) mbar (100 Pa) Ci
liter milliliter micro-liter	l ml μ l
degree Celsius	C

Conversion factors to be given in Methods.

Contents

- 289 EDVITSSON, L., LACOMBE, P., OWMAN, CH., REYNIER REBUFFEL, A. M. & SEYLIZ, J. Oscillatory changes in regional cerebral blood flow of rats induced by alpha- and beta-adrenergic stimulants
 - 297 JENSEN, T. Inhibitory actions from low and high threshold cutaneous afferents on groups I) and II) muscle afferent pathways in the spinal cat
 - 309 AALJAE, C. & MULVANY, M. J. Morphological and mechanical properties of small catecholergic arteries and veins in spontaneously hypertensive rats
 - 313 SYBOM, A. & KARLSSON, T. Relationship between serum IgE levels and anaphylactic histamine release from isolated rat mast cells
 - 319 HÄGGMARK, T. & THORSTENSSON, A. Fibre types in human abdominal muscles
 - 327 PETERSSON, G., AHLMAN, H., BHARGAVA, H. M., DAHLSTRÖM, A., KEWENTER, J., LARSSON, L. & SIEPLER, J. K. The effect of propranolol on the serotonin concentration in the portal plasma after vagal nerve stimulation in the cat
 - 333 LINKOLA, J., FYHRQUIST, F. & YLIKAHRI, R. Adenosine 3',5' cyclic monophosphate, calcium and magnesium excretion in ethanol intoxication and its recovery
 - 339 PERTOVAARA, A. Modification of human pain threshold by specific tactile receptors
 - 343 SKAUGEN, E. & WALLÖE, L. Firing behavior in stochastic nerve membrane model based upon the Hodgkin-Huxley equations
 - 355 GRÄNDE, P.-O., BORGSTRÖM, P. & MELLANDER, S. On the nature of basal vascular tone in cat skeletal muscle and its dependence on transmural pressure across
 - 377 JONSSON, G. E., SHIMIZU, Y., FREDHOLM, B. & GRANSTRÖM, E. & OLUF, E. Efflux of cyclic AMP, prostaglandin E₂ and F_{2a} and thromboxane B₂ in leg lymph of rabbits after scalding injury
- Short Communications*
- 385 CLAUSEN, G., KIRKEBO, A., TYSSEBOTH, L., OFJORD, E. S. & AUKLAND, K. Erroneous estimates of intrarenal blood flow distribution in the dog with radiolabelled microspheres
 - 389 LUNDBERG, J. M., HÖKFELT, T., ÅNGGÅRD, A., PERHOW, S. & EMSON, P. Immunohistochemical evidence for substance P containing fibres in the taste buds of the cat
 - 393 HÖKFELT, T., PHILLIPSON, O. & GOLDSTEIN, M. Evidence for a dopaminergic pathway in the rat descending from the A11 cell group to the spinal cord
 - 397 FUXE, K., GAUTEN, D., JONSSON, G., BOLME, P., AGNATI, L. F., ANDERSSON, K., GOLDSTEIN, M. & HÖKFELT, T. Evidence for a selective reduction of adrenaline turnover in the dorsal midline area of the caudal medulla oblongata of young spontaneous hypertensive rats
- Appended Supplements*
- Supplementum 474. PORSSBERG, H. On integrative motor functions in the cat's spinal cord
- Supplementum 475. OSCARSON, J., HÅKANSON, R., LIEBERG, G., LUNDOVIST, G., SUNDLER, F. & THORELL, J. Varied serum gastrin concentrations: trophic effects on the gastrointestinal tract of the rat

Instructions to authors

Manuscripts (2 copies) should be sent to the National Editor in double spacing on one side of paper of size 21 × 30 cm (A 4) with 4 cm margin. A short title (max. 40 letters) may be suggested. An abstract, not exceeding 200 words should be submitted.

In general, a succinct style and restriction to the necessary of documentation and discussion effectively aids in reducing publication time.

References should be given with full title and name of journals, abbreviated in accordance with 4th Ed. of *World List of Scientific Periodicals*, with volume number and first and last page numbers.

Figures should not be larger than manuscript pages and sent in as glossy prints in a size larger than that required for reproduction. Lettering should be large enough to permit suitable reduction and preferably of uniform size. Photomicrographs should be calibrated on the print (not as enlargement factor in figure text). Figure texts should be assembled on separate sheets.

Tables should be kept at minimum, both in number and size, with text above the table (not on separate sheets). Single numbers in a series should be replaced by mean and S.D. or mean and S.E. In the latter case with number of observations.

Key words (5–10) are recommended in order to facilitate indexing.

For abbreviations, units, and symbols see special list in the Journal and recent articles.

More detailed Instructions to authors are found in *NORDIC BIOMEDICAL MANUSCRIPTS, Instructions & guidelines*, published by the Nordic Publication Committee for Medicine, Ed. G. Svartz Malmberg & R. Goldmann, Universitetsforlaget, Oslo 1978.

The International system of units (SI)

The following symbols and units, recommended by the SI, are being used in *Acta Physiologica Scandinavica*. Certain units, not included in SI, will still be permitted.

SI units with recommended symbols

Units	Symbols
kilogramme	kg
second, millisecond	s ms
mole, millimole, micro-mole, nanomole, picomole	mol mmol μ mol nmol pmol
meter millimeter micrometer nanometer	m mm μ m nm
candela	cd
steradian	sr
hertz (frequency)	Hz (s^{-1})
newton (force)	N ($kg\ m/s^2$)
pascal (pressure)	Pa (N/m^2)
joule (energy)	J ($N\ m$)
watt (effect)	W (J/s)
lumen (lightflow)	lm (cd sr)
lux (illumination)	lx (lm/m^2)

Permitted non SI units

Units	Symbols
gramme	g
minute	min
hour	h
molarity (mol/liter) (calorie) (kilopond) (millimeters of mercury) (millibar)	M cal (4 184 J) kp (9.81 N) mmHg (1,333 mbar) mbar (100 Pa)
curie	Cl
liter milliliter micro liter	l ml μ l
degree Celsius	$^{\circ}C$

Conversion factors to be given in Methods.

Performance of the hypertrophied left ventricle in spontaneously hypertensive rat. Effects of changes in preload and afterload

EDDY NORESSON, SVEN-ERIK RICKSTEN, MARGARETA HALLBÄCK-NORDLANDER and PETER THORÉN

Department of Physiology, University of Göteborg, Sweden

NORESSON E., RICKSTEN S. E., HALLBÄCK-NORDLANDER, M. & THORÉN P. Performance of the hypertrophied left ventricle in spontaneously hypertensive rat. Effects of changes in preload and afterload. *Acta Physiol Scand* 1979; 107: 1-8. Received 13 June 1978. ISSN 0001-6772. Department of Physiology, University of Göteborg, Sweden.

Isolated hearts from adult spontaneously hypertensive rats (SHR, Okamoto 1969) with established hypertension were investigated in an antegrade perfusion apparatus where preload and afterload could be varied independently. Frank-Starling curves were constructed at constant afterloads ranging from 50 mmHg to 150 mmHg. As earlier reported, the SHR hearts exhibited a rightward shift of their Frank-Starling relationships compared to those from the normotensive control hearts, though visible only at afterloads up to about 100 mmHg. At higher afterloads the SHR hearts performed significantly better than the NCR ones as their maximal stroke volume was significantly greater compared to that of controls. Thus, left ventricular hypertrophy obviously increases the work capacity of the heart, though at the cost of an altered Frank-Starling relation dependent on the reduced diastolic compliance. For such reasons the myocardial hypertrophy in established SHR hypertension must be considered physiologic adaptation and not degenerative phenomenon, though naturally degenerative processes may later become superimposed.

Key words: Primary hypertension, spontaneously hypertensive rat, left ventricle, Frank-Starling relation, rightward shift, preload, afterload, maximal cardiac performance.

Left ventricular hypertrophy is a general finding in established hypertension. The increased tension development per myocardial fibre when the left ventricle contracts against an enhanced aortic pressure is considered to be the key stimulus for this hypertrophy. When ventricular hypertrophy has balanced off the elevation of arterial pressure, i.e. afterload, the increased muscle mass contributes to the increased total tension development so that tension per transverse section area of contractile elements is again normalized (cf. Meerson 1969). In the spontaneously hypertensive rat (SHR, Okamoto 1963) being one of the best animal analogues for essential hypertension in man, the first trace of an increase of left ventricular mass appears as early as 3 days after birth and may here contain an element of hyperplasia as well as hypertrophy (Weiss & Lundgren 1978). Later in life left ventricular weight in per cent of body weight increases in due proportion to the increased arterial pressure (Farmer et al

1974). A similar structural adaptation to increased pressure load takes place also within the systemic precapillary resistance vessels where it appears as an increased wall thickness in relation to the internal radius in SHR and in human essential hypertension (Folkow et al. 1973).

Left ventricular hypertrophy as seen in hypertension, has been considered as a principally physiologic adaptation (Hallbäck, Isaksson & Norresson 1975) but it has also been regarded as a more or less degenerative phenomenon (Averil et al. 1975). It has by the former group been shown that an increased filling pressure is required to produce equal stroke volumes in isolated perfused hypertrophied hearts from SHR compared with hearts from normotensive controls (NCR). Thus, the Frank-Starling relationship of hypertrophied hearts was at lower filling pressures displaced to the right of controls in proportion to the degree of left ventricular hypertrophy. However, at higher filling

Table 1 Mean arterial pressure, heart rate, body weight and left ventricular weight in per cent of body weight in adult SHR and matched NCR

Values presented are mean \pm S.E. Levels of significance are given

	Blood pressure (mmHg)	Heart rate (beats/min)	Body weight (g)	Left ventricular weight in per cent of body weight
SHR ($n=17$)	148 \pm 1	374 \pm 1	323 \pm 1	0.304 \pm 0.005
NCR ($n=17$)	100 \pm 1	336 \pm 2	376 \pm 2	0.226 \pm 0.001
<i>P</i>	0.001	n.s.	0.001	0.001
SHR/NCR	1.48	1.05	0.86	1.35

pressures these differences were no longer at hand. This suggests that the rightward shift of the Frank-Starling relationship of the hypertrophied hearts is not a consequence of degenerative phenomena since the differences then would be further accentuated at high filling pressures. It is instead suggested to be due to an altered relationship between enddiastolic pressure and enddiastolic tension in the more thickwalled SHR ventricles (cf Hallbäck 1975).

The present study was undertaken to further investigate these matters and to study how the work performance of hypertrophied hearts differs from that of normotensive control hearts when the cardiac work is altered over a wide range by changing either filling pressures (preload) or peak aortic pressures (afterload). For this purpose isolated beating hearts from adult SHR and from normotensive control rats (NCR) were perfused antegradely in a system where preload and afterload could be varied independently. In this way Frank-Starling curves could be constructed for different levels of constant afterloads.

METHODS

Animals. 17 4–5 months old male SHR (weight around 325 g) and 17 NCR of the same age and sex but slightly heavier (weight around 376 g; Table 1) were included in the study. They were fed a standard pellet diet and had water *ad libitum*.

Preparations. Mean arterial pressure (MAP) measurements were performed one week prior to the actual experiments. During light ether anesthesia a PE 50 catheter was inserted into the tail artery. The rats were allowed to wake up and MAP was then measured during steady state conditions. At the day of experiment the rats were heparinized (50 IU/100 g b.w.) and 15 min later anesthetized with ether. After a midline incision the thymus and the pericardium were removed, the large vessels cut and the heart was immediately placed in ice-cold saline which within 5 s stopped its activity. The aortic transec-

tion was made at least 4 mm above the coronary ostia so that no interference with coronary flow would occur when the heart was mounted in the perfusion apparatus. The aortic cannula, which had an outer diameter of 3 mm, was inserted and tightly ligated. Within 40 s after the excision the heart was perfused via the aorta and the coronaries with a non-recirculating Krebs-Henseleit bicarbonate buffer. Contractions started within seconds after the beginning of the initial washout period. The preperfusion lasted for 6–8 min. Meanwhile a major pulmonary vein was cannulated with the angled cannula shown in Fig. 1 while all other pulmonary veins were ligated.

From now on the heart was instead perfused via left atrium in an antegrad fashion with a recirculating perfusion fluid (Fig. 1). Krebs-Henseleit bicarbonate buffer gassed with 95% O₂ and 5% CO₂ was used as perfusate (Krebs & Henseleit 1932). The volume of the recirculating perfusate was held constant (120 ml) by a reservoir (Fig. 1). The perfusate contained (mM): NaCl 118, KCl 4.7, CaCl₂ 2.5, MgSO₄ 1.2, KH₂PO₄ 1.2, NaHCO₃ 25, NaEDTA 0.5 and glucose 14.

Perfusion apparatus. A modification of the antegrade perfusion apparatus originally described by Morgan and Neely was used (Morgan *et al.* 1965; Neely *et al.* 1967; Isaksson 1972) as shown in Fig. 1. The apparatus consisted of a 130 cm long oxygenating chamber with a micropore filter at the bottom (cf Isaksson 1977). A peristaltic pump with an output of 450 ml/min was collecting the perfusate leaving the oxygenating chamber and pumped it to the top of the chamber and to the airtight bubble trap. The preload could be varied by changing the height of airtight bubble trap over the heart level. The connecting tube (Tygon tube, inner diameter 6 mm) between the heart and the airtight bubble trap contained another small bubble trap because small bubbles could occasionally slip through the first trap. The preload, i.e. left atrial pressure, was recorded via a side tube connected to a Statham 23 DC transducer which was placed at the level of the heart and writing on a Grass polygraph. Compensation was made for the pressure fall in the tube between the transducer and the heart.

The heart was pumping against a modified Starling resistor (Fig. 1). By adjusting the air pressure in the balloon the aortic pressure could be maintained constant at any desired level. The aortic pressure was recorded on a Grass polygraph via a Statham 23 DC transducer (Fig. 1).

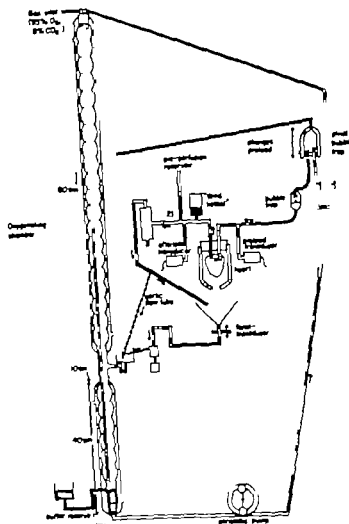


Fig. 1 Schematic illustration of the antegrade perfusion system where preload and afterload can be varied independently

The aortic pulse pressure could be varied by changing the amount of air in the 'Windkessel' (normally 2 ml) and was held between 10-15 mmHg. This implies that the aortic pressure levels were 3-8 mmHg lower than the peak values. Changes in peak aortic pressure were taken as expressions of changes in left ventricular afterload. The coronary flow dripping from the heart and the aortic flow were diverted into a funnel placed on top of Grass FT10 force transducer. An electronic valve was placed on the outlet from the funnel, closing it off during 6 s, every 10th s, so that an intermittent and exact flow registration was obtained by means of the periodic weight increases thus recorded by the force transducer. In this way total cardiac output (CO) was registered but when the aortic output went directly to the oxygenator (Fig. 1 dashed line) only coronary flow was recorded. The overflow in the atrial

bubble trap, the coronary and aortic flow were returned to an extra inlet in the middle of the oxygenator.

Experimental procedures During the actual experiment, which normally lasted 45–60 min, the hearts worked anergically *i.e.* produced an external work. The hearts were throughout paced at 300 beats/min with square wave stimulator at pulse duration of 4 ms and 2–4 V. They were contracting against different levels of peak aortic pressures (50, 80, 110, 130 and 150 mmHg) where for each level of afterload the preload was varied between 1 and 20 mmHg while CO and coronary flow were measured. On the basis of these measurements Frank-Starling curves, representing different levels of afterload, could be constructed.

Fig 3 illustrates short segments of an original recording. There was no substantial change in coronary flow

Modified Starling resistor

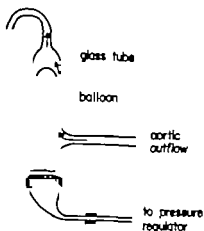


Fig. 2 Modified Starling resistor. By adjusting the air pressure in the balloon, the aortic pressure can be held constant at any desired level.

when the preload was successively raised as long as the afterload was kept constant. Every 10th min during the recording period CO was checked during standardized conditions, i.e. at preload 5.5 mmHg and afterload 80 mmHg to control that the basal performance and general condition of the heart had not been altered. If CO then had decreased more than 10% the experiment was terminated. After the perfusion the wet weight of the left ventricle (including the interventricular wall) was calculated and related to the body weight of the rat.

Statistical analyses were performed according to group comparisons Student's *t* test. Values are presented as mean \pm S.E.

RESULTS

In the awake SHR ($n=17$) mean arterial pressure (MAP) was 148 ± 1 mmHg at an age representing early phases of established hypertension while MAP was 100 ± 1 mmHg in the matched NCR ($n=17$) (Table 1). Heart rates were largely the same during the awake state in the two groups. It is also seen from Table 1 that the weight of the SHR left ventricle was 35% larger than that of NCR per unit body weight.

Fig. 4 shows the compiled experimental results concerning the Frank-Starling relationship for paced SHR and NCR hearts at 5 different levels of constant afterload ranging from 50 mmHg to 150 mmHg. At the lower afterloads (50 mmHg and 80 mmHg) stroke volumes were lower in SHR than in NCR at comparable filling pressures up to 10–17 mmHg where the SHR stroke volume leveled off around $80 \mu\text{l}/100 \text{ g b.w.}$ At an afterload of 50 mmHg the NCR left ventricle reached about the same

maximal stroke volumes as SHR already at preloads between 8 and 10 mmHg. In NCR stroke volume decreased significantly at still higher preloads ($P < 0.05$) which was not the case in the SHR heart even if the filling pressure was here raised to 30 mmHg.

The highest stroke volumes obtained during the experimental procedures were $77 \pm 3 \mu\text{l}/100 \text{ g b.w.}$ for NCR and $82 \pm 2 \mu\text{l}/100 \text{ g b.w.}$ for SHR which for both were obtained at an afterload of 80 mmHg, though SHR needed a higher preload than NCR to reach this maximum, i.e. 15 vs. 10 mmHg. At increasing afterloads the stroke volumes were more reduced in NCR than in SHR at any given diastolic filling pressure. As can be seen from Fig. 4 a rise in afterload from 80 mmHg (arbitrarily set to represent the normotensive level) to 130 mmHg (arbitrarily set to represent the hypertensive level) has much a greater influence on the stroke volumes in NCR than in SHR at any given diastolic filling pressure above 5 mmHg. The maximal stroke volume/100 g b.w. is then reduced 30% in NCR but only 11 per cent in SHR (Fig. 5). These differences are even more pronounced when afterloads of 80 mmHg and 150 mmHg are compared. Thus at a 150 mmHg afterload the maximal stroke volume was in SHR reduced by only 71% but by 48% in NCR compared with those obtained at 80 mmHg (Fig. 5). At afterloads of 130 and 150 mmHg the SHR curve

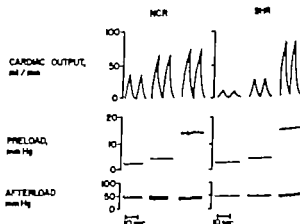


Fig. 3 Original registration of cardiac output from one NCR and one SHR heart. The hearts were paced at a frequency of 300 beats/min. At constant afterload (50 mmHg in peak aortic pressure) the cardiac output was measured at three different preloads. Note the much smaller output, i.e. stroke volume of the SHR left ventricle at low preloads while maximal stroke volumes at high preload are the same in SHR and NCR.

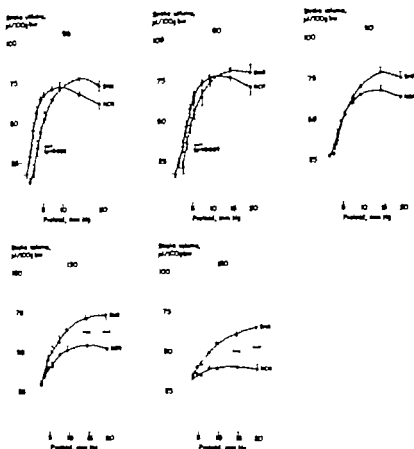


Fig. 4 The effect of increased preload on stroke volume per 100 g b.w. of adult SHR and age-matched NCR left ventricles at 5 different afterloads, ranging from 90 to 50 mmHg. Vertical bars represent \pm S.E. $0.05 > P > 0.01$ $0.01 > P > 0.001$ < 0.001 .

are much steeper than the NCR ones (Fig. 4) indicating that the NCR left ventricle is then working near to its maximal performance already at low filling pressures. In contrast, the SHR left ventricle has at these high afterloads a far better capacity to regulate its work performance by alterations in preload. These findings clearly illustrate that the hypertrophied hearts of SHR can produce a better external work than those of NCR at high afterloads. But at lower afterload the SHR hearts need a higher diastolic filling pressure to produce the same stroke volume as the NCR hearts.

DISCUSSION

A proportionality between the extent of increase in mean arterial pressure (MAP) and left ventricular

hypertrophy has been demonstrated both in hypertensive man and in SHR (cf Pickering 1968, Farmer et al 1974). It has however been discussed whether the left ventricular hypertrophy represents a physiologic adaptation (Beznak 1958, Hallbläck et al 1975, Pfeffer et al 1975) or a degenerative phenomenon (Spurn et al 1969, Ross & Sobel 1972, Averbil et al 1976). Therefore the functional consequences of the left ventricular hypertrophy were examined in a systematic manner in the present study.

The performance of the left ventricle depends on several factors like the enddiastolic filling pressure, the inotropic state of the myocardium as governed by neurogenic and hormonal influences and to some extent on the aortic pressure level (afterload) (Sarnoff & Mitchell 1962). When comparing

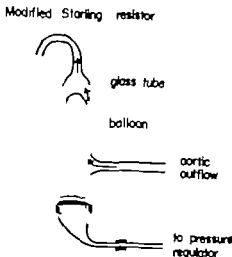


Fig. 2 Modified Starling resistor. By adjusting the air pressure in the balloon the aortic pressure can be held constant at any desired level.

when the preload was successively raised as long as the afterload was kept constant. Every 10th min during the recording period CO was checked during standardized conditions, i.e. at preload 55 mmHg and afterload 80 mmHg to control that the basal performance and general condition of the heart had not been altered. If CO then had decreased more than 10% the experiment was terminated. After the perfusion the wet weight of the left ventricle (including the interventricular wall) was calculated and related to the body weight of the rat.

Statistical analyses were performed according to group comparisons Student's *t*-test. Values are presented as mean \pm S.E.

RESULTS

In the awake SHR ($n=17$) mean arterial pressure (MAP) was 148 ± 1 mmHg at an age representing early phases of established hypertension while MAP was 100 ± 1 mmHg in the matched NCR ($n=17$) (Table 1). Heart rates were largely the same during the awake state in the two groups. It is also seen from Table 1 that the weight of the SHR left ventricle was 35% larger than that of NCR per unit body weight.

Fig. 4 shows the compiled experimental results concerning the Frank-Starling relationship for paced SHR and NCR hearts at 5 different levels of constant afterload ranging from 50 mmHg to 150 mmHg. At the lower afterloads (50 mmHg and 80 mmHg) stroke volumes were lower in SHR than in NCR at comparable filling pressures up to 10–17 mmHg where the SHR stroke volume leveled off around $80 \mu\text{l}/100 \text{ g b.w.}$ At an afterload of 50 mmHg the NCR left ventricle reached about the same

maximal stroke volumes as SHR already at preloads between 8 and 10 mmHg. In NCR stroke volume decreased significantly at still higher preloads ($P < 0.05$) which was not the case in the SHR heart even if the filling pressure was here raised to 30 mmHg.

The highest stroke volumes obtained during the experimental procedures were $77 \pm 3 \mu\text{l}/100 \text{ g b.w.}$ for NCR and $82 \pm 7 \mu\text{l}/100 \text{ g b.w.}$ for SHR which for both were obtained at an afterload of 80 mmHg though SHR needed a higher preload than NCR to reach this maximum, i.e. 15 vs. 10 mmHg. At increasing afterloads the stroke volumes were more reduced in NCR than in SHR at any given diastolic filling pressure. As can be seen from Fig. 4 a rise in afterload from 80 mmHg (arbitrarily set to represent the normotensive level) to 130 mmHg (arbitrarily set to represent the hypertensive level) has much greater influence on the stroke volumes in NCR than in SHR at any given diastolic filling pressure above 5 mmHg. The maximal stroke volume/100 g b.w. is then reduced 30% in NCR but only 11% in SHR (Fig. 5). These differences are even more pronounced when afterloads of 80 mmHg and 150 mmHg are compared. Thus at a 150 mmHg afterload the maximal stroke volume was in SHR reduced by only 21% but by 48% in NCR, compared with those obtained at 80 mmHg (Fig. 5). At afterloads of 130 and 150 mmHg the SHR curve

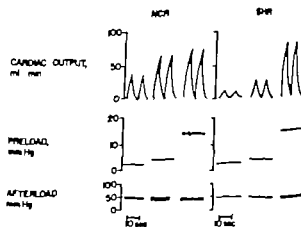


Fig. 3 Original registration of cardiac output from one NCR and one SHR heart. The hearts were paced at a frequency of 300 beats/min. At constant afterload (50 mmHg in peak aortic pressure) the cardiac output was measured at three different preloads. Note the much smaller output, i.e. stroke volume of the SHR left ventricle at low preloads while maximal stroke volumes at high preload are the same in SHR and NCR.

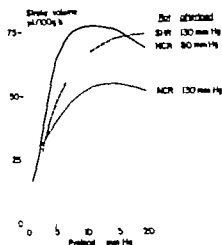


Fig. 6 The effect of increased preload on left ventricular stroke volume per 100 g b.w. for (1) NCR at an afterload of 80 mmHg (corresponding the situation for NCR *in vivo*), (2) SHR at 130 mmHg (corresponding the situation for the SHR left ventricle *in vivo*) and (3) NCR at an afterload of 130 mmHg (corresponding the situation *in vivo* when a normotensive heart is exposed to acute hypertension, about the end of myocardial hypertrophy or if hypertrophy failed to occur in chronic hypertension).

the increased muscle mass of the SHR heart increases its strength proportionally so that it can sustain its stroke volume also when working against high afterload. When comparing stroke volumes in SHR and NCR at given preloads SV is lower in SHR than in NCR at low afterload but higher at high afterload.

However in the *in vivo* situation the SHR heart works against a higher afterload than the NCR heart and this situation is mimicked if the Frank-Starling relationships obtained *in vitro* are compared at an afterload of 80 mmHg for NCR and at 130 mmHg for SHR, which largely represents their MAP levels *in vivo*. In Fig. 6 where this comparison is illustrated the SHR curve is then clearly displaced to the right of the NCR one but when compared to the NCR curve obtained at 130 mmHg afterload, which reflects how a nonhypertrophied heart would work at hypertensive levels, the SHR curve is displaced to the left. Fig. 6 thus illustrates that the SHR left ventricle thanks to its hypertrophy better can maintain an adequate stroke volume at the increased afterload, than would have been possible without any structural myocardial adaptation. However when the cardiac function curves are expressed as in Fig. 6, where the SHR and NCR

hearts are working against afterloads, which could represent their respective *in vivo* situation, the SV for a given preload is reduced in SHR compared to that in NCR. This would indicate that if no compensatory adjustments occur stroke volume would tend to decrease along with the progression of hypertension and left ventricular hypertrophy. Several studies also point in this direction both concerning essential hypertension in man (Frohlich et al. 1971) and in SHR (Frohlich & Pfeffer 1973). At least in the early established phases of essential hypertension in man and in SHR stroke volume is however usually within the normal range after being somewhat increased in early more or less labile phases (Pfeffer & Frohlich 1973; Julius & Schork 1971). The present results were obtained in hearts from SHR in the established phase of hypertension when SV does not differ essentially from age-matched NCR *in vivo* (Frohlich & Pfeffer 1973; Norrison Jones & Hallback 1977). When the pumping ability of hearts in established SHR hypertension was evaluated in open chest animals *in vivo* there were no signs of deteriorated myocardial function (Pfeffer et al. 1976). Therefore some compensation for the altered Frank-Starling relationship would probably be at hand in the intact SHR. This could either be in terms of an increased cardiac filling or by an increased inotropic state where the former alternative seems to be the most pronounced mechanism in the SHR (Norrison et al. 1979).

In conclusion, the present results illustrate that the left ventricular hypertrophy has at least two important functional consequences. First, the reduced diastolic compliance of the left ventricle will decrease the stroke volume at low filling pressures, equivalent with a rightward shift of the Frank-Starling curve. This is most evident in the lower afterload range. Second, the hypertrophy contributes to make the SHR heart correspondingly stronger so it can better cope with the greater work load that it is exposed to in the hypertensive state. Both these phenomena are consequences of the structural adaptation of the heart to an increased pressure load and are not per se evidence of any myocardial degeneration, though such can, of course, be superimposed in later phases of hypertension. Instead, the absence of hypertrophy in hypertension would lead to reduced cardiac performance with lowered stroke volume and lead to deterioration of cardiovascular homeostasis.

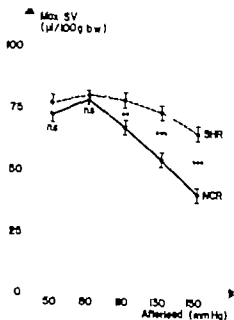


Fig. 5 The relation between maximal stroke volume per 100 g b.w. and afterload for 17 pairs of SHR and NCR left ventricles. Vertical bars indicate \pm S.E. $ns = 0.05 > P \geq 0.01$ $= 0.01 > P \geq 0.001$ $= P < 0.001$

the performance of hearts with and without hypertrophy all these factors must be kept constant which for practical reasons is almost impossible in vivo (Ross 1976). This comparative study was therefore performed on isolated perfused hearts from SHR and NCR in a system where the above-mentioned factors determining cardiac performance could be kept constant or varied independently of each other. The impact of changes in enddiastolic filling pressure on stroke volume i.e. the Frank-Starling relationship was earlier investigated in isolated SHR and NCR at afterloads around 60 mmHg (Hallböck et al 1975). As in the present study a rightward shift in the Frank-Starling relationship was then documented of the SHR heart and the extent of this shift seemed to be proportional to the degree of left ventricular hypertrophy. However in intact animals the SHR hearts work against a higher afterload than the NCR ones which no doubt affects also the work performance. The present results have shown that the work performance of hypertrophied and normal hearts is differently affected by changes in afterload. Thus when the SHR and NCR hearts are compared at lower afterloads the Frank-Starling relationship for SHR is shifted to the right of that in NCR. When however afterload is increased the relationship between filling pressure and SV is better maintained in SHR and at very high afterloads the SHR curve is displaced to the

left of that of the NCR at least at higher filling pressures.

The rightward shift of the SHR curve at low afterloads could theoretically be explained by a depressed myocardial function. This is however an unlikely explanation to judge from the cardiac function curves of SHR and NCR at higher afterloads. As earlier discussed by Braunwald & Ross (1968) other factors than depressed myocardial function can be responsible for an altered Frank-Starling relationship for example a reduced diastolic compliance. Along with hypertension and concomitant left ventricular hypertrophy diastolic compliance is apt to be reduced (Meerson 1969). Then according to Laplace's law the thicker wall of the hypertrophied SHR left ventricle would lead to a correspondingly lower enddiastolic tension per unit wall thickness at a given enddiastolic pressure level (cf. Hallböck 1975). The average muscle fibre stretching which determines stroke volume would then be smaller than in the normal more thin-walled left ventricle. Thus the more the left ventricular wall lumen ratio is increased by hypertrophy the less pronounced is the myocardial prestretch for a given diastolic filling pressure increase particularly so in the outer wall layers. It can hence be concluded that there is an altered relationship between enddiastolic pressure and enddiastolic tension in the presence of an increased myocardial wall thickness [Laplace's law: $T = (P \times r) / h$, T = tension, P = enddiastolic pressure, r = internal radius (unchanged), h = wall thickness (increased)] (Meerson 1969, Hallböck et al 1975). This disproportion is therefore suggested to cause the shift of the SHR Frank-Starling relationship. Such a shift was shown to occur also in renal hypertensive rats by Averill et al (1976) but was here interpreted mainly as signs of degenerative changes.

At low afterloads (50 and 80 mmHg) there was no difference between maximal stroke volumes in the SHR and NCR left ventricles. This indicates that the rightward shift of the Starling curves in SHR at low afterloads and preloads is not a degenerative process but rather reflects the reduced diastolic compliance. Evidently if only the diastolic filling pressure is increased enough as to ensure adequate diastolic prestretch the hypertrophied SHR heart performed just as well as the normotensive one. Further at high afterloads (110, 130 and 150 mmHg) the SHR hearts produced significantly greater stroke volumes than the NCR hearts (Fig. 5). Thus

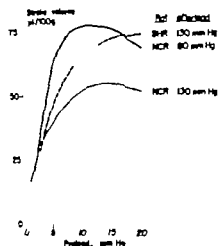


Fig. 6 The effect of increased preload on left ventricular stroke volume per 100 g b.w. for (1) NCR at an afterload of 80 mmHg (corresponding the situation for NCR *in vivo*), (2) SHR at 130 mmHg (corresponding the situation for the SHR left ventricle *in vivo*) and (3) NCR at an afterload of 130 mmHg (corresponding the situation *in vivo* when a nonhypertrophied heart is exposed to acute hypertension, about the aid of myocardial hypertrophy or if hypertrophy failed to occur in chronic hypertension).

the increased muscle mass of the SHR heart increases its strength proportionally so that it can sustain its stroke volume also when working against high afterload. When comparing stroke volumes in SHR and NCR at given preloads SV is lower in SHR than in NCR at low afterload but higher at high afterload.

However in the *in vivo* situation the SHR heart works against a higher afterload than the NCR heart and this situation is mimicked if the Frank-Starling relationships obtained *in vitro* are compared at an afterload of 80 mmHg for NCR and at 130 mmHg for SHR, which largely represents their MAP levels *in vivo*. In Fig. 6 where this comparison is illustrated the SHR curve is then clearly displaced to the right of the NCR one but when compared to the NCR curve obtained at 130 mmHg afterload, which reflects how a nonhypertrophied heart would work at hypertensive levels, the SHR curve is displaced to the left. Fig. 6 thus illustrates that the SHR left ventricle, thanks to its hypertrophy, better can maintain an adequate stroke volume at the increased afterload than would have been possible without any structural myocardial adaptation. However when the cardiac function curves are expressed as in Fig. 6, where the SHR and NCR

hearts are working against afterloads, which could represent their respective *in vivo* situation, the SV for a given preload is reduced in SHR compared to that in NCR. This would indicate that if no compensatory adjustments occur stroke volume would tend to decrease along with the progression of hypertension and left ventricular hypertrophy. Several studies also point in this direction both concerning essential hypertension in man (Frohlich et al 1971) and in SHR (Frohlich & Pfeffer 1973). At least in the early established phases of essential hypertension in man and in SHR stroke volume is, however, usually within the normal range after being somewhat increased in early more or less labile phases (Pfeffer & Frohlich 1973; Julius & Schork 1971). The present results were obtained in hearts from SHR in the established phase of hypertension when SV does not differ essentially from age-matched NCR *in vivo* (Frohlich & Pfeffer 1973; Norellson, Jones & Hallblom 1977). When the pumping ability of hearts in established SHR hypertension was evaluated in open chest animals *in vivo*, there were no signs of deteriorated myocardial function (Pfeffer et al 1976). Therefore some compensation for the altered Frank-Starling relationship would probably be at hand in the intact SHR. This could either be in terms of an increased cardiac filling or by an increased inotropic state where the former alternative seems to be the most pronounced mechanism in the SHR (Norellson et al 1979).

In conclusion: The present results illustrate that the left ventricular hypertrophy has at least two important functional consequences. First, the reduced diastolic compliance of the left ventricle will decrease the stroke volume at low filling pressures, equivalent with a rightward shift of the Frank-Starling curve. This is most evident in the lower afterload range. Second, the hypertrophy contributes to make the SHR heart correspondingly stronger so it can better cope with the greater work load that it is exposed to in the hypertensive state. Both these phenomena are consequences of the structural adaptation of the heart to an increased pressure load and are not per se evidence of any myocardial degeneration, though such can, of course, be superimposed in later phases of hypertension. Instead the absence of hypertrophy in hypertension would lead to reduced cardiac performance with lowered stroke volume and lead to deterioration of cardiovascular homeostasis.

This investigation was supported by grants from the Swedish Medical Research Council (no 14X-00016 and 14X-04764) the Swedish National Association against Heart and Chest Diseases and the Medical Faculty University of Göteborg

AB Hålsjö generally covered part of the expenses for a technician

REFERENCES

- AVERILL, D B, FERRARIO C M, TARAZI R C, SEN S & BAJBUS R. 1976 Cardiac performance in rats with renal hypertension. *Circulat Res* 38, 280-288.
 BEZNAK M. 1958 Cardiac output in rats during the development of cardiac hypertrophy. *Circulat Res* 6, 207-212.
 BRAUNWALD E. & ROSS J. 1963 The ventricular end-diastolic pressure. *Amer J Med* 34, 147-149.
 FARMER, B B, HARRIS R A, JOLLY W W & VAILL, W J. 1974 Studies on the cardiomegaly of the spontaneously hypertensive rat. *Circulat Res* 35, 102-110.
 FOLKOW B, HALLBÄCK M, LUNDGREN Y, SIVERTSSON R & WEISS L. 1973 Importance of adaptive changes in vascular design for establishment of primary hypertension studied in man and in spontaneously hypertensive rats. *Circulat Res* 32 and 33 Suppl. 1, 1-2-1-13.
 FROHLICH E D, TARAZI R C. & DUSTAN H P. 1971 Clinical-physiological correlates in the development of hypertensive heart disease. *Circulation* 44, 446-455.
 HALLBÄCK M. 1975 Interaction between central neurogenic mechanisms and changes in cardiovascular design in primary hypertension. *Acta Physiol Scand* Suppl. 424.
 HALLBÄCK M, ISAKSSON O & NORESSON E. 1975 Consequences of myocardial structural adaptation on left ventricular compliance and the Frank-Starling relationship in spontaneously hypertensive rats. *Acta Physiol Scand* 94, 259-270.
 ISAKSSON O. 1972. Influence on *in vitro* mechanical activity on protein synthesis and amino acid transport in perfused rat hearts. Göteborgs tryckeriet Göteborg.
 JULIUS S & SCHORK M A. 1971 Borderline hypertension - a critical review. *J Chron Dis* 23, 723-754.
 KREBS H A & HENSELEIT K. 1932 Untersuchungen über die Harnstoffbildung im Tierkörper. *Hoppe Seivlers Z Physiol Chem* 210, 33-36.
 MEERSON F Z. 1969 The myocardium in hypertensive hypertension and heart failure. *Circulat Res* 25 Suppl. 7.
 MORGAN H E, NEELY J R., WOOL R E, LIEBECO C, LIEBERMEISTER H & PARK C R. 1965 Factors affecting glucose transport in heart muscle and erythrocytes. *Fed Proc* 4, 1040-1045.
 NEELY J R, LIEBERMEISTER, H, BATTERSBY E J & MORGAN H C. 1967 Effect of pressure development on oxygen consumption by isolated rat heart. *Amer J Physiol* 212, 804-814.
 NORESSON E, JONES J V & HALLBÄCK M. 1977 Hemodynamic changes during tilt after an aortic blockade in spontaneously hypertensive rats. *Cardiovasc Res* 11, 475-480.
 NORESSON E, RICKSTEN S E & THORÉN P. 1979 Left atrial pressure in normotensive and spontaneously hypertensive rats. *Acta Physiol Scand* 110, 9-12.
 OKAMOTO K. 1969 Spontaneous hypertension in rats. *Int Rev Exp Path* 7, 227-270.
 OKAMOTO K & AOKI K. 1963 Development of a strain of spontaneously hypertensive rats. *Jap Circulat J* 27, 282-293.
 PFEFFER M A & FROHLICH E D. 1973 Hemodynamic and myocardial function in young and old normotensive and spontaneously hypertensive rats. *Circulat Res* 32 and 33 Suppl. 1, 1-28-1-35.
 PFEFFER M A, FROHLICH E D, PFEFFER J M & WEISS K. 1974 Pathophysiological implications of the increased cardiac output of young spontaneously hypertensive rats. *Circulat Res* 34 and 35 Suppl. 1, 235-242.
 PFEFFER M A, PFEFFER J M & FROHLICH E D. 1976 Pumping ability of the hypertrophied left ventricle of the spontaneously hypertensive rat. *Circulat Res* 38 No 5.
 PICKERING G W. 1968 High blood pressure. J & A Churchill Ltd. London.
 ROSS J. 1976. The concept of afterload mismatch and its implications in the clinical assessment of cardiac contractility. *Jap Circulat J* 40.
 ROSS J & SOBEL, B E. 1972 Regulation of cardiac contraction. *Ann Rev Physiol* 34, 47-90.
 SARNOFF S J & MITCHELL, J H. 1962 The control of the function of the heart. In *Handbook of physiology*. Circulation vol 1 pp 489-532.
 SPANN J F, MASON D T & ZELIS R F. 1969. The altered performance of the hypertrophied and failing heart. *Amer J Med Sci* 258, 291-303.
 WEISS L. & LUNDGREN Y. 1978 Left ventricular hypertrophy and its reversibility in young spontaneously hypertensive rats. *Cardiovasc Res* 12, 635-638.

Left atrial pressure in normotensive and spontaneously hypertensive rats

UDDY NORESSON, SVEN-ERIK RICKSTEN and PETER THORÉN

Department of Physiology, University of Göteborg, Sweden

NORESSON E, RICKSTEN S. E. & THORÉN P. Left atrial pressure in normotensive and spontaneously hypertensive rat. *Acta Physiol Scand* 1979, 107: 9-12. Received 13 June 1978. ISSN 0001-6772. Department of Physiology, University of Göteborg, Sweden.

The left atrial pressure in adult spontaneously hypertensive rats (SHR) of the Okamoto strain and normotensive control rat (NCR) was measured via chronically implanted catheters. In SHR left atrial pressure in end-expiration was more than twice as high (10.3 ± 0.4 mmHg) as in NCR (4.6 ± 0.3 mmHg). There was no difference in the intrapleural pressure between the two groups of rats; therefore the enhanced left atrial pressure in SHR represents a real rise in the diastolic filling pressure of its left ventricle. This is considered to be the most important compensation for the earlier reported rightward shift of the Frank-Starling curve in SHR (Hallback, Jansson & Norrison 1975; Norrison et al. 1979a). Without this compensation the stroke volume would have been drastically reduced for the hypertrophied heart.

Key words: Essential hypertension, spontaneously hypertensive rat, left atrial pressure, mean arterial pressure.

During the development of arterial hypertension in the spontaneously hypertensive rat (SHR, Okamoto 1963) there is a left ventricular hypertrophy largely proportional to the pressure increase (cf. Folkow et al. 1973). This increased wall thickness of the left ventricle leads to a decreased compliance, shifting the Frank-Starling curve to the right for SHR compared to NCR (normotensive control rat) (Hallback, Jansson & Norrison 1975). To compensate for this Frank-Starling shift, the heart could either work on a higher inotropic state, i.e. shift to another steeper Starling curve, or climb upwards on the prevailing curve by increasing the diastolic filling pressure of the left ventricle, or a combination of both. To explore which of these alternatives is the prevalent one in SHR *in vivo*, the left atrial pressures were measured via chronically implanted catheters at rest in awake NCR and SHR.

Further recent data by Thorén et al. (1979a, b) indicate that the left atrial receptors are reset in SHR. Data on left atrial pressures in NCR and SHR will help to determine the degree of activity *in vivo* in these receptors.

METHODS

4-5 months old male SHR (weighing around 340 g) and NCR of the same age and sex but with moderately higher body weight (around 420 g, Table 1) were used. Seven technically successful expts. were obtained in each strain of rats out of a total of about 40 operated rats. The rats had water *ad libitum* and were fed on a standard pellet diet. During brief ether anaesthesia, PE 50 cannula was inserted into the tail artery. The animals were allowed to wake up and the awake mean arterial pressure (MAP) and heart rate were recorded on Grass polygraph (model 7). Five SHR with MAP below 135 mmHg and one NCR with pressure higher than 110 mmHg were excluded from the study.

After these measurements the animals were anaesthetized with sodium pentobarbital (Nembutal®) 40-50 mg/kg b.w. i.v. and 1/4 of the dose was given when needed. The rats were intubated orally with PE 200 tube and artificially ventilated with positive pressure system (max. inspiration pressure 15 cm water). The thorax was opened in the 4th intercostal space on the right side and great care was taken not to damage the lungs, the intercostal artery or the internal mammary artery.

Two hemostats were placed on the lateral parts of the right middle lung lobe in order to expose the pulmonary vein. The vessel was ligated off distally and a suture was placed around the base of the lobe. Under dissection-

Table 1 Blood pressure, heart rate, body weight and left atrial pressure (at the end of the expiratory phase and the mean value) in adult SHR and matched NCR

Values presented are mean \pm S.E. Levels of significance are given

	Blood pressure (mmHg)	Heart rate (beats/min)	Body weight (g)	Left atrial pressure (mmHg)	
				In end-expiration	Mean
SHR (n = 7)	140 \pm 2	368 \pm 7	340 \pm 2	10.3 \pm 0.4	6.8 \pm 0.3
NCR (n = 7)	102 \pm 2	379 \pm 5	422 \pm 4	4.6 \pm 0.3	2.2 \pm 0.4
P <	0.001	n.s.	0.001	0.001	0.01
SHR/NCR	1.39	0.97	0.81	2.24	3.09

microscope a 1.5–2 cm long PE 10 tube connected to a PE 50 catheter was inserted into the lung vein. By manipulating the snare bleedings could be kept minimal. The tip of the catheter was placed into the left atrium and was connected to a pressure transducer (Statham 23 DC) writing on the Grass polygraph. This catheter passed through the muscle layer in the 5th interstitium and another PE 50 catheter was introduced in the same interstitium with the tip in the thoracic cavity 1 mm inside the wall. Air and exudate could be sucked through the pleural catheter during the closure of the thorax and after the operation.

When closing the thorax the animal lungs were blown up to a respiratory pressure of 20–25 cm water, the respiration switched off and the sutures tightened, whereupon respiration was started again. The two catheters were secured into the thorax wall and then subcutaneously led up to the neck and exteriorized. The catheters were filled with heparinized saline. The muscle and skin layers were sutured with single sutures. The suture lines were more than 1 cm away from the 4th intercostal space in order to prevent leakage of air. During the whole operation the left atrial pressure was followed to ensure good communication. Later the animal was taken off the respirator and subsequently extubated. Body temperature was followed during and after the operation and held at 37°C–38°C. After the operation the remaining air in the thoracic cavity was sucked out. It was important to repeatedly suck the trachea during the postoperative period to avoid respiratory failure. Acute postoperative complications were arterial embolies (hindlimb, kidney) and pneumothorax with a total mortality of about 35%.

After a postoperative rehabilitation period of 7 days in individual cages the left atrial pressure was measured. The two catheters were connected to pressure transducers (Statham 23 DC) placed 30 mm above the cage floor. Thus the zero value for the pressures was 30 mm above the floor, where the left atrium was estimated to be when the rat was in resting position. During 30 min the rats were allowed to rest in the cage, great care being taken to maintain a quiet environment. Both damped and undamped left atrial pressures, and in 4 rats also pleural pressures were measured when the rats were in basal conditions. In 8 operated rats the communication in the left atrial catheter was unreliable and these rats were excluded. The pre- and postoperative MAP levels did not differ by more than 10 mmHg.

RESULTS

MAP levels after light ether anesthesia were 140 \pm mmHg in SHR and 101 \pm 7 mmHg in NCR (Table 1). Table 1 also shows heart rate, body weight, left atrial pressure at the end of the expiratory phase together with mean left atrial pressure, all recorded during rest for the two groups of rats. SHR had then slightly lower heart rates than NCR as earlier reported by Norellson Jones & Hallback (1977). Left atrial pressure at the end of expiratory phase was 124% higher in SHR than in NCR (10.3 \pm 0.4 mmHg and 4.6 \pm 0.3 mmHg, respectively, $P < 0.001$, Table 1). The mean value for left atrial pressure was 209% higher for SHR compared to NCR (6.8 \pm 0.3 mmHg and 2.2 \pm 0.4 mmHg, respectively, $P < 0.01$, Table 1).

Fig. 1 shows the relation between MAP and left atrial pressure in the end of the expiratory phase for SHR and NCR. There is a clear separation between the two groups with the highest atrial pressure at 6 mmHg for NCR and the lowest for SHR at 6.5 mmHg. In two SHR and two NCR the intrapleural pressures at the end of the expiratory phase were the same and varied between 0 and 7 mmHg, indicating that there really is a higher filling pressure of left ventricle in SHR than in NCR. In the other experiments the pleural pressure measurements failed because of the great tendency of fibrin formation around the tip of the pleural catheter.

DISCUSSION

In the present study the left atrial pressure was measured via a thin chronically implanted PE 10 catheter in awake adult spontaneously hypertensive rats (SHR, Okamoto 1969) and normotensive control rats (NCR). SHR is considered to be a good



Fig. 1 Relationship between mean arterial blood pressure (mmHg) and left atrial pressure at end-expiration (mmHg) for adult SHR (●) and matched normotensive controls (NCR ○). Vertical and horizontal bars represent \pm SE. Note that there is no overlapping between the two groups.

animal analogue for essential hypertension in man. The peak left atrial pressure value at the end of expiration averaged 10.3 ± 0.4 mmHg for SHR and 4.6 ± 0.3 mmHg for NCR. These figures are 0.5 to 1.0 mmHg lower if instead the mean pressure at end expiration is registered because the left atrial pulse amplitude measured via the PE 10 tube was 1–2 mmHg at the end of the expiratory phase. Every inspiration was recorded as a shortlasting sharp dip (about 5 mmHg) in the pressure registration, with no differences between SHR and NCR. If the left atrial pressure tracing curve is damped the pressures will be further reduced to 6.8 ± 0.3 mmHg for SHR and 2.2 ± 0.4 mmHg for NCR because of the influence of the low pressure during the inspiratory period. As there is no difference in the intrapleural pressure between the two groups of rats, these higher values for SHR represent greater transmural pressure in the left atrium and an enhanced filling pressure for the hypertrophied left ventricle.

There could be at least two reasons for the increased pressure in the left atrium and the pulmonary veins in the hypertensive animals. First, there may be a centralization of blood to the cardiopulmonary area, as reported in the labile form of essential hypertension in man (Joffes & Esler 1976). Second, the elevated left atrial pressure could be caused

by an increased stiffness of the lung veins and/or of the left atrium. Such a reduced distensibility of these walls could be caused by an increased discharge in the sympathetic nerves to the cardiopulmonary area and/or by a secondary wall hypertrophy caused by the enhanced pressure (cf. Folkow et al 1973).

The functional importance of such an increased filling pressure of left ventricle is obvious. As earlier reported the increased thickness of the SHR left ventricular wall reduced its compliance, which causes a shift of the Frank-Starling relationship to the right (Hallbläck, Isaksson & Norell 1975). This displacement is probably of great importance for the gradual reduction of cardiac output, when the hyperkinetic initiating form of essential hypertension is transverted into the more fixed form with normal or somewhat lowered cardiac output (Lund-Johansen 1978). The raised left ventricular filling pressure is thus of great importance as a compensation for this Frank-Starling shift, helping the heart to preserve its stroke volume in the hypertrophied state. Without this compensation the stroke volume and hence cardiac output would be drastically reduced. The other possible compensatory mechanism for the displaced Starling curve is an enhanced ventricular isotherm, but data from our laboratory indicate that this is of relatively minor importance in SHR (Norell et al 1979b).

Unmyelinated cardiac receptor endings, especially those on the left side, are of importance for the regulation of blood volume (Thoren et al 1976 cf. Thoren 1979). Rats have a large population of cardiac receptors in the atria and all of them seem to transmit their information via unmyelinated fibres (Thoren et al 1979a). The threshold of these receptors is clearly reset to a higher level in SHR with established hypertension (Thoren et al 1979b) compared to NCR (Thoren et al 1979a), probably because of secondary structural changes in the atrial wall.

To summarize: Parallel with the MAP rise in SHR cardiac hypertrophy occurs which makes the left ventricular wall thicker and less distensible leading to a rightward shift of the Frank-Starling curve. This would tend to lower the stroke volume and reduce cardiac output. As a secondary compensatory mechanism there is a rise in left atrial pressure to maintain an adequate filling of the left ventricle. The precise mechanisms behind this left atrial pressure rise are not known.

This work was supported by grants from the Swedish Medical Research Council (14X-00016 and 14X-04764) from the Faculty of Medicine, University of Göteborg and from Svenska Sällskapet för Medicinsk Forskning AB Håssle Göteborg has generously covered part of the expenses for a technician. Thanks to Carl Widmark for skilful technical assistance.

REFERENCES

- FOLKOW B, HALLBÄCK M, LUNDGREN Y, SIVERTSSON R. & WEISS L. 1973 Importance of adaptive changes in vascular design for establishment of primary hypertension. Studies in man and in spontaneously hypertensive rats. *Circulat Res* 33 and 33 Suppl. 1: 1.2-1.13.
- HALLBÄCK M, ISAKSSON O & NORELLSON E. 1975 Consequences of myocardial structural adaptation on left ventricular compliance and the Frank-Starling relationship in spontaneously hypertensive rats. *Acta Physiol Scand* 94: 259-270.
- JULIUS S. & ELSER, M. 1975 The nervous system in arterial hypertension. C. Thomas Publ. Springfield, Ill.
- LUND-JOHANSEN P. Spontaneous changes in central hemodynamics in essential hypertension—a 10 years follow-up study. 1978. To be published.
- NORELLSON E, JONES J. V. & HALLBÄCK M. 1977 Hemodynamic changes during tilt after adrenergic blockade in spontaneously hypertensive rats. *Circulation Res* 11: 475-480.
- NORELLSON E., RICKSTEN S. E., HALLBÄCK M., NORDLANDER M. & THORÉN P. 1979 Performance of the hypertrophied left ventricle in spontaneously hypertensive rat. Effects of changes in preload and afterload. *Acta Physiol Scand* 000: 000-000.
- OKAMOTO K. 1969 Spontaneous hypertension in rats. *Int Rev Exp Path* 7: 227-270.
- OKAMOTO K. & AOKI K. 1963 Development of a strain of spontaneously hypertensive rats. *Japanese Circulation Journal* 27: 282-293.
- THORÉN P. 1978 Role of vagal C-fibers in cardiovascular control. To be published.
- THORÉN P., DONALD D. E. & SHEPHERD, J. T. 1976 Role of heart and lung receptors with non-modulated vagal afferents in circulatory control. *Circulat Res* 38: Suppl. 11: 2-9.
- THORÉN P., NORELLSON E. & RICKSTEN S. E. 1979a. Cardiac receptors with vagal afferents in the rat. *Acta Physiol Scand* 105: 795-803.
- THORÉN P., NORELLSON E. & RICKSTEN S. E. 1979b. Resetting of cardiac C-fibre endings in the spontaneously hypertensive rat. *Acta Physiol Scand* 107: 13-18.

Resetting of cardiac C-fiber endings in the spontaneously hypertensive rat

P THORÉN E. NORESSON and S. E. RICKSTEN

of Physiology, University of Göteborg, Sweden

THORÉN P. NORESSON E. & RICKSTEN S.-E.: Resetting of cardiac C-fiber endings in the spontaneously hypertensive rat. *Acta Physiol Scand* 1979 107: 13-18. Received 13 June 1978. ISSN 0001-6772. Department of Physiology, University of Göteborg, Sweden.

The characteristics of 11 left atrial receptors in 9 adult male spontaneously hypertensive rats (SHR) were investigated. All the receptor afferents were non-medullated with conduction velocities from 0.5 to 1.5 m/s. Elevation of left atrial pressure during graded aortic occlusion always induced a marked increase in receptor discharge with maximal frequencies ranging from 29 to 70 Hz. The threshold for activation was from 7.5 to 13 mmHg in mean left atrial pressure (mean \pm S.E. 10.1 ± 0.6 mmHg). Upon atrial distension all the receptors displayed clear rhythmicity and the discharge correlated closely with the v-wave indicating distension as the cause of receptor activation. The relationship between the mean left atrial pressure and the frequency of discharge was constructed for all the receptors and compared with similar data obtained from normotensive control rats (NCR) (Thorén et al. 1979). It was then obvious that the left atrial receptors are reset in SHR probably secondarily to decreased distensibility of the left atrium.

Key words. Primary hypertension, spontaneously hypertensive rat, volume receptors, C-fiber endings, atrial pressure.

In dogs and cats there is a population of atrial receptors with medullated vagal afferents situated mainly at the crux-atrial junctions (Pamintal 1973). More recently atrial C-fiber endings in the heart of dogs and cats have also been described (Coleridge et al. 1973, Thorén 1976). In the normotensive rat (NCR) heart Thorén et al. (1978) found a large number of afferent C-fiber endings in the atria, but they were not able to find any atrial medullated afferents or any afferents from the ventricles. Most of the atrial C-fiber endings had very high firing frequencies with cardiac rhythmicity up to 50-60 Hz, but some of the receptors showed a more low frequency irregular type of discharge with maximal frequencies less than 25 Hz.

Resetting of cardiac receptors has been shown to occur during chronic severe heart failure in dogs (Greenberg et al. 1973). In their preparation there was a marked derangement of the receptor function, probably due to a severe degeneration of the receptor field and to an altered distensibility of the atrium (Zucker et al. 1977).

The aim of the present study was to examine the characteristics of these left atrial C-fiber endings in the spontaneously hypertensive rat of the

Okamoto-strain (SHR) and to compare these characteristics with similar data earlier obtained from the normotensive control rat (NCR) (Thorén et al. 1979). This study provides for the first time evidence for a resetting of cardiac receptors in a hypertensive animal.

METHODS

Experiments were performed on 9 male spontaneously hypertensive rats (SHR) of the Okamoto strain (300-380 g, age 12-4 weeks). Under light ether anesthesia PE 50 catheter was inserted into the tail artery. The mean arterial pressure (MAP) was recorded on Grass polygraph when the animal was awake after ending the anesthesia. The animals were then anesthetized with sodium pentobarbital (Nembutal® 40-50 mg/kg) administered i.v. and the anesthesia was maintained by repeated doses (Nembutal® 10-15 mg/kg, every 60 min). The trachea was cannulated with a PE-200 tube and positive pressure ventilation with pure oxygen was started with a frequency of 25 per minute and an end-expiratory pressure of 12-15 cm water. All details of the preparation have been published previously (Thorén et al. 1979) and the method will only be described in short here. Muscle movements were prevented by gallamine (Flaxedil® 2-4 mg/kg i.v., repeated every 60 min).

Surgical procedure. The right vagus nerve and the

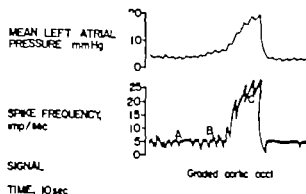


Fig. 1 Mean left atrial pressure and spike frequency in a single left atrial C-fiber during a graded elevation of left atrial pressure induced by a graded aortic occlusion

carotid artery were dissected free in the neck. The thorax was opened by a bilateral intercostal transsternal incision. Snare was placed around the ascending aorta and the inferior caval vein. A thin catheter (PE 10) was placed in the left atrium through the right middle lung lobe vein and connected to a low volume displacement transducer (Gaeltec 3EA). The right upper and middle lung lobe were removed. Arterial blood pressure was recorded in the tail artery via a Statam 23DC transducer. The right jugular vein was cannulated. The vagal trunk was identified just above the lung root and cut in order to eliminate most of the vagal afferents from the lungs and abdominal viscera.

Recordings. The right cervical vagus was placed on a dissection plate and the nerve sheath was carefully dissected away by means of sharp forceps under a dissection microscope. Thin filaments were then obtained and cut centrally and placed on a thin bipolar silver electrode and connected to a nerve amplifier (Grass p. 511). The output of the amplifier was connected to a loudspeaker, a rate meter, an oscilloscope and to an UV-recorder (ABEM 5651) writing intermittently with fast speed. Blood pressure, mean left atrial pressure and the output of the rate meter were recorded on a Grass (mod 7) recorder writing continuously with slow speed. The undamped left atrial pressure and ECG were recorded on the UV-recorder together with the neurogram (Fig. 2).

Experimental procedures. A screening procedure to find receptors in the left side of the heart: the activity in all dissected filaments were observed during short lasting (3–6 s) occlusion of ascending aorta. Every filament that responded with increased activity to this manoeuvre was dissected further until a filament with only one active fiber was found. In most instances an exact localization of the receptors was obtained by probing the heart with a fine probe after killing the animal and opening the heart. The total conduction time was obtained by placing a stimulation electrode connected to a Grass (S4) stimulator over the receptor site and recording the evoked potential in the neck. The conduction velocity was estimated from the approximate length of the conduction pathway and the total conduction time.

Receptor activity was recorded during control conditions and during graded elevation of left atrial pressure

(graded aortic occlusion). The receptor characteristics were compared with the earlier obtained data from the NCR and significance was determined by Student's *t*-test. Values are presented as mean \pm S.E.

RESULTS

This study is based on recording from 11 left atrial receptors in 9 spontaneously hypertensive rats (SHR). The MAP of the awake rats were 151 \pm 1 mmHg. Total conduction time from the receptor site to the recording electrode was from 70–61 ms and the conduction velocity varied from 0.5 to 1.4 m/s (0.8 \pm 0.1 m/s). All the receptors were located in the left atrium as evidenced by probing with a fine plastic probe. Six of the receptors were localized by probing the opened non-beating heart and the other 5 were localized by probing the intact beating heart. The studied receptors were located throughout the entire left atrium also in the atrial appendices and the first part of pulmonary veins.

Receptor discharge during elevation of left atrial pressure. All the receptors responded to elevation of the left atrial pressure induced by a brief occlusion of ascending aorta and their maximal frequency varied from 79 to 70 Hz (55 \pm 3 Hz). The response to a graded increase of the left atrial pressure is shown in Fig. 1. The corresponding neurograms are shown in Fig. 2. Notice that this receptor had a low frequency spontaneous discharge with 1 impulse per cardiac cycle and that upon aortic occlusion the activity increased in parallel with the elevated left atrial pressure.

Fig. 3 shows the individual pressure-response curves for all the 11 receptors. Notice the marked variation in the pressure response curves. The threshold upon activation of the individual receptors varied from 7.5 to 13 mmHg (10.0 \pm 0.6 mmHg) in mean atrial pressure.

The averaged data relating mean left atrial pressure and the activity in the receptors is shown in Fig. 4A.

Firing pattern of the receptors. In the control situation 7 receptors showed a cardiac modulated discharge and when taking the total conduction time into account 4 of them were activated during the a-wave. Upon elevation of left atrial pressure (aortic occlusion) the activity in all the receptors showed a clear cardiac rhythmic discharge pattern and the firing was correlated with the v-wave. However, some endings also discharged with 1 or 2 spikes every a-wave during high atrial pressures.

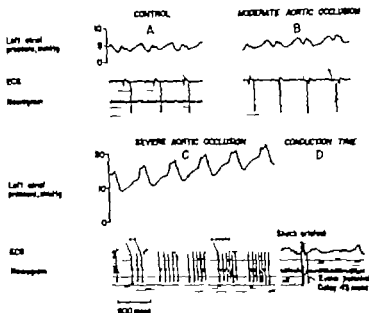


Fig. 2 Left atrial pressure, ECG and nerve impulses in left atrial C-fiber during control conditions (A), moderate aortic occlusion (B), and severe aortic occlusion (C). This receptor is the same as shown in Fig. 1 A. In the control condition the receptor is activated during the a-wave as indicated by the asterisks showing the position in the cardiac cycle of the receptor activation after correction for the total conduction time from the receptor site to the recording electrode as shown in D. Upon a moderate elevation of atrial pressure (B) the firing occurs during the -wave and upon further elevation of the left atrial pressure the v-wave discharge is more prominent with up to 7 up every -wave.

Comparison of left atrial receptor discharge in NCR and SHR. In Fig. 4 A the mean discharge from 3 atrial receptors in NCR (Thorén et al. 1979) and 11 in SHR is compared at increasing mean left atrial

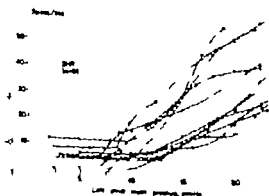


Fig. 3 The pressure-response curves for 11 different left atrial receptors in 9 rats. The activity in the individual receptors is plotted against left atrial mean pressure during an elevation of left atrial pressure induced by a graded aortic occlusion.

pressures. All the receptors in the normotensive rats responded to pressures below 10 mmHg. The thresholds of the SHR receptors were most often above 10 mmHg. Thus, a clear resetting of the atrial C fiber endings in the hypertensive rat is evident.

It has been suggested by Thorén et al. (1979) that there are populations of atrial C-fiber endings in the heart of the NCR. One group of endings has a low frequent irregular discharge and the other type has a more frequent irregular type of discharge. All of the receptors described in the present study were of the high frequency type with cardiac rhythmicity upon activation and maximal frequencies above 25 Hz. If the left atrial receptors in SHR are compared with the earlier obtained data on high frequency receptors in the normotensive animals, the resetting of the left atrial receptors in SHR is still more evident (Fig. 4B).

DISCUSSION

The presence of cardiac vagal receptors has been known since many years. Thus, Paintal (1973) de-

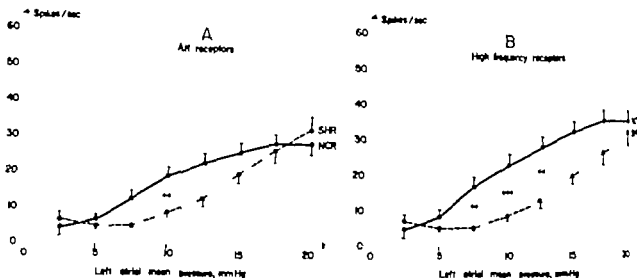


Fig. 4A. Activity in non-medullated vagal afferents from the left atrium during increases in left atrial pressure caused aortic occlusion. The interrupted line shows mean \pm S.E. of recordings from 11 single fibers. For comparison data obtained from NCR are also shown (solid line) (\ast means $P < 0.05$, $\ast\ast$ means $P < 0.01$).

Fig. 4B. The mean activity in 11 left atrial high frequency C-fiber endings in SHR (interrupted line) and similar data from 8 high frequency receptors in NCR (solid line). The data are plotted in the same way as in Fig. 3.

scribed atrial receptors with medullated afferents mainly located at the vein-atrial junctions. More recently Coleridge et al. (1973) and Thorén (1976) examined the characteristics of atrial receptors with non-medullated vagal afferents in dogs and cats. These receptors had somewhat higher thresholds and lower discharge frequencies but many of the atrial C-fiber endings could also respond to moderate elevations of left atrial pressure. There is also a large population of nerve endings with non-medullated vagal afferents in the left ventricle (Coleridge et al. 1964; Sleight & Widdicombe 1965; Öberg & Thorén 1972; Thorén 1977). This group of cardiac C-fiber endings seemed to have a tonic influence on vasomotor center (Thorén et al. 1976).

Thorén et al. (1979) recently suggested the existence of two populations of left atrial C-fiber receptors in the rat. One type of endings showed a fairly low frequent irregular discharge upon elevation of left atrial pressure while the other type was activated with a more high frequent cardiac modulated discharge. The low frequent irregular receptors had higher thresholds than the high frequency ones.

Resetting of cardiac receptors in hypertension. In the present examination the characteristics of such C-fiber endings in the spontaneously hypertensive rat (SHR) have been studied and compared to those in NCR. In this study only high frequency receptors were found but they had a much higher threshold

than the receptors had in the normotensive animal (10.7 ± 0.6 mmHg for SHR in comparison with 4.6 ± 0.6 mmHg for NCR). It is possible that the low frequency receptors in SHR had very high thresholds and were thus difficult to find.

Recent studies by Noreason et al. (1979) indicate that there is a marked elevation of left atrial pressure in the hypertensive rats. A cellular hypertrophy is a general phenomenon in hypertensive animals both in the left ventricle and in the resistance vessels. This is to a great deal considered to be induced by the increased tension per individual cell (Meerson 1969; Folkow et al. 1973). It is therefore likely that this elevated left atrial pressure will induce hypertrophy of the atrial wall which will cause a decreased distensibility of the wall. The decreased distensibility of left atrium will therefore probably be the main reason for the resetting of the receptors.

Physiological consequences of the resetting of the atrial receptors. In cats and dogs the cardiac C-fiber endings induce a tonic vasomotoric inhibition on the vasomotor center and this tonic inhibition seemed to be specifically marked on the vasomotor neurons controlling the sympathetic outflow to the kidneys (cf. Thorén et al. 1976). It has also been postulated that these cardiac vagal reflexes are of importance for the blood volume regulation due to the marked effect on the renal sympathetic outflow. Changes in the renal

sympathetic outflow can influence the sodium excretion via a direct effect on the tubular cells (Dezasa 1977) and via changes in renin release (Auchincloss et al. 1976). It was recently shown by Skaven et al. (1979) that the tonic renal nerve inhibition from cardiac receptors is altered in hypertensive rats. These authors examined the inhibition on the renal nerve upon volume load and found that higher left atrial pressures were needed to reduce the renal nerve inhibition. This further supports the concept that cardiac receptors are reset in spontaneous hypertension, and the altered sympathetic outflow is probably of importance for the reflex control of sodium excretion and renin release.

The resetting of the left atrial C-fibers in the hypertensive rat has several interesting functional consequences. Thus, it has been shown (Hallback et al. 1975) that hypertrophy of the left ventricle induces a clear shift of the Frank-Starling curve to be right meaning that the hypertensive hearts need considerably higher filling pressure to obtain the same stroke volume. As discussed above SHR has a considerably higher left atrial pressure than the normotensive animals. Such a high left atrial pressure would in the absence of left atrial receptor resetting produce a marked inhibition of the sympathetic outflow to the capacitance vessels and it could then be difficult for SHR to ensure an adequate left ventricular filling pressure.

Another interesting point is that the renin release in the spontaneously hypertensive rat seemed to be inhibited (Shiono & Sokabe 1977). The depression seemed to be more pronounced in the very young (5 weeks) hypertensive animals when compared with the older animal with more established hypertension despite the marked increase in left atrial pressure in the older rats. A possible reason might be a resetting of the cardiac C-fibers in established hypertension.

Does the resetting of the cardiac receptors in established hypertension in rats have any significance for pathophysiology of essential hypertension in man? There are some recent studies which might indicate this. Thus patients with mild essential hypertension and low renin values have on average 30% increase in central blood volume without any change in the total blood volume (Julius & Esler 1976). The increased central blood volume is likely to activate the cardiac receptors and cause the reflex inhibition of renin release. Interestingly

enough patients with established and more severe hypertension do not show this inverse relationship between the central blood volume and the renin levels (London et al. 1977). One reason might be a resetting of the cardiac receptors in established hypertension in man.

This study was supported by Swedish Medical Research Council grants 14X-00016 and 14X-04764.

REFERENCES

- DE BONA, G. F. 1977 Neurogenic regulation of renal tubular sodium reabsorption. *Amer J Physiol* 234 F73-F81.
- COLERIDGE H. M., COLERIDGE, J. C. G. & KIDD, C. 1964 Cardiac receptors in the dog, with particular reference to two types of afferent ending in the ventricular wall. *J Physiol (Lond.)* 174 323-339.
- COLERIDGE H. M., COLERIDGE, J. C. G., DANIEL, A., KIDD, C., LUCK, J. C. & SLEIGHT, P. 1973 Impulses in slowly conducting vagal fibers from afferent endings in the ventricle, atria and arteries of dogs and cats. *Circulat Res* 33 87-97.
- FOLKOW, B., HALLBACK, M., LUNDGREN, Y., SIVERTSSON, R. & WEISS, L. 1973 Importance of adaptive changes in vascular design for establishment of primary hypertension studied in man and in spontaneously hypertensive rats. *Circulat Res* 32: 1-16.
- GREENBERG, T. T., RICHMOND, W. H., STOCK, J. G. R. A., GUPTA, P. D., MEE, J. P., MEEHAN, J. P. & HENRY, J. P. 1973 Impaired atrial receptor response in dogs with heart failure due to tricuspid insufficiency and pulmonary artery stenosis. *Circulat Res* 32 and 33 Suppl. 1 2-13.
- HALLBACK, M., ISAKSSON, O. & NORESSON, E. 1975 Consequences of myocardial structural adaptation on left ventricular compliance and the Frank-Starling relationship in spontaneously hypertensive rats. *Acta Physiol Scand* 94 259-270.
- JULIUS, S. & ESLER, M. 1976. Increased central blood volume - possible pathophysiological factor in mild low-renin essential hypertension. *Clin Sci* 51 207-210.
- LONDON, G. M., SAFAR, M. E., WEISS, Y. A., CORVOL, P. L., MENARD, J. E., STON, A. C. & MILLIEZ, P. L. 1977 Relationship of plasma renin activity and aldosterone levels with hemodynamic functions in essential hypertension. *Arch Intern Med* 137 1042-1047.
- MEERSON, F. Z. 1969 The myocardium in hypertension: hypertrophy and heart failure. *Circulat Res* 25 Suppl. ...
- NORESSON, E., RICKSTEN, S. E. & THORÉN, P. 1979 Left atrial pressure in normotensive and spontaneously hypertensive rats. *Acta Physiol Scand* 107 9-12.
- ÖBERG, B. & THORÉN, P. 1972. Studies on left ventricular receptors, signalling in non-medullated vagal afferents. *Acta Physiol Scand* 85 145-163.

- PAINTAL A S 1973 Vagal sensory receptors and their reflex effects. *Physiol Rev* 53 159-227
- RICKSTEN S E, NORESSON E & THORÉN P 1976 Inhibition of renal sympathetic nerve traffic from cardiac receptors in normotensive and spontaneously hypertensive rats. To be published 1979
- SHIONO K & SOKABE, H 1976 Renin-angiotensin system in spontaneously hypertensive rats. *Amer J Physiol* 231 1295-1299
- SLEIGHT P & WIDDICOMBE J G 1965 Action potentials in fibres from receptors in the epicardium and myocardium of the dog's left ventricle. *J Physiol (Lond)* 181 235-258
- THORÉN P 1976 Atrial receptors with non-medullated vagal afferents in the cat. Discharge frequency and pattern in relation to atrial pressure. *Circulat Res* 38 357-362
- THORÉN P 1977 Characteristics of left ventricular receptors with non-medullated vagal afferents. *Circ Res* 40 415-421
- THORÉN P, DONALD D E & SHEPHERD, J 1976 Role of heart and lung receptors with non-medullated vagal afferents in circulatory control. *Circ Res* 38 11 2-9
- THORÉN P, NORESSON E & RICKSTEN, S 1979 Cardiac receptors with vagal afferents in the cat. *Acta Physiol Scand* 105 795-803
- ZANCHETTI A, STELLA A, LEONETTI C, MORGANTI A & TERYOLI L 1976 Control of renin release. A review of experimental evidence and clinical implications. *Amer J Cardiol* 37 675-691
- ZUCKER, I H, EARLE A M & GILMORE, J 1977 The mechanism of adaptation of left atrial ventricular receptors in dogs with chronic congestive heart failure. *J Clin Invest* 60 323-331

The effect of different diets and of insulin on the hormonal response to prolonged exercise

GALBO J. J. HOLST and N. J. CHRISTENSEN

Departments of Medical Physiology B, University of Copenhagen, Department of Clinical Chemistry Bispebjerg Hospital, Medical Department F, Herlev Hospital, and 2nd Clinic of Internal Medicine Aarhus Kommunehospital, Denmark

GALBO J. J., HOLST J. J. & CHRISTENSEN N. J. The effect of different diets and of insulin on the hormonal response to prolonged exercise. *Acta Physiol Scand* 1979, 107: 19-32. Received 12 Dec. 1978. ISSN 0001-6772. Department of Medical Physiology B, University of Copenhagen, Department of Clinical Chemistry Bispebjerg Hospital and 2nd Clinic of Internal Medicine Aarhus Kommunehospital, Denmark.

The importance of carbohydrate availability during exercise for metabolism and plasma hormone levels was studied. Seven healthy men ran on a treadmill at 70% of individual maximal oxygen uptake having eaten a diet low (F) or high (CH) in carbohydrate through 4 days. At exhaustion the subjects were encouraged to continue to run while glucose infusion increased plasma glucose to preexercise levels. Forearm venous blood biopsies from vastus muscle and expiratory gas were analyzed. Time to exhaustion was longer in CH- (106±5 min (S.E.)) than in F-expts. (64±6). During exercise, overall carbohydrate combustion rate, muscular glycogen depletion and glucose and lactate concentrations, carbohydrate metabolites in plasma, and estimated rate of hepatic glucose production were higher. Fat metabolites were lower, and the decrease in plasma glucose slower in CH than in F-expts. Plasma norepinephrine increased and insulin decreased similarly in CH- and F-expts., whereas the increase in glucagon, epinephrine, growth hormone and cortisol was enhanced in F-expts. Glucose infusion eliminated hypoglycemic symptoms but did not substantially increase performance time. During the infusion epinephrine decreased markedly and glucagon even to preexercise levels. Infusion of insulin (to 436% of preexercise concentration) in addition to glucose in F-expts. did not change the plasma levels of the other hormones more than infusion of glucose only but reduced fat metabolites in plasma. At exhaustion muscular glycogen depletion was slow, and the glucose gradient between plasma and sarcoplasm as well as the muscular glucose 6-phosphate concentration had decreased. Conclusions. The preceding diet modifies the energy depot, the state of which (as regards size, receptors and enzymes) is of prime importance for metabolism during prolonged exercise. Plentiful carbohydrate stores (favor both glucose oxidation and lactate production) during exercise norepinephrine increases and insulin decreases independent of plasma glucose changes whereas receptors sensitive to glucose privation but not to acute changes in insulin levels enhance the exercise-induced secretion of glucagon, epinephrine, growth hormone and cortisol. Abolition of cerebral hypoglycemia does not inevitably increase performance time because elimination of the hypoglycemia may not abolish muscular energy lack.

Key words: Glucagon, growth hormone, cortisol, norepinephrine, epinephrine, glucose, glycogen, lipid mobilization, metabolism, fatigue, hypoglycemia.

During prolonged heavy exercise large increases in the uptake and combustion of glucose and free fatty acids occur in the working muscles. At the same time marked changes take place in the plasma concentrations of various hormones, changes which favor glucose production and lipid mobilization. The concentration of insulin decreases, whereas the concentrations of catecholamines, glucagon,

growth hormone and cortisol increase (Galbo et al. 1977c). We have previously investigated the mechanisms which give rise to these hormonal changes. Our studies led to the view that in exercising man plasma norepinephrine mainly reflects a work load dependent activity in the sympathetic nervous system and that α -adrenergic activity inhibits insulin secretion. Furthermore the

hypothesis was put forward that in man during prolonged exercise the secretion of the other hormones is stimulated by cells in CNS and pancreas which respond to glucose privation (Galbo et al 1977c).

In order to examine the validity of this hypothesis we have now measured plasma hormone levels during prolonged exercise which was performed after intake through 4 days of a diet rich in either fat or carbohydrate. Such regimens have been used several times in Scandinavia in this century in studies of exercise metabolism (Boje 1935, Christensen & Hansen 1939, Bergström et al 1967, Hultman 1967, Hultman & Nilsson 1971). They result in small and large glycogen stores respectively and during exercise the plasma glucose concentration declines more rapidly after a fat diet than after a carbohydrate diet. Accordingly if the hormonal response to exercise is enhanced by receptors sensitive to glucose privation also the hormonal changes during exercise would be expected to take place more rapidly after a fat diet than after a carbohydrate diet. In order to further clarify the relationship between the hormonal response and changes in glucose concentrations plasma glucose was at exhaustion restored to pre-exercise levels by glucose infusion during continued exercise.

A decrease in the tissue concentration of insulin may aggravate intracellular glucose privation in glucose sensitive cells regulating hormonal secretion (Müller-Falkow & Unger 1971, Raskin, Fujita & Unger 1975, Szabo & Szabo 1977). Accordingly the decrease of insulin concentration in plasma which takes place during prolonged exercise may enhance hormonal secretion during exercise. If so simultaneous infusion of insulin and glucose may be more efficient in depressing the hormonal response to exercise than infusion of glucose only. Consequently in order to elucidate the importance of insulin for the hormonal response to exercise we infused insulin together with glucose at exhaustion in a group of expts with fat diet. Finally to substantiate the influence of the diets on the glycogen depots and to study the effect of different diets on the metabolic state of working muscles biopsies were taken from the vastus muscle.

METHODS

Subjects and procedure. Seven healthy male students (26 (24-29) years (mean and range)) familiar with the laboratory

gave their informed consent to participate in the study. The students' mean maximal \dot{V}_{O_2} uptake ($\dot{V}_{O_{2max}}$) determined during treadmill running was 4.33 (3.7-5.1) l min⁻¹ and 56 (52-63) ml kg⁻¹ min⁻¹. Mean weight 77 (67-85.5) kg and mean height 184 (180-188) cm. Each subject underwent three diet periods. These periods were 4 days each and were separated by 17 days during which no restrictions concerning physical activity and choice of food were ordered. At the start of each diet period the subjects arrived in the laboratory after an overnight fast. After 30 min rest in a chair they were weighed and had the standing position blood drawn without stasis from the forearm vein. Then in order to produce glycogen depletion the subjects exercised 45 min at a work load corresponding to 80% of individual $\dot{V}_{O_{2max}}$, 30 min on a treadmill at 15 min on a bicycle ergometer. Subsequently a liquid diet (1000 kcal l⁻¹) consisting in the first (F_{10} -expts designated) and third (F_{10} -expts designated) diet period of 76% fat and 13.5% protein, and in the second diet period (C_{10} -expts designated) of 71% carbohydrate and 13.5% protein was delivered. The subjects were asked to consume an amount of diet corresponding to their estimated energy consumption in order to avoid a negative balance of energy in the diet periods. The consumed amount was determined by weighing. Besides the diet only intake of water and vitamin pills were allowed. In the diet periods physical training and smoking were not allowed. In the intervals between the diet periods a supplement of iron (Fe 40 mg day⁻¹) was given. Each diet period was finished by an overnight fast (10 h) after which the students arrived in the laboratory at 8 a.m. They were weighed and had a cannula inserted intravenously in the left forearm whereupon they rested in a chair for 30 min. A sample of urine was examined for ketone bodies, glucose and albumin by stix (Ames). An electrocardiogram was registered with precordial electrodes. While the subjects were standing their oxygen uptake at rest was measured with the Douglas bag method and venous blood samples were drawn without stasis. The glucose concentration in capillary blood from a finger was determined at once with a reflectance meter (Ames) (Schersten et al 1974). Exercise was performed on a motor-driven treadmill with 3% inclination. The speed of the treadmill was chosen so that the work load required 70% of individual maximal oxygen uptake. The subjects ran for repeated 30 min bouts separated by 10-min rest intervals. This sequence was continued until exhaustion. At exhaustion (Exhaustion 1) a 10-min rest was allowed while a cannula was inserted intravenously in the right forearm and connected to a motor-driven infusion pump. Then the subjects were encouraged to resume the running while a 25% (g (100 ml)⁻¹) glucose solution adjusted to pH 7 with 1 M NaHCO₃ was infused from a calibrated glass syringe. Every second min the glucose concentration in capillary blood from a fingertip was determined with the reflectance meter and the speed of the infusion pump adjusted to achieve the pre-exercise blood glucose level and to maintain this level until the subjects were unable to run longer (Exhaustion 2). In the third exercise test (F_{10} -expts) human insulin (Actrapid Novo) was infused as well (1.15 ml min⁻¹ of a solution of 121.8 nmol l⁻¹ of insulin in isotonic sodium chloride containing in addition 1 mM (g

20 ml) human serum albumin) after pruning-dose (575 ml $\text{kg}^{-1} \text{bw}^{-1}$). Expired air was collected through 1.5 mm after 20 min of each exercise period. In each exercise period blood samples were drawn from the catheter after 15 min for analysis of glucose, insulin and oxygen and during the last 2 min for analysis of oxygen, insulin, growth hormone (GH), cortisol, trihydroxybutyrate, glucose, glycerol, FFA (free fatty acids), trihydroxybutyrate, alanine, lactate, pyruvate and creatinine. Capillary blood from fingertips was sampled at the end of each exercise period for glucose determination. Finally blood samples and expired air were collected just after termination, the subjects having recovered for 5 min in the supine and for 5 min in the standing position. Urine after was offered at laboratory 1 (the first (P_1)) as well as in the third (P_3)) experimental series on an average 20 ml of blood were drawn and in the second (CH) 230 ml were drawn. The blood was immediately replaced by isotonic sodium chloride. In the first and second exercise period biopsies (Bergström 1975) weighing about 30 mg are obtained from the lateral head of the quadriceps femoris muscle immediately before exercise and immediately after the first and second run and at exhaustion. The biopsies were obtained through 0.5 cm incisions in the skin 12–16 cm above the knee. The incisions were made in the leg in the first exercise test and in the other leg in the second exercise test.

Analyses. The volume of the collected expired air was measured with a 150 l gasometer (Coflax). The expired air was analysed with an infrared CO_2 -analyser (Beckman LB-1 OA 184) and paramagnetic O_2 analyser (Servomex). The accuracy of the analyses was verified with the Scholander microtechnique (deviation less than 0.06% CO_2 and O_2 , respectively at 12 comparisons performed at intervals of 14 days). Blood for hormone determinations was drawn in ice-cooled test tubes and centrifuged in the cold. Plasma or serum was stored at -20°C until analysis. For catecholamine analysis 10 ml blood were sampled in test tubes which contained 70 mg EDTA and 20 mg ascorbic acid. Plasma, noradrenaline and plasma epinephrine are determined by double-isotope derivative assay (Engelsson & Portnuy 1970) with certain modifications (Christensen 1973). For glucagon and insulin determinations 5 ml blood are drawn in heparinized test tubes containing 0.1 ml 0.25 M Trisylol (Bayer), 1000 U kaolin/embolizing agent. Glucagon was determined with radioimmunoassay after ethanol extraction of plasma (Heding 1971). The antiserum employed 4317 (Holst & Auer 1974) does not cross-react with enteroglucagon. Purified porcine glucagon (NOVO) was used as standard and bound and free hormones are separated by ethanol. Detection limit is below 5.7 pmol l $^{-1}$ and intra- and inter-assay coefficients of variation were about 5% and 15% respectively. Insulin was determined by radioimmunoassay relying on chemical separation (Albano et al 1977). Human insulin (NOVO) was used as standard. The detection limit for the assay system is 0.3 pmol l $^{-1}$ and the intra-assay coefficient of variation is 20% and 3% at 46 pmol l $^{-1}$ (7 pmol l $^{-1}$ of insulin equal 1 μU ml $^{-1}$). Measurements of glucose and insulin concentration in plasma with added exogenous hormone in dilutions of plasma, and in mixtures of plasma with different concentra-

tions yielded results, which deviated less than 10% from the expected values. Serum growth hormone (GH) was determined by a single antibody radioimmunoassay employing Wick chromatography (Orskov, Thomsen & Yde 1968). A Withelini preparation (HIS 968 C) was used as standard. Serum cortisol was measured by commercially available solid phase radioimmunoassay kit (CEA-IRE SORIN). The intra- and inter-assay coefficients of variation of the cortisol assay ($n=8$ triplicate determinations) were 13% (at 606 pmol l $^{-1}$) and 15% respectively. Serum from adrenalectomized rats yielded values which were not significantly different from zero and recovery experiments yielded results which deviated less than 15% from the expected values. Every subject had all analyses of hormone carried out in single assay runs.

The concentration of glucose in blood and plasma was determined by the glucose-oxidase method (Werner, Rey & Wiedinger 1970). In respect to glucose concentrations arterialized capillary blood obtained from fingertips did not differ significantly from blood in the cannulated forearm vein. Free fatty acids (FFA) in serum were determined colorimetrically (Duncombe 1964) with palmitic acid as standard. Glycerol (Eggstein & Kreutz 1966) and alanine (Williamson 1974) in serum and lactate (Gutman & Wahlefeld 1974) in blood were determined by enzymatic spectrophotometric methods and β -hydroxybutyrate and pyruvate by enzymatic fluorimetric microanalyses (Olsson 1971).

Muscle biopsies obtained after exercise were frozen in liquid nitrogen within 10 sec from the end of an exercise bout and stored at -80°C until analysis. About 10 mg of frozen tissue was divided into five pieces and weighed at -20°C on Perkin-Elmer microbalance to the nearest 0.01 mg. Metabolites were extracted during 15 min in 3 N HClO_4 at 4°C . After neutralization with KHCO_3 (2 mol l $^{-1}$) on dry ice the test tubes were centrifuged in the cold. Glucose 6-phosphate, glucose 1-phosphate, glucose lactate and pyruvate were determined on the supernatant by enzymatic fluorimetric microanalyses (Lowry & Passonneau 1973). 1 ml HCl (1 mol l $^{-1}$) was added to the residue and the glycogen was hydrolyzed during 2 h at 100°C . Determination of glucose in the hydrolysates was carried out fluorimetrically (Lowry & Passonneau 1973) and the glycogen concentration is presented as μmol glucosyl units kg^{-1} (wet weight). For determination of the protein concentration about 7 mg of muscle tissue were heated for 30 min at 100°C in 1 ml 1 N NaOH . The protein concentration was determined spectrophotometrically with the Folin phenol reagent (Lowry et al 1951) with bovine serum albumin as the standard. To estimate the precision of the biopsy technique duplicate analyses were performed on five pieces cut from a 31 mg biopsy of human muscle and on 10 pieces cut from a rat leg muscle weighing 80 mg. Mean values (μmol kg^{-1} wet weight) and coefficients of variation for the different analyses on human and rat muscle were: Glucose 6-phosphate: 0.6, 11.5%; Glucose 1-phosphate: 0.7, 17%; Lactate: 2.9, 14.5%; 13.3, 12.8%; Pyruvate: 0.363, 33%; 0.368, 58%; Glycogen: 122, 7.5%; 34.3, 7.3%. The coefficients of variation of the chemical part of the procedures were below 3% except for the coefficient of variation of the pyruvate analysis which was 29%. In

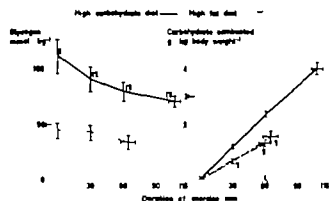


Fig 1 The effect of different diets on the carbohydrate combustion and muscular glycogen concentration during exercise. Mean values (\pm S.E.) of glycogen in the vastus lateralis muscle (expressed as mmol glucosyl units per kg wet weight) and amount of carbohydrate combusted in seven subjects running on a treadmill. In the postabsorptive state each subject exercised three times having eaten through 4 days a diet rich in either carbohydrate or fat. Glycogen concentrations were only measured in one of the two experimental series including a fat enriched diet. + denotes value significantly different ($P < 0.05$) from preexercise (rest) value. ¶ denotes significant difference between experiments including different diets.

the study all chemical analyses were performed at least in duplicate. Enzymes and cofactors were from Boehringer Mannheim.

Statistical evaluation of the data was made by means of correlation analysis and by means of Wilcoxon's non-parametric ranking test and the *t*-test for paired comparisons (Snedecor & Cochran 1965). Differences were considered to be significant if *P* values of less than 0.05 were obtained with both these tests. Concentrations obtained at exhaustion in F_2 - and CH -expts ($n=14$) have been used for correlation analysis when something else is not explicitly stated. The cited correlation coefficients are significant on the 5% confidence level.

RESULTS

Effects of the different diets

Except for hematocrit [$46.7 \pm 0.9\%$ mean and S.E. (F_1 -expts.) significantly higher than 44.1 ± 0.8 (CH -expts.) and 43.5 ± 0.9 (F_2 -expts.)] and FFA [significantly higher in F_1 than in F_2 -expts. (Fig. 4)] values obtained immediately before each of the three diet periods were similar. The energy intake was similar ($P > 0.05$) in periods with fat enriched diet [2492 ± 159 kcal/24 h mean and S.E. (F -expts.) and 2790 ± 90 (F_2 -expts.)] and in periods with carbohydrate enriched diet (2904 ± 195). However during the diet periods a significant loss of body

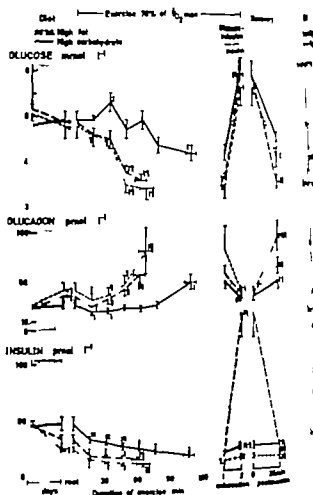


Fig 2 The effects of different diets of exercise and of infusion of glucose and insulin during exercise on glucose, pancreatic glucagon and insulin in plasma. In the postabsorptive state seven subjects ran three times three weeks apart on a treadmill having eaten in advance a diet rich in either carbohydrate or fat (two experimental series). At exhaustion (exhaustion 1) a 10 min rest was allowed. Then the subjects were encouraged to run again as long as possible (to exhaustion 2) while glucose or both glucose and insulin (in one of the experimental series with fat diet designated ---) concentrations were restored by infusion. Values are mean \pm S.E. + denotes significant difference ($P < 0.05$) between values obtained before and after a diet period. * denotes value significantly different from preexercise (rest) value. ¶ denotes value significantly different from value at exhaustion 1. ¶ denotes value significantly different from value at exhaustion 2. ¶ denotes significant difference between experiments including different diets.

weight averaging 2 kg took place in fat expts whereas the 0.6 kg weight loss in carbohydrate expts was insignificant. After the 4 days of diet the muscular glycogen concentration was markedly higher in CH than in F -expts (Fig. 1) and a mild

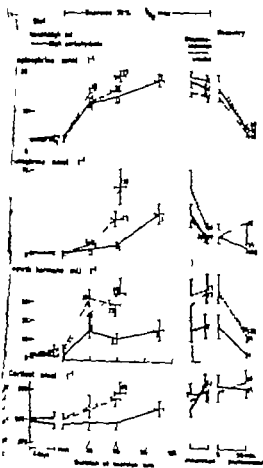


Fig. 3 The effects of different diets, of exercise and of infusion of glucose and insulin during exercise on hormone concentrations in plasma. For further explanation see Fig. 2.

ketonemia had developed in F-expts. The R value (respiratory exchange ratio) was at rest 0.74 ± 0.03 after fat diet and 0.84 ± 0.03 after carbohydrate diet ($P < 0.02$). Fat diet resulted in decreases in "basal" plasma concentrations of insulin, glucose and alanine, and in increases in the concentrations of glucagon, OH-FFA, glycerol and β -hydroxybutyrate (Figs. 2-4). Carbohydrate diet resulted in small increases in norepinephrine and OH concentrations in plasma in the "basal" state (Fig. 3) and in increases in the concentrations of lactate and alanine too (Fig. 5). At the end of the diet periods hematocrit values ($47.8 \pm 1.0\%$ (F), $46.2 \pm 0.6\%$ (CH) and $45.8 \pm 0.6\%$ (F)) had always increased slightly ($P < 0.05$). The changes in alanine and insulin during the diet period correlated mutually ($r = 0.73$).

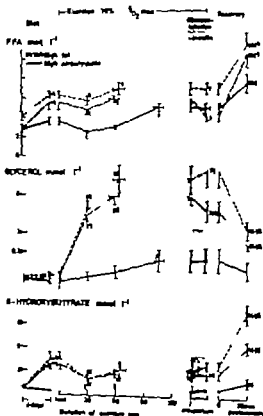


Fig. 4 The effects of different diets, of exercise and of infusion of glucose and insulin during exercise on the concentrations of FFA and glycerol in serum and of β -hydroxybutyrate in blood. For further explanation see Fig. 4.

Responses to exercise

Metabolic rate (kcal min^{-1}) (as calculated from oxygen uptake and R value) and oxygen uptake (69.6 ± 1.7 (F-expts.), 69.7 ± 0.9 (CH-expts.), 68.8 ± 1.5 (F-expts.)) % of individual $\dot{V}_{O_{2\max}}$ ($n = 7$) were constant during all exercise bouts. However the total work time to exhaustion was much longer in CH-expts. (106 ± 5 min) than in F (64 ± 6) and F-expts. (59 ± 6). Heart rate increased from 83 ± 3 (F), 78 ± 4 (CH) and 86 ± 2 (F) beats min^{-1} at rest to 171 ± 2 (F), 163 ± 1 (CH) and 169 ± 1 (F) in the 30th min of exercise. Heart rate rose gradually throughout exercise and was at exhaustion not significantly different in the 3 expts. (181 ± 3 (F), 178 ± 2 (CH) and 176 ± 2 (F)).

In F-expts. the carbohydrate combustion rate during exercise (calculated from O_2 uptake and R value measurements) to be 47 ± 4 (F) and 49 ± 3

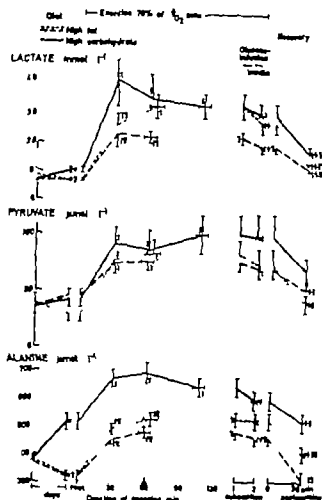


Fig. 5 The effects of different diets of exercise and of infusion of glucose and insulin during exercise on the concentrations of lactate and pyruvate in blood and of alanine in serum. For further explanation see Fig.

(F) % of total energy output per min in the 20th–22nd min) was significantly lower than in CH-expts ($83 \pm 4\%$) (Fig. 1). Furthermore compared with CH-expts the concentration of glucose in plasma declined more rapidly during exercise in F-expts (Fig. 2). This accelerated decrease of glucose concentrations after intake of a fat diet was accompanied by more rapid increases during exercise in the plasma concentrations of glucagon (Fig. 2), epinephrine, GH and cortisol (Fig. 3) than after a carbohydrate diet. During exercise norepinephrine concentrations in plasma always increased progressively above values at rest; the responses to exercise after the different diets did not differ for certain (Fig. 3). Insulin concentrations in plasma always declined gradually during exercise (Fig. 4). At identical times the concentrations were higher in CH than in F-expts.

The concentration of FFA in serum did not change during exercise in F-expts but remained higher than in CH-expts in which an initial decrease was followed by an increase above the concentration at rest (Fig. 4). The serum glycerol concentration gradually increased during exercise in expts but most in F-expts (Fig. 4). The concentration of β -hydroxybutyrate in blood in F-expts, as during exercise lower than at rest but still higher than in CH-expts (Fig. 4). The blood and serum concentrations of lactate, pyruvate and alanine increased during exercise. Lactate and alanine concentrations were higher in CH than in F-expts whereas pyruvate concentrations did not differ significantly (Fig. 5). Hematocrit values did not change significantly during exercise. Comparing the two experimental series with fat diet the responses of hormones and metabolites in plasma to diet and exercise were remarkably similar. However, hematocrit and alanine concentrations were throughout exercise significantly higher in F-expts than in CH-expts. Furthermore, at exhaustion carbohydrate combustion rate, lactate and FFA were higher and insulin lower in F than in CH-expts.

In the vastus muscle the concentration of glycogen gradually decreased during exercise in CH-expts but remained higher than the unchanged concentration in F-expts (Fig. 1). The decrease in glycogen concentration in CH-expts was accompanied by increases in muscular glucose and lactate content (Table 1). The calculated percentage of muscle water in equilibrium with the glucose of plasma water increased in CH-expts from $33 \pm 8\%$ at rest to $58 \pm 9\%$ (mean and S.E.) after 30 min of exercise ($P < 0.1$) at which time it differed ($P < 0.02$) from the value in F-expts ($27 \pm 7\%$). In F-expts the apparent glucose distribution space increased only insignificantly during exercise (from $31 \pm 8\%$ at rest to $40 \pm 5\%$ at exhaustion). The glucose 6-phosphate concentration in muscle tended to decrease

At rest the concentrations of carbohydrate metabolites were slightly higher than mostly reported. Apart from possible influence of the diet, this discrepancy may be ascribed to the fact that the subject in the present study had been standing, not lying, during the 10 min preceding muscle sampling.

Calculated as $(C_{\text{muscle}}/C_{\text{plasma}}) \cdot 100$ where C_{muscle} and C_{plasma} are the calculated glucose concentrations in muscle and plasma water respectively, assuming a water content of 76 and 94% for muscle and plasma respectively.

Table 1 Muscle metabolites during exercise after different diets

	Rest ^a	30 min exercise	60 min exercise	Exhaustion
Glucose, mmol kg ⁻¹				
CH	1.3±0.3	2.4±0.3	1.9±0.4	1.7±0.2 ^a
F	1.2±0.3	1.0±0.2		1.1±0.1
Glucose-6P, mmol kg ⁻¹				
CH	1.4±0.3	1.1±0.2	0.8±0.1	0.6±0.1
F	1.6±0.4	1.1±0.2		0.9±0.1
Lactate, mmol kg ⁻¹				
CH	5.1±0.8	8.1±0.9 ^a	7.4±1.4	5.5±0.7
F	3.8±0.9	4.6±0.9		6.7±1.2
Pyruvate, μmol kg ⁻¹				
CH	207±48	229±47	239±33	14±42
F	184±54	193±27		251±32
Protein, mg g ⁻¹				
CH	183±11	178±6	200±8	184±7
F	207±3	185±6		197±13

^a Values are mean ± S.E. (n=7). The metabolites were measured in wet muscle tissue¹

CH carbohydrate diet F fat diet. Exhaustion was reached after 106±5 min in CH-experiments and after 64±6 min in F-experiments

^a Value significantly different from pre-exercise value

^b Significant difference between F and CH-experiment

^c Value significantly different from pre-exercise value on the 10% probability level (P<0.1)

during exercise while pyruvate and protein concentrations did not change significantly (Table 1). At exhaustion the subjects always reported an overall feeling of fatigue being especially pronounced in the calves. In the fat experiments also symptoms of hypoglycemia (weakness, irritability, mental confusion, nausea, hunger, cold sweating and disturbed co-ordination) were noticed at exhaustion.

Glucagon correlated with the concentrations in plasma of glucose ($r=-0.66$), insulin ($r=-0.64$) and epinephrine ($r=0.57$) and GH ($r=0.56$) and epinephrine, cortisol and GH correlated positively ($P<0.05$) with each other. Glucagon, epinephrine, cortisol and GH correlated negatively ($P<0.05$)

with muscular glycogen at exhaustion. Glycerol correlated with epinephrine ($r=0.54$) and with insulin ($r=0.5$, $P<0.1$). After 30 min of exercise the decrease in muscular glycogen correlated with both the increase in muscular glucose ($r=0.63$) and the increase in lactate ($r=0.76$) and these changes were correlated mutually ($r=0.69$) and the latter with the decrease in glucose 6-phosphate ($r=0.64$). Simultaneously the muscular lactate correlated with blood lactate ($r=0.58$) which in turn correlated with blood pyruvate ($r=0.71$) and alanine ($r=0.60$). At exhaustion in F- and CH-expt (n=7) insignificant positive correlations

existed between glucose 6-phosphate and plasma glucose as well as muscular glycogen.

Glucose infusion during continued exercise

As judged from reflectance meter readings the glucose concentration in capillary blood was stable on the pre-exercise level within 4 mm of glucose infusion. Although symptoms of hypoglycemia disappeared the subjects were only able to run for further 17.8±0.3 min (F-expts.) 15.8±1.6 min (CH-expts.) and 17.5±0.5 min (F-expts.). The average rates of glucose infusion necessary to restore and maintain the blood glucose concentration were significantly higher when both glucose and insulin were infused (1.30±0.09 g min⁻¹ F-expts.) than when only glucose was infused (0.83±0.08 g min⁻¹ (F-expts.) and 0.77±0.06 g min⁻¹ (CH-expts.))

As glucose concentrations were restored plasma glucagon declined to pre-exercise levels (Fig. 2) and plasma epinephrine, too, was markedly reduced (Fig. 3). During glucose infusion the plasma concentrations of norepinephrine, GH and cortisol did not decrease (Fig. 3) and insulin concentrations remained depressed in F- and CH-expts. (Fig. 2). As shown in Figs 4 and 5 the concentrations of fat and carbohydrate metabolites in plasma were not convincingly changed by infusion of glucose alone.

Comparison between F_1 and F_2 -expts reveals that acute elevation of plasma insulin above basal levels did not influence secretion of the other hormones (Figs 2 and 3). The concentrations of FFA, glycerol and β -hydroxybutyrate were reduced by insulin (Fig. 4). During the infusions hematocrit decreased slightly in F -expts (from $47.5 \pm 0.6\%$ to $46.5 \pm 0.6\%$ (F_1), and from $46.3 \pm 0.7\%$ to $45.1 \pm 0.7\%$ (F_2)) whereas heart rate never changed significantly.

The 30 min recovery period

In the recovery periods following glucose or (glucose + insulin) infusions plasma glucose concentrations again decreased below preexercise levels. Plasma glucagon increased above resting levels to mean concentrations which like mean epinephrine and GH concentrations (Fig. 3) were inversely related to the mean glucose concentrations (Fig. 7). The plasma insulin concentration decreased after the end of insulin infusion (F_2 -expts) to a value similar to the unchanged low insulin concentrations in F_1 and CH -expts (Fig. 2). Norepinephrine concentrations decreased after exercise but remained like epinephrine concentrations above preexercise levels (Fig. 3). Cortisol concentrations remained high after exercise whereas GH concentrations decreased significantly (Fig. 3). In the recovery period FFA and β -hydroxybutyrate increased while glycerol concentrations decreased (Fig. 4), the mean values being inversely related to mean insulin concentrations. Just as the plasma concentrations of these fat metabolites throughout the entire experimental course were higher in F than in CH -expts, the concentrations of the carbohydrate metabolites lactate, pyruvate and alanine declining in the postexercise period remained higher in CH than in F -expts (Fig. 5). 30 min after exercise heart rate (109 ± 3 beats/min in F and 122 ± 4 in CH -expts) and mean oxygen uptake (148% and 134% of preexercise values in CH and F -expts, respectively) were still significantly increased. In CH -expts, R value declined in the postexercise period to values below the preexercise value. Hematocrit did not change 30 min after exercise in F and CH -expts. ($n=14$). β -hydroxybutyrate correlated with epinephrine ($r=0.63$) and with insulin ($r=-0.80$). After termination of the insulin infusion the increases in glucagon and epinephrine concentrations correlated mutually

($r=0.67$, $P<0.1$) and both these hormones correlated with plasma glucose ($r=-0.67$ ($P<0.1$); $r=-0.79$ respectively).

DISCUSSION

Regulation of hormonal secretion during exercise

The importance of the plasma glucose concentration. The present study has demonstrated that the hormonal response to prolonged exercise depends upon the preceding diet. After intake of a fat enriched diet the glycogen content in muscle and probably liver (Hultman & Nilsson 1971) was markedly lower than after intake of a diet rich in carbohydrate (Fig. 1). The resulting more rapid decline in plasma glucose concentration during exercise in expts with fat diet was accompanied by faster increases in the concentrations of glucagon, epinephrine, GH and cortisol in plasma (Figs 7 and 8)—a finding which suggests that glucose sensitive receptors are able to modulate the hormonal response to prolonged exercise. This suggestion is further supported by the effects of glucose infusion. When plasma glucose concentrations were restored by exogenous glucose in the final 15 min of exercise plasma epinephrine and glucagon concentrations decreased markedly, glucagon concentrations even to preexercise levels. Irrespective of the preceding diet (Figs 2 and 3). The decreases in the concentrations of these hormones during glucose infusion were due to the glucose infusion and were not a consequence of the 10 min rest period which preceded the infusion. This is so, since we know from the present and our previous studies of prolonged running divided by short breaks that epinephrine and glucagon concentrations do not decrease during a 10 min intermission and a following 15 min run without infusion (Galbo et al 1975, 1976, 1977a, 1977b). The plasma concentrations of GH and cortisol hormones which have considerably longer biological half-lives than epinephrine and glucagon did not decrease during the short lasting glucose infusion. This does not necessarily mean that the plasma glucose concentration is a minor determinant of the response of these hormones to exercise. A delay may be inherent in the stimulus secretion coupling and—although not indicated by our data—GH and cortisol concentrations might have increased further if the last run had not been accom-

by glucose infusion. After termination of exercise and infusion glucose concentrations decreased again while glucagon concentrations increased to values which, relative to glucose concentrations, were not lower than those obtained at exhaustion I (Fig. 2). From this and the above findings it is reasonable to conclude that the glucose concentration in plasma is the determinant of the glucagon response to exercise. 30 min postexercise the concentrations of GH and epinephrine in plasma were inversely related to glucose concentration but the hormone concentrations were lower relative to glucose concentrations than at exhaustion I (Figs. 2 and 3). This indicates that the glucose concentration in plasma is not the sole determinant of the GH and epinephrine responses to heavy exercise. This conclusion is further substantiated by the fact that after 30 min of exercise in expts. on a carbohydrate diet the concentration of both these hormones had increased in the face of an increase in plasma glucose concentration. The persistence of high cortisol concentrations 30 min after exercise at a time when glucose concentrations again were below values obtained at rest, but not lower than concentrations at exhaustion I, is compatible with the assumption that decreased glucose concentrations significantly enhances cortisol secretion during exercise.

Evidence for an influence of plasma glucose concentrations on the hormonal response to exercise in man has previously been published. Thus the rise in glucagon and epinephrine concentrations was markedly reduced when euglycemia was maintained by glucose infusion throughout exercise (Galbo, Christensen & Holst 1977b). Furthermore the rise in glucagon concentration in plasma was abolished when glucose was ingested prior to (Ahlborg & Felig 1977) or during exercise (Luyckx, Pirnay & Lefebvre 1978, Ahlborg & Felig 1976). Also the rise in plasma GH during moderate exercise has been shown to be preventable by carbohydrate ingestion (Hunter, Fonseca & Pastore 1965) and by glucose infusion causing hyperinsulinemia and hyperglycemia (Hansen 1971).

The importance of insulin. On the whole during exercise the concentration of insulin in plasma was inversely related to the concentrations of the other hormones (Figs. 2 and 3). However, a sensitizing effect of a decrease in insulin concentrations on the glucose-sensitive cells modulating the hormonal response to exercise was not proved, since exogenous

insulin + glucose did not depress the concentrations of the other hormones more than exogenous glucose alone. It could be argued that the sampling of blood during the infusions was too infrequent to demonstrate such an effect. Low insulin concentrations might especially act synergistically with low glucose concentrations in plasma. Accordingly a more frequent sampling of blood might have revealed a more rapid decrease in glucagon and epinephrine concentrations during restoration of both insulin and glucose concentrations than during restoration of glucose concentrations only. One could also postulate that the insulin infusion was too brief or the insulin concentrations achieved during insulin infusion too low to restore insulin-mediated cellular glucose turnover in the cells regulating hormonal secretion. In diabetes normalization of the exaggerated growth hormone response to exercise requires a preceding strict insulin treatment (Hansen 1971b). It is possible that the hypoglycemic state induced by fat diet (Fig. 2) in some respect is similar to diabetes and that it was not corrected completely by the short-lasting insulin infusion. Furthermore a decrease in insulin concentration in peripheral blood probably reflects a much larger decrease in insulin concentration in the fluid bathing the pancreatic glucagon secreting A cells. Only about 1% of the blood in the pancreatic vein has passed through the islets of Langerhans and insulin is extracted during hepatic transit. Accordingly the restoration of insulin concentrations in peripheral blood by insulin infusion during exercise possibly was not accompanied by an increase of insulin concentrations to resting values at the A cells. An incomplete restoration of insulin effects on the A cells might explain why glucagon concentrations at the end of the infusions still were 43% above the minimum values obtained 15 min after the beginning of exercise (Fig. 2). Alternatively this finding might be due to the half-life of glucagon being too long in proportion to the infusion periods to allow complete removal of glucagon in excess during these periods.

The importance of sympathetic activity. In the rat the exercise-induced increase in plasma glucagon concentration is mainly caused by increased sympatho-adrenal activity (Galbo et al. 1978). However the present study does not indicate a corresponding influence of the sympatho-adrenal system in man. During exercise as judged from norepinephrine concentrations in plasma, nor-adrenergic

sympathetic nervous activity did not differ with certainty in expts with different diets and did not decrease significantly during glucose infusion (Fig. 3). Thus the enhancement after the fat diet of the glucagon response to exercise and the decline of glucagon concentrations during glucose infusion were probably not secondary to changes in sympathetic nervous stimulation of the pancreatic A cells. Glucagon and epinephrine concentrations varied in parallel during exercise in the different expts. However the lack of parallelism between the changes in the concentrations of these two hormones in the postexercise period (Figs. 2 and 3) indicate that the changes in glucagon concentrations most likely were due to direct effects of glucose on the A cells and not mediated via epinephrine. Further support to this view comes from the fact that the glucagon response to hypoglycemia is normal in sympathectomized (Palmer et al. 1976) and in adrenalectomized (Enslick et al. 1976) man and from the finding that the glucose-glucagon relationship in exercising man is not changed by adrenergic blocking drugs (Galbo et al. 1976; Galbo, Christensen & Holst 1977a). It is unlikely that glucose infusion changed the elimination of glucagon. Thus the marked decline of glucagon concentration upon glucose infusion strongly indicates that the exercise induced increase in glucagon concentrations in plasma reflects an increased A cell secretion.

The present study supports the assumption (Galbo, Christensen & Holst 1977a) that an inhibiting sympathetic nervous activity rather than plasma glucose concentrations determines plasma insulin concentrations during exercise. Early during exercise in spite of unchanged or increased glucose concentrations, insulin levels decreased at the same time as norepinephrine concentrations increased. Furthermore, when glucose was infused norepinephrine concentrations did not decrease and insulin concentrations remained low (Figs. 2 and 3).

Muscular metabolism during exercise

Accumulation of glucose and lactate. The effect of different diets on the muscular concentrations of carbohydrate metabolites have not previously been studied during prolonged exercise. In the present study biopsies were taken from the vastus lateralis muscle. No other muscle has been shown to be a significantly better representative of the working muscles during exhaustive running (Costill et al.

1971; Karlsson & Saltin 1971). We found that the average distribution space for glucose in muscle reached its highest value (58% of muscle wet weight) after 30 min of exercise in expts with carbohydrate enriched diet (Table 1). At least at that time the distribution space was higher than the extracellular space (determined at rest as the raffinose space) being 20–30% in the rat depending on the type of muscle (Kipnis, Helmreich & Cori 1959), determined as the chloride space in man to be 14 and 17% in resting and exercised muscle, respectively (Ahlborg et al. 1967), the negligible change from rest to exercise being in accordance with the constancy of muscular protein concentrations found in the present study (Table 1). The concentration of intracellular free glucose is generally considered to be very low at rest (Elbrink & Bihler 1975; Renne & Holloszy 1977) but it has previously been demonstrated to increase when perfused rat skeletal muscle is stimulated to contract (Renne & Holloszy 1977). The finding of an accumulation of intracellular glucose during exercise at a time when carbohydrate oxidation was increased may be explained by a relative enhancement of glucose transport across the cell membrane (Elbrink & Bihler 1975; Renne & Holloszy 1977) but may also be due to intracellular production of glucose from glycogen (Saha, Lopez Mondragon & Narasimhan 1968; Whalen 1970) and also to a decreased glucose phosphorylation due to an inhibition of hexokinase by glucose 6-phosphate derived from glycogen. The concentration of glucose 6-phosphate did in fact not increase during exercise (Table 1). But compared with expts with fat enriched diet the intracellular glucose concentration was higher during exercise in expts with carbohydrate enriched diet in which also the estimated mean rate of muscular glucose uptake as well as the mean rate of muscular

Concentration of glucose in intracellular space (mmol/l) = [concentration in wet muscle tissue (mmol/kg) - concentration in plasma water (mmol/l) × amount of extracellular water per kg wet muscle tissue (l/kg)] / (amount of intracellular water per kg wet muscle tissue (l/kg)).

Mean rate of muscular glucose uptake (U) = (total amount of carbohydrate combusted - glycogen depletion per kg active muscle × estimated active muscle mass) / increase in glucose concentration in intracellular water × amount of intracellular water in active muscle mass + 0.5 × (sum of increases in concentrations of lactate, pyruvate and alanine in plasma water × amount of extracellular

glycogen breakdown (Fig. 1) were higher. Accompanying the higher rate of carbohydrate oxidation (Fig. 1) the exercise-induced increase in lactate concentrations in muscle (Table 1) and blood (Fig. 5) was higher after carbohydrate diet than after fat diet. Lactate production during exercise has in the past been considered simply a consequence of hypoxia in the working muscles (Elbrink & Bibler 1975). However in the exercising muscles the availability of oxygen (and the exit of lactate over the cell membranes) hardly was lower after carbohydrate enriched diet than after fat enriched diet. Accordingly the present experiments support the view that the magnitude of lactate production rather depends upon the balance between the rate of glycolysis and the capacity for alternative elimination of pyruvate and NADH (Holloszy & Booth 1976).

Effect of exogenous glucose on performance
Low glucose concentrations in plasma (Boje 1935 Christensen & Hansen 1939 Bergstrom et al. 1967) and low muscular glycogen concentrations (Åkblom et al. 1967 Bergstrom et al. 1967 Karlsson & Saltin 1971) have previously been found at exhaustion after prolonged exercise. Furthermore elevation of the initial muscular and hepatic glycogen concentrations by intake of a diet rich in carbohydrate (Boje 1935 Christensen & Hansen 1939 Bergstrom et al. 1967 Karlsson & Saltin 1971) as well as ingestion of glucose at exhaustion in expts. with fat enriched diet (Boje 1935 Christensen & Hansen 1939) have been shown to increase performance time. These findings indicate that continuation of exercise at a given intensity requires that the carbohydrate combustion exceeds a certain lower limit. A lower limit, which probably depends upon the supply of FFA to the working muscles since the carbohydrate combustion as well as plasma glucose and muscular glycogen concentrations at exhaustion are higher in expts. with carbohydrate enriched diet than in expts. with fat enriched diet (Figs. 1 and 2, Boje 1935 Bergstrom et al. 1967), the plasma concentration of FFA being higher in the latter (Fig. 4). At exhaustion in the

present study low muscular glycogen concentration decreased glucose gradient between plasma and muscle water and decreased muscular glucose 6-phosphate concentration (Table 1) indicated that the glucosyl unit turnover in the vastus muscle was lower than earlier during exercise. The simultaneous increase in lipolysis indicated by increased FFA and glycerol concentrations possibly did not completely compensate for the decrease in glucosyl flux and in consequence an energy crisis developed in the working muscles.

In contrast to the findings in the above mentioned earlier studies (Boje 1935 Christensen & Hansen 1939) infusion of glucose did not eliminate the fatigue in the present study. This discrepancy may be due to differences between the different studies as regards the cause of exhaustion. In fact in the earlier studies the improvement of performance by exogenous glucose was ascribed entirely to disappearance of cerebral hypoglycemia, because the overall carbohydrate combustion rate as judged by R-value measurements, did not increase after glucose administration (Boje 1935 Christensen & Hansen 1939). In our expts. with fat enriched diet, however cerebral hypoglycemia was not the major cause of exhaustion, since glucose infusion eliminated the hypoglycemic symptoms but not the fatigue. Although a diet rich in fat was consumed before exercise in the earlier as well as in the present study a muscular lack of energy possibly limited performance only in the present study. This might be the case since in the present study but not in the earlier studies intake of a fat enriched diet was preceded by heavy exercise a regimen known to deplete muscular glycogen stores more than mere intake of fat enriched diet (Hultman 1967). Alternatively exhaustion was in the earlier as well as in the present expts. caused by a muscular lack of energy and the fact that glucose administration improved performance only in the earlier expts. was due to a higher supply of exogenous glucose relative to the minimal glucose need in the earlier than in the present expts. (200 g glucose ingested in 10 min and an estimated previous glucosyl unit turnover of 1.2 g/min in the earlier studies vs an exogenous supply of glucose corresponding to 44 and 26% respectively of previous glucose-unit turnover in the present F₁- and CH-expts.) The conclusion that deficiency of energy substrates in working muscles rather than neuroglycopenia is decisive for exhaustion has previously been drawn from studies. In

after (0.2 body weight) loss of increases in concentration of lactate and pyruvate in intracellular water amount of intracellular water after active exercise)/total work time. Mean rate of hepatic glucose production = 1. decrease in concentration of glucose in plasma water amount of intracellular water volume work time

sympathetic nervous activity did not differ with certainty in expts with different diets and did not decrease significantly during glucose infusion (Fig. 3). Thus the enhancement after the fat diet of the glucagon response to exercise and the decline of glucagon concentrations during glucose infusion were probably not secondary to changes in sympathetic nervous stimulation of the pancreatic A cells. Glucagon and epinephrine concentrations varied in parallel during exercise in the different expts. However the lack of parallelism between the changes in the concentrations of these two hormones in the postexercise period (Figs. 2 and 3) indicate that the changes in glucagon concentrations most likely were due to direct effects of glucose on the A cells and not mediated via epinephrine. Further support to this view comes from the fact that the glucagon response to hypoglycemia is normal in sympathectomized (Palmer et al 1976) and in adrenalectomized (Ensinck et al 1976) man and from the finding that the glucose-glucagon relationship in exercising man is not changed by adrenergic blocking drugs (Galbo et al 1976; Galbo, Christensen & Holst 1977a). It is unlikely that glucose infusion changed the elimination of glucagon. Thus the marked decline of glucagon concentration upon glucose infusion strongly indicates that the exercise induced increase in glucagon concentrations in plasma reflects an increased A cell secretion.

The present study supports the assumption (Galbo, Christensen & Holst 1977a) that an inhibiting sympathetic nervous activity rather than plasma glucose concentrations determines plasma insulin concentrations during exercise. Early during exercise in spite of unchanged or increased glucose concentrations, insulin levels decreased at the same time as norepinephrine concentrations increased. Furthermore, when glucose was infused norepinephrine concentrations did not decrease and insulin concentrations remained low (Figs. 2 and 3).

Muscular metabolism during exercise

Accumulation of glucose and lactate. The effect of different diets on the muscular concentrations of carbohydrate metabolites have not previously been studied during prolonged exercise. In the present study biopsies were taken from the vastus lateralis muscle. No other muscle has been shown to be a significantly better representative of the working muscles during exhaustive running (Costill et al

1971; Karlsson & Saltin 1971). We found that the average distribution space for glucose in muscle reached its highest value (48% of muscle water) after 30 min of exercise in expts with carbohydrate enriched diet (Table 1). At least at that time the distribution space was higher than the extracellular space (determined at rest as the raffinose space) to be 20-30% in the rat depending on the type of muscle (Kipnis, Helmreich & Cori 1959); determined as the chloride space in man to be 14 and 17% in resting and exercised muscle respectively (Ahlborg et al 1967), the negligible change from rest to exercise being in accordance with the constancy of muscular protein concentrations found in the present study (Table 1). The concentration of intracellular free glucose is generally considered to be very low at rest (Elbrink & Bihler 1975; Rennie & Holloszy 1977) but it has previously been demonstrated to increase when perfused rat skeletal muscle is stimulated to contract (Rennie & Holloszy 1977). The finding of an accumulation of intracellular glucose during exercise at a time when carbohydrate oxidation was increased may be explained by a relative enhancement of glucose transport across the cell membrane (Elbrink & Bihler 1975; Rennie & Holloszy 1977) but may also be due to intracellular production of glucose from glycogen (Saha, Lopez-Mondragon & Narahara 1968; Wahren 1970) and also to a decreased glucose phosphorylation due to an inhibition of hexokinase by glucose 6-phosphate derived from glycogen. The concentration of glucose 6-phosphate did in fact not increase during exercise (Table 1). But compared to expts with fat enriched diet the intracellular glucose concentration¹ was higher during exercise in expts with carbohydrate enriched diet in which also the estimated mean rate of muscular glucose uptake as well as the mean rate of muscular

Concentration of glucose in intracellular water (mmol l^{-1}) = [concentration in wet muscle tissue (mmol kg^{-1}) - concentration in plasma water (mmol l^{-1}) \times amount of extracellular water per kg wet muscle tissue (l kg^{-1})] / (amount of intracellular water per kg wet muscle tissue (l kg^{-1})).

Mean rate of muscular glucose uptake (U) = (total amount of carbohydrate combusted - glycogen depletion per kg active muscle \times estimated active muscle mass increase in glucose concentration in intracellular water \times amount of intracellular water in active muscle mass $\times 0.9$) \times (sum of increases in concentrations of lactate, pyruvate and alanine in plasma water \times amount of extracellular

- A SALTIN B 1967 Diet, muscle glycogen and physical performance. *Acta Physiol Scand* 71 140-150.
- BOJE O 1935 Der Blutzucker während und nach körperlicher Arbeit. Thesis. Suppl. *Skand Arch Physiol*.
- CHRISTENSEN E. H. & HANSEN O 1939 Hypoglykämie, Arbeitsfähigkeit und Ernährung. *Skand Arch Physiol* 31 172-179.
- CHRISTENSEN N J 1973 Plasma noradrenaline and adrenaline in patients with thyrotoxicosis and syndromes. *Clin Sci Mol Med* 45 163-171.
- COSTILL D L, SPARKS K., GREGOR R. & TURNER C 1971 Muscle glycogen utilization during exhaustive running. *J Appl Physiol* 31 333-336.
- DUNCAN W G 1964 The colorimetric micro-determination of non-esterified fatty acids in plasma. *Clin Chem Acta* 9 122-125.
- EGOSTEIN M & KREUTZ F H 1966 Eine neue Bestimmung der Neutralfettsäure im Blutserum und Gewebe. *Klin Wochenschr* 44 262-267.
- ELBRINK J & BIHLER L 1975 Membrane transport: its relation to cellular metabolic rates. *Science* 191 1177-1184.
- ENGELMAN K & PORTNOY B 1970 A sensitive double isotope derivative assay for nonesterified and esterified. *Circulat Res* 26: 53-57.
- ENSINCK J W, WALTER R M, PALMER J P, BROODER R G & CAMPBELL R G 1976 Glucose responses to hypoglycemia in adrenalized isolated rats. *Metabolism* 25 227-232.
- GALBO H, HOLST J J & CHRISTENSEN N J 1975 Glucose and plasma catecholamine responses to graded and prolonged exercise in man. *J Appl Physiol* 38 70-76.
- GALBO H, HOLST J J, CHRISTENSEN N J & HILSTED J 1976. Glucose and plasma catecholamines during beta-receptor blockade in exercising man. *J Appl Physiol* 40 835-863.
- GALBO H, CHRISTENSEN N J & HOLST J J 1977 Catecholamines and pancreatic hormones during anesthetic blockade in exercising man. *Acta Physiol Scand* 101 423-437.
- GALBO H, CHRISTENSEN N J & HOLST J J 1977b Glucose-induced decrease in glucagon and epinephrine responses to exercise in man. *J Appl Physiol* 42 525-530.
- GALBO H, RICHTER E A, HILSTED J, HOLST J J, CHRISTENSEN N J & HENRIKSSON J 1977 Hormonal regulation during prolonged exercise. *Ann N Y Acad Sci* 301 72-80.
- GALBO H, RICHTER E A, CHRISTENSEN N J & HOLST J J 1978 Sympathetic control of metabolic and hormonal responses to exercise in rats. *Acta Physiol Scand* 102 441-449.
- GUTMANN I & WAHLEFELD A W 1974 L (+)-Lactate Determination with Lactate Dehydrogenase and NAD. In: *Methods of enzymatic analysis* (ed. H. U. Bergmeyer), vol. 3, pp. 1454-1468. Verlag Chemie Weinheim Academic Press New York San Francisco and London.
- HAGENFELDT L & WAHLEN J 1971 Metabolism of free fatty acids and ketone bodies in skeletal muscle. In: *Muscle metabolism during exercise*. Advances in experimental medicine and biology vol. 11 (ed. B. Pernow and B. Saltin), pp. 153-163. Plenum Press New York and London.
- HANSEN Aa. P 1971 The effect of intravenous glucose infusion on the exercise-induced serum growth hormone rise in normals and juvenile diabetics. *Scand J Clin Lab Invest* 28 195-205.
- HANSEN Aa. P 1971b Normalization of growth hormone hyperresponse to exercise in juvenile diabetics after "normalization" of blood sugar. *J Clin Invest* 50: 1806-1811.
- HEDING L G 1971 Radioimmunochemical determination of pancreatic and gut glucagon in plasma. *Diabetologia* 7 10-19.
- HICKSON R C, RENNETT M J, CONLEE R K, WINDER W W & HOLLOSZY J O 1977 Effects of increased plasma fatty acids on glycogen utilization and endurance. *J Appl Physiol* 43 829-833.
- HOLLOSZY J O & BOOTH F W 1976 Biochemical adaptations to endurance exercise in muscle. *Ann Rev Physiol* 38 773-791.
- HOLST J J & AASTED B 1974 Production and evaluation of glucagon antibodies for radioimmunoassay. *Acta endoc. (Köln)* 77 715-726.
- HULTMAN E 1967 Physiological role of muscle glycogen in man, with special reference to exercise. *Circulation Res. Suppl* 1 20: 99-112.
- HULTMAN E & NILSSON L H 1971 Liver glycogen in man. Effect of different diets and muscular exercise. In: *Muscle metabolism during exercise*. Advances in experimental medicine and biology vol. 11 (ed. B. Pernow and B. Saltin), pp. 143-151. Plenum Press New York and London.
- HUNTER W M, FONSEKA C C & PASSMORE R 1965 The role of growth hormone in the mobilization of fuel for muscular exercise. *Quant J Exp Physiol* 50 406-416.
- ISSEKUTZ B., Jr ISSEKUTZ A. C. & NASH D 1970 Mobilization of energy sources in exercising dogs. *J Appl Physiol* 29 691-697.
- KARLSSON J & SALTIN B 1971 Diet, muscle glycogen and endurance performance. *J Appl Physiol* 31 203-206.
- KIPNIS D M, HELMREICH E. & CORLE F 1959 Studies of tissue permeability IV. The distribution of glucose between plasma and muscle. *J Biol Chem* 234 165-170.
- LOWRY O H & PASSONNEAU J V 1973 A flexible system of enzymatic analysis. Academic Press, New York.
- LOWRY O H, ROSEBROUGH N J, FARR A. L. & RANDALL R J 1951 Protein measurement with the folin phenol reagent. *J Biol Chem* 193 265-275.
- LUYCKX A S, FIRNAY P & LEFEBVRE P J 1978 Effect of glucose on plasma glucagon and free fatty acids during prolonged exercise. *Europ J Appl Physiol* 39: 53-61.
- MÜLLER W A, FALOOKA O R. & UNGER R H 1971 The effect of experimental insulin deficiency on glucagon secretion. *J Clin Invest* 50: 1992-1999.
- NAZAR K, BRZEZINSKA Z. & KOWALSKI W 1972. Mechanism of impaired capacity for prolonged

which an intracarotid glucose infusion given at exhaustion did not restore the work capacity in dogs (Nazar Brzezinska & Kowalski 1972). It may appear strange that performance time was the same when glucose in the present study was infused together with insulin and at a rate corresponding to as much as 74% of the previous carbohydrate combustion rate as it was when a smaller amount of glucose was infused without insulin. The explanation may be that "insulin inhibited lipolysis (Fig. 4) and accordingly increased the glucose need. But how do we explain that the elimination of muscular fatigue by exogenous glucose during exercise may take place without an increase in carbohydrate combustion rate (Boje 1935, Christensen & Hansen 1939)? Let us assume that primarily resting fibers are recruited when primarily recruited fibers are exhausted due to an insufficient glucosyl turnover. Let us in addition assume that an individual feels exhausted when a fixed number of muscle fibers are fatigued or a fixed intensity of innervation is exceeded. In agreement with these assumptions glucose administered at exhaustion may be metabolized in and restore the function of the primarily recruited fibers. In that way saving activity and glycogen combustion in secondarily recruited fibers and accordingly eliminating fatigue without an increase in carbohydrate combustion rate.

CONCLUSION

The present study has shown that in man the rate of carbohydrate combustion is higher during exercise after intake of a diet rich in carbohydrate than after intake of a fat enriched diet, probably as a consequence of both higher hepatic glucose output and muscular glycogen breakdown. However the exercise induced changes in plasma concentrations of norepinephrine and insulin are similar after the two diets, and after the carbohydrate enriched diet the changes in epinephrine, glucagon, cortisol and growth hormone are delayed in parallel with a slower decline in plasma glucose concentration. Hypothetically the regulation of metabolism during prolonged exercise proceeds as follows. Impulses from motor centers in the cerebral cortex or from the working muscles elicit a work load dependent activity in the sympathetic nervous system (Galbo, Holst & Christensen 1975) which in turn depresses insulin secretion (Galbo, Christensen & Holst

1977a). These changes in norepinephrine and insulin levels together with the size of the extramuscular fuel depots as well as the state of receptors and enzymatic machinery in these depots determine the primary mobilization of glucose and free fatty acids from liver and fat tissue. The mobilized substrates are taken up by the exercising muscles, the uptake involving mass effects (Schultz et al 1977, Hagenfeldt & Wahren 1971) and are burned in cooperation with intracellular energy depots (Galbo, Christensen & Holst 1977b, Hickson et al 1977, Rennie & Holloszy 1977) and in mutual competition (Rennie & Holloszy 1977). Excessively mobilized free fatty acids (Issekutz, Issekutz & Nash 1970) may be stored as muscular triglyceride (Zickler 1976). Initiated by decreasing plasma glucose concentration a sensitive secondary safety back up mechanism operates by increasing the secretion of the fuel mobilizing hormones epinephrine, glucagon, cortisol and GH.

The investigation was supported by grants from The Danish Medical Research Council, The P. Carl Petersen Foundation, Forskningsfondene for Storkeundersøgelser, Færøerne og Grønland and The J. Weismann Foundation. Lisbeth Kall, Vibeke Ulrik, Kristensen, Birthe Knudsen, Rikke Grønholdt and E. A. Richter performed skilled technical assistance. Equipment for gas analysis, as kindly lent by the Institute of The Theory of Gymnastics, Copenhagen. Human monocomponent insulin was kindly provided by NOVO Research Institute, Director in chief E. S. Olesen. The Department of Nutritional Physiology, Kommunehospitalet, Copenhagen, composed the diets.

REFERENCES

- AHLBORG B, BERGSTRÖM J, EKELEND L-O & HULTMAN E 1967 Muscle glycogen and muscle electrolytes during prolonged physical exercise. *Acta Physiol Scand* 70: 139-144.
- AHLBORG G & FELIG P 1976 Influence of glucose ingestion on fuel-hormone response during prolonged exercise. *J Appl Physiol* 41: 681-688.
- AHLBORG G & FELIG P 1977 Substrate utilization during prolonged exercise preceded by ingestion of glucose. *Am J Physiol* 233: E188-E194.
- ALJANO J D M, EKINS R P, MARITZ G & TURNER R C 1972 A sensitive precise radioimmunoassay of serum insulin relying on charcoal separation of bound and free hormone moieties. *Acta Endocrin (Kbh.)* 70: 487-509.
- BERGSTRÖM J 1975 Percutaneous needle biopsy of skeletal muscle in physiological and clinical research. *Scand J Clin Lab Invest* 35: 609-616.
- BERGSTRÖM J, HERMANSEN L, HULTMAN F

of muscle temperature on maximal muscle strength power output in human skeletal muscles

J. BERGH and B. EKBLOM

Department of Physiology III Karolinska Institute Stockholm, Sweden

BERGH U & EKBLOM B Influence of muscle temperature on maximal muscle strength and power output in human muscles. *Acta Physiol Scand* 1979 107 33-37. Received 15 Dec. 1978. ISSN 0001-6772. Department of Physiology III Karolinska Institute Stockholm Sweden.

The influence of muscle temperature (T) on maximal muscle strength, power output, jumping, and sprinting performance was evaluated in four male subjects. In one of the subjects the electromyogram (EMG) was recorded from M. vastus lateralis, M. biceps femoris, and M. semitendinosus. T ranged from 30.0°C to 39°C. Maximal dynamic strength, power output, jumping and sprinting performance were positively related to T . The changes were in the same order of magnitude for all these parameters (4-6% °C⁻¹). Maximal isometric strength decreased by 2% °C⁻¹ with decreasing T . The force-velocity relationship was shifted to the left at subnormal T . Thus in short term exercises, such as jumping and sprinting, performance is reduced at low T and enhanced at T above normal primarily as a result of a variation in maximal dynamic strength.

Key words: Muscle temperature, muscle strength, force-velocity, physical performance.

An elevated muscle temperature is known to improve performance in exercises such as short term bicycling (Asmussen & Baye 1945) and 100-800 m running (Hogberg & Ljunggren 1947) whereas a subnormal tissue temperature is accompanied by a decrease in performance (Davies et al. 1975). However in these studies no data were given to illustrate the quantitative aspects of these effects. Therefore, part of the purpose of this investigation is to study the effect of different levels of especially lowered but also enhanced tissue temperatures on short time physical performance.

Furthermore reported data on the effects of different temperatures on muscle strength are conflicting. Thus Asmussen et al. (1976) found a significant correlation between muscle temperature and maximal isometric strength whereas Binkhorst et al. (1977) concluded that maximal isometric strength was independent of muscle temperature. Fall (1972), in his review article, stated that maximal isometric strength seemed to be unaffected by temperature. On the other hand endurance in submaximal isometric exercise was reported by Ed-

wards et al. (1977) to be enhanced at subnormal muscle temperature. Binkhorst et al. (1977) also reported maximal dynamic strength to be higher at elevated muscle temperature while no data are available about the effects of lowered temperature on maximal dynamic strength. Therefore the aim of this study was to study the quantitative effects of different muscle and core temperatures on static and dynamic maximal strength with special emphasis on the force-velocity relationship and its consequence on sprinting and vertical jump performance.

METHODS AND PROCEDURE

Four male subjects aged 24-39 years participated in the study. They were physically well-trained and familiar with the laboratory procedures. Muscle fibre composition expressed as the relative number of type I fibres ranged from 45% to 65%. Temperature may affect the function of the different fibre types differently (Kawabuchi, 1977). Therefore it was considered necessary to use subjects with rather similar fibre type distribution. The experimental protocol is illustrated in Fig. 1. This protocol was repeated at the following levels of core (T_{re}) and vastus lateralis muscle temperature (T).

- muscular work following beta-adrenergic blockade in dogs. *Pflügers Arch ges Physiol* 336: 77-78
- OLSEN C 1971 An enzymatic fluorimetric micro-method for the determination of acetoacetate, β -hydroxybutyrate, pyruvate and lactate. *Clin Chim Acta* 33: 293-300
- ØRSKOV H, THOMSEN H G & YDE H 1968 Wick chromatography for rapid and reliable immunoassay of insulin, glucagon and growth hormone. *Nature (Lond)* 219: 193-195
- PALMER J P, HENRY D P, BENSON J W, JOHNSON D G & ENSINCK J W 1976 Glucagon response to hypoglycemia in sympathetomized man. *J Clin Invest* 57: 522-525
- RASKIN P, FUJITA Y & UNGER R. H 1975 Effect of insulin-glucose infusions on plasma glucagon levels in fasting diabetics and nondiabetics. *J Clin Invest* 56: 1132-1138
- RENNIE M J & HOLLOSZY J O 1977 Inhibition of glucose uptake and glycogenolysis by availability of oleate in well-oxygenated perfused skeletal muscle. *Biochem J* 168: 161-170
- SAHA J, LOPEZ-MONDRAGON R & NARAHARA H T 1968 Effect of epinephrine on permeability to sugar and on the production of free glucose in skeletal muscle. *J Biol Chem* 243: 521-527
- SCHERSTEN B, KÜHL C, HOLLENDER A. & EKMAN R 1974 Blood glucose measurement with dextrostix and new reflectance meter. *Br Med J* 417: 384-387
- SCHULTZ, T A, LEWIS S B, WESTBIE, D A, WALLIN J D & GERICH J E 1977 Glucose delivery: a modulator of glucose uptake in contracting skeletal muscle. *Am J Physiol* 231: E514-E518
- SNEDECOR G W & COCHRAN W G 1965 *Statistical methods*. 5th ed. The Iowa State University Press, Ames, Iowa
- SZABO O & SZABO A J 1977 Evidence for an insulin-sensitive receptor in the central nervous system. *Am J Physiol* 233: 1349-1353
- WAHREN J 1970 Human forearm muscle metabolism during exercise. IV. Glucose uptake at different work intensities. *Scand J Clin Lab Invest* 25: 179-185
- WERNER W, REY H-G & WIELINGER, H 1971 Über die Eigenschaften eines neuen Chromogens für die Blutzuckerbestimmung nach der GOD/POD-Methode. *Z Anal Chem* 252: 4-28
- WILLIAMSON D H 1974 L-Alanine. Determination with alanine dehydrogenase. In *Methods of enzymatic analysis* (ed. H U Bergmeyer), vol 4 pp 1679-1682. Verlag Chemie, Weinheim, Academic Press, New York, San Francisco and London
- ZIERLER K L 1976 Fatty acids as substrates for heart and skeletal muscle. *Circulat Res* 38: 459-463

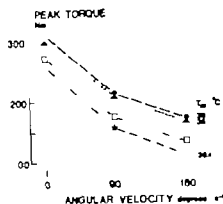


Fig. 3. Peak torque as a function of angular velocity of the knee joint at different levels of T . Average values, $n=4$.

was done at pH 9.4 following alkaline precipitation at pH 6.5.

In one of the subjects an electrocyrogram (EMG) from 4 vastus lateralis, M. semitendinosus, and M. biceps femoris was recorded using skin surface electrodes. The EMG was evaluated only in regard to the timing of onset and termination of activity of these muscles, relative to one another.

RESULTS

The number of subjects was small. Therefore statistical analyses would be of limited value. Individual data for maximal dynamic strength ($90^\circ \times s$) sprinting, and jumping performance are shown in Fig. 4. Average values are presented in Fig. 3 and 4 and in Table 1.

Maximal muscle strength. Peak torque was positively related to T . The changes were $6.5 \text{ N} \times m \times ^\circ C^{-1}$ ($2.1\% \times ^\circ C^{-1}$), $9.8 \text{ N} \times m \times ^\circ C^{-1}$ ($4.7\% \times ^\circ C^{-1}$), and $8.3 \text{ N} \times m \times ^\circ C^{-1}$ ($4.9\% \times ^\circ C^{-1}$) at the angular velocities of 0° , 90° and $180^\circ \times s$ respectively. Thus, the effect of temperature was greater in dynamic than in isometric exercise (vertical jump). The height of the jump decreased with decreasing T at a rate of $2.1 \text{ cm} \times ^\circ C^{-1}$ ($4.2\% \times ^\circ C^{-1}$).

Sprinting performance. The shortest time in which 70 revolutions could be performed was linearly related to T . The work time increased from 10.77 s at $T = 38.3$ to 15.27 s at $T = 31.4^\circ C$. The increment in the average speed of the periphery of the flywheel was $0.5 \text{ m} \times s$ ($4.7\% \times ^\circ C^{-1}$). Peak velocity was also positively related to T and changed by $0.51 \text{ m} \times s \times ^\circ C^{-1}$ ($4.4\% \times ^\circ C^{-1}$).

Power output. During knee extensions the peak power output was positively related to T . The rates of the changes were $28.5 \text{ W} \times ^\circ C^{-1}$ ($5.6\% \times ^\circ C^{-1}$) and $15.8 \text{ W} \times ^\circ C^{-1}$ ($4.9\% \times ^\circ C^{-1}$) at the angular velocities 90° and $180^\circ \times s$ respectively. For the first two revolutions of bicycling average power output increased with increasing temperature at a rate of $45.7 \text{ W} \times ^\circ C^{-1}$ ($5.1\% \times ^\circ C^{-1}$).

EMG. The EMG-activity pattern (defined as in Methods*) of the M. vastus lateralis, M. semitendinosus and M. biceps femoris were similar regardless of muscle temperature.

DISCUSSION

In this study the effect of temperature on jumping and sprinting performance was of the same order of magnitude as indicated by the data reported by Asmussen et al. (1945, 1976). According to the latter studies the changes were $4.4\% \times ^\circ C^{-1}$ for jumping (T range $27\text{--}40^\circ C$) and $5.3\% \times ^\circ C^{-1}$ for sprinting (T range $36\text{--}40^\circ C$) performance compared to $4.2\% \times ^\circ C^{-1}$ and $5.1\% \times ^\circ C^{-1}$ respectively in the present study.

Sprinting and jumping performances were affected in direct proportion to the change in peak torque. This implies that temperature changes had little if any effect on coordination in these rather uncomplicated movements. This is also supported by the fact that the EMG-activity patterns were unaffected by temperature.

Falls (1972) in his review article stated that maximal isometric strength is unaffected by temperature. This is in agreement with the data reported by Binkhorst et al. (1977), Asmussen et al. (1976)

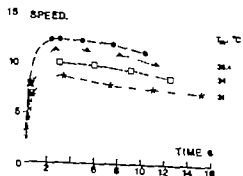


Fig. 4. Speed of the periphery of the fly-wheel as a function of time at 4 different levels of T . Average values, $n=4$.

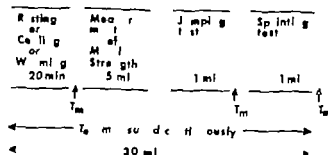


Fig. 1 The experimental protocol. T_m = esophageal temperature, T_m = muscle temperature.

Experimental situations

	1	2	3	4
T_m °C	35–36	35–36	36–37	37–38
T_m °C	30–32	33–35	36–37	38–39

Elevated body temperatures were achieved by intermittent bicycle ergometer exercise. Low muscle temperatures (expts 1 and 2) were produced by immersing the legs (to trochanter major) in cold water.

The order of the experimental situations was varied in order to diminish the influence of a possible training effect with testing day at least 2 days apart.

Maximal muscle strength of the left knee extensors was recorded as torque during maximal voluntary knee extension with fixed angular velocities. The subjects were sitting in an experimental chair and the lower leg moved the lever arm of an isokinetic dynamometer (Cybex II, Lumex Inc., New York).

Maximal strength was measured at 3 different angular velocities: 0° (isometric strength), 90°, 180°/s.

Jumping performance was determined by a vertical jump. The subjects were allowed to start the jump with a countermovement (knee-flexion) and a downward-upward arm swing. The height of the jump was measured by a measuring tape with one end fastened to the subject's waist. The attached tape was sliding through a slit with friction just enough to stop the tape at the peak of the jump.

Sprinting performance was evaluated on using a mechanically braked bicycle ergometer. All subject performed 20 full pedal revolutions (~8.5 kJ) as fast as possible. Time for each revolution was electronically measured with an accuracy of 0.005 s. Time for 2, 5, 10, and 20 revolutions respectively was recorded. Speed of the periphery of the fly-wheel was also calculated at all of the above particular revolutions.

Peak power output during knee extensions was calculated according to $P = M \times \omega$, where P = power (W), M = peak torque (N·m) and ω = angular velocity (rad/s).

Average power output during the first two revolutions of bicycling was determined according to $P = (F \times v) / t$, where P = power (W), F = force (N) necessary to overcome the frictions between the fly-wheel and the friction belt

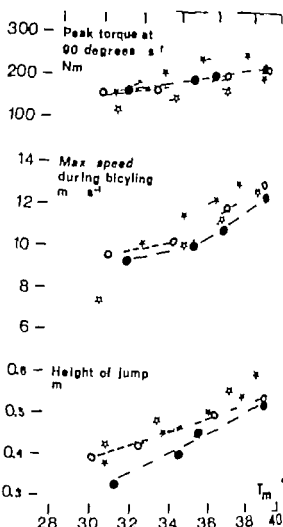


Fig. 2 Individual data for peak torque during knee extension, maximal speed obtained during bicycling and the height of the vertical jump at different vastus lateralis temperatures (T_m).

times the distance covered by a point on the periphery of the fly-wheel and ω = work transferred to the fly-wheel when its mass is accelerated [$I = \frac{1}{2} J \omega^2$, where J = moment of inertia (0.435 kg·m²) and ω = speed of the fly-wheel (rad/s)].

Body temperatures were measured by thermocouples. T_m in the esophagus at the level of the heart. Muscle temperatures were recorded in M. vastus lateralis of the left leg at various depths of 30, 40, and 50 mm and peak after was used (Saltin et al. 1968). T_m was monitored continuously during the experiment. T_m was measured immediately before the strength measurement, after the jumping test and after the sprinting test (cf. Fig. 1). T_m values given in the Results in relation to the different tests are means of values obtained before and after the test.

Muscle samples from M. vastus lateralis were obtained using percutaneous needle biopsy technique (Bergh 1966). The myofibrillar ATP-ase method (Padykula & Herman 1953), as modified by Guth & Samaha (1969), was used for muscle fibre classification. The reaction was carried

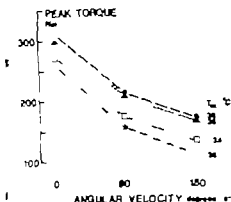


Fig. 3. Peak torque as a function of angular velocity of the knee joint at different levels of T . Average values, $n=4$.

ed out at pH 7.4 following alkaline pretreatment at pH 6.3.

In one of the subjects an electromyogram (EMG) from *M. vastus lateralis*, *M. semitendinosus*, and *M. biceps femoris* was recorded using skin surface electrodes. The EMG was evaluated only in regard to the timing of onset and termination of activity of these muscles, relative to one another.

RESULTS

The number of subjects was small. Therefore statistical analyses would be of limited value. Instead, individual data for maximal dynamic strength (90°) sprinting, and jumping performance are shown in Fig. 4. Average values are presented in Figs 3 and 4 and in Table 1.

Maximal muscle strength. Peak torque was positively related to T . The changes were $6.5 \text{ N} \cdot \text{m} \cdot ^\circ\text{C}^{-1}$ ($2.1\% \cdot ^\circ\text{C}^{-1}$), $9.8 \text{ N} \cdot \text{m} \cdot ^\circ\text{C}^{-1}$ ($4.7\% \cdot ^\circ\text{C}^{-1}$), and $8.3 \text{ N} \cdot \text{m} \cdot ^\circ\text{C}^{-1}$ ($4.9\% \cdot ^\circ\text{C}^{-1}$) at angular velocities of 0°, 90° and 180° s⁻¹ respectively. Thus the effect of temperature was greater in dynamic than in isometric exercise.

Vertical jump. The height of the jump decreased with decreasing T at a rate of $-1 \text{ cm} \cdot ^\circ\text{C}^{-1}$ ($-4\% \cdot ^\circ\text{C}^{-1}$).

Sprinting performance. The shortest time in which 20 revolutions could be performed was inversely related to T . The work time increased from 10.7 s at $T=38.3$ to 15.27 s at $T=31.4^\circ\text{C}$. The increment in the average speed of the periphery of the flywheel was $0.5 \text{ m} \cdot \text{s}^{-1}$ ($4.7\% \cdot ^\circ\text{C}^{-1}$). Peak velocity was also positively related to T and changed by $0.31 \text{ m} \cdot \text{s}^{-1} \cdot ^\circ\text{C}^{-1}$ ($4.4\% \cdot ^\circ\text{C}^{-1}$).

Power output. During knee extensions the peak power output was positively related to T . The rates of the changes were $28.5 \text{ W} \cdot ^\circ\text{C}^{-1}$ ($5.6\% \cdot ^\circ\text{C}^{-1}$) and $15.8 \text{ W} \cdot ^\circ\text{C}^{-1}$ ($4.9\% \cdot ^\circ\text{C}^{-1}$) at the angular velocities 90° and 180° s⁻¹ respectively. For the first two revolutions of bicycling average power output increased with increasing temperature at a rate of $45.7 \text{ W} \cdot ^\circ\text{C}^{-1}$ ($5.1\% \cdot ^\circ\text{C}^{-1}$).

EMG. The EMG-activity pattern (defined as in "Methods") of the *M. vastus lateralis*, *M. semitendinosus* and *M. biceps femoris* were similar regardless of muscle temperature.

DISCUSSION

In this study the effect of temperature on jumping and sprinting performance was of the same order of magnitude as indicated by the data reported by Asmussen et al. (1945-1976). According to the latter studies the changes were $4.4\% \cdot ^\circ\text{C}^{-1}$ for jumping (T range $27-40^\circ\text{C}$), and $5.3\% \cdot ^\circ\text{C}^{-1}$ for sprinting (T range $36-40^\circ\text{C}$) performance compared to $4.2\% \cdot ^\circ\text{C}^{-1}$ and $5.1\% \cdot ^\circ\text{C}^{-1}$ respectively in the present study.

Sprinting and jumping performances were affected in direct proportion to the change in peak torque. This implies that temperature changes had little, if any effect on coordination in these rather uncomplicated movements. This is also supported by the fact that the EMG-activity patterns were unaffected by temperature.

Falls (1972) in his review article stated that maximal isometric strength is unaffected by temperature. This is in agreement with the data reported by Binkhorst et al. (1977). Asmussen et al. (1976)

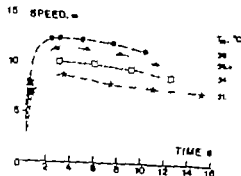


Fig. 4. Speed of the periphery of the fly-wheel as a function of time at 4 different levels of T . Average values, $n=4$.

Table 1 *Average values and range for the data obtained at the four different experimental situations*

		Experimental situation			
		1		3	4
<i>Knee extensions</i>					
T_m °C		35.8 35.3-36.4	35.6 35.2-36.3	37.0 36.8-37.5	37.9 36.6-38.4
T_m °C		30.4 30.0-31.2	33.6 3.8-33.8	36.7 35.2-36.5	38.3 37.7-39.0
0°×s	peak torque (N×m)	262 190-302	282 260-310	301 284-315	31 289-360
90°×s	peak torque (N×m)	148 115-163	177 158-205	211 181-262	16 197-237
90°×s	peak power W	233 181-256	277 248-311	331 284-411	333 309-377
180°×s	peak torque (N×m)	111 84-137	136 126-163	169 139-201	174 167-189
180°×s	peak power W	348 264-430	428 366-512	510 436-631	540 444-691
<i>Vertical jump</i>					
T_m °C		35.8 35.3-36.4	35.6 35.2-36.4	36.9 36.7-37.1	37.8 37.6-38.3
T_m °C		30.6 30.0-31	33.9 32.3-34.4	36.2 35.4-36.9	38.4 37.6-39.0
Height m		0.375 0.325-0.410	0.435 0.395-0.450	0.493 0.450-0.500	0.540 0.510-0.590
<i>Bicycling</i>					
T_m °C		35.7 35.2-36	35.6 35.2-36.3	37.0 36.6-37.3	37.8 37.6-38.3
T_m °C		31.4 30.3-32.3	34.3 33.8-34.9	36.4 36.1-36.6	38.3 37.3-39.8
Time for 70 rev s		15.7 13.19-20.14	11.63 11.61-13.65	11.3 10.51-12.3	10.37 9.95-10.72
Max. speed m×s		8.96 7.40-10.15	10.33 10.00-11.45	11.54 10.70-12.15	11.4 12.25-11.95
Power W 1st rev		683 594-789	797 754-849	921 834-934	999 946-1113

found only a minor effect of temperature on maximal isometric strength, and in the present study the changes in muscle temperature had only a small and probably insignificant influence in this respect. Thus it may be concluded that maximal isometric strength is affected little by changes in muscle temperature.

In contrast, maximal dynamic strength was markedly dependent on T_m . This difference in temperature response may arise from the fact that peak torque can be attained only in a limited part of the range of movement (Thorstensson et al. 1976).

Thus, the time available to attain peak torque is shorter in dynamic than in isometric exercise. In the present study the values were only 0.1-0.2 s during dynamic but 2-4 s in isometric contractions. At low temperature it might be more difficult to activate the motor units during a short time interval, possibly as a result of a lower nerve impulse frequency (Vanggaard 1975). Furthermore, the speed of chemical reactions is decreased at low temperatures. Thus, the breaking and formation of the cross-bridges may be considerably delayed at low temperatures, resulting in a slower rate of tension

development, even though the maximal tension is affected by temperature. However, this seems to be contradicted by the fact that the temperature effect was $4.6\% \times ^\circ\text{C}^{-1}$ independent of contraction velocity over a wide range of movement ($90\text{--}200\text{ s}^{-1}$). The reason for this remarkable independence of speed of contraction is so far obscure.

From the present results it is evident that T has a considerable effect on performance in short term dynamic exercise. In contrast, changes in T have little if any importance during maximal isometric contractions, while dynamic muscle strength will be influenced considerably by T . Finally, the effect of temperature on jumping and sprinting performance is primarily a result of a variation in maximal dynamic strength.

This study was supported by the Research Council of the Swedish Sports Federation (grant 29/77).

REFERENCES

1. ASMUSSEN E & BOJE O 1945 Body temperature and capacity for work. *Acta Physiol Scand* 10: 1–22.
2. ASMUSSEN E, BONDE-PETERSEN F & JØRGENSEN K 1976 Mechano-elastic properties of human muscles at different temperatures. *Acta Physiol Scand* 96: 83–91.
3. BERGSTRÖM J 1961 Muscle electrolytes in man. *Scand J Clin Lab Invest. Suppl.* 68.
4. BINKHORST R A, HOOFT L & VISSERS, A C A. 1977 Temperature and force-velocity relationship of human muscles. *J Appl Physiol Respir Environ Exercise Physiol* 42: 471–475.
5. DAVIES M, EKBLOM, B, BERGH, U & KANSTRUP L-L 1975 The effects of hypothermia on submaximal and maximal work performance. *Acta Physiol Scand* 95: 201–202.
6. EDWARDS R T H, HARRIS, R C., HULTMAN E., KAUSER L., KOH D & NORDENFJÖ L-O 1972. Effect of temperature on muscle energy metabolism and endurance during successive isometric contractions sustained to fatigue of the quadriceps muscle in man. *J Physiol (Lond.)* 226: 335–352.
7. FALLS, H. B. 1972. Heat and cold applications. In: *Exergonic acids and muscular performance* (ed. W P Morgan), pp 119–158. Academic Press, New York.
8. GUTH, L. & SAMAHA F I 1969 Qualitative differences between actomyosin ATPase of slow and fast mammalian muscles. *Exp Neurol* 25: 138–152.
9. HÖGBERG P & LJUNGGREN O 1947 Uppvärmningen (övertan på löpprestationerna. (The influence of warm-up on running performance.) *Svensk Idrott* 40: 668–671.
10. PADYKULA H A & HERMAN E 1955 The specificity of the histochemical method of adenosine triphosphatase. *J Histochem Cytochem* 3: 170–195.
11. RANATUNGA, U W 1977 Changes produced by chronic denervation in the temperature dependent isometric contractile characteristics of rat fast and slow twitch skeletal muscles. *J Physiol (Lond.)* 273: 255–262.
12. SALTIN B, GAGGE A. P & STOLWIJK, J A. J 1968 Muscle temperature during submaximal exercise in man. *J Appl Physiol* 25: 679–682.
13. THORSTENSSON A, GRIMBY G & KARLSSON J 1976. Force-velocity relations and fiber composition in human knee-extensor muscles. *J Appl Physiol* 40: 1216.
14. VANGAARD, L. 1975 Physiological reactions to wet cold. *Aviat Space Environ Med* 46: 33–36.

Measured during bicycling.

Skeletal muscle metabolism, morphology and function in sedentary smokers and nonsmokers

AN ÖRLANDER, KARL HEINZ KIESSLING and LARS LARSSON¹

Institute of Zoophysiology, University of Uppsala, the Department of Animal Nutrition, Swedish University of Agricultural Sciences, Uppsala, and the Laboratory for Human Performance, National Defence Research Institute, Stockholm, Sweden

ÖRLANDER, J., KIESSLING, K.-H. & LARSSON, L. Skeletal muscle metabolism, morphology and function in sedentary smokers and nonsmokers. *Acta Physiol Scand* 1979, 107, 39-46. Received 29 Dec. 1978. ISSN 0001-6772. Institute of Zoophysiology, University of Uppsala, the Department of Animal Nutrition, Swedish University of Agricultural Sciences, Uppsala, and the Laboratory for Human Performance, National Defence Research Institute, Stockholm, Sweden.

Smokers and nonsmokers of a homogeneous population of sedentary men have been compared with respect to skeletal muscle (vastus lateralis) morphological, metabolic and functional characteristics. The percentage type I fibres was lower and that of type IIB fibres higher in the smokers. Fibre areas were almost equal in the two groups. Muscle oxidative capacity was lowered in the smokers, as judged from decreased mitochondrial enzyme activities and lowered fibillar space mitochondrial volume fraction. Isometric and dynamic strengths were lower in the smokers, except at the highest velocity of movement tested. Dynamic strengths expressed in relation to isometric strength were similar at all velocities except the highest, where the smokers were relatively stronger. Muscular endurance, measured in short-term isometric and dynamic tests, was not different. It is suggested that the lowered muscle oxidative capacity and strength in the smokers may be partly consequence of the different fibre type distribution. A possibly lower physical activity level and tobacco smoke constituents (e.g. carbon monoxide) may also be instrumental. It is not clear whether the different fibre type distribution in the smokers is an effect of smoking per se or if background factors are responsible.

Key words: Muscle metabolism, muscle morphology, smoking, strength, tobacco

Tobacco smoking is known to markedly impair the capacity for prolonged exercise, as revealed by performance tests and/or measurements of maximal oxygen uptake (Cooper et al. 1968, Peterson & Kelsey 1969, McDonough et al. 1970, Hrubec & Battig 1970, Shaver 1973, Raven et al. 1974, Ingemann-Hansen & Hallgaard-Kristensen 1977). The impaired working capacity has been attributed to increased oxygen debt and lactate production in smokers (Chevalier et al. 1963, Krimholz et al. 1964, Krimholz & Hedrick 1972, Reece & Ball 1972), although there are conflicting data (Raven et al. 1974). Carbon monoxide has been implicated as a major etiological agent (Chevalier et al. 1966).

The physical working capacity and the metabolic capacity of the working muscles are closely interrelated (Hofman & Booth 1976). It would therefore seem conceivable that part of the impairment of the

working capacity in smokers might be related to effects on muscle. There is but scanty information in the literature concerning possible effects of tobacco smoking on skeletal muscle characteristics. Some early studies (reviewed by Fischer et al. 1960) on the effect of smoking on muscle strength or efficiency showed variable results (increases, decreases or no effect at all). Apparently, no studies on muscle morphology or metabolism in relation to smoking have appeared so far.

In the present study, smokers and nonsmokers of a homogeneous population of sedentary men were compared with respect to skeletal muscle morphological, metabolic and functional characteristics.

¹Present address: Dept. of Physiology III, Karolinska Institute at Gymnasiet och kiropraktiskolan, Stockholm, Sweden.

Table 1 Anthropometrical characteristics

Values are means \pm S.E. FFS fat free soft tissue weight n.s. not significant

Group	No of subjects	Age (y)	Height (cm)	Weight (kg)	FFS (kg)	Skeletal weight (kg)	Body fat weight (kg)	Thigh circumference (cm)
Smokers	18	44 \pm 3	179 \pm	78.4 \pm 2.6	53.9 \pm 1.7	1.4 \pm 0.3	10.0 \pm 0.8	47.8 \pm 0.9
Non-smokers	25	43 \pm 3	180 \pm 1	76.8 \pm 1.6	53.7 \pm 1.3	1.8 \pm 0.2	9.1 \pm 0.3	47.0 \pm 0.7
P		n.s.	n.s.	n.s.	n.s.	n.s.	n.s.	n.s.

MATERIAL AND METHODS

Subjects 43 apparently healthy men (18 smokers and 25 non-smokers) volunteered to participate in the study. They were all white-collar workers (employees of an insurance company) and engaged in little or no physical activity during their spare time. The basis for acceptance of a subject was the desire to get a subject population as homogeneous as possible with regard to physical activity level. Smoking habits were not considered in this selection. An oral consent was obtained from each subject after he had been informed of the procedure and possible risks of the experiments.

Informations regarding smoking habits were obtained by using a questionnaire. Each subject was asked to specify his weekly tobacco consumption: 11 were cigarette smokers and smoked 91 (10–700) cigarettes with or without filters per week; 4 subjects smoked the pipe and consumed 62 (25–125) g of tobacco per week; 3 had "mixed" habits smoking both the pipe and cigars or cigarettes. It was decided to consider all smokers together as one group.

For each subject age, height, weight, skeletal width and skinfold thickness were recorded. Body fat weight, skeletal weight and fat free soft tissue weight (FFS) were calculated according to von Döbeln (1964). The circumference of the left thigh was measured in a horizontal plane just under the gluteal furrow. As shown in Table 1, the two groups were very similar with regard to all studied anthropometrical variables.

All experiments were performed at 8–11 a.m. and followed a fixed protocol with biopsies preceding strength measurements. No restrictions regarding smoking were given, but no subject smoked during at least 70 min preceding the experiments.

Muscle biopsies Muscle tissue was obtained from the left vastus lateralis by the percutaneous needle technique (Bergström 1962). The specimens were used for histochemistry, enzyme assays and electron microscopy.

Histochemistry The muscle samples for fibre typing and area determination were trimmed, mounted frozen in isopentane cooled by liquid nitrogen and stored at -80°C until analysis.

Serial transverse sections (10 μm) were cut with a cryotome at -70°C and the myofibrillar ATPase staining method (Gomori 1941; Padykula & Herman 1955) was used for muscle fibre classification. Photographs of the stained sections were taken and classification into type I (slow twitch) and type II (fast twitch) (Engel 1962) was

made in all 43 subjects. In 34 of the subjects the type I fibres were subclassified into A, B and C subgroups (Brooke & Kaiser 1970; Dubowitz & Brooke 1971). The average number of counted fibres for classification in main groups (type I and type II) and subgroup (type I type IIA, B and C) was 385 ± 5 and 51 ± 35 respectively.

The fibre areas were calculated from the lesser fibre diameter of each fibre type (type I and type II) using an eyepiece micrometer (Dubowitz & Brooke 1973). Assuming each fibre to have a circular cross-section, the diameter equal to the lesser fibre diameter, the average cross-sectional area of each fibre type was calculated. The fibre areas were determined from the NADH tetrazolium reductase staining (Novikoff et al. 1961) and an average of 207 ± 13 diameters were measured per subject. The mean fibre area was calculated according to the formula presented by Haggmark et al. (1978), i.e. fraction type I \times type I fibre area + fraction type II \times type II fibre area.

Biochemical analyses Five enzymes were chosen to represent the major pathways in energy metabolism. Glycolysis was represented by phosphofructokinase (PFK, E.C. 2.7.1.11), lactate fermentation by lactate dehydrogenase (LDH, E.C. 1.1.1.27), fatty acid β -oxidation by 3-hydroxyacyl-CoA dehydrogenase (HAD, E.C. 1.1.3.15), the citric acid cycle by citrate synthase (CS, E.C. 4.1.3.1) and the respiratory chain by cytochrome oxidase (cytochrome c oxidase, E.C. 1.9.3.1). In addition, two enzymes related to the contraction process and the short-term supply of ATP were investigated: Mg^{2+} -stimulated ATPase (F.C. 3.6.1.4) and myokinase (MK, F.C. 2.7.4.3). For PFK, LDH, HAD, CS and cytochrome oxidase were prepared and assays performed as described previously (Örlander et al. 1977). PFK was assayed according to Shonk & Boyer (1961), LDH and HAD by the methods of Bass et al. (1969), CS as described by Srere (1969) and cytochrome oxidase by Srere et al. (1969). For the assays of Mg^{2+} -stimulated ATPase and MK, the procedures described by Thorstensen (1976) were employed. LDH isoenzymes were separated by disc-electrophoresis and relative quantities of H and L subunits were determined as described by Spöck (1976). Protein was estimated by the method of Lowry et al. (1951).

Electron microscopy Small pieces of muscle tissue were processed for electron microscopy and micrographs were taken for stereological analysis by methods described by Weibel (1969). An account of the procedure has been given before (Örlander et al. 1977). It is of note that the values on mitochondrial mean volume and number per

at volume are approximations (see Ölander et al 1977).

The electron microscopical technique is very laborious as part of the investigation was limited to 26 subjects.

Functional measurements. Maximum isometric and dynamic strengths were measured in the left knee-extensor muscles using an isometric dynamometer (Cybex II, Jarnac Inc., New York). The subjects were seated in an adjustable chair with support for the back, shoulders and hips. The top angle was fixed at $\pi/2$ rad (90°) and the lower leg moved the lever of the dynamometer. The lever was at constant length and the centre of the dynamometer axis of rotation was aligned with the anatomical axis of rotation, the knee joint. The angular movement of the knee joint was from 0.55π to 0 rad (100° to 0° , i.e. full knee extension). The angular velocities studied were $\pi/3$, $\pi/3$ and π rad s^{-1} or 60° , 120° and 180° . In addition, comparisons were made with maximum isometric force measured with the same equipment with knee angles of $\pi/6$, $\pi/3$ and $\pi/2$ rad or 30° , 60° and 90° . The peak moment value irrespective of knee angle was defined as the individual maximum isometric strength. Two attempts were allowed at each knee angle and velocity and the highest values were noted. The measurements were made in sequence from slow to fast speeds with 30 recovery between each contraction. The following sequence was used: $\pi/6$ rad, $\pi/3$ rad, $\pi/3$ rad, $2\pi/3$ rad, π rad and π rad. High precision and accuracy for the torque registration have been reported by others (Moffroid et al 1969; Thorstensson et al 1976).

The influence of muscular fatigue due to the testing procedure may be considered negligible (Thorstensson 1976).

Muscular endurance was assessed in both isometric and dynamic terms. Maximum isometric strength (MIS) and maximum endurance respectively were determined for both legs simultaneously (Karlsson & Ölander 1972) by recording the force exerted when the subjects pressed their feet against a stiff bar equipped with force transducer MIS was taken as the highest force value obtained during series of 5 contractions. After 3 min rest isometric endurance time was recorded, measured as the maximum time during which a tension level of 50% of MIS could be maintained.

Dynamic endurance was measured as the ability to maintain tension output during repeated maximal dynamic contractions performed on the isometric dynamometer. The angular velocity was pre-set at π rad s^{-1} (180°).

Endurance was calculated from measuring 50 maximal contractions and determining the relative (%) decline in peak torque from the areas of the three initial contractions.

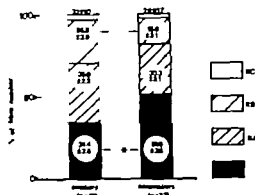


Fig. 1. Fibre type distribution. Values are means \pm S.E. denotes $P < 0.01$.

tions, i.e. subjects with low force decline had high dynamic endurance and vice versa.

A more extensive presentation of the different functional measurements and the functional characteristics in relation to age is given elsewhere (Larsson & Karlsson 1978; Larsson et al 1979).

Statistics. Intergroup differences were evaluated by means of Student's *t*-test, $P < 0.05$ being accepted as significant. The possibility that mass significances (i.e. false significances arising when comparing large numbers of parameters in limited experimental material) might occur was considered. However, since the observed significant differences all seemed physiologically reasonable and coherent, no restrictions were introduced on this ground.

RESULTS

Fibre type distribution and fibre areas. The proportion of type I fibres was significantly lower ($P < 0.001$) in the smokers compared to the nonsmokers ($38.1 \pm 3.9\%$, $n=18$ and $50.7 \pm 3.9\%$, $n=25$ respectively). Type II fibre subclassification revealed a correspondingly increased incidence ($P < 0.01$) of type IIB fibres in the smokers (Fig. 1).

Fibre areas of each fibre type, fibre area ratios and mean fibre areas were almost equal in the two groups. If anything, a tendency towards larger fibre areas was seen in the nonsmokers (Table 2).

Table 2. Fibre areas

Values are means \pm S.E. * denotes not significant

Group	No. of subjects	Type I area (μm^2)	Type II area (μm^2)	Type II/Type I area ratio	Mean fibre area (μm^2)
Smokers	18	2 722 \pm 189	2 933 \pm 19*	1.12 \pm 0.07	2 873 \pm 153
Nonsmokers	25	2 864 \pm 143	3 253 \pm 187	1.15 \pm 0.05	3 050 \pm 168

Table 1 Anthropometrical characteristics

Values are means \pm S.E. FFS fat free soft tissue weight. n.s. not significant

Group	No. of subjects	Age (y)	Height (cm)	Weight (kg)	FFS (kg)	Skeletal weight (kg)	Body fat weight (kg)	Thigh circumference (cm)
Smokers	18	44 \pm 3	179 \pm 7	78.4 \pm 6	53.9 \pm 1.7	1.4 \pm 0.5	10.0 \pm 0.8	54.7 \pm 0.9
Nonsmokers	25	43 \pm 3	180 \pm 1	76.8 \pm 1.6	51.7 \pm 1.3	1.8 \pm 0.2	9.7 \pm 0.5	54.2 \pm 0.7
P		n.s.	n.s.	n.s.	n.s.	n.s.	n.s.	n.s.

MATERIAL AND METHODS

Subjects 43 apparently healthy men (18 smokers and 25 nonsmokers) volunteered to participate in the study. They were all white-collar workers (employees of an insurance company) and engaged in little or no physical activity during their spare time. The basis for acceptance of a subject was the desire to get a subject population as homogeneous as possible with regard to physical activity level. Smoking habits were not considered in this selection. An oral consent was obtained from each subject after he had been informed of the procedure and possible risks of the experiments.

Informations regarding smoking habits were obtained by using a questionnaire. Each subject was asked to specify his weekly tobacco consumption: 11 were cigarette smokers and smoked 91 (10–200) cigarettes with or without filters per week, 4 subjects smoked the pipe and consumed 62 (25–125) g of tobacco per week, 3 had "mixed" habits smoking both the pipe and cigars or cigarettes. It was decided to consider all smokers together as one group.

For each subject age, height, weight, skeletal width and skinfold thickness were recorded. Body fat weight, skeletal weight and fat free soft tissue weight (FFS) were calculated according to von Döbeln (1964). The circumference of the left thigh was measured in a horizontal plane just under the gluteal furrow. As shown in Table 1 the two groups were very similar with regard to all studied anthropometrical variables.

All experiments were performed at 8–11 a.m. and followed a fixed protocol with biopsies preceding strength measurements. No restrictions regarding smoking were given, but no subject smoked during at least 20 min preceding the experiments.

Muscle biopsy Muscle tissue was obtained from the left vastus lateralis by the percutaneous needle technique (Bergström 1962). The specimens were used for his histochemical, enzyme assays and electron microscopy.

Histochemistry The muscle samples for fibre typing and area determination were trimmed, mounted frozen in isopentane cooled by liquid nitrogen and stored at -80°C until analysis.

Serial transverse sections (10 μm) were cut with a cryotome at -20°C and the myofibrillar ATPase staining method (Gomon 1941, Padykula & Herman 1955) was used for muscle fibre classification. Photographs of the stained sections were taken and classification into type I (slow twitch) and type II (fast twitch) (Engel 1964) was

made in all 43 subjects. In 34 of the subjects, the type I fibres were subclassified into A, B and C subgroups (Brooke & Kaiser 1970, Dubowitz & Brooke 1973). The average number of counted fibres for classification in main groups (type I and type II) and subgroups (type II A, B and C) was 585 ± 52 and 251 ± 35 respectively.

The fibre areas were calculated from the "lesser fibre diameter" of each fibre type (type I and type II) using an eyepiece ruler (Dubowitz & Brooke 1973). Averaging each fibre to have a circular cross-section, the diameter equal to the "lesser fibre diameter", the mean cross-sectional area of each fibre type was calculated. The fibre areas were determined from the NADH tetrazolium reductase staining (Novikoff et al. 1961) and an average of 207 ± 13 diameters were measured per subject. The mean fibre area was calculated according to the formula presented by Häggmark et al. (1978), i.e. fraction type I \times type I fibre area + fraction type II \times type II fibre area.

Biochemical analyses Five enzymes were chosen to represent the major pathways in energy metabolism. Glycolysis was represented by phosphofructokinase (PFK, E.C. 2.7.1.11), lactate fermentation by lactate dehydrogenase (LDH, E.C. 1.1.1.27), fatty acid β -oxidation by 3-hydroxyacyl-CoA dehydrogenase (HAD, E.C. 1.1.1.35), the citric acid cycle by citrate synthase (CS, E.C. 4.1.3.1) and the respiratory chain by cytochrome oxidase (cytochrome c, E.C. 1.9.3.1). In addition, two enzymes related to the contraction process and the short-term supply of ATP were investigated: Mg^{2+} -stimulated ATPase (E.C. 3.6.1.4) and myokinase (MK, E.C. 2.7.4.3). For PFK, LDH, HAD, CS and cytochrome c homogenates were prepared and assays performed as described previously (Örlander et al. 1977). PFK was assayed according to Shonk & Boyer (1962), LDH and HAD by the methods of Bass et al. (1969), CS as described by Srere (1969) and cytochrome c according to Whittet et al. (1969). For the assays of Mg^{2+} -stimulated ATPase and MK the procedures described by Thorstensen (1976) were employed. LDH isoenzymes were separated by disc-electrophoresis and relative quantities of M and H subunits were determined as described by Sjödin (1976). Protein was estimated by the method of Lowry et al. (1951).

Electron microscopy Small pieces of muscle tissue were processed for electron microscopy and micrographs were taken for stereological analysis by methods described by Weibel (1969). An account of the procedure has been given before (Örlander et al. 1977). It is of note that the values on mitochondrial mean volume and number per

at volume are approximations (see Örtengren et al 1977) the electron microscopical technique is very laborious part of the investigation was limited to 26 subjects.

Functional measurements. Maximum isometric and dynamic strengths are measured in the left knee-extensor muscles using an isometric dynamometer (Cyber II, Intec Inc., New York). The subjects were seated in an adjustable chair with support for the back, shoulders and feet. The hip angle was fixed at $\pi/2$ rad (90°) and the lower leg moved the lever of the dynamometer. The lever was kept at constant length and the centre of the dynamometer axis of rotation was aligned with the anatomical axis of rotation, the knee joint. The angular movement of the knee joint was from 0.35π to 0 rad (100° to 0°), i.e. full knee extension. The angular velocities studied were $\pi/3$ rad/s and π rad/s or 60°/s and 180°/s. In addition, comparisons were made with maximum isometric force measured with the shank equipment with knee angles of $\pi/6$, $\pi/3$ and $\pi/2$ rad or 30°, 60° and 90°. The peak isometric value irrespective of knee angle, as defined as the individual maximum isometric strength. Two attempts were allowed at each knee angle and velocity and the highest values are noted. The measurements were made in sequence from slow to fast speeds with 30 s recovery between each contraction. The following sequence was used: $\pi/6$ rad/s, $\pi/3$ rad/s, $\pi/2$ rad/s, $\pi/3$ rad/s, $\pi/2$ rad/s, and π rad/s. High precision and accuracy for the torque registrations have been reported by others (Nofftrod et al 1969; Thorenson et al 1976). The influence of isometric fatigue due to the testing procedure may be considered negligible (Thorenson 1976).

Muscular endurance as assessed in both isometric and dynamic terms. Maximum isometric strength (MIS) and isometric endurance respectively are determined for both legs simultaneously (Karlsson & Örtengren 1972) by recording the force exerted when the subjects pressed their feet against a stiff bar equipped with force transducer MIS as taken as the highest force value obtained during series of 5 contractions. After 3 min rest isometric endurance time was recorded, assessed as the maximum time during which tension level of 50% of MIS could be maintained.

Dynamic endurance was measured as the ability to maintain tension output during repeated isometric dynamic contractions performed on the isometric dynamometer. The angular velocity was pre-set at π rad/s (180°/s) while the subject sat as described above. Dynamic endurance was calculated from measuring 50 isometric contractions and determining the relative (%) decline in peak torque from the mean of the three initial contractions.

Table 2. *Fibre areas*

Values are means \pm S.E., n.s. = not significant

Group	No. of subjects	Type I area (μm^2)	Type II area (μm^2)	Type II/Type I area ratio	Mean fibre area (μm^2)
Smokers	18	2 722 \pm 189	2 933 \pm 192	1.12 \pm 0.07	2 873 \pm 153
Non-smokers	25	2 864 \pm 143	3 253 \pm 187	1.15 \pm 0.05	3 050 \pm 166
		n.s.		n.s.	n.s.

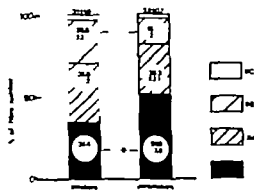


Fig. 1. Fibre type distribution. Values are means \pm S.E. denotes $P < 0.01$.

does subjects with low force decline had high dynamic endurance and vice versa.

A more extensive presentation of the different functional measurements and the functional characteristics in relation to age is given elsewhere (Larsson & Karlsson 1978; Larsson et al 1979).

Statistics. Intergroup differences were evaluated by means of Student's *t*-test, $P < 0.05$ being accepted as significant. The possibility that main significance (i.e. false significances arising when comparing large numbers of parameters in a limited experimental material) might occur as considered. However, since the observed significant differences all seemed physiologically reasonable and coherent, no restrictions were introduced on this ground.

RESULTS

Fibre type distribution and fibre areas. The proportion of type I fibres was significantly lower ($P < 0.001$) in the smokers compared to the non-smokers (38 \pm 2.3% $n=18$ and 50.7 \pm 2.5% $n=25$ respectively). Type II fibre subclassification revealed a correspondingly increased incidence ($P < 0.01$) of type IIB fibres in the smokers (Fig. 1).

Fibre areas of each fibre type, fibre area ratios and mean fibre areas were almost equal in the two groups. If anything, a tendency towards larger fibre areas was seen in the non-smokers (Table 2).

Table 1 Anthropometrical characteristics

Values are means \pm S.E. FFS fat free soft tissue weight n.s. not significant

Group	No of subjects	Age (y)	Height (cm)	Weight (kg)	FFS (kg)	Skeletal weight (kg)	Body fat weight (kg)	Thigh circumference (cm)
Smokers	18	44 \pm 3	179 \pm 7	78.4 \pm 5.6	53.9 \pm 1.7	17.4 \pm 0.5	10.0 \pm 0.8	47.7 \pm 0.9
Nonsmokers	25	41 \pm 3	180 \pm 1	76.8 \pm 1.6	53.7 \pm 1.3	18.0 \pm 0.2	9.2 \pm 0.5	47.0 \pm 0.7
P		n.s.	n.s.	n.s.	n.s.	n.s.	n.s.	n.s.

MATERIAL AND METHODS

Subjects 43 apparently healthy men (18 smokers and 25 nonsmokers) volunteered to participate in the study. They were all white-collar workers (employees of an insurance company) and engaged in little or no physical activity during their spare time. The basis for acceptance of a subject was the desire to get a subject population as homogeneous as possible with regard to physical activity level. Smoking habits were not considered in this selection. An oral consent was obtained from each subject after he had been informed of the procedure and possible risks of the experiments.

Informations regarding smoking habits were obtained by using a questionnaire. Each subject was asked to specify his weekly tobacco consumption: 11 were cigarette smokers and smoked 91 (10–200) cigarettes with or without filters per week; 4 subjects smoked the pipe and consumed 6 (25–125) g of tobacco per week; 3 had 'mixed' habits smoking both the pipe and cigars or cigarettes. It was decided to consider all smokers together as one group.

For each subject age, height, weight, skeletal width and skinfold thickness were recorded. Body fat weight, skeletal weight and fat free soft tissue weight (FFS) were calculated according to von Döbeln (1964). The circumference of the left thigh was measured in a horizontal plane just under the gluteal furrow. As shown in Table 1, the two groups were very similar with regard to all studied anthropometrical variables.

All experiments were performed at 8–11 a.m. and followed a fixed protocol with biopsies preceding strength measurements. No restrictions regarding smoking were given, but no subject smoked during at least 20 min preceding the experiments.

Muscle biopsies Muscle tissue was obtained from the left vastus lateralis by the percutaneous needle technique (Bergström 1962). The specimens were used for histochemistry, enzyme assays and electron microscopy.

Histochemistry The muscle samples for fibre typing and area determination were trimmed, mounted (frozen in isopentane cooled by liquid nitrogen) and stored at -80°C until analysis.

Serial transverse sections (10 μm) were cut with cryotome at -70°C and the myofibrillar ATPase staining method (Gomori 1941; Padykula & Herman 1953) was used for muscle fibre classification. Photographs of the stained sections were taken and classification into type I (slow twitch) and type II (fast twitch) (Engel 1966) was

made in all 43 subjects. In 34 of the subjects, the type I fibres were subclassified into A, B and C subtypes (Brooke & Kaiser 1970; Dubowitz & Brooke 1973). The average number of counted fibres for classification of main groups (type I and type II) and subgroups (type I type IIA, B and C) was 185 ± 57 and 51 ± 35 respectively.

The fibre areas were calculated from the 'lesser fibre diameter' of each fibre type (type I and type II) using a eyepiece micrometer (Dubowitz & Brooke 1973). Averaging each fibre to have a circular cross-section with a diameter equal to the lesser fibre diameter, the mean cross-sectional area of each fibre type was calculated. The fibre areas were determined from the NADH tetrazolium reductive staining (Novikoff et al 1961) and an average of 207 ± 13 diameters were measured per subject. The mean fibre area was calculated according to the formula presented by Haggmark et al (1978): i.e. fraction type I \times type I fibre area + fraction type II \times type II fibre area.

Biochemical analyses Five enzymes were chosen to represent the major pathways in energy metabolism. Glycolysis was represented by phosphofructokinase (PFK, E.C.2.7.1.11), lactate fermentation by lactate dehydrogenase (LDH, E.C.1.1.1.27), fatty acid β -oxidation by 3-hydroxyacyl-CoA dehydrogenase (HAD, E.C.1.1.1.35), the citric acid cycle by citrate synthase (CS, E.C.4.1.1.1) and the respiratory chain by cytochrome oxidase (cytochrome C, E.C.1.9.3.1). In addition, two enzymes related to the contraction process and the short-term supply of ATP were investigated, Mg^{2+} stimulated ATPase (E.C.3.6.1.4) and myokinase (MK, E.C.2.7.4.3). For PFK, LDH, HAD, CS and cytochrome oxidase, muscle homogenates were prepared and assayed as described previously (Örlander et al 1977). PFK was assayed according to Shonk & Boer (1964), LDH and HAD by the methods of Bass et al (1969), CS as described by Srere (1969) and cytochrome oxidase by Srere et al (1969). For the assays of Mg^{2+} stimulated ATPase and MK the procedures described by Thorstensen (1976) were employed. LDH isoenzymes were separated by disc-electrophoresis and relative quantities of M and H subunits were determined as described by Spöck (1976). Protein was estimated by the method of Lowry et al (1951).

Electron microscopy Small pieces of muscle tissue were processed for electron microscopy and micrographs were taken for morphological analysis by methods described by Weibel (1969). An account of the procedure has been given before (Örlander et al 1977). It is of note that the values on mitochondrial mean volume and number per

Table 5. Isometric and dynamic strengths as well as dynamic strength in percent of isometric strength at different angular velocities

Values are means \pm S.E. n.s., not significant

Group		Isometric strength 0° (Nm)	Dynamic strength		120° Nm	%	180° Nm	%
			60° Nm	%				
Smokers	18	180.9 \pm 9.5	165.9 \pm 8.4	93.0 \pm 0.03	143.0 \pm 5.4	80.9 \pm 0.03	117.7 \pm 7.0	68.5 \pm 0.04
Non-smokers	25	216.5 \pm 6.6	194.2 \pm 6.0	90.3 \pm 0.02	161.6 \pm 5.1	75.5 \pm 0.02	131.0 \pm 4.2	60.8 \pm 0.01
		<0.01	<0.01	n.s.	<0.01	n.s.	n.s.	<0.05

Muscular endurance measured both in short term isometric and dynamic endurance tests was not significantly different in the two groups (Table 6).

DISCUSSION

The present investigation has shown some quite clear-cut differences in skeletal muscle morphology, metabolism and function between smoking and non-smoking sedentary men. Significant reductions in muscle oxidative capacity and strength were seen in the smokers, effects which may be partly related to differences in fibre type distribution.

Fibre type distribution

It is evident that the lower proportion of type I fibres and the concomitantly higher percentage type II B fibres in the smokers (Fig. 1) may either be explained as an effect of smoking *per se* or it may be that some background factor is responsible. Both these possibilities will be considered.

There is ample evidence that the 'type' characteristics of a muscle fibre are controlled by

the motor nerve through 'trophic' influences (Guth 1968, Close 1977, Gutmann 1976). Recent evidence indicates that the control may be purely a function of impulse activity (Salmons & Sreter 1976). While human type II A and II B fibres seem to some extent interconvertible by intense training (Andersen & Henriksson 1977, Jansson & Kaijser 1977), it appears that type I-type II interconversions in adult muscle can be achieved only by means such as cross innervation or electrical stimulation (Guth 1968, Salmons & Vrbová 1969, Close 1972, Pettie et al. 1973). It is thus hard to envisage a mechanism whereby tobacco smoking might produce such an alteration. Nicotine would be a conceivable etiological agent, since it stimulates muscle fibres at the motor endplate and interferes with acetylcholine metabolism (Fischer et al. 1960, Larson et al. 1961). A disturbance of the normal neuromuscular interaction by such effects might possibly alter the fibre type distribution pattern.

Negative correlations have been found between the amount of smoking on the one hand and indices of physical fitness and sports interest on the other (Bjerner et al. 1977). In a study of 16-year-old boys and girls, Hedberg & Jansson (1976) found that those with a low percentage type I fibres in vastus lateralis were less active and less interested in physical activities than those with a high percentage. By integrating these observations one might suggest that those with a low proportion type I fibres are more liable to smoke; this would provide an alternative explanation for the present finding. There is evidence for a strong genetic influence on fibre type distribution in man (Komi et al. 1977). It

Table 6. Isometric and dynamic endurance

Values are means \pm S.E. Numbers of subjects within brackets M1S: maximum isometric strength, n.s., not significant

Group	Isometric endurance at 50% M1S (s)	Dynamic endurance: Decline in peak torque, 50 contr. 180° (%)
Smokers	51.9 \pm 4.8 (18)	50.0 \pm 2.9 (12)
Non-smokers	65.2 \pm 6.9 (25)	49.0 \pm 1.1 (21)
P		n.s.

Recent observations by Jansson et al. (1978) do, however, suggest that extreme training might produce type I-type II interconversion.

Table 3 Enzyme activities

Values are means \pm S.E. For full names of enzymes see Material and methods. n.s. not significant

Group	n	PFK $\mu\text{mol} \times \text{min}^{-1} \times (\text{g wet wt})^{-1}$	LDH $\times (\text{g wet wt})$	HAD	CS	Cytox $\mu\text{mol O}_2 \times \text{min}^{-1} \times (\text{g wet wt})^{-1}$	Mg ²⁺ ATPase $\mu\text{mol} \times \text{min}^{-1} \times (\text{g wet wt})^{-1}$	MK $\times (\text{g wet wt})$	H-LDH % of LDH subunit
Smokers	18	8.13 ± 1.16	71.1 ± 7.0	1.77 ± 0.10	3.40 ± 0.20	3.26 ± 0.32	11.1 ± 1.0	150.7 ^a ± 11.4	30.4 ^a ± 3.7
Non smokers	25	8.56 ± 0.73	73.1 ± 6.4	2.25 ± 0.14	4.51 ± 0.22	4.26 ± 0.28	10.9 ^a ± 0.7	177.9 ^a ± 7.3	34.6 ^a +
P		n.s.	n.s.	<0.05	<0.001	<0.05	n.s.	n.s.	n.s.
24 subjects		16 subjects	23 subjects						

Enzyme activities The activities of the 7 studied enzymes in the two groups are shown in Table 3.

PFK, LDH (including subunit percentages), Mg²⁺ stimulated ATPase and MK were not significantly different in the two groups. For the mitochondrial enzymes significantly lower (HAD 21% $P < 0.05$, CS 25% $P < 0.001$, cytox 23% $P < 0.05$) activities were found in the smokers. No difference in muscle protein content was observed.

Ultrastructure Table 4 gives the values on mitochondrial volume fractions as well as apparent numbers and mean volumes in the fibrillar and subsarcolemma spaces of muscle fibres. The volume fraction of lipid droplets is also indicated.

The only significant intergroup difference was a diminished fibrillar space mitochondrial volume fraction (21% $P < 0.01$) in the smokers. A similar trend could be seen for the corresponding mean volume (23% lower in smokers); this difference was however not statistically significant ($P < 0.2$).

No significant difference in lipid droplet content

was present, but when those smokers who smoked 50 g of tobacco or more per week were considered separately a significantly ($P < 0.05$) reduced value was observed ($0.35 \pm 0.08\%$, $n = 5$).

Muscle strength and endurance are shown in Tables 5 and 6. Maximum isometric strength measured either as a one- or a two-leg contraction was found to be higher ($P < 0.05$ – 0.01) in the non smokers (Table 5). This also held true for dynamic strengths ($P < 0.05$ – 0.01) except for the highest angular velocity studied ($\pi \text{ rad} \times \text{s}^{-1}$ or $180^\circ \times \text{s}^{-1}$) which was almost equal in the two groups (Table 5). When dynamic strengths were expressed in relation to maximum isometric strength it was found that the smokers were relatively stronger at the highest angular velocity ($\pi \text{ rad} \times \text{s}^{-1}$) whereas no statistically significant difference was seen at the other velocities studied (Table 5). This seems to indicate a quantitative as well as qualitative difference in muscular strength between the two groups.

Table 4 Ultrastructural parameters

Values are means \pm S.E. Note that numbers and mean volumes are approximations (see Material and methods). n.s. not significant

Group	n	Mitochondria in fibrillar space				Mitochondria in subsarcolemma space			Lipid droplet volume fraction (%)
		Volume fraction (%)	Number μm^{-2}	Sarcomere	$10^6 \times$ Mean volume (μm^3)	Volume fraction (%)	Number μm^{-2}	$10^6 \times$ Mean volume (μm^3)	
Smokers	14	3.79 ± 0.44	1.43 ± 0.17	1.03 ± 0.10	3.63 ± 0.40	77.6 ± 3.6	5.34 ± 0.58	6.18 ± 1.09	0.70 ± 0.15
Non smokers	12	4.79 ± 0.28	1.35 ± 0.1	1.19 ± 0.10	4.70 ± 0.58	23.9 ± 3.1	4.68 ± 0.96	7.1 ± 1.93	0.97 ± 0.14
P		<0.01	n.s.	n.s.	n.s.	n.s.	n.s.	n	n.s.

13 subjects

Research Council (B77-04X-4251-04A, B78-04X-4251-04B), the Research Council of the Swedish Sport Federation, Svenska Allskåpet för medicinsk forskning, Skanska Insurance Company and the Swedish Tobacco Company

REFERENCES

- ANDERSEN P & HENRIKSSON J 1977 Training induced changes in the subgroups of human type II skeletal muscle fibres. *Acta Physiol Scand* 99: 123-135.
- JASS, A., BRDZICKA D, EYER P, HOFER S & PETTE D 1969 Metabolic differentiation of distinct muscle types at the level of enzymatic organization. *Eur J Biochem* 10: 198-206.
- BERGSTRÖM, J 1962. Muscle electrolytes in man. *Scand J Clin Lab Invest*, Suppl. 68.
- BIERSNER, R J, GUNDERSON E K E & RAHE R. H 1972 Relationship of sports interests and smoking to physical fitness. *J Sports Med* 12: 1-4-127.
- BROOKE M H & KAISER K K 1970 Three 'myon' ATPase systems: The nature of their pH lability and mitochondrial dependence. *J Histochem Cytochem* 18: 679-677.
- BURKE, R E & EDGERTON V R 1975 Motor unit properties and selective involvement in movement. *Exercise Sport Sci Rev* 3: 31-41.
- CHERRY N & KIERNAN K 1976 Personality scores and smoking behaviour: A longitudinal study. *Br J Prev Soc Med* 30: 123-131.
- CHEVALIER, R B, BOWERS J A, BONDURANT S & ROSS J C 1963 Circulatory and ventilatory effects of exercise in smokers and nonsmokers. *J Appl Physiol* 18: 357-360.
- CHEVALIER, R B, KRUMHOLZ, R A & ROSS J C 1966 Reaction of non-smokers to carbon monoxide inhalation. *J Amer Med Ass* 198: 1061-1064.
- CLOSE, R 1964 Dynamic properties of fast and slow skeletal muscles of the rat during development. *J Physiol (Lond)* 173: 74-95.
- COOPER, K H, GAY G O & BOTTENBERG R A 1968. Effects of cigarette smoking on endurance performance. *J Amer Med Ass* 203: 123-126.
- DÖBELN W 1964 Determination of body constituents I: Occurrence causes and prevention of overnutrition (ed. G. Blot). Almqvist & Wiksell, Uppsala.
- DUBOWITZ, V & BROOKE, M H 1973 Muscle biopsy: modern approach. Vol 2 in the series *Major Problems in Neurology* W B Saunders, Philadelphia.
- ENGEL, W K 1962 The inevitability of ferro- and cytochrome oxidase of skeletal muscle in the investigation of neuromuscular disease. *Neurology* 12: 778-794.
- ESSEN B, JANSSON E, HENRIKSSON J, TAYLOR, A W & SALTIN B 1975 Metabolic characteristics of fibre types in human skeletal muscle. *Acta Physiol Scand* 95: 153-165.
- FISCHER, E, SILVETTE H, LARSON P S & HAAG H B 1960. Effect of nicotine and tobacco on muscle function. *Am J Phys Med* 39: 63-77.
- GOMORI, G 1941 The distribution of phosphatase normal organs and tissues. *J Cell Comp Physiol* 17: 71-83.
- GUTH L 1968. "Trophic" influences of nerve on muscle. *Physiol Rev* 48: 641-687.
- GUTMANN E 1976. Neurotrophic relations. *Ann Rev Physiol* 38: 177-216.
- HÄGGMARK T, JANSSON E & SVANE, B 1978 Cross-sectional area of the thigh muscle in man measured by computed tomography. *Scand J Clin Lab Invest* 38: 353-360.
- HAKANI N & PIOUS D A 1967 Regulation of cytochrome oxidase in human cells in culture. *Nature* 216: 1087-1090.
- HALLMAN M 1971 Changes in mitochondrial respiratory chain proteins during perinatal development. Evidence of the importance of environmental oxygen tension. *Biochem Biophys Acta* 253: 360-372.
- HEDBERG G & JANSSON E 1976 Skeletal muscle fibre distribution: capacity and interest in different physical activities among students in high school. *Pedagogiska rapporter (Umeå)* 54 (15 Swedish summary in English).
- HOLLOSZY J O & BOOTH F W 1976. Biochemical adaptation to endurance exercise in muscle. *Ann Rev Physiol* 38: 273-291.
- HRUBES, V & BÄTTIG K 1970 Effect of inhaled cigarette smoke on limiting endurance in the rat. *Arch Environ Health* 21: 20-4.
- INGEMANN-HANSEN T & HALKJAER-KRISTENSEN J 1977 Cigarette smoking and maximal oxygen consumption rate in humans. *Scand J Clin Lab Invest* 37: 143-148.
- JANSSON E & KAISER L 1977 Muscle adaptation to extreme endurance training in man. *Acta Physiol Scand* 100: 315-324.
- JANSSON E, SJÖDIN B & TESCH P 1978 Changes in muscle fibre type distribution in man after physical training. A sign of fibre type transformation? *Acta Physiol Scand* 104: 235-237.
- KARLSSON J & ÖLLANDER, B 1972. Muscle metabolites with exhaustive static exercise of different duration. *Acta Physiol Scand* 86: 309-314.
- KINNULU V L 1976 Mitochondrial cytochrome concentrations in rat heart and liver as a consequence of different hypoxic periods. *Acta Physiol Scand* 96: 417-421.
- KLAUSEN K, RASMUSSEN B, GJELLEROD H, MADSEN H & PETERSEN E 1968 Circulation, metabolism and ventilation during prolonged exposure to carbon monoxide and to high altitude. *Scand J Clin Lab Invest* 22: 26-38.
- KOMI P V, VIITASALO J H T, HAVU M, THORSTENSSON A, SJÖDIN B & KARLSSON J 1977 Skeletal muscle fibres and muscle enzyme activities in monozygous and dizygous twins of both sexes. *Acta Physiol Scand* 100: 385-392.
- KRUMHOLZ, R A & HEDRICK E. C 1972. Exercise responses of smoking and non-smoking middle-aged humans: executives. *J Lab Clin Med* 80: 79-87.
- KRUMHOLZ, R A, CHEVALIER, R B & ROSS J C 1964 Cardiorespiratory function in young smokers. *Ann Intern Med* 60: 603-610.

would be tempting to speculate that there exists a hereditary predisposition towards taking up smoking this might be related to the well-established connection between smoking behaviour and personality traits (Cherry & Kiernan 1976 Simon & Primavera 1976). Any conclusions on this point would however be premature at the present time.

Muscle metabolism

The enzyme activity determinations revealed a lower muscle oxidative capacity in the smokers. HAD, CS and cytochrome activities being 21–25% lower than in the nonsmokers (Table 3). Ultrastructurally this was reflected by the equally decreased (21%) fibrillar space mitochondrial volume fraction (Table 4). A lower mean volume per mitochondrion appeared to be the main cause for the decreased volume fraction, even though this difference failed to reach statistical significance.

The impaired oxidative capacity in the smokers' muscles may be due to various causes. Essén et al. (1975) found proportions of 2.5, 1.9, 1.2, 4 for succinate dehydrogenase activity in type I, II A, II B and II C fibres, respectively. By using these values and those in Fig. 1, it can be estimated that some 40–50% of the difference in oxidative capacity may be attributed to the difference in fibre type distribution. A lower physical activity level in the smokers would contribute to the lowered oxidative capacity (cf. Holloszy & Booth 1976). The fact that subjects were recruited on the basis of a low and homogeneous occupational and sparetime physical activity level and the very small differences in anthropometrical characteristics (Table 1) tend to dispute this possibility. The similarities in fibre areas (Table 2) point in the same direction. Furthermore, smokers and nonsmokers reported similar sparetime activities in a questionnaire. It can however not be ruled out that the smokers might have adapted to a somewhat more sedentary way of life since there are indications that smokers generally tend to dislike strenuous physical activities (Björnsäter et al. 1977). Finally, it is conceivable that some of the well over 1 700 substances found in tobacco leaf and/or smoke (Stedman 1968) might influence enzyme levels in muscle. For example, carbon monoxide has been suggested to produce tissue hypoxia (e.g. Klausen et al. 1968; Sagone et al. 1973) which might depress the synthesis of mitochondrial enzymes (e.g. Hakami & Pious 1967;

Simon & Robin 1970; Hallman 1971; Meli et al. 1976; Kinnula 1976).

Functional characteristics

The most striking finding in the functional characteristics of the muscle was the lower muscle strength in the smokers, expressed in isometric as well as dynamic terms. The relative difference amounted to approximately 16% for isometric strength and 15, 12 and 7% for dynamic strength at the different angular velocities corresponding to 60, 120 and 180° × s⁻¹, respectively.

It should be noted that the absolute and relative difference in maximum strength between the two groups decreased with increasing speed of contraction (Table 5). At the highest speed of contraction this difference was not statistically significant. This is not surprising since the smokers had a higher proportion of type II muscle fibres, which is known to be essential to a high force output during fast muscle contractions (cf. Burke & Edgerton 1974). This is most likely due to the short contraction time of type II fibres (Close 1964). In fact, when dynamic strengths were expressed as percent of maximum isometric strength, a significantly higher value was found for smokers at the highest angular velocity (Table 5). This is in accordance with Thorstensson et al. (1976) who demonstrated a positive correlation between percent type II fibres and dynamic strength at 180° × s⁻¹, expressed as percent of maximum isometric strength.

The reason for the lower absolute muscular strength in the smokers is at present not known. Muscular strength is mainly dependent upon the cross sectional area of the muscle and the number of recruited muscle fibres. Since neither thigh circumference (Table 1) nor fibre areas (Table 2) differed between the two groups, a different cross-sectional area does not seem very plausible. A different muscle fibre recruitment pattern thus appears to be the most likely cause for the lower muscular strength in the smoking subjects. It is however too early to speculate upon the mechanism for this, and further studies will be undertaken specifically to analyze these questions.

We are indebted to Mrs Gun-Britt Ölander and M. Maria Ahlberg for skilful technical assistance and to Mr. Carina Eriksson for secretarial assistance. Financial support has been received from Magnus Bergvall's Foundation, Clas Groschinsky Memorial Fund, the Faculty of Science of the University of Uppsala, the Swedish Medical

research Council (B77-04X-4231-04A B78-04X-4231-08), the Research Council of the Swedish Sport Federation, Svenska sjuklöper för medicinsk forskning, Skandinavisk varnare Company and the Swedish Tobacco Company

REFERENCES

- JØRDERSEN P & HENRIKSSON J 1977 Training induced changes in the subgroups of human type II skeletal muscle fibres. *Acta Physiol Scand* 99: 123-125.
- JASS, A., BRDZICKA D, EYER P, HOFER S & PETTE, D 1969 Metabolic differentiation of distinct muscle types at the level of enzymatic organization. *Eur J Biochem* 10: 198-206.
- JERGSTRÖM J 1964 Muscle electrolytes in man. *Scand J Clin Lab Invest. Suppl.* 68.
- JØRNER, R. J. & GUNDERSON E. K. E. & RAHE R. H 1977 Relationship of sports interests and smoking to physical fitness. *J Sports Med* 1: 1-17.
- KROOKE, M. H. & KAISER, K. K. 1970. Three myosin ATPase systems: The nature of their pH lability and sulfhydryl dependence. *J Histochem Cytochem* 18: 670-677.
- KRIEKE, R. E. & EDGERTON V. R. 1975 Motor unit properties and selective involvement in movement. *Exercise Sport Sci Rev* 3: 31-41.
- CHERRY N & KIERNAN K 1976. Personality scores and smoking behaviour: A longitudinal study. *Br J Prev Soc Med* 30: 133-131.
- CHEVALIER, R. B. BOWERS J. A. BONDURANT S. & ROSS J. C 1963 Circulatory and ventilatory effects of exercise in smokers and nonsmokers. *J Appl Physiol* 18: 357-360.
- CHEVALIER, R. B. KRUMHOLZ, R. A. & ROSS J. C. 1966 Reaction of nonsmokers to carbon monoxide inhalation. *J Amer Med Ass* 198: 1061-1064.
- CLOSE, R. 1964 Dynamic properties of fast and slow skeletal muscles of the rat during development. *J Physiol (Lond)* 173: 74-95.
- COOPER, K. H. GAY G. O. & BOTTENBERG R. A. 1964. Effects of cigarette smoking on endurance performance. *J Amer Med Ass* 203: 123-126.
- CRUTCHER, W. 1964. Determination of body constituents for occurrence of cancer and prevention of overnutrition (ed G Blax). Almqvist & Wiksell, Uppsala.
- DUBOWITZ, V. & BROOKE, M. H. 1973 Muscle biopsy: modern approach. Vol. 1 in the series *Major Problems in Neurology* W. B. Saunders Philadelphia.
- ENGEL, W. K. 1962. The essentiality of histo- and cytochemical studies of skeletal muscle in the investigation of neuromuscular disease. *Neurology* 12: 778-794.
- ESSEN B. JANSSON E. HENRIKSSON J. TAYLOR, A. W. & SALTIN B. 1975 Metabolic characteristics of fibre types in human skeletal muscle. *Acta Physiol Scand* 95: 153-165.
- FISCHER, E. SILVETTE H. LARSON P. S. & HAAD, H. B. 1960. Effect of nicotine and tobacco on muscle function. *Am J Phys Med* 39: 63-77.
- GOMORI, G. 1941 The distribution of phosphatase in normal organs and tissues. *J Cell Comp Physiol* 17: 71-83.
- GUTH L. 1968. Trophic influences of nerve on muscle. *Physiol Rev* 48: 645-687.
- GUTMANN E. 1976 Neurotrophic relations. *Ann Rev Physiol* 38: 177-116.
- HÄGGMARK T. JANSSON E. & SVANE, B. 1978 Cross-sectional area of the thigh muscle in man measured by computer tomography. *Scand J Clin Lab Invest* 38: 355-360.
- HAKAMI N & PIOUS D. A. 1967 Regulation of cytochrome oxidase in human cells in culture. *Nature* 16: 1087-1090.
- HALLMAN M. 1971 Changes in mitochondrial respiratory chain proteins during perinatal development. Evidence of the importance of environmental oxygen tension. *Biochim Biophys. Acta* 253: 360-372.
- HEDBERG G & JANSSON E. 1976 Skeletal muscle fibre distribution, capacity and interest in different physical activities among students in high school. *Pedagogiska rapporter* (Umeå) 54. (In Swedish, summary in English.)
- HOLLOSZY J. O. & BOOTH F. W. 1976 Biochemical adaptation to endurance exercise in muscle. *Ann Rev Physiol* 38: 273-291.
- HRUBES, V. & BÄTTIG K. 1970. Effect of inhaled cigarette smoke on swimming endurance in the rat. *Arch Environ Health* 21: 30-4.
- INGEMANN-HANSEN T. & HALKJAER-KRISTEN SEN J. 1977 Cigarette smoking and maximal oxygen consumption rate in humans. *Scand J Clin Lab Invest* 37: 143-148.
- JANSSON E. & KAISER L. 1977 Muscle adaptation to extreme endurance training in man. *Acta Physiol Scand* 100: 315-324.
- JANSSON E. SJÖDIN B. & TESCH, P. 1978 Changes in muscle fibre type distribution in man after physical training: A sign of fibre type transformation? *Acta Physiol Scand* 104: 235-237.
- KARLSSON J. & OLLANDER B. 1972. Muscle metabolites: An exhaustive static exercise of different duration. *Acta Physiol Scand* 86: 309-314.
- KINNULA V. L. 1976 Mitochondrial cytochrome concentrations in rat heart and liver as a consequence of different hypoxic periods. *Acta Physiol Scand* 96: 417-421.
- KLAUSEN K. RASMUSSEN B., GJELLEROD H. MADSEN H. & PETERSEN E. 1968 Circulation, metabolism and ventilation during prolonged exposure to carbon monoxide and to high altitude. *Scand J Clin Lab Invest* 22: 26-38.
- KOMI P. V. VUOLASALO J. H. T. HAVU M. THORSTENSSON A. SJÖDIN B. & KARLSSON J. 1977 Skeletal muscle fibres and muscle enzyme activities in monozygous and dizygous twins of both sexes. *Acta Physiol Scand* 100: 385-392.
- KRUMHOLZ, R. A. & HEDRICK E. C. 1972. Exercise responses of smoking and non-smoking middle-aged business executives. *J Lab Clin Med* 80: 79-87.
- KRUMHOLZ, R. A. CHEVALIER, R. B. & ROSS J. C. 1964. Cardiorespiratory function in young smokers. *Ann Intern Med* 60: 603-610.

- LARSON I S, HAAG H H & SILVITTI H 1961 Some effects of nicotine and smoking on metabolic functions. *Clin Pharmacol Ther* 2: 80-109.
- LARSSON L & KARLSSON J 1978 Isometric and dynamic endurance as a function of age and skeletal muscle characteristics. *Acta Physiol Scand* 104: 179-186.
- LARSSON J, GRIMBY G & KARLSSON J 1979 Muscle strength and speed of contraction in relation to age and muscle morphology. *J Appl Physiol* 46: 451-456.
- LOWRY O H, ROSEBROUGH N J, FARR A I & RANDALL R J 1951 Protein measurement with the Folin phenol reagent. *J Biol Chem* 193: 265-275.
- McDONOUGH J R, KUSUMI I & BRUCI R A 1970 Variations in maximal oxygen intake with physical activity in middle-aged men. *Circulation* 61: 743-751.
- MELA I, GOODWIN C W & MILLER I D 1976 In vivo control of mitochondrial enzyme concentrations and activity by oxygen. *Amer J Physiol* 231: 1811-1816.
- MOTTRID M, WHIPP P R, HOKOSH J, LOWMAN F & THISTLE H 1969 A study of isokinetic exercise. *Phys Ther* 49: 735-747.
- NOVIKOFF A B, SHIN W Y & DRUCKER J 1961 Mitochondrial localization of oxidative enzymes: staining results with two tetrazolium salt. *J Biophys Biochem Cytol* 9: 47-61.
- ÖRLANDER J, HISSING A H, KARLSSON J & LKIBLOM B 1977 Low intensity training: inactivity and resumed training in sedentary men. *Acta Physiol Scand* 101: 351-362.
- PADYKULA H A & HERMAN F 1955 Factors affecting the activity of adenosine triphosphatases as measured by histochemical techniques. *J Histochem Cytochem* 3: 161-169.
- PETERSON P J & KELLY D L 1969 The effect of cigarette smoking upon the acquisition of physical fitness during training as measured by aerobic capacity. *J Amer Coll Health Ass* 17: 230-234.
- PETTI D, SMITH M F, STAUDTE H W & VRBOVÁ G 1973 Effect of long term electrical stimulation on some contractile and metabolic characteristics of fast rabbit muscles. *Pflügers Arch* 338: 257-272.
- RAVIN P B, DRINKWATER B I, HORVATH J M, RUHLING R O, GILNER J A, SUTTON J C & HOLDMAN N W 1974 Age, smoking, lean heat stress, and their interactive effect with carbon monoxide and peroxyacetylnitrate on man's aerobic power. *Int J Biometeorol* 18: 22-32.
- REICH W D, CHALI R A 1977 Inhaled carbon monoxide and treadmill-exercised dogs. *Arch Environ Health* 34: 76-770.
- SAGONE JR A I, LAWRENCE T, CHALCERUS S I 1973 Effect of smoking on tissue oxygen supply. *Blood* 41: 845-851.
- SALMONS S & VRBOVÁ G 1969 The influence of activity on some contractile characteristics of mammalian fast and slow muscle. *J Physiol (Lond)* 201: 535-549.
- SALMONS S & SRETER F A 1976 Significant impulse activity in the transformation of skeletal muscle type. *Nature (Lond)* 263: 30-34.
- SHAPIRO I G 1973 Smoking and selected physical fitness measures. *J Amer Coll Health Ass* 1: 409-412.
- SHONK C J & BOXER G F 1964 Enzyme patterns in human tissues. I. Methods for the determination of glycolytic enzymes. *Cancer Res* 4: 709-724.
- SIMON W J & PRIMAVERA I H 1976 The personality of the cigarette smoker: some empirical data. *Int J Addict* 11: 81-94.
- SIMON L M & ROBIN J D 1970 Changes in heart and skeletal muscle cytochrome oxidase activity during anaerobiosis in the freshwater turtle *Pseudemys scripta elegans*. *Comp Biochem Physiol* 37: 437-441.
- SRI R P A 1969 Climate synthase. *Meth Enzymol* 13: 3-11.
- STEDMAN R I 1968 The chemical composition of tobacco and tobacco smoke. *Chem Rev* 68: 133-201.
- THORSTENSSON A 1976 Muscle strength, fibre type and enzyme activities in man. *Acta Physiol Scand Suppl* 443.
- THORSTENSSON A, GRIMBY G & KARLSSON J 1976 Force-velocity relations and fiber composition in human knee extensor muscles. *J Appl Physiol* 40: 1-16.
- WILKIE L R 1969 Stereological principles for morphometry in electron microscopic cytology. *Int Rev Cytol* 26: 215-302.
- WIERLAT A I, ORISHIMO M W, NELSON J & PHILLIPS S J 1969 The location of different β thioester system for fatty acids in inner and outer mitochondrial membranes from rabbit heart. *J Biol Chem* 244: 6498-6506.

plantar flexion strength and structure

AXEL R. FUGL-MEYER, MICHAEL SJÖSTRÖM
and LENNART WÄHLBY

Department of Physical Medicine and Rehabilitation, Departments of Anatomy and Neurology and Department of Surgery, University of Umeå, S-90185 Umeå, Sweden

FUGL-MEYER A. R., SJÖSTRÖM M. & WÄHLBY L. Human plantar flexion strength and structure. *Acta Physiol Scand* 1979, 107, 47-56. Received 25 May 1978. ISSN 0001-6772. Department of Physical Medicine and Rehabilitation, Departments of Anatomy and Neurology and Department of Surgery, University of Umeå, Sweden.

Plantar flexion strengths were studied in 30 right-handed males. Static and dynamic maximum plantar flexion torques were recorded, knees fully extended (0°) and in 90° flexion. In five of the subjects the soleus and gastrocnemius muscle structure was studied by light microscopy and enzyme histochemistry. Specimens were obtained by needle biopsy usually bilaterally. Intralimbic declines of force were found to be a function of angular motion velocity. Static and dynamic torques correlated significantly. Peak torques were significantly greater (mean 15%) at the 0° than at the 90° knee angle and left maximum plantar flexion torques at 0° were greater (mean 10%) than right. Mean morphometric data on the m. soleus suggested right-left asymmetry which could not be demonstrated for the m. gastrocnemius. Fibres with low stainability for myofibrillar ATPase (Type I fibres) had smaller diameters, but constituted the major part of the cross-sectional area. In these five non-athletes no significant correlation between data on plantar flexion strength and morphometric data on triceps surae structure could be demonstrated. On the other hand, strength covaried with calf circumference.

Key words: Human, skeletal muscle, needle biopsy, morphology, muscle fibres, physiology, strength, isometric, isometric biomechanics.

This investigation was designed to study the plantar flexion strength characteristics in younger adult males and to analyze whether structural details of the triceps surae muscle can predict plantar flexion strength in normal, non-specifically trained subjects. Theoretically, the triceps surae accounts for about 90% of the maximum plantar flexion strength in man (Murray et al. 1976). While the length-tension relationships of the gastrocnemius muscle can be passively altered by changes of knee position such is not the case for the one-joint soleus muscle. This latter part of the triceps surae is of primary importance in stabilizing the talocrural joint when in the upright position (Grant 1970, Campbell et al. 1973).

Human triceps surae muscle contains fibres that can be differentiated on the basis of myofibrillar adenosine triphosphatase activity, aerobic and anaerobic potential (Edström & Nyström 1969, Johnson et al. 1973, Costill et al. 1974, 1976, Gollnick et al. 1974, Taylor et al. 1974, Edgerton et

al. 1975). However, these reports do not include data on fibre size and relative occurrence of the histochemically differentiated fibre categories (cf. Table 4). Thus, hitherto it has not been feasible to estimate the relative cross-sectional fibre area, and to correlate this to the physiological cross-section (Fick 1911). Furthermore, in the field of occupational ergonomics, it is of interest to analyze whether morphological asymmetry occurs in untrained man.

Until recently the methods available for clinical assessment of plantar flexion strength have mostly applied measurements of static strength. Generally semi-objective functional measures (e.g. standing on toes, climbing steps) or strength measurements in standardized positions have been applied (Kendall & Kendall 1969, Daniels & Worthingham 1972). Such methods have, however, been criticized as being too indiscriminate (Herman & Bragis 1967). Objective strength measurements using electronic

- LARSON P S HAAG H B & SILVETTE H 1961 Some effects of nicotine and smoking on metabolic functions. *Clin Pharmacol Ther* 7: 80-109
- LARSSON L & KARLSSON J 1978 Isometric and dynamic endurance as a function of age and skeletal muscle characteristics. *Acta Physiol Scand* 104: 179-186
- LARSSON L, GRIMBY G & KARLSSON J 1979 Muscle strength and speed of contraction in relation to age and muscle morphology. *J Appl Physiol* 46: 431-436
- LOWRY O H ROSEBROUGH N J FARR A L RANDALL R J 1951 Protein measurement with the Folin phenol reagent. *J Biol Chem* 193: 265-275
- McDONOUGH J R KUSUMI F & BRUCE R A 1970 Variations in maximal oxygen intake with physical activity in middle-aged men. *Circulation* 61: 743-751
- MELA L GOODWIN C W & MILLER L D 1976 In vivo control of mitochondrial enzyme concentrations and activity by oxygen. *Amer J Physiol* 231: 1811-1816
- MOFFROID M WHIPPLE R HOFKOSH J LOWMAN E & THISTLE H 1969 A study of isokinetic exercise. *Phys Ther* 49: 735-747
- NOVIKOFF A B SHIN W Y & DRUCKER J 1961 Mitochondrial localization of oxidative enzymes staining results with two tetrazolium salts. *J Biophys Biochem Cytol* 9: 47-61
- ÖRLANDER J KIESSLING K H KARLSSON J & EKBLOM B 1977 Low intensity training inactivity and resumed training in sedentary men. *Acta Physiol Scand* 101: 351-366
- PADYKULA H A & HERMAN E 1955 Factors affecting the activity of adenosine triphosphatases as measured by histochemical techniques. *J Histochem Cytochem* 3: 161-169
- PETERSON F J & KELLEY D L 1969 The effect of cigarette smoking upon the acquisition of physical fitness during training as measured by aerobic capacity. *J Amer Coll Health Ass* 17: 250-254
- PETTE D SMITH M E STAUDTE H W & VRBOVÁ G 1973 Effects of long-term electrical stimulation on some contractile and metabolic characteristics of fast rabbit muscles. *Pflügers Arch* 338: 257-272
- RAVEN P B DRINKWATER B L HORVATH J M RUHLING R O GLINER J A SUTTON J C & BOLDUAN N W 1974 Age, smoking, heat stress and their interactive effect with carbon monoxide and peroxyacetyl nitrate on man's aerobic power. *Int J Biometeorol* 18: 21-32
- REECE W D & BALL R A 1977 Inhaled cigarette smoke and treadmill exercised dogs. *Arch Environ Health* 4: 266-270
- SAGONE JR A L LAWRENCE T & BALCERZAK S P 1973 Effect of smoking on tissue oxygen supply. *Blood* 41: 845-851
- SALMONS S & VRBOVÁ G 1969 The influence of activity on some contractile characteristics of mammalian fast and slow muscle. *J Physiol (Lond)* 201: 535-549
- SALMONS S & SRÉTER F A 1976 Significance of impulse activity in the transformation of skeletal muscle type. *Nature (Lond)* 263: 30-34
- SHAYER L G 1973 Smoking and selected physical fitness measures. *J Amer Coll Health Ass* 1: 489-497
- SHONK C E & BOXER G E 1964 Enzyme patterns in human tissues. I. Methods for the determination of glycolytic enzymes. *Cancer Res* 4: 709-714
- SIMON W E & PRIMAVERA L H 1976 The personality of the cigarette smoker: some empirical data. *Int J Addict* 11: 81-94
- SIMON L M & ROBIN E D 1970 Changes in heart and skeletal muscle cytochrome oxidase activity during anaerobiosis in the freshwater turtle *Pseudemys scripta elegans*. *Comp Biochem Physiol* 37: 437-441
- SRERE P A 1969 Citrate synthase. *Meth Enzymol* 13: 3-11
- STEDMAN R L 1968 The chemical composition of tobacco and tobacco smoke. *Chem Rev* 68: 153-207
- THORSTENSSON A 1976 Muscle strength, fibre types and enzyme activities in man. *Acta Physiol Scand Suppl* 443
- THORSTENSSON A, GRIMBY G & KARLSSON J 1976 Force-velocity relations and fiber composition in human knee extensor muscles. *J Appl Physiol* 40: 116
- WEIBEL E R 1969 Stereological principles for morphometry in electron microscopic cytology. *Int Rev Cytol* 56: 235-302
- WHEREAT A F ORISHIMO M W NELSON J & PHILLIPS S J 1969 The location of different synthetic systems for fatty acids in inner and outer mitochondrial membranes from rabbit heart. *J Biol Chem* 244: 6498-6506

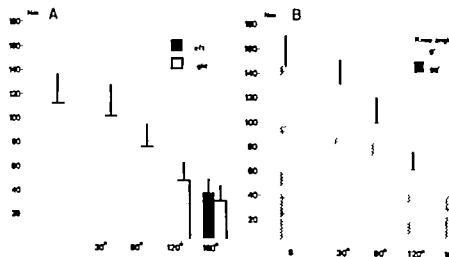


Fig. 3. Relation in 5 healthy sedentary adult males between mean maximum plantar flexion torque of (A) the right and the left legs with knees flexed 90° and (B) the left leg with knee straight (0°) and rightfully flexed (90°). Torque \pm S.D. (Nm) is given as function of angular velocity. S indicates static manoeuvre.

torque was measured with the foot-plate locked in the angular position identical to the peak torque position for the slow (30°/s) dynamic manoeuvre. This angular position was chosen for direct comparison of the static with the dynamic forces.

Morphological studies. 1.5 of the subjects 3 separate muscle biopsies were performed by the same surgeon after strength measurements. The biopsies were taken from both soleus muscles approximately 17 cm above the calcanei and from the maximum bulge of the lateral gastrocnemius using the needle biopsy technique (Bergström 1975). The samples were frozen by immersion in Freon 12 chilled by liquid nitrogen. Serial cross-sections, ten microns thick, were cut in cryostat at 20°C and mounted on glass slides. The specimens were then treated histochemically for myofibrillar adenosine triphosphatase (ATPase) at pH 9.4, 4.6 and 4.2 and succinic dehydrogenase (SDH) and with haematoxylin-eosin (Dubowitz & Brooke 1973).

RESULTS

Strength. The mean maximum static torques in both positions were greater than the peak dynamic torques at 30°/s (Table 1). The relationship between mean maximum plantar flexion torque of the right and left legs is displayed in Fig. 3a. With increasing angular velocity of motion the peak dynamic torques decreased. Static and dynamic peak torques (Table 1) covaried significantly ($P < 0.001$ Pearson correlation) (Table 2) for both legs and for both knee positions. Mean maximum static and dynamic plantar flexion torques in both positions were significantly greater ($P < 0.05$ Student's *t*-test for

paired observations) for the left than for the right legs. Furthermore plantar flexion strength was significantly greater ($P < 0.05$ Student's *t*-test for paired observations) in the 0° than in the 90° knee position (Fig. 3b). Virtually identical plantar flexion strength measurements with the knees in the 90° position were obtained irrelevant of hip position. Dynamic plantar flexion strength at 30°/s straight leg correlated significantly (right 0.59 left 0.49; $P < 0.001$) with calf circumference. In the five subjects studied morphologically right/left strength differences were systematically as pronounced as for the total sample studied with the exception of 30°/s manoeuvres (cf. Table 1). The mean strength difference in maximum plantar flexion strength for the two knee positions were, however, nearly identical for the total sample and the subsample. The plantar flexion strength in the static and in the slow dynamic manoeuvres was about 15–20% and in the two fastest dynamic manoeuvres about 10–15% lower for the 90° than for the 0° knee position. The range of maximum torques was greater for manoeuvres performed with flexed than for those performed with extended knees (cf. Table 1 \pm S.D.).

Structure. The muscle biopsies of which two from the gastrocnemius had to be omitted due to technical failure, showed polygonally packed muscle fibres of equal size (cf. Table 3) interspersed with sparse connective tissue (Figs 4 and 5). A few small rounded muscle fibres were found and one or

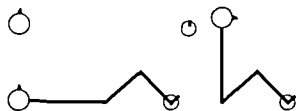


Fig. 1 Testpositions for measurements of static and dynamic plantar flexion strength. In left drawings subjects are placed supine, to the right upright sitting.

equipment have also been described (cf. Darcus 1953, Asmussen & Heeboll Nielsen 1961, Tornvall 1963).

Since the functional demands on plantar flexors are dynamic in character even in their postural alignment function, dynamic force should be the most adequate measurement for their characterization strengthwise. The Cybex II (Lumex, New York) dynamometer offers possibilities of measuring both the maximum static (isometric) and the dynamic forces. For the latter measurements the concept of isokinetics as first described by Hislop & Perrine (1967) and Thistle et al. (1967) is applied. This concept provides opportunities of measuring the dynamic force at any constant predetermined angular velocity of motion greater than zero and up to 300 degrees per second. The validity and reliability of the device has been discussed by Moffroid et al. (1969).

MATERIAL AND METHODS

30 clinically healthy, right-handed men (mean age 30.1 years, S.D. 5.7) were investigated for static and dynamic (isokinetic) plantar flexion strength. None of the subjects were engaged in regular physical training and all had sedentary occupations. Calf circumference, measured in the standing position at the horizontal intersection between the upper and the middle thirds of the lower leg, was 36.9 cm (S.D. 2), for the right and 36.6 cm (S.D. 2), for the left leg. In 5 of the men (mean age 31.4 years, S.D. 4.5) morphological studies were also performed.

Strength measurement. For measurements of strength two Cybex II dynamometers (Lumex, New York) were used, one for each leg. This instrument allows for linear torque measurements from 10 to a maximum of approximately 550 Newtonmetres (Nm) within 1% of the latter maximum registrable torque (Moffroid et al. 1969). Simultaneous registrations of torque and angular motion of the ankle joint were displayed on an X-Y storage-oscilloscope

(Tektronix, Oregon) and registered on an ink writer, as an adequate linear frequency response of 3 dB at 120 Hz (Mingograph, Siemens Elerna, Sweden). The recording instruments were coupled in parallel.

The subjects were placed in the supine position on a plinth. Two leg positions were applied. Either the hips and knees were in the 0° position or knees were in the 90° flexed position and the hips approximately 45° flexed (Fig. 1). In the 0° position the knees and hips were fixed to the plinth by velcro-bands. In the 90° knee position a padded, right angled board was fixed firmly with velcro-band to the dorsal surface of the leg extending 40 cm above and below the knee, thus securing a rigidly standardized 90° knee-angle. In another series of experiments subjects were seated (Fig. 1) with hips virtually maximally flexed and knees 90° flexed. The feet were firmly strapped to the Cybex II foot plate and care was taken to align the flexion/extension axis of the talo-crural joint with that of the apparatus.

Each subject was instructed to perform maximum isokinetic plantar flexions of the ankle joint at preset angular motion velocities of 30°, 60°, 120° and 180°/s, starting at maximum dorsal-flexion. Care was taken that the subject dorsal-flexed slowly pausing shortly in the maximum dorsal-flexed position. The manoeuvres were displayed on the X-Y oscilloscope with force registered on the Y-axis and angle on the X-axis (Fig. 2). This was done to ascertain that the subjects were familiar with the experimental procedure and able to produce virtually similar maximum force-angular curves throughout the range of motion, thus validating the procedure. The maximum static

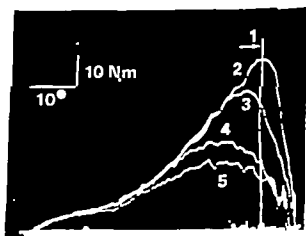


Fig. 2 An example of an X-Y registration of static and dynamic plantar flexion torques. Torque is displayed on the Y-axis and angle on the X-axis. Maximum dorsal flexion is to the extreme right and maximum plantar flexion to the extreme left. (1) denotes maximum static torque in the angular position identical to the peak torque position for the slow (30°/s) dynamic manoeuvre. It was here used for direct comparison of static and dynamic forces. (2) denotes maximum dynamic torque throughout the range of motion of the ankle joint at a preset velocity of 30°/s. (3), (4), (5) denote torque at angular velocities of 60°/s, 120°/s and 180°/s respectively.

Table 2. Coefficients of correlation between maximum static and dynamic peak torques in right (upper figure) and left (lower figure) leg of 30 clinically healthy subjects between 20 and 39 years

Measurements performed in the supine position with knees fully extended (0°)

n	180°/s							10°/s	60°/s	120°/s	180°/s
	90°		0°		90°						
	L Max	R %	L %	R Max	L Max	R %					
69	98	101	40	40	108	80	Static	0.76	0.85	0.65	0.59
95	83	82	51	62	67	65		0.93	0.86	0.76	0.70
59	97	83	36	37	100	84	30°/s		0.84	0.78	0.73
72	96	79	37	48	111	97			0.87	0.81	0.77
88	70	67	30	35	83	86	60°/s			0.88	0.85
71	89	82	39	46	94	87				0.81	0.72
13	13	15	8	11	7	6	120°/s				0.94
63	86	90	36	42	89	93					0.88
14	15	14	9	12	12	11					

cal comparisons of intraindividual structural side differences within the m. gastrocnemius were not performed on account of the small number of bilateral biopsies. In contrast to the tendency towards mean bilateral structural symmetry considerable intraindividual side differences in both fibre composition and diameter were found in several cases exceeding 10%. This was especially noticeable for the fibre composition and fibre diameters for subject B (cf. Table 3). Evidently due to these discrepancies the relative cross-sectional areas also varied. The product of the fibre cross-sectional area and the physiological cross-section was calculated for the

total triceps surae and for its separate components (Table 3). According to Fick (1911) the mean physiological cross-sectional area of the triceps surae is 43 cm² of which the m. soleus represents 47% and the m. gastrocnemius 53%. However the product of the relative morphological and the physiological cross-sectional areas also varied widely intra- and inter-individually. For the latter calculations it was assumed (cf. Johnson et al. 1973) that the biopsy specimens obtained from the deep fascicles of the lateral head of the gastrocnemius muscle possess a structure identical to that of the medial head.



Fig. 5. Serial sections of m. gastrocnemius treated for myofibrillar ATPase at pH 9.4 and for succinyl dehydrogenase at pH 4.6. At pH 9.4 the amount of heavily stained fibres are almost equal of lightly stained fibres. At pH 4.6 the heavily stained fibres show both intermediate and lightly staining characteristics. Also at the SDH staining 3 different fibre types could be differentiated. 100

Table 1 Individual static and dynamic plantar flexion peak torques for the right (R) and left (L) knees healthy sedentary males

	Static				30°/s				60°/s			
	0°		90°		0°		90°		0°		90°	
	R Nm	L Nm	R %	L %	R Nm	L Nm	R %	L %	R Nm	L Nm	R %	L %
A	163	159	71	84	141	130	80	85	108	104	97	91
B	180	191	84	77	162	158	93	80	144	138	70	77
C	179	123	87	91	119	114	85	86	85	96	91	81
D	139	150	81	86	179	135	84	84	96	108	89	71
E	125	140	100	64	105	115	81	74	90	90	77	67
F	147	153	85	80	131	130	85	82	101	107	84	78
±S D (Nm)	74	25	17	2	22	18	24	16	16	19	15	16
\bar{x} (n=30)	139	146	88	84	123	132	84	85	91	101	85	81
±S D (Nm)	73	26	4	26	20	19	25	25	19	20	18	16

Mean values + S D for these and for additionally 25 healthy males are given. Measurements were performed in the 0° position knees either fully extended (0°) or flexed (90°). Values for the 90° position expressed as per cent of the corresponding value at 0°. S D calculated from actual performance (Nm).

two internal nuclei were occasionally found. No diffuse or frequent focal abnormality was seen. In sections treated for myofibrillar ATPase at pH 9.4 fibres with low stainability generally dominated. In the m soleus scattered intensively stained fibres were also seen (Table 3, Fig. 4a) while in some specimens from the m gastrocnemius such high ATPase fibres were more abundant (Fig. 5a). In sections treated for myofibrillar ATPase but pre-incubated at pH 4.2 and 4.6 the picture was reversed. In the m soleus at pH 4.2 less than 1% showed intermediate staining characteristics (Fig. 4b)

while although within a wide range (1%) such fibres occurred more frequently in the lateral gastrocnemius muscle at pH 4.6 (Fig. 5b). High SDH intensity corresponded to fibres with low stainability for ATPase at pH 9.4 and vice versa. In the m soleus these categories showed only subtle variations in SDH stainability and subclassing was considered invalid (Fig. 4c). For the m gastrocnemius such subclassing could be performed (Fig. 5c).

In the m soleus there was no significant left-right asymmetry regarding mean fibre diameter, fibre type (Table 3) or fibre cross sectional area. Stain-

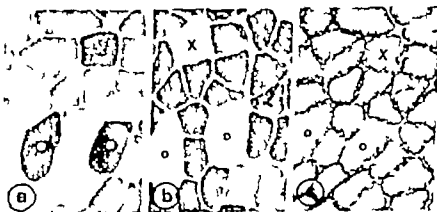


Fig. 4 Serial sections of m soleus treated for myofibrillar ATPase at pH 9.4. (a) At pH 9.4 a dominance of fibres with low stainability is seen with scattered highly stained fibres (• and o). After preincubation at pH 4.2 a few (less than 1% of total) of these latter fibres (x) showed intermediate staining characteristics. $\times 100$.

Table Coefficients of correlation between maximum static and dynamic peak torques in right (upper figure) and left (lower figure) leg of 30 clinically healthy subjects between 20 and 39 years

Measurements performed in the supine position with knees fully extended (0°)

h	90°		180°/s		90°				30°/s	60°/s	120°/s	180°/s
	L	R	L	R	L	R						
	Nm	%	%	Nm	Nm	%	%					
48	96	101	40	50	108	80	Static	0.78	0.85	0.65	0.59	
95	83	82	51	6	67	65		0.93	0.86	0.76	0.70	
59	97	83	34	37	100	86	90°/s		0.84	0.78	0.73	
77	96	79	37	48	111	92			0.87	0.81	0.77	
40	70	67	30	33	83	86	60°/s			0.83	0.85	
71	89	82	39	44	94	82				0.81	0.72	
15	13	15	8	11	7	6	120°/s				0.94	
63	86	90	36	42	89	93					0.88	
14	15	14	9	12	12	11						

oil comparisons of intrasubject structural side differences within the m. gastrocnemius were not performed on account of the small number of bilateral biopsies. In contrast to the tendency towards mean bilateral structural symmetry considerable intrasubject side differences in both fibre composition and diameter were found in several cases exceeding 10%. This was especially noticeable for the fibre composition and fibre diameters for subject B (cf. Table 3). Evidently due to these discrepancies the relative cross-sectional areas also varied. The product of the fibre cross-sectional area and the physiological cross-section was calculated for the

total triceps surae and for its separate components (Table 3). According to Fick (1911) the mean physiological cross-sectional area of the triceps surae is 43 cm² of which the m. soleus represents 47% and the m. gastrocnemius 53%. However the product of the relative morphological and the physiological cross-sectional areas also varied widely intra- and inter-individually. For the latter calculations it was assumed (cf. Johnson et al. 1973) that the biopsy specimens obtained from the deep fascicles of the lateral head of the gastrocnemius muscle possess a structure identical to that of the medial head.



Fig. 5. Serial sections of m. gastrocnemius treated for myofibrillar ATPase at pH 9.4 and for succinate dehydrogenase. At pH 9.4 the amount of heavily stained fibres are almost equal of lightly stained fibres. At pH 4.6 the heavily stained fibres show both intermediate and lightly staining characteristics. Also at the SDH staining 3 different fibre types could be differentiated. $\times 100$

Table 3 Morphometric results on the triceps surae muscle

Muscle fibre appearance and fibre diameter were determined on the basis of low and high stainability in sections cut for myofibrillar ATPase at pH 9.4. R = right, L = left.

Subject Leg	A		B		C		D		E		Mean \pm S.D.	
	R	L	R	L	R	L	R	L	R	L	R	L
<i>Fibre (%)</i>												
<i>Low ATPase</i>												
M soleus	77	69	77	70	70	81	74	82	83	84	75 \pm 1	77 \pm 7
M gastrocnemius	56	77	46	87	67	81	-	87	79	-	-	-
<i>Fibre diameter (μm)^a</i>												
<i>Low ATPase</i>												
M soleus	70	77	71	79	71	68	62	73	83	80	71 \pm 8	75 \pm 5
M gastrocnemius	57	63	61	71	62	65	-	59	64	-	-	-
<i>High ATPase</i>												
M soleus	82	90	80	85	83	75	66	75	97	9	81 \pm 9	83 \pm 8
M gastrocnemius	58	64	64	80	68	65	-	77	81	-	-	-
<i>Product of relative fibre cross-sectional area and physiological cross section</i>												
<i>Low ATPase</i>												
M soleus	1 304	1 511	1 056	1 612	1 304	1 382	1 049	1 61	105	1 985	1 364 \pm 433	1 620 \pm 227
M gastrocnemius	757	1 188	713	1 825	1 071	1 426	-	826	1 348	-	-	-
<i>High ATPase</i>												
M soleus	694	977	543	801	763	393	418	374	531	500	590 \pm 138	599 \pm 251
M gastrocnemius	616	478	939	314	609	503	-	1 118	41	-	-	-

All fibres per biopsy were counted (usually more than 1000).

^aOne hundred fibres of each type were measured according to Schmitt (1976).

(Fibre diameter²)^a \times relative occurrence \times percent of the total physiological cross-section according to Fick (1911).

Spearman rank correlation calculations (r) were performed on the series of ten legs (soleus) and on the eight legs (gastrocnemius) to elucidate whether the structural findings of either the soleus or the gastrocnemius or the combination of these muscles were correlated to maximum torques in static and dynamic manoeuvres. However, no significant strength-structure correlation ($P < 0.05$) was obtained.

DISCUSSION

Strength

Normative data on static and dynamic strengths for left and right plantar flexion in healthy sedentary younger Swedish males between 20-39 years are presented. To our knowledge there are no previous descriptions of dynamic plantar flexion strengths presented elsewhere. A relationship between plantar flexion strength and calf circumference is demonstrated here. Furthermore, because of the design of the experimental procedures, measurements

were monitored (see Methods) and left and right plantar flexion strengths were tested alternately. First, we feel that the intraindividual right/left strength differences were real.

The significant co-variance between static and dynamic strength in both legs or normals corroborates the findings of Asmussen et al. (1965) in the upper extremity. However, in the triceps brachii Osternig et al. (1977) could find only randomized correlations between isokinetic and isometric exercises. The maximum dynamic strength of the human plantar flexor muscles in the untrained males was characterized by a decline at higher angular motion velocities. This finding is in good agreement with that of Thorstensson (1976) in the quadriceps muscle. An interesting deduction is that "non-functional" measurements of static strength are also representative of dynamic manoeuvres, at least in untrained adult males. When measuring maximum plantar flexion torques it seems most appropriate to perform measurements with knee extended as in this position length-tension relationships of all parts of the triceps surae are optimal for development of

plantar force (Herman & Braglin 1967). In the present series of experiments, hip position did not seem to influence plantar flexion strength.

We can offer no obvious explanation for the significant dominance of the left leg plantar flexion strength over the right leg. Coincidence can, however, be excluded as in a greater series of male and female subjects between 20 and 65 ($n=134$) we found a significant dominance of left plantar flexion at identical levels (Fugl-Meyer et al. to be published). The relationship between calf circumference and strength is in agreement with the findings of Lamphear & Montoye (1976) and O'Donovan & Watson (1977) who propose that the maximum strength of muscles in the upper extremities is correlated to different anthropometrical variables.

It is reasonable to assume that of the two chosen positions strength is greater in the 0° than in the 90° knee position. In the former of these positions length-tension relationships are optimal for both the one-joint *m. soleus* and the two-joint *m. gastrocnemius*. In another study of 5 young men (Fugl-Meyer, Burnstedt & Långström in manuscript) we additionally registered the rectified low-pass filtered electromyogram from all three parts of the triceps surae using surface electrodes. The peak tension of the *m. soleus* was identical for manoeuvres performed in the 0° and in the 90° knee position. In contrast for both heads of the *gastrocnemius* the peak tension at the 90° position was significantly lower ($P<0.001$) for the static and for each dynamic manoeuvre. The decrease averaged about 45%. Furthermore in the straight knee position for all the different manoeuvres the peak activation of the three parts of the triceps surae did not differ significantly. In the 90° knee position the *m. soleus* behaved in the same manner. In this position both heads of the *gastrocnemius* had higher peak tensions at the isometric than at the static manoeuvres. This phenomenon may explain the smaller peak torque differences between the 0° and 90° knee position at higher angular velocities.

In younger males the triceps surae constitutes about 70% of the total plantar flexor weight and volume (A. Eriksson et al. unpublished observations). The physiologic cross-section is, according to Fick (1911) of an identical magnitude. As the lever arm of the triceps surae is about double the length of that of the remaining plantar flexors (Jørgensen quoted in Murray et al. (1976)) the triceps surae is by far the dominating plantar flexor. Thus Fick (1911) and

Murray et al. (1976) calculated that in the straight leg position the *m. gastrocnemius* would contribute about 45% and the *m. soleus* about 35–40% to the maximum plantar flexion torque.

The lower peak torques in the 90° as compared to the 0° knee position averaging about 80–90% can thus be explained by the smaller peak activity of the *m. gastrocnemius* in the 90° position. In the straight knee position the *m. soleus* is therefore the dominant plantar flexor contributing at least 50% to the maximum plantar flexion torque.

Structure

The morphometric results from the human triceps surae described here are fairly similar to findings previously presented elsewhere (Table 4). This conclusion is obviously made on the assumption that the fibres by different authors termed as "red", "slow-twitch" and "Type 1" fibres all correspond to the fibres termed here as ATPase low at pH 9.4. We have chosen this terminology simply due to the fact that our only criterium (which is also used by all the other authors listed in Table 4) for classifying the fibres is the degree of stainability in thawed thin cryosections for myofibrillar ATPase at pH 9.4. This classification of muscle fibres is also frequently used in clinical diagnostic work (Dubowitz & Brooke 1973; Engel 1974). It has been pointed out elsewhere (e.g. Edgerton et al. 1975) that myofibrillar ATPase reflects at least one very useful functional parameter, namely the speed of contraction. Direct proofs for this correlation in the *soleus* muscle of the rat have been presented by Kugelberg & Edström (1968) and Kugelberg (1973). However, no such evidence exists concerning the human triceps surae. Furthermore there are morphological differences between the rat and the human *soleus* muscle both at light microscopical level, i.e. the degree of stainability for SDH and distribution of SDH stain precipitate (Edgerton & Simpson 1969) and at electron microscopical level e.g. concerning the myofibrillar M-band (Sjöström & Squires 1977 (rat); Sjöström, unpublished observations (human *soleus*)). Comparisons between different species, even when concerning the same muscle should therefore be made with great caution.

Johnson et al. (1973) found only minor differences between the deep and superficial portions of the human *soleus* muscle regarding the occurrence of Types 1 and 2 fibres. This seems to be analogous with the statements by Collinck et al. (1972) and

Table 4 *Fibre composition of the human triceps surae in different studies*

Source	Age		Biopsy technique	Nomenclature	M. soleus	
	Mean	Range			%	Range \pm SD
Edström-Nyström (1969)*	-	-	Needle	Red	71	65-78
Johnson et al (1973)	-	17-30	Autopsy	Type I	86 deep 89 superficial	70-100 77-100
Costill et al (1974, 1976)	25	13-28	Needle	Slow twitch	81	
Gollnick et al (1974)	-	1-41	Needle or surgical	Slow twitch	80	64-100
Taylor et al (1974)	Adult	-	Needle	Slow twitch	77	
Edgerton et al (1975)	59	1-83	Autopsy	Slow twitch	70	18
Present material	31	4-36	Needle	ATPase low	79	69-94

Bilateral study

Edgerton et al (1975) which were based on findings from the vastus lateralis muscle that the proportion of slow and fast twitch fibres are similar in the superficial and deep regions of human muscles. On the other hand Johnson et al (1973) found that the fibre composition of deep and superficial parts of the lateral m. gastrocnemius could differ considerably. Determinations of fibre population in needle-biopsy specimens from approximately identical sites in the human triceps surae might seem valid. However we found intraindividual differences in fibre composition (low and high ATPase activity respectively see Table 3) with right-left side differences in the soleus of up to eleven and in the lateral gastrocnemius head up to 40%. Therefore we hold the view that for the triceps surae these intraindividual side differences which are eliminated in statistics are based on a heterogeneous fibre distribution even though great care is taken to secure specimens from identical sites. Consequently we dispute the validity of generalizations on compositional muscular homogeneity based on blindly obtained specimens. However qualitatively for diagnoses of muscle pathology this technique has its given place.

The wide variations in fibre population between these five healthy men of which none was actively engaged in competitive sports are in close agreement with the findings of other authors (Table 4). A general feature of both the soleus and the gastrocnemius muscles was the greater diameter of high- in relation to low-ATPase activity fibres. Might this phenomenon in healthy males without special

training reflect relatively high functional demands on this small population of fibres?

Structure and strength

Relationships between structure and strength in leg muscles have previously been demonstrated for knee-extensors in seated man where the one-joint m. vastus lateralis has been subject to morphological analysis and the findings have been generalized as representative for the total knee extension force (cf Thorstensson et al 1976, 1977). In analogy it might be expected that for the triceps surae and especially for the one joint m. soleus which acts as a quadriceps surae (Campbell et al 1973) structure-strength relationships at least for static and slow-dynamic manoeuvres and specifically if the knee is fully extended could be demonstrated. Such was however not the case and several factors must be discussed.

Firstly none of our subjects were actively engaged in regular physical training and only in such individuals have relationships between functional capacity and structure been demonstrated (Sahlin et al 1976, Thorstensson et al 1976, Bylund et al 1977, Thorstensson et al 1977). Secondly the traditional classification of muscle fibres based on stainability for ATPase is more an operational abstract than a real measure of fibre difference and not as such a reliable measure of the structural bases for the functional capacity (cf e.g. Edgerton et al 1975). Thirdly we do not with any degree of certainty know the relationship between fibre properties and the maximum angular force velocity. Fr

stereocenters

	lateral head	
Range/ S.D.	%	Range/ ± S.D.
	63	36-69
45-57	30 deep	43-60
	44 superficial	35-51
	53	38-73
	60	45-82
	57	
20	57	9
	68	14

ally we may in fact, never have reached sufficiently high speeds of angular motion that the possible specific properties of the high glycolytic fibres the triceps surae have dominated. In analogy with other human organs such as liver, kidneys, lungs, the triceps surae may also have a great reserve capacity and we may especially if untrained use only part of it.

This study was supported by grants from the Research Council of the Swedish Sports Federation, The Swedish Medical Research Council and the County of Västernorrland.

REFERENCES

- ASMUSSEN E. & HJEBBØLL-NIELSEN K. 1961 Isometric muscle strength of adult men and women. *Compos Data Natl Ass Indent Par* 11.
- ASMUSSEN E., HANSEN O. & LAMBERT O. 1965 The relation between isometric and dynamic muscle strength in man. *Compos Data Natl Ass Indent Par* 20 211.
- BERGSTRÖM J. 1973 Percutaneous needle biopsy of skeletal muscle in physiological and clinical research. *Scand J Clin Lab Invest* 33 609-616.
- BYLUND A. C., BJURÖ T., CEDERBLAD, G., HOLM, J., LUNDHOLM, K., SÖSTRÖM M., ANOQUIST K. A. & SCHERSTÉN T. 1977 Physical training in men. Skeletal muscle metabolism in relation to muscle morphology and running ability. *Europ J Appl Physiol* 36: 151-169.
- CAMPBELL, K. M., BLOOS, N. L., BLANTON P. L. & LEHR, R. P. 1973 Electromyographic investigation of the relative activity among four components of the triceps surae. *Amer J Phys Med* 52 36-41.
- COSTILL, D. L., JANSSEN E., GOLLNICK, P. D. & SALTIN B. 1974. Glycogen utilization in leg muscles of men during level and uphill running. *Acta Physiol Scand* 91 475-481.
- COSTILL, D. L., DANIELS, L. EVANS, W. FRANK, W. KRAHENBUHL, O. & SALTIN B. 1976. Skeletal muscle enzymes and fiber composition in male and female track athletes. *J Appl Physiol* 40: 149-154.
- DANIELS L. & WORTINGHAM, C. 1972. Muscle testing, techniques of manual examination. Saunders, Philadelphia.
- DARCUS, H. D. 1953. A strain gauge dynamometer for measuring the strength of muscle contraction and for reeducating muscles. *Ann Phys Med* 1 163-176.
- DAUBOWITZ, V. & BROOKE, H. 1973. Muscle biopsy: a modern approach. W. B. Saunders Company, London.
- EDGERTON V. R. & SIMPSON D. R. 1969. The intermediate fibres of rats and guinea pigs. *J Histochem Cytochem* 17: 828-838.
- EDGERTON V. R., SMITH J. L. & SIMPSON D. R. 1975. Muscle fibre type populations of human leg muscles. *Histochem J* 7: 299-306.
- EDSTRÖM L. & NYSTRÖM B. 1969. Histochemical types and sizes of fibres in normal human muscles. *Acta Neurol Scand* 45 257-269.
- ENGEL, W. K. 1974. Fiber types nomenclature of human skeletal muscle for histochemical purposes. *Neurology* 24 344-348.
- FICK, R. 1911. *Anatomie und Mechanik der Gelenke*. Teil III: Spezielle Gelenk- und Muskelmechanik. Fischer, Jena.
- GOLLNICK, P. D., ARMSTRONG R. B., SAUBERT C. W., PFEIL, K. & SALTIN B. 1972. Enzyme activity and fiber composition in skeletal muscle of untrained and trained men. *J Appl Physiol* 33 31-319.
- GOLLNICK, P. D., SJÖDIN B., KARLSSON J., JANSSON E. & SALTIN B. 1974. Human soleus muscle: a comparison of fibre composition and enzyme activities with other leg muscle. *Pflügers Arch* 348: 47-55.
- GRANT R. 1970. The basis of motor control. Academic Press, London-New York.
- HERMAN B. R. & BRAGIN S. J. 1967. Function of the gastrocnemius and soleus muscles. *Phys Ther* 47: 105-113.
- HISLOP H. J. & PERRINE, J. J. 1967. The isokinetic concept of exercise. *Phys Ther* 47 114-117.
- JOHNSON M. A., POLGAR, J., WRIGHTMAN D. & APPLETON D. 1973. Data on the distribution of fibre types in thirty-six human muscles. An autopsy study. *J Neurol Sci* 18: 111-129.
- KENDALL, H. O. & KENDALL, F. P. 1969. *Muscles testing and function*. Williams and Wilkins, Baltimore.
- KUGELBERG, E. 1973. Histochemical composition, contraction speed and fatigability of rat soleus muscle. *J Neurol Sci* 20: 177-198.
- KUGELBERG E. & EDSTRÖM L. 1968. Differential histochemical effects of muscle contractions on phosphorylase and glycogen in various types of fibres: relation to fatigue. *J Neurol Neurosurg Psychiatr* 31 415-423.
- LAMPHEAR, D. E. & MONTGOMERY, H. J. 1976. Muscle

- lar strength and body size. *Human Biology* 48: 147-160.
- MOFFROID M, WHIPPLE R, HOIKOSH J, LOWMAN E. & THISTLE H 1969 A study of isokinetic exercise. *Phys Ther* 49: 735-746.
- MURRAY M P, GUTEN G N, BALDWIN J M & GARDNER G M 1976. A comparison of plantar flexion torque with and without the triceps surae. *Acta Orthop Scand* 47: 122-124.
- O'DONOVAN D J & WATSON A W S 1977 Relationship between muscular strength and body size of postpubertal male adolescents. *J Physiol* 271: 61-62 P.
- OSTERNIG L R, BATES B T & JAMES S L 1977 Isokinetic and isometric torque force relationship. *Arch Phys Med* 58: 254-257.
- SALTIN B, NAZAR K, COSTILL D L, STEIN E, JANSSON E, ESSÉN B & GOLLNICK P D 1976 The nature of the training response. Peripheral and central adaptations to one-legged exercise. *Acta Physiol Scand* 96: 289-305.
- SCHMITT H P 1976 Measurements of voluntary muscle fiber cross sections. A comparative study of different possible methods. *Microscopia Acta* 77: 427-440.
- SJÖSTRÖM M & SQUIRE J M 1977 Cryo-ultrastructure and myofibrillar fine structure: a review. *J Microsc* 111: 239-278.
- TAYLOR A W, ESSÉN B & SALTIN B 1974 Myosin ATPase in skeletal muscle of healthy men. *Acta Physiol Scand* 91: 368-370.
- THISTLE H G, HISLOP H J, MOFFROID M & LOWMAN E W 1967 Isokinetic contraction: a new concept of resistive exercise. *Arch Phys Med* 48: 279-282.
- THORSTENSSON A 1976. Muscle strength, fiber type and enzyme activities in man. *Acta Physiol Scand* Suppl 443.
- THORSTENSSON A, HULTÉN B, VON DÖBEL W & KARLSSON J 1976 Effect of strength training on enzyme activities and fibre characteristics in human skeletal muscle. *Acta Physiol Scand* 96: 397-398.
- THORSTENSSON A, LARSSON L, TESCH P & KARLSSON J 1977 Muscle strength and fibre composition in athletes and sedentary men. *Med Sci Sports* 9: 26-30.
- TORNVALL G 1963 Assessment of physical capabilities. *Acta Physiol Scand* 48: Suppl 701.

The effect of α -aminoisobutyric acid and 2,4-diaminobutyric acid on mouse blastocyst outgrowth in vitro

RELS NÆSLUND, INGER LINDQVIST, GUNNAR RONQUIST[†] and B. OVE NILSSON

[†]Reproduction Research Unit and

Department of Medical and Physiological Chemistry, Biomedical Centre, Uppsala, Sweden

NÆSLUND, G. LINDQVIST, I. RONQUIST, G. & NILSSON, B. O. The effect of α -aminoisobutyric acid and 2,4-diaminobutyric acid on mouse blastocyst outgrowth in vitro. *Acta Physiol Scand* 1979 107 57-61. Received 15 March 1979. ISSN 0001-6772. Reproduction Research Unit and Department of Medical and Physiological Chemistry, Biomedical Centre, Uppsala, Sweden.

Blastocysts recovered from mice in a state of delay of implantation were incubated for 10 h with either α -aminoisobutyric acid (AIB) or 2,4-diaminobutyric acid (DAB), two non-metabolizable amino acids. The incubation medium was composed so as to maintain growth arrest of the inactive, delayed blastocysts in vitro. The blastocysts were then transferred to complete outgrowth medium without the two non-metabolizable amino acids to test the capacity for trophoblast outgrowth. AIB which displays saturation kinetics, was harmless to the blastocysts even at high concentration, while DAB at low concentration irreversibly damaged the trophoblast cell and prevented outgrowth, probably due to non-saturation kinetics resulting in high intracellular accumulation. The harmful effect of DAB could be abolished by concomitant incubation with L-alanine and L-methionine which compete with DAB for the same transport system, while the D-forms of the same amino acids had little or no effect. The results suggest the presence of transport System A in mouse blastocysts; growth arrested in vitro indicating an operative carrier mechanism already during delay of implantation.

Key words: Mouse blastocysts in vitro, α -aminoisobutyric acid, 2,4-diaminobutyric acid

In mice in a state of experimentally delayed implantation it has been found that after induction of implantation by an injection of oestrogen the *in vivo* uptake of the non-metabolizable ^{14}C - α -aminoisobutyric acid (^{14}C -AIB) shows preference for the uterus (Lindqvist et al. 1977). Further, an *in vivo* uptake of ^{14}C -AIB into the blastocysts themselves occurred 8-12 h after the induction of implantation, provided that the blastocysts had been flushed out of the uterine cavity not earlier than 4 h after the ^{14}C -AIB-injection (Lindqvist et al. 1978). Hence, there was a preferential uptake of ^{14}C -AIB into uterine tissue during activation for implantation, and a transport system for this non-metabolizable amino acid was apparently operating to transfer ^{14}C -AIB from the uterine epithelium into the blastocysts via the uterine secretion.

A similar transport system, the System A, is present in Ehrlich ascites tumour cells (Oxender &

Christensen 1963) and also in cultured human glioma cells (Ronquist et al. 1976). This system is Na⁺-dependent and energy-requiring. Short-chain neutral monoamino acids are the physiological substrates, but also diamino acids, such as the non-metabolizable 2,4-diaminobutyric acid (DAB), can share this transport system. However, the diamino acids can usually be transported against a much steeper concentration gradient into the Ehrlich cells than the monoamino acids (Christensen et al. 1973). Therefore DAB, contrary to AIB, showed apparent non-saturation kinetics, resulting in damage to the Ehrlich cells (Christensen et al. 1952).

Delayed mouse blastocysts when flushed out of the uterine cavity and transferred to a serum-containing culture medium start to grow out, a process that has been considered to be analogous to implantation in utero (Gwatkin 1966a) whereas in a medium deprived of glucose, arginine and leucine

- lar strength and body size. *Human Biology* 48: 147-160.
- MOFFROID M, WHIPPLE R, HOFKOSH J, LOWMAN E & THISTLE H 1969. A study of isokinetic exercise. *Phys Ther* 49: 735-746.
- MURRAY M P, GUTEN G N, BALDWIN J M & GARDNER, G M 1976. A comparison of plantar flexion torque with and without the triceps surae. *Acta Orthop Scand* 47: 122-124.
- ODONOVAN D J & WATSON A W S 1977. Relationship between muscular strength and body size of postpubertal male adolescents. *J Physiol* 271: 61-62 P.
- OSTERNIG L R, BATES B T & JAMES S L 1977. Isokinetic and isometric torque force relationship. *Arch Phys Med* 58: 254-257.
- SALTIN B, NAZAR K, COSTILL, D L, STEIN E, JANSSON E, ESSÉN B & GOLLNICK P D 1976. The nature of the training response. Peripheral and central adaptations to one-legged exercise. *Acta Physiol Scand* 96: 289-305.
- SCHMITT H P 1976. Measurements of voluntary muscle fiber cross sections. A comparative study of different possible methods. *Mikroscopia Acta* 77: 427-440.
- SJÖSTRÖM M & SQUIRE J M 1977. Cryo-ultrastructure and myofibrillar fine structure: a review. *J Microsc* 111: 239-278.
- TAYLOR, A W, ESSÉN B & SALTIN B 1973. Myosin ATPase in skeletal muscle of healthy men. *Acta Physiol Scand* 91: 568-570.
- THISTLE H G, HISLOP H J, MOFFROID M & LOWMANN E W 1967. Isokinetic contraction: a new concept of resistive exercise. *Arch Phys Med* 48: 279-282.
- THORSTENSSON A 1976. Muscle strength, fiber type and enzyme activities in man. *Acta Physiol Scand* Suppl 443.
- THORSTENSSON A, HULTÉN B, VON DÖBEL W & KARLSSON J 1976. Effect of strength training on enzyme activities and fibre characteristics in human skeletal muscle. *Acta Physiol Scand* 96: 392-398.
- THORSTENSSON A, LARSSON L, TESCH, P & KARLSSON J 1977. Muscle strength and fibre composition in athletes and sedentary men. *Med Sci Sports* 9: 26-30.
- TORNVALL, G 1963. Assessment of physical capabilities. *Acta Physiol Scand* 58, Suppl 701.

The effect of α -aminoisobutyric acid and 2,4-diaminobutyric acid on mouse blastocyst outgrowth *in vitro*

RELS NÆSLUND, INGER LINDQVIST, GUNNAR RÖNQVIST* and B. OVE NILSSON

*Reproduction Research Unit and

Department of Medical and Physiological Chemistry, Biomedical Centre, Uppsala, Sweden

NÆSLUND G., LINDQVIST I., RÖNQVIST G. & NILSSON B. O. The effect of α -aminoisobutyric acid and 2,4-diaminobutyric acid on mouse blastocyst outgrowth *in vitro*. *Acta Physiol Scand* 1979, 107, 57-61. Received 15 March 1979. ISSN 0001-6772. Reproduction Research Unit and Department of Medical and Physiological Chemistry, Biomedical Centre, Uppsala, Sweden.

Blastocysts recovered from mice in a state of delay of implantation were incubated for 10 h with either α -aminoisobutyric acid (AIB) or 2,4-diaminobutyric acid (DAB), two non-metabolizable amino acids. The incubation medium was composed so as to maintain growth arrest of the inactive delayed blastocysts *in vitro*. The blastocysts were then transferred to complete outgrowth medium without the two non-metabolizable amino acids to test the capacity for trophoblast outgrowth. AIB, which displays saturation kinetics, was harmless to the blastocysts even at high concentration while DAB at low concentration irreversibly damaged the trophoblast cells and prevented outgrowth, probably due to non-saturation kinetics resulting in high intracellular accumulation. The harmful effect of DAB could be abolished by concomitant incubation with L-alanine and L-methionine, which compete with DAB for the same transport system, while the D-forms of the same amino acids had little or no effect. The results suggest the presence of transport System A in mouse blastocysts, growth arrested *in vitro*, indicating an operative carrier mechanism already during delay of implantation.

Key words: Mouse blastocysts *in vitro*, α -aminoisobutyric acid, 2,4-diaminobutyric acid

In mice in a state of experimentally delayed implantation it has been found that after induction of implantation by an injection of oestrogen the *in vivo* uptake of the non-metabolizable ^{14}C - α -aminoisobutyric acid (^{14}C -AIB) shows preference for the uterus (Lindqvist et al 1977). Further, an *in vivo* uptake of ^{14}C -AIB into the blastocysts themselves occurred 8-12 h after the induction of implantation, provided that the blastocysts had been flushed out of the uterine cavity not earlier than 4 h after the ^{14}C -AIB-injection (Lindqvist et al 1978). Hence, there was a preferential uptake of ^{14}C -AIB into uterine tissue during activation for implantation and a transport system for this non-metabolizable amino acid was apparently operating to transfer ^{14}C -AIB from the uterine epithelium into the blastocysts via the uterine secretion.

A similar transport system, the System A, is present in Ehrlich ascites tumour cells (Oxender &

Christensen 1963) and also in cultured human glioma cells (Rönquist et al 1976). This system is Na⁺-dependent and energy-requiring. Short-chain neutral monoamino acids are the physiological substrates, but also diamino acids such as the non-metabolizable 2,4-diaminobutyric acid (DAB) can share this transport system. However, the diamino acids can usually be transported against a much steeper concentration gradient into the Ehrlich cells than the monoamino acids (Christensen et al 1973). Therefore DAB, contrary to AIB, showed apparent non-saturation kinetics, resulting in damage to the Ehrlich cells (Christensen et al 1952).

Delayed mouse blastocysts when flushed out of the uterine cavity and transferred to a serum-containing culture medium start to grow out, a process that has been considered to be analogous to implantation *in utero* (Gwarkin 1966a) whereas in a medium deprived of glucose, arginine and leucine

the inactive delayed blastocysts are kept in a state of growth arrest and therefore remain expanded without signs of trophoblast outgrowth (Naeslund 1979)

The question arose whether delayed blastocysts when incubated in a medium that keeps them in a state of growth arrest would be damaged by the presence of AIB or DAB in the incubation medium indicating an operative carrier already before induction of implantation. To test this mouse blastocysts from animals in delay of implantation were incubated with either AIB, DAB or DAB together with two L amino acids that compete for the same transport system. The blastocysts were then transferred to a serum containing outgrowth medium after 10 h and were observed by light microscopy to judge their viability and capacity for trophoblast outgrowth.

MATERIAL AND METHODS

Pregnant mice of the NMRI strain (Anticimex, Stockholm, Sweden) were ovariectomized on day 3 (day 1 was the day a vaginal plug was found) and given 1 mg of the depot preparation medroxyprogesterone (Depo-Provera, Upjohn Co., USA) subcutaneously to delay implantation (Yoshinaga & Adams 1966). Blastocysts were recovered not earlier than on day 7 when a steady state of blastocyst outgrowth activity is attained (Naeslund & Lundkvist 1978). The uterine horns were dissected free and the blastocysts were flushed into watch glasses with a syringe containing phosphate buffered saline with Mg^{2+} and Ca according to Dulbecco (SBL, Stockholm, Sweden). Dialysed foetal calf serum (Flow Laboratories, Irvine, Scotland) was added in a concentration of 1% to prevent the blastocysts from becoming adhesive. The serum was dialysed in a 100 times excess of a 0.15 M NaCl solution for 3 days with changes twice daily to remove the amino acids and glucose among other things, and was then filter sterilized.

Brinster's medium for ovum culture (Brinster 1963) was used, but with 1.0 mg/ml of glucose instead of sodium lactate (Brinster & Thomson 1966). Reagent grade water from a Milli-Q System (Millipore Corp., Bedford, Mass., USA) was used. This water had a specific resistance of about 18 MΩ/cm. The medium contained 1 mg/ml of bovine albumin, AIB, DAB, L-alanine, L-methionine, D-alanine and D-methionine were added in the combinations given in Table 1. Filter sterilized stock solutions containing 0.1 M of the amino acid were used with addition of 9 mg/ml of NaCl to render them isotonic. To ascertain that the lack of essential amino acids did not damage the blastocysts, a group of blastocysts was maintained in Brinster's medium with glucose but without all amino acids before being transferred to the outgrowth medium. During incubation in droplets under liquid paraffin in an atmosphere of 5% CO_2 in air at 37°C (Brinster 1963) the blastocysts were examined in an inverted micro-

Table 1 Effect of two non-metabolizable amino acids on blastocyst appearance and outgrowth

The blastocysts were first maintained for 10 h in Brinster's medium for ovum culture containing the amino acids and were then transferred to an outgrowth medium. Nine of the blastocysts had a normal appearance and started to grow when transferred into the outgrowth medium. DAB blastocysts damaged: no ability for normal growth in the outgrowth medium.

Amino acid concentration in the incubation medium	Number of blastocysts	Outcome at 10 h
10 mM AIB	18	N
25 mM AIB	20	N
1 mM DAB	17	D
10 mM DAB	78	D
10 mM DAB 5 mM L-alanine 5 mM L-methionine	20	N
10 mM DAB 5 mM D-alanine 5 mM D-methionine	16	D
Brinster's medium with glucose (lacking all amino acids)	6	N

scope to find out whether they were expanded to a normal extent or showed signs of damage. After 10 h they were transferred to an outgrowth medium, namely Brinster's medium with glucose and with addition of the amino acids of Eagle's BME (Eagle 1955) and 1% dialysed foetal calf serum to ascertain the capacity for outgrowth of the trophoblast (Gwatkin 1966b). The blastocyst cultures were observed for 5 days by light microscopy. Each series of experiments was repeated 2–6 times and comprised usually 16–28 blastocysts totally. As a control blastocysts incubated with 10 mM DAB were always matched with blastocysts in other experimental groups.

RESULTS

The results are summarized in Table 1. AIB was harmless to the blastocysts regardless of its concentration within the range 10–25 mM while DAB at a concentration of 10 mM induced a gradual collapse of the blastocysts starting after 3–4 h followed by lysis of the trophoblast cells (Fig. 1a). These cells therefore displayed no ability to grow out after being transferred to the outgrowth medium when examined daily for 5 days. The blastocysts were damaged in a similar way in 1 mM DAB but not so severely as a few trophoblast cells grew out after transfer to the outgrowth medium. The outgrowths were however quite small and abnormal.

Concomitant incubation with 5 mM L-alanine and



Fig. 1 () A blastocyst incubated in 10 mM DAB. The blastocyst is disintegrated. (b) A blastocyst incubated in 10 mM DAB in the presence of L-alanine and L-methionine. The blastocyst is expanded. () Two blastocysts incubated as the blastocyst in Fig. 1b 2 days after transfer to the outgrowth medium. Trophoblast cells are growing. The bars indicate 30 μ m. Bright field () and phase contrast () microscopy.

1 mM L-methionine prevented the effect of 10 mM DAB. Hence, the normal-looking expanded blastocysts showed normal outgrowths in the outgrowth medium after 2 to 3 days (Figs. 1b and). The D-analogues of methionine and alanine also prevented the DAB effect but to a much lower degree. Four out of 16 blastocysts were expanded and the expanded blastocysts only displayed small outgrowths.

Blastocysts that were maintained in Brinster's medium with glucose and albumin but lacking all amino acids were expanded and had a normal appearance after 10 h and showed normal outgrowth after transfer to the outgrowth medium.

DISCUSSION

The effect of AIB and DAB on the blastocysts was evaluated in the present experiments from the capacity of the trophoblast cells of delayed blastocysts to grow out in a serum-containing complete medium after incubation with the respective amino acids. Since the response by the trophoblast cells under the prevailing conditions was unequivocal no graded scaling was decided necessary.

In attempts to achieve as standardized conditions for outgrowth as possible blastocysts flushed out of the uteri from mice in an experimental state of delayed implantation were used. The use of delayed mouse blastocysts in tests of trophoblast outgrowth

offers methodological advantages. These blastocysts no longer possess a zona pellucida (McLaren 1970) which excludes interference of hatching with the outgrowth. Further these blastocysts have a defined capacity for outgrowth (Naeslund & Lundkvist 1978).

The observed blastocyst destruction is most probably due to an extensive accumulation of DAB. This accumulation will lead to exertion of increased osmotic pressure inside the cell by the non-metabolizable amino acid. This high osmotic pressure and perhaps the lowered adenylate charge potential (Atkinson 1977) both caused by the energy-dependent accumulation of DAB will eventually result in lysis of the blastocysts. An accumulation of an artificial amino acid inside the blastocysts does not necessarily per se lead to destruction or inhibited outgrowth of the blastocyst. As observed AIB in the medium did not impede subsequent growth after transfer of the blastocysts into the outgrowth medium. This is explained by the saturation kinetics displayed by AIB which result in a lower intracellular accumulation of this amino acid as compared with DAB.

The transport system involved is most probably the Na-dependent energy-requiring System A since the DAB effect can be abolished by L-alanine and L-methionine which are both to a large extent transported by this system (Oxender & Christensen 1963). The present effect is most probably explained by competitive inhibition between the model amino acid and the two physiological amino acids for the same site at the receptor-carrier complex. Accordingly the D-analogues of alanine and methionine which have a lower affinity for the carrier (Oxender & Christensen 1963) interfered with the DAB transport to a much lower extent.

To prevent activation in vitro of the inactive delayed blastocysts it would seem suitable to use a medium containing no glucose, arginine or leucine since such a medium keeps the delayed blastocysts in a state of growth arrest (Naeslund 1979). In the present experiments the medium had to contain glucose since an energy requiring transport mechanism was being studied during a relatively long observation period but the absence of all essential amino acids however probably prevented the glucose from causing activation of the blastocysts. Further the effect of DAB was observed after only a few hours in culture indicating that the carrier mechanism is already operative in the delayed

blastocysts. This is reasonable since decidual uterine blastocysts are known both to increase in weight (Hensleigh & Weitlauf 1974) and to possess many endocytotic vesicles (Schlafke & Exler 1973) both features indicating metabolic activity.

Further in vitro studies of the transport characteristics for ^{14}C AIB on blastocysts recovered during delay and activation for implantation would reveal whether the increased uptake after induction of implantation (Lindqvist et al. 1978) is caused by a new synthesis of carriers in the plasma membrane or by a changed affinity of the receptor-carrier complex for the amino acids. Such studies are under way.

This study was supported by grants from the Swedish Medical Research Council project No. 1, A 70 and 4 B76-13X 228-1 A. We thank Mrs Barbro Enarsson for skilful technical assistance. Depo-Provera was kindly supplied by Upjohn AB, Sweden.

REFERENCES

- ATKINSON D. 1977. Cellular energy control. Adenylate energy charge is a key factor. *Trends in Biochemical Sciences* 2: N196-N200.
- BRINSTER, R. L. 1963. A method for in vitro culture of mouse ova from two-cell to blastocyst. *Exp Cell Res* 32: 205-208.
- BRINSTER, R. L. & THOMSON, J. L. 1966. Development of eight-cell mouse embryos in vitro. *Exp Cell Res* 4: 308-315.
- CHRISTENSEN, H. N., DE CESPEDES, C. & LOGTEN, M. E. & RONQUIST, O. 1973. Exportation of amino acid transport studied for the Ehrlich ascites tumor cell. *Biochim Biophys Acta* 305: 45-52.
- CHRISTENSEN, H. N., RIGGS, T. R., FISCHER, H. & PALATINE, I. M. 1952. Intense concentration of α - γ -diaminobutyric acid by cells. *J Biol Chem* 198: 17-22.
- EAGLE, H. 1955. Nutrition needs of mammalian cells in tissue culture. *Science* 122: 901-904.
- GWATKIN, R. B. L. 1966a. Amino acid requirements for attachment and outgrowth of the mouse blastocyst in vitro. *J Cell Physiol* 68: 335-344.
- GWATKIN, R. B. L. 1966b. Defined media and development of mammalian eggs in vitro. *Ann NY Acad Sci* 139: 79-90.
- HENSLEIGH, H. C. & WEITLAUF, H. M. 1974. Effect of delayed implantation on dry weight and lipid content of mouse blastocysts. *Biol Reprod* 10: 315-320.
- LINDQVIST, I., NILSSON, O. & RONQUIST, O. 1977. Preferential uptake of ^{14}C - α -aminoisobutyric acid into mouse uterine tissue during early pregnancy. *Acta Physiol Scand* 99: 37-41.
- LINDQVIST, I., EINARSSON, B., NILSSON, O. & RONQUIST, O. 1978. The in vitro transport of ^{14}C - α -aminoisobutyric acid into mouse blastocyst during

- activation for implantation. *Acta Physiol Scand* 102: 477-483.
- KLAREN, A. 1970. The fate of the zona pellucida in mice. *J Embryol Exp Morphol* 23: 1-19.
- LAESLUND, G. 1979. The effect of glucose, arginine and leucine-deprivation on mouse blastocyst outgrowth in vitro. *Upsala J Med Sci* 84: 9-20.
- LAESLUND, G. & LUNDKVIST, Ö. 1978. Effect of the endocrine state of blastocyst donors on the time required for initiation of trophoblast outgrowth. *Upsala J Med Sci* 83: 135-139.
- MENDER, D. L. & CHRISTENSEN, H. N. 1963. Distinct mediating systems for the transport of neutral amino acids by the Ehrlich cell. *J Biol Chem* 238: 3686-3699.
- RONQUIST, G., ÅGREN, G., PONTÉN, J. & WESTERMARK, B. 1976. α -Aminoisobutyric acid transport into human glia and glioma cells in culture. *J Cell Physiol* 89: 433-440.
- SCHLAFKE, S. & ENDERS, A. C. 1973. Protein uptake by rat preimplantation stages. *Anat Rec* 175: 539-560.
- YOSHINAGA, K. & ADAMS, C. E. 1966. Delayed implantation in the spayed, progesterone treated adult mouse. *J Reprod Fertil* 12: 593-595.

Partition of 125 I-iodoantipyrine among erythrocytes, plasma and renal cortex in the dog

J. CLAUSEN, A. HOPE and K. AUKLAND

Institute of Physiology, University of Bergen, Norway

CLAUSEN J., HOPE A. & AUKLAND K. Partition of 125 I-iodoantipyrine among erythrocytes, plasma, and renal cortex in the dog. *Acta Physiol Scand* 1979 107 63-68. Received 17 March 1979. ISSN 0001-6772. Institute of Physiology, University of Bergen, Norway.

The tissue/blood partition coefficient, λ_{wb} , defined as the amount of blood having the same tracer content as one unit of tissue at diffusion equilibrium, was determined for 125 I-iodoantipyrine (I-Ap) and tritiated water (THO) in the dog kidney cortex. Measurements were made after λ_{wb} equilibration for 75 to 300 s and with liver circulation excluded. In 18 kidneys, λ_{wb} for I-Ap averaged 1.38 (S.D. 0.17) w/w (weight/weight), without significant correlation to haematocrit (range 23-43) or to urine pH (range 5.5-8.6). The λ_{wb} for THO averaged 0.97 (S.D. 0.06) v/v (volume/weight), close to the relative water contents. Erythrocyte/plasma partition for I-Ap was 0.82 w/w compared to water partition of 0.71. Thus, at diffusion equilibrium the apparent I-Ap concentration in renal cortical and red cell water exceeds that of plasma water by 14 and 60% respectively. It follows that I-Ap cannot be used as a general indicator for total tissue water content. When used for measurement of local blood flow and modum Kety, λ_{wb} must be determined for each tissue and species.

Key words: Distribution volume, tissue water, renal blood flow, renal medulla, tritiated water.

Due to its lipid solubility and rapid distribution antipyrine has been used to estimate total water content of the whole organism or of individual organs based on the assumption that it distributes freely and exclusively in the whole intra- and extracellular water phase. A similar distribution has been reported for 125 I-iodoantipyrine (I-Ap) and both substances have been used for measurement of local blood flow with the so-called tissue sampling technique and modum Kety (1960). In accordance therewith, recent *in vivo* measurements of the tissue/blood partition coefficient (λ_{wb}) for the rat kidney gave a value close to 1.00 and plausible values for local renal blood flow (Hope & Clausen & Aukland 1976). However, preliminary flow measurements in the dog kidney using the same partition coefficient gave absurdly high cortical flow rates, prompting the present examination of the I-Ap distribution space in the dog kidney.

While I-Ap is readily available, nonvolatile and easily quantitated, it has other less desirable qualities which have to be taken into account. Several investigators have reported a rapid loss of the iodine tag *in vivo* as well as metabolic conversion of the antipyrine molecule itself (Soberman et al. 1949; Straub et al. 1964). The liver has been blamed for both processes. Furthermore, slowly saturating intracellular compartments for antipyrine have been suspected (Hilton & Delfam 1969; Effros & Chinard 1969).

For these reasons and in order to mimic the conditions during flow measurements (8 to 20 s infusion) we decided to measure the kidney tissue/blood partition coefficient (λ_{wb}) (1) *in vivo* (2) without circulation through the liver and (3) with the shortest saturation period compatible with complete diffusion equilibration between arterial blood and tissue.

For the purpose of methodological control λ_{th} for THO (initiated water) was determined by the same experimental procedure.

METHODS

Preparation and control of 125 I-iodoantipyrine

125 I-iodoantipyrine (I Ap) in 0.2% NaHCO₃ solution was obtained from New England Nuclear, Chicago. The amount of free 125 I was determined according to New England Nuclear specifications by silica gel thin layer chromatography (Polygram SIL N HR, Machery Nagel) with chloroform-ethyl ether (85:15) as eluent. Since free 125 I often exceeded the amount recorded by the manufacturer shortly before shipping (1–5%) the preparation was purified on a Sephadex G-10 column with diameter 0.9 cm and height 18 cm using distilled water for elution (Hope et al. 1976; Munck & Andersen 1967). At the time of use the free iodine content was usually 1–2% and never exceeded 5%. Final dilution in saline to about 5 μ Ci/ml was made shortly before infusion.

Experimental procedures

Experiments were performed on 13 mongrel dogs weighing from 15 to 23 kg. Anesthesia was induced by i.v. Nembutal 25 mg/kg b.wt. and supplemented with doses of 3–5 mg/kg when needed. An endotracheal tube was inserted but the ventilation was not assisted. After anesthesia the dogs were given a constant i.v. infusion of 0.9% NaCl and 3% mannitol at a rate of 4 ml/min. Para-aminohippurate (PAH) was added to provide an arterial concentration of 10–20 mg/l. In three experiments an additional infusion of 5% NaHCO₃ was given to obtain alkaline urine and in one experiment dilute HCl was infused for urine acidification. The abdomen was opened by a midline incision and polyvinyl catheters were inserted in both ureters. A nylon snare was placed loosely around each renal pedicle with as little dissection as possible. The spleen was removed, the portal vein dissected free and nylon snares were placed loosely around the origin of the celiac and superior mesenteric arteries. Under short-lasting occlusion of these arteries, a shunt was established from the portal vein to the left common iliac vein by means of polyvinyl tubing, diameter 8 mm. Pressure in the shunt was measured through a T-connection to ascertain free drainage of splanchnic blood. Arterial pressure was measured with a Hewlett Packard transducer through a catheter in a brachial artery. A PE 120 tube was inserted into the femoral artery for blood sampling. After establishing the porta-iliac shunt PAH clearance was determined on each kidney in two or three consecutive 10 min periods, arterial blood samples being drawn at the midpoint of each period. In order to stop also hepatic arterial blood flow the snare on the coeliac artery was tightened. A couple of minutes later an i.v. infusion of I Ap was started. The infusion rate was gradually reduced after a predetermined schedule such as to maintain arterial concentration at a constant level. Simultaneously arterial blood samples were collected continuously at 5 s intervals by free drainage from the femoral artery catheter. After 75 to 300 s infusion the renal pedicles were clamped.

The kidneys were rapidly removed and frozen in CO₂ ethanol and thereafter stored at -70°C.

The procedure described above was followed in 9 dogs with analyses on a total of 13 kidneys. In 4 experiments (kidneys analysed) the procedure was simplified by omitting the porta-iliac shunt. Instead, liver blood flow was stopped by clamping the superior mesenteric and the coeliac arteries as well as the portal vein a couple of mm before tracer infusion. Hemodynamic reactions to the procedure such as changes in arterial pressure and λ_{th} in renal blood flow (Nycotron electromagnetic flowmeter) were found to be small and transitory.

The λ_{th} for THO (initiated water) was determined in 4 of the experiments described above and in 3 additional experiments without interference with liver blood flow.

Treatment of tissue and blood samples

Tissue samples were obtained from the still frozen livers at 4°C as follows: 5–7 mm thick sagittal sections were cut by saw and thereafter 12 to 40 samples of 0.1 to 0.5 g were dissected out by scalpel from the middle two third of the renal cortex. Each sample was immediately transferred to a preweighed counting vial, weighed again and added 4 ml distilled water. Equilibration of I Ap and THO was found to be complete after 24 h. After determining I Ap activity on the whole sample 100 μ l of each sample was transferred to vials containing 6 ml scintillation fluid for measuring THO activity.

Blood samples of 0.1 to 0.3 ml for measurement of I Ap activity were pipetted into preweighed counting vials, weighed again and added 4 ml distilled water. To avoid cumbersome bleaching procedures plasma instead of whole blood was used for determination of THO activity. One glass capillary was filled from each blood sample spun in a hematocrit centrifuge. About 0.02 g plasma was transferred to preweighed counting vials which were weighed again and added 6 ml scintillation fluid. Calculation of whole blood activity was made on the assumption of uniform activity in plasma and red cell water. Plasma and whole blood water content determined in the experiment as described below.

Calculation of λ_{th}

Since it is not possible in every experiment to ensure complete equilibration between tissue and the last kidney sample λ_{th} was calculated by a method which takes into account the whole arterial concentration curve as well as the actual renal blood flow (Hope et al. 1976). Core blood flow was roughly estimated from the PAH clearance (C_{PAH}) under the assumption of 75% extraction, a core flow fraction of 0.90 and cortical volume = 0.7 \times kidney weight (KW).

$$F/W = \frac{C_{PAH} \cdot 0.9}{(1 - Hct) \cdot 0.75 \cdot KW \cdot 0.7} \quad (1)$$

PAH in plasma and urine was determined by the method of Smith et al. (1945).

Under the assumption of complete equilibration between tissue and venous blood the tissue concentration of an inert tracer (C_t) at time T is given by the following equation (Kety 1960):

$$v(T) = \lambda_{\text{tr}} C_{\text{tr}} \int_0^T C_{\text{tr}} e^{-\lambda_{\text{tr}}(T-t)} dt \quad (\text{eq. 2})$$

here C is tracer concentration in arterial blood, λ_{tr} is tissue saturation rate constant, equals $F/W \lambda_{\text{tr}}$, here F/W is blood flow per unit weight, in case cortical and flow obtained from PAH clearance (eq. 1). By testing various values for λ_{tr} , and using the λ_{tr} resulting from F/W and the chosen λ_{tr} , corresponding values for $v(T)$ were obtained from eq. 2. Thereafter the λ_{tr} fitting to observed $C(T)$ was derived by interpolation (Hope et al. 1976).

Erythrocyte/plasma water and I-Ap partition

Blood from 8 dogs gives I-Ap for flow measurements as separated by centrifugation in 10 ml tubes for 10 min at an average g of 1800. ^{125}I radioactivity as well as water content (weighing and drying for 48 h at 90°C) was determined in whole blood, plasma, and packed red cells. ^{125}I distribution was determined by standard microtube centrifugation.

And solubility of I-Ap

The olive oil/water partition of I-Ap was examined by using and shaking equal volumes of water containing I-Ap (0.5% free ^{125}I) and olive oil at room temperature. After three minutes equilibration, water and oil were separated by centrifugation and ^{125}I activity was measured in two phases.

Scintillation measurements

I-Ap activity was determined in a well scintillation gamma counter and THO in Mark I or Isocap 300 liquid scintillation system (Nuclear Chicago) using external standard correct for quenching. Interference by ^{125}I liquid scintillation was minimal because of 10^3 times higher activity of THO in the scintillant.

Medullary blood flow

Determination of λ_{tr} for medullary tissue would require much longer tracer infusion, and was therefore not made. However the present infusion time is ideal for estimation of renal medullary blood flow and samples from inner medulla were therefore discarded in most experiments. Local flow in ml/min per g tissue was calculated from eq. 2.

RESULTS

Since I-Ap was determined per gram blood and tissue λ_{tr} has the dimension of w/w (weight/weight). THO activity was determined per gram tissue and per ml blood, giving λ_{tr} the dimension of l/w (volume/weight).

Tissue/blood partition of I-Ap

The partition coefficient for each kidney was calculated from the average I-Ap concentration of 12 to 40 cortical tissue samples. The concentration scatter in individual kidneys was small, with coefficients

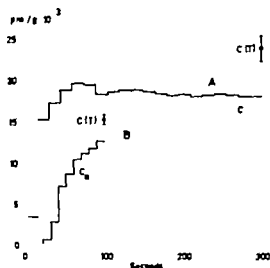


Fig. 1 Two arterial concentration curves (C) and corresponding tissue concentrations ($C(T)$ mean \pm S.D.) for ^{125}I -iodoantipyrine. Calculated λ_{tr} 1.31 in expt. A, 1.39 in expt. B.

of variation ranging from 1.4 to 5.6% (Avg. 3.2%) attesting to uniformity of equilibration and partition coefficient within the cortex.

Two experiments with infusion times of 75 and 300 s respectively shown in Fig. 1 demonstrate clearly a much higher I-Ap activity in the renal cortex than in the last arterial blood samples, indicating a tissue/blood partition coefficient well above unity. The average calculated for 18 kidneys in 13 dogs was 1.38 (S.E. of the mean 0.03). The range was 1.17 to 1.61 and the S.D. 0.13. The individual average for the 13 dogs (2 kidneys in 5 dogs) was 1.35 (S.D. 0.12).

As evident from Fig. 2, λ_{tr} tended to increase with increasing hematocrit, but the correlation was not statistically significant ($p > 0.05$). The λ_{tr} obtained in 3 expts. with saturation periods of 300 s (1.29, 1.35 and 1.39) did not deviate from that of the remaining 10 experiments with 75 to 150 s infusion. No relationship to cortical blood flow to the shape of the blood concentration curve or to uniformity of cortical sample concentrations from each kidney could be detected. Furthermore as evident from Fig. 2, λ_{tr} showed no correlation to urine pH in the range of 5.5 to 8.6.

Erythrocyte/plasma partition of water and I-Ap

The unexpectedly high λ_{tr} for I-Ap might be due to a lower I-Ap concentration in red cell water than in

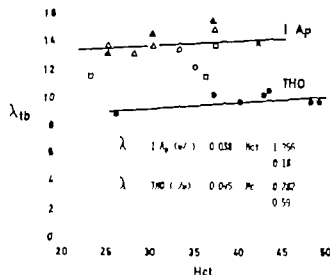


Fig. 2 In vivo partition coefficients for THO (closed circles) and for I Ap as related to hematocrit. The various symbols for I Ap indicate urine pH: Open circles, pH < 6.5; Triangles, 6.5 < pH < 7.5; Squares, pH > 7.5; Crosses, pH unknown.

plasma water λ_{THO} (red cell/plasma partition) for I Ap and water was therefore determined in blood from 8 dogs infused with I Ap. The observed λ_{THO} for I Ap (w/w) averaged 0.85 (S.D. 0.05) or 0.87 when corrected for trapped plasma. Hematocrit averaged 42 (range 37 to 47). The water content (w/w) averaged 0.977 (S.D. 0.006) in plasma, 0.678 (S.D. 0.017) in packed red cells (10 ml tubes) and 0.817 (S.D. 0.019) in whole blood. Taking the corresponding specific weights to be 1.025, 1.090 and 1.050 gives an average red cell water content of 0.657 indicating 4% trapped plasma in packed cells and a true λ_{THO} for H_2O of 0.77 (w/w). The I Ap/ H_2O partition ratio $0.82/0.77 = 1.14$ thus indicates that the apparent I Ap concentration in red cell water is 14% higher than that in plasma water. Similarly it may be calculated that the apparent I Ap concentration in kidney tissue water is 60% higher than that of plasma water at diffusion equilibrium.

Lipid solubility of I Ap

The olive oil/water partition coefficient of I Ap activity at room temperature averaged 1.08 v/v (S.D. 0.06, $n=9$). Correction for free iodine (assumed to be insoluble in oil) gave a true I Ap partition of 1.16.

Tissue/blood partition of THO

The variation of THO concentration among tissue samples from the same kidney was about twice that

for I Ap with an average coefficient of variation of 7.1% (range 3.0 to 12.6 in 8 kidneys). The average tissue/plasma partition coefficient (λ_{THO}) was 0.97 (S.D. 0.05) v/v. Conversion to tissue/blood partition (λ_{THO}) was made on the assumption of a red cell plasma THO distribution equal to that of water, plasma water content of 0.95 (v/v) and individual hematocrits (Avg. 41, range 26 to 49) and blood water contents (Avg. 0.854, S.D. 0.018 v/v). The resulting λ_{THO} averaged 0.97 (S.D. 0.06) v/v as shown in Fig. 2. λ_{THO} for THO tended to increase with increasing Hct but the correlation was not statistically significant ($p > 0.05$).

Inner medullary blood flow

The infusion periods of 75 to 300 s resulted in 1 to 60% saturation of the inner medulla. Using the observed cortical partition coefficients average inner medullary blood flow estimated from I Ap and THO uptake in 15 kidneys was 0.74 (S.D. 0.15) ml/min/g. No difference between I Ap and THO was observed in 6 expts in which both were determined. Cortical blood flow estimate from PAH clearance (eq. 1) averaged 4.39 with range of 7.0 to 6.1 ml/min/g.

DISCUSSION

The average I Ap partition coefficients of 1.34 in kidney/blood and 0.85 for red cell/plasma, compared with the common view that the distribution space for antipyrine and I Ap in cells and tissues is equal to that of water (Hope et al. 1976; Krasnow et al. 1963; Takao et al. 1955) or even lower (Brigbur et al. 1971). However, some literature data suggest differences both among species and among tissues and the present findings are not without precedence. For dog erythrocytes Effros & Chien (1969) found a 10% higher apparent I Ap concentration in cell water than in plasma water in good agreement with the present figure of 14%. While Carlin & Chien (1977) recently reported a surplus of 40% in red cell water. We have no explanation for this discrepancy. In any case, the high solubility of I Ap in erythrocytes with a cell/plasma partition close to unity should imply a tissue/blood partition coefficient rather insensitive to hematocrit changes in agreement with the in vivo experimental findings (Fig. 2).

For the dog kidney Soberman et al. (1949) found

10% higher concentration of antipyrine in tissue than in plasma (two kidneys examined) than in plasma (two kidneys examined) while Hochbee (1956) reported a surplus of 1% (one kidney examined) for aminopyrine. Appreciably higher values were obtained in goat kidneys. Obviously a direct comparison with I Ap is questionable since the observed fat solubility of I Ap is at least 15 times higher than that reported for antipyrine (Renkin 1957). No previous measurements seem available for I Ap partition between kidney tissue and blood in the dog. However, our previous finding of $\lambda_m = 1.00$ for the rat (Hope et al. 1976) and the present rather great individual scatter cloud the surprisingly high average of 1.38 call for close scrutiny of the methods.

Errors due to free iodine or other breakdown products of I Ap would seem to have been reduced to a minimum by (1) excluding the hepatic circulation, and (2) by using the shortest possible infusion period compatible with practically complete equilibration between arterial blood and the renal cortex (saturation half times or more). Extending the infusion period from 75 to 300 s had no consistent effect on the estimated λ_m , giving no evidence for slowly saturating intracellular compartments within this period of time.

The method used for calculating λ_m may need some comments. As a first approximation λ_m was estimated as the ratio between the observed tissue concentration and the average concentration of the first three blood samples. However, because of the infusion time and somewhat changing arterial concentration, a representative arterial value might not be obtained in this way. An intuitive correction for the lack of complete equilibration could be made by using the actual arterial curve and knowledge of the approximate saturation rate constant. Thus, in the case of increasing final arterial concentration one would choose a somewhat lower arterial concentration for comparison with tissue than in the case of falling arterial concentration. The method described above for calculating λ_m replaces this subjective correction by including the whole arterial concentration curve as well as cortical saturation rate derived from PAH clearance. It should be emphasized that the accuracy of the cortical flow estimated from eq. 1 is not critical to the calculation of λ_m . Thus, in both experiments shown in Fig. 1 an error in cortical flow of 20% could change the estimated λ_m by less than 0.01. The intuitive approach outlined above would

usually deviate by less than 0.05 from the calculated value.)

The fact that the pH of certain compartments of the kidney may deviate greatly from that of other biological fluids made us suspect some association between I-Ap uptake and tubular fluid acidification, but experimental evidence did not support that suspicion (Fig. 2).

The finding of a λ_m for THO of 0.97 close to that expected from the average water contents of cortical tissue and blood attests strongly to the validity of the methods and of the measured λ_m for I Ap. However, in spite of smaller analytical errors for I Ap than for THO in tissue and blood (cf. coefficients of variation for individual cortical samples) λ_m for I Ap showed greater scatter than that for THO, suggesting individual differences in the renal I-Ap space.

In conclusion, having excluded gross methodological errors, we must accept that I-Ap has a much higher solubility in kidney tissue than in blood. In fact, calculations show that in comparison to plasma, the tissue has an apparent distribution volume about 60% greater than its water content. The finding is especially surprising in view of the λ_m close to unity measured with the same technique in the rat kidney (Hope et al. 1976) but we have no plausible explanation for this species difference.

Knowledge of λ_m is necessary for estimating local blood flow according to Kety (1960). Since the error in calculated flow resulting from an inappropriate λ_m will increase with increasing degree of saturation (Elkjaer et al. 1974; Hope et al. 1976) the apparent interindividual variations in λ_m for I Ap suggest the use of short infusion periods. On the other hand the effect on calculated flow of inaccurate timing of the infusion duration (about 10 s) will be greater with short infusion periods (Clausen et al. 1979). However, the higher λ_m for I-Ap than for THO implies that the infusion period for I Ap may be prolonged by 40% compared to that of THO to obtain a given degree of saturation, thus adding to the analytical advantage of I Ap over THO.

The values for inner medullary "blood flow" obtained as a byproduct of these experiments should be considered with reservations. (1) The uptake rate is undoubtedly influenced by counter current exchange and urine flow and does therefore reflect "nutritive flow" rather than "true blood flow" (For further discussion see Aukland & Berne 1964; Hope et al. 1976; Clausen et al. 1979) (2)

Total renal blood flow was somewhat lower than we usually observe under control conditions probably because of the rather extensive surgery and the porta-iliac shunt.

While the present study is primarily of interest for the use of I Ap for measuring local renal blood flow in the dog, it also permits some general conclusions. The distribution space for I Ap may deviate greatly from that of water in a given tissue. Furthermore, this deviation may vary considerably among tissues and even among species.

Added in proof: In agreement with the present data Sakurada et al. (Amer J Physiol 234 H59-H66, 1978) reported a much higher solubility for iodo [14 C]antipyrine than for [14 C]antipyrine in nonpolar solvents. However, the brain/blood partition coefficients for both substances, 0.80 and 0.91 respectively, differ markedly from our results on the renal cortex.

REFERENCES

AUKLAND K & BERLINER R. W. 1964 Renal medullary countercurrent system studied with hydrogen gas. *Circulat Res* 15: 430-442.

BRIGHAM K. L., RAMSEY L. H., SNELL J. D. & MERRITT C. R. 1971 On defining the pulmonary extravascular water volume. *Circulat Res* 29: 385-397.

CARLIN R. & CHIEN S. 1977 Partition of xenon and iodoantipyrine among erythrocytes, plasma and myocardium. *Circulat Res* 40: 497-504.

CLAUSEN G., HOPE, A., KIRKEBØ, A., TYSSÉ, BOTN I. & AUKLAND K. 1979 Distribution of blood flow in the dog kidney. I. Saturation rates for inert diffusible tracers. [125 I] iodoantipyrine and tritiated water versus uptake of microspheres under control conditions. *Acta Physiol Scand* 107: 69-81.

EFFROS R. M. & CHINARD F. P. 1969 The in vivo pH of the extravascular space of the lung. *J Clin Invest* 48: 1983-1996.

EKLÖF B., LASSEN N. A., NILSSON L., NORBERG K., SIESJØ B. K. & TORLÖF P. 1974

Regional cerebral blood flow in the rat measured by the tissue sampling technique: a critical analysis using four indicators: C^{14} antipyrine, C^{14} -ethanol, H_2 water and Xenon 133 . *Acta Physiol Scand* 91: 1-16.

HILTON M. A. & DALLAM R. D. 1969 Penetration of rat liver mitochondria to α -ketoglutarate, aspartate and carnitine. *Arch Biochem Biophys* 130: 347-359.

HOPE, A., CLAUSEN G. & AUKLAND K. 1979 Intrarenal distribution of blood flow in rats determined by [125 I] iodoantipyrine uptake. *Circulat Res* 45: 370.

HUCKABEE W. E. 1956 Use of 4-aminocantipyrine in determining volume of body water available for water dilution. *J Appl Physiol* 9: 157-162.

KETY S. S. 1960 Measurement of local blood flow: the exchange of an inert diffusible substance. In: *Methods in medical research*, vol. 8 (ed H. B. Bruner), pp. 228-236. Year Book Medical Publishers, Chicago.

KRASNOW N., LEVINE H. J., WAGMAN R. J. & GORLIN R. 1963 Coronary blood flow measurement. [125 I] Iodo-antipyrine. *Circulat Res* 12: 58-62.

MUNCK O. & ANDERSEN A. M. 1967 Decomposition of iodine-labelled antipyrine. *Scand J Clin Lab Invest* 19: 256-258.

RENKIN E. M. 1952. Capillary permeability to lipid soluble molecules. *Amer J Physiol* 168: 538-545.

SMITH H. W., FINKELSTEIN N., ALIMINOS, L., CRAWFORD B. & GRABER, M. 1945 The renal clearances of substituted hippuric acid derivatives and other aromatic acids in dog and man. *J Clin Invest* 24: 388-404.

SOBERMAN R., BRODIE B. B., LEVY B. I., AXELROD J., HOLLANDER V. & STEELE, J. W. 1949 The use of antipyrine in the measurement of total body water in man. *J Biol Chem* 179: 31-41.

STRAUB W. H., FLANAGAN D. F., AARON R. I., ROSE J. C. 1964 Fate of injected radioiodinated iodoantipyrine in the dog and rat. *Proc Soc Exp Biol Med* 116: 1119-1122.

TALSO P. J., LAHR, T. N., SPAFFORD, N. FE, ENZI G. & JACKSON H. R. O. 1955 A comparison of the volume of distribution of antipyrine, N-acetyl amino-antipyrine and [125 I]-labeled 4-iodoantipyrine in human beings. *J Lab Clin Med* 46: 619-623.

Distribution of blood flow in the dog kidney

¹Saturation rates for inert diffusible tracers, ¹²⁵I-iodoantipyrine and tritiated water versus uptake of microspheres under control conditions

CLAUSEN A. HOPE, A. KIRKEBØ I. TYSSEBOTN and K. AUKLAND

Institute of Physiology, University of Bergen, Norway

CLAUSEN G. HOPE, A. KIRKEBØ A., TYSSEBOTN I. & AUKLAND, K. Distribution of blood flow in the dog kidney. I. Saturation rates for inert diffusible tracers, ¹²⁵I-iodoantipyrine and tritiated water versus uptake of microspheres under control conditions. *Acta Physiol Scand* 1979 107 69-81. Received 17 March 1979. ISSN 0001-6772. Institute of Physiology, University of Bergen, Norway.

Disparate reports on intrarenal blood flow distribution prompted direct comparison between microspheres (Ms) and inert diffusible tracers (DT). The tissue sampling technique for estimating local flow with DT (Kety) was adapted for the dog kidney using ¹²⁵I-iodoantipyrine (I Ap) and tritiated water (THO). M (15 μ m) were injected 3 min prior to 10-15 DT infusion made during continuous 1 arterial blood sampling. Tracers were measured in 7 to 20 samples from each of the following zones: Outer, middle and inner cortex (C₁, C₂, C₃), outer and inner halves of outer medulla (OM₁, OM₂), and inner medulla (IM₁). I Ap and THO gave closely similar flow distributions, and average total renal blood flow (RBF) of 3.90 and 3.78 as compared to 3.94 ml/min/g with Ms. Flow in C₁ (ml/min/g) was similar with all tracers, and as per cent thereof average local flows were: C₁ 102, C₂ 70, OM₁ 34, OM₂ 12, and IM₁ 2 with DT versus 117, 53, 1, 3 and 0 with Ms. Zonal flow fractions of total RBF obtained with DT were: C₁ 0.41, C₂ 0.33 and C₃+medulla 0.26 versus 0.51, 0.33 and 0.16 with Ms. Thus, Ms surplus in C₁ relative to DT flow representing 10% of total RBF matched a Ms deficit in C₂ medulla. This disparity might result from: (1) Failure of M to enter deep afferent arterioles in proportion to blood flow, (2) diffusion of DT from deep portions of the interlobular arteries, and/or (3) postglomerular low and flow of blood and DT.

Key words. Renal blood flow, kidney circulation, local flow measurement, inert diffusible tracers, microspheres.

It is commonly assumed that changes of the intrarenal distribution of blood flow may influence several renal functions. However the verification of such hypotheses is hampered by the fact that various methods for measuring local or regional blood flow in the kidney give different results. This clearly calls for scrutiny of the flow techniques, and two principally different methods will be explored here: (1) The rate of uptake (or removal) of inert diffusible tracers (Kety 1951) and (2) the distribution of intra-arterially injected microspheres (McNay & Abe 1970).

(1) In the case of diffusible tracers the inert gases H₂ and ⁸⁵Kr (or ¹³³Xe) offer the great advantage of practically unlimited repeatability of measurements

(Aukland, Bower & Berliner 1964; Thorburn et al 1963). However with both methods objections may be raised against the techniques used for recording local gas concentration. The H₂ method involves the trauma of inserting platinum electrodes into the tissue. The local trauma is avoided with external monitoring of ⁸⁵Kr-washout, but the deduction of local concentration patterns from the composite desaturation curve involves great uncertainties. For these or other reasons the results obtained with the two methods differ considerably both under control conditions and in various experimental conditions, as recently reviewed by one of us (Aukland 1976).

(2) While the use of microsphere uptake has been

widely accepted. It should be realized that there is only indirect evidence that the microspheres distribute in proportion to blood flow within the kidney. It is especially conspicuous that renal vasodilatation invariably causes an inproportionate rise in microsphere uptake in deep cortex while no such redistribution has been observed with diffusible tracers. (For references see Aukland 1976.)

Because of these discrepancies we decided to study the local uptake of inert diffusible tracers in the dog kidney by the "tissue sampling technique" (Kety 1951) providing atraumatic flow measurements in well defined anatomical regions. This approach permitted simultaneous measurements of microsphere uptake in exactly the same locations.

Since the volatility of gases may cause considerable technical problems we decided to use ^{131}I iodoantipyrine (I Ap) and tritiated water (THO). The uptake of these tracers is commonly assumed to be exclusively flow limited and in the case of I Ap we have recently obtained evidence that this holds true for the rat kidney (Hope, Clausen & Aukland 1976; Clausen & Hope 1977).

A brief account of some of these experiments has appeared in abstract form (Clausen et al. 1977).

METHODS

Inert diffusible tracers. Tissue sampling technique

Principle. The basic assumption underlying the method is that highly diffusible tracers entering the tissue through arterial blood will reach complete equilibrium with the tissue in one single passage. In other words that the tracer activity is equal in venous blood and in the tissue it is drained from. As shown by Kety (1951) blood flow per unit tissue weight (F/W) may be estimated from the tracer concentration in the tissue (C) at time T , arterial tracer concentration (C') in the period 0 to T and the tissue/blood partition coefficient (λ_m)

$$C(T) = \lambda_m k \int_0^T C' e^{-k(T-t)} dt \quad (1)$$

where the rate constant $k = F/(V - \lambda_m)$. Thus if λ_m is known and $C(T)$ and the C' -curve from time zero to T is determined, tissue blood flow can be estimated. Since eq. (1) cannot be solved mathematically, a curve is constructed for corresponding values of $C(T)$ and k using the arterial concentration curve for each particular experiment (Kety 1960).

Tissue/blood partition coefficients. The tissue/blood partition (λ_m) for I Ap, i.e. the amount of blood having the same I Ap content as one gram of tissue, provided the complete diffusion equilibrium has been shown in a separate study to be higher in the dog kidney than in any other tissue studied so far (Clausen et al. 1979). In vivo

equilibration for 75 to 300 s gave an average λ_m of 1.3 (S.D. 0.13, $n=18$) w/w (weight/weight) for the cortex without statistically significant correlation with hematocrit. Since I Ap activity was determined per blood and tissue and λ_m has the dimension of w/w it will give flow in gram per min per gram tissue. Convert to ml/min/g was made by dividing by the specific gravity of blood 1.05.

Tissue blood partition for THO determined in the same in vivo experiments averaged 0.97 (S.D. 0.06) w/w (water weight). For practical reasons a value of 1.00 was used.

Preparation of ^{131}I -iodoantipyrine. ^{131}I -iodoantipyrine (I Ap) in 0.9% NaHCO_3 solution was obtained from New England Nuclear, Chicago. Free iodine was removed on a Sephadex G-10 column and the purity tested by silica gel chromatography as described elsewhere (Hjort et al. 1976; Clausen et al. 1979). At the time of use, the free ^{131}I content was usually 1-2% and did not exceed 5%. Final dilution in saline to an activity of about 5 $\mu\text{Ci}/\text{ml}$ was made shortly before injection of a 50 ml dose.

Experimental protocol. All experiments were performed on mongrel dogs (b.wt. 15 to 25 kg), fasted overnight but with free access to water. Anaesthesia was induced by i.v. injection of Nembutal 25 mg/kg b.wt. and supplemented with doses of 3 to 5 mg/kg when needed. An endotracheal tube was inserted to secure free air ways. Respiration was not assisted. Polyethylene catheters were inserted into a femoral vein for ketamine and in an artery for pressure recording with Hewlett Packard transducer and recorder.

Two series of blood flow measurements will be reported. **Series A** includes 9 experiments with I Ap as the only tracer. One kidney was exposed retroperitoneally through a flank incision. The ureter was catheterized and a nylon sling placed loosely around the renal pedicle. I Ap was given as a constant i.v. infusion over a period of 12 to 20 s. One or several blood samples were collected from a femoral artery PE 60 catheter as described below. The catheter length was 30 cm, and the tip was located about 15 cm from the entry in the femoral artery, i.e. approximately at the aortic bifurcation. Catheter volume was 0.1 ml.

Series B includes 10 experiments with practically simultaneous injection of I Ap/THO and microspheres (^{51}Cr). Both kidneys were exposed retroperitoneally and nylon snares were placed loosely around the renal pedicles. One renal artery was provided with an electromagnetic flow probe (Nycotron, Oslo) and catheterized with a thin polyvinyl tube for infusion of acetylcholine. A catheter was placed in the left ventricle through the right carotid artery for tracer injections. About 5 min before beginning the experiment to be reported here, one Mg batch had been injected under control conditions. Thereafter under continuous intra-arterial infusion of ACh in one kidney, a second Mg batch was injected into the left ventricle, followed within 3 min by a constant infusion of I Ap/THO into the same catheter. The doses of I Ap and THO were 50 μCi and 50 mCi respectively. Arterial blood was sampled from a 50 cm long femoral catheter, the tip being placed in the aorta, approximately at the level of the renal arteries. Both renal pedicles were clamped simultaneously after 10-15 sec infusion.

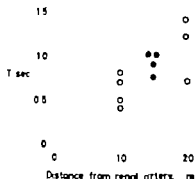


Fig. 1. Difference in appearance times (ΔT) of cold dyes in the aorta at the origin of the renal arteries and 3, 15 and 20 cm further downstream.

This report will give data for blood flow distribution in a control kidney and total flow in both kidneys as estimated from the three tracers. The effect of ACh on flow distribution will be described in a following paper.

Position of arterial sampling catheter. Unexpectedly high cortical flow in a couple of experiments in series A (short sampling catheter) made us suspect that the recorded arterial concentration curves might be more delayed compared to that delivered to the kidney than could be accounted for by catheter passage alone. The transit time in the abdominal aorta was therefore tested in two experiments as follows: Two thermocouples, each mounted at the tip of heart catheter, were introduced into one femoral artery. The temperatures were recorded continuously on a Kuladevski recorder using thermocouples as reference. One probe was advanced 30 cm from the insertion on the thigh, approximately to the level of the renal arteries while the second was placed alternately 10, 15 and 20 cm further downstream. Slug injection of 3–5 ml saline caused sharp deflection at each probe, and the time lag was recorded for the first appearance (calculated from the mean temperature downstroke extrapolated to baseline gave identical results). As shown in Fig. 1 sampling at the aortic bifurcation or in the iliac artery may cause delay of more than 1 s. We have not found it permissible to introduce correction for this delay but calculations showed that flow may have been overestimated by up to 15%. In series B we therefore used 30 cm long sampling catheter (PP 120, volume 0.40 ml), the tip being placed 30 cm from the entrance at the thigh. We thereby obtained measurable delay relative to renal arterial blood and could make appropriate correction of the arterial concentration curve. A usual sampling flow rate would be 0.4 ml/s, giving mean catheter transit time of 1 s.

Catheter siting. was tested as described previously (Hope et al. 1976). Correction of the arterial concentration curve had little influence (magnitude 1%) on calculated flow and was therefore omitted.

Blood and tissue sampling. Blood sampling was started simultaneously with I-Ap/THO infusion by cutting the aortic catheter 15 to 20 cm from its exit from the femoral artery. One sec samples were collected manually into

row of preweighed heparinized vials, and continued until 2–3 s after clamping the renal pedicles. Catheter flow rate and mean transit time were calculated from the timed sample weights and catheter volume. While still clamped, the kidneys were rapidly excised, weighed, plunged into Coy-ethanol, and were thereafter stored at -20°C .

Tissue samples were dissected out at 4°C as follows: 5–7 mm thick transversal or sagittal slices were cut out by circular saw. After scraping off 'saw dust' with a scalpel 7–10 mm broad sectors perpendicular to the kidney surface were cut out and thereafter divided into appropriate zones: The arcuate arteries were used as landmarks for the cortico-medullary border. A further check, the section was also inspected under low-power magnification for vasa recta bundles as indicators for outer medulla. The cortex was usually divided in three zones (C_1 , C_2 and C_3 from capsule to cortico-medullary border), and in some experiments of series A in two zones (OC and IC, outer and inner cortex) of equal thickness (Fig. 2). The border to the inner medulla was judged from the color change and loss of striation. Usually outer medulla (OM) was divided in two layers of equal thickness (OM_1 and OM_2). Samples from the inner medulla were limited to the outer 4–5 mm and did not include the papilla. Immediately after dissection each sample was transferred to preweighed counting vial, weighed again, and was then added 4 ml distilled water. The sample weights varied from 0.05 to 0.16 g. Equilibration of I-Ap and THO between tissue and water was found to be complete after 24 h. I-Ap and M_1 activity was determined on the whole sample. Thereafter 100 μl of each sample was transferred to vials containing 6 ml scintillation fluid for measuring THO activity.

Blood samples of 0.1 to 0.3 ml for measurement of I-Ap activity were pipetted into preweighed counting vials, weighed again, and added 4 ml distilled water. To avoid cumbersome bleaching procedures, plasma instead of whole blood was used for determination of THO activity. One glass capillary was filled from each blood sample and spun in hematocrit centrifuge. The plasma (about 0.02 g) was transferred to preweighed counting vials which were then weighed again and added 6 ml scintillation fluid. Calculation of whole blood THO activity was made on the assumption of uniform activity in plasma and red cell water using plasma and whole blood water content determined in each experiment (Chansen et al. 1979).

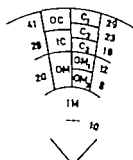


Fig. 2. Zonal division of kidney sector. The numbers give zonal volumes in per cent of total kidney volume.

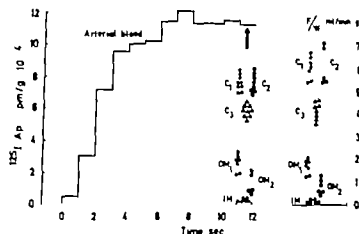


Fig 3 Arterial and tissue concentrations of I Ap in one experiment (Series A). Arrow indicates clamping of the renal pedicle relative to the arterial curve (corrected for catheter delay). Right: Local blood flow calculated for individual tissue samples. Zones defined in Fig 2

Microspheres: Preparation and Injection

Two injections of Ms tagged with ^{86}Sr and ^{141}Ce (3M Co Minnesota) were made in the experiments of series B the second injection preceding I Ap and THO by 2–3 min. Spheres with measured diameters of 16.1 ± 2.4 (S.D.) μm were used in 7 expts. spheres with diameter 19.1 ± 1.3 μm in 3 expts. 4–800 000 spheres ($5\text{--}10 \mu\text{Ci}$) were suspended in 1.0 to 1.5 ml 10% dextran sonificated and injected into the left ventricle in the course of 5 s. A reference arterial blood sample was obtained from the femoral artery catheter by suction pump drawing 12.2 ml/min for a period of 45 s. The number of microspheres trapped in a 100 mg cortical tissue sample was estimated at 100 to 250 corresponding to approximately 0.2 to 0.5 spheres per glomerulus.

Isotope measurements

Radioactivity was measured on the same day in tissue and blood/plasma samples as follows. In series A and partition experiments ^{125}I -activity was measured in a single channel well scintillation counter. In series B the activity of ^{141}Ce and ^{86}Sr was counted in a 3-channel well scintillation gamma counter (Searle Analytic Inc. Model 1185) for 10 min (minimum 1000 counts per cortical sample). Standards were included in each run to check window spillover ratios.

Tritiated water activity was determined in a Mark I or Isocap 300 liquid scintillation system (Nuclear Chicago) using external standard to correct for quenching. Interference by ^{141}Ce scintillation was minimal because of the 10^3 times higher activity of THO in the infusate.

Flow calculations

Average renal blood flow per gram tissue was calculated from the local flow rate and the respective zonal volumes. Cortex, outer and inner medulla (including the papilla) were assumed to account for 70, 20 and 10% of total kidney volume respectively. The further subdivisions of the cortex were considered as 3 mm thick shells of an ellipsoid with diameters 7.3 and 4.3 cm (average for three kidneys of different size) giving the following volume

fractions: C 29%, C₂ 23% and C₃ 18%. Similar estimates for outer medulla gave 12% and 8% for OM₁ and OM₂ respectively (Fig. 2).

RESULTS

Series A

Series A represents our first measurements of I-Ap uptake in dogs and has several imperfections as compared to later experiments (Series B). The use of a short sampling catheter implies an unacceptable delay in the lower aorta and the timing and isotope counting were less accurate in some experiments. While these shortcomings may have influenced absolute flow values, the relative flow distribution should not be seriously affected. The results are reported mainly because these experiments probably represent the best control flow distribution. No experimental intervention was made on any kidney and the I Ap infusion was not preceded by injection of microspheres which theoretically might influence flow distribution.

Table 1 Average coefficient of variation (per cent) of tissue sample tracer concentrations within 100% Series A: 9–10 samples from each zone in 9 kidneys; Series B: 7–10 samples from each zone in 10 kidneys

Zone	Series A		Series B	
	I Ap		I-Ap	THO
C	11.1		4.9	11.7
C ₂	12.7		6.7	10.6
C ₃	16.5		12.2	17.3
OM	1.6		2.1	4.1
OM ₂	42.5		49.0	53.5
Ms				69.8

Table 2. Zonal blood flow per g tissue and zonal fraction of total renal blood flow determined by I Ap \pm S.D.

C_o, C_o=outer, middle and inner third of cortex, OM OM_o=outer and inner half of outer medulla, IM inner medulla, OM+IM IM DF=deep fraction=C_o+IM

Series A (9)		Series B (10)	
Zonal flow (ml/min g)	Zonal fraction (%)	Zonal flow (ml/min g)	Zonal fraction (%)
6.68±1.89	43.5±4.8	5.77±1.94	42.5±3.3
6.50±1.60	33.5±1.4	5.57±1.87	32.6±1.7
4.21±0.89	17.3±2.6	3.79±1.14	17.7±2.3
1.60±0.74	4.4±1.2	1.78±0.69	5.6±1.4
0.57±0.38*	1.0±0.5	0.64±0.37	1.3±0.4
1.14±0.41	5.4±2.5		
0.14±0.05	0.3±0.1		
	5.9±2.3		7.2±1.8*
	23.2±4.3		24.9±3.7
4.45±1.01		3.90±1.25	

5 7 Mean of OM + OM_o + IM in 5 expts. and OM + IM in 4 expts. Added 0.3% for IM

The effective I Ap infusion period defined as the time from first appearance at the entrance of the sampling catheter to clamping the kidney varied from 9 to 18 s (average 11 s). Mean arterial blood pressure (AP) averaged 126 (S.D. 13) mmHg, and hematocrit was 38.6 (S.D. 4.6).

Primary data from one experiment are depicted in Fig. 3 showing the arterial I Ap concentration curve and tissue concentrations in the various zones. For the sake of clarity the symbols representing concentrations in the different zones have been moved apart. Local blood flow calculated from the I-Ap concentrations of individual tissue samples are shown to the right in Fig. 3. It is evident that the concentration pattern with about equal values in C and C_o, somewhat lower in C and sharply decreasing values in the medulla, is retained in the calculated flow. However the nonlinear relationship between tissue concentration and blood flow results in greater scatter of flow rates in each zone and relatively greater differences between the various zones.

The average coefficient of variation for I-Ap concentration within individual cortical zones ranges from 11.1 to 16.5% (Table 1). Since 9 to 20 samples were taken from each zone the S.E. of mean concentration will be 3-5% while calculated mean zonal flow will have a S.E. of 5-10%. In three kidneys, one to three sectors had I Ap concentrations 20 to 50% lower than the average concentration of the remaining 7-10 sectors, but did not differ with respect to interzonal concentration ratios.

Calculation of zonal blood flow from mean zonal

tracer concentration gives a lower value than the average of flows calculated from individual sample concentrations (Hope et al. 1976, Eklof et al. 1974). However even with the rather large scatter observed in this series the average underestimate for cortical samples was only 1.6%. Since even lower intrazonal variations were obtained in later expts. we find it justified to use mean zonal concentrations for flow calculation.

The zonal flow per gram tissue and its fraction of total renal blood flow are averaged for all 9 kidneys in Table 2, and Fig. 4 shows the zonal flow

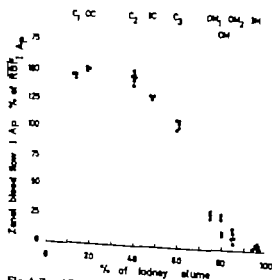


Fig. 4 Zonal flow estimated from I-Ap uptake in 9 kidneys (Series A) in per cent of individual mean RBF_{total}. Zones defined in Fig. 2.

Table 3 Zonal blood flow per g tissue and zonal fraction of total renal blood flow determined in 16 control kidneys (Series B) with microspheres (Ms) 125 I iodoantipyrine (I Ap) and tritiated water (THO) Mean \pm S.D

	Ms		I Ap		THO	
	Zonal flow (ml/min g)	Zonal fraction (%)	Zonal flow (ml/min g)	Zonal fraction (%)	Zonal flow (ml/min g)	Zonal fraction (%)
C	6.34 \pm 2.42	50.8 \pm 7.3	5.77 \pm 1.94	4.5 \pm 3.3	5.31 \pm .57	40.3 \pm 3.7
C	5.42 \pm .50	33.3 \pm 4.6	5.57 \pm 1.87	32.6 \pm 1.7	5.4 \pm .59	32.9 \pm .8
C	7.89 \pm 1.66 *	13.7 \pm 3.8	3.79 \pm 1.14	17.7 \pm .3	3.91 \pm 1.79	18.8 \pm 2.4
OM	0.63 \pm 0.57 *	1.9 \pm 1.1	1.78 \pm 0.69	5.6 \pm 1.4	1.97 \pm 1.15	6. \pm 1.7
OM	0.17 \pm 0.14 *	0.4 \pm 0.1	0.64 \pm 0.3	1.3 \pm 0.4	0.68 \pm 0.37	1.5 \pm 0.5
RBF	3.94 \pm 1.53		3.90 \pm 1.25		3.78 \pm 1.78	
DF		16.0 \pm 4.8		4.9 \pm 3.7		26.8 \pm 4

Significantly different from THO Wilcoxon signed rank test for paired samples. Abbreviations as in Table 1.
Significantly different ($P < 0.05$) from I Ap

in individual expts in per cent of average flow per gram kidney. The flow distribution showed no relationship to the duration of I Ap infusion (9–18 s) or to the degree of saturation of C (30–77%) (Degree of saturation calculated as tissue concentration/ λ_m for I Ap divided by the average concentration of the last three one second blood samples).

Total renal blood flow averaged 4.45 (S.D. 1.01) ml/min g with a range of 3.19 to 5.94 ml/min g.

Series B

As described in Methods Series B provided a direct comparison of blood flow measured in the same tissue samples with Ms and within 2–3 min with I Ap and THO. Acetylcholine was infused continuously into one renal artery raising total RBF_{est} (electromagnetic flowmeter) of the infused kidney by 50 to 100% above control level. Because of the high flow the effective infusion time for I Ap/THO was reduced to average 10.3 s (8 to 13.5 s). \overline{AP} averaged 126 mmHg (S.D. 15) and Hct 38.0 (S.D. 6.6). A moderate (<15%) and shortlasting fall in arterial pressure and RBF_{est} of the acetylcholine infused kidney was occasionally observed after Ms injection but at the time of I Ap/THO infusion RBF_{est} averaged 98% of preinjection control. Data for intrarenal flow distribution are given only for the control kidney whereas calculated total RBF is reported for both kidneys.

Flow distribution within each zone. As evident for intrarenal flow distribution [are] given only for the control kidney whereas calculated total RBF is the scatter was considerably lower than in Series A.

and a coefficient of variation of less than 25% was observed in C and C₂ in 5 expts. Considerably greater scatter was observed for THO concentrations within each zone and without exceptions Ms activity showed the greatest variation (Table 1). However the comparison of concentrations may be somewhat misleading since in the case of Ms the relative scatter for estimated flow will be identical to that of the tissue concentration whereas in the case of I Ap and THO the coefficient of flow variations among samples will be higher than that of the tissue concentrations because of the nonlinear relationship between true concentrations and estimated flow (Fig. 4). Thus the coefficient of variation for I Ap flow will be about 8% in C₁ and C₂ and about 15% in C₃. The corresponding numbers for THO are 16 and 3. Since an average of 9 samples were taken from each zone the standard error of mean zonal flow estimated with I Ap will be about 7.7% in C₁ and C₂ and 5% in C₃. Corresponding numbers for THO are 5 and 8% and for Ms 3.5 and 11%. As evident from Table 1 a much greater scatter was obtained in the medullary zones with all indicators.

In one kidney two sectors had indicator concentrations 70–30% below average.

Flow distribution between zones. Total RBF estimated from I Ap varied considerably among experiments (Fig. 7) with an average about 12% lower than that obtained in Series A (Table 2). The difference reflects lower flow in all cortical zones ($P > 0.05$) whereas little difference was observed in outer medulla. The zonal flow fractions showed less variation and were quite similar in the

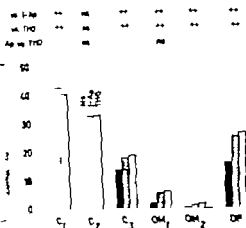


Fig. 5. Zonal flow in per cent of RBF measured with MIs (black columns), I-Ap (hatched columns) and THO (clear columns). Average of 10 control kidneys (Series B). Deep fraction, DF. Medulla, C_3 . Zones defined in Fig. 2. Significance levels: $P < 0.02$, $P < 0.05$ or $P > 0.05$.

no series, except for somewhat lower ($P > 0.05$) outer medullary fractions in Series A (Table 3).

As evident from Table 3 and Fig. 5, the average zonal flow and flow fractions obtained with THO were quite similar to that obtained with I-Ap, except for slightly higher C_3 and outer medullary flow fractions with THO.

A clearly different pattern was observed with MIs. As expected, medullary MIs-activity was low but clearly indicated the presence of microspheres in most tissue samples from OM₁ in some samples from OM₂, and even in occasional IM samples. In addition the flow fraction in C_3 was about 25% lower with MIs than with I-Ap and THO. A significantly higher flow fraction was obtained with MIs in C_2 whereas the three indicators agreed well in the middle cortex C_1 . As will be discussed later the deep flow fraction DF defined as the fraction of total RBF going to C_3 +medulla may provide a useful parameter for comparison. DF averaged 16.0% for MIs compared to 24.9 and 26.8% for I-Ap and THO respectively. As shown in Fig. 6, DF_{MIs} and DF_{I-Ap} agreed well and in spite of considerable scatter DF_{MIs} was lower in all expts. The difference to DF_{I-Ap} and DF_{THO}, averaging about 0.09 and 0.11 respectively, seemed independent of the magnitude of DF and approximately the same difference was maintained also when comparing DF C_3 (Fig. 8).

The distribution of MIs with diameter 12.9 ± 1.3

μm (3 expts.) did not differ from that observed with diameter $16.1 \pm 4.4 \mu\text{m}$.

Inner medullary I-Ap and THO uptake was usually not measured in this series because the infusion time was too short for a meaningful calculation of inner medullary flow. (In calculating DF (Table 3, Figs 5 and 6) the average value of 0.3% of RBF observed in Series A was used.)

Total renal blood flow. The average RBF calculated from the three indicators were not significantly different in the control kidney (Table 3) nor in the acetylcholine infused kidney. In the latter the following means were obtained: I-Ap: 6.40 (S.D. 1.96), THO: 6.35 (S.D. 1.30) and MIs: 6.72 (S.D. 1) ml/min/g. With some exceptions, the agreement was good also in individual experiments, but as shown in Fig. 7 there was a slight tendency for RBF_{I-Ap} and RBF_{THO} to fall off relative to RBF_{MIs} with increasing flow. However the slope of the regression lines did not deviate significantly from unity ($P > 0.05$).

DISCUSSION

Validity of the Kerr model and the tissue sampling technique

A large number of elaborate mathematical models have been designed to describe the blood tissue

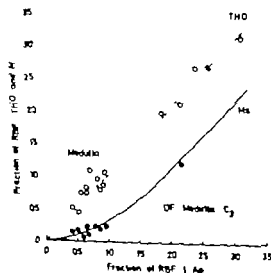


Fig. 6. Fractions of total renal blood flow to medulla and in medulla C_3 (DF), as estimated by THO (open circles), MIs (closed circles) and I-Ap in 10 control kidneys (Series B). Identity line broken. Solid line representing M vs. I-Ap drawn to best visual fit.

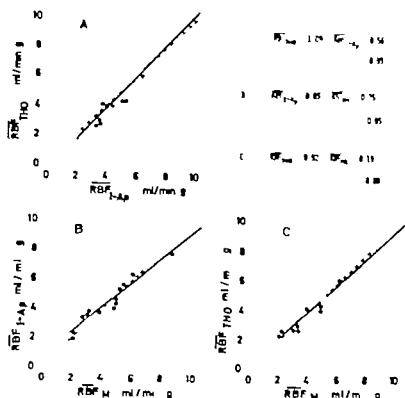


Fig. 7 Comparison of mean RBF in 70 kidneys as measured simultaneously with THO, I-Ap and Ms (Series B). Open circles, Acetylcholine infused kidneys. Filled circles: Control kidneys. Identity lines broken, regression lines solid. Regression coefficient not different from 1.00 ($P > 0.05$).

exchange of inert diffusible substances. However for the purpose of estimating local blood flow from tracer concentrations in tissue and arterial blood the simple exponential model proposed by Kety (1951) would still seem unsurpassed. Two main

assumptions will be briefly discussed with special reference to the kidney: (1) A correct estimate of total renal blood flow requires diffusion equilibrium between each region of the kidney and venous blood leaving that particular region. (2) A true es-

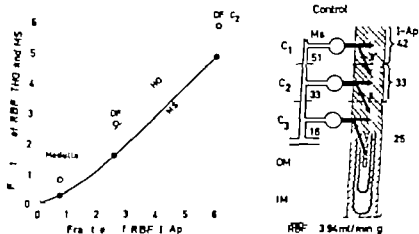


Fig. 8 Left: Average flow fractions in medulla, medulla+C (DF) and DF+C as estimated with THO (open circles), M (filled circles) and I-Ap. 10 control kidneys (Series B). Identity line broken. Solid line representing Ms vs. I-Ap drawn to best visual fit. Right: Hypothetical postglomerular inward flow of blood to account for the difference between zonal flow calculated from Ms and diffusible tracers in control kidneys. The numbers give flow in per cent of total RBF.

mate of regional blood flow requires in addition that the inert tracer is delivered simultaneously to each tissue region exclusively by arterioles/capillaries of that particular region.

The first assumption, venous equilibrium with the tissue is in all probability not satisfied for the medulla. Due to counter current diffusion between arterial and venous vasa recta, blood leaving the medulla during tracer uptake will have a higher tracer concentration than the average concentration in the medulla. The result is an underestimate of blood flow in the medulla as a whole and more so the higher the diffusibility of the tracer. In an attempt to elucidate this point THO was added to the I-Ap infusion in Series B based on the assumption that THO should have a lower diffusion coefficient (D) in tissue than the lipid soluble I-Ap. Evidence for such a relationship has been presented for D_2O versus unlabeled antipyrine in the liver (Thompson et al. 1959).

The lack of direct measurements of D_{I-Ap} and D_{THO} in the kidney prompted the following indirect, and approximate estimates. As Vucelja (1976) recently deduced from large number of literature data, the tissue diffusion coefficients of the 4 gases O_2 , CO_2 , N_2 and H_2 are exponentially related to tissue water content. In the kidney with a water content of 85% the diffusion coefficients should be about 30% of the free diffusion coefficients in water. Assuming the same relationship for I-Ap, and using Graham's law the D_{I-Ap} for the kidney at 37°C may be calculated from Vucelja's data. For instance, from D_{N_2} is obtained

$$D_{I-Ap} = D_{N_2}(MW_{I-Ap}/MW_{N_2})^{0.5} = 1.4 \cdot 10^{-6}(28/31)^{0.5} = 4.2 \cdot 10^{-6} \text{ cm}^2/\text{s}$$

Similarly from H_2 , O_2 and CO_2 , D_{I-Ap} values of $2.4 \cdot 10^{-6}$, $4.8 \cdot 10^{-6}$ and $5.4 \cdot 10^{-6} \text{ cm}^2/\text{s}$ are obtained. Regarding the discrepant values obtained from D_{N_2} , D_{I-Ap} of about $5 \cdot 10^{-6} \text{ cm}^2/\text{s}$ would seem to be a reasonable estimate.

For THO Chazard et al. (1969) estimated from renal venous elution curves kidney diffusion coefficient of 18% of that in water, about $6 \cdot 10^{-6} \text{ cm}^2/\text{s}$. This estimate was based on comparison with Hexanol and the assumption that $D_{Hexanol}$ in the same kidney tissue as in water. If however $D_{Hexanol}$ has the same dependence on tissue water content as the gases mentioned above D_{THO} would come out as $3 \cdot 10^{-6} \text{ cm}^2/\text{s}$. A similar value may be estimated from Fig. 7 in the same study (Chazard et al. 1969), showing D_{THO} of about 40% of D_{I-Ap} . Comparable values may also be estimated from microperfusion studies on tubular THO permeability in rats. The data of Persson (1979) and Persson & Ulfendahl (1970) on permeability and an estimated tubular wall thickness of 10 μm give D_{THO} for proximal tubules of $5.6 \cdot 10^{-6} \text{ cm}^2/\text{s}$ for distal tubules $3.2 \cdot 10^{-6}$ with ADH present, and $1.6 \cdot 10^{-6} \text{ cm}^2/\text{s}$ without ADH.

In conclusion, the diffusibility of I-Ap and THO in the kidney would seem to be quite similar both having a D of $3\text{--}5 \cdot 10^{-6} \text{ cm}^2/\text{s}$. This agrees well with the similar uptake rates for I-Ap and THO in the inner medulla observed in partition experiments (Clausen et al. 1979) indicating that AV shunting in the vasa recta bundles affects the two tracers to the same extent.

It follows that the simultaneous determination of I-Ap and THO does not provide any further insight in the medullary counter current exchange. It must be assumed, however, that both substances will underestimate medullary flow to an unknown extent. Because the medullary flow fraction by all estimates is small this conclusion is not incompatible with the quite good agreement between total renal blood flow estimated from THO, I-Ap and M_s . On the other hand the agreement on total flow provides strong support for the assumption of venous blood/tissue equilibrium and therefore flow-limited uptake for both THO and I-Ap in the renal cortex even at near maximal vasodilation (Fig. 7). Still, both I-Ap and THO could violate the second requirement set out above, i.e. that the tracer should be delivered exclusively by local capillaries. If for instance appreciable amounts of tracer are delivered to the deep cortex by diffusion from the interlobular arteries capillary blood flow in this zone would be overestimated. It would follow that outer cortex were fed by blood having lower tracer concentration than arterial blood leading to an underestimate of outer cortical capillary flow. It should be realized that a "diffusion bypass" (Chazard et al. 1969) of this type does not in itself violate the assumption of venous blood/tissue equilibrium, and is therefore not excluded for either I-Ap or for THO by the good agreement with total flow calculated from M_s uptake. On the other hand this agreement does speak against an appreciable direct arteriovenous diffusion shunt, which is also unlikely for anatomical reasons: While there is close AV proximity for the larger vessels (interlobar and arcuate) interlobular arteries and veins seem to run more separately (von Kögeln et al. 1959; Barger & Herd 1973).

Tracer leaves the blood by diffusion from the peritubular capillaries and—at the same time—by glomerular filtration. The cortical tissue consisting mainly of tubules and their content, will thus be fed from "two sides". This might to some extent help to ensure complete tracer equilibration but since

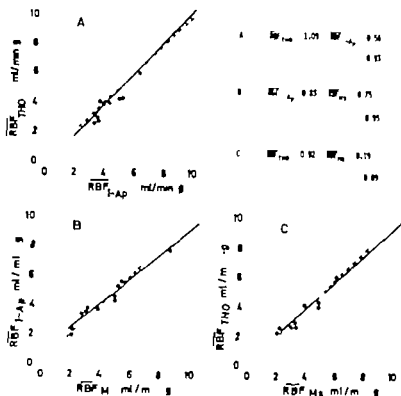


Fig 7 Comparison of mean RBF in 20 kidneys as measured simultaneously with THO I Ap and Ms (Series B). Open circles: Acetylcholine infused kidneys. Filled circles: Control kidneys. Identity lines: broken regression lines: solid. Regression coefficient not different from 1.00 ($P > 0.05$)

exchange of inert diffusible substances. However for the purpose of estimating local blood flow from tracer concentrations in tissue and arterial blood the simple exponential model proposed by Kety (1951) would still seem unsurpassed. Two main

assumptions will be briefly discussed with special reference to the kidney. (1) A correct estimate of total renal blood flow requires diffusion equilibrium between each region of the kidney and venous blood leaving that particular region. (2) A true esti-

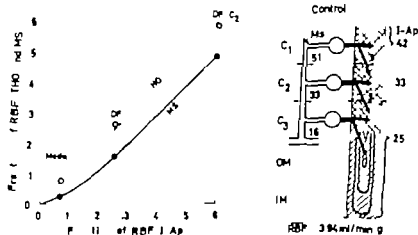


Fig 8 Left: Average flow fractions in medulla, medulla + C_2 (DF) and DF + C as estimated with THO (open circles), Ms (filled circles) and I-Ap in 10 control kidneys (Series B). Identity line: broken. Solid line: representing Ms vs. I Ap drawn to best visual fit. Right: Hypothetical postglomerular inward flow of blood to account for the difference between zonal flow calculated from Ms and diffusible tracers in control kidneys. The numbers give flow in per cent of total RBF.

10 to 20 samples in each zone are averaged the standard error of the mean zonal flow (3.5% in C_1 and C_2 , 11% in C_3) is well acceptable for comparison of flow estimated with M_s to that obtained with I Ap and THO.

All indicators showed much greater intrazonal scatter in C_1 and the medullary zones than in C_2 and C_3 . This does not necessarily signify a greater flow heterogeneity but rather results from the steep concentration (and flow) gradient in this region (Fig. 4), together with the problem of obtaining a consistent zonal division. Even with careful dissection under low power magnification, performed by the same person, there was evidence for considerable variation in dissection both within a single kidney and among different kidneys. Appreciable numbers of M_s might occur in several OM samples and even in OM samples while most samples from these zones were completely free of M_s . These observations emphasize the hazard of comparing results obtained in different laboratories and indicate that reliable comparison of two tracers demands determination of both tracers in the same tissue samples.

Sections with low flow (20–30% below average as estimated with all indicators) were occasionally observed. While no specific faults were detected in these experiments we tend to believe that the phenomenon represents an experimental artifact rather than physiological flow heterogeneity.

Flow distribution between zones

Comparison to other diffusible tracers. As already pointed out above, comparison of data from different laboratories should be made with caution because of the lack of uniform procedures for zonal division of the kidney. In the case of H_2 washout studies made in this laboratory, comparison seems reasonably safe. While the medullary flow patterns are quite similar (Aukland 1967), H_2 measurements tend to give less difference between outer and inner cortical flow than observed with I Ap and THO (Aukland et al. 1973). The difference might result from the greater diffusibility of H_2 causing greater exchange by the interlobular arteries in inner cortex.

In the case of ^{86}Kr autoradiograms suggest a much lower flow in deep (juxtamedullary) than in superficial cortex (Barger and Herd 1973). However, the only quantitative local measurements of ^{86}Kr recently presented by Passmore, Neiberger

and Eden (1977) rather suggest a similar initial washout rate throughout the cortex. Since ^{86}Kr also is more diffusible than I Ap and THO (Chimard et al. 1969) the explanation might be as suggested for H_2 . None of these studies would seem to fit well with the common compartment analysis of externally recorded ^{86}Kr washout indicating that inner cortex and outer medulla can be represented by a common devascularization rate about one third that of outer cortex (Thorburn et al. 1963; Barger & Herd 1973). Outer medullary flow calculated from [I Ap] and THO agrees well with that obtained from ^{86}Kr by Passmore et al. (1977) but are higher than the few in situ measurements reported by Aukland & Wolgast (1968).

Uptake of ^{86}Rb , which depends on the sink effect of the large intracellular potassium pool, gives a cortical flow distribution close to that obtained with I Ap and THO (Bálint, Bartha & Fekete 1969). However, ^{86}Rb shows a relatively much greater uptake in the medulla. Two explanations would seem likely: (1) less counter current exchange of the lipid insoluble ^{86}Rb , or (2) higher extraction of ^{86}Rb in the medulla than in cortex.

In conclusion. While the flow distribution patterns obtained from I Ap and THO uptake is basically similar to that reported for other diffusible tracers, there are discrepancies which in part may be due to differences in diffusibility.

Comparison of diffusible tracers and microsphere uptake. When comparing zonal flow estimated from diffusible tracers versus microsphere uptake, one should keep in mind the different ways of uptake. While practically all M_s (15 μm) are arrested in afferent arterioles or glomeruli (McNay & Abe 1970; Ofstad, Willasven & Egenberg 1973) and therefore reflect glomerular blood flow, the diffusible tracers are probably delivered mainly by the postglomerular peritubular capillaries. Thus the low M_s uptake in the medulla is a simple consequence of the absence of glomeruli in this region. However, if the glomeruli in C_2 , the inner third of the cortex, deliver all blood flow to the medulla through the vasa recta, and in addition all blood flow to the peritubular network in C_2 , the M_s flow in C_2 should equal I Ap/THO flow in C_2 + medulla. This was not the case in any experiment. M_s flow in C_2 was in fact lower than I Ap and THO flow in C_2 alone in all 10 kidneys. Since total flows showed good agreement it follows that there must be a surplus of M_s relative to I Ap/THO flow in

the convoluted proximal tubules are located close to their glomeruli filtration per se will probably not influence the location of tracer uptake. (See below.)

The requirement of simultaneous delivery of tracer to the exchange vessels seems to be well satisfied for the cortex. An estimated passage time through the interlobular arteries of 0.1 s (probably overestimated) leads to an underestimate of outer cortical flow by only 1%.

As discussed previously (Hope et al 1976) the presence of unequilibrated arterial blood in the kidney results in overestimation of blood flow approximately corresponding to its fraction of kidney volume, i.e. only a few per cent. Similar calculations show that the same applies to venous blood present in non-exchange vessels. No appreciable influence on zonal flow ratios would be expected.

Even if the deviations from the theoretical requirements are considered acceptable, the practical problems in determining local uptake rate by the tissue sampling technique are considerable.

Since the high cortical blood flow and rapid tracer uptake necessitate a short infusion period, the timing of the arterial concentration curve to the moment of renal circulatory arrest is critical. As described under Methods (Fig. 1) the transit time through the terminal aorta may, if not accounted for, cause up to 15% overestimate of cortical blood flow. The somewhat higher flow observed in Series A than in Series B may at least in part be due to such errors. Obviously a shortening of the infusion period will increase the effect of timing error and will also preclude measurement in low flow regions. On the other hand, prolongation of the infusion period with a higher degree of saturation will increase the error in calculated flow caused by an inappropriate λ_n and by inaccuracies in the measurement of tracer concentrations in blood and tissue (Hope et al 1976; Eklöf et al 1974). Thus in the experiment shown in Fig. 3 with a 1 Ap saturation of about 50% in C, a 10% error in λ_n (—one S.D. in our estimate of λ_n for 1 Ap (Clausen et al 1979)) will give an error in calculated flow of only 5%. In another experiment with a saturation of 72% which was the highest level accepted, a 10% error in λ_n would lead to 15% error in calculated flow. In the latter case the deep flow fraction would be in error by 1.5% of total RBF, for instance 21.5% instead of 20%.

As described elsewhere, 1 Ap infusion periods of 75–300 s resulted in higher values for flow in IM

(Avg 0.74 ml/min/g) than that observed in Series A (Clausen et al 1979). This finding corroborates previous results showing a considerable initial delay in H_2 washout in IM (Aukland & Berliner 1968). Thus short infusion periods suitable for the cortex consistently cause underestimation of IM flow with diffusible tracers. Although prolonged infusion minimizes the error due to the initial delay, it does not prevent underestimation of flow due to counter exchange of tracer (Hope et al 1976).

Since we found no practical way to determine λ_n for 1 Ap in the medulla, we have assumed a value equal to that determined for the cortex. This is not quite satisfactory, but the error in the medullary flow estimate resulting from an inappropriate λ_n should be small because of the low degree of saturation (well below 50%) and probably of minor importance compared to the error mentioned above. The true total medullary blood flow is presumably considerably higher than that obtained with 1 Ap and THO (or with other diffusible tracers) but any underestimate will only strengthen the conclusion drawn from the comparison with MIs (see below).

While the theoretical and practical problems discussed above may introduce considerable error in absolute flow estimates, none of them are likely to cause great errors in the flow ratios between the various cortical zones.

Flow distribution within each zone

The small scatter of 1 Ap concentrations within cortical zones C₁ and C₂ (coefficient of variation as low as 2.5 in some expts., average 4.9 and 6.7% in C₁ and C₂ respectively) indicates a remarkable intrazonal flow homogeneity among tissue regions of 50 to 150 mg. A rough estimate of the analytical errors involved suggests that the true coefficient of variation for cortical concentrations is on average less than 3% corresponding to a coefficient of variation for blood flow of 5% or less.

The much greater scatter of cortical THO concentration is probably due to less accurate determination of β -activity. While in theory the two tracers might be equally well suited for flow measurement and have been shown to give practically identical average results, there is no doubt that in our hands the 1 Ap is the most reliable.

The greater intrazonal scatter of MIs-activity (Table 1) is explained by the rather small number of spheres in each tissue sample (100–250) (Buckberg et al 1971). However, when the activities of

- LAUSEN G, HOPE, A., KIRKEBO A, TYSSÉ BOTN L. & AUKLAND K 1977 Effect of vasodilation on distribution of microspheres and on zonal blood flow measured with diffusible indicators in the dog kidney (Abstr.) *Proc Internat Union Physiol Sci* 13 141
- KLOF B, LASSEN N A., NILSSON L., NORBERG, K., SIESJÖ B K. & TORLÖF P 1974 Regional cerebral blood flow in the rat measured by the tissue sampling technique: critical evaluation using four indicators C^{14} -antipyrine, C^{14} -ethanol, H^3 -water and Xenon¹³³. *Acta Physiol Scand* 91 1-10
- JOPE, A., CLAUSEN G & AUKLAND K 1976 Intrarenal distribution of blood flow in rats determined by ^{14}C -iodoantipyrine uptake. *Circ Res* 39 36-370.
- LETY S S. 1951 The theory and applications of the exchange of inert gas at the lungs and tissues. *Pharmacol Rev* 1-41
- LETY S S. 1960. Measurement of local blood flow by the exchange of an inert, diffusible substance. In: *Methods in medical research*, vol. 8 (ed. H. D. Brenner), pp. 228-236. Year Book Medical Publishers, Chicago
- KÜGELOHN A, KUHLE, B, KUHLE, W & OTTO K J 1959 *Die Gefäßarchitektur der Niere*. In: *Z. anglöse Abhandlungen aus dem Gebiet der normalen und pathologischen Anatomie* vol. 5 (ed. W. Bergmann and W. Doerr), pp. 9-111 Georg Thieme Verlag, Stuttgart
- McMAY J L & ABE Y 1970 Pressure-dependent heterogeneity of renal cortical blood flow in dogs. *Circ Res* 27 571-587
- MEHRAN A, GUKOD L & HOLLENBERG N K 1974 The role of angiotensin in the cardiovascular and renal response to salt restriction. *Kidney Internat* 5 348-355
- WORKWID L, OFSTAD J & WILLASSEN Y 1976 Effect of static restriction on the intracortical distribution of microspheres in the dog kidney. *Circ Res* 39 608-615
- NISSEN O I 1966. The relation between reabsorption rate and filtration rate in the superficial and deep venous drainage area of the cat kidney. *Acta Physiol Scand* 68 286-294
- OFSTAD, J., WILLASSEN Y & EGENBERG A. E. 1973 Distribution of radioisotope-labeled microspheres in the renal cortex of dogs in hemorrhagic hypotension. *Scand J Clin Lab Invest* 31 277-287
- PASSMORE J C, NEIBERGER, R. E. & EDEN S W 1977 Measurement of intrarenal anastomic distribution of krypton-85 in endotoxic shock in dogs. *Amer J Physiol* 232: H54-H58.
- PERSSON E. 1970 Water permeability in rat distal tubules. *Acta Physiol Scand* 78 364-375
- PERSSON E. & ULFENDAHL, H. R. 1970 Water permeability in rat proximal tubules. *Acta Physiol Scand* 78 353-363
- SLOTKOFF L M, LOGAN A, JOSE, P, D'AVEL LA, J & EISNER, G M 1971 Microsphere measurement of intrarenal circulation of the dog. *Circ Res* 28 158-166.
- SVANES K. & ZWEIFACH B W 1968 Variations in small blood vessel haematocrits produced in hypothermic rats by microocclusion. *Microvasc Res* 1 210-220
- THOMPSON A M, CAVERT H M, LIFSON N & EVANS, R. L. 1959 Regional tissue uptake of D_2O in perfused organs: rat liver, dog heart and gastrocnemius. *Amer J Physiol* 197 897-902.
- THORBURN O D, KOPALD H H, HERD J A., HOLLENBERG M, O'MORCHOE, C. C. C. & BARGER, A. C 1963. Intrarenal distribution of arterial blood flow determined with krypton⁸⁵ in the anaesthetized dog. *Circ Res* 13 290-307
- VAUPEL, P 1976. Effect of percentual water content in tissues and liquids on the diffusion coefficients of O_2 , CO_2 , N and H. *Pflügers Arch* 361 201-204

other parts of the kidney. As evident from Fig 5 good agreement was found in C_2 while the M_s surplus was located in C_1 . This conspicuous and consistent disparity might result from one or several of the following mechanisms:

(1) Microspheres are underrepresented in deep glomeruli relative to glomerular blood flow. This might be caused by axial streaming by a stream line effect (Svanes & Zweifach 1968) or simply by steric exclusion by narrow afferent arterioles (Mørkrid, Ofstad & Willassen 1976). According to previous studies in dogs (Slotkoff et al 1971; Mimran, Guio & Hollenberg 1974) there should be no size-dependent maldistribution of spheres with the average size and the narrow diameter range of the M_s -batches used in the present study. However, available data would not seem to exclude skimming with little or no size-dependency, i.e. even with complete uniformity of M_s diameters deep cortical flow might be underestimated.

(2) Too much IAP and THO are deposited in deep cortex and medulla relative to glomerular flow in this region.

(a) If appreciable diffusion of the tracers takes place across the interlobular arteries or if

(b) a considerable fraction of flow in the peritubular network in one cortical layer is derived from glomeruli situated in more superficial layers as previously proposed for the rat kidney (Hope et al 1976).

A model based on the assumption that mechanisms 1 and 2a are not at work suggests an inward cortical postglomerular flow component corresponding to 9% of total RBF (Fig. 8). A net inward flow of tubular fluid would have a similar effect. However, it may be calculated from the data of Nissen (1966) on the cat kidney that the inward tubular flow could maximally account for one third of the observed disparity between M_s and diffusible tracers. An estimate based on the inward directed flow in the straight segment of the proximal tubules leads to the same conclusion. With a total blood filtration fraction of 0.15 and 60% reabsorption in the proximal convolution the straight segment flow would be 6% of local flow. In comparison the estimated IAP flow from C_2 to C_1 corresponds to 18% of flow in C_1 (Fig. 8). Furthermore, since the tracer will tend to equilibrate with surrounding tissue en route to deeper regions, the actual amount of fluid crossing the zonal borders would probably have to be considerably greater. Inward transport of more

diffusible tracers, for instance H_2 and ^{86}Kr , might accordingly be smaller.

While admittedly speculative, the last explanation (2b) might be the most attractive, but the present experiments do not rule out maldistribution of M_s or interlobular artery exchange of diffusible tracers. Further discussion should therefore await more experimental data.

This work was supported in part by grants from "Eos Langfeldts Fond" and from The Norwegian Research Council for Science and the Humanities.

REFERENCES

- AUKLAND K 1967 Study of renal circulation with inert gas. Measurements in tissue. In Proc 3rd Internat. Congr. Nephrol. Washington D.C., vol. 1 (ed. G.E. Schreiner) pp 188-200. Karger, Basel.
- AUKLAND K 1976 Renal blood flow. In: *Interest. Rev. Physiol. Kidney and urinary tract physiology* 2, vol. 11 (ed. K. Thurau) pp 23-79. University Park Press, Baltimore.
- AUKLAND K & BERLINER R W 1964 Renal medullary countercurrent system studied with hydrogen gas. *Circ Res* 15: 430-442.
- AUKLAND K, BOWER B F & BERLINER R W 1964 Measurement of local blood flow with hydrogen gas. *Circ Res* 14: 164-187.
- AUKLAND K, KIRKEBØ A, LØYNING E & TYSEBØT N 1973 Effect of hemorrhagic hypotension on the distribution of renal cortical blood flow in anesthetized dogs. *Acta Physiol Scand* 87: 514-521.
- AUKLAND K & WOLGAST M 1968 Effect of hemorrhage and retransfusion on intrarenal distribution of blood flow in dogs. *J Clin Invest* 47: 488-501.
- BÄLINT P, BARTHA J & FEKETE A 1969 Intrarenal distribution of blood flow in the dog. *Acta Physiol Acad Sci Hung* 36: 1-11.
- BARGER A C & HERD J A 1973 Renal vascular anatomy and distribution of blood flow. In: *Handbook of physiology*, section 8: Renal physiology (ed. J. Orloff and R. W. Berliner) pp 249-313. American Physiological Society, Washington D.C.
- BUCKBERG G D, LUCK J C, PAYNE D B, HOFFMAN J I E, ARCHIE J P & FLICKER, D E 1971 Some sources of error in measuring regional blood flow with radioactive microspheres. *J Appl Physiol* 31: 598-604.
- CHINARD P P, THAW C N, DELEA A C & PERL, W 1969 Intrarenal volumes of distribution and relative diffusion coefficients of monohydric alcohols. *Circ Res* 25: 343-357.
- CLAUSEN G & HOPE A 1977 Intrarenal distribution of blood flow and glomerular filtration during chronic unilateral ureteral obstruction. *Acta Physiol Scand* 100: 22-32.
- CLAUSEN G, HOPE A & AUKLAND K 1979 Partition of ^{125}I -iodoantipyrine among erythrocytes, plasma and renal cortex in the dog. *Acta Physiol Scand* 107: 63-68.

The effect of transmural field stimulation on the serotonin content in rat duodenal enterochromaffin cells—in vitro

PETTERSSON H, AHLMAN A, DAHLSTRÖM J, KEWENTER J, LARSSON J & LARSSON P. A.

Section of Neurobiology and the Department of Surgery III, University of Göteborg, Sweden

PETTERSSON H, AHLMAN A, DAHLSTRÖM J, KEWENTER J, LARSSON J & LARSSON P. A. The effect of transmural field stimulation on the serotonin content in rat duodenal enterochromaffin cells—in vitro. *Acta Physiol Scand* 1979, 107, 83-87. Received 23 March 1979. ISSN 0001-6772. Institute of Neurobiology and Department of Surgery III, University of Göteborg, Sweden.

The effect of transmural field stimulation (TFS)—*in vitro*—on the serotonin (5-HT) content in enterochromaffin cells (EC) in rat duodenum was studied with a cytofluorimetric method. TFS caused a significant 25% decrease of 5-HT in EC. The presence of tetraoxygen or d,l-propranolol in the stimulation bath antagonized the effect of TFS. In biopsies from rats pretreated with 6-OH-dopamine TFS had no effect on the 5-HT content in EC. The results of the present study strongly suggest that the TFS induced decrease in 5-HT content is due to direct neural, probably β -adrenoceptor mediated influence on the EC.

Key words: Rat enterochromaffin cells, duodenal mucosa, field stimulation, cytofluorimetry, serotonin release, adrenergic mechanism.

The serotonin (5-HT) containing enterochromaffin cell (EC) is a basophilic gut endocrine cell with unique handling properties according to the APUD concept (Pearse 1969). Different populations of EC may store polypeptides beside the amine e.g. histamine, substance P or enkephalin (Pearse et al. 1974; Pearse & Polak 1974; Polak et al. 1976; Almets et al. 1978).

EC are predominantly of the open type, i.e. with a brush of microvilli protruding into the gut lumen (Fujita & Kobayashi 1971). Luminal stimuli e.g. acid pH, hypertonic sugar solution and an increased intraluminal pressure may cause degranulation of the cells and increased levels of 5-HT in the portal blood or in the lumen (Resnick & Gray 1960; Kobayashi & Fujita 1973; O'Hara et al. 1960; Drapanis et al. 1960; Bulbring & Crema 1959). The parallel decrease of 5-HT content in EC and increase of portal 5-HT suggest that the amine is released from the EC upon stimulation. Also neurogenic release mechanisms have been sug-

gested for 5-HT since stimulation of the splanchnic as well as of the vagal adrenergic nerve fibers to the gut causes similar changes (Burks & Long 1966a; Tansy et al. 1971; Ahlman et al. 1976a). Results from cytofluorimetric studies of rat duodenal biopsies incubated *in vitro* with adrenergic agonists and antagonists indicate that at least a β -adrenoceptor mechanism is involved in the release of 5-HT from EC (Pettersson et al. 1978).

In vitro methods offer several advantages in the study of receptor and transmission mechanisms, since (a) a well defined external environment regarding e.g. pH, ionic composition and drug concentrations can be established and (b) secondary effects from changes in secretion and regional blood flow caused by nerve stimulation and drugs do not influence the results. Transmural field stimulation (TFS) of isolated tissues *in vitro* causes an activation of nerve fibers within the specimen (Paton 1955; Farnbo 1977).

The aim of the present investigation was to fur-

Table 1 The effect of TFS (18 V 2 ms 10 Hz, 15 min) on the 5-HT content in duodenal EC from normal rats and rats pretreated with 6-OH DA

Mean value and S.E. of 20 cells from each specimen of each individual rat is shown. Difference from incubated/unstimulated control indicated by * ($P < 0.01$). Original values given within brackets to illustrate variation in fluorescence yield irrespective of simultaneous tissue processing

Normal rats		6-OH DA rats	
Unstimulated	Stimulated	Unstimulated	Stimulated
100 ± 7.3 (525 ± 38)	47 ± 3.2**	100 ± 4.4 (566 ± 25)	89 ± 4.4
80 ± 7.9 (444 ± 35)	72 ± 3.6**	100 ± 5.7 (509 ± 29)	81 ± 4.7*
80 ± 6.5 (385 ± 25)	73 ± 4.4**	100 ± 5.6 (347 ± 22)	98 ± 3.6
80 ± 6.1 (400 ± 4)	64 ± 4.2**	100 ± 7.7 (170 ± 13)	104 ± 6.4
80 ± 9.1 (486 ± 44)	73 ± 6.7**	100 ± 8.7 (137 ± 12)	96 ± 6.3
80 ± 4.3 (540 ± 23)	79 ± 5.0**	100 ± 6.1 (180 ± 11)	107 ± 8.3
80 ± 5.5 (396 ± 22)	101 ± 7.8		
80 ± 2.2 (168 ± 4)	64 ± 5.7**		
80 ± 2.8 (175 ± 5)	92 ± 5.4		
80 ± 5.4 (197 ± 11)	82 ± 5.8**		
80 ± 7.2 (161 ± 12)	89 ± 7.9		
80 ± 5.0 (197 ± 12)	62 ± 3.6**		
Mean 100 ± 1.7	75 ± 4.3*	100 ± 2.6	95 ± 3.9

There was no obvious decrease in the fluorescence intensity of the adrenergic nerve terminals

When tetrodotoxin (10^{-6} M) was added to the stimulation medium no significant change in EC fluorescence was demonstrated in 5/6 animals (Table 2). The contractile response at the TFS was minimal or absent with tetrodotoxin in the bath but the procedure was judged effective by the appearance of gas at the electrodes. Propranolol (10^{-6} M) in the medium had a blocking effect on the decrease of 5-HT in EC (Table 2) but did not block the motor response. The blocking effect of tetrodotoxin and propranolol in the bath was statistically significant ($P < 0.05$) as compared to TFS without drugs added. In the gut specimens of the 6-OH-DA pretreated

rats TFS had no effect in 5/6 animals (Table 1). In these specimens no adrenergic terminals could be observed in the mucosa and submucosa. The almost complete absence of adrenergic nerve terminals was also controlled in stretch preparations of uddes from these animals. A normal motor response was obtained.

DISCUSSION

From nerve stimulation expts in vivo there is evidence for a neurogenic release of 5-HT from EC into the portal stream and possibly also to the gut lumen (Ahlin et al 1978). However such stimulation of the vagal and splanchnic nerves had profound effects on the motility blood flow and secretion of the intestine: effects that may influence the functional state of the EC. Burks and Long (1966b) reported that stimulation of intestinal motility caused release of 5-HT from the gut. Therefore when testing the hypothesis of a neurogenic release of 5-HT from EC, in vitro techniques may offer an advantage being test systems without most of these secondary effects. On the other hand the biopsies are then transferred from their natural environment to artificial media and long neuronal pathways are interrupted.

The TFS procedure used in the present study caused a well reproducible decrease of the 5-HT

Table 2 The influence of tetrodotoxin and propranolol on the effect of TFS on the 5-HT content in duodenal ED

The ratio stimulated/unstimulated is given for each rat. Difference from specimens stimulated in Krebs' solution only indicated by * ($P < 0.05$)

Krebs	Tetrodotoxin 10^{-6} M	Propranolol 10^{-6} M
Mean 0.75 ± 0.04	0.91 ± 0.02*	0.93 ± 0.02*

* See Table 1 - Normal rats

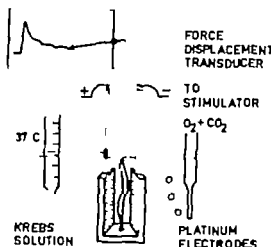


Fig 1 Experimental model. The gut strip was mounted between two parallel platinum meshwork electrodes 7 mm apart in an open plexiglass chamber containing oxygenated Krebs solution (37°C) with the drug to be tested. The lower end of the specimen was fixed to the bottom of the chamber and the upper end connected to a force displacement transducer. The electrodes were connected to a stimulator.

ther study the neural influence on the EC with special regard to adrenergic components using TFS.

MATERIAL AND METHODS

30 Sprague Dawley rats (males, 250 g) were killed by decapitation. The proximal 5 cm of the duodenum was dissected free and placed in ice-cold Krebs solution. The gut was then cut into 12 × 6 mm² longitudinal strips including all 3 layers of the wall. Each strip was then divided into two longitudinal halves, one half to be stimulated and the other to serve as a control. The strip to be stimulated was mounted between two parallel platinum meshwork electrodes (7 × 1 mm²) 7 mm apart in an open plexiglass chamber (Fig. 1). The lower end of the specimen was fixed to the bottom of the chamber and the upper end connected to a force displacement transducer to record the contractile strength developed at TFS. The stimulation bath contained Krebs solution (37°C oxygenated with 5% CO₂, 95% O₂) with the drug to be tested. Each control strip was incubated simultaneously in the same medium during the same period of time as the stimulated strip. The specimens were kept in the medium for equilibration 10 min before stimulation. The stimulation was given from a Grass S9 stimulator using the following parameters: 18 V, 2 ms, 10 Hz during 15 min. The current through the bath was 5–6 mA/mm². The stimulation procedure was judged to be effective by a contractile response from the specimen and by the development of free gas at the electrodes.

Drugs. The drugs used for incubations were tetradotoxin (10⁻⁶ M (Sigma chem.)) and D-1-propranolol (10⁻⁶ M (Indalab[®] ICI)). 6 rats were pretreated with 6-OH dopamine (Sigma chem.) 100 mg/kg b.wt. i.p. 48 h before

the experiments. No further drug incubation with strips from these animals was done.

Histochemistry and cytofluorimetry. After incubation and stimulation the gut specimens were immersed frozen in liquid propane, freeze-dried and treated with formaldehyde vapour generated from paraformaldehyde for fluorescence microscopy according to the Fick strip technique (for description and references see O. & Jonsson 1967). The cytofluorimetric method has been described in detail earlier (Ahlmén et al. 1976). Cytofluorimetry was performed with a Leitz W photometer with an illuminator for incident light positioned to isolate the activation maximum of the fluorophore at 410 nm. The measuring diaphragm fixed at a diameter of about 20 µm, enough to expose the longitudinally cut EC. From each specimen the fluorescence intensity of 20 EC was recorded. A relative measure of the 5-HT level of each EC, fluorescence intensity after 40 s of ultraviolet light was recorded. For each cell the background fluorescence was checked separately and subtracted from the mean intensity of the cell. These values were expressed in arbitrary units and fed into a Hewlett Packard 9811A computer system. The mean value of intracellular 5-HT fluorescence intensity in each control, i.e. the section from parallel-incubated unstimulated strips, was set to 10. The mean value and S.E. for each stimulated specimen was then compared to its unstimulated control. Student's *t*-test was used for comparisons within each animal; a *t*-test for paired and unpaired data were used for comparisons within and between groups of animals. *P*-value < 0.05 was regarded as significant. The frequency distribution of the fluorescence intensities from each sample was normal.

All specimens from one animal were processed simultaneously and all measurements were performed by same person under identical conditions using coded slides. In order to standardize the cytofluorimetric measurements the following criteria were used: (1) Specimens must have no obvious amine diffusion in adrenergic nerves or EC. (2) EC must be sectioned through the lamina propria, the nucleus and the luminal process. (3) Only located in the crypts were measured. (4) In each field view the EC of medium fluorescence intensity (subjectively judged), fulfilling criteria 1–3 was selected for measurement.

RESULTS

Nonstimulated specimens either incubated in Krebs solution only or with any of the drugs added demonstrated distinct beaded adrenergic nerve terminals with blue-green fluorescence and strongly yellow fluorescent EC.

TFS caused a significant 25% decrease of intracellular 5-HT fluorescence after 15 min of stimulation demonstrated by cytofluorimetry (Table 1). The morphology was well preserved. The

- AO C. Y. 1966 Tetradotoxin, section and their significance in the study of excitation phenomena. *Pharmacol Rev* 18: 997-1049.
- OBAYASHI S. & FUJITA, T. 1973 Eosinophilic granule release in the basal-granulated cells of the dog induced by intraluminal application of adequate stimuli in Gastro-entero-pancreatic endocrine system. A cell biological approach (ed. T. Fujita), pp. 49-58. Geka Shoin, Tokyo.
- LUNDBERG J. M., DAHLSTRÖM A., BYLOCK, A., AHLMAN H., PETERSSON G., LARSSON I., HANSSON H. E. & KEWENTER, J. 1978. Ultrastructural evidence for an innervation of epithelial enterochromaffin cells in the guinea pig duodenum. *Acta Physiol Scand* 104: 3-12.
- ALLMÖRS T. & SACHS C. 1968 Degeneration of adrenergic nerves produced by 6-hydroxydopamine. *Europ J Pharmacol* 3: 89-97.
- THARA R. S., FOX, R. D. & COLE, J. W. 1960. Serotonin release mediated by intraluminal mucosa solution. *Surg Forum* 10: 14-218.
- ATON W. D. M. 1955 The response of the guinea pig ileum to electrical stimulation by coxial electrodes. *J Physiol (Lond)* 107: 40-41.
- PEARSE, A. G. E. 1969 The cytochemistry and ultrastructure of polypeptide hormone producing cells of the APUD series and the embryologic, physiologic and pathological implications of the concept. *J Histochem Cytochem* 17: 303-313.
- PEARSE, A. G. E., POLAK, J. M., BLOOM S. R., ADAMS C., DRYBURGH J. R. & BROWN C. 1974. Enterochromaffin cells of the mammalian small intestine: the source of motilin. *Virchows Arch B Cell Pathol* 16: 111-120.
- PEARSE, A. G. E. & POLAK, J. M. 1975 Immunocytochemical localization of substance P in mammalian intestine. *Histochemistry* 41: 373-375.
- PETERSSON G., DAHLSTRÖM A., LARSSON I., LUNDBERG J. M., AHLMAN H. & KEWENTER, J. 1978. The release of serotonin from rat duodenal enterochromaffin cells by adrenoceptor agonists studied in vitro. *Acta Physiol Scand* 103: 219-224.
- POLAK J. M., HEITZ, P. & PEARSE, A. G. E. 1976. Differential localization of substance P and motilin. *Scand J Gastroenterol* 11: 39-42.
- RESNICK, R. H. & GRAY S. J. 1966. Chemical and histologic demonstration of hydrochloric acid-induced release of serotonin from intestinal mucosa. *Gastroenterology* 42: 48-55.
- TANSY M. F., ROTHMAN O., BARLETT J., FARBER, P. & HOHENLEITNER, F. J. 1971. Vagal adrenergic degranulation of enterochromaffin cell system in guinea pig duodenum. *J Pharm Sci* 60: 81-84.
- TOBE, T., IZUMIKAWA F., SANO M. & TANAKA, C. 1976. Release mechanisms of 5-HT in mammalian gastrointestinal tract—especially vagal release of 5-HT. In: *Endocrine gut and pancreas* (ed. T. Fujita), pp. 371-380. Elsevier Scientific, Amsterdam.

content in EC. Addition of tetrodotoxin which inhibits the propagation of action potentials in the nerves (Kao 1966) minimized the motor response and antagonized the effect of TFS on the 5-HT content in EC. Thus the effect of TFS is mainly mediated through activation of nerves within the specimens and not a direct activation of the EC.

The β adrenoceptor antagonist propranolol had a blocking effect equal to tetrodotoxin on the 5-HT decrease in EC upon TFS. This effect of propranolol may be a true β -adrenoceptor blockade or be due to its membrane stabilizing effect or possibly a combination of these mechanisms. However in biopsies from rats pretreated with 6-OH DA which causes a selective chemical destruction of adrenergic nerve terminals (Malmfors and Sachs 1968) no change in intracellular 5-HT levels could be demonstrated after TFS. This gives further support to the hypothesis of an adrenergic probably β -adrenoceptor mediated release of 5-HT from EC upon TFS. Since the motor responses in the propranolol and 6-OH DA groups remained unchanged (as was the 5-HT content in EC) the motor activity per se could not be responsible for the release of 5-HT upon the TFS. In a previous *in vitro* study where rat duodenal biopsies were incubated with various tentative transmitters it was found that not only adrenergic agonists (adrenaline, noradrenaline and isoprenaline) but also acetylcholine caused a decrease of 5-HT in EC (Pettersson et al 1978). In the rat a possible cholinergic release of 5-HT from EC has been suggested also *in vivo* since the decreased tissue concentration in the intestine and elevated portal levels upon vagal nerve stimulation could be partially blocked by atropine (Tobe et al 1976). Thus also neural mechanisms other than an adrenergic mechanism may possibly influence the EC. From a morphological point of view the EC may be influenced by several types of nervous elements. Ultrastructural studies have demonstrated autonomic nerve endings of cholinergic, adrenergic and peptidergic types in very close relation to the base of duodenal EC in the guinea pig (Lundberg et al 1978).

Previous studies (Burks & Long 1966a; Ahlman et al 1976a; Pettersson et al 1978) have indicated that splanchnic and vagal nerve stimulation via an adrenergic mechanism causes a release of 5-HT from EC into the portal circulation and possibly also into the lumen (Ahlman et al 1978). The present study strongly suggests that this release of

5-HT is due to a direct neural influence on the EC. Luminal stimuli e.g. acid pH, glucose, mechanical stimulation (Resnick & Gray 1962; Drapanas et al 1962; Biber 1973) also regulate the release of 5-HT from the EC but the relative importance of neural versus luminal stimuli is not known.

This study was supported by grants from the Swedish Medical Research Council (grants no 17X-05224, 16X-2207, 04P-4173). The Göteborg Medical Society, The Swedish Society of Medical Sciences, the Medical Faculty, University of Göteborg, the M. Bergvall's Foundation and H. and G. Jeansson's Foundation.

REFERENCES

- AHLMAN H, LUNDBERG J M, DAHLSTRÖM A & KEWENTER, J 1976a. A possible vagal adrenergic release of serotonin from enterochromaffin cells in the cat. *Acta Physiol Scand* 98: 366-375.
- AHLMAN H, DAHLSTRÖM A, KEWENTER, J & LUNDBERG J M 1976b. Vagal influence on serotonin concentration in enterochromaffin cells in the cat. *Acta Physiol Scand* 97: 362-368.
- ALUMETS J, HÅKANSSON R, SUNDLER, F & CHANG K J 1978. Leu Enkephalin-like material in nerves and enterochromaffin cells in the gut. *Histochemistry* 56: 187-196.
- BIBER, B 1973. Vasodilator mechanisms in the small intestine. An experimental study in the cat. *Acta Physiol Scand* Suppl 401.
- BURKS T F & LONG J P 1966a. Catecholamine-induced release of 5-hydroxytryptamine from peritoneal vasculature of isolated dog intestine. *J Pharm Surg* 55: 1383-1386.
- BURKS T F & LONG J P 1966b. 5-hydroxytryptamine release into dog intestinal vasculature. *Am J Physiol* 211: 619-625.
- BULBRING E & CREMA A 1959. The release of 5-hydroxytryptamine in relation to pressure exerted on the intestinal mucosa. *J Physiol (Lond)* 146: 18-28.
- CORRODI H & JONSSON G 1967. The formaldehyde fluorescence method for the histochemical demonstration of biogenic monoamines. *J Histochem* 15: 65-78.
- DRAPANAS T, McDONALD J C & STEWART J D 1962. Serotonin release following stimulation of hypertonic glucose into the proximal intestine. *Am Surg* 156: 528-536.
- FARNEBO L-O & HAMBERGER B 1970. Release of norepinephrine from isolated rat uci by field stimulation. *J Pharmacol Exp Ther* 172: 332-341.
- FUJITA T & KOBAYASHI S 1971. Experimentally induced granule release in the endocrine cells of the pyloric antrum. *Z. Zellforsch* 116: 5-40.

Importance of sodium and glucose for the establishment of a villous tissue hyperosmolality by the intestinal countercurrent multiplier

JAN-AXEL HALLBÄCK, MATS JODAL and OVE LUNDGREN

Department of Physiology University of Göteborg, Sweden

HALLBÄCK, J. A., JODAL, M. & LUNDGREN, O. Importance of sodium and glucose for the establishment of villous tissue hyperosmolality by the intestinal countercurrent multiplier. *Acta Physiol Scand* 1979 107: 89-96. Received 28 Feb. 1979. ISSN 0001-6772. Department of Physiology University of Göteborg, Sweden.

The intestinal countercurrent multiplier has earlier been shown to create an increased tissue osmolality in the villi (Jodal et al. 1978). In the present paper the importance of varying the luminal contents on the creation of the villous hyperosmolality was investigated using the cryoscopic technique described by Jodal et al. (1978). The perfusion solutions used contained 0, 25 or 147 mmol Na/l and were either provided with mannitol or glucose (30 mmol/l). It was demonstrated that sodium was of particular importance for the establishment of the villous hyperosmolality while glucose only contributed significantly at low luminal sodium concentrations. It is therefore proposed that glucose only in the absence of sodium in the luminal perfusate may effectively participate in the generation of the villous tissue hyperosmolality via the countercurrent multiplication mechanism.

It has been proposed by Jodal and coworkers (Halljämle et al. 1973, Jodal 1973, Jodal et al. 1978) that the most important physiological implication of the intestinal countercurrent exchanger is its significance for water and sodium absorption by creating a hyperosmolar compartment at the villous tip. Such a hyperosmolality has been inferred to be necessary for explaining water absorption *in vivo* in the absence of or against a lumen to plasma osmotic gradient (Curran & McIntosh 1962, Schultz & Curran 1968). The tissue hyperosmolality is accomplished by the exchanger acting as a countercurrent multiplier. According to the original hypothesis of Jodal and coworkers the hyperosmolality may be established in one of two ways. First, the pumping of sodium by the enterocyte into the villous capillaries would increase sodium plasma concentration in the subepithelial capillary network compared to that in the supplying artery. Sodium may then diffuse along its concentration gradient from capillary to arterial vessel to be brought back towards the villous tip. Second, the same end result could be accomplished if the increased sodium con-

centration produces an osmotic flow of water from the central arterial vessel to the subepithelial capillaries.

It was, however, pointed out by Halljämle et al. (1973) that the absorption of any solute that increases plasma osmolality (e.g. glucose, amino acids) so as to cause a transfer of water from the central artery to the villous capillaries would produce a high tissue osmolality in the way described above for sodium. In the present paper this hypothesis was tested with regard to glucose by determining the villous osmolality when the concentration of sodium and/or glucose was varied in the fluid perfusing the intestinal lumen.

METHODS

A. Operative procedure

The experiments were performed on cats anaesthetized *i.* with chloralose (50 mg/kg b.w.) after induction with ether. The animal had been deprived of food for 24 h and had no obvious signs of intestinal infection. The operative procedures and the recordings of blood flow were similar to those described by Jodal et al. (1975), which should be

able ... Tip and mean osmolality in various portions of intestinal villi ... as total intestinal blood flow ... using different experimental procedures of this study

osmolality ... expressed in mOsm/kg H₂O and blood flow as ml/min 100 g tissue weight. n-Values after each perfusing solution refer to number of observations for the osmolality results. Mean values \pm S.E.

	Tip	From 5 to 30% of villous length	From 5 to 50% of villous length	Whole villous	Total blood flow
Jejunum					
Krebs-glucose (30)	1016 \pm 32	690 \pm 21	579 \pm 17	467 \pm 10	46 \pm 8 (9)
Krebs-mannitol (23)	891 \pm 38	645 \pm 23	579 \pm 18	469 \pm 11	31 \pm 4 (9)
Choline-glucose with 25 mmol Na (15)	737 \pm 56	578 \pm 36	513 \pm 29	429 \pm 20	30 \pm 3 (9)
Choline-mannitol with 25 mmol Na (22)	647 \pm 37	526 \pm 4	480 \pm 19	412 \pm 11	26 \pm 4 (9)
Choline-glucose (11)	658 \pm 52	509 \pm 35	462 \pm 28	401 \pm 17	40 \pm 5 (9)
Choline-mannitol (12)	465 \pm 36	410 \pm 28	391 \pm 25	361 \pm 18	25 \pm 5 (6)
Choline-methionine (15)	571 \pm 29	460 \pm 18	425 \pm 14	381 \pm 9	30 \pm 5 (6)
Ileum					
Krebs-glucose (36)	954 \pm 28	687 \pm 19	596 \pm 16	481 \pm 1	46 \pm 8 (8)
Krebs-mannitol (21)	891 \pm 40	678 \pm 32	596 \pm 16	478 \pm 14	29 \pm 3 (10)
Choline-glucose with 25 mmol Na (14)	776 \pm 46	602 \pm 29	532 \pm 1	436 \pm 11	3 \pm 3 (9)
Choline-mannitol with 25 mmol Na (23)	640 \pm 19	543 \pm 17	499 \pm 15	429 \pm 10	26 \pm 4 (9)
Choline-glucose (23)	613 \pm 19	505 \pm 15	461 \pm 13	400 \pm 8	46 \pm 7 (8)
Choline-mannitol (14)	485 \pm 53	413 \pm 34	387 \pm 26	355 \pm 15	77 \pm 6 (5)
Choline-methionine (16)	651 \pm 27	545 \pm 28	493 \pm 26	423 \pm 20	32 \pm 6 (6)

RESULTS

The results of this study are presented in Tables 4 and 5 and in Figs. 1-4. In Table 2 the measurements of tissue osmolality are presented as tip osmolality and as mean osmolality in the upper 5 to 30, 5 to 50 and 5 to 100% of villous length in the various exper-

imental groups. The figures illustrate the osmolality gradient along the villi when exposing them to the different perfusion solutions. The osmolality measurements obtained with the different solutions are compared in Tables 3 (jejunum) and 4 (ileum) using Wilcoxon's non-parametric test. Two P values are

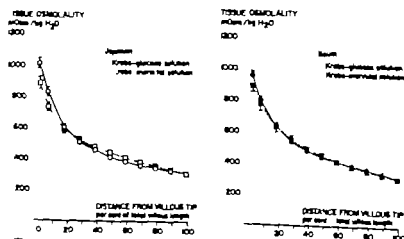


Fig. 1. Tissue osmolality in the villi of jejunum (left panel) and ileum (right panel) when exposed to isotonic Krebs-glucose (circles) and Krebs-mannitol solutions (squares). Bars denote S.E. At many points of the Fig. the S.E. is so small that it falls within the area of the symbols. For number of observations, see Table 2.

Table 1 Composition of the various solutions of this study

Concentrations are expressed in mmol/l

	Na ⁺	K ⁺	Mg ²⁺	Ca ²⁺	Choline	Cl	HCO ₃ ⁻	PO ₄ ³⁻	Glucose	Mannitol	Maltose
Krebs-glucose	147	4.7	1.2	2.5		133	25	1	30		
Krebs-mannitol	147	4.7	1.2	2.5		132	25	1		30	
Choline-glucose											
+25 mmol Na	25	4.7	1.2	2.5	122	132	25	1	30		
Choline-mannitol											
+25 mmol Na	25	4.7	1.2	2.5	122	132	25	1.2		30	
Choline-glucose											
Choline-mannitol											
Choline-maltose											

consulted for details. Briefly, total venous outflow from two sympathetically denervated intestinal segments (mid-jejunum and mid-ileum) was recorded by a drop recorder unit operating an ordinate writer. Mean arterial blood pressure was measured from the left femoral artery by a pressure transducer (Statham P23AC). Cholinergic influences were eliminated by i.v. atropine administration (1 mg/kg b.w.).

B. Recording of intestinal net water transport

Intestinal net water transport was continuously measured with a recirculating system that was coupled to the lumen of the intestinal segments and contained a reservoir (volume 700–1000 ml) to minimize recirculation. The volume change of this system was recorded with a volume transducer connected via a Y-tube to the perfusion system. Provided no motility occurred the recorded change of volume reflected net water absorption or secretion (Jodal et al. 1975). The intraluminal pressure at the outflow end of the segment was kept at about 1 cmHg O and the intestinal segment was perfused at a constant rate of approximately 1 ml/min by means of a roller pump (Model MP-4 Ismatec SA, Zürich, Switzerland). The temperature of the perfusate entering the segment was continuously monitored with a thermocouple thermometer (Electrolab, Copenhagen) and kept at about 38°C.

C. Cryoscopic technique

1. General procedure. The cryoscopic method has been presented in detail by Jodal et al. (1978) also describing the calibration procedures. Briefly, after at least 70–25 min of constant net water transport the segments were rapidly excised and momentarily frozen in isopentane pre-cooled to -150°C in liquid nitrogen. The intestinal wall was then cut obliquely in a cryostat kept at -25°C so as to give cross-sections at different levels of the villi. The tissue sections (15 µm thick) were embedded in kerosene between glass plates and transferred to a temperature controlled unit consisting of an aluminium block mounted on a Zeiss standard microscope provided with a camera. The temperature of the aluminium block could be set at any temperature between -4.5 and +0.5°C. Thawing of the intestinal tissue was achieved by stepwise increases of tissue temperature.

In the first part of this study (about one third of the

experiments) the temperature of the aluminium block was increased manually and the amount of tissue that was thawed at each temperature level was determined from photographs taken manually at the end of an equilibration period usually lasting about 10 min. A Zeiss camera (model C35) adapted to the microscope was used. Some of the results obtained with this technique has been reported in an earlier publication (Jodal et al. 1978, see Results).

In the latter part of this study the temperature of the intestinal tissue was changed automatically by a device constructed by research engineer Lars Ståge. The starting temperature, the temperature increase per step as well as the number of steps (10 or 16) could be varied. The tissue temperature was usually increased in 10 steps with a 5-min equilibration period between each step. An automatic Robot Star 50 camera was used in this series.

Determination of tissue osmolality. The temperature at which the last ice crystals thawed in a villous cross-section was taken as its melting point. The tissue melting point determined in this study was considered to be a measure of the extracellular osmolality. The magnification used (about 50 times) was too low to allow any observation of intracellular ice crystals in the villous tissue.

The thawing of the intestinal tissue always started at the villous tips and spread gradually downwards until both the crypt regions, the submucosa and the muscularis melted at largely the same temperature. The percentage of melted villous tissue for each temperature level was determined from the photographs. The data were fed into a computer which calculated the tissue osmolality at 5, 10, 20, 30, 40, 50, 60, 70, 80, 90% of villous length as well as the mean osmolality between 4 and 30, 4 and 50 and 5 and 100% villous length (Jodal et al. 1978).

D. Solutions

The intestinal mucosa was exposed to seven different solutions. The contents of these are given in Table 1 but only one type of solution was perfused through each segment studied.

E. Statistics

Statistical significance was tested using Wilcoxon's non-parametric tests (Siegel 1956).

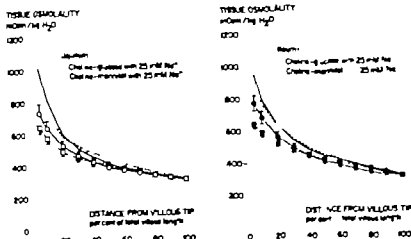


Fig. 2. Tissue osmolality in the villi of jejunum and ileum when exposed to isotonic solutions containing either choline-glucose and 25 mmol NaCl (circles) or choline-mannitol and 25 mmol NaCl (squares). As a comparison the tissue osmolality obtained with Krebs-glucose (continuous line) and Krebs-mannitol (dashed line) solutions are indicated in the Fig. For further details consult legend to Fig. 1.

served when the perfusate contained 147 mmol sodium per liter are indicated by thin lines. Comparing the two solutions with 25 mmol sodium did not reach any statistically significant difference between the osmolality values neither at the tip nor between 5 and 30% of villous length (Tables 3 and 4), although the values for the glucose containing solution always were higher.

Fig. 3 illustrates the osmotic gradients along the villi measured when the intestinal perfusate con-

tained no sodium. Data obtained with perfusates containing glucose or mannitol are presented both for jejunum and ileum in a manner similar to that seen in Figs. 1 and 2. As a comparison the osmotic gradients obtained when the perfusing solutions contained 147 (Fig. 1) or 25 mmol sodium per liter (Fig. 2) are indicated by thin lines. The difference between the tip osmolalities observed with the two sodium free solutions were statistically significant (Tables 3 and 4), the glucose experiments exhibiting

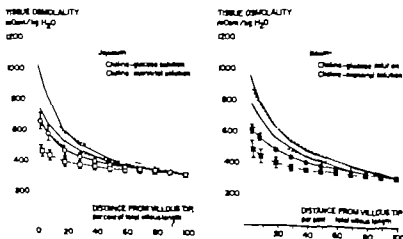


Fig. 3. Tissue osmolality in the villi of jejunum and ileum exposed to choline-glucose (circles) or choline-mannitol (squares) solutions, illustrated in the same way as in Fig. 1. For comparison the tissue osmolalities illustrated in Figs. 1 and 2 are also indicated in the Fig.

Table 3 *P* values when comparing villous tip osmolality (upper value) and mean tissue osmolality in the upper 5 to 30% of villous length (lower value) in the different experimental series performed on the jejunum. The statistical significance was tested using the nonparametric method of Wilcoxon ns = not significant

	Krebs- mannitol	Choline-glucose + 25 mmol Na	Choline-mannitol + 25 mmol Na	Choline- glucose	Choline- mannitol	Choline- mannitol
Krebs-glucose	<0.01	<0.01	<0.01	<0.01	<0.01	<0.01
Krebs-mannitol	ns	<0.01	<0.01	<0.01	<0.01	<0.01
		<0.02	<0.01	<0.01	<0.01	<0.01
		<0.03	<0.01	<0.01	<0.01	<0.01
Choline-glucose + 25 mmol Na		ns	ns	ns	<0.01	<0.02
Choline-mannitol + 25 mmol Na		ns	ns	ns	<0.01	<0.01
Choline-glucose				ns	<0.01	ns
					<0.03	<0.03
Choline-mannitol					ns	ns
						ns

given for each comparison the upper one was obtained when testing the tip osmolality values and the lower one when comparing mean osmolality values in the upper 5 to 30% of the villi.

Fig. 1 illustrates the compiled results of measuring the osmotic gradients along the villus when the perfusing solutions contained either glucose (continuous line) or mannitol (dashed line) and the sodium concentration was 147 mmol/l. Data are presented both for the jejunum (left panel) and the ileum (right panel). In the jejunum the tip osmolality when using glucose solution was significantly higher than when perfusing with mannitol solution but not so in the ileum (Tables 3 and 4). The tip osmolality of the 4 experimental groups presented

in Fig. 1 are somewhat lower than similar values presented in an earlier report (Jodal et al 1978) which may be attributed to the modified cryoscopic technique (see Methods).

Fig. 2 illustrates in the same way as in Fig. 1 the osmotic gradients along the villus when the sodium concentration in the perfusing solutions was 9 mmol/l and the perfusates contained either glucose or mannitol. The osmolality of the perfusates was maintained around 317 mOsm/kg H₂O by addition of choline chloride (Table 1). The results obtained with the perfusate containing glucose (continuous line) or mannitol (dashed line) are presented both for the jejunum (left panel) and the ileum (right panel). For comparison the osmotic gradients ob-

Table 4 *P* Values when comparing villous tip osmolality (upper value) and mean tissue osmolality in the upper 5 to 30% of villous length (lower value) in the different experimental series performed on the ileum. The statistical significance was tested using the nonparametric method of Wilcoxon ns = not significant

	Krebs- mannitol	Choline-glucose + 25 mmol Na	Choline-mannitol + 25 mmol Na	Choline- glucose	Choline- mannitol	Choline- mannitol
Krebs-glucose	ns	<0.01	<0.01	<0.01	<0.01	<0.01
Krebs-mannitol	ns	<0.03	<0.01	<0.01	<0.01	<0.01
		<0.03	<0.01	<0.01	<0.01	<0.01
		ns	<0.03	<0.01	<0.01	<0.01
Choline-glucose + 25 mmol Na		ns	ns	ns	<0.01	ns
Choline-mannitol + 25 mmol Na		ns	ns	ns	<0.01	ns
Choline-glucose				ns	<0.01	ns
					<0.01	ns
Choline-mannitol					ns	<0.01
						<0.01

difference in two cases. In the jejunum a statistically significant difference could be demonstrated between maltose and glucose and in the ileum between maltose and mannitol.

Total blood flow in the two intestinal segments including their lymph nodes are shown in Table 2. The average blood flow in segments perfused with a solution containing glucose was consistently higher than in the corresponding groups with mannitol perfusate. No statistically significant difference could however be demonstrated between individual groups. Comparing all flow values recorded in experiments using a glucose containing perfusate with low rates in all mannitol groups revealed a highly significant difference ($P < 0.01$).

DISCUSSION

The effect of glucose on villous tissue hyperosmolality was investigated by comparing the experimental results recorded when segments of jejunum and ileum were perfused with isotonic solutions containing either glucose or mannitol. Furthermore to evaluate the sodium and glucose interdependence experiments were performed at 3 different sodium concentrations, i.e. 0.25 and 147 mmol/l (Figs. 1-3). Osmolality in the different solutions was kept constant by addition of choline (Table 1). When the sodium concentration in the perfusing solution was high (147 mmol/l) addition of glucose induced only a small rise in villous tissue osmolality compared with the mannitol solution (Fig. 1 Tables 2 and 3). The increase of tissue osmolality produced by the addition of glucose was however larger with diminishing sodium concentration, and thus the largest rise in tissue osmolality was observed when sodium concentration in the perfusing medium was zero (Tables 2 and 3). An increase of tissue osmolality with increasing sodium concentration in the intestinal perfusate was also demonstrated (Figs. 1, 3 and Table 2).

The results of the present study hence suggest that glucose may contribute to the establishment of an osmolar gradient in the villi particularly in the absence of sodium in the perfusate. This hypothesis refers that the absorbed glucose increases the blood glucose concentration in the villous capillaries (see Introduction). This can be accomplished in two ways. *In vitro* studies have provided evidence for a facilitated diffusion process at the baso-lateral membranes of the epithelium (Namer & Hopfer

1977). This process implies among other things the presence of an intracellular glucose concentration that is higher than that of plasma. *In vivo* however no such intracellular accumulation of glucose has been shown indicating the possible presence of an active transport system (Esposito et al. 1977). Both mechanisms are probably able to create the necessary increase in plasma glucose concentration mentioned above.

The insignificant effect on tissue osmolality of glucose at high sodium concentrations in the perfusate may be explained by a highly efficient and fast active transport of sodium into the intestinal capillaries making the transport of glucose quantitatively unimportant. Moreover the slight hyperemia in the glucose experiments as compared to the mannitol ones might have decreased villous osmolality by e.g. reducing the efficiency of the countercurrent multiplier (cf. Jodal et al. 1978). The results with glucose only partly corroborate the hypothesis presented by Fordtran and co-workers (Fordtran et al. 1968; Fordtran 1975), which implies that glucose is the main solute determining net water absorption. However at low or zero sodium concentration in the luminal solution this hypothesis is in better agreement with the results of the present study.

In this context it should be pointed out that the sodium concentration close to the villous surface is probably not zero under *in vivo* conditions even if the entering perfusing solution is devoid of sodium. This is for two reasons. First, there is a continuous sodium diffusion from tissue to lumen along a favorable concentration gradient. Second the sparse sodium ions may have an uneven distribution in the lumen due to a negative charge of the glycocalyx which enhances sodium concentration close to the villous surface. Therefore one cannot entirely exclude the possibility that the effect of glucose on tissue osmolality may in the sodium free perfusate be induced by enhancing active sodium transport at the brush border (Crane 1962; Schultz & Curran 1968, 1970).

In an attempt to test this possibility the intestinal segments were perfused with solutions containing maltose instead of glucose. These experiments were based on the observation by Crane and co-workers (for ref. see Caspary 1977) that glucose molecules produced by a splitting of maltose are absorbed via a sodium independent mechanism into the enterocyte. This mechanism has, however been considered to be of little quantitative impor-

Table 5 Increase in villous osmolality in the upper 5 to 30% of villous length produced by the addition of glucose to the perfusate

The increase is expressed in mOsm/kgH₂O and in % of the osmolality values observed when perfusing the intestinal lumen with a solution containing no glucose

Concentration of sodium in perfusate (mmol/l)	Jejunum		Ileum	
	mOsm/kgH ₂ O	%	mOsm/kgH ₂ O	%
147	45	7	9	1
25	52	10	59	11
0	99	24	92	22

a higher osmolality. A significantly higher mean osmolality in the upper 30% of villous length could only be demonstrated in the ileum.

The results given in Fig. 3 clearly demonstrate the importance of increasing sodium concentration in the solution perfusing the intestinal lumen, particularly in solutions devoid of glucose. Stepwise increases of the sodium content in the mannitol solutions from zero to 147 mmol/l significantly increased villous osmolality (Tables 3 and 4). In the experiments with glucose containing solutions the increase of sodium concentration from 25 to 147 mmol/l produced a statistically significant osmolality increase while the rise from zero to 25 mmol/l induced no significant effect (Tables 3 and 4).

Table 5 illustrates in another way the effect of glucose on tissue osmolality in solutions with varying sodium concentrations. This Table is based on

the average values given in Table 2. The observed increase in tissue osmolality in the upper 30% of villous length upon addition of glucose to the perfusate is most pronounced in the solutions devoid of sodium. Similar results were obtained when expressing the osmolality rise in per cent of the value observed when exposing the tissue to a glucose free solution.

In one series of experiments the intestinal mucosa was exposed to a sodium free solution containing the disaccharide maltose. The observed villous osmolality gradient is illustrated in Fig. 4. As a comparison the osmotic gradients recorded when the perfusate contained glucose or mannitol but no sodium are also shown. Comparing the tip osmolality obtained with the maltose solution with those seen with the two sodium free solutions containing glucose or mannitol showed that they were statistical

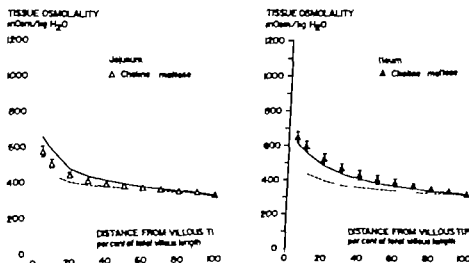


Fig. 4 Tissue osmolality in the villi of jejunum and ileum when exposed to a choline maltose solution (triangles). For comparison the tissue osmolalities obtained with choline-glucose (continuous line) and choline-mannitol (dashed line) solutions are indicated in the Fig.

Release of prostaglandin-like substances during elevations of left atrial pressure in the cat

WIBERG, J. VAAGE and E. SCOTT

Institute of Physiology, University of Oslo, Norway

WIBERG, J. VAAGE, J. & SCOTT, E. Release of prostaglandin-like substances during elevations of left atrial pressure in the cat. *Acta Physiol Scand* 1979 107: 97-103. Received 31 Jan. 1979. ISSN 0001-6772. Institute of Physiology, University of Oslo, Norway.

The purpose of the present work was to measure prostaglandin (PG)-like activity in arterial blood during acute pulmonary hypertension. Anesthetized cats with the chest opened and given positive pressure ventilation were used. A balloon in the left atrium was inflated to elevate hydrostatic vascular pressure in the lungs. Blood was pumped (10 ml/min) from carotid artery to superfuse 3 smooth muscle tissues (rat stomach strip, rat colon and chick rectum); the blood was then returned to the jugular vein by gravity. The assay tissues were pretreated with antagonists against catecholamines, histamine, serotonin and acetylcholine during the experiments. They were sensitive to calibrating doses of 2 ng/ml of PGF_{2α} and 1 ng/ml of PGE₂. 18 periods with elevated left atrial pressure (P_{LA}) (71-89 mmHg), lasting 26 min, were applied in 9 cats. This manoeuvre usually also caused systemic hypotension. 14 of these P_{LA} elevations were accompanied by increased arterial PG-like activity which rapidly subsided when the pressure was released or when indomethacin (7 mg/kg, $n=4$) was given. In 3 additional experiments it was found that pulmonary degradation of PGs was unaffected during P_{LA} elevation. Infusion of angiotensin II contracted the tissues in a pattern different from that caused by pressure elevations and the PG calibrations, and these contractions were not affected by indomethacin. This indicates that the artery tissue contractions cannot be caused by angiotensin II which alone does not increase PG-like activity in arterial blood. Consequently acute pulmonary arterial hypertension appears to stimulate PG synthesis and release in lungs of intact cats.

Key words: cats, lung, pulmonary hypertension, prostaglandins, angiotensin, superfusion method.

The lungs have large capacity for PG synthesis which is stimulated by various mechanical stimuli such as squeezing, stroking or stirring (Piper & Vane 1971; Bakhle & Vane 1974). Distortion of cell membranes has been suggested to be a common denominator in stimulation of PG synthesis and release (Piper & Vane 1971). Stretching of the lungs by increasing airway pressure has been suggested to release PGs (Berry, Edmonds & Wyllie 1971; Saul 1974; Vaage, Wiberg & Scott 1978). Pulmonary congestion and hypertension which lead to stretching of vessel walls and interstitial lung tissue may also stimulate PG synthesis. Pulmonary synthesis and release of PGs may influence pulmonary function (Mathe et al. 1977) and PGs released into the blood stream may have profound effect on the systemic circulation as well (Mabik & McGuff 1976).

We wanted to investigate whether elevation of hydrostatic pressure in the pulmonary circulation caused by elevation of left atrial pressure induced release of prostaglandin-like substances (PGLS) in the intact animal.

Additionally we have tested if increased amounts of PGLS were due to reduced pulmonary inactivation of PGs and whether PGLS were synthesized secondary to release of angiotensin II. Some of our findings have been presented in a preliminary communication (Wiberg et al. 1976).

METHODS

Cats weighing 3.3-4.3 kg were used for the experimental procedure; cats weighing 1.8-3 kg were used as blood donors. All cats were anesthetized with pentobarbitone sodium, 30-40 mg/kg, given i.p. The blood donors were

tance (Caspary 1977 Semenza 1977) and the present experiments also failed to show any conclusive effect on tissue osmolality of the disaccharide.

To summarize the present study has demonstrated that the creation of a villous hyperosmolality is dependent on the contents of the solution perfusing the intestinal lumen. It has been shown that the presence of sodium is of particular importance in this respect while glucose may be contributing at low luminal sodium concentrations.

When comparing blood flow in intestinal segments perfused with isotonic solutions with glucose or mannitol it was noted that the intestinal blood flow was significantly higher in the animals perfused with a glucose solution. It seems reasonable to propose that this vasodilatation represents a functional hyperemia produced by the luminal contents. Two underlying mechanisms seem possible: the release of hormones (Fara et al 1972) and/or the activation of local nervous reflex(es) (Biber 1973 Post et al 1975).

This research was supported by grants from the Swedish Medical Research Council (14X 2835) from the Swedish Society for Medical Sciences from Harald and Greta Jeansson's Fund from Magnus Bergvalls Stiftelse and from the Faculty of Medicine, University of Göteborg.

REFERENCES

- BIBER B 1973 Vasodilator mechanisms in the small intestine. *Acta Physiol Scand Suppl* 401.
- CASPARY W F 1977 Mechanism and specificity of intestinal sugar transport. In *Intestinal permeation* (ed M. Kramer and F. Lauterbach) pp 74-84.
- CRANE R K 1962 Hypothesis for mechanism of intestinal active transport of sugars. *Fed Proc* 21: 891-895.
- CURRAN P R & MACINTOSH J R 1966 A model system for biological water transport. *Nature (Lond.)* 193: 347-348.
- ESPOSITO G, FAELLI A & CAPRARO V 1977 A critical evaluation of the existence of an outward sugar pump in the basolateral membrane of the intestine. In *Intestinal permeation* (ed M. Kramer and F. Lauterbach) pp 107-114.
- FARA J W, RUBINSTEIN E H & NENSCHEN R R 1972 Intestinal hormones and mesenteric vasodilatation after intraduodenal application. *J Physiol* 263: 1058-1067.
- FORDTRAN J S 1975 Stimulation of active and passive sodium absorption by sugars in the large jejunum. *J Clin Invest* 55: 728-737.
- FORDTRAN J S, RECTOR F C & CARTER A S 1968 The mechanisms of sodium absorption in the human small intestine. *J Clin Invest* 47: 884-900.
- HALJAMÄE H, JODAL M & LUNDGREN O 1971 Countercurrent multiplication of sodium in intestinal villi during absorption of sodium chloride. *Acta Physiol Scand* 89: 580-593.
- JODAL M The significance of the intestinal counter-current exchanger for the absorption of sodium and free acids. Thesis, Gotab AB Göteborg 1973.
- JODAL M, HALLBÄCK D-A & LUNDGREN O 1978 Tissue osmolality in intestinal villi during isocal perfusion with isotonic electrolyte solutions. *Acta Physiol Scand* 102: 94-107.
- JODAL M, HALLBÄCK D-A & SVANVIK J A LUNDGREN O 1975 A method for the continuous study of net water transport in the feline small bowel. *Acta Physiol Scand* 95: 441-447.
- MURER H & HOPFER U 1977 The functional polarity of the intestinal epithelial cell: studies with isolated plasma membrane vesicles. In *Intestinal permeation* (ed M. Kramer and F. Lauterbach) pp 284-312.
- POST J A, CHOU C C, KVIETYS P, SIT S P, PITTMAN R & DABNEY J M 1975 Possible mechanisms of postprandial intestinal hyperemia. (Abstract) *Fed Proc* 34: 459.
- SCHULTZ, S G & CURRAN P F 1968. Intestinal absorption of sodium chloride and water. In: *Handbook of physiology* section 6, vol III pp 145-177.
- SCHULTZ, S G & CURRAN P F 1970. Coupled transport of sodium and organic solutes. *Physiol Rev* 50: 637-718.
- SEMENTA G 1977 Intestinal membrane-bound carbohydrases as sugar translocators. In *Intestinal permeation* (ed M. Kramer and F. Lauterbach) pp 171-281.
- SIEGEL S Nonparametric statistics for the behavioral sciences. McGraw-Hill New York 1956.

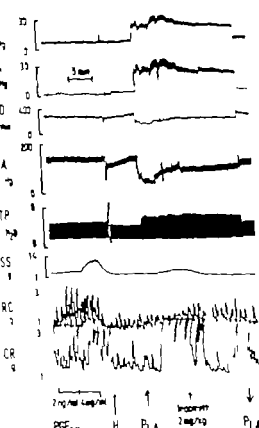


Fig. 1 The effects of elevating left atrial pressure in an anesthetized cat. (a) the chest opened and ventilated with constant tidal volume. The tracings are from the top: pulmonary arterial pressure (P_{PA}), left atrial pressure (P_{LA}), cardiac output (CO), femoral arterial pressure (P_{FA}), transpulmonary pressure (P_{TP}) and aortic tension (P). In 3 bioassay tissues continuously superfused with arterial blood (10 ml/min): rat stomach strip (RSS), rat colon (RC), and clock rectum (CR). The assay tissues are calibrated by direct administration of PGE_{2H} . If P_{LA} elevation is followed by direct administration of PGE_{2H} 10 min later, it denotes hyperinflation of the lungs. During P_{LA} elevation indomethacin was given.

formal, late baseline tension of the assay tissues had stabilized in blood and reacted to standard doses of 1 and 2 ng/kg of PGE_2 and 2 and 4 ng/kg of PGE_{2H} . To counteract the tendency towards spontaneous airways collapse and microvascular leakage the lungs were inflated to peak P_{TP} of 70 cm H_2O for a few seconds 5 min before elevation of P_{LA} . The left atrial balloon, as inflated to give elevation of P_{LA} of 70–80 mmHg. Some cases the highest P_{LA} which the animals could endure with stable, although low level, systemic blood pressure and cardiac output, was employed. Most animals consecutively pressure elevations are performed with intervals of at least 30 min. PO calibrations are performed between each test.

To investigate whether pulmonary hypertension and

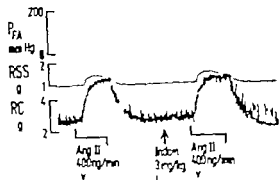


Fig. 2 Effect of infusing angiotensin II (L) to an anesthetized cat (cardiac output 400 ml/min) on femoral blood pressure (P_{FA}) and 2 bioassay tissues continuously superfused by arterial blood (10 ml/min): rat stomach strip (RSS) and rat colon (RC) before and after administration of indomethacin to block PG synthesis.

congestion influenced pulmonary inactivation of PGs, cat were prepared as described but they were given indomethacin (2 mg/kg L) before tests. In the control situation no infusion of PGE_2 was given at dose which contracted the assay tissues corresponding to about 2 ng/ml. When the assay tissues had reached plateau P_{LA} was increased with the infusion of PGE_2 going to test if change in PGE_2 concentration in arterial blood occurred in relation to pressure elevation.

Calculating pulmonary inactivation of PGE_2 . Mixed venous concentration of PGE_2 during infusion was calculated by dividing the amount infused (ng/min) with the cardiac output (ml/min). Per cent inactivation was estimated after the following formula: $[(1 - b)/a] \cdot 100\%$ where a is mixed venous concentration of PGE_2 , and b is the concentration in arterial blood found by bioassay.

Pulmonary and cardiovascular effect of elevation of P_{LA}

When the balloon in the left atrium was inflated P_{LA} and P increased and remained elevated until the balloon was deflated. Simultaneously P_{TP} increased moderately whereas cardiac output P and pulmonary vascular resistance decreased. These changes in P_{LA} and P are presented in Table 1. Pulmonary and cardiovascular changes in the same model have previously been described in more details (Hauge-Øie & Aarneth 1977).

Release of PGLS

A total of 18 P_{LA} elevations were performed in 9 cat (Table 1). During 14 of these elevations the assay tissues contracted suggesting release of PGLS within a couple of min (Fig. 1). The contractions were maintained but subsided rapidly when

Table 1 Effect of increased P_{1A} on PG release

Cat no	Pre-sure elevation (no)	P_{1A} (mmHg)	Duration of P_{1A} elevation (min)	PG-like substances (estimated as PG_{1-5})	P before and during P_{1A} elevation (mmHg)	Indomethacin infused
1	1	4	20	0	130-170	
1	1	4	6	0	130-170	
1	1	43	1	4	110-100	
1	4	1.5	1	1	80-70	
1	5	—	7	PG 1.5	70-65	
	1	5	26	1	110-85	
	1	5	1	0	110-85	
3	1	2	11	4	90-60	
4	1	30	10	—	140-85	
5	1	5	20	3	110-5	+
5	1	33	22	—	110-60	
5	1	30	4	5	90-5	+
6	1	35	16	PG 1.5	110-80	
	1	32	15	—	110-80	
7	1	40	13	0	90-65	
	1	30	10	PG 1.5	80-70	
8	1	30	1	—	90-70	
9	1	31	1	PG 1.5	90-70	+

PG 1.5 indicates that type of PG could not be specified

heparinized with 500 IU/kg and exsanguinated by cardiac puncture. To each 100 ml of this blood was added 1000 IU dry powder heparin. The surgical procedures have previously been described in detail (Vaage, Bæ & Hagenstad 1974).

Ventilation. A tracheal cannula was inserted a muscle relaxant (Allsterrine, Hoffmann-La Roche, 0.5 mg/kg) was given and positive pressure ventilation with constant tidal volume was started. End-expiratory pre-sure was kept at +1.5 cm H₂O by means of a water seal. The respiratory frequency was 4/min and the tidal volume was adjusted so as to keep pH in arterial blood between

7.35-7.45 at the onset of each experiment and was then kept at this level throughout the experiment. Tracheal pressure which in this model equals transpulmonary pressure (P_{1A}) was recorded by a Statham P31Dx transducer via a side-arm of the tracheal cannula.

Systemic and pulmonary pressures. The thorax was opened widely by plating the sternum. Polyethylene catheters were introduced into the femoral artery and into the pulmonary artery through the right ventricular wall for recording of femoral arterial pressure (P_1) and pulmonary arterial pressure (P_{1A}) respectively. A balloon catheter (Dales No. 6) was placed into the left atrium to record left atrial pressure (P_{1A}). P_{1A} could be elevated by inflating the balloon. All pressures were monitored by Statham transducers connected to a Ciba polygraph (Model 7B, Ciba Instrument Co., Quinsy, Mass., U.S.A.). Cardiac output (min. coronary flow) was measured by an electromagnetic flow probe placed around the ascending aorta. Both pulsatile and mean flow were recorded by a Systron square wave flowmeter (type 1 Systron Ltd, Surrey) connected to the Ciba polygraph.

Bleeding. A modification of the blood bath method

technique (Vane 1969) was used as described by Vane, Wiberg & Scott (1976). When the surgical procedure was completed the rat were given 1000 IU/kg of heparin from a catheter in the left arterial artery. 10 ml/min blood was pumped to superfuse a series of a rat stomach strip (RSS), rat colon (RC) and hind leg (CR). The blood then returned to a pig lavage by gravity. The tissues were pretreated with histamine, acetylcholine, histamine, serotonin and acetylcholine (Vaage, Wiberg & Scott 1976). In 4 experiments strips of rabbit aorta (RBA) were included as a flowmeter test in of the aorta tissues were recorded by semiconducting transducer elements connected to the Ciba polygraph. Upstream to the assay tissues standard doses of PG 1.5, PG 1.5 or angiotensin II were infused sublingually.

Experiments. When the extracorporeal circuit was started at whole blood was infused to compensate for the blood loss into the extracorporeal circuit (20-25 ml). The blood alone isotonic saline or dextran (Macrodex 6 Pharmacia, Sweden) was given throughout the experiment whenever necessary to maintain blood pressure and cardiac output.

Effect of PG on PG release. Indomethacin dissolved in phosphate buffer (5 mg/ml) was given 1 mg/kg to inhibit PG synthesis (Vane 1971).

pH measurement. Arterial blood were carried over with an ABL-Base Analyzer PHM 1 Radiometer, Copenhagen, Denmark.

Hematocrit. was determined in triplicate by a microhematocrit centrifuge.

Chemicals. were determined in plasma with a modified Thermo Chromometer (modified instrument, Inc., Needham Heights, Mass., U.S.A.).

Pressure. Pressure of pressure elevation were per-

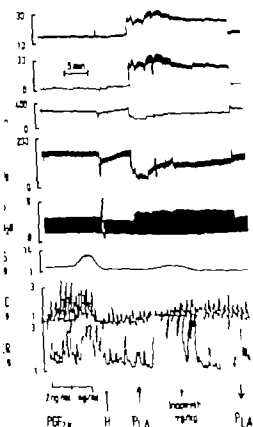


Fig. 1 The effect of elevating left atrial pressure in an anesthetized cat with the chest opened and ventilated with constant tidal volume. The tracings are from the top: pulmonary arterial pressure (P_{fa}), left atrial pressure (P_{la}), cardiac output (CO), femoral arterial pressure (P_{fa}), intrapulmonary pressure (P_{ip}) and nonmetric tension in 3 bioassay tissues continuously superfused with arterial blood (10 ml/min): rat stomach strip (RSS), rat colon (RC), and chick rectum (CR). The assay tissues are calibrated by direct administration of $PGF_{2\alpha}$. H indicates hyperinflation of the lungs. During P_{la} elevation indomethacin was given.

formed then baseline tension of the assay tissues had stabilized in blood and reacted to standard doses of 1 and 2 µg/ml of $PGF_{2\alpha}$ and 2 and 4 µg/ml of $PGF_{2\alpha}$. To counteract the tendency towards spontaneous normoys collapse and microelectrodes the lungs were inflated to peak P_{ip} of 20 cm H_2O for a few seconds 5 min before elevation of P_{la} . The left atrial balloon was inflated to give P_{la} of 20–40 mmHg. In some cases the highest P_{la} which the animals could endure with stable although lowered, systemic blood pressure and cardiac output, was employed. In most animals consecutive pressure elevations are performed with intervals of at least 30 min. PO calibrations are performed between each test.

To investigate better pulmonary hypertension and

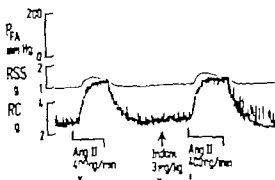


Fig. 2 Effects of infusing angiotensin II (L) to an anesthetized cat (cardiac output 400 ml/min) on femoral blood pressure (P_{fa}) and 2 bioassay tissues continuously superfused by arterial blood (10 ml/min): rat stomach strip (RSS) and rat colon (RC) before and after L administration of indomethacin to block PG synthesis.

congestion influenced pulmonary bioactivity of PGs, cat were prepared as described but they were given indomethacin (2 mg/kg) before tests. In the control situation an infusion of PGE_2 was given at a dose which contracted the assay tissues corresponding to about 50% of the maximum. When the assay tissues had reached plateau P_{la} was increased with the infusion of PGE_2 going, to test if change in PGE_2 concentration in arterial blood occurred in relation to pressure elevation.

Calculation of pulmonary concentration of PGE_2 . Mixed venous concentration of PGE_2 during infusion was calculated by dividing the amount infused (µg/min) with the cardiac output (ml/min). Per cent inactivation was estimated after the following formula: $[(1 - b/a) \times 100\%]$ where a is mixed venous concentration of PGE_2 and b is the concentration in arterial blood found by bioassay.

Pulmonary and cardiovascular effects of raised P_{la}

When the balloon in the left atrium was inflated, P_{la} and P_{fa} increased and remained elevated until the balloon was deflated. Simultaneously P_{ip} increased moderately whereas cardiac output, P_{fa} and pulmonary vascular resistance decreased. These changes in P_{la} and P_{fa} are presented in Table 1. Pulmonary and cardiovascular changes in the same model have previously been described in more details (Hauge-Bo & Aarseth 1977).

Release of PGLS

A total of 18 P_{la} elevations were performed in 9 cats (Table 1). During 14 of these elevations the assay tissues contracted suggesting release of PGLS within a couple of min (Fig. 1). The contractions were maintained but subsided rapidly when

Table 1 Effect of increased P_{LA} on PG release

Cat no	Pressure elevation no	P (mmHg)	Duration of P_{LA} elevation (min)	PG-like substances (estimated as PGE_{2m})	P_i before and during P elevation (mmHg)	Indomethacin infused
1	1	24	70	0	130-170	
1		42	6	0	130-170	
1	3	43	1	4	110-100	
1	4	25		1	80-70	
2	5	1	7	PGLS	70-65	
2	1	79	26	1	110-85	
2	2	26	21	0	110-85	
3	1	3	11	4	90-60	
4	1	30	10	2	140-85	
4		28	70	3	135-75	+
5	1	33	11		125-80	
5	2	30	4		95-75	+
6	1	30	16	PGLS	115-80	
7	1	49	15	2	115-80	
7	2	40	13	0	90-65	
7	3	30	10	PGLS	85-70	
8	1	10	1		90-70	+
9	1	11	1	PGLS	90-70	+

PGLS indicates that type of PG could not be specified

heparinized with 500 I.U./kg and exsanguinated by cardiac puncture. To each 100 ml of this blood was added 1000 I.U. dry power heparin. The surgical procedures have previously been described in detail (Vaae, Bo & Hognestad 1974).

Ventilation. A tracheal cannula was inserted a muscle relaxant (Alloferine® Hoffmann-La Roche 0.5 mg/kg) was given and positive pressure ventilation with constant tidal volume was started. End-expiratory pressure was kept at +1.5 cm H₂O by means of a water seal. The respiratory frequency was 4/min and the tidal volume was adjusted so as to keep pH in arterial blood between 7.35-7.45 at the onset of each experiment and was then kept at this level throughout the expt. Tracheal pressure which in this model equals transpulmonary pressure (P_{TP}) was recorded by a Statham P23 De transducer via a side-arm of the tracheal cannula.

Surgical procedure. Pre- and post-flow recordings. The thorax was opened widely by splitting the sternum. Polyethylene catheters were introduced into the femoral artery and into the pulmonary artery through the right ventricular wall for recording of femoral arterial pressure (P_a) and pulmonary arterial pressure (P_p) respectively. A balloon catheter (Folote No. 8) was placed into the left atrium to record left atrial pressure (P_{LA}). P_{LA} could be elevated by inflating the balloon. All pressures were monitored by Statham transducers connected to Grass polygraph (Model 7B Grass Instruments CO Quincy, Mass. USA). Cardiac output (minus coronary flow) was measured by an electromagnetic flow probe placed around the ascending aorta. Both pulsatile and mean flow were recorded by a Nycotron square wave flowmeter (type 37° Nycotron A/S Norway) connected to the Grass polygraph.

Blood bath. A modification of the blood-bathed organ

technique (Vane 1969) was used as described by Vane, Wiberg & Scott (1978). When the surgical procedure was completed the cats were given 1000 I.U./kg of heparin i.v. From a catheter in the left carotid artery 10 ml/min of blood was pumped to superfuse a series of assay tissues: rat stomach strip (RSS), rat colon (RC) and chick rectum (CR). The blood then returned to a jugular vein by gravity. The tissues were pretreated with blockers against catecholamines, histamine, serotonin and acetylcholine (Vaae, Wiberg & Scott 1978). In 4 expts spirally cut strips of rabbit aorta (RbA) were included as well. Isometric tension of the aorta tissues were recorded by semiconductor transducer elements connected to the Grass polygraph. Upstream to the assay tissues standard doses of PGE_2 , PGE_{2m} or angiotensin II were infused for calibration.

Transfusion. When the extracorporeal circulation was started cat whole blood was infused to compensate for the blood loss into the extracorporeal circuit (70-150 ml). Cat blood alone, isotonic saline or de-tran (Macroderm 6° Pharmacia Sweden) was given throughout the expts whenever necessary to maintain blood pressure and cardiac output.

Inhibition of PG synthesis. Indomethacin dissolved in a phosphate buffer (2.5 mg/ml) was given (1 mg/kg) to inhibit PG synthesis (Vane 1973).

pH measurement. In arterial blood were carried out with an Acid-Base Analyzer PBM 71 Radiometer Copenhagen Denmark.

Hematocrit was determined in duplicate by a microhematocrit centrifuge.

Osmolality was determined in plasma with an Advanced Digimatic Osmometer (Advanced Instruments, Inc. Needham Heights, Ma. USA).

Experimental protocol. Pressure elevations were per-

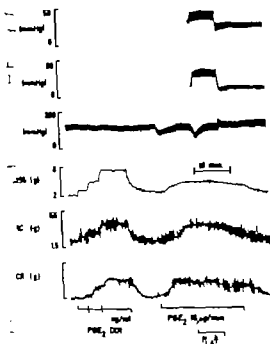


Fig. 4. Effect of P_{LA} elevation on pulmonary degradation of infused PGE_2 . The tracings are pulmonary arterial pressure (P_{PA}), left atrial pressure (P_{LA}), femoral arterial pressure (P_A), and isometric tension in 3 bioassay tissues continuously superfused with arterial blood (10 ml/min): rat stomach strip (RSS), rat colon (RC) and chick rectum (CR). Indomethacin 2 mg/kg was given before the start of the tracings. The tissues were calibrated by PGE_2 and the lungs hyperoxygenated (///). P_{LA} was elevated during an infusion of PGE_2 .

Pulmonary hypertension and inactivation of PGE_2

This was investigated in 3 cats given indomethacin to prevent PG synthesis. After calibration of the assay tissues PGE_2 was infused at a dose which caused assay tissues contractions corresponding to about ng/ml in arterial blood. Inactivation was found to be between 81 and 97% and was not influenced by elevation of P_{LA} (Table 2) (Fig. 4).

Hematocrit (hct) and osmolality

At the onset of each expt. hct was 27–35 (range) and declined to 15–28 (range) throughout the expt., probably due to hemodilution caused by transfusions.

Plasma osmolality was unchanged at 370–328 mosmol/l throughout each expt. It did not change during pressure elevations.

DISCUSSION

In the present work we have focused on increased hydrostatic pressure in the pulmonary circulation as a possible stimulus of PG synthesis and release from intact cat lungs. Inflation of a balloon in the left atrium causes pulmonary hypertension and congestion as well as systemic hypotension (Hauge-Bo & Aarseth 1977). Simultaneously the bioassay tissues contracted indicating release of PGLS. The presently used bioassay tissues are specifically sensitive to PGs (Piper & Vane 1971). Counteracting their contractions by administration of indomethacin, an inhibitor of PG synthesis, is further proof that PGLS really were released since PG release represents de novo synthesis (Piper & Vane 1971).

The assay tissues were calibrated by known concentrations of the "classical" PGE_2 and $PGF_{2\alpha}$. Due to the different contraction pattern of the 3 tissues, the PGLS released could be classified as PGE_2 or $PGF_{2\alpha}$ -like material. However during the conversion of arachidonic acid (AA) in lungs only a minor fraction is transferred into PGE_2 and $PGF_{2\alpha}$. A major fraction of the endoperoxide intermediates (PGG_2 and PGH_2) is converted to the highly unstable but biologically very active thromboxane A (TxA_2) (Hamberg, Svensson & Samuelsson 1975). Conceivably endoperoxides and TxA_2 are released in far higher concentrations than PGE_2 and $PGF_{2\alpha}$ in the present expts. Our assay tissues are also sensitive to TxA_2 and endoperoxides (Hamberg et al 1975; Bunting, Moncada & Vane 1976). The use of the RbA to detect RCS which is a mixture of TxA_2 and endoperoxides (Hamberg, Svensson & Samuelsson 1975; Samuelsson 1976) confirmed the release of these intermediates. Recent investigations have indicated that AA in the lungs is also transformed into the vasodilatory PGI (Dusting et al 1978). PGI is also able to contract the RSS and the CR (Ormrod, Moncada & Vane 1977). Consequently the presently used on-line bioassay may reflect the biological activity and variety of substances formed during the biological conversion of AA.

In the present expts. we could not detect any release of PGLS in 4 of the 18 elevations of P_{LA} . This might indicate that release is not a constant phenomenon, or that in some expts. the amounts released were too small to be detected. The release amounts which were detected, are close to the lower level possible to detect by bioassay. Release of

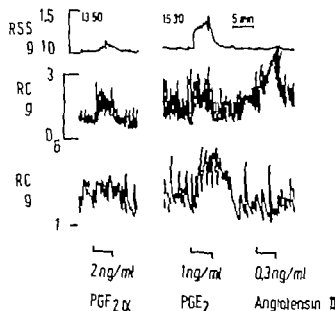


Fig. 3 Typical effects of standard doses PGE_2 , $PGF_{2\alpha}$ and angiotensin II on 3 bioassay tissues superfused with arterial blood (10 ml/min) from an anesthetized cat. The assay tissues are from the top: rat stomach strip (RSS), rat colon (RC) and chick rectum (CR).

P_{1A} was returned to normal. When compared to the pattern of tissue contractions obtained by standard doses of PGE_2 and $PGF_{2\alpha}$, $PGF_{2\alpha}$ like material (1–4 ng/ml) was released in 10 cases. In the remaining 4 the contractions could not be matched by the calibrations. The tissues usually contracted to 1 ng/ml of PGE_2 and 1–2 ng/ml of $PGF_{2\alpha}$. During control periods (P_{1A} 1–5 mmHg) no definite change in PG-like activity was observed.

During 4 elevations of P_{1A} no release of PGLS was detected. The experimental conditions in these 4 situations in 3 cats were not different from the rest of the group (Table 1). In all these cats, however, release of PGLS occurred during other pressure elevations (Table 1).

During 2 pressure elevations gross alveolar edema developed, judged from foam pouring out of the

trachea, and P_{1A} increased throughout pressure elevation and did not normalize afterwards (Hauge & Aarseth 1977). Only one of these cases was accompanied by release of PG-like activity (Table 1).

In cats 6 to 9 a rabbit aorta (RbA) was used in all of the 6 pressure elevations. PGLS were detected in all four tissues.

Effect of indomethacin

During 4 elevations of P_{1A} , accompanied by deflation contractions of the assay tissues, indomethacin (1 mg/kg) was given i.v. to inhibit PG-synthesis. In all these cases the tension of the tissues returned to the control level within a few min (Fig. 1). No further change in tension was observed when P_{1A} later returned to normal after deflating the balloon.

Possible interference of angiotensin II

In all cats a reduction in P_{1A} occurred when P_{1A} was elevated (Table 1). Sometimes a grave hypotension developed. This could activate the renin-angiotensin system with generation of angiotensin II which might interfere with our work, since the tissues were not blocked against angiotensin II. To evaluate this possibility, angiotensin II was infused 6 times in 4 cats both i.v. and directly over the assay tissues to give a blood concentration of 0.1–1.0 ng/ml. The tissue reactions to angiotensin II were independent of the route of administration. In 2 cats angiotensin II was infused twice i.v. Before the second infusion indomethacin (3 mg/kg) was given. However, the tissue contractions before and after indomethacin were identical (Fig. 2), indicating that this blood level of angiotensin II does not increase PG-like activity in arterial blood. Additionally, the pattern of tissue contractions to angiotensin II was dissimilar to that of PGE_2 and $PGF_{2\alpha}$. Angiotensin II especially contracted the RC powerfully (Fig. 3).

Table 2 Effect of increased P_{1A} on pulmonary degradation of PGE

Cat no	Cardiac output (ml/min)	PGE_2 infusion i.v. (μ g/min)	Activity in art. blood (ng/ml)	P (mmHg)	Activity in arterial blood during pre-elevation (ng/ml)	% degradation
10	600	15	3	25	2	9
11	650	10		30	3	81
1	900	15		77	2	88

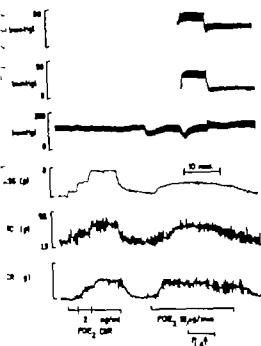


Fig. 4. Effect of P_{LA} elevation on pulmonary degradation of infused PGE_2 . The tracings are pulmonary arterial pressure (P_{PA}), left atrial pressure (P_{LA}), femoral arterial pressure (P_a) and isometric tension in 3 bioassay tissues continuously superfused with arterial blood (10 ml/min): rat stomach strip (RSS), rat colon (RC) and chick rectum (CR). Indomethacin 2 mg/kg was given before the start of the tracings. The tissues were calibrated by PGE_2 and the lungs hyperinflated (H). P_{LA} was elevated during infusion of PGE_2 .

Pulmonary hypertension and relaxation of PGE_2

This was investigated in 3 cats given indomethacin to prevent PG synthesis. After calibration of the assay tissues PGE_2 was infused at a dose which caused assay tissues contractions corresponding to about 10% of arterial blood flow. Inactivation was found to be between 81 and 92% and was not influenced by elevation of P_{LA} (Table 2) (Fig. 4).

Hematocrit (hct) and osmolality

At the onset of each expt. hct was 27–35 (range) and declined to 15–28 (range) throughout the expt., probably due to hemodilution caused by transfusions.

Plasma osmolality was unchanged at 320–328 mosmol/l throughout each expt. It did not change during pressure elevation.

DISCUSSION

In the present work we have focused on increased hydrostatic pressure in the pulmonary circulation as a possible stimulus of PG synthesis and release from intact cat lungs. Inflation of a balloon in the left atrium causes pulmonary hypertension and congestion as well as systemic hypotension (Hauge-Bo & Aarseth 1977). Simultaneously the bioassay tissues contracted indicating release of PGLS. The presently used bioassay tissues are specifically sensitive to PGs (Piper & Vane 1971). Counteracting their contractions by administration of indomethacin, an inhibitor of PG synthetase, is further proof that PGLS really were released since PG release represents de novo synthesis (Piper & Vane 1971).

The assay tissues were calibrated by known concentrations of the 'classical' PGE_2 and $PGF_{2\alpha}$. Due to the different contraction pattern of the 3 tissues, the PGLS released could be classified as PGE_2 or $PGF_{2\alpha}$ -like material. However, during the conversion of arachidonic acid (AA) in lungs only a minor fraction is transferred into PGE_2 and $PGF_{2\alpha}$. A major fraction of the endoperoxide intermediates (PGG_2 and PGH_2) is converted to the highly unstable but biologically very active thromboxane A_2 (TxA_2) (Hamberg, Svensson & Samuelsson 1975). Conceivably endoperoxides and TxA_2 are released in far higher concentrations than PGE_2 and $PGF_{2\alpha}$ in the present expts. Our assay tissues are also sensitive to TxA_2 and endoperoxides (Hamberg et al. 1975; Bunting, Moncada & Vane 1976). The use of the Rha to detect RCS which is a mixture of TxA_2 and endoperoxides (Hamberg, Svensson & Samuelsson 1975; Samuelsson 1976) confirmed the release of these intermediates. Recent investigations have indicated that AA in the lungs is also transformed into the vasodilatory PGI₂ (Dusting et al. 1978). PGI₂ is also able to contract the RSS and the CR (Omine, Moncada & Vane 1977). Consequently the presently used on-line bioassay may reflect the biological activity and variety of substances formed during the biological conversion of AA.

In the present expts. we could not detect any release of PGLS in 4 of the 18 elevations of P_{LA} . This might indicate that release is not a constant phenomenon, or that in some expts. the amounts released were too small to be detected. The release amounts which we detected are close to the lower level possible to detect by bioassay. Release of

smaller amounts of PGLS would have escaped detection.

The systemic hypotension occurring during elevation of P_{1A} might cause generation of angiotensin II which again might contract the assay tissues. Indeed the contraction of the RC during P_{1A} elevation could probably be completely explained by the effect of angiotensin II. However angiotensin II can neither explain the contractions of the RSS and the RC nor the effect of indomethacin. But angiotensin II might be released together with PGLS. What we have characterized as $\text{PGF}_{2\alpha}$ like substances might be PGE_2 like substances plus angiotensin II. Angiotensin II itself is also reported to stimulate PG synthesis and release in several tissues and cells (McGiff et al. 1970; Gimbrone & Alexander 1975). However in the present expts it appears unlikely that PGLS were released secondary to release of angiotensin II. I.v. infusions of angiotensin II did not increase PGLS in arterial blood. The increase in blood level of angiotensin II during our infusion was higher than the maximal blood concentrations (0.33 ng/ml) described during hypovolemia (Hodge et al. 1966).

A main question is the site of origin of the PGs. If they are released from extrapulmonary tissues then they would have to pass the lungs to appear in arterial blood. Since the catabolism and inactivation of PGs is extremely efficient in the pulmonary circulation (70–90%) (Ferreira & Vane 1967; Piper, Vane & Wyllie 1970) this situation would need extremely high levels of PGs in the mixed venous blood reaching the lungs unless PG degradation was impaired. If the pressure elevation significantly increased shunting of blood outside the pulmonary microvasculature during pressure elevation PGs originating in the systemic circulation might escape degradation and thereby increase systemic arterial concentrations of PGs. We tested the degradation of PGE_2 in our model (Table 1) and could show that the pulmonary inactivation of PGE_2 (81–92%) was not changed by elevation of P_{1A} . The values we found for degradation were close to the values given by Ferreira & Vane (1967) in cat. Consequently if the PGLS released do not originate in the lungs then mixed venous blood must have a concentration of PGs higher than 10 ng/ml to cause the activity on the assay tissues. Thus it appears highly unlikely that the PGLS released have an extrapulmonary site of origin.

The mechanical stress due to increased hydro-

static vascular pressure in the pulmonary circulation and extravascular accumulation of fluid might theoretically stimulate PG synthesis. Said & Yoda (1974) reported that lung edema stimulated PG synthesis and release from lungs. However in the presently used model fluid accumulation in the interstitium is usually scarce unless P_{1A} is excessively high (Hauge, Bo and Aarseth 1977). In one of the two cases where fulminant alveolar edema developed no PGLS appeared. Recently we have found in isolated perfused lungs that no PGLS were detected in spite of gross alveolar edema and hypertension (Scott, Vaage & Wiberg 1979), indicating that the release detected in the present work is dependent on the intact state of the animal and probably not due to direct mechanical effect on the lungs.

The elevation of P_{1A} is a marked strain on the animal. It must inevitably be accompanied with increased activity in the sympathetic nervous system and release of catecholamines which again might cause PG release (Hedqvist 1976). Interestingly stimulation of sympathetic nerves to the lungs has been reported to release PGs (Mathé et al. 1977). Release of PGs from lungs secondary to increased activity in the sympathetic nervous system may explain the difference between the findings in intact animals and in isolated lungs during elevated vascular pressure in the pulmonary circulation.

T. Wiberg and J. Vaage were research fellows of the University of Oslo. F. Scott was a research fellow of the Ciba-Geigy Fellowship Trust, London.

This work was supported by grant from the Norwegian Council on Cardiovascular Disease, the Norwegian Research Council for Science and the Humanities, and Norsk Medisinaldepot. PG were the generous gift of Dr J. F. Pike, Upjohn Company.

REFERENCES

- BAKHLE V. S. & VANE J. R. 1974 Pharmacokinetic function of the pulmonary circulation. *Physiol Rev* 54, 1007–1045.
- BERRY T. M., EDMONDS J. F. & WYLLIE J. H. 1971 Release of prostaglandin 1_2 and unidentified factors from ventilated lungs. *Brit J Surg* 58, 184–19.
- HUNTING S., MONCADA S. & VANE J. R. 1976 The effect of prostaglandin endoperoxide and thromboxane A_2 on strips of rabbit coeliac artery and certain other smooth muscle preparations. *Brit J Pharmacol* 57, 463P–463P.
- DUSTING G. J., MONCADA S., MULLANT K. M. & VANE J. R. 1978 B β transformation of arachidonic acid: the circulation of the dog. *Brit J Pharmacol* 61, 339P.

2. JUREIRA, S. H. & VANE, J. 1967 Prostaglandins: their disappearance from and release into the circulation. *Nature (Lond)* 216 868-873.
- IMBRONE, M. A. & ALEXANDER, R. W. 1975 Angiotensin II stimulation of prostaglandin production in cultured human vascular endothelium. *Science* 189 219-220.
- IANBERG, M., HEDQVIST, P., STRANDBERG, K., SVENSSON, J. & SAMUELSSON, B. 1975 Prostaglandin endoperoxides IV. Effects on smooth muscle. *Life Sciences* 16 451-462.
- IANBERG, M., SVENSSON, J. & SAMUELSSON, B. 1975 Thromboxanes: A new group of biologically active compounds derived from prostaglandin endoperoxides. *Proc Natl Acad Sci (Wash.)* 72 2994-2998.
- LAUGE, A., BØG, G. & AARSETH, P. 1977 Hydrostatic pulmonary oedema in the cat. Effects on pulmonary blood and water volumes and on lung compliance. *Acta Anaesthesiol Scand* 1 413-422.
- HEDQVIST, P. 1976 Effects of prostaglandins on autonomic neurotransmission. In: *Prostaglandins: Physiological, pharmacological and pathological aspects* (ed. S. M. M. Karim) pp. 37-62. MTP Press, Lancaster.
- HODGE, R. L., LOWE, R. D. & VANE, J. R. 1966. The effects of alteration of blood-volume on the concentration of circulating angiotensin in anesthetized dogs. *J Physiol (Lond)* 185 613-626.
- MALIK, K. V. & McGIFF, J. C. 1976 Cardiovascular actions of prostaglandins. In: *Prostaglandins: Physiological, pharmacological and pathological aspects* (ed. S. M. M. Karim) pp. 103-200. M. T. P. Press, Lancaster.
- MATHE, A. A., HEDQVIST, P., STRANDBERG, K. & LESLIE, C. A. 1977 Aspects of prostaglandin function in the lung. *New England J Med* 296 830-835.
- McGIFF, J. C., CROWSHAW, K., TERRAGNO, N. A. & LONIGRO, J. A. 1970 Release of prostaglandin-like substance into renal venous blood in response to angiotensin II. *Circulat Res* 26-27 (Suppl. 1), 1121-1130.
- ONINI, C., MONCADA, S. & VANE, J. R. 1977 The effects of prostacyclin (PGI₂) on tissues which detect prostaglandins (PG₂). *Prostaglandins* 13 625-632.
- PIPER, P. J. & VANE, J. 1971 Release of prostaglandins from lung and other tissues. *Ann N Y Acad Sciences* 180 363-385.
- PIPER, P. J., VANE, J. R. & WYLLIE, J. H. 1970 Inactivation of prostaglandins by the lungs. *Nature (Lond.)* 225 600-604.
- SAID, S. I. 1974 Endocrine role of the lung in disease. *Amer J Med* 57 45-463.
- SAID, S. I. & YOSHIDA, T. 1974 Release of prostaglandins and other humoral mediators during hypoxic breathing and pulmonary edema. *Chest* 66, Suppl (part 2), 12a-13a.
- SAMUELSSON, B. 1976. Prostaglandin endoperoxides and thromboxanes. Role in platelets and in vascular and respiratory smooth muscle. *Acta Biol Med Germ* 35 1055-1063.
- SCOTT, E., VAAGE, J. & WIBERG, T. 1979 Lack of release of prostaglandins from isolated perfused lungs during pulmonary hypertension and oedema. *Brit J Pharmacol* 65 197-204.
- VAAGE, J., BØG, G. & HOGNESTAD, J. 1974 Pulmonary responses to intravascular platelet aggregation in the cat. *Acta Physiol Scand* 92, 546-556.
- VAAGE, J., WIBERG, T. & SCOTT, E. 1978 Release of prostaglandin-like substances and lung reactions to induced intravascular platelet aggregation in cats. *Scand J Clin Lab Invest* 38 337-347.
- VAAGE, J., WIBERG, T. & SCOTT, E. 1978 Release of prostaglandin-like substances during increased alveolar pressure. *Microvasc Res* 15 119.
- VANE, J. R. 1969 The release and fate of vaso-active hormones in the circulation. *Brit J Pharmacol* 35 209-242.
- VANE, J. R. 1973 Prostaglandins and aspirin-like drugs. In: *Pharmacology and the future of man* (ed. C. H. Acheson) pp. 35-377. Karger, Basel.
- WIBERG, T., VAAGE, J., SCOTT, E., TEIG, V. & GAUTVIK, K. Increased hydrostatic pressure in the pulmonary circulation of cats induce synthesis and release of prostaglandins. *Acta Physiol Scand Suppl.* 440: 138.

Effects of acute hypotension and hypertension on serum TSH concentrations in male rats

T. MANNISTO, J. KOKKONEN and T. RANTA

Department of Pharmacology, University of Helsinki, Department of Pharmacology, University of Kuopio and Department of Serology and Bacteriology, University of Helsinki, Finland

MANNISTO P. T., KOKKONEN J. & RANTA T. Effects of acute hypotension and hypertension on serum TSH concentrations in male rats. *Acta Physiol Scand* 1979; 107: 105-107. Received 18 Febr. 1979. ISSN 0001-6772. Department of Pharmacology, University of Helsinki, Department of Pharmacology, University of Kuopio and Department of Serology and Bacteriology, University of Helsinki, Finland.

The effect of acute hypertension and hypotension on serum TSH concentration was studied in anesthetized male rats. Intravenous (10 and 30 min) of Na-nitropruside and dihydralazine induced profound hypotension, and angiotensinamide and noradrenaline increased blood pressure, but none of the treatments significantly modified serum TSH concentrations. Also clonidine and noradrenaline when given p.o. caused hypertension, but again the increase of serum TSH levels was not consistent. When the whole material was analysed, there was scarcely significant correlation between the change of blood pressure and the change of serum TSH level. It is inferred that the drugs affecting TSH secretion, do not exert their action solely by changing the blood pressure.

Key words: hypertension, hypotension, serum TSH, noradrenaline, clonidine, dihydralazine, sodium nitropruside, angiotensinamide.

When studying the neurotransmitter control of thyrotrophin (TSH) secretion, we (Tuomisto et al. 1975; Ranta et al. 1977; Mannisto & Ranta 1978) and others (Omaya & Hashizume 1976; Amunizato et al. 1977; Krulich et al. 1977) have used drugs which besides affecting tissue biogenic amines, alter the blood pressure of the animals. There is only a limited information about the effect of some antihypertensive drugs on the brain blood-flow. Na-nitropruside does not significantly affect brain perfusion (Griffiths et al. 1974) but clonidine may initially decrease the brain blood flow both in man (James et al. 1970) and in an animal (Sherman et al. 1968). Concerning the anterior pituitary, Porter & coworkers (1967) have shown that the blood flow in the pars distalis is markedly increased during a profound hypotension. Hence it is possible that rapid change of the blood pressure may alter the blood flow in the pituitary portal vessels, and may so modify the secretion of anterior pituitary hormones. To explore this possibility, we have performed a series of experiments, where the blood pressure, cardiac rate and serum TSH levels were monitored while various drugs, inducing either hypotension or

hypertension were continuously infused. We also used drugs whose primary action is known not to be mediated through the brain biogenic amines.

MATERIAL AND METHODS

Male Wistar albino rats (*Rattus norvegicus*), weighing 200-250 g were used at the age of 7-8 weeks. The animals were fed pelleted rat chow (iodine content about 0.8 mg/kg; Hankkija, Finland) and tap water ad lib. They were kept in groups of 4-6 in dark rooms, artificially illuminated from 7 a.m. to 9 p.m. at temperature of 22-24°C.

The rats were anesthetized with pentobarbital (50 mg/kg, i.p.). Usually 2-3 rats were operated on in one experiment. Arteria carotis (usually left) and Vena jugularis (usually right) were cannulated. The cannula in A. carotis was connected to pressure transducer (Nihon Kohden TMJ MPU-0.5-290-0-113), to an amplifier and a recorder (Nihon Kohden, Medecorder), and the blood pressure was continuously monitored. Pulse rate was calculated from the blood pressure waves every 5th minute. These parameters were measured also at the beginning of the infusions (=control values). Physiological saline or drugs diluted in saline were infused into V. jugularis with constant rate of 0.13 ± 0.003 ml/min (Harvard Syringe Pump model 2681). Some of the rats were killed at 10 min, the rest at 30 min. After the sample for bromocriptin was taken, blood was centrifuged and serum stored at -18°C until

RESULTS AND DISCUSSION

The effect of various drugs and bleeding on the systolic (A) and diastolic blood pressure (B) the cardiac rate (C) and the serum TSH concentrations (D) is shown in Fig. 1.

It became clear from these results that a rapid and profound decrease of the blood pressure as induced by the peripherally acting drugs like Na-nitroprusside and dehydralazine did not significantly depress the TSH secretion, although blood-flow in the pars distalis of the pituitary gland should be increased (Porter et al 1967). The bleeding of the animals caused only a transient hypotension and—after a correction on the basis of the hematocrit—was not associated with any significant fall in the serum TSH levels. The monitoring of hematocrit is important if multiple blood samples are collected for hormone analysis.

The effects of drugs increasing the blood pressure on the serum TSH concentrations were not consistent and with one exception (noradrenaline i.p. at 30 min) did not reach statistical significance.

The pentobarbital anesthesia may contribute to the rather small fluctuations of the serum TSH concentration. We have shown earlier that although various anaesthetics only slightly modified the basal TSH levels they nearly completely inhibited the cold-induced TSH secretion (Männistö et al 1976). Therefore the studies on anesthetized animals cannot directly be compared with those performed on intact animals.

It is concluded that in spite of the major correlation ($r = 0.4562$) between the change of the blood pressure and the change of the serum TSH concentration, the drugs modifying the TSH secretion do not exert their action solely by changing the blood pressure of the experimental animals.

We are grateful to the NIAMDD, the Rat Pituitary Hormone Distribution Program for providing the rat TSH RIA. The study is supported by the grant from the Academy of Finland and Sigrid och Åke Gyllenberg Stiftelse, Helsinki, Finland. The technical help of Dr Jyrki Mäkelä is greatly appreciated.

REFERENCES

- ANNUNZIATO L., DI RENZO G., LOMBARDI G., SCOPACASA F., SCHEITLINI, G., PREZIOSI P. & SCAPAGNINI U. 1977. The role of central noradrenergic neurons in the control of thyrotropin secretion in the rat. *Endocrinology* 100: 734-744.
- GRIFFITHS, D. P. G., CUMMINS B. H., GREENBAUM R., GRIFFITH, H. B., STADDON G. E., WILKINS D. G. & ZORAB, J. M. S. 1974. Cerebral blood flow and metabolism during hypotension induced with sodium nitroprusside. *Brit J Anaesth* 46: 671-679.
- JAMES I. M., LARBI E. & ZAIMIS E. 1970. The effect of the acute intravenous administration of clonidine on the cerebral blood flow in man. *Brit J Pharmacol* 39: 198P-199P.
- KRULICH, L., GIACHETTI A., MARCHLEWSKA KOJ A., HEFCO E. & JAMESON H. E. 1977. On the role of central noradrenergic and dopaminergic systems in the regulation of TSH secretion in the rat. *Endocrinology* 100: 496-505.
- MÄNNISTÖ P., SAARINEN A. & RANTA, T. 1976. Anaesthetics and thyrotropin secretion in the rat. *Endocrinology* 99: 873-880.
- MÄNNISTÖ P. & RANTA, T. 1978. Neurotransmitter control of thyrotropin secretion in hypothyroid rats. *Acta Endocr (Kbh)* 89: 100-107.
- ONAYA, T. & HASHIZUME, K. 1976. Effects of drugs that modify brain biogenic amine concentrations on thyroid activation induced by exposure to cold. *Neuroendocrinology* 20: 47-55.
- PORTER, J. C., HINES M. F. M., SMITH K. R., REPASS, R. L. & SMITH A. J. K. 1967. Quantitative evaluation of local blood flow of the adenohypophysis in rat. *Endocrinology* 80: 583-598.
- RANTA, T. 1975. Effect of dexamethasone on the secretion of thyrotropin in the rat: dose and time relations. *Endocrinology* 96: 1566-1570.
- RANTA, T., MÄNNISTÖ P. & TUOMISTO J. 1977. Evidence for dopaminergic control of thyrotropin secretion in the rat. *J Endocrin* 72: 329-335.
- SHERMAN G. P., GRECA, G. J., WOOD R. J. & BUCKLEY J. P. 1968. Evidence for central hypotensive mechanism of 2-(2,6-dichlorophenylamino)-2-imidazoline (SI 155). *Europ J Pharmacol* 2: 126-128.
- TUOMISTO J., RANTA, T., MÄNNISTÖ P., SAARINEN A. & LEPPÄLUOTO J. 1975. Neurotransmitter control of thyrotropin secretion in the rat. *Europ J Pharmacol* 30: 221-229.

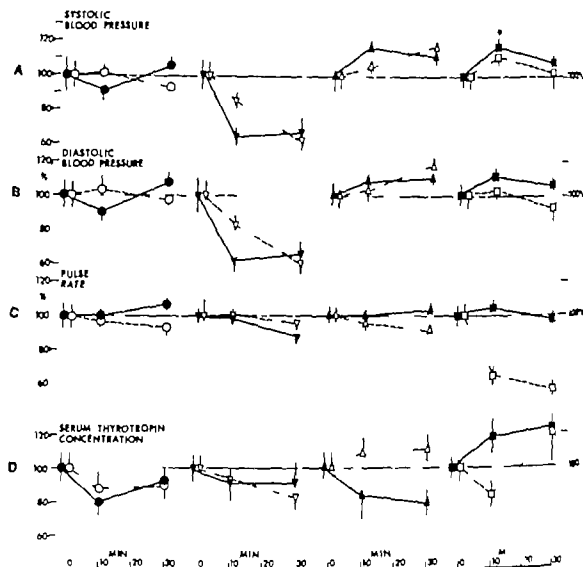


Fig. 1 Effect of the intravenous infusion of 0.9% saline (○-○), dihydralazine (▽-▽), Na-nitropruside (▽-▽), angiotensin amide (△-△) and noradrenaline (●-●) or bleeding (●-●) or the intraperitoneal injection of clonidine (■-■) on the systolic (A), diastolic (B) blood pressure, pulse rate (C) and the serum TSH concentrations (D). The values are expressed as % of the preinfusion values, which were in the following range: systolic blood pressure 135-165 mmHg, diastolic blood pressure 90-120 mmHg, pulse rate 400-480/min and serum TSH level 360-530 ng/ml. Mean \pm S.E. $n=6-7$. The statistical significance of the change from the preinfusion value is shown as follows: * $P<0.05$, ** $P<0.01$, *** $P<0.001$.

analysed for serum TSH concentration by a homologous radioimmunoassay as described earlier (Ranta 1975). Some rats were injected i.p. with clonidine or noradrenaline (1 mg/kg) and killed at 10 or 30 min. Blood pressure, cardiac rate and serum TSH concentration were monitored and saline infused as above. Some rats were bled (about 5 ml) at 0 time and the parameters were followed as above. Several intact rats (not cannulated, unanesthetized) were also killed throughout the experiments.

The following drugs were used: Angiotensin amide (Hypertensin® Ciba, Basle) 0.015 mg/ml, the total dose 0.015 mg in 10 min, 0.035 mg in 30 min; Clonidine HCl (Onon Helsinki) 1 mg/kg i.p.; Dihydralazine mesylate (Nepresol® Ciba Basle) 0.3 mg/ml, 0.37 mg in 10 min, 1.11 mg in 30 min; Noradrenaline bitartrate (Nor-Adrenalin® Star Tampere) either 1 mg/kg i.p. or a 10 min

infusion, 0.015 mg/ml, 0.015 mg in 10 min, 0.035 mg in 30 min; Sodium nitropruside (Nitroside® Roche Basle), 0.1 mg/ml, 0.1 mg in 10 min, 0.37 mg in 30 min. The doses of drugs refer to respective acid or bases.

Blood pressure and cardiac rate are expressed as a percentage of the preinfusion pressure and cardiac rate respectively. Serum TSH concentration is expressed as a percentage of the TSH concentrations of the intact rats. The serum TSH levels were corrected on the basis of the change in haematocrit. The statistical significance of the changes induced by the various treatments was tested by using Student's *t* test and in case of serum TSH concentration also analysis of variance was used. The relation between the change of the blood pressure and the change of the serum TSH concentration was tested with Pearson's regression analysis.

Morphometry of myocardial apex in endurance-trained mice of different ages

HEIKKI KAINULAINEN, LARS PILSTRÖM and VEIKKO VIHKO

Department of Cell Biology, University of Jyväskylä, Finland, and Institute of Zoophysiology, University of Uppsala, Sweden

KAINULAINEN H., PILSTRÖM L. & VIHKO V. Morphometry of myocardial apex in endurance-trained mice of different ages. *Acta Physiol Scand* 1979, 107, 109-114. Received 22 Feb. 1979. ISSN 0001-6772. Department of Cell Biology, University of Jyväskylä, Finland and Institute of Zoophysiology, University of Uppsala, Sweden.

Mitochondrial volume density, surface density of the outer mitochondrial membrane, the mean number and size of mitochondria, and the mean surface density of cristae membranes together with the volume densities of myofibrils and sarcoplasmic space were morphometrically analyzed in cardiac muscle of two groups of sedentary control mice aged 3 and 7 months, and in two groups of mice trained either 1 month rather intensely or 4 months moderately. Of the calculated mitochondrial variables only the surface density of the outer mitochondrial membrane differed between the older controls and the older trained animals, the density being slightly smaller in the trained group. The myofibrillar volume density of the older controls was smaller than that of the younger controls, while the sarcoplasmic volume density was larger. The latter difference possibly function of age, was also observed in the trained groups. The results suggest that at certain steady state level of exercise-induced cardiac muscle hypertrophy the muscle cells of trained mice do not differ markedly in ultrastructural properties from those of sedentary controls.

Key words: Stereology, endurance training, cardiac muscle, mitochondria, mouse.

The effects of endurance training on skeletal and cardiac muscle are different. Endurance training causes typical adaptation in the energy metabolism of skeletal muscle. These adaptations are centred on the aerobic component of the energy-producing mechanism of muscle fibres and have the effect of making skeletal muscle more reminiscent of cardiac muscle (Hollnagel & Booth 1976, Pette 1966). They include increased enzyme activities of β -oxidation (Klotz et al. 1971), citric acid cycle (Hollnagel et al. 1973), and the respiratory chain (Baldwin et al. 1977). Ultrastructural studies show increased mitochondrial volume density (Hoppeler et al. 1973, Kiersing et al. 1974, Vihko et al. 1975). Endurance training does not usually cause either fibre hypertrophy or changes in total protein content (Hollnagel & Booth 1976).

The most typical effect of endurance training on myocardium is an increase in weight (Arcos et al. 1967, Bozner & Meessen 1969, Crews & Aldinger 1967, Osei et al. 1971a, b). No major enzymatic

adaptations have usually been found and the few ultrastructural studies regarding the effects of endurance training on cardiac muscle, especially on its mitochondria, have yielded contradictory results (Bozner & Meessen 1969, Golfinick et al. 1971, Padanilam et al. 1977). It therefore appears that myocardium responds to long-term physical exercise by hypertrophy (Bozner & Meessen 1969, Sahai et al. 1968) and that no major qualitative or quantitative adaptations comparable to those in skeletal muscle occur in energy-producing mechanism of trained cardiac muscle cells.

The aim of the present investigation was to study by stereological methods the effects of two types of endurance training on the ultrastructure of mouse cardiac muscle. A relatively short lasting but intense and a longlasting, moderate running programme on a motor-driven treadmill were used. Using this experimental design limited data were also obtained on the effects of training on the myocardium of mice of different ages.

room temperature. The muscle pieces were then transferred for 2 h into 7.5% saccharose buffered with 0.1 M sodium cacodylate, after which they were postfixed with 1% osmium tetroxide for 1 h at +4°C. The pieces were then immersed for 5 min in veronal buffer (pH 7.4, room temperature) containing 7.5% saccharose, and after that were dehydrated for 3–5 min in 70 and 96% ethanol and for 5 min in 100% ethanol. The dehydrated samples were transferred to propylene oxide for 3–7 min and then to propylene oxide-Epon 812 (1:1) mixture for 1 h, after which they were embedded in Epon (A:B 1:1, DNP 8.2). Samples were kept at room temperature overnight and the Epon was then allowed to polymerize for 48 h at +60°C.

Ultra-thin sections are cut with Porter-Blum ultramicrotome using glass knives. The sections were mounted on 780 mesh grids, stained with lead citrate and examined and photographed with a JEM 100 U electron microscope.

Morphometry

Four blocks were analyzed from each apex. Thin sections were cut at two different levels, separated by at least 15 mm. These sections were mounted on two different grids. Thus two grids per apex were examined. The necessary number of micrographs was estimated as described by Weibel & Goss (1968) and by Herbener et al. (1973) to be approximately 20 (Fig. 2). Accordingly two micrographs per grid were taken resulting in total of 20 prints per myocardium.

Morphometrical volume densities were determined by the point-counting method (e.g. Weibel 1969) and outer mitochondrial and crista membrane areas using curved line grid superimposed on each micrograph (Merz 1968, Weibel 1969). The point-counting lattice included 80 points and the length of the curve as 301 cm at final magnification (Fig. 1). The mean number of mitochondria was calculated according to the method of Weibel & Gomez-Duon (1962). Mean mitochondrial volume was obtained by dividing the mitochondrial volume density by

the number of mitochondria. The surface density of the crista membranes of each apex was estimated from 4 micrographs including at least 200 mitochondria, with a total magnification of 22 830. The other morphological variables were estimated from micrographs with total magnification of 13 630. The abbreviations for variables used are given in Table 1.

The data obtained from the stereological analyses were tested by the Student's *t*-test.

RESULTS

The morphometrical results are given in Table 1. Morphologically the ultrastructure of myocardial apex appeared normal in every group of mice. Very few statistically significant differences were found between groups.

The mitochondrial volume density, the surface density of crista membranes, and the mean number or mean size of mitochondria did not differ between the groups. Almost half of the muscle volume was occupied by mitochondrial mass in the myocardial apex. Depending on the primary magnification used this value varied between 43 and 50% (Table 1).

The surface density of the outer mitochondrial membrane was slightly lower ($P < 0.01$) in the trained TR2 group than in the corresponding control (C2) group. The mean myofibrillar volume density of all animals was slightly lower (43.23%) than the volume density of mitochondria (44.08%). The myofibrillar volume density in group C2 was a little smaller ($P < 0.05$) than that in group C1. The sarcoplasmic volume density was consequently larger ($P < 0.05$) in group C2 than in group C1. In the trained groups a similar difference was also observed: sarcoplasmic volume density in group TR2 was larger ($P < 0.01$) than in group TR1.

There were no significant differences in the volume densities of the extracellular space between the different groups (Table 1).

DISCUSSION

It is generally accepted that morphometrical methods although rather laborious offer a reliable means of carrying out quantitative studies on subcellular structure (e.g. Weibel 1969, Herbener et al. 1973, Hoppeler et al. 1973, Kieckheaf et al. 1974, Panigrahi et al. 1977). They are especially useful in comparative studies and in studies in which the effects of a certain treatment are traced.

In terms of its mitochondrial variables the apex

n	\bar{V}_v	\bar{S}_v ($\mu\text{m}^2/\mu\text{m}^3$)
11 ± 0.04	46 (3 ± 2.5)	9.03 ± 2.00
11 ± 0.06	50 ± 1.85	8.91 ± 0.91
11 ± 0.04	46.39 ± 1.66	8.77 ± 1.43
11 ± 0.03	47.33 ± 1.67	8.10 ± 1.49



Fig. 1 The lattice used for the estimation of mitochondrial volume and surface densities. 80 points were used for the volume densities and point-counting was performed with total magnifications of 13 650 \times and 22 850 \times . The curved line was used for the cristae membrane surface densities with a magnification of 22 850 \times and for the mitochondrial outer membrane density determinations with a magnification of 3 650 \times ; the total length of the line being 301 μ m. The size of the lattice was 19.1 \times 3.8 cm. The sample in the figure was taken from a control animal of group C1.

MATERIAL AND METHODS

Animals and training

F-hybrid mice of the strain B6D.F1/BOM JG 1, Bomholtgård Ltd. Ry, Denmark, aged 60 (13–67) days at the beginning of the experiment, were used. The mice were randomly divided into two training groups (TR1 and TR2) exercising regularly, and into two sedentary control groups (C1 and C2). Controls and the training animals, except while training, lived under ordinary cage conditions with free access to solid food pellets (Hanku, Finland) and tap water. The training in the TR1-group was intense. These mice ($n=9$) were made to run on a motor-driven treadmill with horizontal tracks daily for 30 min at a speed of 20 m/min and for 45 min at 18 m/min before noon, and for 75 min at 18 m/min in the afternoon. This training programme lasted for 30 days and the exercises were performed 7 days a week.

In the training group TR2 ($n=10$) training was moderate but lasted for a longer period than that in the TR1-group. The programme consisted of a run on the treadmill for 10 min at a speed of 20 m/min 5 days a week over a period of 120 days.

Two trained animals and two controls were killed on day after the last exercise during each experiment. Animals in the first control group (C1) ($n=9$) were then of the same age as the animals in the first training group (TR1) and the animals in the second control group (C2) ($n=10$) were as old as those in the second training (TR2) group. The age difference between the younger and older animal groups was 3 months.

Electron microscopy

Mice were killed by dislocation of the neck and the heart was immediately removed. The apex of each myocardium was cut off and immersed in ice-cold 2% glutaraldehyde buffered with 0.1 M sodium cacodylate at pH 7.4. The tissue samples were cut into small (approx. 1 mm³) pieces and left in the fixative for 24 h at +4°C and then for 1 h at

Table 1 Results of morphometrical analysis of myocardial apex in two groups of sedentary control mice in two groups of endurance trained mice. Mean \pm S.D.

Data in the left part of the Table are calculated from micrographs taken with primary magnification 4 000 \times and 11 μ m; the right part with primary magnification 6 700 \times . $V_{1,mt}$ = volume density of mitochondria, $V_{1,fb}$ = volume density of fibrils, $V_{1,sc}$ = volume density of sarcoplasmic space, $V_{1,ec}$ = volume density of extracellular space, $N_{1,mt}$ = average number of mitochondria, $S_{1,mt}$ = surface density of outer mitochondrial membrane, $\bar{V}_{1,mt}$ = average size of mitochondria, $S_{1,mt}$ = surface density of cristae.

Group	Age (months)	Volume densities				$N_{1,mt}$ / 10 μ m	$S_{1,mt}$ (m ² /cm ²)
		$V_{1,mt}$	$V_{1,fb}$	$V_{1,sc}$	$V_{1,ec}$		
C1	3	43.74 \pm 1.43	44.36 \pm 1.15	9.16 \pm 0.64	2.77 \pm 0.70	5.24 \pm 0.29	2.06 \pm 0.77
C2	6	45.18 \pm 1.05	40.95 \pm 0.68*	11.53 \pm 0.86*	2.33 \pm 0.4	4.93 \pm 0.70	2.10 \pm 0.61
TR1	3	43.81 \pm 1.00	44.95 \pm 0.87	9.17 \pm 0.52	2.09 \pm 0.6	4.76 \pm 0.31	0.1 \pm 0.09
TR2	6	43.59 \pm 1.01	4.66 \pm 0.76	11.62 \pm 0.61	2.0 \pm 0.77	4.65 \pm 0.09	0.0 \pm 0.07

Statistically significant ($P<0.05$) difference compared to group C1.

Statistically significant ($P<0.01$) difference compared to group TR1.

Statistically significant ($P<0.01$) difference compared to group C2.

mitochondrial number and mass after long-term exercise.

Endurance training did not cause any major qualitative changes in mitochondria. The surface density of cristae was similar in every animal group suggesting unchanged oxidative capacity in the trained myocardium. Panagou et al (1977) reported no significant changes in the amount of mitochondrial protein nor in the specific activities of malate dehydrogenase, cytochrome c oxidase and ATPase in rat myocardium after swimming training. Myofibrils and mitochondrial volume densities and the number of mitochondria were also unchanged in our study. In the present study, small decrease due to training was recorded in the surface density of outer mitochondrial membrane. The results of Edington & Cosmas (1972) and Cosmas & Edington (1975) showed a decrease in the average volume of mitochondria resulting in an increased outer surface area, if the volume density remains unchanged. In the present study the mitochondrial volume density and the average number of mitochondria per unit volume were slightly smaller in the TR2 group than in the C2 group, resulting the same average volume ($0.94 \mu\text{m}^3$) of a mitochondrion in both groups. Evidently the difference in the surface density of outer mitochondrial membrane is caused by the slightly smaller average number of mitochondria in trained muscle.

The volume density of myofibril was larger in the younger C1 than in the older C2 control group. By contrast, the volume fraction of sarcoplasm (in this study all other cellular contents than mitochondria, myofibrils and nuclei) was larger in the C2 than the C1 group. The latter difference was also observed in the trained animals. It is possible that this difference is due to the age difference between the groups.

The entire left ventricle, especially those of the left atricle, might be better objects for ultrastructural studies concerning exercise-induced cardiac muscle hypertrophy. However, the present results from myocardial apex lend confirmation to earlier observations of the proportionality of mitochondrial biogenesis to hypertrophy in situations in which the stimulus causing the hypertrophy has acted for relatively long time (Bozner & Meerson 1969; Meerson 1975; Meerson & Breger 1977). The early phases of endurance training programme before the hypertrophied cellular steady state has been attained might yield more informa-

tion concerning the mechanisms of exercise-induced myocardial hypertrophy.

We thank Raimo Vassilinen and Paavo Niemi for excellent technical assistance.

REFERENCES

- ALDINGER, E. E. & SOHAL, R. S. 1970. Effects of depletion on the ultrastructural myocardial changes in the rat subjected to chronic exercise. *Amer J Cardiol* 26, 369-374.
- ARCOS J. C., SOHAL, R. S., SUN S.-C., ARGUS M. F. & BURCH, G. E. 1967. Changes in ultrastructure and respiratory control in mitochondria of rat heart hypertrophied by exercise. *Exptl Mol Path* 8, 49-65.
- BALDWIN K. M., KLINKERFUSS O. H., TERJUNG, R. L., MOLE, P. A. & HOLLOSZY J. O. 1972. Respiratory capacity of white and later mediate animals: adaptive response to exercise. *Amer J Physiol* 222, 373-378.
- BOZNER, A. & MEESSEN, H. 1969. Die Feinstruktur des Herzmuskels der Ratte nach einmaligem und nach wiederholtem Schwimmtraining. *Virchows Arch Zellpath.* Abt. B 3, 242-269.
- COSMAS, A. C. & EDINGTON D. W. 1975. Mitochondrial distributions in hearts of male rats as a function of long-term physical training. In: *Metabolic adaptation to prolonged physical exercise* (ed. H. Howald and J. R. Poortmans), pp. 350-356. Birkhäuser Verlag, Basel.
- CREWS, J. & ALDINGER, E. E. 1967. Effect of exercise on myocardial function. *Amer Heart J* 74, 536-542.
- EDINGTON D. W. & COSMAS, A. C. 1972. Effect of maturation on mitochondrial size distribution in rat hearts. *J Appl Physiol* 33, 715-718.
- GOLLNICK, P. D., LANUZZO, C. D. & KING, D. W. 1971. Ultrastructural and enzyme changes in muscles with exercise. In: *Muscle metabolism during exercise* (ed. B. Pernow and B. Saltin), pp. 69-85. Plenum Press, New York.
- HERBENER, G. H., SWIGART, R. H. & LANG, C. A. 1973. Morphometric comparison of the mitochondrial populations of normal and hypertrophied hearts. *Lab Invest* 28, 96-103.
- HOLLOSZY J. O. & BOOTH, F. W. 1976. Biochemical adaptations to endurance exercise in muscle. *Ann Rev Physiol* 38, 173-191.
- HOLLOSZY J. O., OSCAL, L. B., DON, J. J. & MOLE, P. A. 1973. Mitochondrial citric acid cycle and related enzymes: adaptive response to exercise. *Biochem Biophys Res Commun* 40, 1368-1373.
- HOPPELER, H., LUTHI, P., CLAASSEN, H., WEIßEL, E. R. & HOWALD, H. 1973. The ultrastructure of the normal skeletal muscle. A morphometric analysis on contracted and relaxed and well-trained and untrained. *Pflügers Arch Ges Physiol* 314, 17-32.
- KIESSLING, K.-H., MLLSTRÖM, L., BYLUND, A.-C., SALTIN, B. & PHL, K. 1974. Enzyme activities and

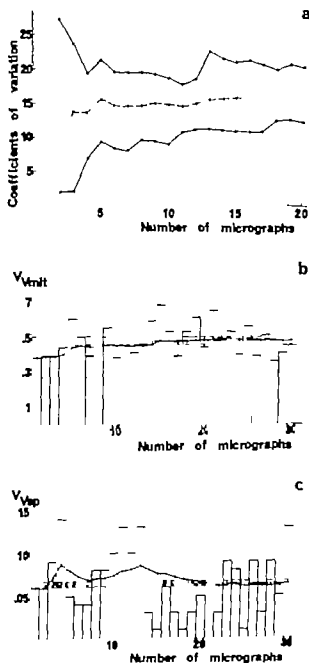


Fig. 2 (A) Determination of the requisite number of micrographs per muscle sample according to Herbener et al (1973). The broken line represents the average value for the variation coefficient and the two unbroken lines the extreme values of the coefficient. Data are taken from the mitochondrial volume densities in group C1. (B) Determination of the requisite number of micrographs for estimation of mitochondrial volume density. Columns represent the volume density estimated per micrograph the fraction line represent the average value of the volume density as a function of increasing number of micrographs and the two lines of dashes indicate the 5% confidence limits of the mean volume density estimated from 30 micrographs. V_{mit} = volume density of mitochondria. (C) Determination of the requisite number of micrograph for estimation of the volume density of sarcoplasmic space. V_{scp} = volume density of sarcoplasmic space other explanations as in Fig. 2B.

of the myocardium seems to be between the atrial and ventricular parts of mouse heart muscle. The values of mitochondrial volume density measured in the apex in the present study were rather similar to those reported by Herbener et al (1973) in the ventricle muscle of mouse heart. In the atrium of the myocardium the mitochondrial volume density reported by Herbener et al (1973) is smaller (33–35%) than that in the apex (41–45%) in this study. Estimations of the mitochondrial volume density based on micrographs taken at the more powerful magnification gave even higher values (48–50% Table 1) as observed earlier (Rohr et al 1976). This is partly due to the method of choosing such areas for electromicrographs which contained large numbers of mitochondria to facilitate the analysis of the surface density of cristae.

In respect of the number of mitochondria per unit volume of myocardium the apex ($4.65 \pm 0.47 \mu\text{m}^3$) was also between the atrium (5.69 ± 0.77) and the ventricle (7.01 ± 1.10) (Herbener et al 1973). The volume of an average mitochondrion was greatest in the ventricle ($1.45 \pm 0.83 \mu\text{m}^3$), medium in the apex (0.83 ± 0.94) and smallest in the atrium (0.56 ± 0.80).

No significant effects of training were observed in the indices of mitochondrial volume density, number or average volume. This is in agreement with the previous results of Arcos et al (1967), Bozner & Meeusen (1961), Gollnick et al (1971), and Paniagua et al (1977) observed with rats. A training programme consisting of 1 h daily running at a speed of 20 m/min for 5 days a week caused an 8–12% significant increase in the heart weight of mice after 20 exercises (Vihko & Salminen unpublished). The lack of training effects in mitochondrial variables or in myofibrillar volume density therefore suggests that myofibrillar or mitochondrial biogenesis occurs in proportion to cardiac muscle hypertrophy. According to Bozner & Meeusen (1969) mitochondrial volume fraction increases at early phases of training being at its highest on the fourth day after the beginning of training. Therefore it is also possible that at early phases of hypertrophy mitochondrial capacity first increases and improved capacity for energy production enables rapid protein biosynthesis resulting in a new hypertrophied steady state relatively soon, e.g. after one month of training as in this study (TR1-group). However Aldinger & Sohal (1970) and Arcos et al (1967) have reported increased

Villous tissue osmolality and intestinal transport of water and electrolytes

AN-AXEL HALLBÄCK, MATS JODAL, ANDERS SJÖQVIST
and OVE LUNDGREN

Department of Physiology, University of Göteborg, Sweden

HALLBÄCK A, JODAL M, SJÖQVIST A. & LUNDGREN O. Villous tissue osmolality and intestinal transport of water and electrolytes. *Acta Physiol Scand* 1979; 107: 115-126. Received 28 Febr. 1979. ISSN 0001-6772. Department of Physiology, University of Göteborg, Sweden.

The villous tissue hyperosmolality created by the intestinal countercurrent multiplier has been proposed to be of importance for fluid transport across the intestinal epithelium *in vivo*. This study was performed to test this hypothesis. Net transport of fluid and electrolytes (sodium, potassium and chloride), as well as unidirectional fluxes of water and sodium were determined in the small intestine of the cat. The villous osmolality was altered by varying the composition of sodium and glucose in the isotonic solutions perfusing the intestinal lumen. Net transport of fluid was correlated to tissue osmolality mainly due to an increase of the unidirectional flux of water from lumen to tissue with augmented tissue osmolality. The results are thus consistent with the view that the intestinal countercurrent multiplier is of essential importance for net water transport. A correlation was found between net water and net sodium intestinal transport. A similar correlation was also demonstrated between net sodium and net chloride absorption rates in the jejunum while in the ileum net loss of sodium into the intestinal lumen was not accompanied by any corresponding loss of chloride loss. This observation suggests the presence of sodium independent transport mechanisms for chloride in the ileum but not in the jejunum.

The vascular arrangement in the cat intestinal villi is consistent with the existence of a countercurrent exchanger, as also supported by experimental observations (for reviews, see Lundgren 1967, 1974). Jodal and co-workers (Haljamae et al. 1973; Jodal 1973; Jodal et al. 1978) proposed that a villous countercurrent exchanger would be particularly important for water and solute absorption by creating a hyperosmolar compartment at the villous tip as a result of its countercurrent multiplying effects. It is as recently possible to quantify this hyperosmolality with a cryoscopic method (Jodal et al. 1978). Such revealed a villous tip osmolality beyond 1000 mOsm/kg H₂O in the feline gut during luminal perfusion with an isotonic solution containing sodium and glucose.

The efficiency of countercurrent multiplier is among other things dependent on the rate of active solute uptake. By varying the composition of the luminal perfusate, it is possible to vary the rate of active absorption of solutes (e.g. sodium) which

influences the concentration gradient between the two limbs of the countercurrent exchanger. This, in turn, affects the degree of tissue hyperosmolality at the villous tips (Jodal et al. 1978; Hallbäck et al. 1979b).

The present study was designed to investigate the effects on water and solute absorption when tissue osmolality in the intestinal villi was varied. The efficiency of the countercurrent multiplier was altered by changing the sodium and/or glucose contents of the luminal perfusate. Bidirectional fluxes of water and sodium as well as net potassium and net chloride transport were determined and correlated to tissue osmolality.

METHODS

The experiments of this study were included in those recently reported by Hallbäck et al. (1979b). Consequently operative procedures, recordings of net water transport, the cryoscopic technique and the solutions used are identical, and described in the mentioned paper. The determi-

- morphometry in skeletal muscle of middle-aged men after training. *Scand J Clin Lab Invest* 33: 63-69.
- MEERSON F Z. 1975. Role of synthesis of nucleic acids and protein in adaptation to external environment. *Physiol Rev* 55: 79-123.
- MEERSON F Z. & BREGER A M. 1977. Common mechanisms of hearts adaptation and deadaptation—hypertrophy and atrophy of heart muscle. *Basic Res Cardiol* 72: 228-234.
- MERZ, W. A. 1968. Die Streckenmessung an gerichteten Strukturen im Mikroskop und ihre Anwendung zur Bestimmung von Oberflächen-Volumen-Relationen im Knochengewebe. *Mikroskopie* 22: 132-142.
- MOLE P A, OSCAI L B & HOLLOSZY J O. 1971. Adaptation of muscle to exercise. Increase in the levels of palmityl CoA synthetase, carnitine palmitate transferase and palmityl CoA dehydrogenase and in the capacity to oxidize fatty acids. *J Clin Invest* 50: 2323-2330.
- OSCAI L B, MOLE P A, BREID B & HOLLOSZY J O. 1971a. Cardiac growth and respiratory enzyme levels in male rats subjected to a running programme. *Amer J Physiol* 220: 1238-1241.
- OSCAI L B, MOLE P A & HOLLOSZY J O. 1971b. Effects of exercise on cardiac weight and mitochondria in male and female rats. *Amer J Physiol* 220: 1944-1948.
- PANIAGUA R, VAZQUEZ, J J & LOPEZ MORA TALLA N. 1977. Effects of physical training on rat myocardium. An enzymatic and ultrastructural morphometric study. *Rev Esp Fisiol* 33: 273-282.
- PETTE D. 1966. Mitochondrial enzyme activities. Regulation of metabolic processes in muscle. (ed J M Tager, S Papa, E Quagliariello and E Slater) vol 7 pp 75-49. Elsevier Publishing Co, Amsterdam.
- ROHR H, OBERHOLZER M, BARTSCH G J, KELLER M. 1976. Morphometry in cytoenergetics pathology. Methods, baseline data and applications. *Int Rev Exp Path* 15: 233-325.
- SOHAL, R S, SUN S C, COLCOLOUGH, R L J, BURCH G E. 1968. Ultrastructural changes with intercalated disc in exercised rat hearts. *Lab Invest* 18: 49-53.
- VIHKO V, SARVIHARJU P J, HAVU M, HIRVIMÄKI Y, SALMINEN A, RAHNILA P & AHTILA A U. 1975. Selected skeletal muscle variables and aerobic power in trained and untrained men. *J Sports Med (Torino)* 15: 296-304.
- WEIBEL, E. R. 1969. Stereological principles for morphometry in electron microscopic cytology. *Int Rev Cytol* 26: 235-302.
- WEIBEL, E. R. & GNAGI H R. 1968. Improvements in efficiency of stereologic methods in electron microscopic cytology. Fourth Eur Regional Conf on Electron Microscopy, Rome, pp 601-602.
- WEIBEL, E. R. & GOMEZ DUMM D M. 1962. A principle for counting tissue structures on random sections. *J Appl Physiol* 17: 343-348.

able — Absorption of water (net and fluxes) and the corresponding tissue osmolality in various portions of intestinal villi during the different experimental procedure of this study

— Net values for net absorption means absorption, negative values secretion. Mean values \pm S.E.

	Net water movement (ul/min 100 cm ²)	Water flux from lumen to tissue (ul/min 100 cm ²)	Water flux from tissue to lumen (ul/min 100 cm ²)	Villous tip osmolality (mOsm/kg H ₂ O)	Mean osmolality (mOsm/kg H ₂ O) in upper	5 to 30 % of villous length	5 to 90 % of villous length	5 to 100 % of villous length
jejunum								
rebo-glucose (—9)	344 \pm 69	1114 \pm 157	791 \pm 116	1022 \pm 30	669 \pm 23	590 \pm 23	461 \pm 13	
rebo-sucrose (—8)	21 \pm 59	1065 \pm 182	830 \pm 189	901 \pm 50	652 \pm 34	580 \pm 28	468 \pm 15	
rebo-glucose								
25 g/mol Na (8)	77 \pm 33	822 \pm 177	747 \pm 106	701 \pm 77	560 \pm 47	497 \pm 38	421 \pm 25	
rebo-sucrose								
25 g/mol Na (—9)	46 \pm 35	705 \pm 75	659 \pm 74	633 \pm 54	518 \pm 35	475 \pm 27	410 \pm 15	
rebo-glucose (—9)	40 \pm 26	1141 \pm 75	1182 \pm 65	631 \pm 64	491 \pm 41	448 \pm 33	395 \pm 21	
rebo-sucrose (—6)	97 \pm 32	779 \pm 206	867 \pm 701	495 \pm 58	430 \pm 43	405 \pm 37	368 \pm 15	
rebo-sucrose (—6)	20 \pm 42	737 \pm 129	717 \pm 107	579 \pm 37	463 \pm 21	428 \pm 17	383 \pm 12	
ileum								
rebo-glucose (8)	252 \pm 6	931 \pm 178	713 \pm 163	940 \pm 33	679 \pm 22	591 \pm 19	478 \pm 15	
rebo-sucrose (8)	188 \pm 51	1110 \pm 129	905 \pm 119	895 \pm 57	680 \pm 43	601 \pm 34	482 \pm 19	
rebo-glucose								
25 g/mol Na (9)	109 \pm 32	779 \pm 97	670 \pm 88	764 \pm 53	603 \pm 36	535 \pm 28	437 \pm 15	
rebo-sucrose								
25 g/mol Na (—9)	3 \pm 32	597 \pm 72	565 \pm 59	643 \pm 12	545 \pm 13	501 \pm 11	430 \pm 8	
rebo-glucose (—8)	43 \pm 79	776 \pm 138	734 \pm 125	629 \pm 34	513 \pm 19	466 \pm 16	403 \pm 10	
rebo-sucrose (—6)	86 \pm 53	434 \pm 11	539 \pm 122	463 \pm 67	399 \pm 43	381 \pm 34	343 \pm 19	
rebo-sucrose (—6)	6 \pm 65	961 \pm 67	623 \pm 72	658 \pm 46	554 \pm 30	504 \pm 48	431 \pm 37	

as zero in both the jejunum and the ileum. The studies of unidirectional fluxes (Fig. 1) revealed that the increased rate of net water absorption along with augmented tissue osmolality was largely ex-

plained by a marked increase of lumen to tissue flux of water (about 410 and 490 μ l/min \times 100 cm² in jejunum and ileum respectively right panel of Fig. 1) in both intestinal segments. The corresponding

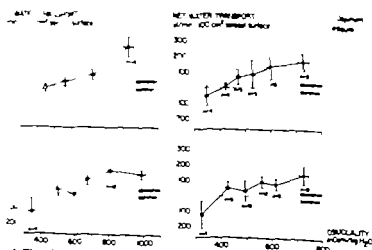


Fig. 1. The relationship between intestinal net water transport and villous tip osmolality (left panels) or mean tissue osmolality in the upper 5 to 30 % of villous length (right panels) in jejunum (upper panels) and ileum (lower panels). The results obtained with the different perfusates were classified according to tissue osmolality. Bars denote S.E.

nations of water and electrolyte fluxes will be described below

A. Biochemical and radioactive measurements

To determine water and electrolyte fluxes across the intestinal epithelium, samples (2–3 ml) collected in plastic tube (1) were taken of the perfusate entering and leaving the intestinal segments after a perfusion period lasting at least 15 min. Sodium and potassium concentrations of these samples were measured by flame photometry (Eppendorf) and chloride concentrations with a chloride meter (Corming Eel 970 Chloride meter, Halstead, Essex, England).

To determine unidirectional water and sodium transport from lumen to tissue, 50–60 μCi $^3\text{H}_2\text{O}$ and 4–8 μCi ^{22}Na (0.05 μg) were added per liter perfusate and the β -radiation was estimated in a Packard Tri-carb liquid scintillation spectrometer. The time of counting was prolonged so that the coefficient of variation was below 1%. An external γ -standard was used to correct for quenching. All analyses were carried out in duplicates.

In 20 animals the arterial concentrations of the two tracers were determined at the end of the experiment. They never exceeded 3% of the luminal concentration. In most experiments they were about 1% of that of the perfusate.

B. Calculation

1. *Intestinal net water transport* was calculated from the continuously recorded change in perfusate volume in the recirculating system (see Jodal et al. 1975).

2. *Intestinal net transport of electrolytes* were calculated according to the following formula:

$$J_{\text{net}} = C_{\text{in}} \times V_{\text{in}} - C_{\text{out}} \times (V_{\text{in}} - J_{\text{net}}^{\text{H}_2\text{O}}) \quad (1)$$

For explanation of symbols used see Table 1.

3. *Unidirectional rate and sodium transport* were calculated according to Levitan et al. (1962) and Skadhauge (1969) modified to fit our direct net water transport determinations. Mean luminal concentrations of sodium and tracers (^{22}Na and $^3\text{H}_2\text{O}$) were calculated assuming logarithmic reductions along the intestinal segment. The following formulas were used:

$$J_{\text{in}}^{\text{H}_2\text{O}} = \frac{[\text{H}_2\text{O}]_{\text{in}} \times V_{\text{in}} - [\text{H}_2\text{O}]_{\text{out}} (V_{\text{in}} - J_{\text{net}}^{\text{H}_2\text{O}})}{10 \log([\text{H}_2\text{O}]_{\text{in}}) - \log([\text{H}_2\text{O}]_{\text{out}})} \quad (2)$$

$$J_{\text{in}}^{\text{Na}} = \frac{[^{22}\text{Na}]_{\text{in}} \times V_{\text{in}} - [^{22}\text{Na}]_{\text{out}} (V_{\text{in}} - J_{\text{net}}^{\text{H}_2\text{O}})}{10 \log([^{22}\text{Na}]_{\text{in}}) - \log([^{22}\text{Na}]_{\text{out}})} \times 10 \log([Na]_{\text{in}}) - \log([Na]_{\text{out}})} \quad (3)$$

$$J_{\text{out}} = J_{\text{in}} - J_{\text{net}} \quad (4)$$

The fluxes were related to serosal area and expressed as $\mu\text{l}/\text{min} \times 100 \text{ cm}^2$ serosal surface (water) or $\mu\text{mol}/\text{min} \times 100 \text{ cm}^2$ serosal surface (electrolytes).

C. Statistics

Statistical significance was tested using Wilcoxon's non-parametric tests. A *P* value of 0.05 or less was considered as significant (Siegel 1956).

RESULTS

Water transport Table 3 summarizes the results of net and unidirectional water fluxes when the intestinal mucosa was exposed to the 7 different perfusates (see Table 1 Hallböök et al. 1979b). Table 4 also gives the tissue osmolality data recorded in the different perfusates. These results are presented as villous tip osmolality and mean tissue osmolality in upper 5 to 30% of villi and 5 to 100% of villi length.

Fig. 1 gives rates of net water transport in jejunum (upper panels) and ileum (lower panels) plotted against villous tip osmolality (left panels) and against mean tissue osmolality in the upper 5 to 30% of villous length (right panels). The results are classified according to tissue osmolality regardless of perfusate used. In Fig. 2 the unidirectional water transport rates are plotted in a similar manner.

In Fig. 1 negative values denote net water transport from tissue to lumen and positive values indicate net transport in the opposite direction. Both in jejunum and in ileum net water transport changed from secretion to considerable absorption when tip or mean osmolality in upper 5 to 30% of villi length was enhanced and transport tended to level off with increasing osmolality. At villous tip osmolalities around 500 mOsm/kg H_2O or at a mean tissue osmolality around 400 mOsm/kg H_2O in upper 5 to 30% of villous length, net water transport rate

Table 1. Explanation of symbols used in formula 1–4

J_{net}	net transport
J_{in}	unidirectional transport of fluid or solute from lumen to tissue
J_{out}	unidirectional transport of fluid or solute from tissue to lumen
V_{in}	rate of perfusate entering the intestinal segment
C_{in}	concentration of solute in the solution entering the intestinal segment
C_{out}	concentration of solute in the solution leaving the intestinal segment
$[Na]_{\text{in}}, [Na]_{\text{out}}$	concentration of sodium in the solution entering or leaving the intestinal segment
$[^{22}\text{Na}]_{\text{in}}, [^{22}\text{Na}]_{\text{out}}$	concentration of ^{22}Na entering or leaving the intestinal segment
$[^3\text{H}_2\text{O}]_{\text{in}}, [^3\text{H}_2\text{O}]_{\text{out}}$	concentration of tritiated water entering or leaving the intestinal segment

Table 3 Net sodium absorption as well as sodium flux from lumen to tissue and from tissue to lumen measured with the different perfusates used in the study

Positive values denote absorption, negative secretion. Mean values \pm S.E.

	Net sodium movement ($\mu\text{mol/min}$ 100 cm^2)	Sodium flux from lumen to tissue ($\mu\text{mol/min}$ 100 cm^2)	Sodium flux from tissue to lumen ($\mu\text{mol/min}$ 100 cm^2)
Jejunum			
rebo-glucose (6)	49.2 \pm 13.6	91.0 \pm 13.0	46.6 \pm 5.3
rebo-mannitol (7)	6.6 \pm 16.3	79.7 \pm 15.9	77.7 \pm 7.1
soluc-glucose 25 mmol Na ⁺ (=6)	10.8 \pm 4.1	17.8 \pm 5.7	30.1 \pm 2.7
soluc-mannitol 25 mmol Na ⁺ (=7)	-1.9 \pm 6.9	11.2 \pm 1.4	4.1 \pm 7.3
soluc-glucose (=9)	-26.0 \pm 9.2		
soluc-mannitol (7)	24.8 \pm 5.2		
soluc-sucrose (=6)	-28.0 \pm 8.5		
Ileum			
rebo-glucose (8)	38.5 \pm 11.1	100.5 \pm 15.3	6.0 \pm 16.4
rebo-mannitol (=5)	77.6 \pm 12.9	105.0 \pm 0.6	45.5 \pm 14.4
soluc-glucose 25 mmol Na ⁺ (=8)	-5.1 \pm 3.6	21.7 \pm 5.5	27.2 \pm 6.4
soluc-mannitol 25 mmol Na ⁺ (=8)	17.7 \pm 4.3	12.5 \pm 1.7	30.2 \pm 3.7
soluc-glucose (=8)	-9.0 \pm 2.8		
soluc-mannitol (6)	-25.8 \pm 9.9		
soluc-sucrose (6)	26.9 \pm 9.0		

and no statistically significant difference could be demonstrated between the two groups.

In Fig. 5 the net rate of water transport is plotted vs. that for sodium, showing that this relationship is almost linear in both jejunum and ileum. Addition of glucose to the perfusates tended to increase the rate of water absorption in the jejunum though the effect was not statistically significant. In the ileum glucose addition had no effect.

Chloride transport Table 4 summarizes the measured rates of net chloride transport in the jejunum and the ileum. In Fig. 6 net rate of chloride transport is plotted vs. tissue osmolality in a similar way as for net water transport (Fig. 1). In the jejunum the net rate of chloride transport was enhanced from secretion of 10 to an absorption of 30 $\mu\text{mol/min}$ 100 cm^2 serosal surface with increasing tissue osmolality. A net secretion of chloride was recorded in 13 of the 19 expts. with the lowest villous tissue osmolality. In the ileum, on the other hand, secretion was only observed in 4 of the 19 expts. with the lowest osmolality. In Fig. 7 net rate of chloride transport is plotted vs. net rate of sodium transport. In the jejunum these two variables showed good correlation. In the ileum on the other hand, net sodium secretion was not accompanied by any chloride loss into the lumen.

Potassium transport The results on net potassium transport rate are presented in Table 4 and Fig. 8. In both jejunum and ileum a small absorption of potassium was seen in all the experimental series.

Fig. 4 The relationship between unidirectional sodium transports and tissue osmolality illustrated in the same way as Fig. 2. Results obtained with solutions containing 25 mmol Na/l are depicted with dashed lines and those with 147 mmol Na/l solutions with solid lines. Bars denote S.E.

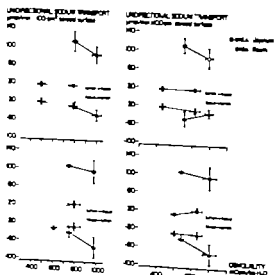


Fig. 4 The relationship between unidirectional sodium transports and tissue osmolality illustrated in the same way as Fig. 2. Results obtained with solutions containing 25 mmol Na/l are depicted with dashed lines and those with 147 mmol Na/l solutions with solid lines. Bars denote S.E.

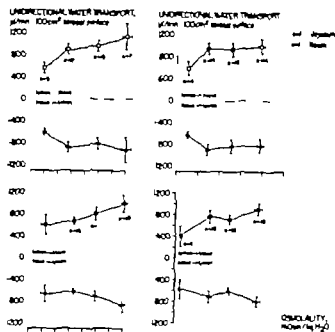


Fig. 2 The relationship between the unidirectional transports of water and tissue osmolality. The abscissa in the left panels denotes villous tip osmolality and in the right panels the mean tissue osmolality in the upper 5 to 30% of the villi. The upper panels show results from jejenum, the lower panels from ileum. The observations were classed according to tissue osmolality. Bars denote S.E.

flux from tissue to lumen also showed a tendency to increase with enhanced tissue osmolality (about 190 and 250 $\mu\text{mol}/\text{min} \times 100 \text{ cm}^2$ in jejenum and ileum, right panel of Fig. 2) an effect that was most pronounced in jejenum at low osmolality.

Sodium transport. Data on sodium transport in

jejenum and ileum are presented in Table 3 showing both rates of net sodium transport as well as rates of unidirectional sodium transport (in the seven perfusates used, negative signs indicating net sodium loss into the lumen).

Fig. 3 illustrates the compiled data on net sodium transport in jejenum (upper panels) and ileum (lower panels) plotted against villous osmolality. The left panels show osmolality at the tip and the right panels mean tissue osmolality in upper 5 to 30% of villous length. Only experiments where the luminal perfusates contained 25 or 147 mmol Na are included and plotted separately.

When the intestinal lumen was exposed to a perfusate containing 25 mmol Na/l, net secretion occurred amounting to about 10 μmol sodium/min 100 cm^2 serosal surface. This secretion tended to be constant despite varying tissue osmolality. When the perfusate contained 147 mmol Na/l there was a net sodium absorption of 50–70 μmol Na/min 100 cm^2 serosal surface, which appeared to be constant or even to decrease with increasing villous osmolality. This decrease of net sodium transport was not statistically significant.

Fig. 4 summarizes the calculations on unidirectional sodium transport, classified in the same manner as for net sodium transport. It is evident that the difference in net sodium absorption between the 25 mmol and the 147 mmol Na solution (Fig. 3) was mainly caused by a marked increase in sodium transport from lumen to tissue. Transport in the opposite direction was fairly constant.

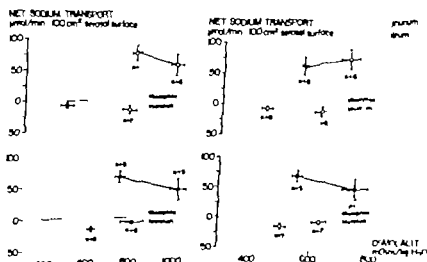


Fig. 3 The relationship between net sodium transport and villous osmolality illustrated in the same way as in Fig. 1. The results from the solutions containing 25 (dotted lines) or 147 mmol Na/l (solid lines) are included. Bars denote S.E.

Table 3 Net sodium absorption as well as sodium flux from lumen to tissue and from tissue to lumen measured with the different perfusates used in the study

Positive values denote absorption, negative secretion. Mean values \pm S.E.

	Net sodium movement ($\mu\text{mol/min}$ 100 cm^2)	Sodium flux from lumen to tissue ($\mu\text{mol/min} \times$ 100 cm^2)	Sodium flux from tissue to lumen ($\mu\text{mol/min}$ 100 cm^2)
jejunum			
free-glucose (6)	49.0 ± 13.6	91.0 ± 13.0	46.6 ± 5.5
free-mannitol (7)	62.6 ± 16.3	79.7 ± 15.9	27.7 ± 7.1
glucose-glucose + 25 mmol N (6)	-10.8 ± 4.1	17.8 ± 5.7	30.1 ± 2.7
glucose-mannitol 25 mmol N (7)	12.9 ± 6.9	11.2 ± 1.4	4.1 ± 7.3
glucose-glucose (9)	-26.0 ± 9.2		
glucose-mannitol (7)	-24.8 ± 5.2		
glucose-methose (6)	28.0 ± 8.5		
ileum			
free-glucose (8)	38.5 ± 11.1	100.5 ± 15.3	61.0 ± 16.4
free-mannitol (5)	72.6 ± 12.9	105.0 ± 0.6	45.5 ± 14.4
glucose-glucose 25 mmol Na (8)	-5.1 ± 3.6	21.7 ± 5.5	77.2 ± 6.4
glucose-mannitol 25 mmol Na (8)	-17.7 ± 4.3	12.5 ± 1.7	30.2 ± 3.7
glucose-glucose (8)	9.0 ± 2.8		
glucose-mannitol (6)	25.8 ± 9.9		
glucose-methose (6)	26.9 ± 9.0		

no statistically significant difference could be demonstrated between the two groups.

In Fig. 5 the net rate of water transport is plotted against sodium concentration, showing that this relationship is almost linear in both jejunum and ileum. Addition of glucose to the perfusates tended to increase the rate of water absorption in the jejunum though the effect was not statistically significant. In the ileum glucose addition had no effect.

Chloride transport Table 4 summarizes the measured rates of net chloride transport in the jejunum and the ileum. In Fig. 6 net rate of chloride transport is plotted vs. tissue osmolality in a similar way as for net water transport (Fig. 1). In the jejunum the net rate of chloride transport was enhanced from a secretion of 10 to an absorption of $30 \mu\text{mol/min}$ 100 cm^2 serosal surface with increasing tissue osmolality. A net secretion of chloride was recorded in 13 of the 19 experiments with the lowest villous tissue osmolality. In the ileum, on the other hand, secretion was only observed in 4 of the 19 experiments with the lowest osmolality. In Fig. 7 net rate of chloride transport is plotted vs. net rate of sodium transport. In the jejunum these two variables showed good correlation. In the ileum on the other hand, net sodium secretion was not accompanied by any chloride loss into the lumen.

Potassium transport The results on net potassium transport rate are presented in Table 4 and Fig. 8. In both jejunum and ileum a small absorption of potassium was seen in all the experimental series.

Figure 4 illustrates the relationship between unidirectional sodium transport and tissue osmolality. The results are presented in the same way as in Figure 1. Results obtained with solutions containing 25 mmol Na/l are depicted with dashed lines and those with 147 mmol Na/l solutions with solid lines. Bars denote S.E.

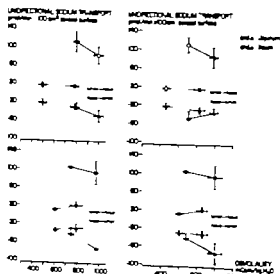


Fig. 4 The relationship between unidirectional sodium transport and tissue osmolality illustrated in the same way as Fig. 1. Results obtained with solutions containing 25 mmol Na/l are depicted with dashed lines and those with 147 mmol Na/l solutions with solid lines. Bars denote S.E.

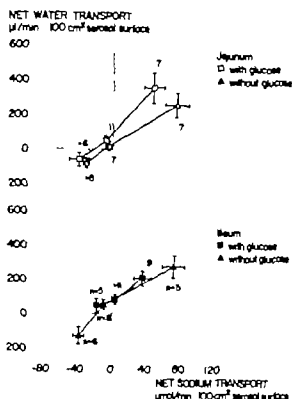


Fig. 5 The relationship between net water transport and net sodium transport in jejunum (upper panel) and ileum (lower panel). Squares illustrate results obtained with solutions containing glucose and triangles depict experiments with glucose-free solutions. Bars denote S.E.

DISCUSSION

There is no evidence to suggest that water transport across epithelia is an active process. It is generally assumed that water passively follows actively

transported solutes (House 1974). To explain water absorption *in vivo* in the absence of a lumen to plasma osmolar gradient, a hypotonic compartment has been postulated to exist in the intestinal mucosa (Curran & Mclennan 1968; Schultz & Curran 1968) which according to Schultz & Curran (1968) should be localized to the space between the epithelial cells and the basolateral membrane. Diamond & Bossert (1967) on the other hand proposed that a standing hyperosmolar gradient is localized to intercellular spaces of epithelium. Such hypertonic spaces around the epithelium have however never been experimentally demonstrated *in vivo* in the small intestine. Later Machen & Diamond (1969) and Simmons & Valin (1976) provided indirect support for the existence of a hyperosmolar compartment in the mammalian gall bladder and small intestine respectively. Gupta, Hall & Naftalin (1978) localized intercellular hyperosmolar region between the epithelial cells by electron microprobing but the observed profiles of $[Na^+]$, $[K^+]$ and $[Cl^-]$ around the enterocytes were not consistent with the steady gradient hypothesis of Diamond & Bossert (1967) or its modifications by Sackin & Boulpaep (1973).

An alternative hypothesis explaining water transport *in vivo* across the epithelia in villous structures was proposed in reports from this laboratory. According to this hypothesis a counterion exchanger exists in most villous structure

Table 4 Net absorption of chloride and potassium in jejunum and ileum during the different experimental procedures of this study

Positive values denotes absorption; negative value secretion. Mean values \pm S.E.

	Net Cl ⁻ movement ($\mu\text{mol}/\text{min} \times 100 \text{ cm}^2$)	Net K ⁺ movement ($\mu\text{mol}/\text{min} \times 100 \text{ cm}^2$)
Jejunum		
Krebs-glucose	38.6 ± 10.4 ($n=9$)	0.69 ± 0.48 ($n=8$)
Krebs-mannitol	37.4 ± 8.6 ($n=8$)	46 ± 0.78 ($n=6$)
Choline-glucose + 25 mmol Na	18.8 ± 8.2 ($n=9$)	-0.69 ± 1.23 ($n=9$)
Choline-mannitol + 25 mmol Na	-0.5 ± 6.5 ($n=9$)	0.77 ± 0.25 ($n=9$)
Choline-glucose	-18.1 ± 8.5 ($n=9$)	0.12 ± 1.20 ($n=10$)
Choline-mannitol	-6.3 ± 9 ($n=4$)	0.83 ± 0.59 ($n=6$)
Choline-maltose	-4.8 ± 7.9 ($n=6$)	-0.55 ± 0.98 ($n=6$)
Ileum		
Krebs-glucose	57.7 ± 6.6 ($n=9$)	1.31 ± 0.33 ($n=9$)
Krebs-mannitol	47.3 ± 14.6 ($n=8$)	4 ± 0.45 ($n=6$)
Choline-glucose + 25 mmol Na	13.4 ± 6.8 ($n=8$)	1.57 ± 0.54 ($n=9$)
Choline-mannitol + 25 mmol Na	1.2 ± 9.2 ($n=9$)	0.87 ± 0.38 ($n=9$)
Choline-glucose	-3.5 ± 4.8 ($n=8$)	0.56 ± 0.33 ($n=8$)
Choline-mannitol	-3.5 ± 11.8 ($n=4$)	1.6 ± 0.56 ($n=7$)
Choline-maltose	0 ± 7.8 ($n=6$)	-0.20 ± 0.40 ($n=6$)

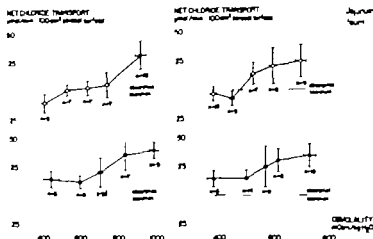


Fig. 6 The relationship between net chloride transport and tissue osmolality illustrated in the same way as in Fig. 1. Bars denote S.E.

functioning as a countercurrent multiplier to create marked increases in villous osmolality (cf Halpern et al. 1973; Jodal 1973; Jodal et al. 1978; Hallback et al. 1979b). Similar mechanisms have been proposed to exist also in papillary structures of the tongue (Hallback et al. 1979). The evidence for these mechanisms includes the demonstration of very high electrolyte concentrations (Halpern et al. 1973; Zentzen & Monge 1975) and marked hyperosmolality (Jodal et al. 1978; Hallback et al. 1979) in the villous core *in vivo*. A close correlation between rate of net water absorption and villous core osmolality is, however, a prerequisite for accepting this hypothesis and the present report is devoted to such an analysis.

The efficiency of a villous countercurrent multiplier and, hence, the extent of villous hyperosmolality depend on several variables, such as blood supply characteristics (including capillary permeability and blood flow), epithelial hydraulic conductivity, epithelial solute permeability, rate of active solute transport in the villi. In the present study tissue hyperosmolality is altered primarily by changing the last-mentioned variable, accomplished by varying the composition of the isotonic perfusates used to supply the intestinal lumen. Based on observations in both *in vitro* and *in vivo* experiments it is generally accepted that sodium is the main ion determining intestinal water absorption (Schultz & Curran 1968). It is also known that passage of sodium across the luminal border of the enterocyte is facilitated when glucose is present in the intestinal lumen (Craze 1964; Schultz & Curran 1970). For

such reasons the concentrations of sodium and glucose in the luminal perfusate were altered in the present experiments.

The results presented in Fig. 1 show a close cor-

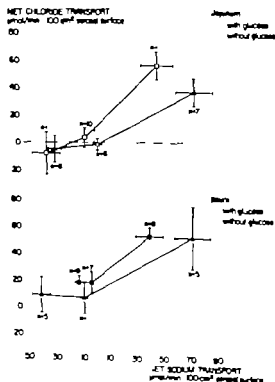


Fig. 7 The relationship between net chloride transport and net sodium transport in jejunum (upper panel) and ileum (lower panel). Squares depict results obtained with solutions containing glucose and triangles illustrate experiments with glucose-free solutions. Bars denote S.E.

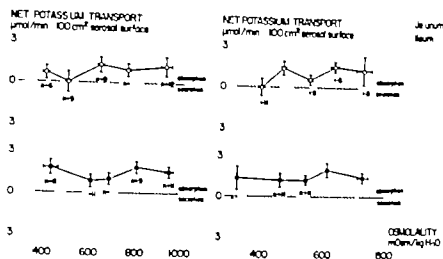


Fig. 8 The relationship between net potassium transport and tissue osmolality illustrated in the same way as in Fig. 1. Bars denote S.E.

relation between net water transport and tissue osmolality. Net water secretion changed into net absorption as villous osmolality increased from just above isotonicity to a marked hyperosmolality. This increase in villous osmolality augmented primarily the flux rate of water from lumen to tissue, thus supporting the hypothesis that the villous countercurrent exchanger is crucial for intestinal water absorption.

Assuming that the tissue osmolality measured in this study represents the only driving force for net water absorption, it is possible to calculate a hydraulic conductivity coefficient of the intestinal epithelium (L_p). This assumption represents of

course an oversimplification of the physiological situation. It should however be pointed out that the osmotic forces created by the tissue osmolality are very large indeed as discussed in previous reports (Jodal et al. 1978; Hallböök et al. 1978). The calculations presented in Table 5 are based on the net water absorption rates and the tissue osmolality measurements reported in Table 1. The L_p values were calculated from the difference between the choline-mannitol group and the other groups and they are expressed per cm^2 mucosal surface, whereas the ratios for mucosal to serosal surface area reported by Wood (1944). The reflection coefficient was set to 0.60 for the jejunum and to 0.85 for the

Table 5 The diffusional permeability to water (P_d) and the hydraulic conductivity (L_p) in the jejunum and the ileum of the cat

All calculations were made assuming that the exchange of water occurred across varying portions of the villi. The details of the calculations are described in text.

	Jejunum			Ileum	
	Length (cm)	P_d ($\text{cm} \times \text{s} \times 10^6$)	L_p ($\text{cm} \times \text{s} \times 10^{12}$)	P_d ($\text{cm} \times \text{s} \times 10^6$)	L_p ($\text{cm} \times \text{s} \times 10^{12}$)
Arabs-glucose	30	2.6	36	1.8	23
	50	1.7	34	1.2	20
	100	0.87	34	0.60	16
Arabs-mannitol	30	2.6	31	1.8	18
	50	1.7	26	1.2	15
	100	0.87	22	0.60	11
Choline-glucose	30	2.6	19	1.8	22
	50	1.7	17	1.2	19
	100	0.87	14	0.60	14

um, since it was assumed that the tissue osmolality increase was mainly made up of sodium chloride (Fordtran et al. 1965). Table 5 includes calculations L_p assuming that the water absorption takes place along the whole villus or only at the upper 30–50% of the villi. When doing the calculations in the two last-mentioned groups the assumed mucosal surface areas were altered correspondingly. The values of this study are of the same order of magnitude as those reported in earlier investigations on the small intestine in vivo (cf. House 1974), compared with the L_p values for various capillaries reported earlier ($(20\text{--}45) \times 10^{-12}$ cm/s Pa; Biber et al. 1973), the hydraulic conductivity of the intestinal epithelium is much smaller.

It is also possible to roughly estimate the diffusive permeability of water (P) from the present results. For these calculations we have chosen the mean influx rate of tritiated water in the experiments with the lowest villous osmolality, i.e. when bovine mannitol was used as luminal perfusate (Table 1). In these experiments diffusion ought to be the dominating process by which tritiated water moves into the tissue. The values obtained are given in Table 5. The diffusive water permeability recorded in the present study is similar to that noted in other studies in vivo (House 1974).

The result presented in Fig. 5 on the relationship between net transport of fluid and net transport of sodium suggests a clear relationship between these two transport processes as has also been shown in a large number of other studies (in vitro: Curran 1960; Clarkson & Rothstein 1960; Barry et al. 1965; α Curran & Salomon 1957; Phillips & Sumner 1967; Fordtran et al. 1968; Sladen & Dawson 1969).

The result of the present study indicate that addition of glucose to a perfusate containing 147 mmol NaCl caused no significant change in sodium transport in the jejunum or in the ileum. However, addition of glucose to solutions containing 25 mmol NaCl enhance the mucosal to serosal flux of sodium.

Two different mechanisms have been proposed to explain the effect of glucose on the lumen to tissue transport of sodium. The sodium gradient hypothesis implies that sodium and glucose interact with a common carrier-transport system at the apical border of the enterocyte and that both solutes are transported transcellularly (Crane 1962; Schultz & Curran 1970; Schultz & Fritzel 1972). On the other hand, in *in vivo* experiments on humans

Fordtran and coworkers (Fordtran et al. 1968; Turnberg et al. 1970; Fordtran 1975) obtained evidence in jejunum but not in ileum for a passive absorption of sodium via a solvent drag phenomenon secondary to an active glucose transport. It is not possible to differentiate between these two mechanisms on the basis of the present results. However, the results do not support the proposal by Fordtran and collaborators that sodium transport is governed by different mechanisms in jejunum and ileum.

Although the present results do not suggest any difference for glucose transport between the jejunum and the ileum, the observations on chloride transport clearly indicate that it differs in the two parts of the small intestine. Thus, the results presented in Figs 6 and 7 and Table 4 suggest the presence of a sodium independent transport mechanism of chloride ions in the ileum while no such mechanism seems to exist in the jejunum. This observation corroborates earlier reports that have proposed the presence of a chloride-bicarbonate exchange mechanism in the ileum (Turnberg et al. 1970b) as well as a sodium dependent transport (Nellans et al. 1974). In jejunum no sodium independent mechanism can be detected either with the present experimental technique or by Turnberg et al. (1970a). The conclusions regarding a chloride-bicarbonate interaction in vivo are based on the observation of a high intraluminal P_{CO_2} . It should however be underlined that the high carbon dioxide concentration in the small intestinal lumen may at least in part, be produced by the presence of the intestinal countercurrent exchanger which very effectively tends to delay the net absorption of lipophilic solutes such as CO_2 (Lundgren 1967; Hamilton et al. 1967, 1968; Bond et al. 1977).

Potassium is generally believed to be passively absorbed through solvent drag (for ref. see Turnberg 1972). Our study indicates that net potassium transport is rather constant in spite of a rising villous tissue osmolality and an increasing net water absorption. However, an augmented passive potassium absorption by solvent drag into the intestinal tissue may be balanced by an increased loss of potassium from the epithelium cells into the lumen. This, in turn, may be secondary to a rise in intracellular K^+ produced by the increased, active pumping of potassium at the baso-lateral membrane by the Na-K dependent ATP-ase pump.

The hypothesis that a countercurrent multiplica-

tion of sodium provides the driving force for passive water and electrolyte absorption in the small intestine implies that the *in vivo* system is extremely complicated. In a previous study the importance of different vascular parameters for the efficiency of the countercurrent exchanger was investigated (Jodal et al 1978). Furthermore experiments were performed by Hallbäck et al (1979b) which studied the dependence of villous tissue osmolality on varying the active solute transport. The present study relates tissue osmolality to transport of water across the epithelium. However to get a detailed knowledge of the interaction between the counter current multiplier and the transport of water and solutes across the intestinal epithelium the influence of a large number of other factors has to be evaluated.

One important factor in this context is the ability of the enterocyte to transport solutes against considerable lumen to tissue concentration gradients. The rate of active transport depends on a large number of factors such as the thickness of the unstirred layer in the lumen, the intracellular concentration of the various solutes, the number of pumping sites per unit plasma membrane surface area. The latter factor may in some instances vary along the villus due to an adaptation to the extracellular environment (cf Csáky & Fischer 1977). Furthermore the active transport of electrolytes together with the extracellular and intracellular ion concentrations determine the potential difference across the plasma membrane of the enterocytes, one further driving force for epithelial movement of ionized solutes.

The established tissue hyperosmolality forces water and dissolved solutes into the tissue through pores, by most workers believed to be mainly located in the epithelial tight junctions. The rate of fluid transfer in the paracellular routes is among other things determined by the width of this space and the leakiness of the tight junctions. The size of the intercellular space is in turn dependent on the interstitial hydrostatic pressure created by the presence of the tissue hyperosmolality according to Curran's double membrane hypothesis. The rate of fluid transfer is also one factor that governs the thickness of the unstirred layer by varying the convective stirring at the lumen-tissue interface.

It is important to realize that all the factors discussed above probably vary quantitatively along

the villous length. The situation is further complicated by a decreasing oxygen tension and increasing carbon dioxide tension in the tissue base to tip, also a result of the intestinal countercurrent exchanger (Lundgren 1967). Finally the probable existence of active secretory mechanisms, perhaps mainly localized in the crypts, have to be taken into the account as well as a diffusion of solutes into the lumen in the villi along favorable concentration gradients.

The description above clearly indicates that a large number of technically very difficult experiments are needed before a detailed understanding of the villous transport mechanisms *in vivo* are obtained and further that one should be cautious transferring *in vitro* results to the *in vivo* situation (cf Corbett et al 1977).

This research was supported by grants from the Swedish Medical Research Council (14X-285), from the Swedish Society for Medical Sciences, from Harald's and Greta Jonsson Fund from Magnus Bergvall's bequest and from the Faculty of Medicine, University of Göteborg.

REFERENCES

- BARRY J C, SMYTH D H & WRIGHT E W 1965 Short-circuit current and solute transfer by a jejunal. *J Physiol* **181** 410-431.
- BIBER B, LUNDGREN O & SVANVİK J 1971 Intramural blood flow and blood volume in the small intestine of the cat as analyzed by an indicator-dilution technique. *Acta Physiol Scand* **87** 391-401.
- BOND J H, LEVITT D G & LEVITT M D 1977 Quantitation of countercurrent exchange during passive absorption from the dog small intestine. *JCI Invest* **59** 308-318.
- CLARKSON T W & ROTHSTEIN A 1960 Transport of monovalent cations by the isolated small intestine of the rat. *Amer J Physiol* **199** 898-906.
- CORBETT C L, ISAACS P F T, RILEY A K & TURNBERG I A 1977 Human intestinal transport *in vitro*. *Gut* **18** 116-140.
- CRANE R K 1966 Hypothesis for mechanism of small intestinal active transport of sugars. *Fed Proc* **1** 891-895.
- CSÁKY T Z & FISCHLER E 1977 Induction of intestinal epithelial sugar transport by high NaCl sugar. *Experientia (Basel)* **33** 223-224.
- CURRAN P F 1960 NaCl and water transport by rat ileum *in vitro*. *J Gen Physiol* **43** 1137-1148.
- CURRAN P F & MACINTOSH J R 1966 A mechanism for biological water transport. *Nature (Lond)* **191** 347-348.
- CURRAN P F & SOLOMON A K 1957 Ion and

- water fluxes in the ileum of rats. *J Gen Physiol* 41: 143-148.
- ANOND J M & BOSSERT W H 1967 Steadily-gradient osmotic flow: A mechanism for coupling of salt and solute transport in epithelia. *J Gen Physiol* 50: 2081-2083.
- SCHER R B & PARLSONS D S 1950. The gradient of mucosal surface area in the small intestine of the rat. *J Anat* 84: 771-782.
- FORDTRAN J S 1975 Stimulation of active and passive sodium absorption by sugars in the human jejunum. *J Clin Invest* 55: 728-737.
- FORDTRAN J S, RECTOR F C, EWTON M F, SOTER N & KINNEY J 1965 Permeability characteristics of the human small intestine. *J Clin Invest* 44: 1935-1944.
- FORDTRAN J S, RECTOR F C & CARTER, N W 1968 The mechanism of sodium absorption: the human small intestine. *J Clin Invest* 47: 884-900.
- ROVIV D, DEBALA, R P & SULLIVAN H W 1975 Ion transport by rabbit jejunum in vivo. *Am J Physiol* 228: 166-168.
- UPTA B J, HALL, T A & NAFTALIN R J 1978 Microprobe measurement of Na, K and Cl concentration profiles in epithelial cells and intercellular spaces of rabbit ileum. *Nature (Lond)* 272: 70-73.
- ALLMÄE H, JODAL, M & LUNDGREN O 1973 Countercurrent multiplication of sodium in intestinal ileum during absorption of sodium chloride. *Acta Physiol Scand* 99: 580-593.
- ALLMÄE H, JODAL, M & LUNDGREN O 1978 Evidence for the existence of countercurrent exchange in the small intestine in man. *Gastroenterology* 74: 682-690.
- HALLMÄE H, JODAL, M & LUNDGREN O 1979 Vascular anatomy and tissue osmolality in the ileum and jejunum papillae of the cat. *Am J Physiol* 236: 101-108.
- HALLMÄE H, JODAL, M & LUNDGREN O 1978a Importance of sodium and glucose for the establishment of villous tissue hyperosmolality by the intestinal countercurrent multiplier. *Acta Physiol Scand* 107: 89-96.
- HAMILTON J D, DAWSON A M & WEBB J 1967 Limitation of the use of inert gases in the measurement of small gut mucosal blood flow. *Gut* 8: 409-421.
- HAMILTON J D, DAWSON A M & WEBB J P W 1968 Observations upon small gut mucosal pO_2 and pCO_2 in anesthetized dogs. *Gastroenterology* 55: 71-80.
- HOUSE, C R 1974 Water transport in cells and tissues. Edward Arnold (Publ.) London.
- JODAL, M 1973 The significance of the intestinal countercurrent exchanger for the absorption of sodium and fatty acids. Thesis, Gösta AB Göteborg.
- JODAL, M, HALLMÄE, H & SVANVIG J & LUNDGREN O 1979 A method for the continuous study of net salt and water transport in the feline small bowel. *Acta Physiol Scand* 95: 441-447.
- JODAL, M, HALLMÄE, H & LUNDGREN O 1978 Tissue osmolality in intestine with during jejunal perfusion with isotonic electrolyte solutions. *Acta Physiol Scand* 102: 94-107.
- LEVITAN R., FORDTRAN J S, BURROWS B A & INGELFINGER, F J 1962 Water and salt absorption in the human colon. *J Clin Invest* 41: 1754-1759.
- LUNDGREN O 1967 Studies on blood flow distribution and countercurrent exchange in the small intestine. *Acta Physiol Scand* Suppl 303.
- LUNDGREN O 1974 The circulation of the small bowel mucosa. *Gut* 15: 1005-1013.
- MACHEN T E. & DIAMOND J M 1969 An estimate of the salt concentration in the lateral intercellular spaces of rabbit gallbladder during maximal fluid transport. *J Membrane Biol* 1: 194-213.
- NELLANS H N, FRIZZELL, R A & SCHULTZ, S G 1974 Brush-border processes and transmembrane Na and Cl transport by rabbit ileum. *Am J Physiol* 226: 1131-1141.
- PHILLIPS S F & SUMMERSKILL, W H J 1967 Water and electrolyte transport during maintenance of motility in human jejunum and ileum. *J Lab Clin Med* 70: 686-696.
- SACKIN H & BOULPAEP E L 1975 Models for coupling of salt and water transport. Proximal tubular reabsorption in vertebrate kidney. *J Gen Physiol* 66: 61-73.
- SCHULTZ, S G & CURRAN P F 1968 Intestinal absorption of sodium chloride and water. In: *Handbook of Physiology* sec 6, vol III pp. 1245-1275.
- SCHULTZ, S G & CURRAN P F 1970 Coupled transport of sodium and organic solutes. *Physiol Rev* 50: 637-718.
- SCHULTZ, S G & FRIZZELL, R A 1972 An overview of intestinal absorptive and secretory processes. *Gastroenterology* 63: 161-170.
- SIEGEL, S 1956 Nonparametric statistics for the behavioral sciences. McGraw-Hill Kogakusha, Tokyo.
- SIMMONS N L & NAFTALIN R J 1976 Factors affecting the compartment of sodium ion within rabbit ileum in vitro. *Biochim Biophys Acta* 448: 411-425.
- SKADHAUGE, E. 1969 The mechanism of salt and water absorption in the intestine of the eel (*Anguilla anguilla*) adapted to waters of various salinities. *J Physiol* 204: 135-158.
- SLADEN G E & DAWSON A. M. 1969 Interrelationships between the absorptions of glucose, sodium and water by the normal human jejunum. *Clin Sci* 36: 119-133.
- TURNBERG L. A. 1972 Mechanism of potassium transport in the human small intestine. In: *Transport across the intestine* (ed W L. Barlow & P D. Seaman) Edinburgh and London.
- TURNBERG L. A., FORDTRAN J S, CARTER, N W & RECTOR, F C 1970a Mechanism of bicarbonate absorption and its relationship to sodium transport in the human jejunum. *J Clin Invest* 49: 548-556.
- TURNBERG L. A., BIEBERDORF P A, MORAWSKI S O & FORDTRAN J S 1970b Interrelationships of chloride, bicarbonate, sodium

- and hydrogen transport in the human ileum. *J. Clin. Invest.* 49: 557-567.
- WOOD H. O. 1944 The surface area of the intestinal mucosa in the rat and in the cat. *J. Anat.* 78: 103-105.
- ZEUTHEN T. & MONGE E. 1975 Intra- and ex-

tracellular gradients of electrical potential and activities of the epithelial cells of the rabbit ileum recorded by microelectrodes. *Phil. Trans. R. Soc. Lond.* 271: 277-281.

Influence of Intravenous Infusion on heart rate, sympathetic and vagal efferentation and left atrial and aortic baroreceptor activity in dogs

MARTTI O. K. HAKUMÄKI

Department of Physiology, University of Kuopio, Finland, and Department of Physiology, University of Helsinki, Finland

HAKUMÄKI M. O. K. Influence of intravenous infusion on heart rate, sympathetic and vagal efferentation and left atrial and aortic baroreceptor activity in dogs. *Acta Physiol Scand* 1979, 107, 127-133. Received 3 March 1979. ISSN 0001-6772. Department of Physiology, University of Kuopio, Finland, and Department of Physiology, University of Helsinki, Finland.

The influence of 42 infusions of saline on heart rate, sympathetic and vagal cardiac efferent activity and on the aortic baroreceptor and left atrial B-type nerve impulse activity was studied in 37 morphine-chloralose anesthetized dogs. The responses in heart rate were tachycardic in 31 infusions and bradycardic in 11 infusions. In tachycardia, sympathetic activity increased in majority of the cases but also decreases and nonsignificant changes were observed. Vagal efferentation decreased in most of the cases but also nonsignificant changes or increases in activity occurred. Sympathetic efferentation notably decreased in bradycardic responses while vagal efferentation diverged in different directions in its nerve activity rate. The ratio of sympathetic to vagal impulses significantly correlated to the heart rate in most of the cases in tachycardia but not in bradycardia. It is concluded that sympathetic and vagal cardiac efferentation plays significant role in heart rate regulation in volume load-induced tachycardia but in bradycardia only the changes in sympathetic cardiac efferentation are important in respect to heart rate changes. The aortic baroreceptor and left atrial B-type receptor activity rate increased both in tachycardia and bradycardia. Changes in the activities of these receptors do not explain the different heart rate responses. It is supposed that bradycardic responses result from changes in cardiac contraction associated with some reflex mechanism suppressing the excitatory influence of the activity of atrial receptors on sympathetic cardiac efferentation.

Key words: autonomic nervous system, sympathetic efferent cardiac discharges, vagal efferent cardiac discharges, left atrial receptor discharges, baroreceptor discharges, heart rate.

Since Bainbridge's (1915) observation on the influence of infusion on the heart rate in dogs numerous investigations have been done in order to investigate the phenomenon and to find the local receptor area of the afferent pathway and the role of sympathetic and vagal efferentation in this reflex. In these studies it has been shown that a tachycardic response to infusion can be elicited (Sawa & Miyazaki 1970, Anrep & Seppälä 1926) but not always (DeGraff & Sand 1925, Ball & Katz 1941), and it seems to depend on the control heart rate (Colledge & Linden 1955, Pathak 1959, Jones 1966, Ahmed & Nicoll 1963, Horich et al. 1964) and the grade of the local stretch (Goetz 1965). Also

tachycardia can be elicited in denervated hearts (Pathak 1959, Donald & Shepherd 1963). The possible reflex area of afferentation has been studied by Ledson & Linden 1964, Kurim et al. 1977 and Kappagoda, Linden & Soow 1977 and was found to be localized at the junction of the atria and blood vessels. Also in conscious dogs i.v. infusion induced tachycardia (Bishop & Peterson 1976) and the same reflexogenic pathways have been observed as in anesthetized dogs.

The findings and observations on the activity in afferent and efferent cardiac nerves during i.v. infusions or local distensions are sparse. It has been demonstrated that atrial B-type activity and sym-

pathetic efferent cardiac activity increase during the distension of the atrial—blood vessel junction (Lindén 1973). An increase in sympathetic cardiac efferentation during *i.v.* infusion has been reported by Bergström, Hakumäki & Sarajärvi (1971) as well as a decrease in vagal efferentation and an increase in sympathetic cardiac activity (Hakumäki 1972). The difference between the left and right atrium has been studied by Koizumi *et al.* (1975) who observed that distension of the right atrium always induced an increase in sympathetic efferent cardiac activity but on the left side the response to stretch was immediately a decrease and after that an overshooting in efferentation and heart rate. In blood cats sympathetic afferent activity from the heart also increased after an injection of saline (Malliani *et al.* 1975). Previous works have demonstrated that different types of local stimuli and also *i.v.* infusions induce both tachycardia and bradycardia and different types of responses in sympathetic and vagal efferentation while changes in afferentation and afferentation—efferentation relationships are unknown.

The aim of this work was to study the function of left atrial receptors, aortic baroreceptors and sympathetic and vagal efferent cardiac activity before during and after *i.v.* infusion in Bainbridge type experiments in anesthetized dogs in order to find out what kind of changes in afferentation and efferentation can be observed in cardio-acceleratory or bradycardic responses.

METHODS

37 dogs weighing 8–15 kg were premedicated with morphine hydrochloride (1 mg/kg) and 1 h later anesthetized with an *i.v.* infusion of α -chloralose (100 mg/kg). The dog was then intubated and artificial respiration was started with a gas mixture of air and 20% oxygen. When the chest was opened an expiratory resistance of 3 cm of water was placed in the expiratory outlet of the respirator. The left side of the chest was opened and the fourth rib was removed. The upper lobe of the lung was resected and a paraffin oil pool was formed inside the thorax cavity from pleura parietale. The femoral vein was cannulated for *i.v.* infusions. In some of the experiments catheters for recording aortic arch and left atrial pressure were introduced through the femoral artery and pulmonary vein. The catheters were flushed with heparin solution (50 IU/100 ml) of saline during the course of the experiment. On the left side of the neck the vagosympathetic trunk was prepared in order to record vagal efferentation, baroreceptor afferentation and left atrial afferent activity. Response in vagal efferentation was tested by stimulating electrically the cranial end of the baroreceptor nerve. Those efferent

fibres of the vagus nerve which showed spontaneous efferent activity capable of being increased by aortic receptor nerve stimulation were selected for the recording of cardiovascular efferent vagal activity. The acid-base balance of the experimental animal was monitored by taking blood samples anaerobically from the femoral artery. The corrections to acid-base balance and fluid balance were made by adjusting the ventilated gas mixture and respirator rate and by giving *i.v.* 7.5% sodium bicarbonate. The pO_2 of arterial blood was adjusted to 140 mmHg, pCO_2 to 20–40 mmHg and pH to 7.35–7.45. The temperature of the animal was measured from the esophagus and temporarily from the left atrium by means of an electric thermometer and regulated with a water-heated operation table. Additional doses of α -chloralose were given when needed. The urinary bladder was cannulated. The *i.v.* infusions were performed through the femoral vein and the temperature of the infused saline was equal to the temperature of the left atrial blood of the experimental animal. The sympathetic activity was recorded from the few-fibres preparation of the third efferent cardiac nerve. Vagal efferentation was recorded from its fibres. The afferent activities in all the experiments were recorded from single fibres. The action potentials were filmed from the screen of a cathode ray tube at a speed of 15.2 cm/s. The impulses were calculated usually from the film. The number of impulses per second or one heart cycle was calculated and the values for statistical analyses were the mean of the impulses from several periods of 4 s. The significance of the changes in heart rate and nerve activities were studied by a Student's *t*-test. The correlations between two parameters were tested with regression analysis. The changes were significant if P was less than 0.05. All the calculated values were determined from a period before (control), during and after the infusion and from a 10 s period after a 2 s break in the recording following the infusion period.

RESULTS

In all the experiments attempts were made to record simultaneously as many different nerve fibres as possible, usually from 2 to 4 different nerves. In 32 dogs with 42 infusions the discharge rates of 8 aortic baroreceptors, 1 left atrial B-type receptor, 31 sympathetic efferent nerves and 31 vagal cardiac efferent nerves were studied.

Heart rate responses to infusion

The 42 *i.v.* infusion of 80–150 ml of body warm saline in 37 dogs within 40–80 s induced tachycardia in 31 cases and bradycardia in 11 cases. The control values of heart rate in tachycardic responses varied from 54 beats/min to 158 beats/min, mean 91 beats/min and the maximal effect during or after infusion was 118 beats/min to 185 beats/min, mean 125 beats/min. The difference in heart rate between the mean of control and the mean of the tachycardic

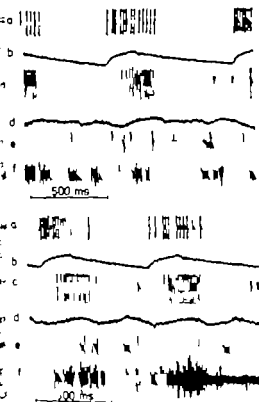


Fig. 1 Influence of saline infusion upon nerve activities before (A) and 20 s after (B) infusion of 170 ml of saline. The traces from top to bottom: (a) Aortic baroreceptor activity (b) aortic arch pressure (c) left atrial B-type activity (d) left atrial pressure (e) vagal efferent cardiac activity and (f) sympathetic efferent cardiac activity. The weight of the animal was 10.2 kg and the response to saline tachycardia.

response was highly significant ($P < 0.001$). In 10 out of 31 infusions the beginning of the infusion induced a decrease in heart rate during the first 4–10 heart beats which was followed by tachycardia. Fig. 2 (a) bradycardic responses the control heart rate values varied from 101 beats/min to 169 beats/min, mean 122 beats/min and during the infusion from 78 beats/min to 153 beats/min, mean 117 beats/min. The difference between the mean values of the two groups was highly significant ($P < 0.001$).

Nerve activities in tachycardia

In tachycardic responses with 31 infusion the sympathetic efferentation increased in 24 (78%) de-

TACHYCARDIA

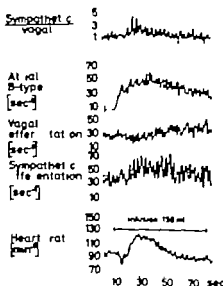


Fig. 2 Influence of saline infusion on the ratio of the number of sympathetic and vagal impulses, number of left atrial B-type impulses, number of vagal cardiac efferent impulses, number of sympathetic postganglionic efferent cardiac impulses and on the heart rate where the response to infusion is tachycardia. Note the decrease in heart rate at the beginning of the infusion. The values represent results calculated from cycle to cycle. The weight of the animal was 12.7 kg.

creased in 1 (3%) ($P < 0.05$ – 0.001) and was not changed in 6 (19%) ($P > 0.01$) of the infusions. Vagal efferentation increased in 4 (13%) decreased in 20 (64%) and no changes were observed in 7 (23%) of the cases. The ratio of sympathetic to vagal impulses increased in 26 (83%) decreased in 0 (0%) and was not significantly changed in 5 (17%) of the cases. Aortic baroreceptor activity rate increased significantly in all the tachycardic responses as did the left atrial B-type activity rate. Typical changes in afferentations and efferentations are demonstrated in Figs. 1 and 2. The correlation coefficients (r) between the heart rate and the sympathetic efferentation varied from 0.144 to 0.917 mean of 0.702 , $n=18$, $P < 0.001$ of mean value and from -0.226 to -0.865 mean of -0.577 , $n=1$, $P < 0.01$ of mean value. The correlation coefficients between heart rate and vagal efferentation varied from -0.377 to -0.983 mean of -0.678 , $n=18$, $P < 0.001$ of mean value and from 0.275 to 0.799 mean of 0.478 , $n=19$, $P < 0.001$ of mean value and

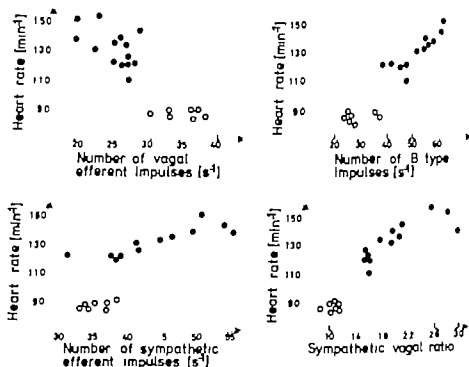


Fig. 3 Heart rate as a function of the number of vagal cardiac efferent imp/s ($r = -0.891$ upper left) number of left atrial B-type imp/s ($r = 0.930$ upper right) number of sympathetic postganglionic efferent cardiac imp/s ($r = 0.866$ lower left) and as the ratio of the numbers of sympathetic and vagal cardiac efferent imp/s ($r = 0.887$ lower right). Each point represents a mean of the results calculated in respect to successive periods of 4 s before (open circles) during and after (closed circles) infusion of saline of 80 ml within 40 s. The weight of the animal was 10.6 kg and the response tachycardia.

the correlation coefficient between the heart rate and sympathetic-vagal ratio varied from 0.222 to 0.937 mean of $r = 0.691$ $n = 19$ $P < 0.001$ of mean value. The correlation between the B-type impulses and heart rate was from 0.546 to 0.976 mean of $r = 0.828$ $n = 19$ $P < 0.001$ of mean value. Fig. 3 represents a typical example in correlations between the heart rate and calculated nervous parameters in tachycardic responses.

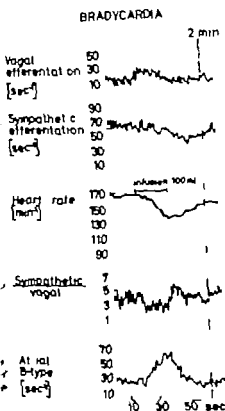
Nerve activities in bradycardia

In bradycardic responses with 11 infusions sympathetic efferentation increased in 0 (0%) decreased in 8 (75%) ($P < 0.05$ – 0.001) and was not changed ($P > 0.05$) in 3 (25%) of the cases. Vagal efferentation increased in 3 (27%) decreased in 2 (18%) and was not changed in 6 (55%) of the cases. The ratio of sympathetic to vagal impulses increased in 3 (28%) decreased in 4 (36%) and was not changed in 4 (36%). The aortic baroreceptor and left atrial B-type activity rate increased in all of the cases. In bradycardic responses the correlation coefficient (r) between the heart rate and sympathetic efferentation

varied from 0.199 to 0.914 mean of $r = 0.661$ $n = 18$ $P < 0.01$ of mean value and between heart rate and vagal efferentation from -0.360 to 0.879 mean of $r = -0.466$ $n = 18$ $P < 0.05$ of mean value. The correlation coefficient between the heart rate and the sympathetic-vagal ratio varied from 0.207 to 0.912 mean of $r = 0.691$ $n = 17$ $P < 0.05$ of mean value and from -0.471 to 0.737 mean of $r = -0.605$ $n = 21$ $P < 0.01$ of mean value. The correlation coefficients between B-type impulses and the heart rate varied from -0.115 to -0.885 mean of $r = -0.430$ $n = 17$ $P < 0.01$ of mean value. Fig. 4 represents changes in vagal and sympathetic efferentation heart rate the sympathetic-vagal ratio and left atrial B-type activity in a bradycardic response to i.v. saline infusion.

DISCUSSION

In this study attempts were made to record simultaneously the changes in left atrial aortic baroreceptor and sympathetic and vagal efferent ac-



4 Influence of saline infusion upon the number of vagal cardiac efferent impulses, number of sympathetic postganglionic efferent cardiac impulses, the heart rate, the ratio number of sympathetic to vagal impulses and upon the number of left atrial B-type impulses. The response to infusion in bradycardia. The values represent result calculated from cycle to cycle. The weight of the animal was 33 kg.

tries and to find out what is their role separately and together in heart rate regulation. One of the difficulties met in this work was to find and get most of the four different types of nerves studied functioning together and simultaneously. For this reason the recording of aortic and atrial pressures and atrial and baroreceptor activities was done only in a few experiments. The use of heparin addition to the use of cannulae caused an increased tendency to bleed in nerve preparations. It is clear that single and few fibre recordings from sympathetic and vagal nerves are a practical way of studying efferentiation and efferentiation but it is also obvious that they represent only a small part of all the information transfer between the central nervous system and the heart. However, changes in

the activity of these fibres would give some new information on their role in the phenomenon studied.

The morphine premedication may augment the vagal tone (Page & Hoff 1969) which of course has a favourable effect on eliciting the tachycardic reflex. Anaesthesia with α -chloralose was chosen, because it leaves the autonomic balance and reflexes largely intact (Price 1960, Greisholmer 1965, Cox 1972). Pentobarbital was not considered to be proper because it has been proved to depress the cardiovascular reflexes and nervous activities (Hälinen, Hakumäki & Sarajärvi 1978). In spite of the fact that it has been widely used in cardiovascular research physiology.

The main reaction with 42 i.v. infusions of saline in 32 dogs was tachycardia. In 10 infusions of these a decrease in heart rate at the beginning of the infusion during the first 4–10 heart beats was found. It is possible that these temporary heart rate changes are merely due to the augmented mechanical load on the heart induced by increased venous return at the beginning of the infusion. However, it seems that also constant bradycardia is one of the responses to i.v. infusion in anesthetized dogs in addition to tachycardia. The mean of the control heart rate in tachycardia was significantly lower than the mean of the control heart rate in bradycardia, but also the bradycardic responses were observed with a low control heart rate.

The findings about efferentiation in tachycardia in the present work are in agreement with the earlier works of Bergström, Hakumäki & Sarajärvi (1971), Hakumäki (1972) that sympathetic efferent cardiac activity increases in tachycardic responses. Also opposite reactions were observed in the present work, which implies that there might be more specific reflex arches so that different cardiac nerves might be activated separately and independently.

Vagal efferentiation showed diminution in most of the cases in tachycardia, although increases in activity were also observed. It is possible that all the nervous activity recorded as cardiac efferent impulses might have contained impulses of efferent fibres to some other organs which increased their activity by cardiovascular stimulation. It is clear that vagal efferentiation alone does not regulate heart rate but the sympathetic-vagal ratio seems to be one of the most effective regulators in tachycardic responses. This ratio was increased in 83% of the cases, a decrease was not observed. The re-

sults of efferentation in this work support the hypothesis of a reciprocal function of the sympathetic and vagal cardiac efferentation reported earlier by Marguth, Raule & Schaefer (1951) and later Weidinger, Hetzel & Schaefer (1967). However, this antagonism seems not to be the rule, because different types of reactions were also seen in vagal and sympathetic cardiac activity. It is obvious that the heart rate is a result of the sum function of the sympathetic and vagal activities and the ratio of sympathetic to vagal impulses as a main regulator allows different types of reactions in both the autonomic nervous activities.

In bradycardic results the findings in efferentation are quite opposite to the findings during tachycardia. In most cases a very clear decrease in sympathetic cardiac efferent activity was observed although there were some nonsignificant changes. There was never an increase in activity. A very important point in these results is that in vagal efferentation activity was not greatly increased and in half of the cases was not changed significantly. It is also confusing that the sympathetic/vagal ratio does not correlate clearly to the heart rate in bradycardia. It is possible that bradycardia during volume load is a result of a combination of cardiac contractility changes and neural factors. So the bradycardic response can be explained in the following way. The pumping capacity of the heart has decreased in the course of the experiment and by i.v. infusion the increased volume load thus stretches the weakened ventricles and stimulates the ventricular receptors more than usual. This overwhelms the tachycardia initiating neural systems and decreases the sympathetic efferentation to the heart. This hypothesis supports the findings of this work that 10 tachycardic reactions were preceded by a short period of 5–10 heart beats of bradycardia at the beginning of the infusions. Also the recent observations of Wennergren, Thorén & Lisander (1977) support this hypothesis of the role of the ventricular receptors in bradycardia.

What is the role of the left atrial B-type receptor and aortic arch baroreceptor activities in these results? In all the tachycardic and bradycardic responses the activity rates of these receptors increased. The left atrial B-type receptor has both an inhibitory (Hakumäki 1970) and excitatory influence on sympathetic efferentation (Kappagoda et al. 1975; Koizumi et al. 1975) so that initial response to left atrial stretch is inhibitory and the later re-

sponses excitatory in sympathetic cardiac efferent activity. It is obvious that the increased activity of atrial receptors is responsible for the increase in cardiac sympathetic efferentation and heart rate. It is difficult to explain why atrial receptors do not influence the sympathetic system in bradycardic responses though they increased their activity. The aortic arch baroreceptor may inhibit atrial receptor influence in CNS in bradycardia but why they do not do it in tachycardic responses where the baroreceptors also increased their activity is unclear. It may be concluded that baroreceptors do not play a significant role in heart rate regulation during volume load as Bishop & Peterson (1976) have earlier suggested in conscious dogs. It is possible that a more detailed analysis of the baroreceptor activity would give new information on their role in heart rate regulation at the CNS level.

It is interesting that most of the observational conclusions made in this field on neural cardiovascular regulation have been correct or partly correct. It can be assumed that the so-called Bainbridge reflex is a sum function of different kinds of overlapping inhibitory and excitatory components which are working simultaneously during and after the i.v. infusion and the responses in the heart rate are dependent upon that reflex arch which is stronger and overwhelming the others. It seems that there are still numerous open questions in the nervous control of heart efferentation and efferentation and in their interrelationships in different kinds of cardiovascular conditions and more experimental work is needed with anesthetized and conscious animals before the details of cardiovascular regulation are well-known.

This work was supported by the Academy of Finland, North-Savo Regional Fund of the Finnish Cultural Foundation and the Paavo Nurmi Foundation. I wish to express my gratitude to Miss R. Rajala (Hokapaino) and Miss E. Holma for typing the manuscript and drawing the figures.

REFERENCES

- AHMED, O. & NICOLL, P. A. 1963. Chronotropic response to intravenous infusion in the anaesthetized dog. *Am. J. Physiol.* **204**, 4, 3–7.
- ANREP, G. V. & SEGALL, H. N. 1926. The central reflex regulation of the heart rate. *J. Physiol.* **61**, 21–31.
- BAINBRIDGE, F. A. 1915. The influence of cardiac filling upon the rate in the heart. *Proc. R. Soc. Lond.* **40**, 65–68.

- LLIN, I. R. & KATZ, L. N. 1941 Observations on the localization of the receptor area of the Bainbridge reflex. *Am J Physiol* 135: 202-13.
- ROSTROM, R. M., HAKUMAKI, M. O. K. & SARA, J. S. H. S. 1971 Heart rate in relation to sympathetic efferentation associated with the Bainbridge reflex in dogs. *Acta Physiol Scand* 83: 571-573.
- THOP, V. S. & PETERSON, D. F. 1976 Pathways regulating cardiovascular changes during volume loading in awake dogs. *Am J Physiol* 231 (3): 854-859.
- LEBRIDGE, J. C. G. & LINDEN, R. J. 1955 The effect of intravenous infusions upon the heart rate of the anaesthetized dog. *J Physiol* 128: 310-319.
- XX, R. H. 1977 Influence of chloralose anesthesia on cardiovascular function in trained dogs. *Am J Physiol* 233: 660-667.
- GRAFF, A. C. & SANDS, J. 1925 Are reflexes from the large veins or sense of importance in the regulation of the circulation. *Am J Physiol* 74: 400-415.
- YALD, D. E. & SHEPHERD, J. T. 1963 Changes in heart rate on intravenous infusion in dogs with chronic cardiac denervation. *Proc Soc Exp Biol Med* 113: 315-317.
- DETZ, K. L. 1965 Effect of increased pressure within right heart cavities on heart rate in dogs. *Am J Physiol* 209 (3): 507-511.
- REINHEIMER, E. M. 1965 The circulatory effects of anesthetics. I. *Handbook of physiology* Section 2, Circulation, ed. III (ed. W. F. Hamilton and P. Dow). pp. 2477-2510. Amer. Physiol. Soc. Washington D.C.
- YAKUMAKI, M. O. K. 1970 Function of the left atrial receptors. *Acta Physiol Scand* 344: 1-54.
- AKUMAKI, M. O. K. 1972 Vagal and sympathetic efferent discharge in the Bainbridge reflex of dogs. *Acta Physiol Scand* 85: 414-417.
- YALINEN, M. O., HAKUMAKI, M. O. K. & SARA, J. S. H. S. 1978 Suppression of autonomic postganglionic discharges by pentobarbital in dogs. 1st or 2nd endocrinum. *Acta Physiol Scand* 104: 167-174.
- YITTSCH, L. J., BOYD, E. & KATZ, L. N. 1964 Effect of intravenous volume infusion on heart rate in anaesthetized dogs. *Am J Physiol* 206: 997-996.
- ONES, J. J. 1941 The Bainbridge reflex. *J Physiol* 100: 98C-105C.
- KAPPAGODA, C. T., LINDEN, R. J. & SNOW, H. M. 1972 A reflex increase in heart rate from distension of the junction between the superior vena cava and the right atrium. *J Physiol* 220: 177-197.
- KAPPAGODA, C. T., LINDEN, R. J. & SNOW, H. M. 1975 Atrial receptors and heart rate: the efferent pathway. *J Physiol* 249: 581-590.
- KARIM, F., KIDD, C., MALPUS, C. M. & PENNA, P. E. 1972 The effects of stimulation of the left atrial receptors on sympathetic efferent nerve activity. *J Physiol* 227: 43-260.
- KOIZUMI, K., ISHIKAWA, T., NISHINO, H. & McBROOKS, C. 1975 Cardiac autonomic system reactions to stretch of the atria. *Brain Res* 87: 247-261.
- LEDSOME, J. R. & LINDEN, R. J. 1964 A reflex increase in heart rate from distension of the pulmonary vein-atrial junctions. *J Physiol* 170: 456-473.
- LINDEN, R. J. 1973 Function of cardiac receptors. *Circulation* 48: 463-480.
- MALLIANI, A., LOMBARDI, F., PAGANI, M., RE, CORDATI, G. & SCHWARTZ, P. J. 1973 Spinal cardiovascular reflexes. *Brain Res* 87: 239-248.
- MARQUH, H., RAULE, W. & SCHAEFER, H. 1951 Aktionsströme im zentrifugalen Herznerven. *Pflügers Arch Ges Physiol* 254: 224-245.
- PAGE, C. P. & HOFF, H. E. 1969 Cardiovascular and respiratory relationships in the morphine-pentobarbital anesthetized dog. *Arch Int Pharmacodyn* 177: 311-331.
- PATHAK, C. L. 1959 Alternative mechanism in cardiac acceleration in Bainbridge reflexion experiments. *Am J Physiol* 197: 441-444.
- PRICE, H. L. 1960 General anesthesia and circulatory homeostasis. *Physiol Rev* 40: 187-218.
- SASSA, K. & MIYAZAKI, H. 1920 The influence of venous pressure upon heart rate. *J Physiol* 54: 203-212.
- WEIDINGER, H., HETZEL, R. & SCHAEFER, H. 1962 Aktionsströme im zentrifugalen vagen Herznerven und deren Bedeutung für den Kreislauf. *Pflügers Arch* 276: 266-279.
- WENNERGREN, G., THORÉN, P. & LISANDER, B. 1977 Cardiac receptors activated during the hypothalamic defence reaction. *Acta Physiol Scand* 101: 41-246.

The chromaffin system of the African lungfish *Protopterus aethiopicus*¹

MIMY ABRAHAMSSON, SUSANNE HOLMGREN, STEFAN NILSSON and
JUT PETTERSSON

Department of Zoophysiology, University of Göteborg, Sweden

ABRAHAMSSON T, HOLMGREN S, NILSSON S & PETTERSSON K. On the chromaffin system of the African lungfish, *Protopterus aethiopicus*. Acta Physiol Scand 1979, 107, 135-139. Received 5 March 1979. ISSN 0001-6772. Department of Zoophysiology, University of Göteborg, Sweden.

The distribution of chromaffin tissue was studied in the African lungfish using Falck-Hillarp fluorescent histochemistry together with quantitative analysis of catecholamines in plasma and tissue extracts. Intensely fluorescent cells form chromaffin tissue in the wall of the atrium, the wall of the most anterior part of the left cardinal vein and the walls of the segmentally arranged intercostal arteries. The arrangement thus appears to be a combination of the situations in cyclostomes, elasmobranchs and teleosts. Adrenaline is present in larger quantities than noradrenaline in the intercostal arteries and the cardinal vein, while noradrenaline dominates in the atrium. During stress, induced by physical disturbance of the animals, a strong increase in especially the noradrenaline concentration of the plasma was detected.

Key words: Lungfish, *Protopterus aethiopicus*, chromaffin tissue, catecholamines.

In 1900, Kohts introduced the term 'chromaffin' for cells which are stained brown by certain chrome salts, a phenomenon first described by Henle (1865) in experiments with the adrenal gland. Coupland (1963, 1971) defines a normal chromaffin cell as one which develops from neuroectoderm, is innervated by pre-ganglionic sympathetic nerve fibres, is capable of synthesizing and secreting catecholamines and of storing them in sufficient concentration to give a positive chromaffin reaction.

In studies of chromaffin systems of lower vertebrates it has rarely been possible to obtain enough evidence to fulfill all these criteria, and the term chromaffin is therefore used in a less exact sense to indicate cells storing large quantities of catecholamines.

Well developed chromaffin systems are found in a number of lower vertebrates, but contrary to mammals the chromaffin tissue is not arranged as a distinct adrenal medulla. In cyclostomes (hagfish and lampreys), chromaffin tissue has been described in the walls of major veins (Guacanti 1902, Gaskell 1912) and there are also large quantities of

catecholamines stored in chromaffin cells of the heart (both ventricle and atrium) and in the portal vein heart of Myxine (Östlund 1954, Augustinsson et al. 1956, Östlund et al. 1960, Euler & Fluge 1961, Bloom et al. 1961, Lagerstrand & Nilsson 1972). Elasmobranchs have their chromaffin tissue arranged segmentally along the vertebral column into chromaffin bodies. These are sometimes referred to as 'supra-renal' bodies as opposed to the 'inter-renal' tissue which is the adreno-cortical tissue of the elasmobranchs. The 'supra-renal' bodies of the elasmobranchs are associated with sympathetic ganglia and may be innervated by pre-ganglionic fibres of sympathetic origin. Especially large chromaffin bodies lie in the anterior part of the cardinal sinus in contact with the gastric ganglion on each side ('auxiliary bodies') (Young 1933, Nicol 1957, Coupland 1965, Gannon et al. 1972, Nilsson et al. 1975, Abrahamsson 1979).

In teleosts the chromaffin tissue is embedded in

¹Part of this work, as presented at the meeting of the Scandinavian Physiological Society in Lund, Acta Physiol Scand 1978, 102: 33A-34A.

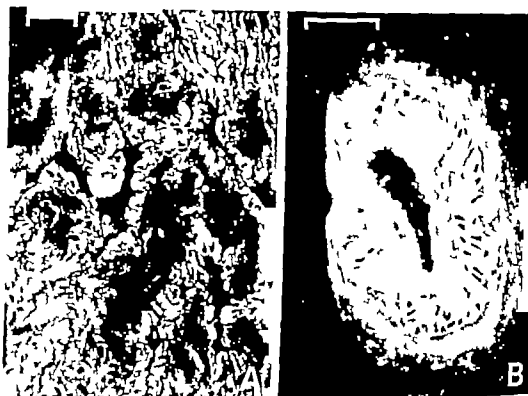


Fig. 1 (A) Intensely fluorescent cells lining the lumen of the atrium. Calibration = 100 μ m. (B) Intensely fluorescent cells in the wall of an intercostal artery very close to the dorsal aorta. Calibration = 100 μ m.

the walls of the posterior cardinal veins inside the head kidney (Oguri 1960; Mazeaud 1977; Grove et al. 1972; Nilsson 1976). The chromaffin tissue in the head kidney of the cod is innervated by pre-ganglionic cholinergic fibres which control release of adrenaline and noradrenaline into the blood stream (Nilsson et al. 1976; Holmgren 1977).

Chromaffin cells in the lungfish *Protopterus annectens* were described by Giacomini (1906). They were found in the walls of the intercostal arteries and also in the anterior part of the left cardinal vein ('azygos vein'). Holmes (1950) confirmed the finding of chromaffin cells in the intercostal arteries of the same species but was unable to verify Giacomini's finding of such cells in the cardinal vein. Sympathetic fibres reach the left cardinal vein and an innervation of the chromaffin tissue in the intercostal arteries has been described (Jenkin 1978; Holmes 1950).

This work was started to clarify the distribution and function of chromaffin cells in a Dipnoan fish by use of Falck-Hillarp fluorescence histochemistry and analyses of catecholamine content in the organs which from findings in other lower vertebrates can be suspected to store catecholamines.

MATERIAL AND METHODS

African lungfish (*Protopterus annectens*) of various sizes with a body length of 35–50 cm were used in the experiments. The animals were captured near Kisumu, Kenya and flown from Nairobi to Göteborg where they were kept in fresh water at 25°C and regularly fed before the experiments.

Measurement of catecholamine levels in plasma and tissues were made by the method of Bertler et al. (1958) modified by Haggendal (1963). The catecholamines in perchloric acid extracts of plasma and tissues were purified on Dowex 50W X8 resin and fluorimetric measurement were made using a Farrand Mark I spectrofluorimeter. The recovery of known amounts of adrenaline (100 ng) and noradrenaline (100 ng) from the columns was determined and found to be $82 \pm 5\%$ (mean \pm S.E., $n=11$) and noradrenaline $83 \pm 5\%$ (mean \pm S.E., $n=11$). The values given below have been corrected for these recoveries. All values are presented as means \pm S.E. Stress was induced by chasing the animal around its tank for 10–15 min. Blood samples were taken with a heparinized syringe from the dorsal aorta immediately after killing.

Fluorescent histochemistry was carried out by the Falck-Hillarp method as described by Falck & Owman (1963). Freeze-dried pieces of tissue were treated in formaldehyde vapour at 80°C for 1 or 3 h. Tissue sections of 10 μ m were mounted in Entellan (Merck) and viewed on a Leitz Ortholux fluorescence microscope with top light illumination and barrier filter. Photographs

Table 1. Catecholamine level in some tissues and plasma of the African lungfish expressed as $\mu\text{g/g}$ tissue or $\mu\text{g}/100 \text{ ml}$ plasma spect etc.

Values are given as mean \pm S.E. Number of estimations =

Tissue	Adrenaline	Nonadrenaline	% adrenaline	
Heart	4.18 \pm 1.10	70.77 \pm 17.31	5	6
Intercostal arteries proximal part of	5.10 \pm 2.06	0.26 \pm 0.4	98	5
Distal part of intercostal arteries	216.2	94.3	70	1
Intercostal arteries distal portion	0.33 \pm 0.08	0.05 \pm 0.03	87	8
Cardinal vein (left)	0.55 \pm 0.23	0.03 \pm 0.02	95	6
Pool plasma (control)	2.29 \pm 0.77	2.36 \pm 1.15	49	6
Pool plasma ("stressed")	6.41 \pm 1.85	29.10 \pm 14.28	18	4

Photomicrographs taken by Leitz Orthomat automatic camera on Kodak Tri-X film.

RESULTS

Large quantities of intensely fluorescent chromaffin cells were found by the Falck-Hillarp fluorescent histochemical technique in the atrium of the heart, most proximal part of the intercostal arteries and in the anterior 5 mm of the left cardinal vein (Figs 1 and 2).

In the atrium, the fluorescent cells line all inner surfaces of the pearly tissue (Fig. 1A). No such cells were present in the ventricle. A similar lining of the vessel wall by fluorescent cells was observed in the left cardinal vein (Fig. 1), while in the intercostal arteries there appeared to be a layer of non-fluorescent tissue between the chromaffin tissue and the vessel lumen (Fig. 1B). It was not possible to detect any differences in the intensity related to formaldehyde incubation times (1 or 3 h). Table 1 shows the result of the catecholamine analysis of the different tissues and plasma. It is notable that nonadrenaline dominates over adrenaline in the heart and also in the plasma of the "stressed" animals. In the adrenal gland, adrenaline appears to dominate in the other chromaffin tissues. In one animal the exact part of the intercostal arteries containing the chromaffin tissue was carefully dissected out giving a higher catecholamine content per g tissue (Table 1).

DISCUSSION

Chromaffin tissue and sympathetic fibres innervating this tissue was described by Giacomini (1906) in the intercostal arteries of *Protopterus annectens*

and later by Holmes (1950). The present findings of the position of the chromaffin tissue in the intercostal arteries of *P. annectens* agree well with these earlier descriptions. A further claim by Giacomini (1906) that chromaffin cells were also present in the left cardinal vein was refuted by Holmes (1950) on the grounds that the chromaffin reaction used was not specific enough to allow such a statement. From the present work, where the highly specific fluorescent histochemical technique was used, it is evident that Giacomini was right, and that there is a well developed chromaffin tissue in the anterior part of the left cardinal vein ("azygos vein").



Fig. 2. Intensely fluorescent cells lining the walls of the most anterior part of the left cardinal vein. Photomontage. Calibration = 200 μm .

In addition to confirmation of earlier findings large quantities of chromaffin cells were found in the atrium of the heart. This is similar to the situation in cyclostomes where adrenaline and noradrenaline in large amounts have been found in both atrium and ventricle (*Lampetra Petromyzon Myxine*) and also in the portal vein heart (*Myxine*) (Östlund 1954 Lagerstrand & Nilsson 1972).

Thus it is clear that *Protopterus* has a remarkably well developed chromaffin system with its chromaffin tissue organized as a "combination" of the systems seen in several of the other groups of lower vertebrates.

Although the main catecholamine of the chromaffin tissue in the intercostal arteries and the left cardinal vein appears to be adrenaline noradrenaline is the circulating amine showing the most dramatic increase during "stress". This amine is stored in large quantities in the atrium and it is possible that a large portion of the circulating catecholamines are released from the heart. An innervation of chromaffin tissue in the intercostal arteries and left cardinal vein has been described (Jenkin 1928 Holmes 1950) but the nature of the control of catecholamine release from the atrium is not known.

The estimation of the catecholamine content of the heart must be evaluated considering the fact that only the atrium contains fluorescent cells. The amount of amines per gram tissue present in the atrium is therefore more than twice the figure given in Table 1. Similarly the weight of chromaffin tissue proper embedded in the vessels (intercostal arteries/dorsal aorta and cardinal vein) is very small compared to the total weight of the vessel tissues and therefore the amounts of amines per gram chromaffin tissue are much higher than indicated by the presented figures. This is also shown by the much higher catecholamine content in the sample of carefully dissected intercostal arteries (Table 1).

The strong increase in the concentration of especially noradrenaline in blood plasma following physical disturbance ("stress") indicates that circulating amines play a role in the over-all control of circulation and other organ functions. The effects of circulating amines may be of particular importance in *Protopterus* since the sympathetic adrenergic system is very poorly developed (Abrahamsson et al 1979a).

It is concluded from the present study that the chromaffin system of the African lungfish is com-

posed of chromaffin tissue in at least three different regions: the walls of the intercostal arteries; the wall of the left cardinal vein and the wall of the atrium. Adrenaline is present in larger quantities than noradrenaline in the intercostal arteries and the left cardinal vein while in the atrium—and also in the blood plasma of "stressed" animals—there is a dominance for noradrenaline. Preliminary results indicate that the noradrenaline in the *Protopterus* heart can be synthesized locally and not only taken up and stored as suggested in certain ideas (Saetersdal et al 1974 Abrahamsson et al 1979b).

Our thanks go to Mrs M. Fernandes and Prof M. H. R. Zoology Department University of Nairobi, for direct help in obtaining the animals. We also sincerely thank Mr B. Egnér and Mrs G. Rydgren for their expert technical assistance. This work was supported by grants from the Swedish Natural Science Research Council, the Magnus Bergvall Foundation and the Lars Hierta Memorial Foundation.

REFERENCES

- ABRAHAMSSON T. 1979 Phenylethanolamine methyl transferase activity and catecholamine synthesis and release from chromaffin tissue of the spiny dogfish *Squalus acanthias*. *Comp. Biochem. Physiol.* In press.
- ABRAHAMSSON T., HOLMGREN S. & NILSSON J. & PETERSSON K. 1979a Adrenergic and cholinergic effects on the heart, the lung and the spleen of the African lungfish *Protopterus aethiopicus*. *Physiol. Scand.* 107: 141-147.
- ABRAHAMSSON T., JÖNSSON A.-C. & NILSSON S. 1979b Catecholamine synthesis in chromaffin tissue of the African lungfish *Protopterus aethiopicus*. *Acta Physiol. Scand.* 107: 149-151.
- AUGUSTINSSON K. B., FÄNGE R., JOHNSON J. & ÖSTLUND E. 1956. Histological, physiological and biochemical studies on the heart of the cyclostomes, *Myxine* and *Lampetra*. *J. Physiol.* 131: 257-276.
- BERTLER, A., CARLSSON A. & ROSENGREN F. 1958. A method for the fluorimetric determination of adrenaline and noradrenaline in tissues. *Acta Physiol. Scand.* 44: 273-292.
- BLOOM G., ÖSTLUND E., EULER, U. S. v. & HAJKO P., RITZEN M. & ADAMS-RAJ J. 1979. Studies on catecholamine-containing granules of specific cells in cyclostome hearts. *Acta Physiol. Scand.* 113: 185-193.
- COUPLAND R. E. 1965. The natural history of the chromaffin cell. Longmans, London.
- COUPLAND R. E. 1972. The chromaffin system. In: *Handbook of experimental pharmacology* (ed. H. Blaschko and E. Mutschler) pp. 16-45.
- EULER, U. S. v. & FÄNGE R. 1961. Catecholamine nerve and organ of *Myxine*. *Acta Physiol. Scand.* 107: 141-147.

- nerveles and *Gadus callarias*. *Gen Comp Endocrinol* 1 191-194.
- LOCK, B. & OWMAN, CH. 1965. A detailed methodological description of the fluorescence method for the cellular demonstration of biogenic monoamines. *Acta Univ Lundensis* 7 Sect. II 1-3.
- MONROE, B. J., CAMPBELL, O. D. & SATCHELL, G. H. 1972. Monoamine storage in relation to cardiac regulation in the Port Jackson shark *Heterodontus portusjacksoni*. *Z Zellforsch* 131 437-450.
- OSKELL, J. F. 1911. The distribution and physiological action of the suprarenal medullary tissue in *Petromyzon fluviatilis*. *J Physiol* 44 59-67.
- ACONINI, E. 1902. Contributo alla conoscenza delle capsule surrenali nei Cyclostomi. *Sulle capsule surrenali dei Petromyzonti*. *Monitore Zool Ital* 13 143-162.
- ACONINI, E. 1906. *Sulle capsule surrenali nel simplesse dei Dipnoi*. *Ricerche in Protogerma anverre*. *R C Acad Lincei* 15 394-398.
- ROVE, D. J., STARR, C. R., ALLARD, D. R. & DAVIES, W. 1972. Adrenaline storage in the pro-nephros of the plaice *Pleuronectes platessa* L. *Comp Gen Pharmacol* 3 205-212.
- AGGENDAL, J. 1963. An improved method for fluorimetric determination of small amounts of adrenaline and noradrenaline in plasma and tissues. *Acta Physiol Scand* 59 42-254.
- ENLE, J. 1865. Über das Gewebe der Nebenniere und der Hypophyse. *Z Rat Mat* 4 143-152.
- OLMES, W. 1948. The adrenal homologues in the lungfish *Protopterus*. *Proc Roy Soc B* 137 549-565.
- HOLMGREN, S. 1977. Regulation of the heart of teleost, *Gadus morhua*, by autonomic nerves and circulating catecholamines. *Acta Physiol Scand* 99 62-74.
- TENKIN, P. M. 1928. Note on the sympathetic nervous system of *Lepidosteus paradoxus*. *Proc Roy Soc Edinburgh* 48 45-49.
- JOHN, A. 1900. Über den Bau und die Entwicklung der Nierenarterie Carotidarterie. *Arch Mikr Anat* 56 81 184.
- LAGERSTRAND, G. & NILSSON, S. 1972. Effects of 6-hydroxydopamine on the catecholamine levels in the systemic and portal hearts of *M. xian glauconus*. *Acta Reg Soc Scient Linc Goth* 8 39-41.
- MAZEAUD, M. 1972. Epinephrine biosynthesis in *Petromyzon marinus* (Cyclostoma) and *Salmo gairdneri* (Teleost). *Comp Gen Pharmacol* 3 457-468.
- NICOLL, J. A. C. 1952. Autonomic nervous system in lower vertebrates. *Biol Rev* 27 1-49.
- NILSSON, S. 1976. Fluorescent histochemistry and cholinesterase staining of sympathetic ganglia in a teleost, *Gadus morhua*. *Acta Zool (Stockh)* 57 69-77.
- NILSSON, S., HOLMGREN, S. & GROVE, D. J. 1975. Effects of drugs and nerve stimulation on the spleen and arteries of two species of dogfish, *Scyliorhinus canicula* and *Squalus acanthias*. *Acta Physiol Scand* 95 219-230.
- NILSSON, S., ABRAHAMSSON, T. & GROVE, D. J. 1976. Sympathetic nervous control of adrenaline release from the head kidney of the cod, *Gadus morhua*. *Comp Biochem Physiol* 55C 123-127.
- OGURI, M. 1960. Studies of the adrenal glands of teleosts-III. On the distribution of chromaffin cells and interrenal cells in the head kidneys of fishes. *Bull Jap Soc Scienc Fish* 26 443-447.
- ÖSTLUND, E. 1954. The distribution of catecholamines in lower animals and their effect on the heart. *Acta Physiol Scand* 31 Suppl. 112: 1-67.
- ÖSTLUND, E., BLOOM, O., ADAMS-RAY, J., RITZEN, M., SIEGMAN, M., NORDENSTAM, H., LISHAJKO, F. & EULER, U. S. 1960. Storage and release of catecholamines and the occurrence of specific submicroscopic granulation in the hearts of cyclostomes. *Nature* 188, 324-325.
- SAETERSDAL, T. S., JUSTESSEN, N. P. & KROHNSTAD, A. W. 1974. Ultrastructure and innervation of the teleostean struma. *J Molec Cell Cardiol* 6 415-437.
- YOUNG, J. Z. 1933. The autonomic nervous system of teleosts. *Quart J Micro Sci* 75 571-624.

adrenergic and cholinergic effects on the heart in lung and the spleen of the African lungfish *Protopterus aethiopicus*

JIMMY ABRAHAMSSON, SUSANNE HOLMGREN,
TEFAN NILSSON and KNUT PETTERSSON

Department of Zoophysiology, University of Göteborg, Sweden

ABRAHAMSSON J., HOLMGREN S., NILSSON T. & PETTERSSON K.
Adrenergic and cholinergic effects on the heart, the lung and the spleen of the African
lungfish *Protopterus aethiopicus*. *Acta Physiol Scand* 1979, 107, 141-147. Received
5 March 1979. ISSN 0001-6772. Department of Zoophysiology, University of Göteborg,
Sweden.

Effects of adrenergic and cholinergic drugs were studied on isolated preparations from the
heart, the lung and the spleen of the African lungfish. In addition, nerve-lung preparation
was employed for the study of the autonomic nervous control of the lung. Falck-Hillarp
fluorescent histochemistry was used in the search for adrenergic neurons in the sympathetic
chains and trunks. The *Protopterus* lung received cholinergic excitatory innervation via
the pulmonary branches of the vagi. The presence of parasympathetic ganglia in the lung
trunks is indicated. Adrenergic drugs, when producing response, either contracted or
relaxed lung strips. Spleen strips were contracted by cholinergic drugs acting on muscarinic
receptors and, to a lesser extent, by adrenergic drugs. A strong negative inotropic effect
was produced by carbachol on paced atrial but not ventricular strips, while adrenalin
increased the contraction force in ventricular but not atrial strips. The sympathetic ganglion
cell did not contain enough catecholamines to give off any visible fluorescence, nor was it
possible to show any adrenergic nerve terminals in the trunks studied. It is concluded that
the adrenergic control in the lungfish is mainly due to circulating catecholamines, rather
than adrenergic nerve fibres, since concentrations of catecholamines in *Protopterus* plasma
are high enough to affect the spleen, lung and ventricle.

Key words: Lungfish *Protopterus aethiopicus*, drug effects, autonomic nervous system.

The anatomy of the sympathetic nervous system in
lungfish was first described by Guicconi (1906)
(*Protopterus annectens*) and in more detail by Jen-
kin (1928) using another species of the fami-
ly *Lepidosauridae* (*Lepidosaur paradoxus*). The
sympathetic chains in both animals are extremely
fine chords extending from the posterior part of the
body cavity and ending anteriorly (in *Lepidosaur*)
in the 1st spinal nerve. Segmental sympathetic
ganglia lie in close connection with the intercostal
arteries and sympathetic innervation of the
chromaffin cells in the wall of these arteries has
been described (Holmes 1940, *Protopterus an-
nectens*). A sympathetic branch to the left cardinal
vein (Cargos *et al.*), which may also control
chromaffin tissue in this vein has also been de-
scribed (Jenkins 1928).

There are no direct connections between the
sympathetic chains and the vagi but sympathetic
fibres might at least theoretically reach the vagi via
the nerve joining the vagus ganglion and the 1st
spinal nerve (Jenkins 1928).

The lung is innervated by autonomic nerve fibres
running in the pulmonary branches of the vagi: the
left pulmonary vagus innervates the right part of the
lung and vice versa. Ganglion cells in the pulmo-
nary vagi have been described (Parker 1892, Guic-
coni 1906, Jenkins 1928). Acetylcholine contracts
and catecholamines relax the *Protopterus* lung, the
effect of acetylcholine being blocked by atropine
(Johansen & Rente 1967).

The heart does not appear to be under a
cholinergic vagal tone, since atropine does not
change the heart rate while high doses of

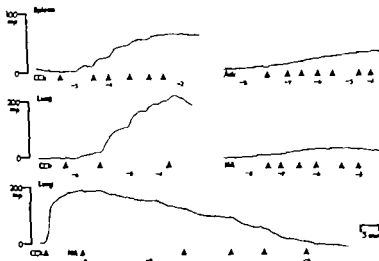


Fig. 1. Recordings of drug-induced tension changes in isolated strip preparations from the spleen (upper traces) and lung (middle and lower traces) of *Protopterus*. Numbers refer to the logarithm for the agonist concentration in mol/litre (M). The following agonists were used: adrenaline (Adr), noradrenaline (NA) and carbachol (CCh). Note that the preparation represented by the lower trace was precontracted by carbachol (10^{-4} M).

Adrenaline or noradrenaline either contracted (pD_2 for adrenaline 5.89 ± 0.97 , $n=3$) or after pre-contraction with carbachol, relaxed (pD_2 for adrenaline 5.48 , 5.05 , $n=2$) the lung strips (Fig. 1). Low concentrations (10^{-7} – 10^{-6} M) of the beta-adrenergic agonist isoprenaline relaxed precontracted lung strips, while high concentrations (10^{-4} – 10^{-3} M) produced contraction of previously untreated strips. Similar to the spleen strips, lung strips showed a much lower sensitivity of adrenergic drugs compared to cholinergic drugs tested on the same preparation, and in 4 fish no recordable response at all to adrenergic drugs was obtained.

A strong negative inotropic effect was caused by carbachol on atrial strip from one fish tested, while the effect on ventricular strip was small or absent (Fig. 4) (Fig. 7). Positive inotropic responses were obtained with adrenaline on ventricular ($pD_2 = 6.69 \pm 0.17$, maximal increase in beat force $30.0 \pm 1.0\%$, $n=3$) but not atrial ($n=1$) strips (Fig. 4).

Isolated non-lung preparation

Contractions of the lung could be obtained by electrical stimulation of the pulmonary branch of

the vagus every 2 min for at least 6 h. Preparations from 2 animals were used. The force of contraction and the duration of each contraction could be increased by addition of eserine (10^{-6} M) to the organ bath (Fig. 3). Addition of α -tubocurarine (7.6×10^{-6} M) or atropine (10^{-6} M) strongly diminished or abolished the responses to nerve stimulation (Fig. 3).



Fig. 2. Recordings of isotropic responses of *Protopterus* ventricle (upper traces) and atrium (lower traces) to adrenaline (Adr) and carbachol (CCh). Numbers refer to the logarithm for the agonist concentration in mol/litre (M). The isolated strip preparations were stimulated with pulses of 10 V and 1 ms duration at 0.8 Hz.

acetylcholine produces bradycardia (Johansen & Relte 1968). Positive ino- and chronotropic effects of adrenaline have been recorded, the chronotropic effect being most pronounced in aestivating animals (Mohsen et al. 1974).

The spleen is an elongated organ embedded in the gut wall and is rich in lymphoid tissue (Parker 1897). No direct sympathetic innervation of the type seen in other vertebrates (splanchnic nerves) appears to be present in lungfish (Jenkin 1928) and if any sympathetic fibres at all reach the spleen they must run with the intestinal branches of the vagus.

This work aims to elucidate the significance of the autonomic nervous system in the African lungfish and the effects of cholinergic and adrenergic drugs on the lung, the heart and the spleen.

MATERIALS AND METHODS

African lungfish. *Protopterus aethiopicus* of either sex with a body length of 35–50 cm were used in the experiments. The animals were captured near Khumu, Kenya, and flown from Nairobi to Göteborg where they were kept in fresh water at 25°C and regularly fed before the experiments.

Isolated strip preparations

Strips with a thickness of 3 mm were cut from the atrium and ventricle of the heart, the spleen and the lung of freshly killed lungfish. The strips were attached to GRASS FTO3 isometric transducers and suspended in organ baths containing a lungfish ringer of the following composition: NaCl 5.5, KCl 0.33, CaCl₂ 2H₂O 0.32, MgSO₄ 7H₂O 0.19, NaHCO₃ 2.0, NaH₂PO₄ 2H₂O 0.43, glucose 1.0 g/litre. The ringer was kept at 25°C and bubbled throughout the experiment with 97% O₂/3% CO₂. Strips kept in ringer at +4°C could be used for up to 4 days without detectable changes in responses. A basic tonus of 25 mp (1 mp = vertical force of 1 mg = 9.81×10^{-6} N) was initially applied to the strips which were then left to recover for 1 h before the start of experiments.

The atrial and ventricular strips were paced by electrical pulses of 0.8–1 Hz, 1 ms and 7–10 V delivered from GRASS S6 stimulators through two thin platinum wires attached around the lower parts of the suspended strip.

Concentration/response curves were obtained by cumulative addition of drugs and affluence for the drugs determined as pD_2 -values ($pD = -\log EC_{50}$) (van Rossum 1963). pD_2 values are given \pm S.E.M. and n indicates number of animals. From each animal 1–6 preparations were used for pD determinations and mean values used for further determinations. The pA_2/pA_{10} -values for atropine on spleen strips were determined with carbachol as agonist as described by Ariens & van Rossum (1957) and van Rossum (1963).

Isolated nerve-lung preparation

2–3 cm of the pulmonary branch of the splanchnic nerve were carefully dissected free from the underlying lung lobe and a 1 cm

wide ring of the lung was cut posterior to the splanchnic nerve. The nerve/lung preparation was suspended in an organ bath as described for the isolated strip preparation and the nerve placed over two fine platinum hook electrodes regularly stimulated for 70 s with 20 Hz 1 ms duration at 10 V with 1 min intervals.

Fluorescent histochemistry

Pieces of the dorsal aorta, spleen, lung and intestine chain were quick-frozen in liquid propane cooled in liquid nitrogen. After freeze-drying, the tissue pieces were treated as described by Falck & Owman (1970). Paraformaldehyde treatment at 80°C was carried out for 1 or 3 h. Sections of 10 μ m were viewed in a Leitz Ortholux microscope with top light illuminator and a barrier filter 470 nm. With this treatment the presence of ornithine decarboxylase in the preparations can be identified by a blue-green (specific) fluorescence.

Drugs

The following drugs were used in the experiments: acetylcholine chloride, L-adrenaline bitartrate, atropine sulphate, carbachol chloride, ephedrine hydrochloride, isoprenaline hydrochloride, L-noradrenaline bitartrate, d-tubocurarine chloride. Concentrations are expressed in mol/litre (M).

RESULTS

Isolated strip preparations

Spleen strips contracted in response to the cholinergic agonists carbachol ($pD_2 = 4.59 \pm 0.11$, $n=6$) and acetylcholine ($pD_2 = 4.09 \pm 0.14$, $n=3$) and the adrenergic agonist adrenaline ($pD_2 = 6.36 \pm 0.09$, $n=10$) (Fig. 1). Noradrenaline produced very weak or not recordable responses not allowing any quantified estimations ($n=6$). The effects of ornithine decarboxylase were invariably weaker than the effects of the cholinergic agonists when tested on the same preparations. Atropine (10^{-10} M) caused a parallel shift of the concentration/response curve for carbachol giving $pA_2 = 8.2$ and $pA_{10} = 9.4$ estimated from 7 antagonized curves from 3 fish, which indicates a competitive blockade of muscarinic receptors.

Lung strips were contracted by acetylcholine ($n=2$, $pD_2 = 4.96 \pm 0.14$) and carbachol ($pD_2 = 5.38 \pm 0.11$, $n=8$) (Fig. 1). The effects of both acetylcholine and carbachol were antagonized by atropine (10^{-10} M) but no evaluation of pA values was made since consecutive control curves with the agonists showed irregular depression of the sensitivity of the strips, making absolute determinations of the shift produced by the antagonist impossible.

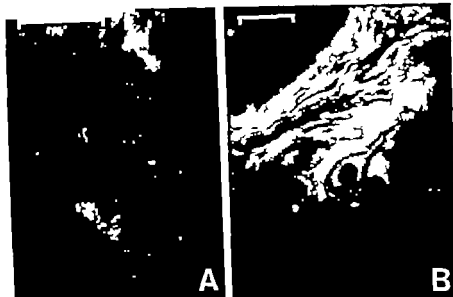


Fig. 4. Sympathetic ganglion cells from *Protopterus*, detectable in the fluorescence microscope only by their weak α -specific "back-ground" fluorescence and weak orange-yellow fluorescence emitted by cytoplasmic granules. The outline of the cells are clearly visible. In B elongated cells emitting an intense specific fluorescence can be seen alongside nerve cell bodies. Calibration in both A and B = 90 μ m.

The results obtained with atropine and eserine on the nerve-lung preparations are compatible with the view that the pulmonary branches of the vagi carry cholinergic excitatory fibres to the lung. The blocking effect of α -tubocurarine which serves as a good ganglionic blocker in toad (Nilsson 1978) could indicate the presence of autonomic ganglia in the lung. However, no tests to elucidate the identity of the ganglionic blockade were performed in this study. The effect of eserine suggests the presence of cholinesterases in the preparation.

An antagonistic adrenergic inhibitory control of the lung could be exerted by circulating catecholamines. The plasma concentrations of adrenaline increases from 0.13 μ M in control animals to 0.33 μ M in "stressed" animals, while the corresponding figures for noradrenaline are 0.14 μ M and 1.7 μ M respectively (Abrahamsson et al. 1979). These concentrations of the catecholamines will influence the lung musculature as judged from the concentration/exposure curves for adrenaline and noradrenaline on isolated lung strips.

No studies of chronotropic effects of drugs on the heart were performed in the present work, but possible chronotropic effect of adrenaline on the heart of *Protopterus* annectens, particularly aestivating

animals, have been described (Mjøsnes et al. 1974). Positive inotropic effects of catecholamines on isolated ventricular strips were seen in the present study. Again it is possible that the levels of circulating catecholamines affect the heart in a manner similar to the situation in elasmobranchs and teleosts (Gannon et al. 1972, Wahlqvist & Nilsson 1977, Holmgren 1977, Short et al. 1977, Butler et al. 1978).

A lack of a negative inotropic effect of cholinergic agonists on the ventricle is found in other vertebrates (Gannon 1971, Hedberg & Nilsson 1976, Holmgren 1977). Similarly in *Protopterus* the carbachol effect on the ventricle is absent or very small compared to the effect on the atrium. In a teleost (Holmgren 1977) and a reptile (Hedberg & Nilsson 1976) where the inotropic effects of drugs were studied in the same way as in the present work, a distinct positive inotropic effect of catecholamines was observed in the atrium. The lack of this effect in the isolated strip preparations from the lungfish atrium may in some way be linked to the presence of very large quantities of catecholamines in this organ (Abrahamsson et al. 1979). Similarly exogenous catecholamines have no effect on the adrenaline and noradrenaline rich

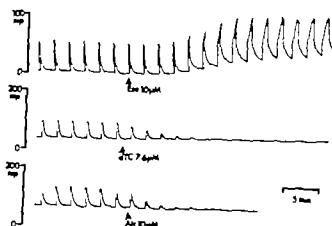


Fig. 3 Effects of cholinergic agents on the concentrations of the *Protopterus* lung produced by electrical stimulation of the pulmonary branch of the vagus nerve with 20 Hz, 1 ms duration and 10 V for 70 s every 2 min. Addition of eserine (Ese , 10^{-5} M) produces an increase in contraction force and duration (upper trace) while *d* tubocurarine (*dTC*, 7.6×10^{-4} M) and atropine (*Atr*, 10^{-5} M) abolishes the response to nerve stimulation (middle and lower traces).

Fluorescent histochemistry

No fluorescent nerve terminals were observed in any of the organs studied and this may at least in part be due to the presence of strongly autofluorescent material in the tissues. However, no specific catecholamine fluorescence was observed in the cell bodies of the sympathetic ganglion cells either but only a dull orange yellow granular fluorescence (Fig. 4A, B). In a few cases cells emitting a very strong specific fluorescence were observed in close proximity to sympathetic ganglion cells (Fig. 4B).

DISCUSSION

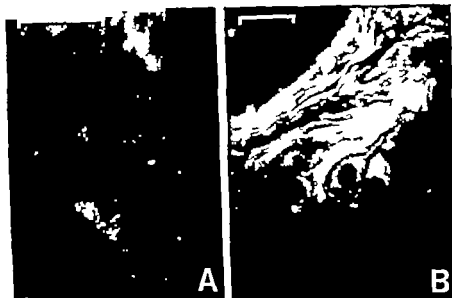
The sympathetic ganglia are diffusely arranged in elasmobranchs and chondrosteans while distinct sympathetic chains of the type seen in the tetrapods are present in holosteans and especially teleosts (Nicol 1957). Regularly arranged sympathetic chains are also found in the dipnoans (Giacomini 1906, Jenkin 1928) although early anatomists overlooked the very delicate strands (Parker 1897, Wiedersheim 1889 quoted in Jenkin 1928). The present findings that the sympathetic cells do not contain enough catecholamines to produce a visible fluorescence with the Falck-Hillarp technique suggests that the sympathetic system of *Protopterus* plays a very small role as an adrenergic nervous control function. The sympathetic system may however be important in the control of catechol

amine release from the chromaffin tissue in some parts of the animal (Giacomini 1906, Jenkin 1928, Holmes 1950, Abrahamsson et al. 1979). The L₁ of a prominent sympathetic adrenergic chain may in part be compensated for by a more powerful adrenergic control by circulating catecholamines.

The elongated intensely fluorescent cells in the sympathetic ganglia are similar to cells observed in other vertebrates and may have some local regulatory function like the SIF-cells of mammalian ganglia (McLean & Burnstock 1966, Nishio 1971, Tosaka & Kobayashi 1977).

The mammalian spleen is contracted by catecholamines acting via α adrenoceptors of the splenic smooth musculature but the effects of acetylcholine are weak and variable (for review see Davies & Withrington 1973). The contractile adrenergic excitatory effect is also seen in spleen strip preparations from lower vertebrates (Opdyke & Opdyke 1971, Nilsson et al. 1975, Elasmobranchs Vairal 1933, Nilsson & Grove 1974, Holmgren & Nilsson 1975, Teleosts, Vairal 1933, Nilsson 1978, Amphibians). The effects of acetylcholine are inconsistent in elasmobranchs, weakly excitatory in the toad (*Bufo marinus*) and very strongly excitatory and consistent in the eel (*Gadus morhua*) where a double sympathetic adrenergic/cholinergic innervation of the spleen has been postulated (Nilsson & Grove 1974, Holmgren & Nilsson 1975). It is notable that the *Protopterus* spleen strips were more sensitive to cholinergic agonists than to the adrenergic drugs. The spleen of *Protopterus* is somewhat special with its anatomical position embedded in the gut wall and covered with muscular fibres and peritoneum (Parker 1897). In the present experiments this muscle coat was carefully removed to avoid interference from gut musculature.

Also the lung strip preparations contracted strongly in response to acetylcholine and carbachol while the contractory effects of catecholamines were weak if at all present. In precontracted preparations a consistent relaxing effect of catecholamines was observed which is in agreement with the previous findings of Johansen & Reite (1967). This dual effect of catecholamines might be due to different receptor properties in different regions of the lung tissue as found in a toad (*Bufo marinus*) where the lung wall was predominantly β -relaxatory while the septal edges were excitatory (Holmgren & Ca 1978).



4. Sympathetic ganglion cells from *Protopterus*, detectable in the fluorescence microscope only by their weak 'back-ground' fluorescence and weak orange-yellow fluorescence emitted by cytoplasmic granules. The lin of the cells are clearly visible. In B elongated cells emitting an isoenzyme specific fluorescence can be seen alongside nerve cell bodies. Calibration in both A and B = 50 μ m.

The results obtained with atropine and eserine on nerve-lung preparations are compatible with the view that the pulmonary branches of the vagus carry cholinergic excitatory fibres to the lung. The blocking effect of *at* tubocurarine, which serves as a good ganglionic blocker in a toad (Nilsson 1978), would indicate the presence of autonomic ganglia in the lung. However, no tests to elucidate the specificity of the ganglionic blockade were performed in this study. The effect of eserine suggests the presence of cholinesterases in the preparation. As an antagonistic adrenergic inhibitory control of the lung could be exerted by circulating catecholamines. The plasma concentrations of adrenaline increases from 0.13 μ M in control animals to 0.33 μ M in stressed animals, while the corresponding figures for noradrenaline are 0.14 μ M and 1.77 μ M respectively (Abrahamsson et al 1979). These concentrations of the catecholamines will influence the lung musculature as judged from the concentration/response curves for adrenaline and noradrenaline on isolated lung strips.

No studies of chronotropic effect of drugs on the heart were performed in the present work, but possible chronotropic effect of adrenaline on the heart of *Protopterus* annectans, particularly activating

animals have been described (Mohsen et al 1974). Positive inotropic effects of catecholamines on isolated ventricular strips were seen in the present study. Again it is possible that the levels of circulating catecholamines affect the heart in a manner similar to the situation in elasmobranchs and teleosts (Garmon et al 1972, Wahlqvist & Nilsson 1977, Holmgren 1977, Short et al 1977, Butler et al 1978).

A lack of a negative inotropic effect of cholinergic agonists on the ventricle is found in other vertebrates (Garmon 1971, Hedberg & Nilsson 1976, Holmgren 1977). Similarly in *Protopterus* the carbachol effect on the ventricle is absent or very small compared to the effect on the atrium. In a teleost (Holmgren 1977) and a reptile (Hedberg & Nilsson 1976) where the inotropic effects of drugs were studied in the same way as in the present work, a distinct positive inotropic effect of catecholamines was observed in the atrium. The lack of this effect in the isolated strip preparations from the lungfish atrium may in some way be linked to the presence of very large quantities of catecholamines in this organ (Abrahamsson et al 1979). Similarly exogenous catecholamines have no effects on the adrenaline and noradrenaline rich

hearts of cyclostomes (Östlund 1954 Fänge 1957 quoted in Östlund 1954). The role of the large quantities of catecholamines in the hearts of cyclostomes and *Protopterus* in the control of the cardiac work is not known but some local regulatory influence may be suspected.

It is concluded from the results of the present work that the sympathetic nervous system plays a minor role as an adrenergic nervous control system in the African lungfish although sympathetic fibres may be responsible for an adrenergic humoral control by release of catecholamines from stores in chromaffin tissue. The sensitivity of the lung, spleen and ventricle to catecholamines suggests the possibility of a regulatory function of circulating levels of amines in these organs.

Our thanks go to Mrs M. Fernandes and Prof. M. Hyder Zoology Department University of Nairobi for their help in obtaining the animals. We also sincerely thank Mrs Lena Utter for her expert technical assistance and angelic patience. This work was supported by grants from the Swedish Natural Science Research Council, the Magnus Bergvall Foundation and the Anna Ahrenberg Foundation.

REFERENCES

- ABRAHAMSSON T, HOLMGREN S & NILSSON S & PETTERSSON K 1979 On the chromaffin system of the African lungfish *Protopterus aethiopicus*. *Acta Physiol Scand* 107: 135-139.
- ARIENS E J & VAN ROSSUM J M 1947 pD, pA and pD values in the analysis of pharmacodynamics. *Arch Int Pharmacodyn* 110: 275-299.
- BUTLER P J, TAYLOR E W, CAPRA M F & DAVISON W 1978 The effect of hypoxia on the levels of circulating catecholamines in the dogfish *Scyliorhinus ca tula*. *J Comp Physiol* 127: 325-330.
- DAVIES B N & WITHRINGTON P G 1973 The action of drugs on the smooth muscle of the capsule and blood vessels of the spleen. *Pharmacol Rev* 25: 373-414.
- FALCK B & ÖWMAN CH 1965 A detailed methodological description of the fluorescence method for the cellular demonstration of biogenic monoamines. *Acta Univ Lundens* 7: 1-3.
- GANNON B J 1971 A study of the dual innervation of teleost heart by a field stimulation technique. *Comp Gen Pharmacol* 175-183.
- GANNON B J, CAMPBELL G D & SATCHELL G H 1977 Monoamine storage in relation to cardiac regulation in the Port Jackson shark *Heterodontus portus jacksoni*. *Z Zellforsch* 131: 437-450.
- GIACOMINI E 1906 Sulle capsule surrenali e sul simpatico dei Dipnoi. *Ricerche in Protopterus aethiopicus*. *R Acad Lincei* 15: 394-398.
- HEDBERG A & NILSSON S 1976 Vago-sympathetic innervation of the heart of the puff adder, *Bitis arietans*. *Comp Biochem Physiol* 53C.
- HOLMES W 1940 The adrenal homologues in the fish *Protopterus*. *Proc Roy Soc B* 137: 489-491.
- HOLMIGREN S 1977 Regulation of the heart of a teleost *Gadus morhua* by autonomic nerves and circulating catecholamines. *Acta Physiol Scand* 99: 6-7.
- HOLMIGREN S & CAMPBELL G 1978 Receptors in the lung of the cod *Bass* regional differences in responses to intratracheal sympathetic nerve stimulation. *Comp Biochem Physiol* 60C: 11-18.
- HOLMIGREN S & NILSSON S 1975 Effects of adrenergic and cholinergic drugs on isolated strips from the cod *Gadus morhua*. *Eur J Pharmacol* 32: 163-169.
- JENKIN P M 1928 Note on the sympathetic nervous system of *Lepid sthen parichthys*. *Proc Roy Soc Edinburgh* 48: 55-69.
- JOHANSEN K & REITE O B 1967 Effects of acetylcholine and biogenic amines on pulmonary smooth muscle in the African lungfish *Protopterus aethiopicus*. *Acta Physiol Scand* 71: 48-57.
- JOHANSEN K & REITE O B 1968 Effects of acetylcholine and biogenic amines on bronchopulmonary and systemic vascular resistance in the African lungfish *Protopterus aethiopicus*. *Acta Physiol Scand* 74: 465-471.
- MCCLEAN J R & BURNSTOCK G 1966 Histochemical localization of catecholamines in the urinary bladder of the toad (*Bufo marinus*). *J Histochem Cytochem* 14: 538-548.
- MOHSEN T, LATTOUF H & JADOUN G 1971 Variations des effets de l'adrénaline sur le cœur de *Protopterus annectens* (Poisson Dipnoïde) en la dose et selon la phase du cycle biologique de l'animal. *C R Soc Biol* 168: 915-919.
- NICOL J A C 195... Autonomic nervous system in lower chordates. *Biol Rev* 7: 1-49.
- NILSSON S 1973 Fluorescent histochemistry of catecholamines in the urinary bladder of a teleost (*Gadus morhua*). *Comp Gen Pharmacol* 4: 17-1.
- NILSSON S 1978 Sympathetic innervation of the spleen of the cane toad *Bufo marinus*. *Comp Biochem Physiol* 61C: 133-139.
- NILSSON S & GROVE D J 1974 Adrenergic cholinergic innervation of the spleen of the cod *Gadus morhua*. *Eur J Pharmacol* 24: 135-143.
- NILSSON S, HOLMIGREN S & GROVE D J 1974 Effects of drugs and nerve stimulation on the spleen and arteries of two species of dogfish *Scyliorhinus ca tula* and *Squalus acanthias*. *Acta Physiol Scand* 95: 19-30.
- OPDYKE D F & OPDYKE N E 1971 Splenic responses to stimulation in *Squalus acanthias*. *Am J Physiol* 221: 623-625.
- ÖSTLUND F 1954 The distribution of catecholamine in lower animals and the effect on the heart. *Acta Physiol Scand* 31 (Suppl. 11): 1-67.
- PARKER W N 1897 On the anatomy and physiology of *Protopterus annectens*. *Trans Roy Irish Acad* 7: 109-130.

- ORTS, S., BUTLER, P. J. & TAYLOR, E. W. 1977
 The relative importance of nervous, hormonal and in-
 trinsic mechanisms in the regulation of heart rate and
 stroke volume in the dogfish (*Squalus acanthias*). *J.*
Exp Biol 70: 77-92.
- SAKA, T. & KOBAYASHI, H. 1977 The SIF cell as
 a functional modulator of ganglionic transmission
 through the release of dopamine. *Arch Histol Jap*
 38: 187-196.
- DREL, J. 1933 Action de l'adrénaline et de l'acé-
 tyldoline sur la rate. *J. Physiol. Pathol. Gén.*
 31: 42-52.
- VAN ROSSUM, J. M. 1963 Cumulative dose-response
 curves. II. Technique for the making of dose-response
 curves in isolated organs and the evaluation of drug
 parameters. *Arch Int Pharmacodyn Ther*
 143: 299-330.
- WAHLQVIST, L. & NILSSON, S. 1977 The role of
 sympathetic fibres and circulating catecholamines in
 controlling the blood pressure and heart rate in the
 cod, *Gadus morhua*. *Comp Biochem Physiol* 57C: 65-
 67.

Catecholamine synthesis in the chromaffin tissue of the African lungfish *Protopterus aethiopicus*

ANN ABRAHAMSSON, ANN-CATHRINE JONSSON and STEFAN NILSSON

Department of Zoophysiology, University of Göteborg, Sweden

ABRAHAMSSON A, JONSSON A-C & NILSSON S. Catecholamine synthesis in the heart and intercostal arteries of the African lungfish *Protopterus aethiopicus*. *Acta Physiol Scand* 1979, 107, 149-151. Received 5 March 1979. ISSN 0001-6772. Department of Zoophysiology, University of Göteborg, Sweden.

The activities of dopamine- β -hydroxylase (DBH, E.C. 1.14.17.1) and phenylethanol-N-methyl transferase (PNMT, E.C. 2.1.1.10) were determined in tissue homogenates from the chromaffin tissue containing atrium and intercostal arteries from the African lungfish. Clearly measurable activities of DBH were found in both kinds of tissues, while PNMT activity was ascertained only in the intercostal arteries. The activity of DBH in the atrium indicates possibly for local synthesis of the large amounts of catecholamines, especially noradrenaline, found in this tissue. Catecholamines synthesized in and released from the chromaffin tissues of *Protopterus*, may be of great importance for the adrenergic control in this animal in the absence of a well developed sympathetic nervous system.

Key words: African lungfish, *Protopterus aethiopicus*, catecholamines, dopamine- β -hydroxylase, phenylethanolamine-N-methyl transferase.

Large quantities of catecholamines are stored in chromaffin cells in the systemic and portal vein parts of cyclostomes (Giacomini 1902, Gaskell 1911, Östlund 1954, Lagerstrand & Nilsson 1977). Storage of catecholamines in endothelial cells of teleosts (*Gadus morhua* and *Lebistes reticulatus*) and these endothelial catecholamines are thought to be taken up from the plasma and stored rather than locally synthesized (Saetersdal et al. 1974).

The last two steps in the biosynthesis of adrenaline in the 'Blaschko pathway' (Blaschko 1939) are the hydroxylation of dopamine to noradrenaline and the subsequent methylation of noradrenaline to adrenaline. The enzymes responsible for these reactions are dopamine- β -hydroxylase (DBH, E.C. 1.14.17.1) and phenylethanolamine-N-methyl transferase (PNMT, E.C. 2.1.1.10) respectively. These enzymes have been demonstrated in lower vertebrates such as elasmobranchs (Abrahamsson 1979, PNMT), teleosts (Abrahamsson & Nilsson 1976, Marezal 1972, Abrahamsson 1979b, PNMT; Jonsson & Nilsson 1979, DBH) and amphibians (Wurtzman et al. 1968, PNMT; Wooten & Saavedra

1974, PNMT and DBH). The properties of DBH and PNMT from lower vertebrates appear to be similar to those of mammalian enzymes, with the possible exception of a lower temperature optimum (Wurtzman et al. 1968, Wooten & Saavedra 1974, Abrahamsson 1979b, Jonsson & Nilsson 1979).

In a study of the chromaffin system of the African lungfish large quantities of adrenaline (4.2 μ g/g whole heart) and especially noradrenaline (70.7 μ g/g whole heart) were shown to be present in the atrium (Abrahamsson et al. 1979). Chromaffin tissue also lies embedded in the walls of the intercostal arteries, and in the left posterior cardinal vein (Giacomini 1906, Abrahamsson et al. 1979).

This very preliminary work was carried out to investigate the presence of DBH and PNMT in chromaffin tissue from the African lungfish.

MATERIALS AND METHODS

Tissues from two specimens of the African lungfish (*Protopterus aethiopicus*) were used in this study. The animals were captured in Lake Victoria near Kijunjo, Kenya, and flown to Göteborg where they were kept in fresh water tanks at 25°C until the experiments.

Table 1

Tissue sample	Tissue weight (mg)	DBH activity (nmol octopamine formed/h \times g tissue)	PNMT activity (nmol norepinephrine formed/h \times g tissue)
Intercostal arteries animal 1	10.1	53.8	3.6
Intercostal arteries animal 2	9.4	79.9	117.2
Atrium animal 1	286.4	401.9*	
Atrium animal 2	511.2	176.8*	

Mean value from triplicate incubations.

The atria of the hearts or pooled samples of the intercostal arteries were homogenized in 4 and 2 ml 0.14 M KCl respectively. The homogenate was then divided into two parts, for the determination of the activities of PNMT and DBH respectively.

PNMT was determined by the method of Axelrod (1962) exactly as described by Abrahamsson (1979b). Incubation with DL-normetanephrine as substrate was carried out for 30 min at 30°C and pH=7.9 using 3 H-S-adenosyl-methionin as the methyl donor.

DBH was determined essentially according to the method of Nagatsu & Udenfriend (1977) as described by Jönsson & Nilsson (1979). One drop of Triton X 100 was added to the homogenate and 0.4 ml samples were incubated for 1 h at 30°C and pH=5.4 with tyramine as the substrate.

RESULTS AND DISCUSSION

No optimization of the various incubation parameters were performed on this very small material. The determinations of enzymatic activities were made under conditions shown to be optimal for the respective enzyme from other fish (Abrahamsson & Nilsson 1976; Abrahamsson 1979a, b; Jönsson & Nilsson 1979) giving the results presented in Table 1. The exact determination of the enzymatic activities for comparison with other chromaffin tissues is also made difficult by the great variability in the amounts of non-chromaffin vascular and other tissues homogenized together with the small amounts of chromaffin tissue proper. It is however evident from the present preliminary results that both PNMT and DBH are present in the intercostal arteries and that DBH in addition is present in the atrium of the heart. The possible presence of PNMT in the atrium cannot be ascertained in the present study due to very high blank values. These high blank values presumably arise due to conversion of endogenous catecholamines to 3 H-methylated metabolites. The activity of PNMT in the atrium can however be expected to be low since

noradrenaline greatly dominates over adrenaline in this tissue (Abrahamsson et al. 1979a).

The role of catecholamines thus locally synthesized in the atrium is not known, but a local regulatory function may be speculated. The chromaffin tissue of *Protopterus* may also be of great importance in the general adrenergic function of the animal, since a sympathetic adrenergic nervous system appears to be lacking (Abrahamsson et al. 1979a).

Our thanks go to Mrs M. Fernandez and Prof M. H. Zooloogy Dept. University of Nairobi for their help obtaining the animals. This work was supported by grants from the Swedish Natural Science Research Council and the Magn. Bergvall Foundation.

REFERENCES

- ABRAHAMSSON T. 1979a. Phenylethanolamine-N-methyl transferase activity and catecholamine degradation and release from chromaffin tissue of the spiny dogfish *Squalus acanthias*. *Comp. Biochem. Physiol.* In press.
- ABRAHAMSSON T. 1979b. Axonal transport of a renal ne-noradrenaline and phenylethanolamine-N-methyl transferase (PNMT) in sympathetic neurons of the eel *Gadus morhua*. *Acta Physiol. Scand.* 107: 316-323.
- ABRAHAMSSON T. & NILSSON S. 1976. Phenylethanolamine-N-methyl transferase (PNMT) activity and catecholamine content in chromaffin bodies and sympathetic neurons in the eel *Gadus morhua*. *Acta Physiol. Scand.* 96: 94-99.
- ABRAHAMSSON T., HOLMIGREN S. & NILSSON S. & PETTERSSON K. 1979a. On the chromaffin system of the African lungfish *Protopterus annectans*. *Acta Physiol. Scand.* 107: 135-139.
- ABRAHAMSSON T., HOLMIGREN S. & NILSSON S. & PETTERSSON K. 1979b. Adrenergic and cholinergic effects on the heart, the lung and the spleen of the African lungfish *Protopterus annectans*. *Acta Physiol. Scand.* 107: 141-147.
- AXELROD J. 1962. Purification and properties of phenylethanolamine-N-methyl transferase. *J. Biol. Chem.* 237: 1657-1660.

- USCHKO H 1939 The specific action of L-dopa de-carboxylase J Physiol 96: 50-51P
- SKELL, J P 191. The distribution and physiological action of the suprarenal medullary tissue in *P. monacanthus* J Physiol 44: 59-67
- ACOMINI E 1902 Contributo alla conoscenza delle capsule surrenali dei Ciclostomi. Sulle capsule surrenali dei Petromyzonti. *Monitore Zool Ital* 13: 143-146
- ACOMINI E 1906 Sulle capsule surrenali e sul sistema dei Dymoi. Ricerche su *Protoperus nasuetens* R.C Acad Lincei 15: 394-398
- SSON A-C & NILSSON S 1979 Effects of pH temperature and Cu^{2+} on the activity of dopamine- β -hydroxylase from the chromaffin tissue of the cod, *Gadus morhua* Comp Biochem Physiol 62C: 5-8
- GELSTRAND G & NILSSON S 1977 Effect of β -hydroxydopamine on the catecholamine levels in the systemic and portal hearts of *M. xiphioides*. Acta Reg Soc Scient Linn Goth 8: 39-41
- MAZEAUD M 1972. Epinephrine biosynthesis in *Petromonacanthus* (Cyclostoma) and *Salmo gairdneri* (Teleost). *Comp Gen Pharmacol* 3: 457-468
- NAGATSU T & UDENFRIEND S 1972. Photometric assay of dopamine- β -hydroxylase activity in human blood. *Clin Chem* 18: 980-983.
- ÖSTLUND E 1954. The distribution of catecholamines in lower animals and their effect on the heart. *Acta Physiol Scand* 31 Suppl. 112: 1-67
- SAETERSDAL T S, JUSTESEN N P & KROHNSTAD A W 1974. Ultrastructure and innervation of the teleostean atrium. *J Molec Cell Cardiol* 6: 415-437
- WOOTEN G F & SAAVEDRA J M 1974 Axonal transport of phenylethanolamine-N-methyl transferase in toad sciatic nerve. *J Neurochem* 22: 1059-1064.
- WURTMAN R J, AXELROD J, VESSELL, E. S. & ROSS G T 1968 Species differences in hydroxylability of phenylethanolamine-N-methyl transferase. *Endocrinology* 82: 584-590

Estimation of cerebral extraction of circulating compounds by the brain uptake index method: influence of circulation time, volume of injection and cerebral blood flow

HARDEBO and B. NILSSON

Departments of Histology and Neurology and Laboratory of Experimental Brain Research, University of Lund, Sweden

HARDEBO J. E. & NILSSON B. Estimation of cerebral extraction of circulating compounds by the brain uptake index method: Influence of circulation time, volume of injection and cerebral blood flow. *Acta Physiol Scand* 1979, 107, 153-159. Received 3 April 1979. ISSN 0001-6772. Department of Histology and Neurology and Laboratory of Experimental Brain Research, University of Lund, Sweden.

The Oldendorf-brain uptake index method for estimating and characterizing the transport of circulating substances across the blood-brain barrier in the rat has been widely applied. The present study illustrates that minimizing the volume injected into the circulation to 10 μ l or less is necessary. Otherwise the flow artefacts, induced by the injected volume and the rate of injection, will influence the index. This principle is also relevant to techniques using intracarotid injections for the direct study of cerebral blood flow. The study also elucidates the need for reducing the circulation time after injection to about 5 sec, to avoid artefacts due to metabolism and back diffusion to the circulation of the substances studied.

Key words. blood-brain barrier, cerebral blood flow, cerebral extraction

The method originally described by Oldendorf has been widely applied for estimating the transport across the blood-brain barrier (BBB) of various substances (Oldendorf 1971, 1973; Wade & Katzman 1971; see also Oldendorf & Szabo 1976; Pardridge & Oldendorf 1977). The method involves injection into the common carotid artery in the rat of a bolus of the radiolabelled test substance together with a highly diffusible reference substance, usually water. The animal is decapitated after 15 sec, and the percentage of residual test substance in the ipsilateral brain hemisphere relative to the reference substance is expressed as the brain uptake index (BUI).

Critical analyses of this technique have shown that BUI is not strictly a quantitative measure of brain uptake function, mainly since the uptake of the reference substance is a complex function being influenced by both diffusion limitation and back diffusion (clearance) of the substance and thus highly dependent upon cerebral blood flow (CBF) (Botting & Lassen 1975; Bradbury et al. 1975; Oldendorf & Braun 1976; Raichle et al. 1976).

The present study is an attempt to evaluate the importance of some reasonable modifications of the technique, i.e. (1) reducing the volume of the bolus and thus the CBF response, (2) using a more diffusible reference substance than water, and (3) reducing the time interval between bolus injection and tissue fixation.

(1) Injection of a large bolus volume may change the cerebral hemodynamics (Hardebo & Nilsson 1979). Since the uptake of the test and reference substances may be influenced both by the actual cerebral blood flow (CBF) and the available capillary exchange surface, the effects on CBF and intravascular pressure of various volumes of the injected bolus were studied and related to the BUI.

(2) Ideally, blood-brain equilibration of the reference substance should occur instantaneously and the substance be virtually totally extracted from the brain circulation. In the present study, ethanol was chosen as reference substance, since it is more freely diffusible across the BBB than water (Raichle et al. 1976).

(3) In the original experiments (Oldendorf 1970)

1971) the animal was decapitated 15 s after injection. This interval was an estimation of the time required for wash out of the test substance from the blood compartment after a single capillary passage. However, as shown by Furlow & Bass (1976) a non-diffusible substance appears on the venous side (external jugular vein) already after a few seconds with a peak after 2.5 s. It is almost totally washed out after 5–6 s and reappears due to recirculation after 7–8 s. Hence a time interval of about 5 s between injection and decapitation should be preferable. At any prolongation of the interval the BUI obtained will not only reflect brain uptake but also clearance from the brain into the blood stream and may as well be influenced by brain metabolism of the test substance.

METHODS

Preparation of animals. The experiments were performed on male rats weighing 300–350 g. Wistar rats were used for determination of cerebral blood flow and Sprague-Dawley rats for BUI studies. The rats had free access to pellet food and tap water until operation. Anaesthesia was induced with 3% halothane to allow tracheotomy and immobilization with tubocurarine chloride (1 mg/kg i.v.). Halothane 0.6–0.8% was given during the operation procedure then withdrawn. The animals were artificially ventilated on 70% N_2O and 30% O_2 (Braun) the $PaCO_2$ being adjusted to about 35 mmHg. The body temperature was kept at 37°C by means of intermittent heating.

Cerebral blood flow. In 4 animals catheters were placed just distal to the aortic bifurcation via the femoral artery on one side for recording of the systemic blood pressure (AoP) via a pressure transducer (Elema, Sweden) and sampling of arterial blood for blood gas measurements (BMS Mk II Radiometer, Copenhagen). One femoral vein was cannulated for infusion of fresh donor blood during the period of blood sampling. Both external carotid arteries were cannulated as described below. The intracranial pressure (ICP) was measured through a needle inserted into the cisterna magna connected to a pressure transducer (Elema).

CBF was continuously measured with the technique developed by Nilsson & Sjöström (1976, 1979). Thus the cerebral venous outflow was measured by drop counting in a closed circuit diverting blood from one retrograde vein during compression of the contralateral vein and returning the blood—drained from the forebrain on both sides—through a catheter in the external jugular vein on one side into the central venous system. The outflow volume was calculated by the use of a diagram relating drop rate to volume. It was controlled that hemodilution did up to 40% (volume) with Krebs-Ringer buffer solution did not increase the drop volume more than 5%. Hence no attempts were made to correct for the possible influence upon drop volume of the infused solution.

The outflow volume was converted into CBF values

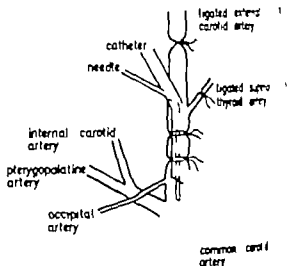


Fig. 1. Position of catheter for infusions in the external carotid artery. The infusions are carried into the external carotid artery and in addition to the test substance pterygopalatine and occipital arteries. Position of hole for measurement of intracarotid pressure at the level of the carotid bifurcation is indicated.

expressed in ml/100 g \times min by measurement of the cerebral arterio-venous difference in oxygen content (AVDO₂) in the control situation. Assuming a cerebral oxygen consumption (CMRO₂) of 7.58 ml/100 g \times min (Nilsson & Sjöström 1976) the CBF (in ml/100 g \times min) could be calculated from $7.58/AVDO_2$ and related to the actual venous outflow volume.

The effect on the CBF as reflected in the cerebral venous outflow rate as well as the effect on ICP recorded following simultaneous infusion into each external carotid artery of 10, 25 or 40 μ l during 1 s of Krebs-Ringer buffer solution or blood. Several experiments were run in each animal but a new experiment was not made until the venous outflow rate had returned to control level. Adequate reactivity of the CBF to hyperventilation was tested in each animal after the experiments had been completed.

Intracarotid pressure. In one group of 4 animals a needle was inserted into the external carotid catheter on one side with the opening just distal to the carotid bifurcation (Fig. 1). The outer diameter of the needle was 0.1 mm compared to the inner diameter of the catheter 0.6 mm, thus allowing a free flow past the needle during the infusion. In addition a catheter was placed in one femoral artery for recording of AoP and sampling of arterial blood for blood gas measurements. These animals were used to measure the effect on intracarotid pressure (CarP) during the venous intracarotid infusion (10, 25 or 40 μ l during 1 s).

Brain uptake index. After ligation of all branches of the main trunk of the right internal carotid artery as cannulated centrifugally in 71 animals with the catheter opened placed within one mm distal to the bifurcation.

Table 1 Changes in CBF (cerebral blood flow as determined by the cerebral venous outflow rate), ICP (intracranial pressure), CarP (intracarotid pressure at the level of the carotid bifurcation) and AoP (aortic blood pressure measured at the level of the aortic bifurcation) induced by an infusion of 10, 25 or 40 µl of Krebs-Ringer buffer solution or blood into each internal carotid artery

± S.E., number of observations in brackets

Infused intracarotid fluid during 1 s	Duration of increase in CBF (s)	CBF maximum increase in % of the resting CBF	ICP maximum increase in % of the resting ICP	Increase in CarP (mmHg)	Increase in AoP (mmHg)
10 µl buffered saline blood	5.8 ± 0.4 (10) 5.7 ± 0.5 (7)	6.7 ± 0.7 3.3 ± 0.4	3.1 ± 0.8 3.0 ± 0.7	4.0 ± 0.3 (23)	1.2 ± 0.4 1.3 ± 0.5
25 µl buffered saline blood	10.6 ± 1.2 (7) 10.8 ± 0.7 (5)	15.9 ± 2 9.3 ± 0.9	12.4 ± 0.3 11.6 ± 0.7	12.2 ± 1.2 (23)	4.6 ± 1.0 4.8 ± 1.1
40 µl buffered saline blood	18.9 ± 1.7 (8) 17.5 ± 1.1 (6)	28.0 ± 1.8 17.7 ± 1.1	26.4 ± 2.5 26 ± 3.1	25.4 ± 2.5 (16)	7.2 ± 0.4 8.0 ± 1.0

sections through the catheter in the external carotid artery then carried into the internal carotid artery supplying the brain (and in addition to the territory of the external pterygopalatine and occipital arteries) (Fig. 1). A catheter was also placed into one femoral artery for sampling of arterial blood for blood gas measurements. Determination of BUI was performed by intracarotid infusion of 10 or 40 µl of Krebs-Ringer buffer solution containing a mixture of the reference substance ^{14}C (Amersham, specific activity 27.1 mCi/mmol, concentration 100 nmol/ml), and either of the 3 different ^3H substances: L-isodrenaline-7- ^3H (NA) (New England Nuclear, specific activity 9.1 Ci/mmol, concentration 10 nmol/ml), ^3H -insulin (Amersham, specific activity 9 Ci/mmol, concentration 120 nmol/ml) or ^3H -ster (Amersham, 5 Ci/ml, concentration 7.5 nmol/ml). Respiratory arrest was induced by an intravenous injection of saturated potassium chloride 1 or 15 s after administration of the bolus. The animal was instantaneously decapitated and the head frozen in liquid nitrogen. Various regions supplied by the internal carotid artery on the injected side (frontal, parietal, frontal part of occipital cortex, thalamus and caudate nucleus) were cryosectioned on a cryostat at -15°C , weighed and placed in liquid scintillation vials containing 1.0 ml Soluene (Packard), where the tissue had been desiccated. 10 ml of Instagel was added. The tissue samples from each animal were counted in β -emissions in a Nuclear Chicago liquid scintillation counter. Quench correction was performed along conventional principles. According to Oldendorf (1971), the brain uptake index (BUI) is calculated from the specific activity of ^3H (test substance) and ^{14}C (reference substance) in the tissue and in the injected area as follows:

$$\text{BUI} = \frac{\text{tissue } ^3\text{H}/\text{tissue } ^{14}\text{C}}{\text{arterial } ^3\text{H}/\text{arterial } ^{14}\text{C}} \times 100$$

Statistical differences between mean values are assessed by the Student's t -test for unpaired data.

RESULTS

Cerebral blood flow and intracranial pressure. The resting mean (\pm S.E.) AoP was 120 ± 5 mmHg, resting ICP 12.8 ± 1.3 mmHg, CBF 73.7 ± 2.2 ml/100 g \times min, AVDO_2 10.3 ± 0.31 ml/100 ml, PaO_2 104 ± 3 mmHg, PaCO_2 35.3 ± 1.2 mmHg and pH 7.34 ± 0.16 . The effects of intracarotid infusions are listed in Table 1 and illustrated in Fig. 2, showing data of representative experiments with an infused volume of 10 and 40 µl, respectively of buffered saline. Infusion of 10 µl buffered saline during 1 s induced a very slight increase in CarP and CBF and a small change in ICP. AoP was almost unchanged. Increasing the infused volume over 25 to 40 µl gave rise to more pronounced and prolonged increase in CBF, ICP and CarP. The increase in intracranial pressure caused by the infusion was even reflected within the vascular tree at the level of AoP measurement. The CBF had not returned to a resting level until about 20 s after injection of 40 µl of buffered saline. When blood substituted saline as infusate the CBF changes were less pronounced, evidently due to absence of hemodilution, while the effects upon CarP, AoP and also ICP were similar to those induced with buffered saline (Table 1). These findings thus show the purely pressure-induced changes in CBF and ICP. A transient fall in CBF and ICP was observed upon infusion of 25 or 40 µl buffered saline or blood a few seconds after the initial increase (Fig. 2). This may be due to an autoregulatory vasoconstriction.

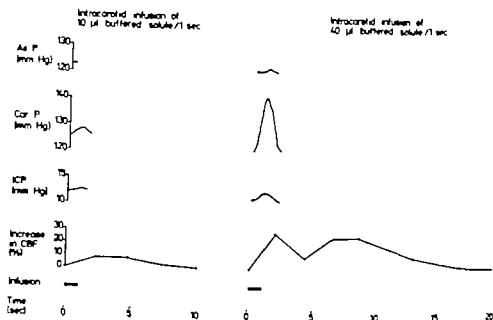


Fig. 2 Representative experiment performed in one animal (intracarotid pressure was measured in a separate animal) illustrating changes in cerebral blood flow (CBF) as reflected by the cerebral venous outflow drop rate, intracranial pressure (ICP—measured in the cisterna magna), intracarotid pressure (CarP—measured at the level of the carotid bifurcation) and aortic (systemic) blood pressure (AoP) induced by an intracarotid infusion on each side of 10 or 40 μ l Krebs-Ringer buffer solution over 1 s.

Brain uptake index The BUI in a brain hemisphere for inulin, NA and water after various circulation times (5 and 15 s) and injected volumes (10 and 40 μ l) are listed in Table 2. Injection of 40 μ l gave a significantly higher index than 10 μ l for water. A similar tendency was noticed for NA and also inulin. Further 15 s circulation time gave significantly lower index values than 5 s for NA.

DISCUSSION

According to the original technique (Oldendorf 1970, 1971) the radiolabelled mixture in an aqueous

solution is injected through a needle into a common carotid artery on one side. A high rate of injection is chosen to minimize mixing with circulating blood during the brain passage, thereby preventing from binding of the test substance to plasma proteins. Of the bolus mixture of 200 μ l injected within approx. 0.25 s, about 40 μ l is estimated to enter the internal carotid distribution (Oldendorf 1971). However, the blood flow to one hemisphere is normally only about 10 μ l/s (equivalent to 6 ml/100 mg and min) (Nilsson & Siesjö 1976) for a 0.75 g brain hemisphere. Therefore it is not surprising to find that 40 μ l of an aqueous solution in

Table 2 Brain uptake index (BUI) for tritiated water, 1-noradrenaline and inulin using 14 C-ethanol as reference substance after intracarotid injection of a radioactive bolus of 10 or 40 μ l, and circulation time of 5 or 15 s.

The values represent mean uptake (\pm S.E.) in regions supplied by the internal carotid artery from 6 animals (for water 6 μ l/15 s, 5 animals). Comparison of mean values according to Student's *t*-test for water 10/40 μ l: $*P < 0.01$, $**P < 0.05$; 1-noradrenaline 5/15 s: $P < 0.001$, otherwise non-significant difference.

Substance	10 μ l		40 μ l	
	5	15	5 s	15
Water	8.0 ± 1.0	79.4 ± 1	87.9 ± 1.3	85.4 ± 1.1
1-Noradrenaline	5.41 ± 0.00	3.16 ± 0.11	5.84 ± 0.15	3.54 ± 0.09
Inulin	1.64 ± 0.05	1.64 ± 0.10	1.70 ± 0.04	1.68 ± 0.05

ted over 1 down to the external carotid bilaterally to reach the internal carotid distribution induces a substantial increase in CBF and ICP though part of the infused volume enters the extracerebral circulation (via the pterygopalatine and ophthalmic arteries). It is notable that the flow in these vessels beyond the point of tissue sampling used in Oldendorf's model (i.e. 15 s after injection of 2) 50 μ l injected over approximately 0.5 s directly into one carotid internal artery in its flow region (the common and external carotid ligated) gives an even more marked increase in CBF and retrovascular volume (Furrow & Bass 1976) as will probably the volume injected in the original Oldendorf technique and in e.g. the CBF technique used by Crooke (1963) and Hertz et al. (1977). Apart from hemodilution this increase in CBF is caused by pressure-induced distension of vessels which may open closed microvessels thereby increasing the available capillary exchange surface. It should be noted however that, for technical reasons, the recent CBF studies had to be undertaken with lateral injection, thus not exactly mimicking the effects of unilateral injections used for BUI studies.

Clearly the use of water as reference substance will give BUI values that are overestimated as compared to the values obtained with a more diffusible reference substance. The higher BUI values for water found in the present series when a bolus of 40 μ l was used (Table 1) should primarily be explained by the increase in CBF provoked by the injection. This explanation would however imply an increasing flow dependence of the extraction also for the more diffusible substance (used as reference) which is not supported by the findings by Raichle et al. (1976). These authors found that about 90% of an injected bolus of labelled water was exchanged with brain at a CBF of 40 ml/100 g min, while the comparable figure for ethanol was 98%. However the extraction was reduced to about 77 and 87% respectively at CBF of about 100 ml/100 g min. This should lower the ethanol/water uptake quotient. Possibly other factors come into play. Thus, an increased back diffusion of ethanol during the clearance phase may influence the result even during the 5 s interval. The finding of an unchanged BUI for insulin at 15 s compared to 5 s further indicates that back diffusion of the reference substance is involved. Thus definite washout of insulin should have occurred during the 15 s period and yet the quotient insulin/ethanol is unaltered. With increasing

flow represented here by 40 μ l instead of 10 μ l the uptake will be overestimated even when ethanol is used. Using tritiated water as standard, Oldendorf (1971) found a mean BUI in the hemisphere of 4.5% for NA at a circulation time of 15 s, whereas in the present experiments, using 3 C-ethanol as standard (10 and 40 μ l volume respectively 15 s circulation time) values of 3.36–3.54 were obtained. Oldendorf's (1971) and the present values for insulin were 1.99 and 1.64–1.68, respectively.

The significantly lower BUI value for NA after 15 s circulation time compared to the value after 5 s elucidates another mechanism that necessitates reduction of the circulation time. It is generally considered that circulating neurotransmitter monoamines are not able to reach the brain parenchyma (for review see Edvinsson & MacKenzie 1976, see also Hardebo et al. 1979a). To a high extent, the structural unity of the endothelial lining at the level of the BBB (Reese & Karnovsky 1967) prevents the polar and water-soluble NA from being extracted from the brain circulation as reflected in the low BUI after 5 s circulation time. The few per cent of NA that do penetrate into the endothelial cells of brain microvessels and—at the level of brain parenchymal arterioles and pial vessels—further into the smooth muscle cell layer are metabolized by monoamine oxidase and catechol-O-methyl transferase present in these structures (Bertler et al. 1966, Spector et al. 1977, Hardebo et al. 1977, 1979b) probably constituting a further enzymatic barrier for monoamines. That a small fraction of NA actually can reach the brain vascular smooth muscle cells and induce a transient vasoconstriction (before the amine is metabolized)—if administered in sufficient amounts—is consistent with the finding of a shortlasting reduction in CBF upon intracarotid injection in the rat of a bolus of NA (Hardebo, Nilsson & Owman 1979). It is highly likely that the main explanation for the lower BUI value for NA at 15 s—apart from simple back-diffusion to the circulation and washout from the brain—is metabolism in the brain vessel wall and subsequent clearance back to the circulation. Rapid degradation by catechol-O-methyl transferase may be mainly responsible since metabolism via monoamine oxidase is a slower process. It should be noted that reduction of circulation time does not substantially influence the BUI for water (i.e. a non-metabolized substance). However as a general principle, it

should be advantageous to avoid the possible influence of secondary metabolic effects by using a short circulation time.

In the present series of experiments a further modification of the Oldendorf technique comprised injection into the internal carotid artery via the cannulated external carotid and not through a needle in the common carotid artery. This procedure eliminates any interruption or diminution of the blood flow through the internal carotid artery and also lowers the risk of vasospasm of this artery frequently occurring when the common carotid artery is manipulated.

CONCLUSIONS

The present study clearly illustrates that minimizing the volume injected into the rat brain circulation is necessary. Otherwise the flow artefacts induced by the injected volume and the rate of injection will influence the BUI. This principle should also be relevant to techniques using intracarotid injections for the direct study of CBF. 10 μ l was the smallest precise volume that could be administered in our model. If possible in the rat the use of even smaller volumes would be an advantage. The results further elucidate the need for reducing the circulation time from 15 s to about 5 s (cf. Oldendorf & Braun 1976) to avoid as far as possible effects of clearance and metabolism. The use of ethanol as reference substance is advantageous even if it is maybe not the ideal substance.

This work was supported by grants from the Swedish Medical Research Council (grant No. 04X 732 and 14X 263).

The skilful technical assistance of Mrs Camilla Hultman is gratefully acknowledged.

REFERENCES

- BERTLER, Å, FALCK, B., OWMAN, CH. & ROSENBERG, E. 1966. The localization of monoaminergic blood-brain barrier mechanisms. *Pharmacol. Rev.* 18, 369-385.
- BOLWIG, T. G. & LASSEN, N. A. 1975. The diffusion permeability to water of the rat blood-brain barrier. *Acta Physiol. Scand.* 93, 415-422.
- BRADBURY, M. W. B., PATLAK, C. S. & OLDENDORF, W. H. 1975. Analysis of brain uptake and loss of radiotracers after intracarotid injection. *Am. J. Physiol.* 229, 1110-1115.
- CRONE, C. 1963. The permeability of capillaries in various organs as determined by use of the indicator diffusion method. *Acta Physiol. Scand.* 58, 297-301.
- EDVINSSON, L. & MACKENZIE, E. T. 1976. Mechanisms in the cerebral circulation. *Pharmacol. Rev.* 28, 275-348.
- FURLOW, TH. W. & BASS, N. H. 1976. Cerebral hemodynamics in the rat assessed by a radiolabelled indicator-dilution technique. *Brain Res.* 110, 164-179.
- HARDEBO, J. E. & NILSSON, B. 1979. Hemodynamic changes in brain caused by local infusion of hyperosmolar solutions. In particular relation to blood-brain barrier opening. *Brain Res.* 000, 000-000.
- HARDEBO, J. E., NILSSON, B. & OWMAN, CH. 1979c. Influence upon cerebral blood flow of a short-lasting intracarotid injection of neurotransmitter monoamines as measured by a venous outflow method. *Acta Neurol. Scand.* 60, Suppl. 72, 136-137.
- HARDEBO, J. E., EDVINSSON, L., EMSON, P. C. & OWMAN, CH. 1977. Isolated brain microvesicles: enzymes related to adrenergic and cholinergic function. In: *Neurogenic control of the brain circulation* (Ed. O. Owman and L. Edvinsson), pp. 105-113. Pergamon Press, Oxford.
- HARDEBO, J. E., EDVINSSON, L., MACKENZIE, E. T. & OWMAN, CH. 1979a. Histofluorescence study on monoamine entry into the brain before and after opening of the blood-brain barrier by osmotic mechanisms. *Acta Neuropath. (Berl.)* 47, 145-150.
- HARDEBO, J. E., EMSON, P. C., FALCK, B., OWMAN, CH. & ROSENBERG, E. 1979b. Enzymes related to monoamine metabolism in brain microvessels. *J. Neurochem.* In press.
- HERTZ, M. M., HEIMINGSEN, R. & BOLWIG, T. G. 1977. Rapid and repetitive measurement of blood flow and oxygen consumption in the rat brain using intrarterial xenon injection. *Acta Physiol. Scand.* 101, 501-503.
- NILSSON, B. & SIESJÖ, B. K. 1976. A method for determining blood flow and oxygen consumption in the rat brain. *Acta Physiol. Scand.* 96, 77-82.
- NILSSON, B. & SIESJÖ, B. K. 1979. A venous outflow method for continuous measurement of the cerebral blood flow and oxygen consumption in the rat. *Stroke* 10, In press.
- OLDENDORF, W. H. 1970. Measurement of brain uptake of radiolabelled substances using a modified internal standard. *Brain Res.* 24, 372-376.
- OLDENDORF, W. H. 1971. Brain uptake of radiolabelled amino acids, amines and hexoses after arterial injection. *Am. J. Physiol.* 221, 1629-1638.
- OLDENDORF, W. H. 1973. Saturation of blood-brain barrier transport of amino acid in phenylethylamino. *Arch. Neurol.* 28, 45-48.
- OLDENDORF, W. H. & BRAUN, L. D. 1976. [³H]-Tryptamine and [³H]-water: a diffusible internal standard for measuring brain extraction of radiolabelled substances following carotid injection. *Brain Res.* 113, 219-224.
- OLDENDORF, W. H. & SZABO, J. 1976. Amino acid transport to one of three blood-brain barrier transporters. *Am. J. Physiol.* 230, 94-98.
- PARRIDGE, W. M. & OLDENDORF, W. H. 1977. Transport of metabolic substrates through the blood-brain barrier. *J. Neurochem.* 28.

- 1 SCHLE, M. E., EICHLING, J. O., STRAATMAN,
2 M. G., WELCH, M. J., LARSON, K. B. & TER-
3 POGOSSIAN, M. M. 1976 Blood-brain barrier
4 permeability of ^{14}C -labelled alcohols and ^{18}O -labelled
5 water. *Am J Physiol* 230: 543-552.
- 6 ESE, T. S. & KARNOVSKY, M. J. 1967 Fine
7 structural localization of blood-brain barrier to ex-
8ogenous peroxidase. *J Cell Biol* 34: 207-217.
- 9 SPECTOR, S., BAIRD-LAMBERT, J. & LAI, P. M.
10 1977 Disposition of norepinephrine in isolated brain
11 microvessels. In: *Neurogenic control of the brain*
12 *circulation* (ed. Ch. Owman and L. Edvinsson) pp.
13 115-120. Pergamon Press, Oxford.
- 14 WADE, L. A. & KATZMAN, R. 1975 Rat brain regional
15 uptake and decarboxylation of L-DOPA following
16 carotid injection. *Am J Physiol* 228: 352-359.

Comparative study on the uptake and subsequent carboxylation of monoamine precursors in cerebral microvessels

HARDEBO B, FALCK B and CH ÖWMAN

Departments of Histology and Neurology, University of Lund, Sweden

HARDEBO J. E., FALCK, B. & ÖWMAN, CH. A comparative study on the uptake and subsequent decarboxylation of monoamine precursors in cerebral microvessels. *Acta Physiol Scand* 1979, 107, 161-167. Received 3 April 1979. ISSN 0001-6772. Departments of Histology and Neurology, University of Lund, Sweden.

The endothelial cells and pericytes of brain microvessels (capillaries and small veins) are equipped with an enzymatic barrier impeding the passage of circulating amino acids, such as amine precursors, into the brain. The properties of this mechanism was studied in brain slices and isolated microvessels from various species including man and also fetal material following incubation in dihydroxyphenylalanine (DOPA), 5-hydroxytryptophan (5-HTP) and dihydroxyphenylserine (DOPS). A stereospecific, energy-dependent uptake leading to accumulation in the brain microvessel walls was found in all species studied; this process was found to exist already prenatally. The capacity of decarboxylation, the second step in the trapping mechanism at the blood-brain interphase, showed considerable species variation. The enzyme was present also in fetal brain microvessels. Incubation experiments provided support for the presence of monoamine oxidase, but absence of catechol-O-methyl transferase, in the microvessel walls.

Key words: brain microvessels, aromatic amino acid decarboxylase, monoamine oxidase, blood-brain barrier.

The microvessel (capillaries and small veins) in the central nervous system are capable of taking up and carboxylate monoamine precursors, such as L-3,4-dihydroxyphenylalanine (L-DOPA) (Bertler et al. 1964, 1966; Öwman & Rosengren 1967; Bartholomew et al. 1971; Dawson & Laszlo 1971; Wade & Kalz 1975a, b); L-5-hydroxytryptophan (L-5-HTP) (Bertler et al. 1964) and 3,4-dihydroxyphenylserine (DOPS) (Constantinides et al. 1975). The presence of aromatic L-amino acid decarboxylase (AAD) in the endothelial cells and pericytes of these vessels constitutes an enzymatic barrier impeding the passage of the monoamine precursors into the brain, as shown in the rat and mouse (Bertler et al. 1966). The present study was undertaken to investigate the presence of the uptake mechanism for monoamine precursors, as well as the AAD activity, in brain microvessels of various species including man. The appearance of these functions in the fetal brain was also studied.

MATERIALS AND METHODS

Animals. The majority of the study was performed on adult animals of either sex: 8 albino mice, 67 Sprague-Dawley rats, 8 hamsters, 6 guinea-pigs, 6 albino rabbits, 4 cats, 4 dogs, 4 pigs, 4 cows, 3 baboons and brain tissue from 5 baboons (obtained during neurosurgical operations). The laboratory animals had free access to standard pellet food and water. They were killed under light ether or nembutal anesthesia. In addition, fetuses of various age from rat (32 fetuses from 4 animals), rabbit (8 from 3 animals) and human (1 black pregnancy was interrupted at 20 and 22 weeks of gestation) was studied. Blood vessels appear in the central nervous system of the rat on day 1-14 of gestation (Blur & Wolff 1972). In the rabbit at 11 days of gestation (Donahoe 1964), and are present in human fetuses at the 10th week of gestation (Povlishock et al. 1977).

Incubation of tissue slices. One mm thin slices of the parietal cortex, caudate nucleus, cerebellum, spinal cord and hippocampus from 4 animals of each species studied (from temporal cortex, frontal cortex or cerebellum of man) were cut with razor blade and transferred to incubation dishes containing ice-cold Krebs-Ringer buffer solution. Slices were also taken from the brain hemispheres—pref-

essentially cortical tissue—of fetuses of various ages from rat, rabbit and man. The buffer solution had the following composition (mM): NaCl 118, KCl 4.5, CaCl₂ × H₂O 2.5, MgSO₄ × 7H₂O 1.0, NaHCO₃ 25, KH₂PO₄ 1.0 to which was added 1 mg/ml glucose and 0.2 mg/ml ascorbic acid. The solution was continuously aerated with a mixture of 95% O₂ and 5% CO₂ giving a pH of 7.4.

The vials were placed in an incubation bath at 37°C for preincubation during 70 min in the presence of the decarboxylase inhibitors, carbidopa or benserazide (10⁻⁴ M) followed by incubation during 70 min after the addition of the various monoamine precursors at a dose of 1/10 or 100 µg/ml L-DOPA, D-DOPA, (+)-erythro-DOPS, (-)-erythro-DOPS, (±)-threo-DOPS and L-5-HTP. In some of the incubations the monoamine oxidase inhibitor nialamide (10⁻⁴ M) or the catechol-O-methyltransferase inhibitor U-0511 (10⁻⁴ M), replaced carbidopa or benserazide. Control slices were incubated without addition of any drugs.

The uptake of L-DOPA, L-5-HTP and (+)-erythro-DOPS (in the presence of carbidopa) was further characterized in the presence of ouabain (10⁻⁴ M) at low sodium and high potassium concentrations (in the buffer solution KCl substituted for all NaCl) under combined anoxia (continuous bubbling with 95% N₂ and 5% CO₂) and absence of glucose. In the presence of dimethylphenol and also at 0°C.

Fluorescence microscopy. Following incubation the various tissue pieces were frozen to the temperature of liquid nitrogen and further processed for fluorescent monoamine histochemistry according to the Falck-Hillarp method (Björklund, Falck & Owman 1977). The paraformaldehyde used in the histochemical procedure had previously been equilibrated with air of 70% humidity. The formaldehyde-induced histochemically visible fluorophores of noradrenaline, adrenaline, dopamine, DOPA and DOPS are indistinguishable since they have the same spectral characteristics and exhibit a green light under the optical conditions used (Björklund et al. 1977). 5-HTP and 5-hydroxytryptamine exhibit a yellow, rapidly fading light under these conditions (Björklund et al. 1977). When evaluating the changes in fluorescence intensity after incubations under various conditions, the material to be compared was always freeze-dried and further processed on the same occasion.

Isolation of cerebral microvessels. Whole brains from rats were used. After removal they were kept in an ice-cold 67 mM phosphate buffer (pH 7.4) throughout the procedure. The meninges, including the pial membrane and its vessels, were carefully torn off and the choroid plexus were removed. White matter, including the whole brain stem, was dissected away. Tissue obtained from 4–6 rats was chopped with a razor blade and then gently further disrupted by some 10 strokes up and down through 3 different 10–20 ml plastic syringes equipped with a nylon net (pore size 1000 µm, 500 µm and 80 µm, respectively) placed to their open cut end. The material was subsequently homogenized by hand with a loosely fitting Teflon pestle in a smooth glass tube (1 mm clearance). The homogenate was washed through one nylon sieve with 0.5 µm pore size. The material remaining on the sieve after a tensile washing was re-homogenized and re-sieved 3–4 times through the same carefully

washed sieve. The tissue passing these sieves was collected and sieved through another sieve with 75 µm size. The material remaining on this sieve was also washed and re-homogenized and re-sieved in the same carefully washed sieve. The tissue fraction remaining on the sieve after extensive washing consists of capillary venules and a few larger vessels, whereas most of the larger vessels and vessels branching off into clusters of small vessels, as well as a few small clusters of neurons and glia, remain on the 75 µm sieve. Microvessels (Neurons, glia, small microvessel segments, and cellular fragments) pass the 75 µm sieve. The capillary fraction is pure with regard to vessels and is only contaminated with a few glial endfeet stuck onto the vessel wall (Hardebo et al. 1977) and possibly perivascular nerve fibers. The yield of microvessels is less than 1/1000 of the original weight of the grey matter. Brendel, Metten & Oelz (1974) have shown that a mixed fraction of microvessels prepared under similar conditions is metabolically active.

Incubation of isolated microvessels. The mixture fractions were transferred to incubation vials containing ice-cold Krebs-Ringer buffer solution (composition as above). The vials were placed in an incubation bath allowed to equilibrate for 70 min at 37°C in the presence of the decarboxylase inhibitor benserazide (10⁻⁴ M) before incubation, which was started by adding 7H-L-DOPA to the solution. The tissue preparations were incubated 15 min at a temperature of 37°C. The buffer solution was continuously aerated with 95% O₂ and 5% CO₂. Incubation was terminated by transferring the buffer to ice-cold buffer solution. The microvessel fraction was collected by centrifugation at 4°C at 110 g and washed in isotonic-free cold buffer for each 10 min.

In order to further characterize the uptake microvessel fractions were also incubated in the presence of ouabain (10⁻⁴ M) and at 0°C.

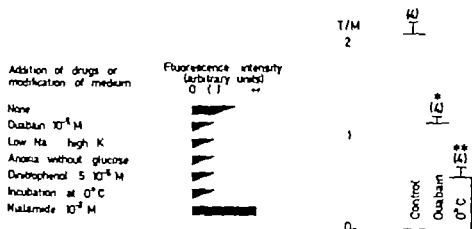
Measurement of radioactivity. After incubation 5 microvessel samples were weighed and transferred to liquid scintillation vial. They were solubilized in 6 ml Soluene (Packard) and liquid scintillation counting performed in 10 ml Instagel (Packard), as are appropriate samples (5 µl) of the incubation medium. Corrections were obtained according to conventional principles.

Drugs. L-DOPA and D-DOPA (Sigma), (±)-erythro-DOPS (+)-L and (-)-D-erythro-DOPS (all gifts from Roche), L-5-HTP (Sigma), carbidopa (MSD), benserazide (Roche), ouabain (Sigma), nialamide (Bayer), and 7H-L-DOPA (Radiochemical Centre, Amersham, UK).

Statistics. Mean values were compared according to Student's *t*-test for unpaired data.

RESULTS

Fluorescence microscopy. Of the various brain regions from control slices incubated in buffer solution alone, showed a dense network of delicate catecholamine-containing nerve terminals emitting



1. Accumulation of L-DOPA in the walls of microvessels in rat parietal cortex pretreated with benzerazide 10^{-4} M and incubated in the presence of $10 \mu\text{g/ml}$ L-DOPA alone and after addition of drugs or modification of the medium (following decarboxylase inhibition by 10^{-4} M benzerazide). For comparison the fluorescence intensity following pretreatment with malamide instead of benzerazide is shown (the accumulated fluorophore now consists of L-DOPA). The fluorescence ratio (U/M: μg tissue per μl medium) following 15 min incubation of isolated cerebral vessels with ^3H -L-DOPA (and after decarboxylase inhibition by 10^{-4} M benzerazide) under control conditions (C) and in the presence of ouabain (10^{-4} M) or during hypothermia (0°C). Values are means \pm S.E. number of experiments (in parentheses). Control vs. experimental according to Student's *t*-test. $^{*}0.01 < P < 0.05$, $^{**}0.01 < P < 0.01$.

roen fluorescence in the cerebellum only a small number of isolated green-fluorescent axons were seen. The parenchymal blood vessels were supplied with varying amounts of sympathetic nerves. In the heart tissue adrenergic nerves were seen in the myocardium and in association with the nodal vessels. All tissues showed a slight diffuse, non-specific greenish background fluorescence. No clear wall proper was in all regions essentially non-fluorescent except for the intense autofluorescence in the internal elastic membrane of peripheral arteries.

After incubation with the known monoamine oxidase inhibitors, carbonylcholine or benzerazide, an accumulation of fluorophore, weak but above the diffuse background fluorescence, was seen in the brain microvessel walls (endothelial cells and pericytes of pial vessels and small veins) to a similar degree in all test species studied and irrespective of whether benzerazide or carbonylcholine was used as decarboxylase inhibitor. The intensity of the general background fluorescence was also increased. No clear accumulation above the diffuse background fluorescence had occurred in the walls of

the brain parenchymal arterioles, pial vessels, or heart vessels. Of the various amino acids tested (at an identical concentration in the incubation bath) L-DOPA induced the strongest fluorescence in the microvessel wall of brains from adult and newborn animals. L-5-HTP and (+)-erythro-DOPS a somewhat weaker fluorescence, whereas the fluorescence induced by D-DOPA, (-)-erythro-DOPS or (\pm)-threo-DOPS was considerably weaker. The discrepancy in fluorescence intensity between L-DOPA on one hand and L-5-HTP and (+)-erythro-DOPS on the other is well explainable by the varying fluorescence yield in the standard formaldehyde reaction used (Björklund et al. 1972). Also in brain slices from fetal and newborn animals a clear-cut uptake of the monoamine precursors was seen.

Fig. 1 and 2 show the inhibitory influence on the uptake of L-DOPA (in the presence of a decarboxylase inhibitor) into brain microvessel walls by various drugs or by modification of the medium as studied in brain slices as well as in isolated fractions of microvessel (using radioactive L-DOPA). The pattern of inhibition, being the same for L-5-HTP and (+)-erythro-DOPS, indicates the presence of an

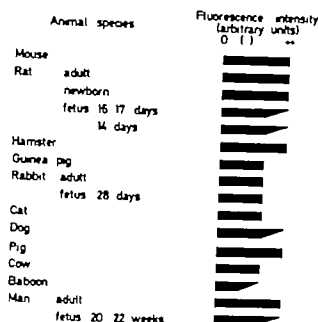


Fig. 2 Accumulation of fluorophore (L-DOPA and dopamine) in the microvessel wall of brain cortical slices from various species (adult unless otherwise stated) incubated for 30 min in the presence of $10 \mu\text{g/ml}$ L-DOPA following monoamine oxidase inhibition (10^{-4} M nialamide) and processed according to the formaldehyde histochemistry method. The comparison refers to the combined presence of L-DOPA and dopamine (formed by decarboxylation within the microvessel wall) since the fluorophores are undistinguishable under the optical conditions used. Tapering part of the bars indicate intermediate intensities.

energy-dependent uptake mechanism into the cells of the brain microvessel wall.

Inhibition of monoamine oxidase by nialamide (but with intact decarboxylase activity) clearly enhanced the accumulation of the fluorophores in the microvessel wall as evidenced by a stronger fluorescence intensity in relation to the background fluorescence as compared to that obtained after inhibition of the AAD activity (Fig. 1a). This provides indirect evidence for the presence of microvascular AAD activity in all species studied as well as the presence of a subsequent breakdown mechanism via monoamine oxidase in these vessel walls. However considerable species differences were now revealed indicating variations in AAD activity (Fig. 2). Also in slices from fetal brains inhibition by nialamide revealed an enhanced accumulation in the microvessel wall indicating the presence of microvascular AAD activity already at this age (Fig. 2). On the other hand inhibition of

catechol-O-methyl transferase by U-0512 did not affect the accumulation of fluorophore in the microvessel wall.

DISCUSSION

The integrity of the endothelial lining along with the paucity in transendothelial vesicular transport and absence of fenestrae in brain vessels (Renehan & Karnovsky 1967; Westergaard & Brightman 1973) constituting the morphological blood-brain barrier impedes the passage of a large variety of compounds from the circulation into the brain. However substances may pass this barrier by virtue of lipid solubility or with the aid of carrier mechanisms. The present study provides evidence for the existence in various species including rat of an energy-dependent uptake mechanism for the immediate precursors to neurotransmitters, monoamines at the level of the endothelial cell pericytes of brain microvessels in contrast to the endothelium of brain parenchymal arterioles. The study does not show whether the uptake occurs across the luminal or the abluminal side of the microvessel wall or both. An avid uptake of L-DOPA *in vivo* into brain microvessel walls of the rat has been reported following intracarotid administration of radioactive L-DOPA (Oldendorf 1971; Wade & Katzman 1975a; own unpublished observations) but simple diffusion also contributes to some extent (Wade & Katzman 1975a). An energy-dependent uptake of L-DOPA into rat brain slices (thus reflecting both an uptake into neurons and into vessel walls) has also been characterized (Yoshida et al. 1963a and b) in a similar way as presently for microvessels. Also in the newborn and fetal brains this is noticed.

The present uptake mechanism at the level of the blood-brain barrier is supposed to be shared with other neutral amino acids as shown for the D-phenylalanine, methionine, histidine, cysteine, valine, isoleucine, leucine, tryptophan and threonine (Chirigos et al. 1969; Oldendorf 1973; Pardo et al. 1977). Moreover this movement across the membranes is bidirectional (Christensen 1969; Wade & Katzman 1975b) which is consistent with the finding that L-DOPA is readily taken up into the microvessel wall also when administered into the brain parenchyma (Bertler et al. 1966). A facilitated diffusion of L-DOPA into the microvascular endothelial cell and pericytes would mean that the uptake of

along a concentration gradient so that the uptake from the circulation—or brain parenchyma (Bertler et al 1977)—ceases when the intracellular concentration of free L-DOPA is equal to that on the outside of the cell membrane. That histologically visible accumulation of fluorophore is more than of the background fluorescence in fact is proved, even when the conversion to dopamine is efficiently blocked by a decarboxylase inhibitor, indicating that some kind of intracellular trapping of L-DOPA occurs in the microvessel wall. Another possibility is that the uptake is not solely simple facilitated diffusion, but has a component of active transport of the 'uphill' type as indicated by the mode of inhibition found in the present in vitro studies, in line with the reasoning made by de Waele & Kitzman (1975).

Of the two decarboxylase inhibitors used, especially carbidopa has a structural similarity with L-DOPA. It would, therefore, be possible that this inhibitor shares an uptake mechanism in common with L-DOPA across the endothelial membrane, leading to reduce the absolute amount of L-DOPA being able to reach the endothelial cytoplasm when the two agents are present together in the incubation bath. Even so, the uptake of L-DOPA is still high enough for adequate fluorescence histochemical visualization.

The degree of intracellular L-DOPA accumulation as reflected in the ratio of radioactivity in the microvessel fraction and the medium, was less than that reported for the uptake of noradrenaline into sympathetic nerves under similar conditions (Edvinsson & Olsson 1977; Alm et al 1979) but considerably higher than the extraneuronal amine uptake into smooth musculature (Alm et al 1979). The energy-dependency of the microvessel uptake was confirmed by the inhibition accomplished with hypothermia, combined anoxia and glucose deprivation, or uncoupling of the oxidative phosphorylation with dinitrophenol. The result from the incubation with low sodium and high potassium, as well as in the presence of ouabain, suggest that the uptake is linked with Na^+ -dependent ATPase. The uptake of monoamine precursors is stereoselective, since L-DOPA and (1R)-erythro-DOPS are taken up more readily than D-DOPA, (1S)-erythro-DOPS and (1R)-threo-DOPS in brains from adult and newborn animals (see also Bertler et al 1976; Olsendorff 1973; Constantinidis et al 1975). However, the possible existence of a stereospecificity was not possible to establish in the fetal material.

Pretreatment with the monoamine oxidase inhibitor nialamide enhanced the accumulation in the endothelial cells and pericytes of the microvessel wall. This finding offers support for the presence of monoamine oxidase in these cells (Bertler et al 1966; Spector et al 1977; Liu & Spector 1978; Hardebo et al 1977, 1979). When studying the effect of pretreatment with nialamide, no decarboxylase inhibitor was present in the bath. Hence, the enhanced accumulation of fluorophore in this situation is primarily due to the formation of the corresponding monoamine (dopamine, 5-hydroxytryptamine or noradrenaline) from the respective precursor (L-DOPA, L-5-HTP or DOPS) within the microvessel wall. It should be recalled that the fluorescence of the precursor and the corresponding monoamine are indistinguishable under the optical conditions used. The decarboxylase activity thus revealed was found to vary between species, as reflected in the difference in accumulation of fluorophore. This species difference agrees with findings from chemical determinations on isolated cerebral microvessels (Hardebo et al 1979) and in histofluorescence studies following administration of L-DOPA in vivo (Langelier et al 1971) or after incubation of brain slices in the presence of the amino acid (Downson & Laszlo 1971; Downson 1973). Decarboxylase activity was indicated also in the microvessel wall of the newborn and fetal brain. This supports the findings in vivo on rats (Kellogg et al 1973).

Inhibition of catechol-O-methyltransferase did not affect the accumulation of fluorophore in the microvessel wall, indicating that this enzyme is not present in the endothelial cells and pericytes (see also Hardebo et al 1979; cf. Spector et al 1977).

L-DOPA, and probably 5-HTP too, is found in the circulation (where the normal L-DOPA concentration is about 3×10^{-6} M; Hansson et al 1978) despite the presence of a considerable decarboxylase activity in many visceral organs. Apart from metabolizing circulating DOPA and 5-HTP that would otherwise have been taken up across the blood-brain barrier by the neutral amino acid carrier system, the decarboxylase activity in brain microvessel wall may be involved in a more complex enzymatic barrier mechanism for other circulating amino acids such as phenylalanine, tyrosine and tryptophan or may be involved in a hitherto un-

known metabolic pathway across the blood-brain interphase

The efficiency of the blood-brain barrier to impede the passage of L-DOPA into the brain by decarboxylation. In addition to the decarboxylation activity in the peripheral tissues, have required high doses of L-DOPA in the medical treatment of Parkinson's disease with disturbing side-effects as a frequent result. Therefore a decarboxylase inhibitor (carbidopa or benserazide) effective in peripheral tissues as well as in brain microvessel walls but only to a negligible extent in the brain parenchyma is now added to L-DOPA in the therapy. Under these conditions the amine precursor can be administered in lower doses, reducing the incidence of undesired side-effects.

This work was supported by grants from the Swedish Medical Research Council (grants No. 04X 732 and 04X 56).

The skilful technical assistance of Mrs Inga-Margit Hägg is gratefully acknowledged.

REFERENCES

- ALM P, ÖWMAN CH, SJÖBERG N-O & THORBERT G 1979 Uptake and metabolism of ³H-norepinephrine in myometrial adrenergic nerves of the guinea-pig. Effect of pregnancy. *Am J Physiol* 236 C277-C285.
- BÄR TH & WOLFF J R 1977 The formation of capillary basement membranes during internal vascularization of the rat's cerebral cortex. *Z Zellforsch* 133 231-248.
- BARTHOLINI G, CONSTANTINIDIS J, TISSOT R & PLETSCHER A 1971 Formation of monoamines from various amino acids in the brain after inhibition of extracerebral decarboxylase. *Biochem Pharmacol* 20 1241-1247.
- BERTLER A, FALCK B & ROSENGREN F 1964 The direct demonstration of a barrier mechanism in the brain capillaries. *Acta Pharmacol (Ahh)* 20:317-318.
- BERTLER A, FALCK B, ÖWMAN CH & ROSENGREN E 1966 The localization of monoaminergic blood-brain barrier mechanisms. *Pharmacol Rev* 18 369-385.
- BJÖRKLUND A, FALCK B & ÖWMAN CH 1977 Fluorescence microscopic and microspectrofluorometric techniques for the cellular localization and characterization of biogenic amines. In: *Methods in Investigative and Diagnostic Endocrinology*, vol. 1. The thyroid and biogenic amines (ed. J E Rall and I J Kopin) pp. 318-368. North-Holland Publ. Comp. Amsterdam.
- BRENDEL K, MEEZAN E & CARLSON E C 1974 Isolated brain microvessels: a purified metabolically active preparation from bovine cerebral cortex. *Science* 185 951-955.
- CHIRIGOS M, A GREENGARD P & FRIEND S 1960 Uptake of tyrosine by rat brain *in vivo*. *J Biol Chem* 235 2075-2079.
- CHRISTENSEN H N 1969 Some special barrier problems of transport. *Adv Enzymol* 1, 1-30.
- CONSTANTINIDIS J, GEISSBUHLER F, GIL LARD J M, AUBERT C, HOVAGIMIAN N & TISSOT R 1975 Formation de monoamines dans le cerveau du rat après administration de 1-(α -ro-3,4-dihydroxyphenyl)serine. *Psychopharmacol (Berl)* 44 201-209.
- DONAHUE S 1964 A relationship between fine structure and function of blood vessels in the central nervous system of rabbit fetuses. *Am J Anat* 135 17-23.
- DOWSON J H 1973 Animal models for an intact blood-brain barrier mechanism for therapeutically administered L-DOPA. *Life Sci* 13 25-29.
- DOWSON J H & LASZLO I 1971 Quantitative histochemical studies of formaldehyde-induced pericythyl fluorescence following L-DOPA administration. *J Neurochem* 18 2501-2508.
- EDVINSSON I & ÖWMAN CH 1977 Quantitation of the uptake of ³H-norepinephrine into rabbit vessels and its relation to the degree of sympathetic nerve supply. In: *Neurogenic control of the heart* (ed. Ch. Öwman and L. Edvinsson) pp. 13-13. Pergamon Press, Oxford.
- HANSSON C, EDHOLM L E, AGRIFF G, RORSMAN H, ROSENGREN A M & ROSENGREN E 1978 The quantitative determination of 5-hydroxytryptophan and dopa in normal serum and serum from patient with malignant melanoma by means of high-pressure liquid chromatography. *J Chromatogr* 183 419-427.
- HARDEBO J E, EDVINSSON L, EMISON P C & ÖWMAN CH 1977 Isolated brain microvessels. Enzymes related to adrenergic and cholinergic functions. In: *Neurogenic control of the brain circulation* (ed. Ch. Öwman and L. Edvinsson) pp. 105-111. Pergamon Press, Oxford.
- HARDEBO J E, EMISON P C, FALCK B & ÖWMAN CH & ROSENGREN E 1979 Quantitative measurement of the formation and degradation of neurotransmitter monoamines at the blood-brain interphase in various species including man. *J Neurochem* In press.
- KFELLOGO C, LUNDBERG P & RAUSTEDT L 1973 Analysis of capillary and parenchymal monoamine L-amine acid decarboxylase activity in regional brains during ontogenic development in the rat. *Brain Res* 50 369-378.
- LAI F M & SPECTOR S 1978 Studies on the monoamine oxidase and catechol-O-methyltransferase of the rat cerebral microvessels. *Arch Int Pharmacodyn* 233 227-234.
- LANGELIER P, PARENT A & POIRIER L J 1974 Decarboxylase activity of the brain capillary walls and parenchyma in the rat, cat and monkey. *Brain Res* 45 620-629.
- OLDENDORF W H 1971 Brain uptake of radiolabelled amino acids, amines and hormones after arterial perfusion. *Am J Physiol* 221 1629-1639.

2. ENDORF W. H. 1973 Stereospecificity of blood-brain barrier permeability to amino acids. *Am J Physiol* 224 967-969.
3. VAN CH. & ROSENGREN E. 1967 Dopamine formation in brain capillaries—an enzymatic blood-brain barrier mechanism. *J Neurochem* 14 547-550.
4. IDRIDGE, W. M. 1977 Kinetics of competitive inhibition of neutral amino acid transport across the blood-brain barrier. *J Neurochem* 28 103-108.
5. LISHOCK, J. T., MARTINEZ A. J. & MOOSSY J. 1977 The fine structure of blood vessels of the telencephalic perivascular space in the bovine fetus. *Am J Anat* 149 439-443.
6. ESE, T. S. & KARNOVSKY M. J. 1967 Fine structural localization of blood-brain barrier: exogenous peroxidase. *J Cell Biol* 34 207-17.
7. CTOR, S., BAIRD-LAMBERT J. & LAI, F. M. 1977 Disposition of norepinephrine in isolated brain microvessels. I. Neurogenic control of brain circulation (ed. Ch. Owman and L. Edvinsson), pp. 115-120. Pergamon Press, Oxford.
8. WADE L. A. & KATZMAN R. 1975a Rat brain regional uptake and decarboxylation of L-DOPA following carotid injection. *Am J Physiol* 228 352-359.
9. WADE, L. A. & KATZMAN R. 1975b Synthetic amino acids and the nature of L-DOPA transport at the blood-brain barrier. *J Neurochem* 25 837-842.
10. WESTERGAARD E. & BRIGHTMAN M. W. 1973 Transport of proteins across the normal cerebral arterioles. *J Comp Neurol* 152 17-44.
11. YOSHIDA, H., KANIKE, K. & NAMBA J. 1963 Properties of carrier system to transport L-dopa into brain slices. *Nature* 198 191-192.
12. YOSHIDA, H., NAMBA, J., KANIKE, K. & ISAI ZUMI E. 1963b Studies on active transport of L-dopa (dihydroxyphenylalanine) into brain slices. *Jap J Pharmacol* 13 1-9.

The vagal control of the feline pyloric sphincter

EDIN H. AHLMAN and J. KEWENTER

from the Department of Surgery III, University of Göteborg, Sweden

EDIN H. AHLMAN, H. & KEWENTER, J. The vagal control of the feline pyloric sphincter. *Acta Physiol Scand* 1979; 107: 169-174. Received 5 April 1979. ISSN 0001-6772. Department of Surgery III, University of Göteborg, Sweden.

In acute experiments on cats in chloralose anaesthesia the effects of efferent and afferent electrical stimulation of the cervical vagi on an applied constant flow of saline through the feline pylorus was studied. The motor activity of the stomach was recorded simultaneously with volume recording technique. Efferent cervical vagal stimulation caused a decrease in the transpyloric flow and an increased gastric motor activity. In a few animals the decreased transpyloric flow was preceded by a short period of increased flow. When the transpyloric flow was reduced by splanchnic nerve stimulation or noradrenaline infusion, vagal nerve stimulation induced an increased flow through the pylorus indicating the presence of relaxatory fibres to the pylorus within the vagi. Electrical stimulation of the central end of the ipsilateral vagal nerve in the neck, with the contralateral vagal nerve left intact, resulted in a decreased transpyloric flow and relaxation of the stomach. This response could be reduced with or without intact splanchnic nerves, and disappeared when the intact contralateral vagus was cut. It is concluded that the vagi mediate both excitatory and inhibitory fibres to the pyloric sphincter in the cat. A vago-vagal excitatory reflex to the pylorus can be elicited by afferent vagal nerve stimulation together with vago-vagal relaxatory response of the stomach.

Key words: Pyloric sphincter, gastric motility, electrical stimulation, vagal nerves, cat.

The presence of an anatomical well-defined pyloric sphincter has been demonstrated in some species but is strongly questioned in others (Dadlo 1968; Edwards 1968 and Kaye et al. 1976). However, Forgren (1941) demonstrated the presence of such a sphincter at the gastroduodenal junction of the cat. Histochemical studies have verified a high number of cholinergic ganglion cells and adrenergic nerve terminals in this region compared with surrounding parts of the gastrointestinal tract indicating the presence of a specific sphincter region (Scharb et al. 1974).

A high pressure zone at the gastroduodenal junction has been documented (Brink et al. 1965). Antral peristalsis caused a decreased pressure within this zone while duodenal perfusion with amino acids, glucose and fat increased the pressure (Fisher & Cohen 1973). Thus physiological characteristics for gastrointestinal sphincter are fulfilled for the gastroduodenal junction according to the definition given by Fisher & Cohen (1973).

In numerous studies have indicated that the vagal nerves contain noncholinergic relaxatory fibres to

the pylorus in dogs (Mir et al. 1977). If these fibres are identical to those which mediate the non-cholinergic non-adrenergic gastric relaxation is still unclear since volume recordings of gastric motility were not recorded simultaneously in their experiments. Whether the vagi convey nerve fibres to the pyloric region, which can control this sphincter independently of the gastric motor activity is not known.

The aim of the present investigation was to study the effect of efferent and afferent vagal nerve stimulation on an externally applied flow of saline through the feline pyloric sphincter. It was also judged to be of interest simultaneously to study the gastric motility in order to investigate whether the vagal nerves might exert specific effects on the pylorus separated from those on the stomach.

MATERIAL AND METHODS

The experiments were performed in 77 cats of both sexes. The animals were fasted for about 24 h prior to the experiment but had free access to water. The anaesthesia

16 The vagal control of the feline pyloric sphincter

EDIN H. AHLMAN and J. KEWENTER

from the Department of Surgery III, University of Göteborg, Sweden

EDIN H. AHLMAN & KEWENTER J. The vagal control of the feline pyloric sphincter. *Acta Physiol Scand* 1979; 107: 169-174. Received 5 April 1979. ISSN 0001-6772. Department of Surgery III, University of Göteborg, Sweden.

In acute experiments on cat, in chloralose anaesthesia the effects of efferent and afferent electrical stimulation of the cervical vagi on an applied constant flow of saline through the feline pylorus was studied. The motor activity of the stomach was recorded simultaneously with volume recording technique. Efferent cervical vagal stimulation caused decrease in the transpyloric flow and an increased gastric motor activity. In few animals the decreased transpyloric flow was preceded by a short period of increased flow. When the transpyloric flow was reduced by splanchnic nerve stimulation or noradrenaline infusion, vagal nerve stimulation induced an increased flow through the pylorus indicating the presence of relaxatory fibres to the pylorus within the vagi. Electrical stimulation of the central end of the ipsilateral vagal nerve in the neck, with the contralateral vagal nerve left intact resulted in decreased transpyloric flow and relaxation of the stomach. This response could be induced with or without intact splanchnic nerves, and disappeared when the intact contralateral vagus was cut. It is concluded that the vagi mediate both excitatory and inhibitory fibres to the pyloric sphincter in the cat. A vago-vagal excitatory reflex to the pylorus can be elicited by afferent vagal nerve stimulation together with vago-vagal relaxatory response of the stomach.

Key words: Pyloric sphincter, gastric motility, electrical stimulation, vagal nerves, cat.

The presence of an anatomical well-defined pyloric sphincter has been demonstrated in some species but strongly questioned in others (Dedio 1968; Edwards 1968 and Kaye et al. 1976). However, Jorgensen (1941) demonstrated the presence of such a sphincter at the gastroduodenal junction of the cat. Histochemical studies have verified a high number of cholinergic ganglion cells and adrenergic nerve terminals in this region compared with surrounding parts of the gastrointestinal tract indicating the presence of a specific sphincter region (Schardt et al. 1974).

A high pressure zone at the gastroduodenal junction has been documented (Bræk et al. 1965). Antral peristalsis caused a decreased pressure within this zone. Intra-duodenal perfusion with amino acids, glucose and fat increased the pressure (Fisher & Cohen 1973). Thus, physiological characteristics for a gastrointestinal sphincter are fulfilled for the gastroduodenal junction according to the definition given by Fisher & Cohen (1973).

In *in vitro* studies have indicated that the vagal nerves convey noncholinergic relaxatory fibres to

the pylorus in dogs (Mir et al. 1977). If these fibres are identical to those which mediate the non-cholinergic non-adrenergic gastric relaxation is still unclear since volume recordings of gastric motility were not recorded simultaneously in their experiments. Whether the vagi convey nerve fibres to the pyloric region which can control this sphincter independently of the gastric motor activity is not known.

The aim of the present investigation was to study the effect of efferent and afferent vagal nerve stimulation on an externally applied flow of saline through the feline pyloric sphincter. It was also judged to be of interest simultaneously to study the gastric motility in order to investigate whether the vagal nerves might exert specific effects on the pylorus separated from these on the stomach.

MATERIAL AND METHODS

The experiments were performed in 27 cats of both sexes. The animals were fasted for about 24 h prior to the experiments but had free access to water. The anaesthesia

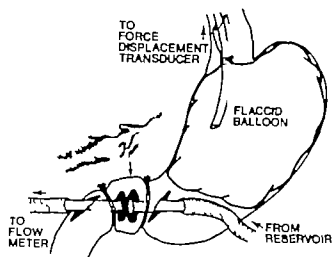


Fig. 1 Schematic drawing of the technique used to study transpyloric flow. Note histology sections from this region demonstrating a circular valve/sphincter.

was initiated with ether and was continued with chloralose (50 mg/kg b.w.) slowly injected through one of the femoral veins. The animals were placed on an operation table on a thermostatically regulated heating pad in order to maintain the body temperature at about $+38^{\circ}\text{C}$. A tracheal cannula was inserted to guarantee free airways. A femoral artery was cannulated and connected to a pressure transducer (Statham p.3 DC) for continuous recording of the arterial blood pressure. The abdomen was opened with a midline incision. The catecholamine secretion from the adrenal medulla is known to be a potent intestinal inhibitor. To eliminate this effect the arterial and venous vessels of the adrenal glands were ligated.

Nerve operations and stimulation procedures. Through the tracheostomy incision the cervical vagi were isolated from the sympathetic trunk and divided uni- or bi-laterally. The cut ends of the vagi were inserted separately into insulated ring electrodes which were cautiously placed deep into the wound before nerve stimulation. In 16 cats given efferent vagal nerve stimulation the splanchnic nerves were left intact in 5 animals and divided bilaterally in 11 animals at the preganglionic level subdiaphragmatically prior to the stimulation.

In animals given unilateral afferent nerve stimulation the splanchnic nerves were left intact in 7 and divided bilaterally in 11 cats. In 4 animals both splanchnic and vagal nerves were divided during the experiment. All nerve stimulations were performed using square wave pulses from a Grass stimulator (S4E) during 5 min. The stimulation parameters (8–15 V, 0.5 ms, 8–12 Hz) were divided into 2 groups activating high (5 ms) and low threshold (0.5 ms) efferent fibres selectively according to Martenson (1965a). The same groups of parameters were applied for the afferent nerve stimulations.

Recording of transpyloric flow. A non-compressible plastic tube (diameter 8 mm) was inserted through a small longitudinal incision along the greater curvature on the anterior wall of the lower corpus region of the stomach and fixed with a loose ligature immediately proximal to the pylorus. Consequently atrial motor activity could not

influence the transpyloric flow. A similar plastic tube was inserted through a longitudinal incision in the serosal portion of the duodenum opposite the sphincter. There it was brought up to the pylorus opposite the proximal tube. In this position the distal tube was fixed by a suture around the duodenum (see Fig. 1).

A reservoir containing normal saline thermostatically regulated to be at body temperature was connected to the proximal tube. The distal tube was connected to a piezoelectric flow meter which records volume changes of the transpyloric flow within 0–1000 ml/min. The volume from the flow meter was collected and constantly perfused into the perfusion reservoir. Since the fluid surface of the reservoir was large (370 cm²), the inflow pressure during the sphincter could be kept almost constant by means of recirculation of the saline. The pressure gradient between both reservoirs and the pylorus was variable. The new height between the reservoirs was 40 cm. To initiate the inflow a pressure of 70 cmH₂O was induced and immediately thereafter reduced to about 10 cmH₂O (Fig. 2).

Recording of gastric tone. A flaccid plastic balloon of about 1000 ml volume was introduced orally into the corpus-fundus part of the stomach in the anaesthetized animal. The balloon was connected by a rubber tube to a water tank mounted on a weight recorder (Grass Force Displacement Transducer FT 10C) and connected to an amplifier. The water level in the tank could be varied by changing the level of the weight transducer. By effecting the system with the tank at different water levels in relation to the stomach, water was allowed to fill the periballoon. In most experiments an hydrostatic pressure gradient was accomplished at 5 cmH₂O. Recording of the pressure, intragastric tone and transpyloric flow were simultaneously recorded by means of a Grass polygraph (Grass S4E) (Fig. 2).

RESULTS

Efferent vagal nerve stimulation. Uni- and bilateral efferent cervical vagal stimulation with activated

Table 1 Effect of bilateral and unilateral efferent vagal stimulation respectively on the transpyloric flow and gastric motor activity

Low stimulation of low threshold fibres. High stimulation of high threshold fibres. (For details see text)

	Unilateral		Bilateral	
	Low	High	Low	High
Pylorus				
Contract	4/5	14/14	1/4	15/16
Inhibition	0/5	5/14	0/4	
No effect	3/5	0/14	3/4	1/16
Stomach				
Contract	4/5	14/14	3/4	14/14
Inhibition	0/5	0/14	0/4	
No effect	1/5	0/14	1/4	0/14

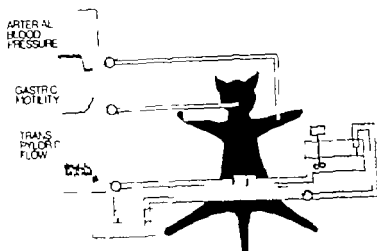


Fig. 2. Schematic illustration of experimental setup and preparation of the pylorus in vivo. For details see text.

threshold fibres elicited a reduction or cessation of the transpyloric flow after about 70 s while a mild (10–15 s) contraction was obtained in the stomach (Fig. 3, Table 1). In 5 of 14 animals given bilateral stimulation of the high threshold fibres there was a small but clear immediate initial increase of the transpyloric flow followed by a reduction of the flow. In 9 of these cats the gastric contraction was followed by a prompt decrease in tone, some at the cessation of stimulation. There is no difference in the pyloric or gastric response whether the splanchnic nerves were cut or left intact.

Unilateral vagal stimulation activating the low threshold set of fibres, reduced the transpyloric flow within 20 s in 2 out of 5 cats. Bilateral stimulation activating the low threshold fibres reduced the transpyloric flow; only one of 4 animals (Table 1).

Afferent vagal nerve stimulation. The effect of afferent cervical vagal nerve stimulation with the other vagal nerve left intact is seen in Fig. 4. A reduction of the transpyloric flow and a concomitant gastric relaxation was obtained when the high threshold fibres were activated. Activation of the low threshold set of fibres resulted in a pyloric and gastric contraction in a few animals (see Table 2).

Reduction of the transpyloric flow at afferent nerve stimulation had a delay of 5–10 s while the gastric relaxation always was prompt. In 4 animals,

with cut splanchnic nerves, the cut distal cervical vagal nerve was stimulated in afferent direction before and after the contralateral side had been divided in the neck. Vagal stimulation elicited a pyloric contraction and gastric relaxation in all 4 animals. The responses disappeared completely af-

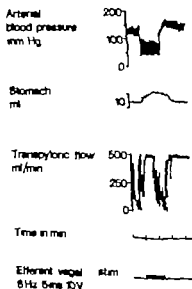


Fig. 3. Effect of efferent cervical vagal stimulation on arterial blood pressure, gastric motor activity and transpyloric flow. Note the initial increase of transpyloric flow before the contraction.

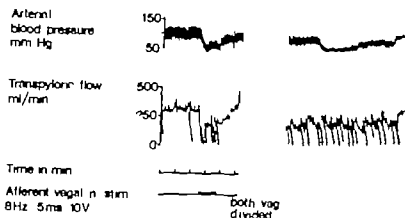


Fig. 4 Effect of afferent vagal stimulation on blood pressure and transpyloric flow before (left panel) and after (right panel) dividing of the contralateral cervical vagal nerve

ter the intact vagal nerve had been cut (Fig. 4). Efferent stimulation of the cut vagal nerves again induced a contraction of the pylorus.

Efferent vagal nerve stimulation during concomitant splanchnic nerve stimulation or noradrenaline-infusion. In order to investigate if the vagal nerves also convey relaxatory fibres to the pylorus region the vagal nerves were stimulated when the sphincter tone was increased by a concomitant splanchnic nerve stimulation or local infusion of noradrenaline. The effect of vagal stimulation during simultaneous splanchnic stimulation was studied in 5 expts. A typical expt. is illustrated in Fig. 5. Splanchnic nerve stimulation with supra-maximal currents at 8 Hz elicited a contraction of the pylorus. Bilateral efferent vagal stimulation with

activation of the high threshold fibres caused increased transpyloric flow.

In 7 animals the effect of vagal stimulation before and during noradrenaline infusion (0.01–0.02 mg/kg b.w./min i.a.) was studied. The infusion caused contraction of the sphincter. Efferent vagal stimulation during concomitant noradrenaline infusion caused an increase of the reduced flow in 4 of 7 animals studied.

DISCUSSION

In postmortem studies in cats we could confirm the presence of an anatomical pyloric sphincter circular or semilunar in shape (see Fig. 1 inset) as earlier described by Torgersen (1942). The vast majority of previous in vivo studies of the pylorus region have been performed by means of recordings of pressure or electrical activity within the pyloric area. Pressure recording systems have some disadvantages when gastrointestinal sphincters are investigated. It can be difficult to keep the pressure receptor within the sphincter region which also might be difficult to exactly identify. Furthermore the recording device might interfere with the sphincter activity. Recordings with strain gauge force transducers do not allow the study of overall motor function of the gastrointestinal tract. This may explain some of the differences in previous studies of the pyloric sphincter.

In order to avoid some of these disadvantages and to be able to study the overall motor function of the pylorus region a flow recording method was used. Such a method has previously been used in the study of the ileo-cecal sphincter (Pahlm & Kjaer

Table 2 Effect of unilateral afferent vagal stimulation with the other vagal nerve left intact on the transpyloric flow and gastric motor activity

Low: stimulation of low threshold fibres. High: stimulation of high threshold fibres (For details see text)

	Low	High
<i>n</i>	5	11
<i>Pylorus</i>		
Contract.	2	11
Inhibition	—	—
No effect	3	—
<i>Stomach</i>		
Contract.	1	—
Inhibition	—	10
No effect	4	1

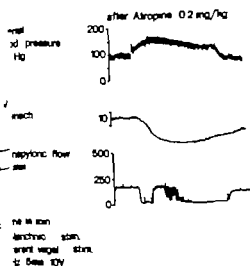


Fig. 5. Effect of bilateral efferent vagal stimulation on ad pressure, gastric motor activity and transpyloric flow during concomitant splanchnic nerve stimulation.

ner 1976) and has been shown to have several advantages. Thus, the interference from a balloon catheter within the sphincter region is avoided and even small variations in sphincter tone can be noted. However, when perfusion method is used several factors have to be taken into consideration. First, the perfusion pressure has to be kept at a constant level by using a reservoir with a large cross-sectional area and a recirculation pump. The perfusion and drainage tube must have a capacity which is larger than the maximal flow through the sphincter and the tubes have to be placed close to the sphincter area in order to avoid secondary effects from the caecum-entrum area and the blood vessels. As saline was used as perfusion fluid interference due to viscosity could be excluded. The temperature of the perfusion fluid has been shown to be of great importance (Pahlén 1975). Therefore, the temperature of the perfusion fluid was kept around 38°C. Great care was taken not to tie the ligature around the proximal tube too tight. At the end of each experiment no sign of ischemic injury to this region was observed.

Electrical field stimulation of isolated strips of nerves from the pylorus of cat, dogs and opossum suggests an inhibitory innervation of the gastro-duodenal junction (Aurias et al 1974). Efferent vagal stimulation in dogs, after pretreatment with atropine, caused an inhibition of spontaneous

pyloric activity indicating an atropine-resistant inhibitory innervation of the pylorus (Mir et al. 1977). In the present experiments, efferent vagal stimulation caused an initial relaxation of the pylorus with an increased transsphincteric flow followed by a contraction of the sphincter also indicating the presence of relaxatory vagal fibres to this region. To further confirm the existence of such fibres within the vagi, these were stimulated during concomitant increase of the sphincter tone as the intestinal tone has been considered to determine which type of intestinal response to vagal stimulation that can be induced (Garry 1957, Van Harn 1963). Thus, low tone of the intestine was said to favour excitatory responses and high tone inhibitory responses. Therefore, the vagal nerves were stimulated when the sphincter tone was increased by either an intraarterial noradrenaline infusion or a concomitant splanchnic nerve stimulation. Efferent vagal stimulation caused an increased flow in both these series of experiments indicating the presence of relaxatory fibres within the vagi to the pylorus. Thus, the present experiments support the assumption that the vagal nerves convey both excitatory and inhibitory fibres to the pyloric sphincter.

The physiological significance of the vago-vagal excitatory reflex to the pylorus is unclear. Pajntal (1954), Andrew (1957) and Iggo (1957) have shown an increased discharge in vagal afferent fibres on stimulation of either chemo- or mechanoreceptors of the intestine, stomach and oesophagus. Harper et al. (1959) and Jansson (1969) directly stimulated the efferent fibres within the vagi and found a reflex activation of the vagal relaxatory fibres to the stomach. This gastric response was abolished by vagotomy of the contralateral vagus, indicating a vago-vagal relaxatory reflex. In the present study a gastric relaxation at afferent vagal stimulation and a concomitant contraction of the pylorus was always obtained. This reflex response disappeared after bilateral vagotomy, indicating the presence of a vago-vagal excitatory reflex to the pylorus. Jansson (1969) suggested that the vago-vagal relaxatory gastric reflex may form part of the normal gastric emptying. It is possible that even the vago-vagal excitatory pyloric reflex may participate in the normal gastric emptying and in the prevention of bile reflux.

In the present experiments, the latency of the pyloric responses was much shorter at efferent (5–10 s) than at afferent (20 s) stimulation of the cervical

vagi. These rather long latencies might indicate activation of composite neurohumoral mechanisms e.g. the release of gastrointestinal hormones or simply reflect that the innervation of the sphincter regions is far more complex than of the gut itself (Goyal & Rattan 1975). The faster responses to afferent vagal stimulation might then be due to a more selective neuronal activation through a polysynaptic pathway rather than the crude mixed effects on smooth muscle cells, intramural ganglia and gut endocrine cells elicited at efferent stimulation.

It has previously been shown that the vagal nerves contain at least 2 groups of efferent nerve fibres which control the gastric motor activity (Martinson & Muren 1963; Martinson 1965a). Thus excitatory fibres could be selectively activated when comparatively low threshold parameters were used. If the duration of the stimulatory pulses was increased to high threshold values vagal relaxatory fibres were activated as well. The high threshold fiber group also include fibres stimulating the acid and pepsinogen secretion in the stomach as well as vasodilatory fibres (Martinson 1965b). In the present study contractions were regularly obtained when stimulating parameters activating the high threshold fibres were used e.g. the same parameters which activate the non-cholinergic non-adrenergic relaxatory fibres to the stomach. This vagal response with pyloric contraction and gastric relaxation, acid and pepsinogen secretion and vasodilatation seems all suitable for the digestive gastric activity.

Supported by the Swedish Medical Research Council (grant no. 17X-05220) and by Östergötlands Läkaresällskap.

REFERENCES

- ANDREW B. L. 1957 Activity in afferent nerve fibres from the cervical oesophagus. *J. Physiol. (Lond)* 135 54p-55p.
- ANURAS S., COOKE A. R. & CHRISTENSEN J. 1974 An inhibitory innervation at the gastroduodenal junction. *J. clin. Invest.* 54 529-535.
- BRINK B. M., SCHLEICHEL J. F. & CODE C. F. 1963 The pressure profile of the gastroduodenal junctional zone in dogs. *Gut* 6 162-171.
- DIDO L. J. A. & ANDERSSON M. C. 1968 The sphincters of the digestive system, pp. 15-196. W.B. Saunders and Wilkins, Baltimore.
- EDWARDS D. A. W. & ROWLANDS F. V. 1964 Physiology of the gastroduodenal junction. In: *Handbook of physiology*, sect. 6, vol. IV, p. 1935.
- FISHER R. & COHEN S. 1973 Physiological characteristics of the human pyloric sphincter. *Gastroenterology* 64 67-75.
- GARRY R. C. 1957 Innervation of abdominal viscera. *Med. Bull.* 13 70-206.
- GOYAL R. K. & RATTAN S. 1975 Nature of the vagal inhibitory innervation to the lower esophageal sphincter. *J. Clin. Invest.* 55 1119-1126.
- HARN G. L. v. 1963 Responses of muscles of cat intestine to autonomic nerve stimulation. *Am. J. Physiol.* 204 35-358.
- HARPER A. A., KIDD C. & SCRATCHERD T. M. 1966 Vago-vagal reflex effects on gastric acid secretion and gastrointestinal motility. *J. Physiol. (Lond)* 148 417-436.
- IGGO A. 1957 Gastric mucosal chemoreception and vagal afferent fibres in the cat. *Quart. J. Exp. Physiol.* 42 398-409.
- JANSSON G. 1969 Extrinsic nervous control of peristalsis. An experimental study in the cat. *Acta Physiol. Scand. Suppl.* 196.
- KAYE M. D., MEHTA S. J. & SHOWALTER J. F. 1976 Manometric studies of the human pylorus. *Gastroenterology* 70 477-480.
- MARTINSON J. & MUREN A. 1963 Excitation and inhibitory effects of vagus stimulation on gastric motility in the cat. *Acta Physiol. Scand.* 57 309-316.
- MARTINSON J. 1965a Vagal relaxation of the stomach. Experimental reinvestigation of the concept of the transmission mechanism. *Acta Physiol. Scand.* 64 453-462.
- MARTINSON J. 1965b The effect of graded stimulation on gastric motility, secretion and flow in the cat. *Acta Physiol. Scand.* 65 300-309.
- MIR S. S., MASON G. R. & ORMSBEE III H. S. 1967 An inhibitory innervation at the gastroduodenal junction in anesthetized dogs. *Gastroenterology* 73 434-434.
- PAHLIN P. E. 1975 Extrinsic nervous control of the ileo-cecal sphincter in the cat. *Acta Physiol. Scand. Suppl.* 476.
- PAHLIN P. E. & KEWENTER J. 1976 Sympathetic nervous control of cat ileo-cecal sphincter. *Am. J. Physiol.* 231 796-803.
- PAINTAL A. S. 1954 A study of gastric stretch receptors. Their role in the peripheral mechanism of sensation of hunger and thirst. *J. Physiol. (Lond)* 116 267-270.
- SCHARDT M. & van der ZYPEN E. 1974 Funktionelle und qualitative Untersuchungen über die regionalen Unterschiede des intramuralen Nervensystems im Magen-Darm-Kanal des wachen Laborsäugetiers. *Acta Anat.* 90 403-470.
- TORGERSEN J. 1942 The muscular bulk and movement of the stomach and duodenal bulb. *Acta Pathol. Suppl.* 45 1-191.

A note on the bolus injection residue detection method for measurement of capillary permeability

J. SEJRSSEN

Institute of Medical Physiology B, University of Copenhagen, Denmark

The bolus injection external registration method for measurement of capillary extraction was introduced by Sejrssen in 1970. An elaboration of this method and further experimental support has been given in a later article (Sejrssen 1979). In a note on this method Garby & Gronlund (1978) perform a theoretical analysis on the basis of some conditions and assumptions of the method. The present note is aimed at correcting the errors introduced by Garby & Gronlund (1978) in their analysis in order to show the irrelevance of the analysis performed.

From the article presenting the bolus injection residue detection method for measurement of capillary extraction (Sejrssen 1970) the following quotation is taken: A large fraction of the bolus of chromium-51 EDTA will pass through the muscle vessels very fast, vascular transit and extraction E, will be extracted over the capillary membrane and thus have also an extravascular transit. By this sentence it was made explicit that the extracted fraction, E, of the intra-arterially injected indicator bolus has both an intra- and an extra-vascular transit, while the complementary fraction, denoted the transmitted fraction, T, does not permeate the capillary membrane and consequently has only vascular transit through the muscle.

In the note by Garby & Gronlund (1978) equation (11), it is erroneously reproduced from the article by Sejrssen (1970) that the registered curve supplemented by a retropolation from the time when the vascular transit is finished is an expression of the washout of the extracted fraction located exclusively in the interstitial space. This part of the indicator bolus cannot be measured separately by residue detection which must register the total amount in the area under study given as a relative measure. This implies that their equation (14) also becomes wrong.

From an estimate of the volume of arterial vessels and the actual blood flow level it can be calculated that more than 10% of the indicator molecules must be present in the arterial vessels at time of maximum height of the curve in the actual experiments (Sejrssen 1970, 1979). This part of the indicator will be separated in an E and T fraction later on in the following part of the washout. But these conditions do not involve that a separation of the E and T fraction is impossible by the retropolation procedure. These considerations then imply that equations (9), (10), (11) and (13) in the article by Garby & Gronlund (1978) become unnecessary demands.

For the applicability of the method the essential question is how accurately the registered residue curve can be resolved in the E fraction which enters the interstitial space, and the T fraction with an exclusively intravascular transit. Due to the considerable difference in transit times of the extracted and the transmitted fractions resolution can be performed with good approximation. In average a factor of 26 has been found between the values of rate constants of the two types of transit within the first minutes of the washout curves for chromium-51 EDTA in skeletal muscle. Even for the fastest part of the transit of the extracted molecules compared to that of the slowest part of the transit of the transmitted molecules there is a difference in rate constants of at least a factor of 7 (Sejrssen 1979). It is important to notice that the time interval for the retropolation is relatively short. It is assumed that the tissue to blood exchange of indicator in the retropolation interval has the same washout kinetics as the curve part used for the retropolation. It is observed that the fractional washout rate is almost constant for the curve part employed. This is presumably effected by diffusional mixing of the indicator in that part of the interstitial compartment

positioned in close relation to the capillary wall which constitutes a pronounced diffusional resistance for the actual molecules.

By residue detection the total amount of indicator in the area under study will contribute to the registered counting activity. When the total input to the system has a shorter duration than the shortest transit time of the system (Sejrsven 1969) then the maximum height of the registered washout curve is a relative measure of the total bolus input. The washout of the extracted fraction from the total system is expressed relatively by the registered curve after some time when the vascular transit of the transmitted fraction for all practical purposes has come to an end. This curve part can be simulated by some mathematical expression employed for the retropolation of the curve. The value of this curve at the time of maximum height of the registered curve yields the extraction fraction when expressed relative to the maximum value of the registered curve. As the total amount of indicator is present in the area under study at this time the total amount of the extracted fraction is also present at that time. The location of the extracted fraction will at that time be partly in the different segments of the vascular bed and partly in the interstitial space. There is no demand of complete spatial separation of the extracted and the transmitted fraction at that time and in principle no demand concerning an insignificant back diffusion from interstitial to vascular space.

Subtraction of the retropolated curve from the registered curve gives the transit curve for the transmitted fraction through the vascular system expressed as a relative measure. The vascular volume (calculated from the mean transit time of an

intravascular indicator and the directly measured blood flow in separate experiments) divided by the mean transit time of this vascular transit curve yields the value of the blood flow. This value can be compared to the directly measured blood flow. The configuration of the intravascular transit curve can be compared to that of an intravascular indicator. These comparisons have been performed in order to investigate the validity of the suggested retropolation procedure (Sejrsven 1979). The conditions and assumptions necessary for the method are listed and discussed in detail in the article by Sejrsven (1979).

A correction of the erroneous proposition introduced by Garby & Grönlund (1978) has the effect that all the supplementary conditions and corrections proposed by them do not constitute requirements for the method. One might speculate that their approach could be used as basis for an alternative analysis, but the unrealistic demand that the E and T fractions are separated at the time for maximum of the registered curve eliminates such possibility.

REFERENCES

- GARBY I & GRÖNLUND J 1978. A note on a single injection residue function method to determine capillary permeability. *Acta Physiol Scand* 104: 363.
- SEJRSVEN P 1970. Single injection external retropolation method for measurement of capillary extraction. In: *Capillary permeability* (Alfred Benzon Symp. 1) (ed C Crone and N A Lassen) pp 145-5. Munksgaard, Copenhagen.
- SEJRSVEN P 1979. Capillary permeability measured by bolus injection residue and venous detection. *Acta Physiol Scand* 105: 73-92.

Reduction of adrenaline turnover in cardiovascular area of rat medulla oblongata by clonidine

L. FUXE, GÖSTA JONSSON, PER BOLMJE, KURT ANDERSSON, LUIGI F. AONATI,
JEK GOLDSTEIN and TOMAS HÖKFELT

Department of Histology, Karolinska Institute, Stockholm, Sweden, Department of Pediatrics,
Surgery Hospital, Stockholm, Sweden, Department of Human Physiology, University of Bologna, Bologna,
and Department of Biochemistry, New York University Medical Center, New York, USA

It has recently been postulated that clonidine is an
adrenaline (A) agonist in the central nervous system
and that this action could be of importance for its
depression activity (Fuxe et al. 1976, 1979).
Therefore, in the present paper the acute effect of
clonidine in clinically relevant doses have been
studied on noradrenaline (NA) and adrenaline
turnover in the hypothalamus and in the dorsal
lateral area of the caudal medulla oblongata
(DCMO), using inhibitors of dopamine β -hy-
droxylase, FLA 63 (bis-(4-methyl-1-homo-
enzymyl-isoocarbonyl)-disulphide) and of
methylglanamine N-methyltransferase SK&F
139 (7,8-dichloro-1,2,4-tetrahydroisoquinoline
dichloride) (Corrodi et al. 1970; Pendleton
et al. 1976).

Male specific pathogen free Sprague-Dawley rats
have been used (150 g b.w.). The rats were kept 5
per cage under regular light-dark conditions (light
from 6 a.m. and off at 8 p.m.). They were given
ad libitum pellets and water ad libitum. They were killed
by decapitation between 9 and 11 a.m. Clonidine
was given into the jugular vein under light ether
anesthesia. Immediately before the clonidine injection
FLA 63 or SK&F 64139 were given in doses of
1 mg/kg (i.p.) and 40 mg/kg (i.p.) respectively 1 or
2 h before killing.

By means of a rectangular punch (3-4 mm) the
hypothalamus was dissected out from a frozen
coronal section of the diencephalon. The DCMO
was also dissected out by means of a rectangular
punch (1x3 mm) from a frozen coronal 1 mm thick
section of the medulla oblongata, the caudal plane
being located immediately behind the obex. DCMO
obtains, after also, the nucleus tractus solitarius,
nucleus dorsalis motorus nervi vagi and parts of the
nucleus commissuralis (see Fuxe et al. 1979). The
catecholamine levels were determined by means of
high pressure liquid chromatography in combina-

tion with electrochemical detection, using α -methyl
dopamine as an internal standard (Keller et al. 1976;
Medford et al. 1977).

Clonidine in a dose of 30 μ g/kg significantly re-
duced the SK&F 64139 induced A depletion in the
DCMO (Fig. 1). An i.v. injection of clonidine in a
dose of 7.5 μ g/kg significantly reduced the FLA 63
induced A depletion in the DCMO, while the FLA
63 induced NA depletion in this area was un-
influenced (Table 1). In the hypothalamus, however

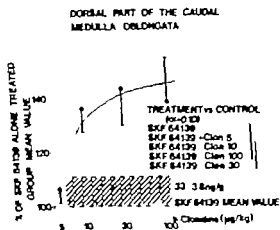


Fig. 1. The effects of clonidine on the SK&F 64139 induced A depletion in the dorsal lateral area of the caudal medulla oblongata (DCMO). For treatment, see text. The values are expressed in per cent of SK&F 64139 untreated group mean value. Means \pm S.E. are shown out of 3 rats. The hatched area represents the S.E. of the SK&F 64139 alone group mean value. The A levels in the untreated group was 60 ± 6 ng/g tissue (mean \pm S.E.). Thus, 2 h of treatment with SK&F 64139 (40 μ g/kg) produced approximately 50% depletion of the A stores in the DCMO (33 ± 3 ng/g tissue). The statistical analysis is given in the table of the figure. The Dunn test was used with an experimental wise error rate of $\alpha = 0.1$. The groups not embraced by the same line are significantly different.

Table 1 Effects of clonidine on FLA 63 induced changes in CA stores in dorsal midline area of the *L. medulla oblongata* (DCMO) and hypothalamus

Treatment	Dose of clonidine ($\mu\text{g/kg}$)	DCMO			Hypothalamus
		NA % (ng/g tissue)	A % (ng/g tissue)	DA % (ng/g tissue)	NA % (ng/g tissue)
Saline		100 \pm 8 (5) (4 668 \pm 354)	100 \pm (5) (104 \pm 23)	100 \pm 3 (5) (396 \pm 17)	100 (5) (3 938 \pm 99)
Clonidine 1 h	10	89 \pm (5)	1.5 \pm 11 (5)	102 \pm 4 (5)	104 (5)
Clonidine 2 h	30	94 \pm 9 (5)	116 \pm 13 (5)	105 \pm 6 (5)	106 \pm 11 (5)
FLA 63 1 h		100 \pm 6 (4) (3 064 \pm 15)	100 \pm 7 (3) (79 \pm 5)	100 \pm 10 (4) (1 148 \pm 77)	100 (5) (3 971 \pm 129)
Clonidine + FLA 63 1 h		109 \pm 6 (8)	134 \pm 17 (7)	147 \pm 10 (8)	115 (8)
FLA 63 2 h		100 \pm 1 (5) (7 653 \pm 317)	116 \pm 13 (5) (47 \pm 7)	100 \pm 11 (5) (948 \pm 107)	100 (15) (1 577 \pm 17)
Clonidine + FLA 63 2 h	7.5	100 \pm 11 (8)	123 \pm 21 (8)	99 \pm 13 (8)	130 \pm 11 (8)

For treatment, see text. Means \pm S.E. are shown. The values are given in per cent of untreated group mean value of FLA 63 1 h group mean value and of FLA 63 2 h group mean value respectively. The absolute levels are given in parentheses in $\mu\text{g/g}$ tissue. As seen from the absolute levels, 1 h of treatment with FLA 63 reduces noradrenaline contents and also contents in the DCMO to 36% and 43% respectively of untreated group mean value. In the hypothalamus the noradrenaline contents are reduced to 38% and 6% respectively of untreated group mean value. Number of animals in parentheses. Statistical analysis was made by means of Mann-Whitney U-test. $P < 0.05$, $P < 0.01$.

clonidine in the same dose instead significantly reduced the FLA 63 induced NA depletion without influencing the FLA 63 induced A depletion in this area (Table 1).

The present findings give evidence that clonidine administered into the jugular vein can reduce A turnover in the DCMO since clonidine reduced both the FLA 63 and the SK&F 64139 induced A depletion in the DCMO in doses from 7.5 to 30 $\mu\text{g/kg}$. However, no evidence was obtained that A turnover was reduced in the hypothalamus by 7.5 $\mu\text{g/kg}$ of clonidine. These results are in agreement with recent reports that clonidine can reduce A turnover in brain (Fuxe et al. 1979b; Scatton et al. 1979). The present results therefore support our hypothesis that clonidine at least in the DCMO can be an A agonist in clinically relevant doses. It is known that injections into the jugular vein of clonidine in the doses used produce vasodepressor actions (Bolme et al. 1974). It is unclear, however, if the reduction of A turnover observed is due to activation of post- or pre-synaptic α component of central A receptors.

It is of interest that hypothalamic NA was more responsive to clonidine treatment than hypothalamic A. Thus clonidine in a dose of 7.5 $\mu\text{g/kg}$ seemed to reduce hypothalamic NA turn-

over since it significantly reduced the FLA 63 induced NA depletion in the hypothalamus. Therefore, when discussing the mechanism of action of the cardiovascular effects of clonidine, both the NA and A mechanisms must be considered. Adrenaline mechanisms in the medulla oblongata and NA mechanisms in the hypothalamus seem to have a similar sensitivity to clonidine. In conclusion, the present paper gives evidence that clonidine in doses from 7.5 $\mu\text{g/kg}$ can reduce A turnover in the DCMO and NA turnover in the hypothalamus.

This work was supported by a grant (04X-4626) from the Swedish Medical Research Council. Clonidine was generously supplied by Boehringer Ingelheim (Germany).

REFERENCES

- BOLME P, CORRODI H, FUXE K, HÖKfelt U, LIDBRINK O & GOLDSTEIN M (1974) Pharmacological control of central adrenaline neurons in motor and respiratory control. Studies with clonidine and its interaction with piperazine and its derivative. *Europ J Pharmacol* 28: 89-94.
- CORRODI H, FUXE K, HAMBERGER B & LJUNGBÄCK H (1970) Studies on central and peripheral noradrenaline neuron using a new dopamine- β -hydroxylase inhibitor. *Europ J Pharmacol* 14: 145-155.

	DA
(μ g/kg)	% (ng/g tissue)
1 (5)	100 \pm 11 (5)
	(697 \pm 79)
2 (5)	103 \pm 10 (5)
3 (5)	104 \pm 7 (5)
4 (5)	100 \pm (4)
5	(990 \pm 26)
1 (10)	114 \pm 8 (8)
2 (5)	100 \pm 7 (5)
3	(728 \pm 60)
1 (10)	108 \pm 6 (10)

FUXE, K., BOLME, P., HÖKFELT, T. & GOLDSTEIN, M. 1976 Central adrenaline receptors and blood pressure regulation. Evidence for an adrenergic vasodepressor system mediating the actions of clonidine. In *Recent advances in hypertension*, vol. 3 (ed. P. Mallet, & M. Sefler), pp. 72-80. Laboratoires J. Boehringer Ingelheim, Reims, France.

- FUXE, K., BOLME, P., JONSSON, G., AGNATI, L., F. GOLDSTEIN, M., HÖKFELT, T., SCHWARZ, R. & ENGEL, J. 1979a On the cardiovascular role of noradrenaline, adrenaline and peptide containing neuron systems in the brain. In *Nervous system and hypertension* (ed. P. Mey, & H. Schmitt), pp. 1-17. Wiley-Flammarion, Paris.
- FUXE, K., GANTEN, D., JONSSON, G., AGNATI, L., F. BOLME, P., ANDERSSON, K., GOLDSTEIN, M., HALLMAN, H., UNGER, T. & RASCHER, W. 1979 Catecholamine turnover changes in hypothalamus and dorsal midline area of the caudal medulla oblongata of spontaneously hypertensive rats. *Neurosci Lett* 1, *in press*.
- KELLER, R., OKE, A., MEDFORD, I. & ADAMS, R. N. 1976 Liquid chromatographic analysis of catecholamines-routine assay for regional brain mapping. *Life Sci* 19, 995-1004.
- MEDFORD, I., OKE, A., ADAMS, R. N. & JONSSON, G. 1977 Epinephrine localization in human brain stem. *Neurosci Lett* 5, 141-145.
- PENDLETON, R. G., KAISER, C. & GESSNER, G. 1976 Studies on adrenal phenylethanolamine N-methyltransferase (PNMT) with SH-64139, selective inhibitor. *J Pharmacol Exp Ther* 197, 623-632.
- SCATTON, B., PELAYO, F., DUBOCOVICH, M. L., LANGER, S. Z. & BATHOLINI, G. 1979 Effects of clonidine on the cerebral adrenaline turnover and the adrenaline release in nucleus tractus solitarius of the rat. I. Presynaptic receptors (ed. S. Langer, K. Starke & M. Dubocovich), pp. 31-34. Pergamon Press, Oxford.

Table 1 Effects of clonidine on FLA 63 induced changes in CA stores in dorsal midline area of the medulla oblongata (DCMO) and hypothalamus

Treatment	Dose of clonidine ($\mu\text{g/kg}$)	DCMO			Hypothalamus
		NA % (ng/g tissue)	A % (ng/g tissue)	DA % (ng/g tissue)	NA % (ng/g tissue)
Saline		100 \pm 8 (4) (4 668 \pm 354)	100 \pm 22 (4) (104 \pm 13)	100 \pm 3 (5) (396 \pm 17)	100 (14) (3 938 \pm 99)
Clonidine 2 h	10	89 \pm 5 (5)	115 \pm 11 (5)	102 \pm 4 (5)	104 \pm 15 (5)
Clonidine 1 h	30	94 \pm 9 (5)	116 \pm 13 (5)	103 \pm 6 (5)	106 \pm 15 (5)
FLA 63 1 h		100 \pm 6 (4) (3 064 \pm 15)	100 \pm 7 (3) (79 \pm 5)	100 \pm 10 (4) (1 148 \pm 77)	100 (54) (2 391 \pm 126)
Clonidine + FLA 63 1 h		109 \pm 6 (8)	134 \pm 17 (7)	142 \pm 10 (8)	115 \pm 16 (8)
FLA 63 2 h		100 \pm 1 (5) (653 \pm 317)	100 \pm 15 (5) (47 \pm 7)	100 \pm 11 (5) (948 \pm 107)	100 (16) (1 127 \pm 179)
Clonidine + FLA 63 2 h	7.5	100 \pm 11 (8)	113 \pm 21 (8)	99 \pm 13 (8)	102 \pm 11 (8)

For treatment see text. Means \pm S.E. are shown. The values are given in per cent of untreated group mean value and 1 h group mean value and of FLA 63 2 h group mean value respectively. The absolute levels are given in parentheses. As seen from the absolute levels, 2 h of treatment with FLA 63 reduces noradrenaline contents and stores in the DCMO to 56% and 45% respectively of untreated group mean value. In the hypothalamus the corresponding noradrenaline and adrenaline levels to 38% and 61% respectively of untreated group mean value. Number of animals in parentheses. Statistical analysis was made by means of Mann-Whitney U test. $P < 0.05$, $P < 0.01$.

clonidine in the same dose instead significantly reduced the FLA 63 induced NA depletion without influencing the FLA 63 induced A depletion in this area (Table 1).

The present findings give evidence that clonidine administered into the jugular vein can reduce A turnover in the DCMO since clonidine reduced both the FLA 63 and the SK&F 64139 induced A depletion in the DCMO in doses from 7.5 to 30 $\mu\text{g/kg}$. However, no evidence was obtained that A turnover was reduced in the hypothalamus by 7.5 $\mu\text{g/kg}$ of clonidine. These results are in agreement with recent reports that clonidine can reduce A turnover in brain (Fuxe et al. 1979b; Scatton et al. 1979). The present results therefore support our hypothesis that clonidine at least in the DCMO can be an A agonist in clinically relevant doses. It is known that injections into the jugular vein of clonidine in the doses used produce vasodepressor actions (Bolme et al. 1974). It is unclear however if the reduction of A turnover observed is due to activation of post- or pre-synaptic α components of central A receptors.

It is of interest that hypothalamic NA was more responsive to clonidine treatment than hypothalamic A. Thus clonidine in a dose of 7.5 $\mu\text{g/kg}$ seemed to reduce hypothalamic NA turn-

over since it significantly reduced the FLA induced NA depletion in the hypothalamus. Therefore, when discussing the mechanism of action of the cardiovascular effects of clonidine, both central NA and A mechanisms must be considered. Adrenaline mechanisms in the medulla oblongata and NA mechanisms in the hypothalamus seem to have a similar sensitivity to clonidine. In conclusion, the present paper gives evidence that clonidine in doses from 7.5 $\mu\text{g/kg}$ can reduce A turnover in the DCMO and NA turnover in the hypothalamus.

This work was supported by a grant (04X-4626) from the Swedish Medical Research Council. Clonidine was previously supplied by Boehringer Ingelheim (Germany).

REFERENCES

- BOLME P, CORRODI H, FUXE K, HÖNIGT L, LIDBRINK O & GOLDSTEIN M (1974) A involvement of central adrenaline neurons in locomotor and respiratory control. Studies with clonidine and its interactions with papezian and yohimbine. *Europ J Pharmacol* 28, 89-94.
- CORRODI H, FUXE K, HAMBERGER B & LJUNGBÄCK A (1970) Studies on central and peripheral noradrenaline neurons using a noradrenaline- β -hydroxylase inhibitor. I. *Acta Pharmacol* 1, 145-155.

The influence of prostaglandin synthetase inhibition on the spontaneous contractile activity and induced responses of the human oviduct

TONPE and B. LINDBLOM

Department of Obstetrics and Gynecology, University of Göteborg, Sweden

The isthmus portion of the human Fallopian tube comprises three muscle layers with different fibre content: the outer longitudinal, the intermediate circular and the innermost longitudinal, the latter appearing towards the distal end of the isthmus (Daniel & Czernobitsky 1968; Daniel et al. 1975). We have recently demonstrated that in the outer longitudinal layer at the distal end of the isthmus, i.e. at the ampullary-isthmus junction (AIJ), there is a response of α -mediated excitatory response after exposure to noradrenaline, adrenaline, phenylephrine and transmural nerve stimulation (Lindblom et al. 1979). Moreover, prostaglandin $F_{2\alpha}$ ($PGF_{2\alpha}$) has been shown to be a potent stimulator of the longitudinal smooth muscle in this region (Lindblom et al. 1979).

The present report concerns the influence of indomethacin, an inhibitor of PG synthesis, on spon-

taneous activity and α -adrenoceptor responses of longitudinal smooth muscle at the AIJ of the human oviduct.

Tissues from 20 women, 25-40 years of age, were included in the study. All patients had regular menstrual cycles and hormonal contraception had been withdrawn for at least 3 months prior to bilateral tubal resection. Routine premedication and general anesthesia were given to all patients. A 4-5 cm long portion of the tube was excised without clamping and immediately placed in chilled oxygenated Krebs-Ringer bicarbonate buffer. The particular phase of the menstrual cycle was estimated by serum levels of progesterone and estradiol-17 β . Muscle strips from the longitudinal layer of the isthmus were dissected under a stereo microscope.

The strips were approximately 4 mm long, with a cross-sectional area of approx. 1 mm². The muscle strips were suspended in 50 ml organ baths containing Krebs-Ringer buffer at a temperature of 37°C and aerated continuously with 5% CO₂ in O₂. One end of the strip was tied to a tissue holder by a silk ligature and the other end was connected to an isometric force transducer by a ligature.

The contractile activity was recorded under passive tension of 4 mN (for further methodological details, see Lindblom et al. 1979). The drugs used were: Phenylephrine hydrochloride (Sigma Chemicals Company, Mo, USA), $PGF_{2\alpha}$ (triamethamine salt, kindly supplied by the Upjohn Company, Kalamazoo, Mich.), Phenoxylbenzamine hydrochloride (Dibenzyl S K & F Laboratories Ltd., U.K.) and indomethacin (kindly supplied by Merck Sharp & Dohme International, Rahway, N.J.). Phenylephrine and $PGF_{2\alpha}$ were dissolved in



Fig. 1. Left panel: Spontaneous contractile activity (upper tracing) and the effect of indomethacin (40 μ g/ml) (lower tracing) on the spontaneous contractile activity of oviductal musculature from the human oviductal isthmus. Middle panel: The stimulatory effect of phenylephrine (10 μ M) (upper tracing) and the effect of phenylephrine after total inhibition of spontaneous activity induced by indomethacin (40 μ g/ml) (lower tracing). Right panel: The stimulatory effect of $PGF_{2\alpha}$ (0.1 μ g/ml) (upper tracing) and the effect of $PGF_{2\alpha}$ after total inhibition of spontaneous activity induced by indomethacin (40 μ g/ml) (lower tracing). Vertical calibration = 4 mN; horizontal calibration = 3 min.

Present address: S. C. B. Medical College Campus, Cutback 753 007 Orissa, India.

Key words: Smooth muscle, oviduct, human, prostaglandins, adrenoceptors, calcium.

REFERENCES

- EN J W 1974. Prostaglandins and prostaglandin synthetase inhibitors. Studies on uterine motility and function. In: Prostaglandin synthetase inhibitors (ed. H J Robinson & J R Vane) pp 289-301. Raven Press, New York.
- EF I & HAFEZ, E S. E. 1973. Utero-ovascular motility: its emphasis on ov. transport. *Obstet Gynaecol Survey* 28, 679-703.
- NIEL, E E, POSEY V A & PATON D M 1975. A structural analysis of the myogenic control systems of the human Fallopian tube. *Am J Obstet Gynecol* 121, 854.
- VIA, A & CZERNOSILSKY B 1968. A comparative histologic study of the utero-tubal junction in the rabbit, rhesus monkey and the human female. *Am J Obstet Gynecol* 101, 417.
- ELDER, M G, MYATT L & CHAUDHARI G. 1977. The role of prostaglandins in the spontaneous motility of the Fallopian tube. *Fertil Steril* 28, 86-90.
- LINDBLOM B, HAMBERGER, L. & WIKVIST N 1978. Differentiated contractile effect of prostaglandins E and F on the isolated circular and longitudinal smooth muscle of the human oviduct. *Fertil Steril* 30, 553-559.
- LINDBLOM, B, LJUNG, B & HAMBERGER L 1979. Adrenergic and non-1 non-adrenergic neuronal mechanisms in the control of smooth muscle activity in the human oviduct. *Acta Physiol Scand* 106, 15-220.

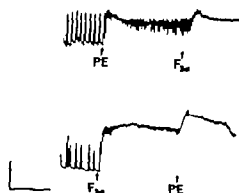


Fig. 2 The effect of $\text{PGF}_{2\alpha}$ 1 $\mu\text{g}/\text{ml}$ on longitudinal muscle maximally contracted by phenylephrine 10 μM (PE) (upper record) and the effect of phenylephrine 10 μM on a similar preparation maximally contracted by $\text{PGF}_{2\alpha}$ 1 $\mu\text{g}/\text{ml}$ (lower record). Vertical calibration = 4 mN, horizontal calibration = 5 min.

buffer whereas indomethacin was dissolved in 0.9% sodium chloride with 0.05% Tween 80.

Some 10–30 min after the mounting of the specimens in the organ chambers spontaneous contractile activity appeared. Addition of indomethacin to the bath in a final concentration of 10–40 $\mu\text{g}/\text{ml}$ caused a concentration-dependent reversible inhibition of the spontaneous contractile activity. The inhibitory effect appeared within 2–5 min after the addition of the drug to the bath. Total inhibition of the spontaneous activity was achieved at 30–40 $\mu\text{g}/\text{ml}$ (Fig. 1). The inhibitory effect lasted for approximately 15 min. Phenylephrine (10 μM) caused a marked stimulatory effect on the preparations characterised by a tetanic contracture. After total inhibition of spontaneous activity induced by indomethacin the effect of exogenous PE was unaltered (Fig. 1). The excitatory effect of $\text{PGF}_{2\alpha}$ (0.1 $\mu\text{g}/\text{ml}$) was similar to that of PE and also this response was unaffected by indomethacin (Fig. 1). Maximum contraction evoked by PE could be further augmented by $\text{PGF}_{2\alpha}$. Similarly preparations maximally contracted by $\text{PGF}_{2\alpha}$ exhibited a further increase in tone after the addition of PE (Fig. 2). After α -adrenoceptor blockade with phenoxybenzamine (0.1 μM) the effect of PE was abolished whereas the response of $\text{PGF}_{2\alpha}$ was unaffected. In nominally calcium-free solution both the spontaneous activity as well as the responses to $\text{PGF}_{2\alpha}$ or PE were abolished.

Both adrenergic nerves and local hormones such as prostaglandins (PGs) have been claimed to be of crucial importance in the regulation of oviductal

contractility which in turn is considered to influence the transport of the ovum through the tube (for review see Aref & Hafez 1973). Studies on the uterine tissues from the pregnant rat have similarly indicated that an intact PG synthesis is essential for spontaneous myometrial contractility (Aiken 1974). In the latter study, indomethacin concentration of 0.01–3.0 $\mu\text{g}/\text{ml}$ was found to inhibit spontaneous contractions and high concentrations also abolished the stimulatory effect of the precursor arachidonic acid. On the other hand, Fuder et al. (1977) failed to demonstrate an inhibitory effect of indomethacin on human oviductal muscle in vitro and concluded that PGs are not directly involved in the regulation of myogenic activity in this tissue. The very poor spontaneous activity of the large tubal segments used in that study can be doubted, however, as to the validity of their conclusions.

The present investigation performed on strips from the longitudinal musculature of the human oviductal isthmus demonstrates that indomethacin in concentrations between 10–40 $\mu\text{g}/\text{ml}$ inhibits spontaneous contractile activity in a reversible and concentration-dependent manner. Moreover, the initial contractile patterns can be restored by the addition of small amounts of $\text{PGF}_{2\alpha}$. Together these results suggest that PG synthesis is of crucial importance for spontaneous activity in the human oviduct in vitro. Both PE and $\text{PGF}_{2\alpha}$ elicit powerful excitatory responses and these effects are not reduced by indomethacin at concentrations that cause total inhibition of spontaneous activity. These observations demonstrate that the inhibitory effects of indomethacin are not unexpected in nature and that α -adrenoceptor-mediated contraction is not mediated via an influence on PG synthesis, indicating that the sympathetic nerve may utilize other paths in the activation of the muscle cells. This suggestion is strengthened by the finding that after maximum contraction evoked by $\text{PGF}_{2\alpha}$ a further increase in tension could be achieved by the addition of PE and vice versa. Nevertheless, the excitatory actions of PGs are α -adrenoceptor stimulation certainly involve a common final mechanism since both effects are abolished in nominally calcium-free solution.

This investigation was supported by grants from Knut and Alice Wallenberg Foundation, The Swedish Medical Research Council (2873) and The Göteborg Medical Society, Sweden.

on the VIP-ergic innervation of the feline pylorus

EDEN J M LUNDBERG H AHLMAN A DAHLSTRÖM
FAHRENKRUG, T HÖKFELT and J KEWENTER

Institute of Neurobiology and the Department of Surgery III, University of Göteborg,
Department of Histology, Karolinska Institute, Stockholm, Sweden, and the
Department of Chemical Chemistry, Bispebjerg Hospital, Copenhagen, Denmark

nonactive intestinal polypeptide (VIP), isolated and sequenced by Said and Mutt (Said & Mutt 1970, Mutt & Said 1974) has been localized by immunohistochemistry to peripheral neurons in various nerves (Lundberg et al 1978) and organs, i.e. the gastrointestinal region (Larsson et al 1976). Furthermore VIP has been localized to sphincter zones (Alm et al 1979) and found to relax the antral smooth muscle (Morgan et al 1978) and the cardiac sphincter (Rattan et al 1977). In addition, VIP can be released from the gut by electrical stimulation of the vagal nerves in the pig (Fahrenkrug et al 1978).

It was also recently demonstrated that close relations of this peptide caused a gastric relaxation and an increased blood flow to the stomach (Ekblad et al 1979), a response similar to the vagally induced effect at high threshold stimulation (Martinson 1965). Together these findings strongly suggest that VIP may be one of the neurotransmitters in the gastrointestinal tract (see Fahrenkrug et al 1978b). The purpose of the present study was to demonstrate VIP-ergic neurons within the feline pylorus by immunohistochemistry and to further study the simultaneous effects on gastric and pyloric motility when VIP was injected in local gastric artery.

The immunohistochemical studies were performed as described previously (for references, see Eden et al 1979b), using VIP antiserum 5603-5 (Fahrenkrug et al 1977, 1978). Gastric motility was studied by volume recordings of a flaccid intragastric balloon at constant intraluminal pressure (Martinson 1965). Pyloric motility was recorded as changes of an applied constant flow of body warm saline across the sphincter (Eden et al 1979). 6 cats (2.5-3 kg) of either sex in chloralose anaesthesia (50 mg/kg) were used. A fine bipolarized plastic catheter (1 mm) was introduced along the greater curve of the stomach via the splenic artery in retro-

grade direction. In its final position ink infusion after the experiments showed distribution to the first part of the duodenum, the pylorus and the stomach. VIP (kindly donated by Prof. Viktor Mutt, Karolinska Institute, Stockholm) was dissolved in saline and given as single bolus doses (0.03-1.3 nmol) via this catheter. The VIP injections induced a prompt gastric relaxation and a marked increase of the transpyloric flow at all doses given, but only in 50% of the experiment with the lowest dose (0.03 nmol). The effects lasted about 10-15 min and 4-5 min respectively (Fig. 1).

The VIP-containing neurons within the pylorus had a characteristic distribution pattern. VIP immunoreactive nerve cells were observed in moderate numbers in the myenteric and high numbers in the submucous plexus. Numerous VIP immunoreactive fibres were seen in the lamina propria, in the circular smooth muscle layer (Fig. 2) and in the myenteric plexus.

In the stomach VIP-immunoreactive nerve cells were observed both in the myenteric plexus (fewer than in pylorus) and in the submucous plexus (as in pylorus). In the corpus-antrum the circular muscle layer contained a medium dense network of nerve fibres, the lamina propria mucosae a dense network, and the longitudinal muscle layer few single nerve fibres.

In a previous study we have demonstrated enkephalin immunoreactive nerve cells and fibres mainly in the myenteric plexus and the circular smooth muscle layer of the pylorus (Eden et al 1979b). Furthermore, enkephalin as well as vagal stimulation caused a pyloric contraction effects which were blocked by naloxone (Eden et al 1979b). The VIP immunoreactive fibres in the circular muscle layer had a distribution very similar to the enkephalin nerves. Nevertheless the two peptides have antagonistic effects since VIP causes pyloric relaxation. It is interesting to note that, in

- WZEWSKI J F 1973 The inhibitory effect of vasoactive intestinal polypeptide on the mechanical and electrical activity of canine antral smooth muscle. *J Physiol* 232: 437-450.
- MUTT V & SAID S I 1974 Structure of the porcine vasoactive intestinal octacosia peptide. *Europ J Biochem* 42: 581-599.
- RATTAN S, SAID S I & GOYAL R K 1977 Effect of vasoactive intestinal polypeptide (VIP) on the lower esophageal sphincter pressure (LESP). *Proc Soc Exp Biol Med* 155: 40-43.
- SAID S I & MUTT V 1970 Polypeptide with broad biological activity: isolation from small intestine. *Science* N.Y. 69: 17 1218.

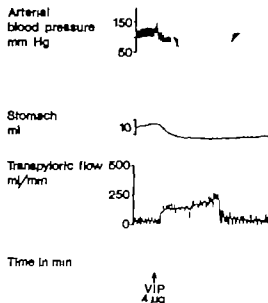


Fig. 1 Recordings of intraarterial blood pressure, gastric motility and transpyloric flow in the cat at i.a. bolus injection of VIP (1.3 nmol). Note the long-lasting relaxation of the stomach (10–15 min) and the more short-lasting dilatation of the pylorus (4–5 min).

agreement with the results of Eklund et al. (1979) the VIP-induced receptive relaxation has a very long duration, whereas the pyloric relaxation seen in this study was more short-lasting. It seems therefore possible that neuropeptides may play important roles in the regulation of the pyloric sphincter tone.

The technical assistance of Mrs. Waldtraut Hlort and Mrs. Harriet Andersson is gratefully acknowledged. This study was supported by the Swedish Medical Research Council (grants nos. 17X-5220, 04X-2887, 04X-2207 and 04P-4173) by the Medical Faculty, University of Göteborg, Göteborgs Läkaresällskap and Harald och Greta Jeansson's Stiftelse, Sweden.

REFERENCES

- ALUMETS, I., FAHRENKRUG, J., HÄKANSSON, R., SCHAFFALITZKY DE MUCKADELL, O. B. & UDDMAN, R. 1979. A rich VIP nerve supply is characteristic of sphincters. *Nature* 280, 155–156.
- EDLIN, R., AHLMAN, H. & KEWENTER, J. 1979a. The vagal control of the feline pylorus. *Acta Physiol. Scand.* In press.
- EDLIN, R., LUNDBERG, J. M., AHLMAN, H., DAHL, STRÖM, A., KEWENTER, J., TERENIUS, L. & HÖKFELT, T. 1979b. Evidence for an enkephalic neural control of the pylorus. *Gastroenterology*. Submitted.
- EKLUND, S., JODAL, M., LUNDGREN, O. & SJÖQVIST, A. 1979. Effects of vasoactive intestinal
- polypeptide on blood flow, motility and fluid transfer in the gastrointestinal tract of the cat. *Acta Physiol. Scand.* 105, 461–468.
- FAHRENKRUG, J. & SCHAFFALITZKY DE MUCKADELL, O. B. 1977. Radioimmunoassay of vasoactive intestinal polypeptide in plasma. *Lab. Invest.* 37, 1379–1388.
- FAHRENKRUG, J., GALBO, H., HOLST, J. J. & SCHAFFALITZKY DE MUCKADELL, O. B. 1978a. Influence of the autonomic nervous system on the release of vasoactive intestinal polypeptide from the gastrointestinal tract. *J. Physiol. (Lond.)* 290, 481–491.
- FAHRENKRUG, J., HAGLUND, U., JODAL, M., LUNDGREN, O., OLBE, L. & SCHAFFALITZKY DE MUCKADELL, O. B. 1978b. Release of vasoactive intestinal polypeptide in the gastrointestinal tract of cats: possible functional implication. *J. Physiol. (Lond.)* 284, 791–805.
- FAHRENKRUG, J. & SCHAFFALITZKY DE MUCKADELL, O. B. 1978c. Distribution of vasoactive intestinal polypeptide in the porcine central nervous system. *J. Neurochem.* 31, 1445–1451.
- LARSSON, L. I., FAHRENKRUG, J., SCHAFFALITZKY DE MUCKADELL, O., SUNDLER, F., HÄKANSSON, R. & REHFELD, J. F. 1978. Localization of vasoactive intestinal polypeptide (VIP) to central and peripheral neurons. *Proc. Natl. Acad. Sci.* 75, 3197–3200.
- LUNDBERG, J. M., HÖKFELT, T., NILSSON, G., TERENIUS, L., REHFELD, J., ELDE, R. & SAID, S. 1978. Peptide neurons in the sympathetic and somatic nerves. *Acta Physiol. Scand.* 104, 499–501.
- MARTINSSON, J. 1965. Studies on the efferent vagal control of the stomach. *Acta Physiol. Scand.* 65, Suppl. 255.
- MORGAN, A. O., SCHMALZ, P. F. & SZUTZ

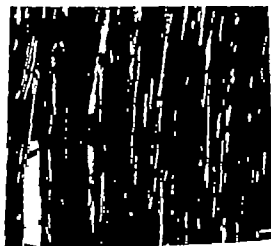


Fig. 2 Immunofluorescence micrograph of the cross-smooth muscle layer of the feline pylorus. A dense network of longitudinally sectioned VIP-immunoreactive nerve fibres is seen. Bar indicates 50 µm.

3 to 2 coupling of the Na-K pump responsible for the transepithelial Na transport in frog skin occluded by the effect of Ba

XBERT NIELSEN

Institute of Biological Chemistry A, Aug. Kroghs Vej 1, Copenhagen, Denmark

According to the two-membrane hypothesis (Jensen & Ussing 1958) one would expect an increase in the K^+ permeability of the outside facing membrane to result in an active outward transport of K^+ (Fig. 4). Polyene antibiotics increase the permeability of cell membranes for K^+ and other ions (De Kruijff & Demel 1974). Addition of polyene antibiotics (filipin and amphotericin B) to the outside bathing solution of the isolated frog skin in fact result in an active outward transport of K^+ (Nielsen 1971, Nielsen 1972). In a recent paper (Nielsen 1979) it is shown that the filipin-induced active outward K^+ transport is coupled to the active Na^+ transport and the data suggest that the coupling ratio between the active transepithelial Na^+ and K^+ transport is 1.5 (3 Na^+ /2 K^+). If the active Na^+ transport across the isolated frog skin is carried

out by a Na^+ - K^+ pump with a coupling ratio of 1.5 then the addition of a component which completely inhibits the passive K^+ current across the inward facing membrane should in the absence of filipin initially result in 66.6% inhibition of the short-circuit current (SCC) (see below).

The experiments were performed on male and female frogs (*Rana temporaria*) as described previously (Nielsen 1977). The epithelia were dissected from collagenase treated skins (Jensen & Nielsen 1978) and mounted in perspex chambers (area 0.7 cm²) and bathed in stirred Ringer's solution (Na⁺ 115, K⁺ 2.5, Ca²⁺ 1, Mg²⁺ 1, Cl⁻ 117, CO₃²⁻ .5, PO₄³⁻ 1, glucose 5 mM, pH 7.8).

Addition of 5 mM Ba²⁺ to the inside bathing solution (IBS) resulted in an inhibition of the SCC and in an increase in the transepithelial resistance (Fig. 1). About 5 min after the addition of Ba²⁺ the SCC started to recover and the resistance started to decrease. The recovery phase was completed 70-90 min after the addition of Ba²⁺. The recovery varied from 30% to complete recovery. In the present paper only the initial effect of Ba²⁺ will be discussed. When Ba²⁺ is added to the IBS of isolated epithelia the same result is obtained as in whole skins (Fig. 2) but the inhibition is faster because the thickness of the unstirred layer on the inside has been reduced by removal of the connective tissue.

The primary inhibitory effect of Ba²⁺ is much faster than the secondary effect (the recovery) of Ba²⁺ so the two effects are separated in time. Therefore it is possible to measure the Ba²⁺ induced initial inhibition without getting interference from the subsequent recovery. The initial Ba²⁺ induced inhibition is plotted against the Ba²⁺ concentration in the IBS (Fig. 3), the Ba²⁺ induced inhibition of the SCC increases with increasing Ba²⁺ concentration until a maximum inhibition is reached. Addition of Ba²⁺ (5 mM) to the IBS a

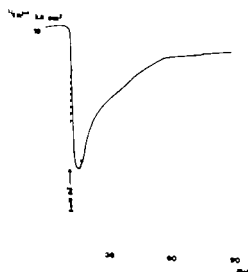


Fig. 1. Effect of Ba²⁺ on the short-circuit current across isolated frog skin. At the arrow Ba²⁺ (5 mM) is added to the inside bathing solution. — Short-circuit current (μA/cm²). - - - Transepithelial resistance (kΩ/cm²).

intracellularly in the cells the net Na flux across outward facing membrane has to be reduced by amount of K which is pumped into the cells. If coupling ratio for the Na-K pump is 1.5 a complete blocking of the K flux via the K channel will initially result in a 66.6% inhibition of the SCC. Thereafter the SCC will change probably because presence of Ba causes secondary increase in K permeability of the membranes as shown in rabbit muscle (Hermismeyer & Sperelakis 1970). The observations that maximum Ba-induced inhibition of the SCC is not significantly different from 66.6% (Fig. 3) supports the idea that the unipathetic Na transport in frog skin is carried out by a Na-K pump with a coupling ratio of 1.5. In metazoal cells (such as erythrocytes, muscle and nerve) it is generally accepted that the coupling ratio for the Na-K pump is 1.5 (Thomas 1977).

REFERENCES

- KRUIFF B. & DEMEL, R. A. 1974. Polyene antibiotic-sterol interactions in membranes of archaebacteria, eukaryotic cells and lecithin liposomes. *Biochim. Biophys. Acta* (Amst.) 339, 57-70.
- ENDERSON E. C. 1974. Scorpion toxin sensitive electrogenic mechanism in frog sartorius muscles exposed to barium. *Pflügers Arch. Ges. Physiol.* 340, 81-95.
- HERMISMEYER, A. & SPERELAKIS, N. 1970. Decrease in K⁺ conductance and depolarization of frog cardiac muscle produced by Ba. *Am. J. Physiol.* 19: 1108-1114.
- JOHNSEN A. H. & NIELSEN R. 1978. Effect of the antidiuretic hormone arginine vasotocin, theophylline, flupar and A23187 on cyclic AMP in isolated frog skin epithelium (*Rana temporaria*). *Acta Physiol. Scand.* 102: 281-289.
- KOEFOTD-JOHNSON V. & USSING H. H. 1958. The nature of the frog skin potential. *Acta Physiol. Scand.* 42: 298-308.
- NAGEL, W. 1978. Ba²⁺ decreases C₁ in frog skin. *Fed. Proc.* 37, 569.
- NIELSEN R. 1971. Effect of amphotericin B on the frog skin in vitro. Evidence for outward active potassium transport across the epithelium. *Acta Physiol. Scand.* 83, 106-114.
- NIELSEN R. 1972. The effect of polyene antibiotics on the aldosterone induced changes in sodium transport across the isolated frog skin. *J. Ster. Biochem.* 3, 11-128.
- NIELSEN R. 1977. Effect of the polyene antibiotic flupar on the permeability of the inward- and the outward-facing membrane of the isolated frog skin. *Acta Physiol. Scand.* 99, 399-411.
- NIELSEN R. 1979. Coupled transepithelial Na and K transport across isolated frog skin. Effect of ouabain, ionophore and the polyene antibiotic flupar. *J. Membrane Biol.* In press.
- THOMAS R. C. 1972. Electrogenic sodium pump in nerve and muscle cells. *Physiol. Rev.* 52, 563-594.

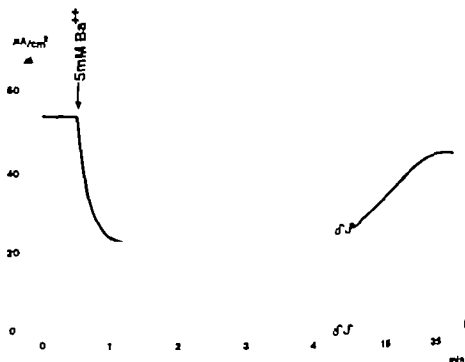


Fig. 2 Effect of Ba^{2+} on the short-circuit current across an isolated epithelium

concentration which gave maximum inhibition resulted in a $65.0 \pm 1.9\%$ ($n=10$) inhibition of the SCC. This inhibition is not significantly different from 66.6%. Ba^{2+} has been shown to reduce the K conductance in frog heart (Hermesmeier & Sperelakis 1970), in frog muscle (Henderson 1974) and in frog skin (Nagel 1978; Nielsen 1979).

According to the two-membrane hypothesis (Koefoed-Johnsen & Ussing 1958) the active Na transport across the isolated frog skin occurs in two steps: passive diffusion across the outward facing

membrane of the epithelium followed by an active extrusion across the inward facing membrane, the Na-K pump. If the active Na transport is carried out by a Na-K pump with a coupling ratio 1.5 then according to this model (Fig. 4) $\frac{1}{2}$ of the SCC across the inward facing membrane is carried by K ions and $\frac{1}{2}$ by Na ions. Addition of a component (Ba^{2+}) which completely blocks the K channel would abolish the K current via the K channel; the K which is pumped into the cell via the Na-K pump cannot leave the cells. In order to maintain

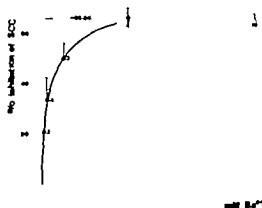


Fig. 3 Maximum percentage reduction of the short-circuit current elicited by various concentrations of Ba^{2+} . Values are the mean \pm S.E. Figures at the curve are number of expts.

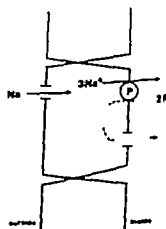


Fig. 4 The two-membrane hypothesis. P, Na-K pump with a coupling ratio of 1.5 ($3Na/2K$).

Chloride transport by self exchange and by KCl salt diffusion in gramicidin treated human red blood cells

BERT CASS and MADS DALMARK

Department of Biophysics, University of Copenhagen, Physics Institute and the Department of Medicine M, Frederiksberg Hospital, Denmark

CASS, A. & DALMARK, M. Chloride transport by self-exchange and by KCl salt diffusion in gramicidin-treated human red blood cells. *Acta Physiol Scand* 1979, 107, 193-203. Received 10 Jan. 1979. ISSN 0001-6772. Department of Biophysics, University of Copenhagen, Physics Institute and the Department of Medicine M, Frederiksberg Hospital, Denmark.

The permeability of gramicidin-treated human red blood cell membranes to K^+ and Cl^- has been measured at normal ionic strength (1) by tracer exchange at steady-state distribution of salt, and (2) by net transport of salt in the presence of a salt concentration gradient. Under both conditions KCl was the only inorganic salt in cells and medium. In the studies of self-exchanges the electrical driving force on the ions was zero. Calculation of permeability coefficients from net salt transport was simplified because the experiment was designed as a special case of the Nernst-Planck diffusion regime I—the single salt case. Gramicidin altered the cell membranes from being anion to become cation selective. Gramicidin increased the potassium exchange without affecting the chloride exchange measurably. The chloride exchange showed saturation kinetics as does chloride exchange in normal cells. The net transport of KCl in the presence of a constant concentration gradient increased to a constant value with increasing gramicidin concentration. At high gramicidin concentrations (0°C, pH 7.2) the chloride permeability coefficient calculated from tracer exchange ($1.9 \cdot 10^{-4}$ cm/s) was 290 times the chloride permeability coefficient calculated from net salt transport ($0.65 \cdot 10^{-4}$ cm/s). The latter value corresponds to chloride conductance of $4.2 \cdot 10^{-4}$ ohm $^{-1}$ cm $^{-2}$. The chloride permeability coefficient was $1 \cdot 10^{-4}$ cm/s at 25°C (pH 6.8) indicating a value of 3 for the Q_{10} . It appears that normal red cells are anion selective in the sense that anion permeability exceeds cation permeability with a factor of more than hundred between 0°C and body temperature. The anion exchange, i.e. the Hamburger shift, is a tightly coupled transport process which is several orders of magnitude faster than anion transport by salt diffusion.

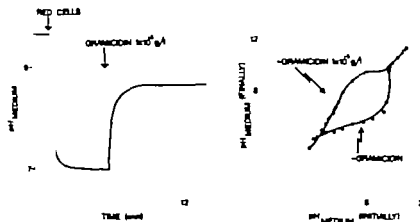
Key words: Chloride transport, red blood cells, gramicidin.

It was suggested by Warburg (1922) and Van Slyke et al. (1923) that the human red blood cell is selectively anion permeable in the sense that anion permeability exceeds cation permeability by orders of magnitude. The electroneutrality condition dictates that chloride transport is limited to exchange for other anions like chloride (Chloride self-exchange) or bicarbonate (the Hamburger shift) because the cation permeability is low. However it is impossible from studies on normal cells to decide whether (1) all the anions are transported by independent migration, or whether (2) greater or smaller fraction of anion efflux and influx is linked together as an electroneutral—chemically coupled—anion ex-

change. The latter alternative is favoured by the characteristics of chloride self-exchange which shows features of facilitated diffusion (reviewed by Dalmark 1976). The low electrical membrane conductance relative to the chloride tracer exchange in the red cell of the giant salamander *Amphiuma*, is consistent with this view (Lassen et al. 1974, 1978).

The cation permeability of red cell membranes is increased by addition of various ionophores. In these modified cells the electroneutrality restriction is fulfilled when the chloride transport takes place as

Present address: The Finsen Institute, Dept. Med., Strandboulevarden, Copenhagen, DK 2100, Denmark.



1 The pH-shifts of low ionic strength medium following suspension of red cells in the medium and, later on, after addition of gramicidin to the cell suspension (Fig. 1a). Acidification and alkalization of low ionic strength medium following suspension of red cells in the medium (haematocrit 0.01 v/v) as functions of the pH in the media prior to the addition of the cells in absence (●) or in presence (○) of gramicidin (10^{-6} g/l) (Fig. 1b). The cells were washed in salt solution (130 mM KCl, 27 mM sucrose) and titrated to pH 6.6 (38°C) before the cells were suspended in the low ionic strength media (1 mM KCl, 302 mM sucrose) at 38°C. The pH of the suspending medium was adjusted with NaOH/KCl before the cells were suspended.

measured either (a) by coulometric titration (CMT) (Radiometer, Copenhagen, Denmark), or from the distribution of ^{36}Cl between cell water and bath together with the chloride concentration in bath. The potassium content in the cells was determined either (a) by flame photometry (Radiometer, Copenhagen, Denmark), or (b) from the potassium concentration in medium and the distribution of ^{40}K . The sodium and chloride concentration in medium was determined by flame photometry and coulometric titration. An equation of the permeability coefficient employed in transport experiments is derived in Results.

RESULTS

The results will be presented in 4 sections. The first section describes the effect of gramicidin on ionic selectivity of the red cell membrane at low ionic strength. The second and third section contain experimental data on (a) potassium and chloride self exchange, and (b) net transport of potassium chloride and water at normal ionic strength. The last section contains an analysis of the net transport experiments and the estimate of the chloride permeability coefficient.

Effect of gramicidin on selectivity

A rapid acidification of the medium occurs when normal red cells are suspended in low ionic strength media at neutral pH (Davson 1939; Wilbrandt 1940).

It is generally believed that anions like chloride and hydroxyl ions rapidly reach thermodynamic equilibrium. The distribution of chloride across the untreated membrane determines the pH of an unbuffered KCl solution because the cellular pH is constant owing to the high buffer capacity of hemoglobin. Fig. 1 shows the acidification of a low ionic strength medium following suspension of red cells in the medium. Subsequent addition of gramicidin to the cell suspension shifts the pH in the alkaline direction. Although the mechanism of the acidification is debated the alkalization of the medium following addition of gramicidin appears to be a transport of protons because proton permeability is greatly increased in gramicidin-treated thin lipid membranes (Myers & Haydon 1972). The potassium diffusion potential in gramicidin-treated red cells determines the distribution of protons across the cell membranes in the experimental situation employed.

Fig. 1b (filled circles) demonstrates the acidification of the medium as a function of the pH prior to normal cells were suspended in an unbuffered low ionic strength medium: the change in pH increased with the pH initially present in the medium. No change in pH was observed at an initial pH of 4.6. This pH value was predictable from the chloride distribution across the cell membranes: the activity

(1) an anion exchange or (2) a net anion transport accompanied by cations (net salt transport) in the presence of a concentration gradient. The effect of ionophores on net salt transport has been interpreted as if the anion transport by salt diffusion was much slower than anion transport by self-exchange (Harris & Pressman 1967; Scarpa et al. 1970; Tosteson et al. 1973; Wieth et al. 1973; Hunter 1977; Parker et al. 1977; Knauf et al. 1977). Estimates of the chloride permeability coefficient were obtained by using the Nerst-Planck formalism with the Goldman constant field assumption or by flux ratio measurements. The absence of an inhibitory action of the ionophores on chloride exchange was not directly disproved.

We used an ionophore, gramicidin, to increase the cation permeability. Gramicidin is a linear polypeptide antibiotic of molecular weight c. 1880 isolated from *Bacillus brevis* (Sarges & Witkop 1965). Gramicidin contains many non-polar side chains and no ionizable groups as both the C and N terminals are blocked. Gramicidin forms channels consisting of gramicidin dimers through thin lipid membranes. The channels include monovalent cations and exclude anions like chloride and divalent cations (Myers & Haydon 1972). Reviews on gramicidin have been presented by Haydon & Hladky (1972), Hladky (1974) and Bamberg et al. (1977).

We demonstrate that gramicidin turns the human red blood cell into a highly cation selective membrane with an unaltered chloride self-exchange which at neutral pH is orders of magnitude faster than the KCl diffusion. The calculation of permeability coefficients from net salt transport was simplified because the experiment was designed as a special case of the Nerst-Planck diffusion regime, i.e. the single salt diffusion case. The term of the electrical driving force is eliminated in the equation of the permeability coefficient in this experimental situation. Some of the results have been cited previously (Cass & Dalmark 1974).

METHODS AND CALCULATIONS

Freshly drawn heparinized human red blood cells were washed three times to pH 6.8 (25°C) and resuspended to a hematocrit of 0.25 in a salt solution (140 mM KCl, 27 mM sucrose). The buffy coat was removed.

The temperature sensitivity of the gramicidin effect (cf. Fig. 1) demanded that gramicidin—in all experiments—had to be added to the cell suspension at a high tempera-

ture in order to increase the cation permeability. All temperature experiments were started once gramicidin was added to the cell suspension. (b) Low temperature experiments were carried out with cells isolated with gramicidin at room temperature for half an hour before experiments were started. Only insignificant anion-potassium exchange was observed after subsequent washes of the (b)-cells in gramicidin-free salt solution at low temperature. The gramicidin-treated cells were titrated to pH 7 (0°C) and resuspended in a salt solution (150 mM KCl, 7 mM sucrose). The distribution of KCl between cell water and medium was unity in these conditions (Dalmark 1975b). Gramicidin was added as a methanolic solution of Gramicidin N.F. monomer (Lundbeck and Co., Copenhagen, DK 2000) which was composed of gramicidin A 50%, gramicidin B 7%, gramicidin C 25%. Three types of experiments were carried out with gramicidin-treated cells and normal cells.

(1) The low ionic strength experiments were performed by injection of approx. 200 mg packed cells into 30 ml vigorously stirred medium containing 1 mM KCl, 302 mM NaCl. The medium pH was monitored by a pH-meter (Radiometer, Copenhagen, Denmark). A steady pH-value was obtained approx. 1 min after an acid or base pulse.

(2) The exchange experiments were carried out as described by Dalmark & Wieth (1972) by injection of 200 mg packed and isotope labelled cells into 30 ml vigorously stirred medium and, subsequently, by serially adding cell-free efflux medium by rapid filtration of the suspension. The exchange kinetics of potassium chloride was well described by a closed two-compartment model with constant volumes up to at least 10% isotopic equilibrium value. The half-time of K⁺ exchange was determined from a plot of $\ln(1 - a_{\infty}/a_t)$ versus time, where a_t or a_{∞} are the specific activities at the time of sampling or at isotopic equilibrium. The slope of the graph was equal to the rate coefficient k for KCl efflux under the conditions employed. The cell equilibrium flux (influx = efflux) was calculated from the equation

$$J_{Cl} (\text{mmol}/3 \times 10^8 \text{ cells} \cdot \text{min}) = k \cdot (Cl_i) \cdot V_i \cdot F$$

where k is the rate coefficient of tracer efflux (s⁻¹), Cl_i is the cellular chloride concentration (mmol/L water), V_i is the cellular water content (kg water/kg solids) and F has the dimension kg cell solids per J cells (Dalmark 1975a). The 3×10^8 cells have a surface area of 4890 m² (Ponder 1948) and contain 1 kg cells at an ionic strength of 0.15 (Funder & Wieth 1966).

(3) The net salt transport experiments were carried out with cells pretreated exactly as the cells of the exchange experiments. The experiments were initiated by resuspending the cells to a hematocrit of 0.25 in a salt solution (165 mM NaCl, i.e. there was a salt concentration difference of 15 mM across the cell membrane at the beginning of the experiment) and subsequently the cells began to take up salt. At time of sampling the cells were separated from the suspending medium with an amount of trapped extracellular fluid of 7% (w/w) by ultrafiltration. The cellular content was measured by drying packed cells to constant weight (105°C, 4 h). The cellular content of chloride

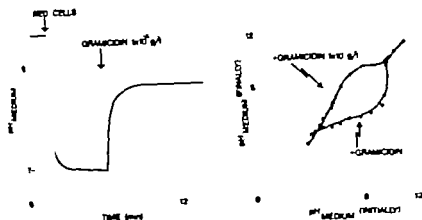


Fig. 1. The pH-shifts of low ionic strength medium following suspension of red cells in the medium and later on, after addition of gramicidin to the cell suspension (Fig. 1a). Acidification and alkalization of low ionic strength media following suspension of red cells in the media (hematocrit 0.01 v/v) as functions of the pH in the media prior to the suspension of the cells in absence (●) or in presence (○) of gramicidin (10^{-6} g/l) (Fig. 1b). The cells were washed in salt water (150 mM KCl, 27 mM sucrose) and titrated to pH 6.6 (34°C) before the cells were suspended in the low ionic strength media (150 mM KCl, 302 mM sucrose) at 34°C. The pH of the suspending medium was adjusted with KOH or HCl before the cells were suspended.

measured either (a) by coulometric titration (CMT) (Radiometer Radiometer Copenhagen Denmark), or (b) from the distribution of ^{36}Cl between cell water and medium together with the chloride concentration in medium. The potassium content in the cells was determined either (a) by flame photometry (Radiometer Copenhagen, Denmark), or (b) from the potassium concentration in medium and the distribution of ^{40}K . The potassium and chloride concentration in medium was determined by flame photometry and coulometric titration. The equation of the permeability coefficient employed in transport experiments is derived in Results.

RESULTS

The results will be presented in 4 sections. The first section describes the effect of gramicidin on ionic conductivity of the red cell membrane at low ionic strength. The second and third section contain experimental data on (a) potassium and chloride self exchange and (b) net transport of potassium, chloride and water at normal ionic strength. The last section contains an analysis of the net transport experiments and the estimate of the chloride permeability coefficient.

Effect of gramicidin on selectivity

A rapid acidification of the medium occurs when normal red cells are suspended in low ionic strength media at neutral pH (Davson 1939; Wilbrandt 1940).

It is generally believed that anions like chloride and hydroxyl ions rapidly reach thermodynamic equilibrium. The distribution of chloride across the untreated membrane determines the pH of an unbuffered KCl solution because the cellular pH is constant owing to the high buffer capacity of hemoglobin. Fig. 1 shows the acidification of a low ionic strength medium following suspension of red cells in the medium. Subsequent addition of gramicidin to the cell suspension shifts the pH in the alkaline direction. Although the mechanism of the acidification is debated the alkalization of the medium following addition of gramicidin appears to be a transport of protons because proton permeability is greatly increased in gramicidin-treated thin lipid membranes (Myers & Haydon 1972). The potassium diffusion potential in gramicidin-treated red cells determines the distribution of protons across the cell membranes in the experimental situation employed.

Fig. 1b (filled circles) demonstrates the acidification of the medium as a function of the pH prior to normal cells were suspended in an unbuffered low ionic strength medium: the change in pH increased with the pH initially present in the medium. No change in pH was observed at an initial pH of 4.6. This pH value was predictable from the chloride distribution across the cell membranes: the activity

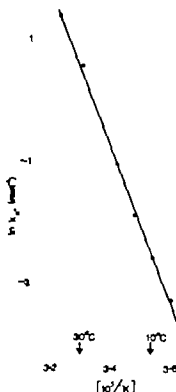


Fig. 2. The Arrhenius plot showing the rate constant k (ml/s) of proton flux across the red cell membrane after addition of gramicidin (10^{-6} g/l) to cells suspended in an unbuffered low ionic strength medium (hematocrit 0.01 v/v) as a function of the reciprocal absolute temperature ($^{\circ}\text{K}$). The cells were washed in a salt solution (150 mM KCl, 27 mM sucrose) and titrated to pH 6.8 (25°C) before the cells were suspended in the low ionic strength medium (1 mM KCl, 302 mM sucrose, neutral pH). The relationship between $\ln k$ (Y) vs. $10^3/T^{\circ}\text{K}$ (X) was described by the equation $Y = -12.7X + 42.3$, $r = -0.99$. The Arrhenius activation energy of proton flux following addition of gramicidin was 105 kJ/mole (25 kcal/mole).

coefficients of chloride and the intracellular pH of 6.6 at 38°C . The selectivity of the membranes disappeared at pH above nine. A large increase in cation permeability has previously been demonstrated as an effect of a high pH in the suspending medium (Passow 1964; LaCelle & Rothstein 1966).

Addition of gramicidin alters the cell membrane to a highly cation permeable membrane as demonstrated by the upper curve (open circles) in Fig. 1b. A pH shift was measured of a similar size but of an opposite sign as that observed with an anion selective membrane under identical conditions except for gramicidin. The disappearance of selectivity above pH nine was also observed with gramicidin-treated cells.

Fig. 1b demonstrates that the potassium permea-

bility is increased relative to chloride permeability in the pH range from five to nine in the presence of gramicidin. The gramicidin molecule contains ionizable groups as both the C and N termini are blocked (Sarges & Wilkop 1965) and gramicidin modified artificial lipid bilayers are highly cation selective even at low pH (Myers & Hayden 1977).

Formation of cation permeable channels is a complicated process since gramicidin is slightly soluble both in water and in lipids and furthermore the cation permeable unit is believed to be a dimer (reviewed e.g. Hladky 1974). Fig. 7 demonstrates the high temperature sensitivity of the formation of cation selective membranes following addition of gramicidin to the suspending medium. Fig. 8 is an Arrhenius plot of the rate constant of the proton flux initiated by addition of gramicidin to a suspension of red cells in an unbuffered low ionic strength medium. The rate constant was determined from the slope of a plot of $\ln(\Delta H/\Delta H_{\infty})$ vs. time where $\Delta H/\Delta H_{\infty}$ are the cumulative proton transport at the time t and at the new steady state. No change in medium pH was observed at 0°C within approximately 1 h after addition of gramicidin. This temperature sensitivity demanded that the cells had to be treated with gramicidin at room temperature before the cells were employed in low temperature experiments (cf. Methods).

Effect of gramicidin on potassium and chloride exchange

The potassium and chloride exchange across the human red cell membrane can be determined simultaneously at 0°C using a simple filtration technique (Dalmark & Wieth 1977). The chloride exchange in normal cells has been studied extensively at 0°C temperature (Dalmark & Wieth 1970; Gunn et al. 1973; Dalmark 1975a). Fig. 3 shows the effect of gramicidin on potassium and chloride exchange. The half-time of potassium exchange decreases drastically with gramicidin concentration (Fig. 3a) in contrast to an unaltered half-time of chloride exchange (Fig. 3b). The half-time of potassium exchange in normal cells in 35 days under unaltered conditions (Dalmark 1975b) but the half-time decreased to 1 s in the presence of 50 μM gramicidin. The slope of the line (Fig. 3a) is smaller than the expected slope of two for a dimer channel. However, the relationship between the conductance of artificial bilayers and the gramicidin concentration also demonstrates a slope of less than

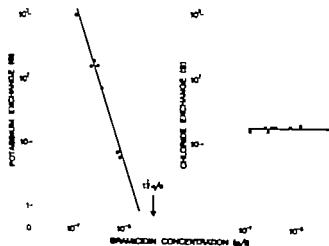


Fig. 3 The effect of gramicidin on potassium exchange (Fig. 3a) and on chloride exchange (Fig. 3b) determined simultaneously at distribution ratio of potassium chloride between cell water and medium of unity (pH 7.4, 0°C). The composition of the medium (mM): 150 KCl, 27 sucrose. The lines were drawn by eye (—) with slope of 1.3 (Fig. 3a), and (—) with slope of zero (Fig. 3b). Assuming that the membrane potential difference is equal to zero, reasonable assumption in view of the salt distribution ratio of unity the "tracer permeability coefficient" (P) is given by the equation: $P \text{ (cm/s)} = (3 \cdot 10^{-12} \text{ s}) / t$ where t is the half-time of tracer exchange (seconds). The gramicidin was added to the cells at room temperature (cf. Methods).

probably because a true partition equilibrium between medium and membrane can never be reached (Haydon & Hladky 1972, Bamberg et al 1977).

Gramicidin had no inhibitory effect on chloride exchange at physiologic ionic strength as the half-time of chloride exchange was independent of the gramicidin concentration (Fig. 3b).

The ability of the gramicidin channels to exclude chloride can be tested by measuring the chloride equilibrium flux vs. chloride concentration. Assuming that the gramicidin channel has a chloride conductance different from zero the chloride transport through this pathway is linearly related to chloride concentration. Such a transport pathway will be superimposed the chloride exchange observed in normal cells. Fig. 4 shows the concentration dependence of chloride transport in the presence of gramicidin compared with chloride exchange in normal cells (Cass & Dalmark 1973). Chloride transport shows saturation kinetics as well as self-inhibition both in absence and in presence of gramicidin indicating that the postulated chloride flux through the gramicidin channel is less than a few per cent of the total chloride transport.

Similar exchange studies were performed at 25°C at pH 6.8 because the electrical net charge on the intracellular buffers is zero at this pH and temperature. Chloride exchange in normal cells has a half-time of approx. 0.2 s (Tosteson 1959, Brahm 1977). We demonstrated with our manual filtration technique that chloride tracer was at isotopic equilibrium within 2 s regardless the gramicidin concentration although potassium exchange increased drastically at 25°C as at 0°C (Fig. 3a).

Effect of gramicidin on net potassium chloride transport

The cells of the exchange experiments were suspended in 150 mM KCl plus 27 mM sucrose at pH 6.8 (25°C) or at pH 7.2 (0°C). The potassium chloride distribution ratio between the concentrations in cell water and medium was unity under these conditions (Dalmark 1975b) and no net transport of salt took place.

The cells of the following net salt transport experiments were pretreated with gramicidin as described in Methods and resuspended in 165 mM KCl where upon the cells began to take up potassium chloride and water in the presence of a concentration differ-

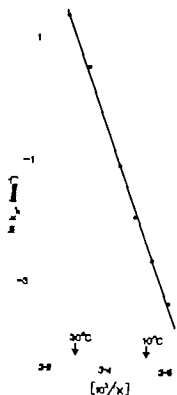


Fig. 2 The Arrhenius plot showing the rate constant k (min^{-1}) of proton flux across the red cell membrane after addition of gramicidin (10^{-6} g/l) to cells suspended in an unbuffered low ionic strength medium (hematocrit 0.01 v/v) as a function of the reciprocal absolute temperature ($^{\circ}\text{K}$). The cells were washed in a salt solution (150 mM NaCl, 77 mM sucrose) and titrated to pH 6.8 (25°C) before the cells were suspended in the low ionic strength medium (1 mM KCl, 302 mM sucrose, neutral pH). The relationship between $\ln k$ (Y) vs. $10^3/K$ (X) was described by the equation $Y = -12.7X + 42.3$, $r = -0.99$. The Arrhenius activation energy of proton flux following addition of gramicidin was 105 kJ/mole (25 kcal/mole).

coefficients of chloride and the intracellular pH of 6.6 at 38°C . The selectivity of the membranes disappeared at pH above nine. A large increase in cation permeability has previously been demonstrated as an effect of a high pH in the suspending medium (Passow 1964; LaCelle & Rothstein 1966).

Addition of gramicidin alters the cell membrane to a highly cation permeable membrane as demonstrated by the upper curve (open circles) in Fig. 1b. A pH-shift was measured of a similar size but of an opposite sign as that observed with an anion selective membrane under identical conditions except for gramicidin. The disappearance of selectivity above pH nine was also observed with gramicidin-treated cells.

Fig. 1b demonstrates that the potassium permea-

bility is increased relative to chloride permeability in the pH range from five to nine in the presence of gramicidin. The gramicidin molecule contains 2 ionizable groups as both the C and N termini are blocked (Sarges & Witkop 1965) and gramicidin modified artificial lipid bilayers are highly cation selective even at low pH (Myers & Haydon 1970).

Formation of cation permeable channels is a complicated process since gramicidin is not soluble both in water and in lipids and, furthermore, the cation permeable unit is believed to be dimeric (reviewed e.g. Hladky 1974). Fig. 3 demonstrates the high temperature sensitivity of the formation of cation selective membranes following addition of gramicidin to the suspending medium. Fig. 3a is an Arrhenius plot of the rate constant of the proton flux initiated by addition of gramicidin to a suspension of red cells in an unbuffered low ionic strength medium. The rate constant was determined from the slope of a plot of $\ln(\Delta H/\Delta H_{\infty})$ vs. time, where ΔH and ΔH_{∞} are the cumulative proton transport at the time t and at the new steady state. No change in medium pH was observed at 0°C within 1 h after addition of gramicidin. This temperature sensitivity demanded that the cells had to be treated with gramicidin at room temperature before the cells were employed in low temperature experiments (cf. Methods).

Effect of gramicidin on potassium and chloride exchange

The potassium and chloride exchange across the human red cell membrane can be determined simultaneously at 0°C using a simple filtration device (Dalmark & Wieth 1972). The chloride exchange in normal cells has been studied extensively at different temperatures (Dalmark & Wieth 1970; Gunn et al. 1973; Dalmark 1975a). Fig. 3 shows the influence of gramicidin on potassium and chloride exchange. The half time of potassium exchange decreases drastically with gramicidin concentration (Fig. 3a) in contrast to an unaltered half time of chloride exchange (Fig. 3b). The half time of potassium exchange in normal cells is 35 days under standard conditions (Dalmark 1975b) but the half time is decreased to 1 s in the presence of $50 \mu\text{M}$ gramicidin. The slope of the line (Fig. 3a) is smaller than the expected slope of two for a dimer channel. However, the relationship between the conductance of artificial bilayers and the gramicidin concentration also demonstrates a slope of less than

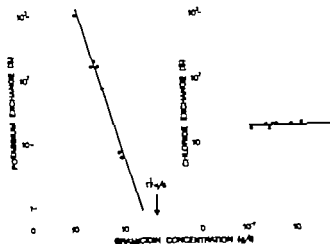


Fig. 3 The effect of gramicidin on potassium exchange (Fig. 3a) and on chloride exchange (Fig. 3b) determined simultaneously at a distribution ratio of potassium chloride between cell water and medium of unity (pH 7.2, 0°C). The composition of the medium (mM): 150 KCl, 27 sucrose. The lines were drawn by eye (—) with slope of 1.3 (Fig. 3a) and (---) with slope of zero (Fig. 3b). Assuming that the membrane potential difference is equal to zero, a reasonable assumption in view of the salt distribution ratio of unity, the "tracer permeability coefficient" (P) is given by the equation $P \text{ (cm}^2\text{ s}^{-1}) = (1/10^{-6})[t]$ where t is the half-time of tracer exchange (seconds). The gramicidin was added to the cells at room temperature (cf. Methods).

probably because a true partition equilibrium between medium and membrane can never be reached (Haydon & Hladky 1972, Bamberg et al 1977).

Gramicidin had no inhibitory effect on chloride exchange at physiologic ionic strength as the half-time of chloride exchange was independent of the gramicidin concentration (Fig. 3b).

The ability of the gramicidin channels to exclude chloride can be tested by measuring the chloride equilibrium flux vs. chloride concentration. Assuming that the gramicidin channel has a chloride conductance different from zero the chloride transport through this pathway is linearly related to chloride concentration. Such a transport pathway will be superimposed on the chloride exchange observed in normal cells. Fig. 4 shows the concentration dependence of chloride transport in the presence of gramicidin compared with chloride exchange in normal cells (Cane & Dalmark 1973). Chloride transport shows saturation kinetics as well as self-inhibition both in absence and in presence of gramicidin indicating that the postulated chloride flux through the gramicidin channel is less than a few per cent of the total chloride transport.

Similar exchange studies were performed at 25°C at pH 6.8 because the electrical net charge on the intracellular buffers is zero at this pH and temperature. Chloride exchange in normal cells has a half-time of approx. 0.2 s (Tosteson 1959, Brahm 1977). We demonstrated with our manual filtration technique that chloride tracer was at isotopic equilibrium within 2 s regardless the gramicidin concentration although potassium exchange increased drastically at 25°C as at 0°C (Fig. 3a).

Effect of gramicidin on net potassium chloride transport

The cells of the exchange experiments were suspended in 150 mM KCl plus 27 mM sucrose at pH 6.8 (25°C) or at pH 7.2 (0°C). The potassium chloride distribution ratio between the concentrations in cell water and medium was unity under these conditions (Dalmark 1975b) and no net transport of salt took place.

The cells of the following net salt transport expts. were pretreated with gramicidin as described in Methods and resuspended in 165 mM KCl whereupon the cells began to take up potassium chloride and water in the presence of concentration differ-

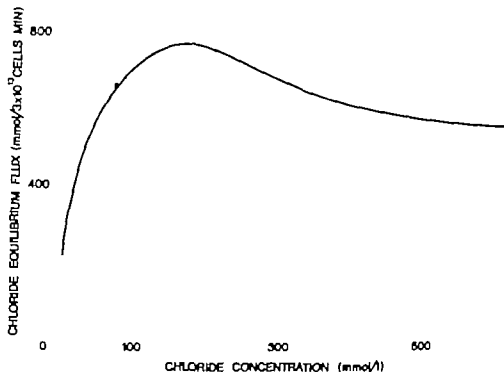


Fig. 4 The dependence of chloride equilibrium flux on chloride concentration (pH 7.2, 0°C) in the presence of gramicidin (10^{-4} g/l) compared with chloride exchange in normal cells (—) taken from Dalmark (1975a). The cell concentration of salt was altered by the nystatin technique (Cass & Dalmark 1973). The electrolyte solutions employed (mM): 50–500 KCl, 27 sucrose. The distribution ratio of KCl between cell water and medium was unity. The cells were treated with gramicidin at room temperature (cf. Methods).

ence of 15 mM KCl across the cell membrane. Fig. 5 shows simultaneous values of the cellular potassium and chloride content in a net transport experiment. One observes that the cells took up potassium chloride. Fig. 6a shows the cellular water content as a function of time after addition of gramicidin in a net transport experiment. Fig. 6b shows the cellular water content as a function of the sum of cellular potassium and chloride content. The transported fluid was slightly hyperosmotic as 2.64 g water was transported concomitantly with one mmol ion against the expected 3.03 g water/mmol ion for a solution of 165 mM KCl. The imperfect osmotic behaviour of red cells has been described under various experimental conditions (Ponder 1948; Dalmark 1975b). A net uptake of potassium chloride accompanied by a hyperosmotic water transport was also demonstrated at 0°C (pH 7.2).

Theoretical analysis and the estimate of chloride permeability

In this section we develop expressions for the net transport of a uni-univalent salt across a membrane having a highly cation selective region and a highly anion selective region. We imagine these two re-

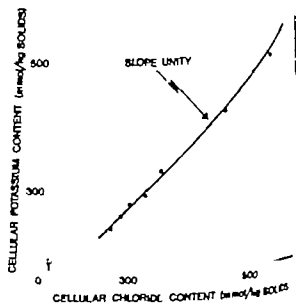


Fig. 5 The cellular content of potassium vs. the cellular content of chloride in cells from one net transport experiment (25°C, pH 6.8). The cells were prior to the experiment equilibrated with a salt solution (150 mM KCl, 150 mM sucrose) and resuspended in another salt solution (150 mM KCl). The experiment was started by addition of gramicidin (10^{-4} g/l) and the cells took up KCl in the presence of a KCl concentration difference across the cell membrane. At the appropriate times the cells were analyzed for potassium, chloride and water.

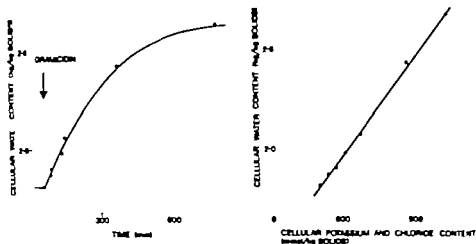


Fig. 6 The cellular water content as a function of time after addition of gramicidin (Fig. 6a) and as a function of the sum of the cellular content of potassium and chloride (Fig. 6b) in a net transport experiment (25°C, pH 6.8). The experimental conditions are described in legend to Fig. 5. The following equation was obtained by regression analysis of the cellular water content, Y , vs. the sum of the cellular content of potassium and chloride, X : Y (kg water/kg cell solids) = $0.00264X$ (mmol ion, potassium or chloride/kg cell solids) + 0.34963 , $r^2 = 0.998$.

ions to be physically separated in the membrane through the expressions we obtain will be similar to those derived from the Nernst-Planck flux equations assuming that the ions pass through a single and homogeneous regime. The reason for assuming the regions in our red cell membrane are physically separated is that we have created the cation selective region artificially using gramicidin. We want to determine the permeability of the naturally occurring chloride selective region—or in any case demonstrate which fraction the chloride transport by diffusion constitutes of the total chloride transport in gramicidin-treated human red cells.

We want to calculate net potassium chloride flux, J_{KCl} , through a mosaic membrane containing gramicidin channels in the presence of a potassium chloride concentration difference $\Delta(KCl)$. The only permeating species in cells and medium is potassium chloride and the potassium and chloride concentrations are under the conditions employed described by

$$[K]_i = [Cl]_i + [K]_o = [Cl]_o \quad (1)$$

This condition is only fulfilled at a given temperature at one single pH value, i.e. where the electrical net charge on hemoglobin is zero.

We assume that (1) the gramicidin-induced permeability is much greater than the endogenous

potassium permeability in the membrane, which we neglect, and (2) the chloride permeability is unaffected by gramicidin.

Fig. 7 shows the suggested equivalent circuit of the membrane. The batteries, E or E_{Cl} represent

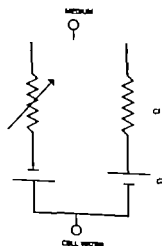


Fig. 7 The equivalent circuit representing the cell membrane of gramicidin-treated human red blood cells. The potassium and chloride concentration cells, E_K and E_{Cl} , arranged in parallel are the main sources of membrane current while R and R_{Cl} represent the resistance of the regions through which these ions pass. The dependence of R on gramicidin concentration is depicted by the arrow.

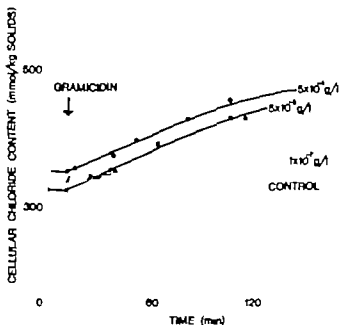


Fig. 8. The cellular content of chloride as a function of time after addition of various doses of gramicidin in 4 net transport experiments (25°C, pH 6.8). The experimental conditions are described in legend to Fig. 5 except for the gramicidin doses. The drawn curves are parallel at the two highest gramicidin doses indicating that chloride at high gramicidin concentration is the rate-limiting ion of the KCl flux.

the potassium and chloride concentration cells while R_k or R_{Cl} represent the resistances of the regions through which the ions pass. The R_k varies with the gramicidin content in the membrane.

The current through either limb of the circuit may be written

$$I_k = g_k (E_k - E_m) \quad (2a)$$

$$I_{Cl} = g_{Cl} (E_{Cl} - E_m)$$

where I_k or I_{Cl} are the potassium or chloride current densities in the inward direction, g_k or g_{Cl} are the corresponding conductances per unit area, and E_m is the electrical membrane potential difference with the outside solution as a reference. The potassium and chloride batteries are defined by (cf. (1))

$$E_k = (RT/F) \ln((K)_m / (K)_s) \\ = (RT/F) \ln((KCl)_m / (KCl)_s) \quad (3a)$$

$$E_{Cl} = (RT/F) \ln((Cl)_m / (Cl)_s) \\ = (RT/F) \ln((KCl)_m / (KCl)_s) \quad (3b)$$

where R is the universal gas constant, T is the

absolute temperature, the valence and F is Faraday's constant.

Hence

$$E_k = -E_{Cl}$$

At steady state of transport we have the zero-current condition

$$I_k + I_{Cl} = g_k (E_k - E_m) + g_{Cl} (E_{Cl} - E_m) = 0 \quad (4)$$

and the membrane potential difference is given by

$$E_m = (g_k - g_{Cl}) E_k / (g_k + g_{Cl}) \quad (5)$$

At steady state of transport the fluxes are given by

$$M_{KCl} = M_k = M_{Cl} = I_k / F = I_{Cl} / F \quad (6a)$$

where M_{KCl} , M_k and M_{Cl} are the fluxes of neutral salt of potassium and of chloride per unit area. From (2a), (3a), (5b) and (6a) we obtain the flux of neutral salt

$$M_{KCl} = (RT/F^2) (2g_k g_{Cl} / (g_k + g_{Cl})) \\ \ln((KCl)_m / (KCl)_s) \quad (6b)$$

We expand the natural logarithm after defining the potassium-chloride concentration difference $\Delta(KCl) = (KCl)_m - (KCl)_s$, noting that $\Delta(KCl)/KCl_s$ is much less than unity and we obtain

$$M_{KCl} = 2\Delta(KCl) / ((F^2(KCl)_s / RTg_k) \\ + (F^2(KCl)_s / RTg_{Cl})) \quad (6c)$$

Defining the potassium permeability coefficient P_k and the chloride permeability coefficient P_{Cl} by

$$P_k = RTg_k / F^2(KCl)_s \quad \text{and}$$

$$P_{Cl} = RTg_{Cl} / F^2(KCl)_s \quad \text{we obtain from (6c)}$$

$$M_{KCl} = P_k P_{Cl} \Delta(KCl) / (P_k + P_{Cl}) = P_{KCl} \Delta(KCl) \quad (6d)$$

which is Fick's equation of single salt flux where P_{KCl} is an operationally defined apparent permeability coefficient of KCl equal to $P_k P_{Cl} / (P_k + P_{Cl})$.

indicating an Arrhenius activation energy of app. 40 kJ/mole (10 kcal/mole)

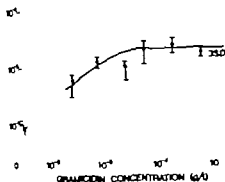


Fig. 8. The permeability coefficient of potassium chloride, P_{KCl} , as a function of gramicidin concentration in a suspending medium (pH 6.8, 25°C). The P_{KCl} is an experimentally defined apparent permeability coefficient of 3 derived in Results for the net transport experiment, the single salt diffusion case.

The salt flux will increase with gramicidin—as a potassium permeability increases—to a finite J_{Cl} which is determined by the chloride permeability (cf. (6d)). If experimentally we have that w_{Cl} is much less than the measured P then P_{Cl} will determine the value of P_{KCl} and chloride will be the rate-limiting ion of salt flux, since

$$J_{KCl} = Q P_{KCl} / (1 + (P_{Cl}/P_{KCl})) \approx 2P_{Cl} \quad (7)$$

and we have

$$J_{KCl} = P_{KCl} \Delta(KCl) \approx 2P_{Cl} \Delta(KCl) \quad (8)$$

Fig. 8 shows that net potassium chloride flux increased with gramicidin concentration to a finite J_{Cl} in contrast to the continuously increasing potassium flux (cf. Fig. 1 and Fig. 3a). So the experiments performed with a high gramicidin concentration fulfilled the requirements of eq. 8.

Fig. 9 shows the calculated P_{KCl} as a function of gramicidin concentration. One observes that P_{KCl} increased with gramicidin concentration until a plateau where P_{KCl} was gramicidin-insensitive. The gramicidin-insensitive P_{KCl} (pH 6.8, 25°C) was 4.2×10^{-5} cm/s S.D. 2.9×10^{-5} = 16, indicating a $P_{Cl} = 1.3 \times 10^{-4}$ cm/s.

The gramicidin-insensitive P_{KCl} at 0°C (pH 7.2) was 1.3×10^{-5} cm/s S.D. 0.7×10^{-5} = 17 indicating a P_{Cl} of 6.5×10^{-5} cm/s. The Q_{Cl} was app. three

DISCUSSION

The paper demonstrates a marked discrepancy in gramicidin-treated human red blood cells between the chloride permeability coefficient calculated from (1) chloride exchange and (7) net salt transport in the presence of a concentration gradient of salt. The calculation of the chloride permeability coefficient in the net salt transport study was simplified since the experiment was designed as a special case of the Nernst-Planck diffusion regime i.e. the single salt diffusion case. It is unnecessary in this situation to know the actual membrane potential difference as the term of the electrical driving force is eliminated in the equation of the permeability coefficient. The electrical membrane potential difference and therefore the electrical driving force was supposed to be zero in the exchange study because the distribution ratio of potassium chloride between cell water and medium was unity.

The chloride permeability coefficient calculated from tracer experiments at anion equilibrium is 1.9×10^{-4} cm/s (0°C, pH 7.2) regardless the gramicidin concentration (Fig. 3b). This value is 290 times the chloride permeability coefficient calculated from net salt transport experiments at high gramicidin concentrations (0°C, pH 7.2). These observations demonstrate that the slow chloride net transport compared to chloride exchange is not a gramicidin-induced decrease in the transport rate of the chloride transport apparatus which only for the reason of electroneutrality has to work like a chloride exchange mechanism in normal cells.

Are these results on chloride transport in gramicidin-treated cells valid in normal cells? Qualitatively it appears that chloride transport by diffusion also in normal cells only makes up a small fraction of the total chloride transport since (1) the characteristics of chloride exchange is unaffected by gramicidin (Fig. 4) and (2) cells containing gramicidin channels have a chloride permeability coefficient much less than expected from chloride exchange. The magnitude of this fraction is difficult to assess since the exact value depends on the selectivity of the gramicidin channels. Myers & Haydon (1972) noted that the transference number of chloride was 0.2 in gramicidin-treated artificial bilayers separated by calcium chloride. These

membranes are very low conductance membranes as calcium is almost totally excluded from the gramicidin channels. Consequently it is difficult to exclude the possibility that the chloride diffusion in red cells increases with gramicidin concentration. However (1) the chloride permeability coefficient is independent of gramicidin concentration at high gramicidin concentrations (Fig. 8) and (2) the value of the chloride permeability coefficient presented here agrees roughly with values obtained by investigators using valinomycin as cation transport inducing substance (Hunter 1977; Knauf et al. 1977).

Gramicidin has previously been used to investigate the chloride permeability in human red cells under various conditions. Qualitatively Scarpa et al. (1970) pointed out that the electrogenic chloride transport was much smaller than expected from data on chloride exchange given in the literature. Wieth, Dalmark, Gunn & Tosteson (1973) determined a chloride permeability coefficient of 1.2×10^{-7} cm/s (25°C, pH 6.8) from potassium chloride net flux into a low ionic strength medium in the presence of gramicidin and phloretin, a potent inhibitor of chloride exchange. This value is 6 times greater than the value presented here. The difference might be an effect of either the low ionic strength which is known to increase cation permeability (LaCelle & Rothstein 1966) or the presence of phloretin, a aglycone of phlorizin which is known to increase chloride permeability (Kaplan & Passow 1974).

The chloride permeability coefficient in unmodified red cells can be determined by measuring the electrical conductance of the cell membrane as the measuring technique is insensitive to a large electro-neutral chloride transport by exchange. However impalement of the tiny cells with glass electrodes invariably causes a leak around the electrode by which a rapid discharging of the membrane potential takes place. This difficulty is especially pronounced with the small human red cells (Lassen & Sten-Knudsen 1968; Jay & Burton 1969). The problem with the rapid discharging has probably been circumvented in the measurements of the membrane resistance in the large red blood cell of the *Amphura*. In that case resistances as high as 10 ohmcm² (18°C) has been reported (Hoffman & Lassen 1971; Lassen 1972; Lassen et al. 1974, 1978). These values should be compared with a "chloride resistance" of 4 ohmcm² calculated from chloride exchange in the same type of cells.

The chloride diffusion has a low temperature sensitivity with an activation energy of app. 4 kJ/mole (10 kcal/mole) in contrast to chloride exchange with an activation energy of 84–116 kJ/mole (20–28 kcal/mole) (Dalmark & Wieth 1972; Brahm 1977). The chloride exchange is orders of magnitude faster than chloride diffusion with a highly temperature-dependent factor: 2.9×10^4 (0°C) 0.7×10^4 (25°C) and 7×10^4 (body temperature).

In conclusion the original suggestion by Katch (1922) is still valid: the red cell membrane is relatively anion permeable in the sense that anion permeability exceeds cation permeability. The membrane is anion selective with a factor of 1.3×10^2 (0°C, pH 7.2) as the passive potassium permeability coefficient under identical conditions (temperature, pH, cell and medium composition): 5×10^{-11} cm/s (Dalmark 1975b). The anion selectivity lasts from 0°C to body temperature; both chloride and potassium diffusion has a low temperature sensitivity. The physiologic anion exchange, i.e. the Hamburger shift, is a temperature coupled transport process where anion influx and efflux are linked together by interaction between the anions and groups attached to the cell membrane. This anion transport by exchange is orders of magnitude faster than chloride transport by independent migration.

I am glad to express my indebtedness to Mrs B. Olsen for her valued technical assistance. This work supported by a grant from The Danish Heart Foundation, Copenhagen, Denmark.

REFERENCES

- BAMBERG E., ALPES H., APELLI, H. J., BENI, JANKO K., KOLB H. A., LAUGER, P. & GRUBER E. 1977. Studies on the gramicidin channel. *Biochemistry of membrane transport*. Proc. 4th Sciences (ed. G. Semenza and E. Carafoli), p. Springer Verlag, Berlin.
- BRAHM J. 1977. Temperature-dependent changes in chloride transport kinetics in human red cells. *J. Physiol.* 70, 281.
- CASS A. & DALMARK M. 1973. Equilibrium distribution of ions in nystatin-treated red cells. *Nature New Biol.* 44, 47.
- CASS A. & DALMARK M. 1974. Personal communication. In: *The red blood cell* (ed. D. M. Surge), p. 662. Academic Press, New York.
- DALMARK M. 1975a. Chloride transport in human cells. *J. Physiol. (Lond.)* 250, 39.
- DALMARK M. 1975b. Chloride and water distribution in human red cells. *J. Physiol. (Lond.)* 250, 63.

membranes are very low conductance membranes as calcium is almost totally excluded from the gramicidin channels. Consequently it is difficult to exclude the possibility that the chloride diffusion in red cells increases with gramicidin concentration. However (1) the chloride permeability coefficient is independent of gramicidin concentration at high gramicidin concentrations (Fig. 8) and (2) the value of the chloride permeability coefficient presented here agrees roughly with values obtained by investigators using valinomycin as cation transport inducing substance (Hunter 1977, Knauf et al. 1977).

Gramicidin has previously been used to investigate the chloride permeability in human red cells under various conditions. Qualitatively Scarpa et al. (1970) pointed out that the electrogenic chloride transport was much smaller than expected from data on chloride exchange given in the literature. Wieth, Dalmark, Gunn & Tosteson (1973) determined a chloride permeability coefficient of 1.2×10^{-7} cm/s (25°C, pH 6.8) from potassium chloride net flux into a low ionic strength medium in the presence of gramicidin and phloretin, a potent inhibitor of chloride exchange. This value is 6 times greater than the value presented here. The difference might be an effect of either the low ionic strength which is known to increase cation permeability (LaCelle & Rothstein 1966) or the presence of phloretin, a glycone of phlorizin which is known to increase chloride permeability (Kaplan & Passow 1974).

The chloride permeability coefficient in unmodified red cells can be determined by measuring the electrical conductance of the cell membrane as the measuring technique is insensitive to a large electroneutral chloride transport by exchange. However, impalement of the tiny cells with glass electrodes invariably causes a leak around the electrode by which a rapid discharging of the membrane potential takes place. This difficulty is especially pronounced with the small human red cells (Lassen & Sten-Knudsen 1968, Jay & Burton 1969). The problem with the rapid discharging has probably been circumvented in the measurements of the membrane resistance in the large red blood cell of the Amphibia. In that case resistances as high as 10^7 ohmcm² (18°C) has been reported (Hoffman & Lassen 1971, Lassen 1977, Lassen et al. 1974, 1978). These values should be compared with a "chloride resistance" of 4 ohmcm² calculated from chloride exchange in the same type of cells.

The chloride diffusion has a low temperature sensitivity with an activation energy of approximately 10 kcal/mole in contrast to chloride exchange with an activation energy of 84–126 kJ/mole (20–30 kcal/mole) (Dalmark & Wieth 1972, Brahm 1977). The chloride exchange is orders of magnitude faster than chloride diffusion with a highly temperature dependent factor: 2.9×10^4 (0°C), 0.7×10^4 (25°C) and 7×10^4 (body temperature).

In conclusion, the original suggestion by Brahm (1922) is still valid: the red cell membrane is not only anion permeable in the sense that anion permeability exceeds cation permeability. The cell membrane is anion selective with a factor of 1.3×10^2 (0°C, pH 7.2) as the passive potassium permeability coefficient under identical conditions (temperature, pH, cell and medium composition) is 5×10^{-1} cm/s (Dalmark 1975b). The anion selectivity lasts from 0°C to body temperature in both chloride and potassium diffusion has a low temperature sensitivity. The physiological anion change, i.e. the Hamburger shift is a tightly coupled transport process where anion influx and efflux are linked together by interaction between the anions and groups attached to the cell membrane. This anion transport by exchange is an order of magnitude faster than chloride transport by independent migration.

I am glad to express my indebtedness to Mrs. B. T. Olsen for her valued technical assistance. This work is supported by a grant from The Danish Heart Foundation, Copenhagen, Denmark.

REFERENCES

- BAMBERG, E., ALPES, H., APELL, H. J., BENZ, E., JANKO, K., KOLB, H. A., LAÜGER, P. & GRÖS, E. 1977. Studies on the gramicidin channel. In: *Biochemistry of membrane transport*. Proc. 1st Int. Conf. on Membrane Transport, Prague, 1976. J. Biol. Sci. (ed. G. Semenza and E. Carafoli), p. 179. Springer Verlag, Berlin.
- BRAHM, J. 1977. Temperature-dependent changes in chloride transport kinetics in human red cells. *J. Gen. Physiol.* 70: 283.
- CASS, A. & DALMARK, M. 1973. Equilibrium distribution of ions in nystatin-treated red cells. *Nature* 242: 44–47.
- CASS, A. & DALMARK, M. 1974. Personal communication. In: *The red blood cell* (ed. D. M. Surraort), p. 662. Academic Press, New York.
- DALMARK, M. 1975a. Chloride transport in human red cells. *J. Physiol. (Lond.)* 250: 39.
- DALMARK, M. 1975b. Chloride and water distribution in human red cells. *J. Physiol. (Lond.)* 250: 65.

Metabolic properties of nerve endings isolated from rat brain

E. JANSSON, M. H. HÄRKÖNEN and H. HELVE†

Department of Clinical Chemistry, University of Helsinki, Meilahdi Hospital, Helsinki, Finland

JANSSON, E.-E., HÄRKÖNEN, M. H. & HELVE, H. Metabolic properties of nerve endings isolated from rat brain. *Acta Physiol Scand* 1979, 107, 205-212. Received 23 Jan. 1979. ISSN 0001-6772. Department of Clinical Chemistry, University of Helsinki, Finland.

Energy metabolism was studied in nerve endings isolated from 3-week-old rat brain. Concentrations of glycogen, glucose, ATP, phosphocreatine and lactate were lower in synaptosomes than in the intact brain. The consumption of these endogenous substrates, the ability to generate high-energy phosphate and the production of acetylcholine were determined in aerobic and anaerobic conditions. Unlike nerve tissue in general, synaptosomes preferentially utilized endogenous ATP and phosphocreatine stores which, on incubation in the absence of exogenous substrates, were emptied long before glycogen stores were exhausted. The optimal medium for respiratory studies was found to have electrolyte concentrations equal to the extracellular fluid. The synaptosomes had an endogenous respiration rate of 6.3 nmol O₂/mg prot./min, measured with an oxygen electrode, and it probably reflects consumption of their glycogen stores. Glucose usually had no effect on the respiration rate of synaptosomes, but sometimes increased it slightly. However, after incubation in the presence of ascorbate synaptosomes showed an increase in respiration when glucose was added. ADP, when added with glucose, also stimulated respiration. Pyruvate and succinate always increased respiration, succinate usually having the stronger effect. The present results show that isolated nerve endings are metabolically intact, which justifies their use in research on neurotransmission. In addition, opposite to the present consensus, synaptic transmission does not seem primarily to depend on the availability of glucose but rather on local stores of high-energy phosphate compounds.

Key words: Synaptosomes, respiration, energy metabolism, synaptic function.

Present knowledge of the metabolism of nerve endings is limited and based mainly on the results of studies on the oxygen consumption of isolated nerve endings (synaptosomes). Such studies have shown that synaptosomes respire using glucose, pyruvate (Bradford 1969), glutamate and succinate (Verity 1972) as substrates, and that ATP and phosphocreatine can be synthesized in the presence of glucose (Bradford 1969). Little attention has been paid to the substrates that provide energy for synaptosomes, despite the observations that synaptic transmission is the aspect of nerve function most vulnerable to shortages of glucose (Larrabee & Klingman 1966; Härkönen et al. 1969).

The present study concerned the oxygen consumption, high-energy phosphate production and rates of energy usage by synaptosomes in various conditions. The results indicate that synaptosomes are metabolically intact and that local energy metabolism plays an important role in synaptic transmission.

MATERIAL AND METHODS

Preparation of synaptosomes. Three-week-old Sprague-Dawley rats of both sexes were decapitated and the brain, except for the cerebellum, was dissected out and homogenized in 0.32 mol/l ice-cold, oxygenated sucrose in glass homogenizer with Plexiglass pestle (clearance 250 µm) at 850 rpm for 2 min. In some experiments, the cerebral cortices were dissected out and used instead of whole-brain homogenates. The nuclear and crude mitochondrial fractions, and the subfractions containing myofibrils, synaptosomes and mitochondria, are isolated as described by Gray & Whittaker (1962). After one wash the synaptosomes were resuspended in 0.32 mol/l sucrose. The protein of the synaptosome suspension was determined according to Lowry et al. (1951). The purity of the fractions was checked by electron microscopy.

Incubation techniques. When oxygen consumption was determined, samples of the synaptosome suspension in sucrose were diluted with 1 ml of incubation medium and incubations were carried out in thermostated Plexiglass vessels at 30°C. In other experiments, the diluted synaptosome preparations were incubated at 37°C in stoppered 50-ml polypropylene centrifuge tubes (gentle shaking), into which gases (95% O₂+5% CO₂ or N₂) were bubbled through vented needles. Samples were withdrawn

Table 2. The concentrations of various substrates of energy metabolism in isolated nerve endings and in cerebral cortex of the rat (nmol/kg prot.)

— values referring to synaptosomes and cerebral cortex are means of at least two determinations or means \pm S.E. of 4 determinations

substrate	Synaptosomes	Cerebral cortex	
		Immediately frozen*	Delayed frozen*
glucose	4.20 \pm 0.51	28.8 \pm 0.66	18.0 \pm 0.22
lactate	0.30	4.05 \pm 0.68	1.47 \pm 0.36
pyruvate	2.81 \pm 0.34	17.8 \pm 0.06	5.86 \pm 0.82
succinate	2.29 \pm 0.43	11.4 \pm 1.98	2.19 \pm 0.65
citrate	5.22 \pm 1.41	24.4 \pm 0.83	34.0 \pm 2.64
ATP	94 \pm 0.36		
ADP	4.93 \pm 0.95		
AMP	0.031	0.020	

*— frozen in liquid nitrogen immediately after decapitation.

Skull opened and brain removed before freezing in liquid nitrogen.

Determined according to Raj & Harkness 1976.

mol/l. At 0.5–4 mmol/l Ca^{2+} respiration was slightly enhanced (8–10%) but at higher concentrations (8 mmol/l) clearly depressed. Mg^{2+} also slightly enhanced respiration at concentrations of 0.5–5.0 mmol/l. Neither ion had any stimulatory effect on respiration in the presence of 10 mmol/l pyruvate or succinate. No change in oxygen uptake occurred in glucose, pyruvate or succinate medium when the O_2^{2-} (0.5–10 mmol/l) or K^+ (1–20 mmol/l) concentration was increased stepwise. The negative results with high K^+ concentrations could in part be due to the fact that the synaptosomes might have been depolarized during storage in the cold sucrose solution. The short incubation time in the electrolyte medium was not sufficient to repolarize the synaptosomal membrane. In tests with various buffers imidazole-HCl, Tris-HCl, glycylglycine, bicarbonate) none seemed to be superior to the others.

The isolated synaptosomes contained large amounts of endogenous substrates and respired at an appreciable rate without addition of substrates (16.3 ± 1.0 nmol O_2 /mg prot./min, mean \pm S.E. of 5 synaptosomal preparations, range 4.02–12.4 nmol O_2 /mg prot./min). Oxygen consumption was linear during the first 3–5 min (the values given in Table 1 were measured within this time) but then often tended to decrease. Thus, when synaptosomes were incubated in oxygenated substrate-free medium at 30°C, respiration fell to about 50% in 30 min and to 20% in 60 min. Endogenous respiration was not significantly lowered when synaptosomes were stored at 0°C for as long as 6 h, although

sometimes the response to added substrates seemed to be weaker than that of freshly prepared synaptosomes.

Addition of 10 mmol/l glucose to the incubation medium did not have a constant effect (Table 1). Mostly respiration was unaffected, but in some experiments small increase was seen. Even with synaptosomes which had been aged by incubation at 30°C for 30–60 min in the absence of substrates, addition of glucose did not raise oxygen consumption significantly. However when synaptosomes were first incubated in 40 mmol/l arsenate for 1 h, which by itself did not stimulate respiration addition of glucose induced a 4-fold increase in oxygen consumption. Addition of 5 mmol/l ADP to a glucose medium produced a 70–100% increase in respiration (Table 1). The response was not linear and the highest values were measured during the first few minutes.

Pyruvate and succinate at a concentration of 10 mmol/l stimulated oxygen uptake, raising it to twice the level without any added substrate (Table 1). Respiration with pyruvate was not linear and after a few minutes only 40% of the effect remained.

FCCP (carbonyl cyanide *p*-trifluoromethoxy phenylhydrazone) and oligomycin were used to study the mechanisms controlling the respiration of synaptosomes. In a glucose medium, 1 mmol/l of FCCP had a slight stimulatory effect (34% mean increase) on the rate of oxygen consumption (Table 1). The effect of oligomycin was also small but in 4 expts. the addition of 1 $\mu\text{g/ml}$ oligomycin after

Table 1 Effect of substrates or inhibitors on endogenous respiration of synaptosomes

Endogenous respiration was 6.3 ± 1.0 nmol O_2 /mg prot./min (mean \pm S.E. of 8 expts.). All expts. were carried out at 30°C. The increase (+) or decrease (-) in oxygen uptake induced by an agent was calculated in comparison to the endogenous respiration in the particular experiments. Values are means \pm S.E. of 4-14 expts. indicated as the number of different batches of synaptosomes/the total number of tests.

Agent added	Effect of oxygen uptake nmol O_2 /mg protein $^{-1}$ min	Change (%)	No. of expts.
Glucose 10 mmol/l	+0.33 \pm 0.30	+5	8/14
Pyruvate, 10 mmol/l*	+5.90 \pm 0.45	+89 \pm 6	3/10
Succinate 10 mmol/l	+6.4 \pm 0.48	+83 \pm 4	4/12
ADP 1 mmol/l ^b	+1.46 \pm 0.16	+4 \pm 3	2/7
ADP 5 mmol/l	+5.08 \pm 1.35	+52 \pm 2	4/4
FCCP 10 ⁻⁶ mmol/l	+2.54 \pm 0.48	+34 \pm 6	2/7
Oligomycin 1 μ g/ml ^c	-0.10	-7	4/4

* During the first linear minute.

^b The effect of ADP was studied in the presence of 10 mmol/l glucose.

FCCP was added after glucose or glucose plus 1 or 5 mmol/l ADP.

^c The effect of oligomycin was studied in the presence of 10 mmol/l glucose.

with a long needle without interruption of incubation and fixed immediately with an equal volume of 0.6 mol/l ice-cold perchloric acid containing 2 mmol/l EDTA. The mixture was centrifuged in the cold at 3500 \times g for 5 min and a portion of the supernatant was neutralized (pH 6.5) with 2.5 mol/l $KHCO_3$.

Determination of oxygen consumption. The oxygen consumption of synaptosome suspensions was determined with a Clark-type oxygen electrode (Clark et al. 1953).

Determination of metabolites. Glycogen, ATP, ADP, AMP and lactate in the neutralized perchloric acid extract were measured by fluorometric enzymatic methods with a Farrand A 3 fluorometer (Lowry et al. 1964; Passonneau et al. 1967). As sucrose is partially hydrolysed in perchloric acid, glucose was determined in a $Ba(OH)_2$ - $ZnSO_4$ extract of synaptosomes (Härkönen et al. 1969). Ammonia production was determined by a fluorometric enzymatic method (Folbergrova et al. 1969).

Semi-quantitative evaluation of the vesicle content of incubated synaptosomes. For electron microscope studies a sample of the synaptosome suspension was diluted with ice-cold 2.5% glutaraldehyde solution in 0.1 mol/l phosphate buffer, pH 7.4. After fixation the synaptosomes were centrifuged and the pellet processed according to a conventional EM routine. Photographic negatives of representative areas were taken at 10500 \times magnification and after framing and coding projected onto a white lined background. The entire coded negative was independently inspected by two of the authors and every recognizable synaptosome was evaluated for its vesicle content by expressing the area filled with vesicles as a percentage of the whole area of the synaptosomes (except for the intrasynaptosomal mitochondria). Thus 100% denotes synaptosomes packed with vesicles whereas 0% denotes particles identified as synaptosome ghosts or as synaptosomes without intact vesicles. Every negative contained about 20 synaptosomes and each author evaluated about 100 synaptosomes in various states for each of the different incubation conditions. The validity of this subjective

method of quantification was confirmed by placement of actual counting of vesicles.

Reagents. The water used had been deionized, as it passed through charcoal and Millipore filters. Salts, amino acids and pyridine nucleotides were obtained from the Sigma Chemical Company (St. Louis, Mo., USA) or from Boehringer and Sohne (Mannheim, West Germany). L-lactate dehydrogenase was purchased from Worthington (Freehold, N.J., USA). Other chemicals used were commercially available products of analytical grade.

RESULTS

Purity of the synaptosomal fraction

The purity of every synaptosomal fraction prepared was checked by electron microscopy. The microendings were mainly well-preserved but the fractions also contained some unidentified membrane profiles, either empty nerve endings or fragments of glial origin. Mitochondrial contamination was less than 10% of all particles and consisted almost exclusively of small, apparently synaptosomal mitochondria.

Oxygen consumption

Respiration was studied routinely in a medium consisting of NaCl 136 (values in mmol per liter), KCl 5.6, $CaCl_2$ 2.2, NaH_2PO_4 1.2, $MgCl_2$ 1.3 and an imidazole buffer, pH 7.4-8.0.

The effects of Ca^{2+} , Mg^{2+} , K and PO_4^{3-} on synaptosomal consumption of oxygen in the presence of 10 mmol/l glucose were tested by measuring the concentration of each ion from zero to 10⁻⁴ M.

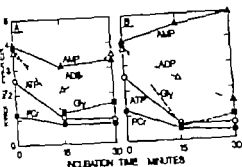


Fig. 4. Metabolism of high-energy phosphate compounds in synaptosomes in an oxygenated electrolyte medium at 37°C. The medium was supplemented with 10 mmol/l glucose (A) or with 10 mmol/l glucose + 5 mmol/l ADP (B) (ADP content of the blank incubation solution was subtracted from the ADP values). Results of typical experiment.

cal to prepare, glucose was not measured during incubation studies. During the first 5 min glycogen dropped to 65% of the initial level and after 15 min only about half of the original concentration was left (Fig. 1). The rate of consumption then slowed down, but at 3 h practically all glycogen had been used up. Lactate increased during the first 5 min and then decreased at a constant rate and at 3 h only trace amounts were detected. ATP and phosphocreatine fell at comparable rates after 5 min; their values were only about half the initial level after 1 h less than 10% was left.

Changes in metabolism during

incubation in nitrogen

When synaptosomes (3 separate preparations) were incubated in a nitrogen-saturated medium in the absence of added energy substrates, glycogen fell to 40% of the initial concentration in 10 min then decreased more slowly (Fig. 2). After an initial lag of 1 min the lactate concentration rose and the increase was roughly proportional to the decrease in glycogen. ATP and phosphocreatine fell rapidly during the first min reaching 30% and 15% of the respective initial levels. After 10–15 min, there was still less than 10% of these substrates left. An approximate metabolic rate can be calculated for the synaptosomes from the rate of use of high-energy phosphate ($\sim P$) seen as changes in ATP and phosphocreatine, glucose and glycogen (see e.g. Erlanson et al. 1969). During the first min of anoxia $\sim P$ was used at a rate of 10 $\mu\text{mol/kg prot./min}$. If

the P/O ratio is taken as 3 this rate of use of $\sim P$ is equivalent to an oxygen consumption of 3.3 nmol/mg prot./min . This is somewhat lower than the value measured with an oxygen electrode.

Generation of ATP and phosphocreatine

Synaptosomes were incubated with constant oxygenation in a medium containing 10 mmol/l glucose alone or 10 mmol/l glucose and 5 mmol/l ADP in order to study their ability to synthesize high-energy phosphate. Neither alone nor with ADP could glucose maintain the initial level of these high-energy phosphate compounds (Fig. 3). However, in the presence of glucose the decrease was smaller than during endogenous respiration, e.g. ATP decreased by 1.3 μmol compared with 2.2 μmol and phosphocreatine by 0.3 μmol compared with 1.7 μmol per kg protein during the first 15 min (values are means of 2 separate expts.). Furthermore, after this initial fall, the level of both compounds remained the same (ATP 1.0 and phosphocreatine 0.8 $\mu\text{mol/kg prot.}$) for 1 h while during endogenous respiration, high-energy phosphates were practically exhausted.

The presence of 10 mmol/l glucose could not prevent the concentrations of ADP and AMP from decreasing during incubation, especially during the first 15 min (Fig. 4A). In Fig. 4B (incubation medium supplemented with 10 mmol/l glucose + 5 mmol/l ADP) the linear decrease of ADP and the linear increase of AMP as a function of time, suggest the presence of enzymatic ADPase activity. Generation of high-energy phosphate was also studied in a Ca-free medium containing 20 mmol/l

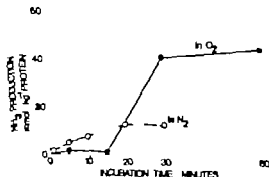


Fig. 5. Anaerobic production in isolated nerve endings in an electrolyte solution without added energy substrates in the presence or absence of oxygen at 37°C. Results of typical experiment.

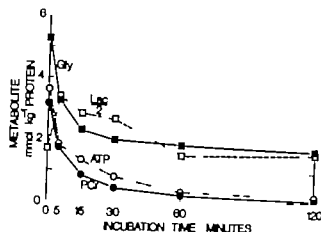


Fig. 1 Utilization of energy metabolites in isolated nerve endings. Synaptosomes were incubated at 37°C in oxygenated substrate-free electrolyte solution buffered with imidazole-HCl pH 7.4. At the times indicated samples were withdrawn from the suspension. Results of a typical experiment. Gly=glycogen, Lac=lactate and PCr=phosphocreatine.

glucose inhibited the respiration by 7%. Likewise when oligomycin was added after 40 mmol/l arsenate 18% inhibition was obtained.

Metabolite levels

Table 2 shows the concentration of energy metabolites measured in perchloric acid extracts of freshly prepared synaptosomes. The metabolite concentrations were considerably lower in the synaptosomes than in cerebral cortex which had been frozen immediately. The decrease was very rapid during the initial 15–20 s following decapitation while the brain was being dissected out and thus before it was

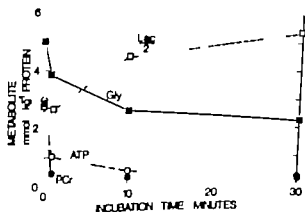


Fig. 2 Effect of anoxia on the utilization of energy metabolites in isolated nerve endings. A suspension of synaptosomes was incubated under nitrogen in the absence of added substrates at 37°C, and samples were taken at the times indicated. Results of a typical experiment.

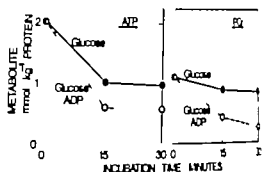


Fig. 3 Generation of ATP and phosphocreatine in synaptosomes in an oxygenated electrolyte medium at 37°C. The medium was supplemented with 10 mmol/l glucose with 10 mmol/l glucose + 5 mmol/l ADP. Results of a typical experiment.

chilled. This became evident when the metabolites were measured in extracts of cerebral cortex obtained either after freezing the head of the rat in liquid nitrogen immediately after decapitation or after dissection in the same way as for preparation of synaptosomes followed by freezing (Table 2). ATP and phosphocreatine concentrations were only a little lower in the synaptosomes than in the "delayed frozen" cerebral cortex and corresponded well to levels previously reported (Barber & Mellor 1976; Hawthorne & Pickard 1977; von Krause & Howard 1978). Thus during the actual isolation procedure the decrease was relatively slow. This was apparently due to the fact that the synaptosomes had adequate supplies of oxygen and nutrients and metabolism was slowed down by chilling. The differences in glucose and lactate levels between the synaptosomes and the "delayed frozen" cerebral cortex is probably due to diffusion of these compounds into the surrounding medium.

Changes in metabolites during incubation in oxygen

The concentrations of glycogen, ATP, phosphocreatine and lactate were followed during incubation in oxygen for 2–3 h in a substrate-free medium in 3 different synaptosomal preparations (Fig. 1). When synaptosomes are isolated in a sucrose gradient measurement of glucose is difficult because perchloric acid produces glucose via hydrolysis of sucrose. For measurements in freshly prepared synaptosomes we therefore used the Ba(OH)₂/ZnSO₄ precipitation method and found glucose to be approximately 0.3 mmol/kg prot. (Table 1). As the concentration was so low and extracts at

and synaptosomes we were only occasionally able to show a slight stimulation of oxygen consumption by glucose.

The insensitiveness of our synaptosome preparation to glucose is probably due to the short initial incubation time during which they were still respiring on endogenous glycogen stores. The failure to raise respiration in aged synaptosomes which had consumed most of their glycogen stores, may have been due to tissue catabolism and damage to all enzymatic structures during the aging process. This explanation is supported by the observation that during the first 30 min of incubation, ammonia production was considerable.

The insensitiveness of our synaptosome preparation to uncouplers apparently reflects the fact that the complex metabolic system which the synaptosome represents, respiration is controlled at a step which is not affected by uncouplers.

The stimulating effect of ADP on glucose respiration leads us to assume that ADP, despite its positive charge, does to some extent penetrate the synaptosomal membrane. Taking the ratio of the respiration rate in the presence of ADP to that in its absence as an indication of the respiratory control of the system (Chance & Williams 1956) a ratio of 1.7 is obtained with 5 mmol/l ADP which would suggest fair respiratory control. When synaptosomal mitochondria have been isolated in Ficoll-density media they have also shown good metabolic activity and respiratory control (Lau & Clark 1976).

Utilization of high-energy phosphates

Bradford (1969) reported that, with glucose as substrate, synaptosomes synthesized both ATP and phosphocreatine. Closer scrutiny of his data, however, shows that actually he measured the levels of ATP and phosphocreatine in synaptosomes after incubation for 1 h in various media in the presence of metabolic poisons. In our generation experiments we followed the concentration of both compounds during the course of incubation. The rapid initial decrease in ATP concentration could be due to the membrane Na^+/K^+ -ATPase (Abdel-Latif & Abood 1964) activated by temperature and Na^+ and K^+ in the incubation medium. The simultaneous decrease in phosphocreatine could thus be due to creatine kinase activity tending to synthesize ATP from ADP and phosphocreatine. After the initial fall

there was hardly any change in ATP or phosphocreatine concentration during the next 2-3 h. Our interpretation of these results is that Na^+/K^+ -ATPase activity, creatine kinase activity and oxidative phosphorylation supported by glucose (or glycogen), came to equilibrium and ATP and phosphocreatine reached a steady-state-concentration in the synaptosomes. The AMP deaminase activity localized in the synaptosomes (Jansson & Häkkinen to be published) would explain the decreasing sum of adenylates during incubation.

Energy metabolism and synaptic function

The function of nerve tissue, especially synaptic transmission (Larrabee & Klingman 1962, Häkkinen et al. 1969) is very sensitive to glucose deprivation. It has been shown that failure of transmission occurs long before ATP and phosphocreatine are exhausted in the ganglion, and this seems to coincide with depletion of hexoses (Häkkinen et al. 1969). Evidence also indicates that the locus of the failure is at the synaptic level and several explanations have been offered without direct experimental support (see Larrabee & Klingman 1962, Nicolescu et al. 1966, Häkkinen et al. 1969). The present results show that 2 h after the start of incubation (when transmission through the ganglion is known to fail Häkkinen et al. 1969) the synaptosomes were depleted of ATP and phosphocreatine, although glycogen was still present. Therefore, blockage of impulse propagation at the synaptic level appears to be due to local depletion of ATP in the nerve endings, followed by failure of the ion pump. The other possible explanation would be the catabolism of tissue elements in the absence of glucose; this hypothesis gains support from the high production of ammonia and disappearance of vesicles containing the transmitter. It might well be that failure of chemical transmission is due to the two phenomena together. The earlier hypothesis of depletion of acetyl-CoA, suggested because failure of transmission coincides with depletion of hexoses, seems no longer tenable (Häkkinen et al. 1969).

This work was supported by grants from the Medical Research Council in the Academy of Finland, the Sigrid Juselius Foundation, Helsinki, and the Finska Läkaresällskapet.

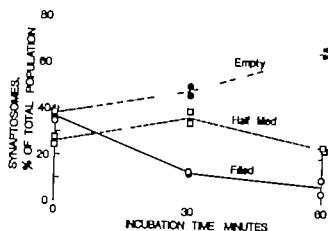


Fig. 6 The effect of incubation at 37°C in oxygenated electrolyte solution without added energy substrates on the preservation of synaptosomes. The "filled" synaptosomes contain the normal quantity of vesicles (occupying 60–100% of the synaptosome area) those which are "half filled" have lost about half their vesicles and the "empty" synaptosomes contain few if any vesicles (occupying at most 20% of the synaptosome area). The points represent the result of two independent investigators.

PO_4^{3-} . During the first 15 min 50% of the ATP and phosphocreatine were lost, but after this initial fall there was no further loss of either compound.

Ammonia production and vesicle preservation in incubated synaptosomes

For synaptosomes incubated in an oxygenated substrate free medium ammonia production was, after an initial lag about 1.5 mmol/kg prot./min during the first 30 min and then levelled off (Fig. 5). Under nitrogen ammonia production was much slower averaging 0.4 mmol/kg prot./min (Fig. 5).

Synaptosomes incubated at 37°C without substrates showed clear-cut morphological alterations as compared with unincubated synaptosomes stored at 4°C on ice. The number of vesicles decreased drastically and often enlarged vesicles as well as swollen intrasynaptosomal mitochondria could be seen. These changes were apparent after as little as 30 min but after incubation for 1 h most synaptosomes contained hardly any intact vesicles and were filled with debris. These changes were evaluated semi-quantitatively (see Material and methods). At zero time well preserved synaptosomes and synaptosomes with a very low vesicular content were about equal in number (Fig. 6). However after 1 h at 37°C only about 10% of the synaptosomes were in good condition and nearly 70%

were badly damaged (empty of vesicles). When performed in the absence or presence of oxygen incubation had the same morphological effect.

DISCUSSION

Pattern of utilization of energy reserves

Despite the low concentration of endogenous substrates the metabolic changes that occurred when the tissue was incubated in an oxygen or nitrogen atmosphere show that the synaptosomes are viable and utilize their energy reserves according to their requirements. In both conditions glycogen, ATP and phosphocreatine the major energy-yielding compounds in nervous tissue (besides glucose which *in vivo* originates from blood), were consumed in a pattern quite different from that seen in immature nerve cells (Hemminki & Härlid 1971) or in the sympathetic ganglion (Härlid *et al.* 1969). In synaptosomes ATP and phosphocreatine were used rapidly in both the presence and the absence of oxygen while in the other tissues they lasted much longer especially in oxygen. The initial decline of glycogen in synaptosomes as compared to ganglion cells or in immature nerve cells could be due to the fact that they are practically devoid of endogenous glucose which is the substrate utilized initially at least in the ganglia. In most of our synaptosome preparations, glucose was detectable at substantial concentrations only after ATP and phosphocreatine were used up. It is obvious from the small decrease in glycogen after 15 min in oxygen that this is not the main substrate supporting the substantial respiration. However, a considerable amount of ammonia was produced between 15 and 30 min after the start of incubation. This would explain the oxygen consumption, because most of the ammonia formed in nervous tissue during incubation *in vitro* originates from amino acids that are oxidatively deaminated (Weil-Malherbe 1962).

Oxygen consumption in isolated nerve endings

It has been shown previously that synaptosomes have an adequate endogenous respiration rate which can be stimulated by glucose or pyruvate (Bradford 1969, Venty 1972, Diamond & Finkelstein 1973, Bradford *et al.* 1978). With our technique the endogenous respiration rate was higher than in manometric techniques (Bradford 1969) but even

of synaptosomes, we were only occasionally able to show a slight stimulation of oxygen consumption by glucose.

The insensitiveness of our synaptosome preparation to glucose is probably due to the short incubation time during which they were still respiring on endogenous glycogen stores. The failure to resume respiration in aged synaptosomes, which consumed most of their glycogen stores, may have been due to tissue catabolism and damage to enzymatic structures during the aging process. An explanation is supported by the observation that during the first 30 min of incubation, ammonia production was considerable.

The insensitiveness of our synaptosome preparations to uncouplers apparently reflects the fact that the complex metabolic system which the synaptosome represents, respiration is controlled at a step which is not affected by uncouplers.

The stimulating effect of ADP on glucose respiration leads us to assume that ADP, despite its positive charge, does to some extent penetrate the synaptosomal membrane. Taking the ratio of the respiration rate in the presence of ADP to that in its absence as an indication of the respiratory control of the system (Chance & Williams 1956) a ratio of 7 is obtained with 5 mmol/l ADP which would suggest fair respiratory control. When intrasynaptosomal mitochondria have been isolated in Ficoll-across media they have also shown good metabolic activity and respiratory control (Lai & Turk 1976).

Generation of high-energy phosphates

Jefford (1969) reported that, with glucose as a substrate, synaptosomes synthesized both ATP and phosphocreatine. Closer scrutiny of his data, however, shows that actually he measured the levels of ATP and phosphocreatine in synaptosomes after incubation for 1 h in various media in the presence of metabolic poisons. In our generation experiments we followed the concentration of both compounds during the course of incubation. The rapid initial decrease in ATP concentration could be due to the membrane Na^+/K^+ -ATPase (Abdel-Latif & Abood 1964) activated by temperature and Na^+ and K^+ in the incubation medium. The simultaneous decrease in phosphocreatine could thus be due to creatine kinase activity tending to synthesize ATP from ADP and phosphocreatine. After the initial fall

there was hardly any change in ATP or phosphocreatine concentration during the next 2–3 h. Our interpretation of these results is that Na^+/K^+ -ATPase activity, creatine kinase activity and oxidative phosphorylation supported by glucose (or glycogen), came to equilibrium, and ATP and phosphocreatine reached a steady state-concentration in the synaptosomes. The AMP deaminase activity localized in the synaptosomes (Jansson & Häkkinen, to be published) would explain the decreasing sum of adenylates during incubation.

Energy metabolism and synaptic function

The function of nerve tissue, especially synaptic transmission (Larrabee & Klingman 1962, Häkkinen et al. 1969), is very sensitive to glucose deprivation. It has been shown that failure of transmission occurs long before ATP and phosphocreatine are exhausted in the ganglion, and this seems to coincide with depletion of hexoses (Häkkinen et al. 1969). Evidence also indicates that the locus of the failure is at the synaptic level and several explanations have been offered without direct experimental support (see Larrabee & Klingman 1962, Nicolescu et al. 1966, Häkkinen et al. 1969). The present results show that 2 h after the start of incubation (when transmission through the ganglion is known to fail, Häkkinen et al. 1969), the synaptosomes were depleted of ATP and phosphocreatine although glycogen was still present. Therefore, blockage of impulse propagation at the synaptic level appears to be due to local depletion of ATP in the nerve endings, followed by failure of the ion pump. The other possible explanation would be the catabolism of tissue elements in the absence of glucose: this hypothesis gains support from the high production of ammonia and disappearance of vesicles containing the transmitter. It might well be that failure of chemical transmission is due to the two phenomena together. The earlier hypothesis of depletion of acetyl-CoA, suggested because failure of transmission coincides with depletion of hexoses, seems no longer tenable (Häkkinen et al. 1969).

This work was supported by grants from the Medical Research Council in the Academy of Finland, the Sigrid Juselius Foundation, Helsinki, and the Finnish Lääkäriliiketoiminta.

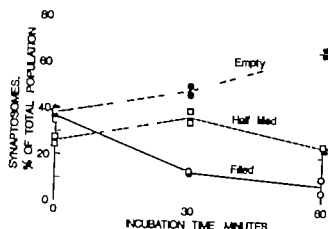


Fig. 6 The effect of incubation at 37°C in oxygenated electrolyte solution without added energy substrates on the preservation of synaptosomes. The "filled" synaptosomes contain the normal quantity of vesicles (occupying 60–100% of the synaptosome area) those which are "half filled" have lost about half their vesicles and the "empty" synaptosomes contain few, if any vesicles (occupying at most 20% of the synaptosome area). The points represent the result of two independent investigators.

PO_4^{3-} . During the first 15 min 50% of the ATP and phosphocreatine were lost but after this initial fall there was no further loss of either compound.

Ammonia production and vesicle preservation in incubated synaptosomes

For synaptosomes incubated in an oxygenated substrate free medium ammonia production was after an initial lag about 1.5 mmol/kg prot./min during the first 30 min and then levelled off (Fig. 5). Under nitrogen ammonia production was much slower averaging 0.4 mmol/kg prot./min (Fig. 5).

Synaptosomes incubated at 37°C without substrates showed clear-cut morphological alterations as compared with unincubated synaptosomes stored at 4°C on ice. The number of vesicles decreased drastically and often enlarged vesicles as well as swollen intrasynaptosomal mitochondria could be seen. These changes were apparent after as little as 30 min but after incubation for 1 h most synaptosomes contained hardly any intact vesicles and were filled with debris. These changes were evaluated semi-quantitatively (see Material and methods). At zero time well preserved synaptosomes and synaptosomes with a very low vesicular content were about equal in number (Fig. 6). However after 1 h at 37°C only about 10% of the synaptosomes were in good condition and nearly 70%

were badly damaged (empty of vesicles). This was performed in the absence or presence of oxygen; incubation had the same morphological effect.

DISCUSSION

Pattern of utilization of energy reserves

Despite the low concentration of endogenous substrates the metabolic changes that occurred when the tissue was incubated in an oxygen or nitrogen atmosphere show that the synaptosomes are able to utilize their energy reserves according to their requirements. In both conditions glycogen and phosphocreatine the major energy rich compounds in nervous tissue (besides those which in vivo originates from blood) were consumed in a pattern quite different from that seen in immature nerve cells (Hemminki & Harkonen 1969) or in the sympathetic ganglion (Harkonen *et al.* 1969). In synaptosomes ATP and phosphocreatine were used rapidly in both the presence and absence of oxygen while in the other tissues it lasted much longer especially in oxygen. The initial decline of glycogen in synaptosomes as compared to ganglion cells or in immature nerve cells could be due to the fact that they are practically devoid of endogenous glucose which is the substrate utilized initially at least in the ganglia. In most of our synaptosome preparations, glycogen was detectable at substantial concentrations only after ATP and phosphocreatine were used up. It is obvious from the small decrease in glycogen after 15 min in oxygen that this is not the main substrate supporting the substantial respiration. However a considerable amount of ammonia was produced between 15 and 30 min after the start of incubation which would explain the oxygen consumption, because most of the ammonia formed in nervous tissue during incubation in vitro originates from amino acids that are oxidatively deaminated (Weid-Müller 1962).

Oxygen consumption in isolated nerve endings

It has been shown previously that synaptosomes have an adequate endogenous respiration rate which can be stimulated by glucose or pyruvate (Bradford 1969; Venty 1972; Diamond & Iversen 1973; Bradford *et al.* 1978). With our technique the endogenous respiration rate was higher than with manometric techniques (Bradford 1969) but even

tryptophylglycine dipeptide in ACTH/MSH cells of the human hypophysis: its identification and studies on its antinociceptive effects in mice

PPO PARTANEN, SEPPÖ KAAKKOLA and ILPO KÄÄRIÄINEN

Unit of Pathology, Jorvi Hospital, Espoo and Department of Pharmacology,
University of Helsinki, Finland

PARTANEN S., KAAKKOLA S. & KÄÄRIÄINEN I. Tryptophylglycine dipeptide in ACTH/MSH cells of the human hypophysis: its identification and studies on its antinociceptive effects in mice. *Acta Physiol Scand* 1979 107 213-218. Received 26 Feb. 1979. ISSN 0001-6772. Unit of Pathology, Jorvi Hospital, Espoo and Department of Pharmacology, University of Helsinki, Finland.

The ACTH/MSH cells of the pars distalis and pars intermedia of the mammalian hypophysis contain peptides with amino-terminal tryptophan which exhibit a strong fluorescence after treatment with modified formaldehyde vapour methods and with glyoxylic acid in the tissue sections from freeze-dried specimens. By homogenization of the hypophyses in ethanolic glyoxylic acid and subsequent heating the peptides can be converted to highly fluorescent β -carboline derivatives, these can then be extracted with glacial acetic acid, separated by silica gel thin-layer chromatography and identified in UV light. Amino-terminal tryptophyl peptide from adult human hypophysis extracted and treated in this way gave the structure L-tryptophylglycine after acid hydrolysis. This structure was subsequently confirmed by producing a fluorescent derivative from authentic L-tryptophylglycine using the same reaction conditions as for the tissue homogenate. This derivative moved in the same way in thin-layer chromatography as fluorescent amino-terminal tryptophyl peptide extracted from human hypophyses. Thereafter study was made of the antinociceptive effects of authentic L-tryptophylglycine administered subcutaneously in mice both alone and together with morphine. L-tryptophylglycine had no antinociceptive effects alone and neither did it change morphine antinociception. Also it had no apparent effects on the behaviour of mice. Thus, ACTH/MSH cells contain a dipeptide whose physiological function differs from the effects of ACTH, MSH and endorphins.

Key words: Antinociception, extraction, hypophysis, tryptophyl peptide

The hormone storage granules of ACTH/MSH cells in both the pars distalis and the pars intermedia of all mammals studied contain substance(s) which exhibits a strong specific fluorescence after treatment with modified formaldehyde fluorescence histochemical methods and after treatment with glyoxylic acid (see Partanen 1978a). Previously this substance was thought to be serotonin, primary catecholamine, tryptamine or a tryptamine-like compound, but according to Sephadex G-5 chromatographic studies by Häkkinen et al (1972, 1974) it is a polypeptide or polypeptides with amino-terminal tryptophan. The hypophyseal fluorescent peptide can be demonstrated by immersion of freeze-dried hypophyseal sections in an alkaline solution of glyoxylic acid followed by heating leading to formation of highly fluorescent

dihydro- β -carboline derivatives (Partanen 1975). In model experiments glyoxylic acid treatment also appeared to induce the formation of a highly fluorescent product from amino-terminal tryptophyl dipeptide without breaking the peptide bond (Partanen 1976).

Following the same reaction principle, when rat hypophyses were homogenized and heated in glyoxylic acid-ethanol a strongly fluorescent substance could thereafter be extracted from the precipitate and separated by silica gel thin-layer chromatography (Partanen 1978b).

In the present work a study was made of the nature of this hypophyseal fluorogenic tryptophyl peptide extracted from human hypophysis. After its identification as L-tryptophylglycine research was carried out on its opioid-like effects *in vivo* in mice.

REFERENCES

- ABDEL-LATIF A. A. & ABOOD L. G 1964 Biochemical studies on mitochondria and other cytoplasmic fractions of developing rat brain. *J Neurochem* 11, 9-15.
- BARBERIS C & McILWAIN H 1976. 5 Adenine mononucleotides in synaptosomal preparations from guinea pig neocortex: their change on incubation, superfusion and stimulation. *J Neurochem* 26, 1015-1021.
- BRADFORD H F 1969 Respiration in vitro of synaptosomes from mammalian cerebral cortex. *J Neurochem* 16, 675-684.
- BRADFORD H F, WARD H K & THOMAS A. J 1978. Glutamine—a major substrate for nerve endings. *J Neurochem* 30, 1453-1459.
- CHANCE B & WILLIAMS G R 1956. The respiratory chain and oxidative phosphorylation. *Adv Enzymol* 17, 65-134.
- CLARK L. C. Jr, WOLF R. GRANGER, G & TAYLOR Z 1953 Continuous recording of blood oxygen tensions by polarography. *J Appl Physiol* 6, 189-193.
- DIAMOND I & FISHMAN R A 1973 Development of glucose oxidation in isolated nerve endings. *Nature* 243, 519-520.
- FOLBERGROVA J, PASSONNEAU J V, LOWRY O H & SCHULZ, D W 1969 Glycogen ammonia and related metabolites in the brain during seizures evoked by methionine sulfoximine. *J Neurochem* 16, 191-203.
- GRAY E G & WHITTAKER, V P 1962. The isolation of nerve endings from brain. An electron microscopic study of cell fragments derived by homogenization and centrifugation. *J Anat (Lond)* 96, 79-88.
- HÄRKÖNEN M H A, PASSONNEAU J V & LOWRY O H 1969 Relationships between energy reserves and function in rat superior cervical ganglion. *J Neurochem* 16, 1439-1450.
- HAWTHORNE, J N & PICKARD M R 1977 Phosphatidate metabolism in stimulated synaptosomes. *Biochem Soc Trans* 5, 57-59.
- HEMINKI K. & HÄRKÖNEN M 1974. Effect of energy reserves by cells isolated from embryonic brain. *Acta Physiol Scand* 91, 69-74.
- LAI J C K. & CLARK, J B 1976. Preparation and properties of mitochondria derived from synaptosomes. *Biochem J* 154, 43-432.
- LARRABEE M G & KLINGMAN J D 1964. Metabolism of glucose and oxygen in mammalian sympathetic ganglia at rest and in action. In: *Neurochemistry* (ed. by A. C. Elliott, L. H. Page and H. Quastel) pp. 150-176. Thomas, Springfield.
- LOWRY O H, ROSEBROUGH N J, FARR, A L & RANDALL, R J 1951 Protein measurement with Folin phenol reagent. *J Biol Chem* 193, 265-275.
- LOWRY O H, PASSONNEAU J V, HUSSEY, B E, BERGER, F X & SCHULZ, D W 1964 Effect of ischemia on known substrates and co-factors of the glycolytic pathway in brain. *J Biol Chem* 239, 12-17.
- NELSON KRAUSE D. C. & HOWARD, B D 1973 Energy utilization in the induced release of γ -aminobutyric acid from synaptosomes. *Brain Res* 147, 91-105.
- NICOLESCU P, DOLIVO M, ROUILLET, C & FOROGLIOU-KERAMEUS C 1966. The effect of deprivation of glucose on the ultrastructure and function of the superior cervical ganglion of the rat in vitro. *J Cell Biol* 7, 267-285.
- PASSONNEAU J V, GATFIELD, P D, SCHULZ, D W & LOWRY O H 1967 An enzymatic method for measurement of glycogen. *Analyt Biochem* 19, 1-6.
- RAU K. & HÄRKÖNEN M 1976. Determination of cyclic adenosine 3',5'-monophosphate in tissue. *Anal J Clin Lab Invest* 36, 161-168.
- WEIL-MALHERBE H 1962. Ammonia metabolism in the brain. In: *Neurochemistry* (ed. by A. C. Elliott, L. H. Page and J. H. Quastel), pp. 321-336. Thomas, Springfield.
- VERITY M A 1972. Cation modulation of synaptic respiration. *J Neurochem* 19, 1305-1317.

Tryptophylglycine dipeptide in ACTH/MSH cells of the human hypophysis: its identification and studies on its antinociceptive effects in mice

PPO PARTANEN, SEPPO KAAKKOLA and ILPO KÄÄRIÄINEN

Unit of Pathology, Jorvi Hospital, Espoo and Department of Pharmacology, University of Helsinki, Finland

PARTANEN S., KAAKKOLA, S. & KÄÄRIÄINEN I. Tryptophylglycine dipeptide in ACTH/MSH cells of the human hypophysis: its identification and studies on its antinociceptive effects in mice. *Acta Physiol Scand* 1979, 107: 213-218. Received 26 Feb. 1979. ISSN 0001-6772. Unit of Pathology, Jorvi Hospital, Espoo and Department of Pharmacology, University of Helsinki, Finland.

The ACTH/MSH cells of the pars distalis and pars intermedia of the mammalian hypophysis contain peptides with amino-terminal tryptophan which exhibit strong fluorescence after treatment with modified formaldehyde vapour methods and with glyoxylic acid in the tissue sections from freeze-dried specimens. By homogenization of the hypophyses in ethanolic glyoxylic acid and subsequent heating the peptides can be converted to highly fluorescent β -carboline derivatives; these can then be extracted with glacial acetic acid, separated by silica gel thin-layer chromatography and identified in UV light. Amino-terminal tryptophyl peptide from adult human hypophysis extracted and treated in this way gave the structure L-tryptophylglycine after acid hydrolysis. This structure was subsequently confirmed by producing fluorescent derivative from authentic L-tryptophylglycine using the same reaction conditions as for the tissue homogenate. This derivative moved in the same way in thin-layer chromatography as fluorescent amino-terminal tryptophyl peptide extracted from human hypophysis. Thereafter, study was made of the antinociceptive effects of authentic L-tryptophylglycine administered subcutaneously in mice both alone and together with morphine. L-tryptophylglycine had no antinociceptive effects alone and neither did it change morphine antinociception. Also it had no apparent effects on the behaviour of mice. Thus, ACTH/MSH cells contain dipeptide whose physiological function differs from the effects of ACTH, MSH and endorphins.

Key-words: Antinociception, extraction, hypophysis, tryptophyl peptide

The hormone storage granules of ACTH/MSH cells in both the pars distalis and the pars intermedia of all mammals studied contain substance(s) which exhibits a strong specific fluorescence after treatment with modified formaldehyde fluorescence histochemical methods and after treatment with glyoxylic acid (see Partanen 1978a). Previously this substance was thought to be serotonin, primary catecholamine, tryptamine or tryptamine-like compound but according to Sephadex G25 chromatographic studies by Håkansson et al. (1972, 1974) it is a polypeptide or polypeptides with amino-terminal tryptophan. The hypophyseal fluorogenic peptide can be demonstrated by immersion of freeze-dried hypophyseal sections in an ethanolic solution of glyoxylic acid followed by heating leading to formation of highly fluorescent

dihydro- β -carboline derivatives (Partanen 1975). In model experiments glyoxylic acid treatment also appeared to induce the formation of a highly fluorescent product from amino-terminal tryptophyl dipeptide without breaking the peptide bond (Partanen 1976).

Following the same reaction principle, when rat hypophyses were homogenized and heated in glyoxylic acid-ethanol a strongly fluorescent substance could thereafter be extracted from the precipitate and separated by silica gel thin-layer chromatography (Partanen 1978b).

In the present work a study was made of the nature of this hypophyseal fluorogenic tryptophyl peptide extracted from human hypophysis. After its identification as L-tryptophylglycine research was carried out on its opioid-like effects *in vivo* in mice.



Fig. 1 The pars distalis of the hypophysis obtained within 48 h after death from a cadaver stored at 4°C. Yellow cytoplasmic fluorescence in some pars distalis cells induced by immersion of freeze-dried deparaffinized sections in 4% glyoxylic acid monohydrate in ethanol at 22°C for 5 min followed by heating at 100°C for 5 min. $\times 200$.

The project was stimulated by recent findings of substances of hypophyseal origin possessing strong opiod-like effects.

MATERIALS AND METHODS

Source of human hypophyse. Six human macroscopically normal hypophyses were obtained at autopsy from adult patients within 48 h after death. The cadavers were stored at 4°C. The hypophyses were stored after dissection at -50°C.

Fluorescence histochemistry. Two hypophyses were freeze-dried and embedded in paraffin wax without formaldehyde vapour treatment. The deparaffinized sections were briefly rinsed in absolute ethanol and immersed in 4% glyoxylic acid monohydrate (Sigma) in absolute ethanol for 5 min at 22°C, blotted dry and heated at 100°C for 5 min and then embedded in Diatex (AB Wilh. Becker) (Partanen 1975). The sections were examined and photographed with a Leitz Orthoplan fluorescence microscope equipped with an HBO 700 high pressure mercury lamp (Osram) as UV light source, the primary filters were BG 38, BG 3 and UG 1 and the secondary filter was K 470.

Extraction of hypophyseal fluorogenic peptide. Four

hypophyses (wet weight 1.1 g) were homogenized at 4°C with a glass homogenizer in 5 volumes of 4% glyoxylic acid monohydrate (GA) in ethanol. The homogenate was transferred to a glass tube, which was stoppered and heated at 65°C for 1 h. After cooling to 22°C the homogenate was centrifuged for 15 min at a speed of 3000 rpm. The precipitate was washed with 2 volumes of GA-ethanol and recentrifuged. The precipitate was washed 3 times with 3 volumes of diethyl ether and extracted three times with 3 volumes of glacial acetic acid (Sigma 1978b). The extract was allowed to evaporate and the volume was finally adjusted with glacial acetic acid to 500 μ l.

Thin-layer chromatography. Ascending thin-layer chromatography was carried out on precoated silica gel plates without a fluorescence indicator (by γ -radiation 0.25 mm, Silica gel 60 E, Merck). All solvents were analytical grade. The following solvent systems (v/v) were used: 1) *n*-butanol-glacial acetic acid-water (1:1:2), 2) *n*-butanol-ethanol-glacial acetic acid-water (2:1:1:3), 3) isopropanol-water (4:1), 4) *n*-butanol-glacial acetic acid-water (4:1:1), 5) *n*-butanol-glacial acetic acid (5:1:4, upper phase), 6) *n*-butanol-acetone-water-NH₃ (15:15:5:1). The fluorescence on the plate was studied with excitation light at 370 nm and photographed through a secondary cut-off filter (460 nm). Ninhydrin reagent (0.1% ninhydrin, E. Merck) in *n*-butanol-glacial acetic acid (9:1) or 0.1% amino black (E. Merck) in acetic acid was used to visualize the chromatograph extract and the reference amino acids.

Acid hydrolysis. The fluorescent bands separated for hypophyseal extract in thin-layer chromatography in solvent system 1 were scraped off and extracted at 22°C with 400 μ l of glacial acetic acid for 30 min and with 200 μ l for 10 min. As a control the same area as above was scraped off from the pure plate and treated in the same way. The glacial acetic acid extracts were allowed to evaporate to dryness and dissolved in 0.5 ml of 6 N HCl, transferred to glass tubes filled with N₂, stoppered and heated at 25°C for 26 h or 72 h. The hydrolysates were then evaporated to dryness and dissolved in 90 μ l of 0.1 N HCl. Amino acids (United States Biochemical Corporation) dissolved in 0.1 N HCl (1 mg/ml) were used as a reference. They were pipetted in amounts of 1 μ l (1 μ g); thereafter the plates were aerated for 30 min and chromatographed.

Fluorescence model experiments. 1) L-Tryptophan solution 0.5 ml (1 mg/ml dissolved in 0.1 N HCl) and 1 μ l of 4% GA-ethanol were heated at 65°C for 1 h, in a reaction producing highly fluorescent β -carbolines (Björklund et al. 1972). 3 μ l of this solution, which turned yellow, was used as a reference substance for hypophyseal fluorogenic substance and for its hydrolysate. 2) Small amounts of pure L-tryptophan and L-tryptophylglycine (Sigma) were treated in the same way as the hypophyses, and glacial acetic acid extract (coloured yellow) were used in amounts of 2-3 μ l as a reference for hypophyseal extract and for its hydrolysate.

Assessment of antinociception. In the antinociception experiments male white mice of the NMRI strain, aged 36-40 g were used. They were kept on a standard diet and given tap water ad libitum. The nociceptive responses were tested using the hot plate method (Eddy & Lemmon).

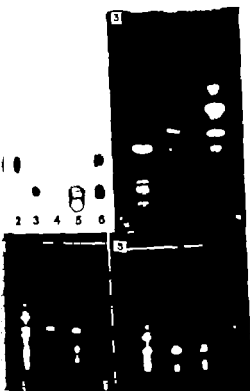


Fig. 2. A silica gel chromatograph of 15 μ l of acid hydrolysate of hypophyseal fluorescent band (5) developed in α -butanol-acetic acid-water-25% NH_3 (15:15:15:1 v/v) and sprayed with ninhydrin. 4: control acid hydrolysate of pure silica gel plate treated in the same way as the fluorescent hypophyseal band. Glycine is seen in the acid hydrolysate of the fluorescent band. 1: Pro. 2, Ser. 3: Gly. 6: Ser+Ser+Gly.

Fig. 3. A fluorescence photomicrograph of silica gel thin layer chromatograph of original hypophyseal extract. Lich was homogenized in 4% ethanolic glyoxylic acid (left), of acid hydrolysate of hypophyseal fluorescent band (centre) and of L-tryptophan (right) treated with glyoxylic acid. Solvent system α -butanol-glacial acetic acid-water (4:1:1 v/v). One strongly yellow fluorescent band seen in the original hypophyseal extract. Two weak blue fluorescent bands are seen near the origin. Acid hydrolysis of the strongly fluorescent band produces an additional blue fluorescent band, which moves in the same way as the blue fluorescent band of L-tryptophan treated with glyoxylic acid.

Fig. 4. 5 Fluorescence photomicrographs of silica gel thin layer chromatograph of the original hypophyseal extract (centre), of L-tryptophan (left) and of L-tryptophylglycine (right) treated and extracted in exactly the same way as hypophyseal homogenate. The hypophyseal fluorescent band moves in the same way as the fluorescent derivative of L-tryptophylglycine and as both the colour of fluorescence is yellow. Although these bands move in the same way as the fluorescent derivative of L-tryptophan, L-tryptophan gives different pattern of fluorescent bands,

1953). All injections were given s.c. in doses of 0.1 ml/10 g. The substances used were L-tryptophylglycine and (α -)morphine hydrochloride (Pharmacospecta Nordica). They were dissolved in 0.9% NaCl solution. The doses of morphine given refer to the base. Student's *t*-test was used in the statistical treatment of the results.

RESULTS

Fluorescence histochemistry In the hypophyseal sections treated with GA-ethanol numerous oval to round cells in the pars distalis and the invaginating cells of the pars nervosa exhibited moderate to strong yellow fluorescence restricted to the cytoplasm (Fig. 1).

Thin-layer chromatography of hypophyseal extract Two chromatographic plates were given an application of 200 μ l of hypophyseal extract as one band 18 cm in length. The plates were developed in solvent system 1. In UV light one strongly yellow fluorescent band (corresponding to 46.7 mg of hypophyseal wet weight/1 cm) was seen. In addition, one strongly fluorescent band or spot was observed when the extract (3–20 μ l) was chromatographed in solvent systems 2, 3, 4 and 6 (Figs. 3–5). The fluorescent spots did not stain with ninhydrin but did stain weakly with amido black. A chromatographed strongly fluorescent band was scraped off from the 200 μ l extracts and extracted with glacial acetic acid. From the new extract, 360 μ l was evaporated and subjected to acid hydrolysis. The hydrolysis times were 26 and 72 h. Twenty μ l of extract were also pipetted as a band (10 mm) onto chromatographic plates and the plates were developed in solvent systems 2 and 3. One strongly fluorescent band was seen in UV light the R_f values were 0.33 and 0.61 respectively. The spots did not stain with ninhydrin and no stained bands were seen on the plates.

Thin-layer chromatography of acid hydrolysate Five μ l of acid hydrolysate (corresponding to 42 mg of original hypophyseal wet weight) was applied as one spot together with the control hydrolysate of pure silica gel and with reference amino acids, and developed in solvent system 4. The front was allowed to move 118 mm, and the following R_f values were obtained after visualization of amino acids

and some fluoresce blueably Fig. 4 solvent system as in Fig. 3. Fig. 5 solvent system α -butanol-ethanol-glacial acetic acid-water (2:1:1:1 v/v).



Fig. 1 The pars distalis of the hypophysis obtained within 48 h after death from a cadaver stored at 4°C. Yellow cytoplasmic fluorescence in some pars distalis cells induced by immersion of freeze-dried deparaffinized sections in 4% glyoxylic acid monohydrate in ethanol at -2°C for 5 min followed by heating at 100°C for 5 min. $\times 700$.

The project was stimulated by recent findings of substances of hypophyseal origin possessing strong opioid-like effects.

MATERIALS AND METHODS

Source of human hypophyses Six human macroscopically normal hypophyses were obtained at autopsy from adult patients within 48 h after death. The cadavers were stored at -40°C. The hypophyses were stored after dissection at -40°C.

Fluorescence histochemistry Two hypophyses were freeze-dried and embedded in paraffin wax without formaldehyde vapour treatment. The deparaffinized sections were briefly rinsed in absolute ethanol and immersed in 4% glyoxylic acid monohydrate (Sigma) in absolute ethanol for 5 min at 22°C, blotted dry and heated at 100°C for 5 min and then embedded in Duxtex (AB Wih. Beckert) (Partanen 1975). The sections were examined and photographed with a Leitz Orthoplan fluorescence microscope equipped with an HBO 700 high pressure mercury lamp (Osram) as UV light source; the primary filters were BG 38, BG 3 and UG 1 and the secondary filter was K 470.

Extraction of hypophyseal fluorogenic peptide Four

hypophyses (wet weight ≈ 1 g) were homogenized with a glass homogenizer in 5 volumes of 4% glyoxylic acid monohydrate (GA) in ethanol; the homogenate was transferred to a glass tube, which was stoppered, heated at 65°C for 1 h. After cooling to $\approx 20^\circ\text{C}$, the homogenate was centrifuged for 15 min at a speed of 3000 r/min. The precipitate was washed with 5 volumes of GA-ethanol, recentrifuged. The precipitate was washed 3 times with 3 volumes of diethyl ether and extracted 30 min with 3 volumes of glacial acetic acid (E. Merck 1978b). The extract was allowed to evaporate to dryness and the volume was finally adjusted with glacial acetic acid to 400 μl .

Thin-layer chromatography Ascending thin-layer chromatography was carried out on precoated silica plates without a fluorescence indicator (layer 0.1–0.5 mm, Silica gel 60 E, Merck). All solvents were analytical grade. The following solvent systems were used: 1) *n*-butanol–glacial acetic acid–water (1:1:1), 2) *n*-butanol–ethanol–glacial acetic acid–water (1:1:3), 3) isopropanol–water (4:1), 4) *n*-butanol–glacial acetic acid–water (4:1:1), 5) *n*-butanol–glacial acetic acid (5:1:4, upper phase), 6) *n*-butanol–acetic acid–NH₃ (15:15:5:1). The fluorescence in the plates was studied with excitation light at 370 nm, and photographed through a secondary cut-off filter (460 nm, Schott reagent) (0.1% ninhydrin, E. Merck) in *n*-butanol–glacial acetic acid (9:1) or 0.1% amino black (E. Merck) in glacial acetic acid was used to visualize the chromatographic extract and the reference amino acids.

Acid hydrolysis The fluorescent bands separated from hypophyseal extract in thin-layer chromatography in solvent system 1 were scraped off and extracted at 25°C with 400 μl of glacial acetic acid for 30 min and with 200 μl for 15 min. As a control, the same area as above was scraped off from the pure plate and treated in the same way. The glacial acetic acid extracts were allowed to evaporate to dryness and dissolved in 0.5 ml of 6 N HCl, transferred to glass tubes filled with N₂, stoppered and heated at 70°C for 26 h or 7 h. The hydrolysates were then evaporated to dryness and dissolved in 90 μl of 0.1 N HCl. Amino acids (United States Biochemical Corporation) dissolved in 0.1 N HCl (1 mg/ml) were used as a reference. They were precipitated in amounts of 1 μl (1 μg), thereafter the plates were aerated for 30 min and chromatographed.

Fluorescence model experiments 1) Tryptophan solution 0.5 ml (1 mg/ml) dissolved in 0.1 N HCl and 1 μl of 4% GA-ethanol were heated at 65°C for 1 h, as a reaction producing highly fluorescent β -carbolines (Bjorklund et al. 1977). 3 μl of this solution, which turned yellow, was used as a reference substance for hypophyseal fluorogenic substance and for its hydrolysis. 2) Small amounts of pure L-tryptophan and L-tryptophylglycine (Sigma) were treated in the same way as the hypophyses, and glacial acetic acid extract (coloured yellow) were used in amounts of 3 μl as a reference for hypophyseal extract and for its hydrolysis.

Mouse formalin experiments In the animal experiments male white mice of the NMRI strain (approx. 16–40 g) were used. They were kept on a standard diet and given tap water ad libitum. The nociceptive response was tested using the hot plate method (Daly & Leinhardt

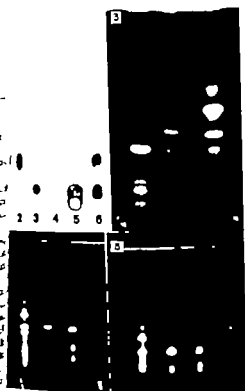


Fig. 2. A silica gel chromatograph of 15 μ l of acid hydrolysate of hypophyseal fluorescent band (5) developed in *n*-butanol-acetone-water-25% NH₄OH (15:15:15:1) and sprayed with ninhydrin. 4: control acid hydrolysate of pure silica gel plate treated in the same way as the fluorescent hypophyseal band. Glycine is seen in the acid hydrolysate of the fluorescent band. 1: Pro 2, Ser 3, Gly 6, His 5, Arg 4.

Fig. 3. A fluorescence photomicrograph of silica gel thin layer chromatograph of original hypophyseal extract, which was homogenized in 4% ethanolic glyoxylic acid (left), of acid hydrolysate of hypophyseal fluorescent band (centre) and of L-tryptophan (right) treated with glyoxylic acid. Solvent system: *n*-butanol-glacial acetic acid-water (4:1:1). (v) One strongly yellow fluorescent band is seen in the original hypophyseal extract; two weak yellow fluorescent bands are seen near the origin. Acid hydrolysate of the strongly fluorescent band produces an additional blue fluorescent band, which moves in the same way as the blue fluorescent band of L-tryptophan treated with glyoxylic acid.

Fig. 4. 5 Fluorescence photomicrographs of silica gel thin layer chromatograph of the original hypophyseal extract (centre), of L-tryptophan (left) and of L-tryptophylglycine (right) treated and attracted in exactly the same way as hypophyseal homogenate. The hypophyseal fluorescent band moves in the same way as the fluorescent derivative of L-tryptophylglycine and in both the colour of fluorescence is yellow. Although these bands move in the same way as the fluorescent derivative of L-tryptophan, L-tryptophan gives different pattern of fluorescent bands.

1953). All injections were given s.c. in a volume of 0.1 ml/10 g. The substances used were L-tryptophylglycine and (-)-morphine hydrochloride (Pharmacopecta Nordica). They were dissolved in 0.9% NaCl solution. The doses of morphine given refer to the base. Student's *t*-test was used in the statistical treatment of the results.

RESULTS

Fluorescence histochemistry In the hypophyseal sections treated with GA-ethanol numerous oval to round cells in the pars distalis and the invading cells of the pars nervosa exhibited moderate to strong yellow fluorescence restricted to the cytoplasm (Fig. 1).

Thin-layer chromatography of hypophyseal extract Two chromatographic plates were given an application of 200 μ l of hypophyseal extract as one band 18 cm in length. The plates were developed in solvent system 1. In UV light one strongly yellow fluorescent band (corresponding to 46.7 mg of hypophyseal wet weight/1 cm) was seen. In addition, one strongly fluorescent band or spot was observed when the extract (3–20 μ l) was chromatographed in solvent systems 2, 3, 4 and 6 (Figs. 3–5). The fluorescent spots did not stain with ninhydrin but did stain weakly with amido black. A chromatographed strongly fluorescent band was scraped off from the 200 μ l extracts and extracted with glacial acetic acid. From the new extract 360 μ l was evaporated and subjected to acid hydrolysis. The hydrolysis times were 26 and 72 h. Twenty μ l of extract were also pipetted as a band (10 mm) onto chromatographic plates and the plates were developed in solvent systems 2 and 3. One strongly fluorescent band was seen in UV light, the R_f values were 0.33 and 0.61 respectively. The spots did not stain with ninhydrin and no stained bands were seen on the plates.

Thin-layer chromatography of acid hydrolysate Five μ l of acid hydrolysate (corresponding to 42 mg of original hypophyseal wet weight) was applied as one spot together with the control hydrolysate of pure silica gel and with reference amino acids, and developed in solvent system 4. The front was allowed to move 118 mm and the following R_f values were obtained after visualization of amino acids

and some fluorescence bluishly (Fig. 4, solvent system as in Fig. 3). Fig. 5 solvent system *n*-butanol-ethanol-glacial acetic acid-water (2:1:1:1) (v).

Table 1 The effect of L-tryptophylglycine on the reaction times of mice in the hot plate test (mean \pm S.E.)

Saline or L-tryptophylglycine were injected s.c. 5–9 mice in each group. The values of L-tryptophylglycine group are significantly different from those of corresponding saline group.

Time after injection (min)	Treatment			
	Saline	L-tryptophylglycine		
		1 mg/kg	10 mg/kg	100 mg/kg
10	7.8 \pm 0.9	8.2 \pm 0.6	—	—
20	7.8 \pm 0.7	9.1 \pm 0.7	7.6 \pm 0.4	—
30	7.8 \pm 0.7	8.8 \pm 0.4	—	6.5 \pm 0.6
40	8.4 \pm 0.7	8.0 \pm 0.5	—	—

with ninhydrin. Ser 0.21 Phe 0.53 Asp 0.18 Val 0.42 Tyr 0.49 Glu 0.74 Arg 0.08 CysH 0.07 Trp 0.55 His 0.07 Thr 0.27 Met 0.45 Cys-SCy 0.07 Lys 0.06 Ala 0.28 Ile 0.51 Asn 0.18 Pro 0.21 Gly 0.22 Leu 0.53 and the acid hydrolysate of fluorescent band 0.21. The colour was violet as in the serine and glycine spots, thus differing from the proline spot which was yellow. The hydrolysate of pure silica gel plate did not give any definite spot. The results were the same after 26 and 77 h of hydrolysis. Thus the conclusion was drawn that hypophyseal amino-terminal tryptophyl peptide contains either Ser or Gly or Pro or some combination of these amino acids. Thereafter acid hydrolysate from a fluorescent band was developed in several solvent systems and only in system 6 did Ser and Gly move clearly separately. Pro and Gly also moved separately (Fig. 7). Glycine was thus identified in the hydrolysate.

Thin layer chromatography of fluorescent bands. When portions of acid hydrolysate of hypophyseal extract (2.5–20 μ l) were chromatographed in the

solvent systems described two fluorescent spots/bands were seen in all except solvent system 3. One moved as a hypophyseal fluorescent band, and the spots were yellow fluorescent; the second moved as one fluorescent spot or band of GA-tryptophan nature and the spots were bluish fluorescent (Fig. 3). Taking together the observations of the presence of both amino-terminal tryptophan and glycine in the hypophyseal fluorogenic peptide, the original hypophyseal extract and products of L-tryptophyl and L-tryptophylglycine treated in the same way, the tissue extract were chromatographed in solvent systems 2 and 4. The hypophyseal fluorogenic substance moved in the same way as L-tryptophylglycine and both fluoresced yellow. In L-tryptophan extract several fluorescent spots were observed which moved in a slightly different way. In addition blue fluorescent spots were present (Figs 4–5). The present results gave L-tryptophylglycine for the structure of the hypophyseal fluorogenic peptide and its antinociceptive effect were thereafter studied.

Table 2. The effect of L-tryptophylglycine on the antinociceptive effect of morphine in the hot plate test mice

The second injection was given 5 min after the first one; all the injections were given s.c. The reaction time was measured 20 min after the first injection. n = number of animals. $P < 0.001$ compared to the saline + saline group. The values of L-tryptophylglycine + morphine group are not significantly different from those of saline + morphine group.

Treatment (mg/kg)	n	Reaction time (seconds \pm S.E.)
Saline + saline	10	7.8 \pm 0.5
Saline + morphine (15)	10	13.9 \pm 1.0*
L-Tryptophylglycine (10) + morphine (15)	1	11.8 \pm 0.9
Saline + morphine (30)	7	46.7 \pm 3.4
L-Tryptophylglycine (1) + morphine (30)	7	39.9 \pm 4.4
L-Tryptophylglycine (10) + morphine (30)	10	45.4 \pm 3.2

L-Tryptophylglycine and testing of antinociceptive activity. *L*-Tryptophylglycine alone even at high doses, had no significant antinociceptive effects assessed by the hot-plate method (Table 1). Morphine at doses of 15 and 30 mg/kg significantly prolonged the hot-plate time but *L*-tryptophylglycine did not change the antinociceptive effect of morphine (Table 2). *L*-Tryptophylglycine did not have any clear effects on the behaviour of mice at the doses used.

DISCUSSION

The yellow cytoplasmic fluorescence in certain hypophyseal cells induced by GA-ethanol indicated that a fluorogenic substance remains unaltered in histochemical reactivity when hypophyses are obtained about 48 h after death from cadavers stored at 4°C. Because other hypophyseal cells did not exhibit any specific fluorescence it seems justifiable to assume that the fluorogenic substance obtained after GA-ethanol treatment of hypophyseal extract is the same as that demonstrated histochemically. In previous works this fluorogenic substance has been localized in hormone storage granules of ACTH/MSH cells of the mammalian hypophysis (in both histochemical and biochemical separation methods) (Häkkanen et al. 1975; Partanen 1978a). The present results gave the structure *L*-tryptophylglycine for the hypophyseal fluorogenic substance. The molecular weight of this dipeptide is 41 and differs from the previously reported molecular weight (over 5000) of the main fraction of amino-terminal tryptophyl peptides separated by reversed-phase chromatography from hypophyseal anterior parts of the central nervous system although the presence of smaller amino-terminal tryptophyl peptides was not excluded (Häkkanen et al. 1972; Edrén et al. 1973; Häkkanen et al. 1974). In addition, the extraction methods used by Häkkanen and co-workers (Häkkanen et al. 1972; Edrén et al. 1973; Häkkanen et al. 1974) and by the present authors differed which could explain the differences concerning the molecular weight.

It has been demonstrated histochemically that amino-terminal tryptophyl peptides of the hypophyseal cells decreased concomitantly with a decrease in the immunohistochemically demonstrable ACTH in anterior parts distal to the pars intermedia (Häkkanen & Sundler 1977) and in the number of electron microscopically demonstrable hormone storage granules in the pars intermedia (Partanen &

Back, to be published). Thus, amino-terminal tryptophyl peptides are released into the peripheral circulation and possibly also directly into the central nervous system via the retrograde hypophyseal portal circulation (Oli et al. 1977) together with other hormones of ACTH/MSH cells. It has been shown that β -endorphin shows parallel changes both in blood and in the hypophysis with ACTH (Guillemin et al. 1977). The sequence Try-Gly is present in β -lipotropin, ACTH and MSHs but it has no ACTH or MSH-like activity which requires at least a tetrapeptide in which Try-Gly is in the carboxyl terminal position (Wallis 1975). In addition, the present results showed that *L*-tryptophylglycine alone administered subcutaneously into mice had no antinociceptive effects and no influence on morphine antinociception even at high doses. The content of amino-terminal tryptophyl peptides in the mouse hypophysis expressed in the form of tryptophylalanine equivalents has been reported to be about 10 μ g/g of wet weight (Häkkanen et al. 1974). Thus, although it is possible that *L*-tryptophylglycine is hydrolyzed by peptidases as enkephalins if given systemically (Pert et al. 1976) the doses were so large that intact tryptophylglycine was probably present in the circulation at times when the measurements were made. Also it seems that *L*-tryptophylglycine does not exert any physiological effect in its hydrolysis to tryptophan which subsequently leads to increased serotonin synthesis in the central nervous system (Fenstrom & Wurtman 1972). Serotonin has been shown to modify the effects of opiates, and it has been suggested that opiates exert their effect by changing the serotonin content (Hosobuchi et al. 1977). Further *L*-tryptophylglycine had no apparent effect on the behaviour of mice. Thus, the physiological significance of *L*-tryptophylglycine seems to be different from the effects of ACTH, MSH and hypophyseal opiate-like peptides. It might be a physiologically inactive part of a larger molecule or a dipeptide with its own unknown function.

This work was supported by grants from E. Astrom Foundation and J. K. Paasikivi Foundation.

REFERENCES

- BÖRKLUND, A., LINDVALL, O. & SVENSSON, L.-Å. 1972. Mechanism of biogenic amine formation in the histochemical glyoxylic acid method for monoamines. *Histochemistry* 32: 113-133.

- EDDY N B & LEIMBACH D 1953 Synthetic analgesics. II Dithienylbutenyl- and dithienylbutylamines. *J Pharmacol Exp Ther* 107: 385-393
- EDVINSSON L, HÅKANSON R, RÖNNBERG A L & SUNDLER F 1973 Tryptophyl-polypeptides in rat brain. *J Neurochem* 20: 897-899
- FERNSTROM J D & WURTMAN R J 1972 Brain serotonin content: physiological regulation by plasma neutral amino acids. *Science* 178: 414-416
- GUILLEMIN R, VARGO T, ROSSIER J, MINICK S, LING N, RIVIER, C, VALE, W & BLOOM F 1977 β -Endorphin and adrenocorticotropin are secreted concomitantly by the pituitary gland. *Science* 197: 1367-1369
- HOSOBUCHI Y, MEGLIO M, ADAMS J E, & LI C H 1977 β -Endorphin: development of tolerance and its reversal by 5-hydroxytryptophan in cats. *Proc Natl Acad Sci USA* 74: 4017-4019
- HÅKANSON R, SUNDLER F, NOBIN A, LARSSON L, I, SJÖBERG N-O, EDVINSSON L & LARSSON L, I 1974 Peptides with NH_2 -terminal tryptophan in the adenohypophysis. *Cell Tiss Res* 150: 281-290
- HÅKANSON R, SUNDLER F, LARSSON L, I, SJÖBERG N-O, EDVINSSON L & LARSSON L, I 1974 Peptides with NH_2 -terminal tryptophan in the adenohypophysis. *Cell Tiss Res* 150: 281-290
- HÅKANSON R, SUNDLER F, LARSSON L, I, EKMAN R. & SJÖBERG N-O 1975 Peptides with NH_2 -terminal tryptophan in adrenocorticotrophic hormone and melanocyte-stimulating hormone granules of adenohypophysis. *J Histochem Cytochem* 23: 65-74
- HÅKANSON R. & SUNDLER F 1977 Facultative dehydro-ozone-induced fluorescence in pituitary ACTH cells: effect of adrenalectomy. *Cell Tiss Res* 183: 419-421
- OLIVER C, MICAL, R. S & PORTER, J. C 1977 Hypothalamic-pituitary vasculature: evidence for retrograde blood flow in the pituitary stalk. *Endocrinology* 101: 598-604
- PARTANEN S 1975 Simultaneous fluorescent histochemical demonstration of catecholamines and tryptophyl-peptides in endocrine cells. *Histochemistry* 41: 295-303
- PARTANEN S 1976 Fluorophore formation of tryptophyl-peptide in histofluorescence methods and carbonyl compounds. *Proc Fifth Int Congr Histochem Cytochem (Bucharest)* 269
- PARTANEN S 1978a Carbonyl compound induced fluorescence of biogenic monoamines in the calyx cells of the hypophysis. *Progr Histochem Cytochem* 8 (3): 1-47
- PARTANEN S. 1978b Isolation and thin layer chromatographic identification of several peptides with NH_2 -terminal tryptophan and their histochemical demonstration in the ACTH cells of the hypophysis. *Histochemistry* 56: 147-154
- PERT C B, BOWIE D. L, FONG, B. T & J, CHANG J. K. Synthetic analogues of met-enkephalin which resist enzymatic destruction. In: *Opiates and endogenous opioid peptides* (ed H W Kosterlitz) 77: 79-86. Elsevier, Amsterdam 1976.
- WALLIS M 1975 The molecular evolution of pituitary hormones. *Biol Rev* 50: 35-98.

Comparison of effects of pentobarbital and ethanol on the neuronal activity in the posterior parietal association cortex

HYVÄRINEN M, LAAKSO R, ROINE R and L. LEINONEN

From the Department of Physiology, University of Helsinki, Finland

HYVÄRINEN J, LAAKSO M., ROINE, R. & LEINONEN L. Comparison of effects of pentobarbital and ethanol on the neuronal activity in the posterior parietal association cortex. *Acta Physiol Scand* 1979 107: 219-225. Received 28 Febr. 1979. ISSN 0001-6772. Department of Physiology, University of Helsinki, Finland.

The problem of this study was whether the effects produced by alcohol in the posterior parietal association cortex are specific to this drug or shared by other centrally acting depressant drugs such as barbiturates. The effect of graded doses of pentobarbital on multisensorial popliteal activity was recorded with transdural microelectrode technique in 30 expl. in Brodmann's area 7 of five stump-tailed monkeys (*Macaca speciosa*). The results were compared with those from 32 expls. performed with alcohol and published separately. The dosage of the two drugs was determined on the basis of the monkeys' sensor-motor coordination which was assessed with a rating scale of reaching accuracy for food rewards. There were several recording sites where the actions of the two drugs were similar at similar behavioural levels of intoxication. However, in the distribution of effects among various functional types of recording sites, significant differences were found between pentobarbital and alcohol. Alcohol commonly diminished cellular activity related to motor behaviour (reaching, grasping) and only rarely responses to somesthetic stimuli, whereas the effects of pentobarbital were the opposite being most common on somatosensory responses and least common on activity related to motor behaviour. Also responses to visual stimuli were more sensitive to pentobarbital than to alcohol. The actions of pentobarbital and alcohol on responses evoked by sensory stimulation differed significantly ($P < 0.01$). We conclude that significant differences exist in the mechanisms of action of alcohol and barbiturate on the associative systems of the brain.

Key words: Ethanol, pentobarbital, parietal association cortex, multisensorial activity

It has been suggested that the effects observed in the CNS after administration of alcohol are non-specific and similar to the effects produced by other centrally acting depressant drugs such as barbiturates (Kakani 1975). With EEG and evoked potential techniques it has been demonstrated that cortical associative zones and midbrain reticular formation are sensitive to the actions of alcohol (DiPerni et al. 1968, Petrait et al. 1974). We have shown previously that the cellular activity in the posterior parietal association cortex is sensitive to the action of alcohol (Hyvärinen et al. 1978), and that often the behavioural action of alcohol is closely paralleled by its action on the cellular activity in this cortical region that normally participates in the sensor-motor control of hand- and eye-movements

(Hyvärinen & Ponanen 1974, Mountcastle et al. 1975). It was therefore of interest to study whether the effects produced by alcohol in the posterior parietal association cortex are specific to alcohol or whether barbiturates would produce similar results. We performed this study using pentobarbital in doses that produced effects in the monkeys' sensor-motor coordination comparable to those produced by alcohol. The results indicate that although similarities exist in the actions of these two drugs there are also significant differences.

MATERIAL AND METHODS

This study was performed with 5 *Macaca speciosa* monkeys weighing 6 to 10 kg. It was not possible to hold single units long enough for the study of the drugs, because the

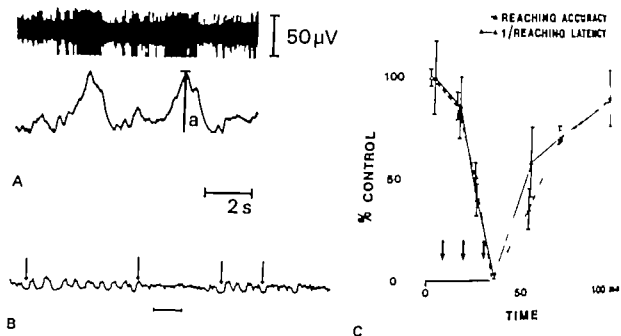


Fig. 1 (A) Multineuronal impulse activity (upper trace) and the same activity rectified and integrated (lower trace). The control responses during reaching with ipsilateral arm toward a food reward are seen. Measurement of the amplitude of an integrated response from the base-line of the recording is indicated (a). Mean amplitudes and their standard deviation were calculated of ten consecutive responses. The mean and standard deviation values obtained during the action of the drug were then expressed as percentage of the mean control value. (B) Spontaneous activity in an integrated multineuronal recording showing two periods of rhythmic discharge. The beginning and the end of the rhythmic periods are indicated by arrows. Pentobarbital was injected 12.5 mg/kg divided in 4 doses; the sample was recorded in the remount phase 53 min after the last dose. For measurement of the percentage of time of rhythmic discharge 40 s of spontaneous activity was recorded; the duration of rhythmic periods was measured and expressed as percentage of the total duration of the recording. (C) The effect of pentobarbital on the reaching accuracy score and the inverse value of the reaching latency measured electrically. At each arrow 4 mg/kg of pentobarbital was given through the intracardial catheter. The mean and standard deviation values of 10 trials expressed as per cent of control values. The same notation is used in all figures.

induction of and recovery from the drug effects took several hours. Therefore multiple unit recordings were made. Multineuronal impulse activity was recorded in the same part of Brodmann's area 7 as in our previous paper (Hyvärinen et al. 1978) in chronic experiments with movable microelectrodes. No other anesthesia except the drugs studied was used during the experiments. The recording methods have previously been described in detail (Hyvärinen & Poranen 1974; Hyvärinen et al. 1978, 1979). In this study multineuronal activity was recorded with glass-insulated tungsten electrodes moved into the cortex through the intact dura with a hydraulic micromanipulator. The multineuronal activity (Fig. 1A) was filtered, rectified and integrated using the apparatus described by Weber & Buchwald (1965). High-pass filtering at 300, 500 or 1000 Hz eliminated completely slow wave signals from the recording leaving only action potential spikes. Judging from the variance in the amplitudes of the action potentials recorded these were discharged by approximately 5–10 neurons. Many things influence the amplitude of the multineuronal responses, such factors as the size of the elec-

trode, the size of the neurons recorded and movement of the electrode in reference to the cells studied. To eliminate the influence of these variables, the electrodes were not moved during the study of the drugs and the amplitudes of the integrated multineuronal responses were expressed as percentages of the amplitudes in the recordings made prior to the administration of the drug (Fig. 1A). The drugs were infused through an intracardial catheter permanently implanted in the right atrium of the heart as previously described (Hyvärinen et al. 1974). In some experiments pentobarbital (Nembutal RI) was given in 30 experiments were performed using pentobarbital and the results of these experiments were compared with those from experiments performed with alcohol and published previously (Hyvärinen et al. 1978). The dosage of the drugs was adjusted by following the behavioural actions. For the purpose a rating scale was constructed for estimation of the monkey's reaching accuracy for food reward. Ten points were given for normal rapid and accurate reaching for food rewards offered by the experimenter. With increasing dosage of the drugs the reaching became slow

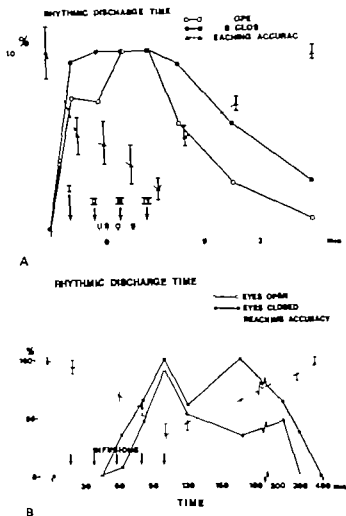


Fig. 2. The development of the rhythm during the action of the drug. The percentage of recording time when the spontaneous discharge was rhythmic is indicated together with the reaching accuracy. (A) Pentobarbital infusions (arrow) of 5 (first arrow) + 3 2.5 mg/kg. (B) Alcohol infusions 5 0.5 g/kg. More rhythm was present when the monkey's eyes were closed.

and accurate and finally ceased altogether. Zero points were given for no attempt to reach and intermediate values were given for intermediate accuracies and speeds. These eleven criteria used to do these scorings getting consistent results. For one drug level their estimates did not differ from each other more than $\pm 10\%$. In some experiments the adequacy of this arbitrary rating scale was compared with electrical measurements of the monkey's reaching latency using specially constructed food well. A close correlation was observed between the reaching scores and the average values of reaching latency (Fig. 1C). The appearance of rhythm in the spontaneous multielectrode discharge was studied by measuring the time that the

discharge was rhythmic. This time was expressed as percent of total recording time as indicated in Fig. 1B. At least 3 successive waves were required for a period to be considered rhythmic. The dominant frequency of the rhythm was determined by counting the number of distinct waves per time unit during the rhythmic periods.

RESULTS

Both pentobarbital and alcohol produced a rhythmic spontaneous multielectrode discharge

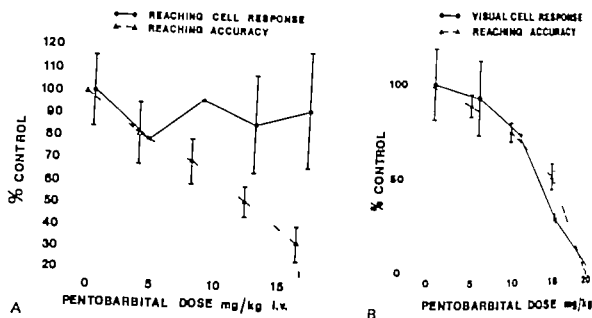


Fig. 3 (A) Lack of effect of pentobarbital on the amplitude of integrated responses at a recording site responding to reaching movements performed with the contralateral hand. Although the reaching accuracy fell with increasing dose of pentobarbital the cellular responses remained unaffected. Means and standard deviations of 10 responses. (B) The effect of pentobarbital dose on the amplitude of a visual response and reaching accuracy. At this recording site new objects brought into the monkey's visual field close to the animal triggered a response but visual fixation of familiar food did not produce responses. At each dose level 10 new objects were presented to the monkey as stimuli and the means and standard deviations of the responses are plotted in the figure.

This rhythmicity appears to be related to the slow EEG rhythms produced by centrally depressant drugs. In the multiple unit records the proportion of time that the spontaneous activity was rhythmic increased with increasing dose. Closing of the eyes increased the prevalence of the rhythmic activity. It was also evident that the amount of rhythmic discharge correlated inversely with the performance of the animal expressed as reaching accuracy and that this relationship was similar for alcohol and pentobarbital (Fig. 7). In alcohol experiments the frequency of the rhythm became slower with increasing dose (Hyvärinen et al. 1978) but such a relationship was not seen in pentobarbital experiments in which the dominant rhythm stayed at approximately 7 Hz when present.

7 expts with pentobarbital were performed at sites where the cellular activity correlated with reaching movements performed with the contralateral arm and hand as described before (Hyvärinen & Poranen 1974; Mountcastle et al. 1975). The results were compared with those obtained from 1 alcohol experiments on functionally similar recording sites. The effects on motor responses were less common in the pentobarbital group in which three

of eight sites were affected by the drug whereas 12 sites were sensitive to alcohol (Table 1). The negative result of one pentobarbital experiment is illustrated in Fig. 3A. The differences of the effect of pentobarbital and alcohol on cellular activity related to motor behaviour were not statistically significant however.

Visual stimuli activated 13 recording sites in pentobarbital experiments. Eleven of these were sensitive to the action of pentobarbital whereas two were not. These expts are compared with results from 10 similar expts. performed with alcohol in 5 of which there was an effect of the drug (Table 1). These sites responded to following type of visual stimuli: visual approach towards the animal, visual fixation of objects, visual presentation of new objects, uncovering of the eyes, and movement in the visual field.

Fig. 3B illustrates amplitudes of visual responses as a function of pentobarbital dose at a site where the cells responded to new visual stimuli. Movement of indifferent visual stimuli in the visual field of the animal or visual fixation of food did not activate this recording site. The effect of pentobarbital on this response was strongly decremental.

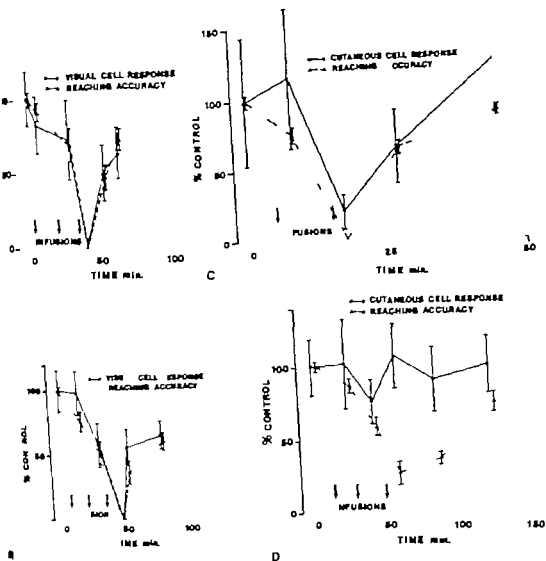


Fig. 4 Effects of pentobarbital (A) and alcohol (B) on the responses at site responding to large moving stimuli brought to the visual field from the contralateral side. The two experiments were performed at the same cortical site with an interval of four days. Pentobarbital infusions (arrows) 5 mg/kg each and alcohol infusions 1 g/kg each. Means and standard deviations of 10 responses. (C) Effect of pentobarbital on responses to cutaneous touch and on reaching accuracy. Two infusions of 5 mg/kg each are given at arrows. (D) Effect of alcohol on similar responses and reaching accuracy. Infusions of 1 g, 1 g and 0.5 g/kg were given at arrows. Means and standard deviations of 10 responses. The two experiments are performed at the same cortical site with an interval of eight days. This site responded to touch of the meat.

Fig. 4A and B show decrement of visual responses recorded at another site during the action of pentobarbital and alcohol. At this site both drugs produced close to identical effects.

Somesthetic responses were less often affected by alcohol than by pentobarbital. Alcohol reduced the response amplitudes at only 3 of 10 recording

sites (Table 1), whereas 7 of 9 recording sites responding to somesthetic stimulation were sensitive to pentobarbital. The effect of pentobarbital on the somesthetic responses was statistically significantly more common ($P < 0.05$ χ^2 -test) than the effect of alcohol.

Fig. 4C and D show an example of different ef-

Table 1 Effect of alcohol and pentobarbital on multilineuronal impulse responses at different recording sites in area 7

Type of activity	Pentobarbital effect				Alcohol effect				Total
	Yes		No		Yes		No		
	N	%	N	%	N	%	N	%	
Motor (reaching, grasping, manipulation)	3	37	5	63	8	67	4	33	20
Visual (complex visual phenomena)	11	85	2	15	5	50	5	50	20
Somatosensory (skin, muscle, joint)	7	78	2	29	3	30	7	70	19
Total	21	70	9	30	16	50	16	50	62

The differences between the effect of alcohol and pentobarbital are statistically significant (χ^2 -test) on the somatosensory responses ($P < 0.05$) and on the sensory responses (somatosensory and visual combined $P < 0.01$). The difference between the effects on motor responses and sensory responses is significant for pentobarbital ($P < 0.05$).

effects of pentobarbital and alcohol on responses to similar cutaneous stimuli. As reported previously no effect of alcohol on the cellular activity was observed in the primary somatosensory cortex (Hyvärinen et al. 1978). One experiment performed with pentobarbital in SI indicated a small effect also in this region.

Table 1 indicates the distribution of effects of alcohol and pentobarbital in 62 experiments. The level of dosage of the two drugs was comparable, since both reduced the reaching accuracy close to zero. The effect of pentobarbital on all sensory responses (somesthetic and visual combined) was significantly more common than the effect of alcohol ($P < 0.01$, χ^2 -test). On the other hand an effect of alcohol was more often observed on cellular responses related to movements although this difference was not statistically significant.

DISCUSSION

The multiple unit recording method used in this study can be considered as an intermediate technique between recording of intracortical slow wave activity and single unit activity. For the study of the action of drugs this recording method proved suitable as the effects of the drugs on the multiple unit activity were quite distinct. To sample sufficiently single unit data for firm conclusion on the action of the drugs would have required considerably more experiments. Several factors may influ-

ence the magnitude of multiple unit activity. Such factors are for instance the size of the electrode tip and the size of the cells recorded as well as the distance between the cells and the electrode. The influence of these factors was eliminated from the present study of drug effects by leaving the electrode in place prior to and during the study of the drugs and by expressing the amplitude values as percentage of the control values obtained prior to the injection of the drugs.

It has been known that sensory areas of the cortex are less sensitive to anesthetic than the associative areas (Albe-Fessard & Fessard 1961; Thompson et al. 1963) and this fact has been applied to delineate the sensory and motor areas by the evoked potential and electrical stimulation techniques in deep pentobarbital narcosis (Woolsey et al. 1942; Woolsey 1958). On the other hand it has been suggested that the neural effects of alcohol are similar to those of other centrally acting depressant drugs such as barbiturates (Kalant 1975). The effects observed in this study were indeed similar in many respects. For instance both drugs produced a rhythmic spontaneous activity that was similarly related to the behaviour of the animal, i.e. the rhythmicity increased as the reaching accuracy decreased (Fig. 1). Also the effects of the two drugs on cellular responses to stimuli were comparable at several recording sites in area 7.

Behaviourally the actions of the two drugs appeared different, however. Whereas small doses of pentobarbital produce a general appearance of sedation

and a tendency to fall asleep the motor performance is not much disturbed when awake. Alcohol, however, produces often a euphoric state in which the motor behaviour increases but becomes incoordinated. Therefore one would expect the effects of the two drugs to differ at some level.

This work indicates that although there are many similarities in the action of alcohol and pentobarbital on the multimodal impulse activity in the anterior parietal association cortex the effects also differ from each other. The differences are most clear on the sensory responses (somesthetic and smell) that are significantly more often affected by pentobarbital than by alcohol. Cellular activity related to motor behaviour on the other hand was more often affected by alcohol than by pentobarbital (Table 1) although this difference was not statistically significant. The difference in the distribution of effects appears consonant with the behavioural effects of the two drugs. The general sedation produced by pentobarbital correlates with its depressant action on the sensory responses in area 7 whereas the motor incoordination produced by alcohol correlates with the effect that this drug has on the cellular discharges related to motor performance.

Studies on the neural effects of alcohol performed with EEG- and evoked potential-techniques have indicated that cortical association zones and the circular formation are more sensitive to the drug than the specific cortical projection areas (DiPerrri et al. 1968, Perrin et al. 1974). Consequently it has been suggested that the polysynaptic structures are more susceptible to the actions of alcohol than sensory systems that have simpler synaptic connections (Wallgren & Barry 1970, Himwich & Callison 1972, Kalant 1975). On the basis of these results the effect of pentobarbital appears to accumulate in the successive sensory synapses and this may be true for alcohol also (Hyvärinen et al. 1978). However the lesser effect of pentobarbital on the discharges related to motor performance complicates this interpretation. Although the number of synapses in a neural pathway may be important in determining the action of this kind of drugs there appear to be differences in the details of the mechanisms involved.

This work has been supported by a grant from the Finnish Foundation for Alcohol Studies.

REFERENCES

- ALBE FESSARD, D. & FESSARD, A. 1963. Thalamic integrations and their consequences at the teleencephalic level. *Progr Brain Res* 1: 115-148.
- DiPERRI, R., DRAVID, A., SCHWEIGERDT, A. & HIMWICH, H. E. 1968. Effects of alcohol on evoked potentials of various parts of the central nervous system of cat. *Quart J Stud Alc* 29: 20-37.
- HIMWICH, H. E. & CALLISON, D. A. 1972. The effects of alcohol on evoked potentials of various parts of the central nervous system of the cat. In: *The biology of alcoholism* (ed. B. Krasn and H. Begleiter), vol. 2, pp. 62-84. Plenum Press, New York.
- HYVÄRINEN, J. & PORANEN, A. 1974. Function of the parietal associative area 7 as revealed from cellular discharges in alert monkeys. *Brain* 97: 673-692.
- HYVÄRINEN, J., LAAKSO, M., RÖTNE, R. & LEINONEN, L. 1979. Effects of phencyclidine, LSD and amphetamine on neuronal activity in the posterior parietal association cortex of the monkey. *Neuropharmacology* 18: 237-242.
- HYVÄRINEN, J., LAAKSO, M., RÖTNE, R., LEINONEN, L. & SIPPPEL, H. 1978. Effect of ethanol on neuronal activity in parietal association cortex of alert monkeys. *Brain* 101: 701-715.
- KALANT, H. 1975. Direct effects of ethanol on the nervous system. *Federation Proc* 34: 1930-1941.
- MOUNTCASTLE, V. B., LYNCH, J. C., GEORGOPOULOS, A., SAKATA, H. & ACUNA, C. 1975. Posterior parietal association cortex of the monkey: Command functions for operations within extrapersonal space. *J Neurophysiol* 38: 871-908.
- PERRIN, R. O., HOCKMAN, C. H., KALANT, H. & LIVINGSTON, K. E. 1974. Acute effects of ethanol on spontaneous and sensory evoked electrical activity in cat brain. *Electroenceph Clin Neurophysiol* 36: 19-31.
- THOMPSON, R. F., JOHNSON, R. H. & HOOPES, J. J. 1963. Organization of somatic sensory and visual projection to association fields of cerebral cortex in cat. *J Neurophysiol* 26: 343-364.
- WALLGREN, H. & BARRY III, H. 1970. *Actions of alcohol*, p. 175. Elsevier, Amsterdam.
- WEBER, D. S. & BUCHWALD, J. S. 1963. A technique for recording and integrating multiple unit activity simultaneously with the EEG in chronic animals. *Electroenceph Clin Neurophysiol* 19: 190-192.
- WOOLSEY, C. N. 1959. Organization of somatic sensory and motor areas of the cerebral cortex. In: *Biological and biochemical bases of behaviour* (ed. H. F. Harlow and C. N. Woolsey), pp. 63-81. The University of Wisconsin Press, Madison.
- WOOLSEY, C. N., MARSHALL, W. H. & BARD, P. 1942. Representation of cutaneous tactile sensibility in the cerebral cortex of the monkey as indicated by evoked potentials. *Bull Johns Hopk Hosp* 70: 399-441.

We wish to thank Mr Mika Lomakoski, Mrs Katrina Luoma and Mrs Ritta Kuitunen for technical assistance.

Table 1 Effect of alcohol and pentobarbital on multilineuronal impulse responses at different recording sites in area 7

Type of activity	Pentobarbital effect				Alcohol effect				Total	
	Yes		No		Yes		No			
	N	%	N	%	N	%	N	%		
Motor (reaching, grasping, manipulation)	3	37	5	63	8	67	4	33	20	52
Visual (complex visual phenomena)	11	83	2	15	5	50	5	50	23	77
Somatosensory (skin, muscle, joint)	7	78	2	22	3	30	7	70	19	54
Total	1	70	9	30	16	50	16	50	6	30

The differences between the effect of alcohol and pentobarbital are statistically significant (χ^2 -test) on the somatosensory responses ($P < 0.05$) and on the sensory responses (somatosensory and visual combined $P < 0.01$). The difference between the effects on motor responses and sensory responses is significant for pentobarbital ($P < 0.05$).

effects of pentobarbital and alcohol on responses to similar cutaneous stimuli. As reported previously no effect of alcohol on the cellular activity was observed in the primary somatosensory cortex (Hyvärinen et al. 1978). One experiment performed with pentobarbital in S1 indicated a small effect also in this region.

Table 1 indicates the distribution of effects of alcohol and pentobarbital in 62 expts. The level of dosage of the two drugs was comparable since both reduced the reaching accuracy close to zero. The effect of pentobarbital on all sensory responses (somesthetic and visual combined) was significantly more common than the effect of alcohol ($P < 0.01$, χ^2 test). On the other hand an effect of alcohol was more often observed on cellular responses related to movements although this difference was not statistically significant.

DISCUSSION

The multiple unit recording method used in this study can be considered as an intermediate technique between recording of intracortical slow wave activity and single unit activity. For the study of the action of drugs this recording method proved suitable as the effects of the drugs on the multiple unit activity were quite distinct. To sample sufficiently single unit data for firm conclusion on the action of the drugs would have required considerably more experiments. Several factors may influ-

ence the magnitude of multiple unit activity. Such factors are for instance the size of the electrode tip and the size of the cells recorded as well as the distance between the cells and the electrode. The influence of these factors was eliminated from the present study of drug effects by leaving the electrode in place prior to and during the study of the drugs and by expressing the amplitude values as percentage of the control values obtained prior to the injection of the drugs.

It has been known that sensory areas of the cortex are less sensitive to anesthetic than the associative areas (Albe Fessard & Fessard 1961, Thompson et al. 1963) and this fact has been applied to delineate the sensory and motor areas by the evoked potential and electrical stimulation techniques in deep pentobarbital narcosis (Woolsey et al. 1942, Woolsey 1958). On the other hand it has been suggested that the neural effects of alcohol are similar to those of other centrally acting depressant drugs such as barbiturates (Kailant 1979). The effects observed in this study were indeed similar in many respects. For instance both drugs produced rhythmic spontaneous activity that was similar related to the behaviour of the animal, i.e. the rhythmicity increased as the reaching accuracy decreased (Fig. 1). Also the effects of the two drugs on cellular responses to stimuli were comparable at several recording sites in area 7.

Behaviourally the actions of the two drugs appeared different however. Whereas small doses of pentobarbital produce a general appearance of sedation

Increase in local cerebral blood flow induced by circulating adrenaline: involvement of blood-brain barrier dysfunction

LI ABUL RAHMAN, NILS DAHLGREN, BARBRO B. JOHANSSON and BO K. SIESJÖ

Laboratory of Experimental Brain Research and Departments of Anaesthesia and Neurosurgery, University of Lund, Sweden

ABUL RAHMAN, A., DAHLGREN, N., JOHANSSON, B. B. & SIESJÖ, B. K.: Increase in local cerebral blood flow induced by circulating adrenaline: involvement of blood-brain barrier dysfunction. *Acta Physiol Scand* 1979; 107: 227-232. Received 22 March 1979. ISSN 0001-6772. Laboratory of experimental Brain Research and Departments of Anaesthesia and Neurosurgery, University of Lund, Sweden.

The influence of ultra-venous infusion of adrenaline ($8 \mu\text{g} \cdot \text{kg}^{-1} \cdot \text{min}^{-1}$) upon local cerebral blood flow (CBF) in paralyzed and artificially ventilated rats was measured autoradiographically with ^{14}C -iodoantipyrine as the diffusible tracer. At this dose adrenaline invariably increased local CBF even though blood pressure was close to normal at the time of the CBF measurement. In average, local CBF increased to 400% of control. In 6 of 9 animals the increase in flow was inhomogeneous with randomly distributed areas of very high flow rates. Experiments with ^3H -administration of Evans blue prior to infusion of adrenaline showed that areas of Evans blue extravasation appeared in 3 of 4 animals. Although areas of extravasation often corresponded to areas of high flow rates the former were much more circumscribed. Furthermore, very high flow rates were found in areas showing no signs of blood-brain barrier dysfunction. It is concluded that the increase in CBF was at least partly due to pressure-mediated passage of adrenaline across the blood-brain barrier but that such passage can occur in the absence of microscopically visible extravasation of proteins.

Key words: adrenaline, local CBF, blood-brain barrier dysfunction

During recent years, it has become increasingly evident that biologically active amines influence cerebral metabolic rate for oxygen (CMR_{O_2}) and cerebral blood flow (CBF). Thus, at least under some circumstances, intravenously or intracarotidally administered noradrenaline or isoprenaline can give increases in CMR_{O_2} and CBF (James & MacDonnell 1975; MacKenzie et al. 1976a; for further literature see Kuschinsky & Wahl 1978). Since catecholamines are supposed not to penetrate the blood-brain barrier (Weil-Malherbe et al. 1961; Benier et al. 1966; Oldendorf 1971) it has been tentatively concluded that the barrier must be "opened" by increasing the blood pressure or the osmolarity of the blood perfusing the brain, before circulating amines can exert their effects on intracerebral receptors (MacKenzie et al. 1976a and b). However, this point may not be settled since others have concluded that the balance between α

(constrictory) and β (dilatory) adrenoreceptor activity in the cerebral vessels is such that a precipitous increase in local amine concentration, one that would result from an opening of the blood-brain barrier, actually may transform a dilatory response to a constrictory one (McCalden et al. 1977).

Results from this laboratory have shown that CMR_{O_2} and CBF may rise appreciably in certain stressful situations and that these increases are minimized or prevented by pretreating the animals with propranolol, or by adrenalectomy (Carlsson et al. 1977). Since it could be suspected that circulating catecholamines were involved the cerebral metabolic and circulatory effects of i.v. infusions of noradrenaline and adrenaline were tested in lightly anesthetized rats. The results showed that nor-

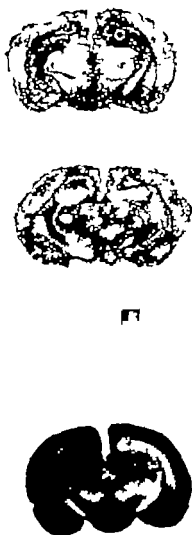


Fig. 2. Diagram illustrating effects on local CBF of hypercapnia (top) and adrenaline infusion (middle), as extravasation of Evans blue-protein complex as result of adrenaline infusion (bottom). The colour scales for I-CBF are only qualitative, and not internally comparable. They therefore only illustrate the distribution of high flow (yellow - red) and low flow (green - blue). Note homogeneous increase in I-CBF in hypercapnia and patchy increase after adrenaline infusion. The colour images were processed in the automatic microscanning system developed in the Laboratory of Cerebral Metabolism, National Institute of Health, by courtesy of dr. L. Sokoloff.

Table 1 Physiological parameters for the experimental groups

The values are means \pm S.E.

Experimental group	Body temp (°C)	MABP mmHg		During measurement of CBF	PaO ₂ (mmHg)	PaCO ₂ (mmHg)	pH
		Pre-infusion	Max				
Control (n=6)	37.0 \pm 0.4		148 \pm 5	144 \pm 4	103 \pm 2	37.0 \pm 0.7	7.42 \pm 0.08
Adrenaline (n=9)	37.3 \pm 0.1	137 \pm 4	181 \pm 7	138 \pm 7	96 \pm 5	39.3 \pm 5	7.32 \pm 0.08

drenaline in doses of 5 and 8 μ g kg⁻¹ min⁻¹ gave rise to a moderate (average 50%) increase in CMR_{O₂} which was blocked by propranolol. However following adrenaline in a dose of 8 μ g kg⁻¹ min⁻¹ CMR_{O₂} was doubled and in many animals CBF rose 4- to 5-fold (Bertman et al. 1978).

Various vasoactive substances like metamizol, angiotensin, noradrenaline and adrenaline can induce acute arterial hypertension in experimental animals leading to blood brain barrier (BBB) dysfunction. It has been shown that areas with BBB dysfunction as revealed by Evans blue or sodium fluorescein extravasation have higher CBF than non-damaged areas suggesting a local failure ('break through') of autoregulation (for review of literature see Johansson 1974a and 1976; MacKenzie et al. 1976b).

The present experiments were undertaken to provide answers to the following three questions: (1) Is the previously recorded increase in cortical CBF following adrenaline infusion a generalized phenomenon affecting all brain regions? (2) Is the flow homogeneously increased or does it occur in a 'spotty' fashion? (3) If the latter is true, is the local increase in CBF correlated with signs of BBB dysfunction induced by the increase in blood pressure? In order to provide answers to these questions adrenaline was infused i.v. in rats in a dose of 8 μ g kg⁻¹ min⁻¹. We measured local CBF with an autoradiographic technique using ¹⁴C-iodoantipyrine as diffusible tracer and evaluated BBB dysfunction by recording the penetration of Evans blue from blood to tissue.

METHODS

Operative procedure. Male Wistar rats, weighing 320-400 g, were allowed free access to pellet food and tap water until the day of operation. Anaesthesia was induced with 3% halothane. The animals were then tracheotomized, immobilized with tubocurarine chloride (1.5 mg kg⁻¹ i.v.) and artificially ventilated with 75% N₂O and 25% O₂. At

this point, halothane supply was discontinued. All femoral arteries and femoral veins were cannulated, the arteries to allow blood pressure recording and sampling of arterial blood for measurements of blood gases, pH and ¹⁴C-iodoantipyrine activity during CBF measurement, and the veins to allow infusion of adrenaline and of local CBF measurement. Body temperature was adjusted to 37°C and arterial P_aO₂ to 35-40 mmHg. Heparin was given i.v. in a dose of 5 IU kg⁻¹.

Infusion of adrenaline. Adrenaline, as obtained as the bitartrate dissolved in physiological saline at a concentration of 1 mg ml⁻¹ (ACO Stockholm). Before infusion, 1 ml of this stock solution was mixed with physiological saline to a final volume of 10 ml yielding an adrenaline concentration of 80 μ g ml⁻¹. About 30 min following the completion of the operative procedures the adrenaline was infused at a rate of 8 μ g kg⁻¹ min⁻¹. Local CBF was measured after an infusion period of 10 min.

Measurement of local CBF. We measured local CBF with an autoradiographic technique utilizing ¹⁴C-iodoantipyrine as a tracer (Sakurada et al. 1978). Details of methodology was as described in a preceding communication (Abdul-Rahman et al. 1979). It should be emphasized that the method is of limited accuracy at very high flow rates. Thus although quantitative figures have been given even for flow rates exceeding 5 ml g⁻¹ min⁻¹ these values are only approximations.

Measurement of BBB dysfunction. To test the function of the blood-brain barrier (BBB) Evans blue in a dose of 1 ml kg⁻¹ was given i.v. as a 1% solution in saline before the adrenaline infusion was started. In this dose the dye binds to serum albumin in vivo. Extravasation of the dye-protein complex could be macroscopically observed. However, in all 4 animals infused with Evans blue the brains were sectioned in a microtome and photographed. In order to allow a correlation between local CBF and Evans blue extravasation alternate sections were taken for autoradiography and photography respectively.

Statistics. Statistical differences were calculated using Student's *t* test.

RESULTS

As stated, adrenaline was infused i.v. in a dose of 8 μ g kg⁻¹ min⁻¹ in 9 rats with subsequent autoradiographic determination of local CBF 10 min following the start of the infusion. Physiological parameters are given in Table 1. In 4 of the animals

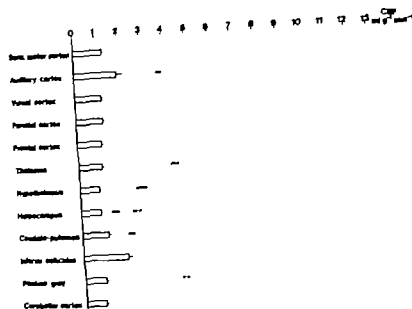


Fig. 1. Local CBF in same animals in which adrenaline ($8 \mu\text{g kg}^{-1} \text{ min}^{-1}$) had been infused for 10 min. Control values (staples) are given as means \pm S.E. in each animal, the symbols (dots) represent the average CBF within any one structure. Within each animal the average increase in CBF in various structures were similar and there were three animals in which very marked increases were observed throughout the brain, and others showing moderate or mild changes in CBF. Flow rates exceeding $5 \text{ ml g}^{-1} \text{ min}^{-1}$ are of limited accuracy (see Methods).

BB dysfunction was simultaneously determined by evaluating the extravasation of administered Evans blue. In all rats infusion of adrenaline was accompanied by a rise in mean arterial pressure of 30–50 mmHg. However as Table 1 shows the blood pressure subsequently fell and at the time of the CBF measurement, mean arterial blood pressures ranged between 120 and 170 mmHg. The table also shows that arterial P_{O_2} was close to control values, excluding the possibility that increases in local flow rates were related to hypercapnia. A previous study (Dahlgren et al. 1979) showed that infusion of adrenaline in a dose of $8 \mu\text{g kg}^{-1} \text{ min}^{-1}$ increased blood glucose concentration from 9 to 14 mmol/l.

The local CBF measurements gave 3 main results. First, following adrenaline infusion flow increased markedly in all brain structures. Second, in the majority of animals there were clear differences in flow rates even within the same area. Third, although 3 of 4 animals showed Evans blue extravasation marked increases in flow occurred even when no signs of protein extravasation were observed.

The first point is illustrated in Fig. 1 which gives local CBF values in each separate animal and compares them to the appropriate control values (means \pm S.E. see Abdul-Rahman et al. 1979). In making this graph no attention was paid to differences in flow within a structure. Instead an average value was obtained by making 5–7 densitometric readings from different parts of the structure in question. The results show that in many structures, the lowest CBF was twice the mean control value while the highest was 5-fold control. In most structures, the average increase in CBF was to 400% of control. In two structures (hippocampus and caudate putamen) the mean increase was only 2.5-fold and in one (cerebellar cortex) it was 5-fold. These pronounced increases in flow were not due to increased perfusion pressure and abolished autoregulation. Thus when the CBF values for any one structure were plotted against the mean arterial blood pressure at peak value as well as at the time of CBF measurement, no correlation between CBF and pressure was apparent (not shown). In fact, local CBF increased 3- to 4-fold even in animals that had mean arterial blood pressures below the

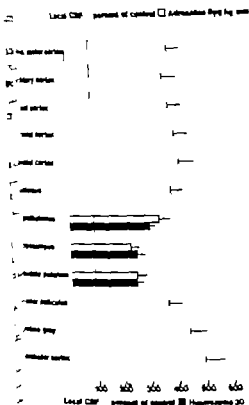


Fig. 3. Increases in local CBF in adrenaline-infused animals (filled staples) and in those exposed to hypertension (hatched staples). The values are means \pm S.E. in percent of normotensive controls.

etc., e.g. an increase in osmolarity did not contribute to the circulatory and metabolic effects observed presently.

The magnitude of the increase in local and regional CBF following adrenaline infusion is surprising. Previous results obtained in man and in a variety of experimental animals indicate that "maximal" vasodilatation in the brain is obtained in hypercapnia (see Berntman et al. 1979). In order to allow a comparison of increases in CBF, 4 animals were exposed to marked hypercapnia (P_{CO_2} 78.9 \pm 2 mmHg) with subsequent measurement of local CBF using techniques identical to those used in the adrenaline-infused animals. Mean arterial blood pressure in these animals was 149 ± 4 mmHg at 30 min. Fig. 3 compares local CBF to adrenaline-infused and in hypercapnic animals. Clearly adrenaline gave rise to increases in flow that were comparable to, or even more pronounced than, those observed

in hypercapnia. It should be emphasized that the infusion of adrenaline does not lead to signs of EEG activation nor does it cause accumulation of lactic acid in the tissue (Dahlgren et al. 1979). All these results point to the fact that adrenaline exerts its effects of cerebral resistance vessels by other mechanisms rather than an activation of the reticular activation system or an accumulation of acid.

This study was supported by grants from the Swedish Medical Research Council (Project No. B79-1AX-263), the Wallenberg Foundation and from U.S. PHS Grant No. 1 R01 NS-07838.

REFERENCES

- ABDUL-RAHMAN A., DAHLGREN N., INGVAR, M., REHNCRONA, S. & SIESJÖ B. K. 1979. Local versus regional cerebral blood flow in the rat at high (hypoxia) and low (phenobarbital anaesthesia) flow rates. *Acta Physiol Scand* 106: 53-60.
- BERTMAN L., DAHLGREN N. & SIESJÖ B. K. 1979. Influence of moderate and extreme hypercapnia on cerebral blood flow and oxygen consumption in the rat brain. *Anesthesiology* 50: 299-305.
- BERTMAN L., DAHLGREN N. & SIESJÖ B. K. 1978. Influence of intravenously administered adrenaline on cerebral oxygen consumption and blood flow in the rat. *Acta Physiol Scand* 104: 101-108.
- BERTLER, A., FALCK, B., OWMAN CH. & ROSENGREN E. 1966. The localization of monoamineergic blood-brain barrier mechanisms. *Pharmacol Rev* 18: 369-383.
- CARLSSON C., HÄGERDAHL, M., KAASIK, A. E. & SIESJÖ B. K. 1977. A catecholamine-mediated increase in cerebral oxygen uptake during immobilization stress in rats. *Brain Res* 119: 223-231.
- DAHLGREN N., SAKABE, T., ROSEN L. & SIESJÖ B. K. Cerebral functional, metabolic and circulatory effects of intravenous infusion of adrenaline in the rat. *Brain Res.* Submitted for publication.
- JAMES, I. M. & MACDONNEL, L. 1975. Factors affecting the cerebrovascular response to noradrenaline in the dog. *Brit J Pharmacol* 54: 129-143.
- JOHANSSON B. 1974a. Blood-brain barrier dysfunction in acute arterial hypertension. Thesis, University of Gothenburg.
- JOHANSSON B. 1974b. Regional cerebral blood flow in acute experimental hypertension. *Acta Neurol Scand* 50: 366-372.
- JOHANSSON B. 1976. Brain barrier pathology in acute arterial hypotension. In: *Transport phenomena in the nervous system* (ed. G. Levi, L. Battaglia and A. Lajtha), pp. 517-527. Plenum Publ. Corp. New York.
- JOHANSSON B. 1978. Effect of an acute increase of the intravascular pressure on the blood-brain barrier. A comparison between conscious and anesthetized rats. *Stroke* 9: 582-590.

normal mean (142 ± 4 mmHg) at ICBF measurement

The second point is illustrated in Fig. 2 which shows autoradiographs from two high flow situations. In one (top) CBF was increased by raising arterial P_{CO_2} to 80 mmHg and in the other (middle) adrenaline was infused i.v. (This section was taken from the brain that showed the most pronounced inhomogeneities in flow.) In hypercapnia local CBF in grey matter areas increased in a fairly homogenous fashion while the adrenaline infused animal showed pronounced intrastuctural differences in flow. For example in the parietal cortex CBF varied between 2.4 and 4.7 ml g⁻¹ min⁻¹ and in the brainstem and the hippocampus comparable differences were observed. Of the 9 adrenaline-infused animals 6 showed clear intrastuctural differences in CBF predominantly in parietal cortex hippocampus brain stem and cerebellum. In the remaining 3 animals CBF was increased but intrastuctural differences were not observed.

As remarked 4 animals were used to identify areas of Evans blue extravasation. In 3 of these multiple areas of extravasation were observed an example of which is shown in Fig. 3 (bottom). In general areas of extravasation corresponded to CBF values that were 3- to 5-fold control. However a quantitative comparison could not be made since the areas of extravasation were much more circumscribed than the areas of excessively high flow rates. Furthermore equally high CBF values were observed in areas visibly devoid of extravasated Evans blue. Thus although the infusion of adrenaline gave evidence of blood-brain barrier dysfunction in 3 of 4 animals local CBF was markedly increased in the absence of macroscopically visible signs of such dysfunction.

DISCUSSION

The present results have confirmed our previous observation that intravenous infusion of adrenaline in a dose of 8 µg kg⁻¹ min⁻¹ leads to a pronounced increase in CBF (Bertman et al. 1978). This result and that showing an accompanying increase in CMR_{O_2} corroborate previous observations in man (King et al. 1957) although the circulatory and metabolic effects induced by adrenaline were far more pronounced in the rat. However it is difficult to compare doses in the two studies. The present results have also shown that although adrenaline

increases mean arterial pressure, the marked rise in local CBF was present at a time when pressure was again close to normal values. Furthermore although local CBF rose in all brain structures studied some animals showed signs of a marked inhomogeneity. For practical reasons Evans blue-albumin extravasation was only estimated macroscopically. As the brains under the present circumstances could not be perfused and the concentration of Evans blue was high in the blood, the conditions were not optimal for detecting low grade of tracer extravasation. Moreover when the more diffusible BBB tracer sodium fluorescein is given together with Evans blue in acute hypertension the fluorescent areas in the brain are more extensive than the blue areas and Evans blue-albumin extravasation is not observed in all fluorescent areas (Johansson 1974b). Thus it seems not unlikely that the BBB was disturbed also in areas with macroscopically apparently intact BBB to protein tracers. The very high CBF in the cerebellum is interesting in light of a recent study in which the BBB dysfunction in adrenaline-induced acute hypertension was quantified with ¹²⁵I-HSA (human serum albumin). Although multifocal protein leakage was noted in all parts of the brain the highest concentration of the tracer was found in the cerebellum (Johansson 1978). In contrast acute hypertension induced by angiotensin or metaraminol results in extravasation mainly in cortical structures. In an accompanying study (Dahlgren et al. 1979) it could be shown that when blood pressure was kept constant during infusion of adrenaline in a dose of 8 µg kg⁻¹ min⁻¹ neither CBF nor CMR_{O_2} rose. The combined results strongly indicate that the initial increase in blood pressure allows adrenaline to pass the blood-brain barrier and that the enhancement of oxygen consumption and blood flow is caused by the action of the amine on intracerebral adrenoceptors. We tentatively conclude that the increase in pressure leads to an enhanced translocation of adrenaline across the blood-brain barrier e.g. by vesicular transport even when any concomitant translocation of Evans blue protein complex is macroscopically undetectable. As shown in another study (Dahlgren et al. 1979) the infusion of adrenaline is accompanied by a rise in blood glucose concentration to about 150% of control. Since such relatively moderate changes in glucose concentration have not previously been found to influence CBF or CMR_{O_2} we tentatively conclude that peripheral of

Inhibition of fast axonal transport and microtubule polymerization in vitro by colchicine and colchicine

J. ANDERS EDSTRÖM, MATS HANSON, MARGARETA WALLIN
and BO CEDERHOLM

Department of Zoophysiology, University of Lund, Sweden

EDSTRÖM, A. HANSON, M. WALLIN, M. & CEDERHOLM, B. Inhibition of fast axonal transport and microtubule polymerization in vitro by colchicine and colchicine. *Acta Physiol Scand* 1979; 107: 233-237. Received 23 March 1979. ISSN 0001-6772. Department of Zoophysiology, University of Lund, Sweden.

The effects of colchicine and colchicine on fast axonal transport in frog sciatic nerves were studied in vitro. Colchicine inhibited the transport to about the same extent as colchicine. Preincubation at low temperature potentiated the inhibitory effect of either drug. The polymerization of purified brain tubulin was inhibited by colchicine at 5-10 times higher concentrations than colchicine. The similarity of the effects obtained with colchicine and colchicine indicates that both drugs arrest axonal transport by interfering with microtubule function. Colchicine and colchicine did not affect the levels of high energy phosphates (ATP and CrP) in frog nerves indicating that reduced energy supply was not responsible for the arrested transport.

Key words: Axonal transport, microtubules, colchicine, colchicine, energy supply

Microtubules (MT) are supposed to play a role in axonal transport (for recent reviews see Dustin 1972, Hanson & Edström 1978a). This idea is based mostly on the transport inhibiting effects of antimitotic drugs. No direct proofs exist and contradicting results with various inhibitors have been reported (Byer 1974, Schönbarth et al 1977).

Colchicine blocks axonal transport and inhibits polymerization of tubulin in cell-free systems (Norenberg & Timasheff 1970, Banks & Tili 1975). Differences in degree and time-course of inhibition of axonal transport could be ascribed to its slow penetration into myelinated fibers (Fink et al 1973, Paulson & McClure 1974). Colchicine is presumed to bind only to tubulin and not to affect MT, thereby shifting the equilibrium towards tubulin (Wilson & Metz 1973). This process is accelerated by cold and the inhibitory effect of colchicine on axonal transport is potentiated by preincubation at low temperature (Hanson & Edström 1978b, Ochs 1976). On the other hand arrested transport has been observed without visible ultrastructural changes (Dustin et al 1975, Norström et al 1977, Serron 1971), indicating that subtler effects can be sufficient.

The role of MT is central for the understanding of axonal transport and other intracellular motile processes. Colchicine derivatives which retain some of the properties of colchicine while lacking others are therefore useful tools in studies of axonal transport mechanisms. The possibility of transport inhibition by colchicine due to effects on cellular processes unrelated to MT has been discussed. Such effects were considered less likely since humicolchicine, which does not bind to tubulin, lacked transport effects (Banks & Tili 1975, Dahlström et al 1975, Paulson & McClure 1974, Price 1974). To obtain further information about this problem another derivative, colchicine, was recently used. It was found to inhibit fast as well as slow axonal transport in the fish optic system (Schönbarth et al 1977) in spite of its inability to bind to rat brain tubulin. Neither did the authors observe ultrastructural changes in colchicine-treated nerves. In contrast, results in this report raise the possibility that transport inhibitory effects by colchicine are due to interference with MT and closely similar to those of colchicine.

Axonal transport is closely dependent on energy through ATP (Ochs & Hollingsworth 1971). Col-

- KING B D SOKOLOFF L. & WECHSLER R. L. 1952 The effects of 1-epinephrine and 1-nor-epinephrine upon cerebral circulation and metabolism in man. *J Clin Invest* 31 773-79
- KUSCHINSKY W & WAHL, M 1978 Local chemical and neurogenic regulation of cerebral vascular resistance. *Physiol Rev* 58 656-689
- MACCADDEN T A EIDELMAN B H & MENDELOW A. D 1977 Barrier and uptake mechanisms in the cerebrovascular response to noradrenaline. *Am J Physiol* 4 H458-H465
- MACKENZIE, E T MCCULLOCH J & HARPER, A M 1976a Influence of endogenous norepinephrine on cerebral blood flow and metabolism. *Amer J Physiol* 31 489-494
- MACKENZIE, E T STRANDSGAARD S GRAHAM D I JONES J V HARPER, A M & FARRAR, J A 1976b Effects of acutely induced hypertension in cats on pial arteriolar caliber but cerebral blood flow and the blood-brain barrier. *Circ Res* 39 33-41
- MACKENZIE E. T MCCULLOCH J OKEANS, W PICKARD J D & HARPER, A. M. 1976c Cerebral circulation and norepinephrine: Relevance of the blood-brain barrier. *Amer J Physiol* 31 483-484
- SAKURADA O KENNEDY C JENLE, J BROWN, J D CARBIN G L. & SOKOLOFF L. 1973 Measurement of local cerebral blood flow with ^{14}C iodoantipyrine. *Amer J Physiol* 34 (1) H39-H46
- WEIL MALHERBE H WHITBY L. G. & ALLROD J 1961 The blood-brain barrier for catecholamines in different regions of the brain. In *Regional neurochemistry* (ed S. S. Kety and J. E. L. pp. 284-292 Pergamon Press, Oxford.

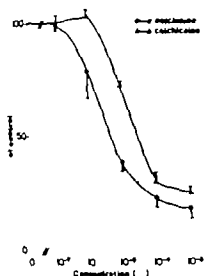


Fig. 1. Effects of colchicine and colchicene on the polymerization of MT in vitro. Protein samples were incubated for 5 min at 4°C with or without drugs (10^{-8} – 10^{-4} M) and the polymerization was measured at 37°C during an experimental period of 25 min. The results are presented as per cent of albumin control levels (mean values of 3 experiments).

RESULTS

Colchicine at 0.1 mM and 0.025 mM reduced the accumulation of labelled material in front of a ligature to 47% and 87% respectively of control. The corresponding values for colchicene were 54% and 9% (Table 1). Colchicine and colchicene thus showed about the same inhibitory effect on axonal transport. Neither drug affected protein synthesis in the ganglia. Preincubation at 1°C for 3 h in the presence of 0.1 mM colchicine or colchicene reduced the accumulated activity to a third of that in nerves treated with drug but without cold (data not shown). Colchicine was slightly more effective than colchicene under these circumstances.

The levels of ATP and CrP in control nerves after incubation for 17 h were 0.35 ± 0.03 and 1.49 ± 0.10 nmol per mg wet weight (mean \pm S.E., $n=4$) respectively. These values are only slightly lower than in freshly excised nerves. Paired nerves incubated in the presence of 0.1 mM concentrations of colchicine or colchicene showed unchanged levels of high energy phosphates.

The effects of colchicine and colchicene on polymerization of calf brain MT are presented in

Fig. 1. Both mitosis-inhibitors were found to inhibit the polymerization at high concentrations (10^{-4} and 10^{-5}) and to nearly the same extent. Colchicine was shown to be a more potent inhibitor than colchicene since it affected the polymerization process even at its low concentrations as 10^{-8} M. At this concentration no effect was resolved in the presence of colchicene.

The activities of calf brain MT associated Mg^{2+} and Ca^{2+} ATPases did not deviate from normal values, 2.9 and 3.1 nmol Pi liberated/mg/min at pH 6.8 (Wallin et al. 1979) at colchicene concentrations ranging from 10^{-4} to 10^{-6} M.

DISCUSSION

Colchicene is a metabolite of colchicine in some animals (Schönharting et al. 1974). It is less toxic than colchicine but its effects on the organism are similar, e.g. cell division, urate induced edema and ^{125}I release from the thyroid are all affected to some extent (Zweig & Chignell 1973; Fitzgerald et al. 1971).

In the optic system of fish colchicene was reported to be a more effective inhibitor of axonal transport than colchicine (Schönharting et al. 1977). In contrast, the two drugs had almost equal effects on transport in the frog sciatic nerve in the present study. The two agents differ in some properties. Colchicene is more lipophilic than colchicine and has an affinity for SH-groups (Schnell et al. 1976). It also inhibits phosphatases, probably by interaction with divalent cations (Siebert et al. 1975). Its affinity for tubulin is much lower than colchicine. Schönharting et al. (1977) could not detect any binding of [3H]-colchicene to tubulin but to several other components in a rat brain supernatant. However, it has earlier been shown to inhibit [3H]-colchicine binding to tubulin to some extent (Zweig & Chignell 1973). Another criterion for MT affinity is its effects on tubulin polymerization. Colchicene was shown, in the present investigation, to inhibit MT assembly at concentrations five to ten times higher than colchicine.

The differences in transport inhibitory effects obtained with the two drugs in the optic and sciatic system might depend on permeability factors and be related to the lipophilic characters of the substances. We have previously shown that several drugs with weak antimitotic activity reduce axonal

Table 1 Mean values \pm S.E. of radioactivity in ganglia and 4 mm segment of nerve proximal to a ligature 30 mm from the ganglia

From each animal one nerve was used as a control. The ganglion compartments contained 30 μ Ci [3 H]-leucine in Ringer. Colchicine or colchicine was added to the ganglionic compartments of the experimental nerves and 10 μ Ci to all other compartments. *P* values were obtained by use of a two-tailed *t* test for paired preparations

	Conc mM	Counts/min ganglia $\times 10^3$	% of control	Counts/min at ligature $\times 10^3$	% of control	<i>P</i>	No. of animals
Colchicine	0.1	1793 \pm 140	96.4	113 \pm 18	46.8	<0.005	10
Control		1861 \pm 120		241 \pm 29			
Colchicine	0.025	1330 \pm 48	97.5	13 \pm 21	87.1	<0.02	4
Control		1364 \pm 54		245 \pm 23			
Colchicine	0.1	1961 \pm 324	96.0	104 \pm 23	53.5	<0.01	4
Control		2044 \pm 342		195 \pm 69			
Colchicine	0.025	1312 \pm 161	112.6	144 \pm 70	90.2	n.s.	6
Control		1165 \pm 180		160 \pm 27			

chicine has been shown not to affect energy-dependent neuronal processes other than axonal transport (protein synthesis, electrical activity) except at very high concentration. However, no direct measurements of high energy phosphates (ATP and CrP) have been made in the presence of colchicine or colchicine and the evidence for an unaffected energy metabolism is indirect. In the present study we have measured the effects of transport inhibitory concentrations on the levels of ATP and CrP.

MATERIALS AND METHODS

Frogs (*Rana temporaria*) were used in this study. A preparation consisting of the 8th and 9th dorsal ganglia together with the sciatic nerve was dissected out. A ligature was placed on the nerve 30 mm from the ganglia. The two preparations from the same frog were used for experiment and control respectively and were incubated in an apparatus where the ganglia could be separated from the nerve by silicone grease barriers (Edström & Mattsson 1972). Frog Ringer solution with L-[4,5- 3 H]-leucine (105 Ci/mole, 1 mCi/ml, The Radiochemical Centre, Amersham) and colchicine or colchicine were added to the ganglionic compartments of the experimental nerve and ordinary Ringer to the other compartments. After incubation for 17 h at 18°C the nerves were cut into 4 mm pieces and treated with 5% trichloroacetic acid at 80°C for 1 h. After washing in water the ganglia and the nerve piece were solubilized in Soluene 350 (Packard Co.). The protein incorporated radioactivity was assessed with a Packard 3375 liquid scintillation spectrophotometer in a 0.55% Permafluor III solution (Packard Co.) in toluene.

ATP and CrP were assayed according to Lowry & Passmore (1972). Nerves were incubated for 17 h at 18°C in 0.1 mM colchicine or colchicine solution in Ringer. Subsequently the nerves were weighed, dropped into liquid nitrogen and crushed with a pre-cooled steel pestle. ATP and CrP were extracted with 1 M perchloric acid, the supernatant neutralized and the formation of NADPH from glucose and ATP by hexokinase and glucose-6-phosphate dehydrogenase assayed by spectrophotometry. CrP was subsequently converted to Cr and ATP by creatine kinase and the assay repeated.

Calf brain tubulin was purified by two cycles of polymerization-depolymerization as described by Borej et al. (1974) and modified by Larsson et al. (1976). One part of brain cortex was homogenized with 1.5 parts of PEG-buffer (PIPES 100 mM, EGTA 1 mM, GTP 1 mM, pH adjusted to 6.8 with NaOH). The homogenate was centrifuged at 25000 *g* for 1 h at 0-4°C. Tubulin in the supernatant was polymerized at 37°C for 15 min and centrifuged. Pellets were stored at -40°C. Prior to experiment the pellets were resuspended in PEG-buffer to the desired protein concentration (2.8-3.1 mg/ml) as determined by the method of Lowry et al. (1951) using bovine serum albumin as standard. The tubulin sample was preincubated for 5 min at 4°C with or without drugs (10^{-6} to 10^{-4} M). The time-course of polymerization at 37°C was followed by isometry in the presence of various concentrations of colchicine or colchicine.

ATPase activity was assayed in samples of MT preparations by measuring liberated inorganic phosphate according to Weil-Malherbe & Green (1951) and modified by Ledig et al. (1975).

Colchicine (C=C⁺-demethylcolchicine) was prepared from colchicine by acid hydrolysis (Boyland & Mills 1938). The resulting precipitate was washed with acetone, dissolved in alcohol, crystallized from water-alcohol and dried.

- EDSTRÖM, A. HANSSON, H. A. & SJÖSTRAND J. 1971. Effects of colchicine on axonal transport and ultrastructure of the hypothalamo-neurohypophyseal system of the rat. *Z. Zellforsch.* 113: 771-293.
- CHIL, S. 1976. Mechanism of axoplasmic transport and block of transport by pharmacological agents. *South Afr. Congr. Pharmacol., Heidelberg, Pretoria*, p. 78.
- CHIL, S. & HOLLINGSWORTH, D. 1971. Dependence of fast axoplasmic transport in nerve on oxidative metabolism. *J. Neurochem.* 18: 107-114.
- WILSON, J. C. & McCURE, W. O. 1974. Microtubules and axoplasmic transport. *Brain Res.* 73: 333-337.
- KICE, M. T. 1974. The effects of colchicine and leurocolchicine on the rapid phase of axonal transport in the rabbit nasal system. *Brain Res.* 77: 497-501.
- ANDERSON, P. E. 1971. Mechanism of axoplasmic transport. *J. Neurobiol.* 2: 347-360.
- CHIGNELL, E. SCHÖNHARTING, M. & SIEBERT, G. 1976. On the interaction of colchicine and colchicine with sulfhydryl compounds. *Z. Physiol. Chem.* 357: 567-571.
- SCHÖNHARTING, M., BREER, H., RAHMANN, H., SIEBERT, G. & RÖSNER, H. 1977. Colchicine, a novel inhibitor of fast axonal transport without tubulin binding properties. *Cytobiol.* 16: 106-117.
- SCHÖNHARTING, M., MENDE, G. & SIEBERT, G. 1974. The metabolism of colchicine by mammalian liver microsomes. *Z. Physiol. Chem.* 355: 1391-1399.
- SIEBERT, G., SCHÖNHARTING, M., OTT, M. & SURJANA, S. 1975. Inhibition of phosphatases by the metabolite O^6 -desmethylcolchicine (colchicine) and their reactivation by divalent cations. *Z. Physiol. Chem.* 356: 855-860.
- WALLIN, M., LARSSON, H. & EDSTRÖM, A. 1979. Effects of sulfhydryl reagents on brain microtubule associated ATP-ase activity *in vitro*. *J. Neurochem.* in press.
- WEIL-MALHERBE, H. & GREEN, R. H. 1951. The catalytic effect of acetylcholine on the hydrolysis of organic phosphate bonds. *Biochem. J.* 49: 286-292.
- WEISENBERG, R. C. & TIMASHEFF, S. N. 1970. Aggregation of microtubule subunit protein. Effects of divalent cations, colchicine and vinblastine. *Biochem. J.* 41: 4110-4116.
- WILSON, L. & MEZA, I. 1973. The mechanism of action of colchicine. Colchicine binding properties of sea urchin sperm tail outer doublet tubulin. *J. Cell Biol.* 58: 709-719.
- ZWENG, M. H. & CHIGNELL, C. F. 1973. Interaction of some colchicine analogs, vinblastine and podophyllotoxin with rat brain microtubule protein. *Biochem. Pharmacol.* 22: 2141-2150.

transport at mM concentrations in a way which is related to their amphiphilic character (Edström & Hanson 1975). Direct comparisons between the concentrations used in the MT polymerization and transport experiments are probably not possible. The sources of nervous tissue and the incubation times differ considerably. The present results suggest that the transport inhibitory action by colchicine is on MT or associated proteins of importance for the polymerization process.

Very little is known about the exact mechanisms by which colchicine blocks axonal transport. In most cases there is a decreased number of microtubules after colchicine administration (Banks & Tüll 1975; Hökfelt & Dahlström 1971; Fink et al 1973). However, in some nerves transport can be blocked by colchicine without visible structural changes. In rabbit optic nerves Karlsson et al (1971) found a normal number of MT in spite of transport block after colchicine administration. Identical findings have also been made in the hypothalamo-pituitary system (Dustin et al 1975). Low doses of colchicine might therefore affect the function of MT without degrading them. It is possible that the primary transport inhibitory action of both colchicine and colchicine is on the function of some MT associated protein important for both axonal transport and MT stability.

Neither colchicine nor colchicine affected the ATP or CrP levels of frog nerves. Since colchicine in contrast to colchicine is known to inhibit phosphatases (Siebert et al 1975) its interference with ATPases necessary for the utilization of ATP for axonal transport cannot be excluded. Very little is known about transport ATPases in nerves but a possible candidate is brain dynein, an MT associated ATPase which however was unaffected by colchicine.

This work was supported by grants from The Swedish Natural Science Research Council (grant no. 2535-015). M. Bergvall's Stiftelse and Kungliga Fysiografiska Sällskapet, Lund. The skilful technical assistance of Inger Antonsson is gratefully acknowledged.

REFERENCES

- BANKS P. & TULL, R. 1975. A correlation between the effects of antimitotic drugs on microtubule assembly in vitro and the inhibition of axonal transport in noradrenergic neurones. *J Physiol (Lond)* **253**, 283-294.
- BORISY G. G., OLMSTED J. B., MARCUM J. M. & ALLEN C. 1974. Microtubule assembly in vitro. *Folia Pharmacol. Exp. Biol.* **33**, 167-174.
- BOYLAND E. & MAWSON E. H. 1948. The conversion of colchicine into colchicine. *Biochem. J.* **42**, 1204-1206.
- BYERS, M. R. 1974. Structural correlates of rapid axonal transport: evidence that microtubules may not be directly involved. *Brain Res.* **75**, 97-113.
- DAHLSTRÖM A., HEIWAALL, P.-O. & LARSSON, H. A. 1975. Comparison between the effect of colchicine and vincristine on axonal transport in rat brain neurons. *J. Neural Transm.* **37**, 305-311.
- DUSTIN P. 1978. Microtubules. Springer, Berlin.
- DUSTIN P., HUBERT J. P. & FLAMENT-DURANT, J. 1975. Action of colchicine on axonal flow and pericytes in the hypothalamo-pituitary system of the rat. *Ann. NY Acad. Sci.* **253**, 670-684.
- EDSTRÖM A. & HANSON M. 1975. The mechanism of fast axonal transport. A pharmacological approach. *Neuropharmacology* **14**, 181-188.
- EDSTRÖM A. & MATTSSON H. 1972. Fast axonal transport in vitro in the sciatic system of the frog. *J. Neurochem.* **19**, 205-221.
- FINK B. R., BYERS, M. R. & NIDDAUGH, M. F. 1973. Dynamics of colchicine effects on rapid axonal transport and axonal morphology. *Brain Res.* **64**, 311.
- FITZGERALD T. J., WILLIAMS, B. & UYENAI, E. H. 1971. Colchicine on sodium urate-induced psoriasis in mice: structure-activity relationships of colchicine derivatives. *Proc. Soc. Exp. Biol. Med.* **136**, 170.
- HANSON M. & EDSTRÖM A. 1978a. Microtubule inhibitors and axonal transport. *Int. Rev. Cytol.* **56**, 373-402.
- HANSON M. & EDSTRÖM A. 1978b. Fast axonal transport. Effect of antimitotic drugs and inhibition of energy metabolism on the rate and amount of transported protein in frog sciatic nerves. *J. Neurobiol.* **8**, 97-108.
- HÖKFELT T. & DAHLSTRÖM A. 1971. Effects of two mitotic inhibitors (colchicine and vinblastine) on the distribution and axonal transport of noradrenergic storage particles, studied by fluorescence and electron microscopy. *Z. Zellforsch.* **119**, 460-484.
- KARLSSON J.-O., HANSSON H. A. & SJÖSTRAND J. 1971. Effect of colchicine on axonal transport morphology of retinal ganglion cell. *Z. Zellforsch.* **115**, 65-283.
- LARSSON H., WALLIN M. & EDSTRÖM A. 1973. Induction of a sheet polymer of tubulin by Zn²⁺. *Folia Pharmacol. Exp. Biol.* **32**, 104-110.
- LEDIG M., CIESIELSKI, TRESKA, J. & CAM, Y. MONTAGNON D. & MANDEL, P. 1975. ATP activity of neuroblastoma cell in culture. *J. Neurochem.* **25**, 635-640.
- LOWRY O. H. & PASSONNEAU, J. V. 1972. A flexible system of enzymatic analysis. Academic Press, New York.
- LOWRY O. H., ROSEBROUGH, N. J., FARR, A. L. & RANDALL, R. J. 1951. Protein measurement with the Folin phenol reagent. *J. Biol. Chem.* **193**, 265-274.

Effects of cholera toxin on villous tissue osmolality and fluid and electrolyte transport in the small intestine of the cat

JAN-AXEL HALLBÄCK, MATS JODAL and OVE LUNDGREN

Department of Physiology, University of Göteborg, Sweden

HALLBÄCK J.-A., JODAL M. & LUNDGREN O. Effects of cholera toxin on villous tissue osmolality and fluid and electrolyte transport in the small intestine of the cat. *Acta Physiol Scand* 1979, 107:239-249. Received 4 Apr 1979. ISSN 0001-6772. Department of Physiology, University of Göteborg, Sweden.

The effects of cholera toxin on tissue osmolality and on net transport rates of water, sodium, chloride and potassium as well as on unidirectional fluxes of water and sodium were studied *in vivo* in all experiments the toxin caused net secretion of water, sodium, chloride and potassium. The unidirectional sodium transport from tissue to lumen was increased while the flux in the opposite direction was reduced 180 min after cholera toxin ligation. Cholera toxin produced only a small reduction in the villous tissue hyperosmolality created by the intestinal countercurrent exchanger. This reduction was far too small to explain the observed net secretion of fluid and solutes induced by the cholera toxin. Other mechanisms underlying the cholera secretion are discussed.

It reports from this laboratory experimental evidence has been presented for the existence of a countercurrent multiplier in the villi of the feline small intestine (Hallbjörk et al. 1973; Jodal et al. 1978). This mechanism establishes the hyperosmolar tissue compartment which, according to Curran & McLoosh (1963) is a prerequisite to explain mucosal water absorption in the absence of or against a lumen to plasma osmolality gradient. In the study by Hallbjörk et al. (1979) it was demonstrated that intestinal absorption changed into secretion when the osmolar gradient along the intestinal villi was abolished by substituting sodium ions in the luminal perfusate with choline.

A pronounced fluid loss from the small intestine can also be produced by exposing the intestinal mucosa to various bacterial toxins. The most thoroughly investigated among such agents is the cholera toxin. The present study was performed to elucidate to what extent cholera toxin influences the osmolar gradient normally present along the intestinal villi during fluid absorption. Fluid and electrolyte transport across the intestinal epithelium was also followed in the experiments.

METHODS

A. Operative procedures

The experiments were performed on cats anesthetized i. v. with chloralose (30 mg/kg b.w.) after induction with ether. The animals had been deprived of food for 24 h and had no obvious signs of intestinal infection. The operative procedures and the recordings of blood flow were similar to those described in the paper by Jodal et al. (1975), which should be consulted for details. Briefly total venous outflow from two sympatrically denervated ileal segments (mid-jejunum and mid-ileum) was recorded by a drop recorder and operating as ordinate writer. Mean arterial pressure was measured from the left femoral artery by a pressure transducer (Statham P23AC). Cholinergic influences were eliminated by atropine administration 1 mg/kg b.w.

B. Recording of intestinal net water transport and experimental procedures

Net water absorption or secretion were determined according to the method described by Jodal et al. (1973). In short, a recirculating system was coupled to the lumen of each intestinal segment. The volume change of this system was continuously recorded with a volume transducer connected to the system via Y-tube. Provided no motility occurred the recorded changes of volume reflected net water absorption or secretion. The intraluminal pressure at the outflow end of the segment was kept at about 1

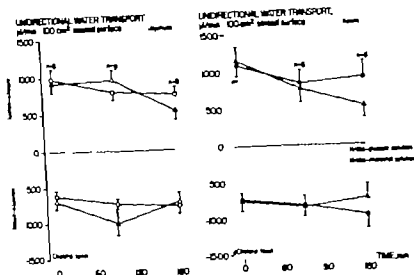


Fig. 2. Unidirectional water transport rates in jejunum and ileum from lumen to tissue (upper panel) and from tissue to lumen (lower panel) before and following 30 min incubation with cholera toxin. Bars denote \pm S.E.

value (water) or $\mu\text{mol}/\text{mm}^2$ 100 cm^2 serosal surface (electrolyte).

Cryoscopic technique

General procedure. The cryoscopic method, including calibration procedures, has been presented in detail by Jodal et al. (1978). Briefly, the frozen intestinal segment (as an obliquely cut cryostat kept at -5°C so as to make 15 μm thick cross-sections at different levels of the villi. The tissue sections were embedded in kerosex between glass plates and transferred to temperatures controlled and consisting of an aluminium block mounted on a Zeiss standard microscope connected with an automatic camera (Robot Star 50). The temperature of the aluminium block could be set at any temperature between

-4.5 and $+0.5^\circ\text{C}$. Thawing of the intestinal tissue was achieved by stepwise increases of tissue temperature which was done automatically with 5 min equilibration period between each step. At the end of each period the tissue section was photographed.

2. Determination of tissue osmolality. The temperature, at which the last ice crystal thawed in villous cross-section, was taken as its melting point. The tissue melting point determined in this study was considered to be a measure of the villous core osmolality. The magnification used (about 50 times) was too low to allow any observation of intracellular ice crystals in the villous tissue. The thawing of the intestinal tissue always started at the villous tips and spread gradually downward until finally the crypt region, the submucosa and the muscularis melted at largely the same temperature. The percentage of melted villous tissue for each temperature level was determined from the photographs. The data were fed into a computer which calculated the tissue osmolality at 5, 10, 20, 30, 40, 50, 60, 70, 80, 90% of villous length as well as the mean osmolality between 5 and 30, 5 and 50 and 5 and 100% villous length as described in more detail by Jodal et al. (1978).

E. Solutions

The lumen of the intestinal segments was perfused with modified Krebs-Henseleit solution containing (mmol/l): 147 Na, 4.7 K, 1.2 Mg^{2+} , 2.5 Ca^{2+} , 132 Cl^- , 25 HCO_3^- , 1.2 PO_4^{3-} and either 30 glucose or 30 mannitol. The osmolality of the solution was 312 ± 10 mOsm kgH_2O (i.e. isotonic with cat plasma).

F. Statistics

Statistical significance was tested using the sign test or Wilcoxon nonparametric tests (Siegel 1956).

or flux from lumen to lumen
mm² 100 cm²

Time	Cholera
2.76 (4)	774 \pm 108 (8)
3.0 (5)	717 \pm 122 (9)
1.76 (4)	847 \pm 172 (4)
1.132 (4)	716 \pm 185 (7)

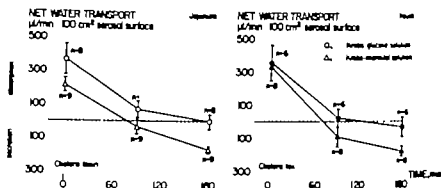


Fig. 1 Net water transport in jejunum and ileum before and following a 30 min exposure to cholera toxin. Bars denote \pm S.E.

cmH₂O and the intestinal segment was perfused at a constant rate of approximately 1 ml/min by means of a roller pump (Model mp-4 Ismatec Sa, Zürich Switzerland). The temperature of the perfusate entering the segment was continuously monitored with a thermocouple thermometer (Electrolab Copenhagen) and kept at about 38°C by a heating pad. Recirculation was prevented by including a large reservoir (700–1 000 ml) in the circulating system.

After a control period of 45 min samples of the perfusing medium entering and leaving each segment were collected. Thereafter 200–300 mg of crude cholera toxin (freeze dried culture filtrate, NIH lot 001) per 10 cm intestine dissolved in 5–6 ml bodywarm physiologic saline solution was placed in the lumen of each segment. Both ends of the segments were closed and the toxin was exposed to the mucosa for 30 min. The toxin was then gently washed out with 30–50 ml warm perfusing medium and the perfusion was again started. Samples of the perfusate entering and leaving the segments were taken at 90 and 180 min after the start of cholera toxin exposure. Immediately after the collection of the last samples from the perfusion system the segments were rapidly extirpated and momentarily frozen in isopentane precooled to about -150°C in liquid nitrogen.

C. Biochemical and radioactive measurements

In order to calculate water and electrolyte fluxes across the intestinal epithelium samples (2–3 ml) were taken from the perfusates entering and leaving the intestinal segments. The samples were collected in plastic tubes. The sodium and potassium concentrations in the samples were determined with a flame photometer (Eppendorf) and the chloride concentrations were determined with a chloride meter (Corning Eel 970 Chloride Meter, Halstead Essex, England).

For determination of water and sodium unidirectional transport from lumen to tissue $62.5 \mu\text{Ci}$ $^3\text{H}_2\text{O}$ and $5 \mu\text{Ci}$ ^{22}Na ($0.05 \mu\text{g}$) were added per liter of the perfusate fluid. Radioactivity was measured by a liquid scintillation (Pak) and Tri-carb liquid scintillation spectrometer model 3300. Quenching was corrected for by using an external standard. The coefficient of variation of the radioactive measurements was below 1%. All analyses were carried out in duplicates.

Intestinal net transport of sodium, potassium and chloride as well as unidirectional transport of water and sodium were calculated as described by Hallböök et al. (1979). The net transport and the fluxes are related to serosal area and expressed as $\mu\text{l}/\text{min}/100 \text{ cm}^2$ serosal

Table 1 Rates of net water transport and unidirectional water fluxes before and 180 min after a 45 min intestinal incubation with cholera toxin

The intestinal segment were perfused with Krebs-glucose or a Krebs-mannitol solution. Mean values \pm S.E. * asterisk denotes statistical significance.

	Net water movement ($\mu\text{l}/\text{min} \times 100 \text{ cm}^2$)		Water flux from lumen to tissue ($\mu\text{l}/\text{min} \times 100 \text{ cm}^2$)	
	Control	Cholera	Control	Cholera
Jejunum				
Krebs-glucose	370 \pm 90 (8)	-1 \pm 44 (8)	997 \pm 139 (8)	773 \pm 110 (8)
Krebs-mannitol	15 \pm 4 (9)	-174 \pm 70 (9)	928 \pm 170 (9)	542 \pm 118 (9)
Ileum				
Krebs-glucose	356 \pm 106 (6)	-3 \pm 58 (6)	1 091 \pm 145 (6)	915 \pm 18 (6)
Krebs-mannitol	330 \pm 87 (8)	-179 \pm 30 (8)	1 15 \pm 184 (6)	579 \pm 157 (7)*

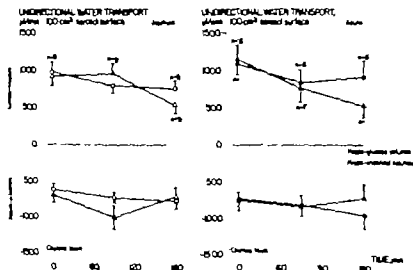


Fig. 2. Unidirectional water transport rates in jejunum and ileum from lumen to tissue (upper panel) and from tissue to lumen (lower panel) before and following a 30 min incubation with cholera toxin. Bars denote \pm S.E.

rice (water) or μ mol/100 cm² serosal surface (electrolyte).

Cryoscopic techniques

General procedure. The cryoscopic method including calibration procedures, has been presented in detail by Jodal et al. (1978). Briefly, the frozen intestinal segment was cut obliquely as a crystal kept at -25°C so as to give 15 μ m thick cross-sections at different levels of the ile. The tissue sections were embedded in kerestane between glass plates and transferred to a temperature-controlled unit consisting of an aluminium block mounted on Zeiss standard microscope connected with an automatic camera (Reuter Star 30). The temperature of the aluminium block could be set at any temperature between

-4.5 and $+0.5^{\circ}\text{C}$. Thawing of the longitudinal tissue was achieved by stepwise increases of tissue temperature, which was done automatically with a 4 min equilibration period between each step. At the end of each period the tissue section was photographed.

2. Determination of tissue osmolality. The temperature, at which the last ice crystal thawed in villous cross-section, was taken as its melting point. The tissue melting point determined in this study was considered to be a measure of the villous core osmolality. The magnification used (about 90 times) was too low to allow any observation of intracellular ice crystals in the villous tissue. The thawing of the longitudinal tissue always started at the villous tips and spread gradually downward until finally the crypt region, the submucosa and the muscularis melted at largely the same temperature. The percentage of melted villous tissue for each temperature level was determined from the photographs. The data were fed into a computer which calculated the tissue osmolality at 5, 10, 20, 30, 40, 50, 60, 70, 80, 90% of villous length as well as the mean osmolality between 5 and 30, 5 and 50 and 5 and 100% villous length as described in more detail by Jodal et al. (1978).

E. Solutions

The lumen of the intestinal segments was perfused with modified Krebs-Henseleit solution containing (mmol/l): 147 Na⁺, 4.7 K⁺, 1.2 Mg²⁺, 2.5 Ca²⁺, 132 Cl⁻, 25 HCO₃⁻, 1.2 PO₄³⁻ and either 30 glucose or 30 mannitol. The osmolality of the solution was 312 ± 10 mOsm/kg H₂O i.e. isotonic with cat plasma.

F. Statistics

Statistical significance was tested using the sign test or Wilcoxon nonparametric tests (Siegel 1956).

or from tissue to lumen
mm: 100 cm²

Cholera	
1-7% (7)	774 (108 (8))
4-9% (9)	717 (122 (9))
1-5% (4)	947 \pm 172 (4)
7-13% (4)	716 (185 (7))

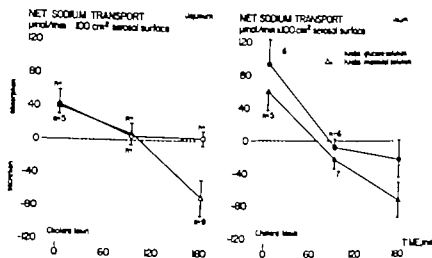


Fig. 3 Net sodium transport in the small intestine before and following a 30 min exposure to cholera toxin. Bars denote \pm S.E.

RESULTS

Water transport Fig. 1 illustrates the net water transport rate in the jejunum (left panel) and in the ileum (right panel) before 90 and 180 min after cholera toxin exposure. Table 1 summarizes net and unidirectional water transport in the jejunum and the ileum during control and after 180 min cholera toxin incubation. A positive value denotes a net water transport from lumen to tissue (absorption) and a negative value a net transport in the opposite direction (secretion). Statistically significant differences are indicated in the Table.

It is evident from Table 1 and Fig. 1 that cholera toxin caused a marked and statistically significant reduction in net water transport, particularly when the intestinal segments were perfused with a krebs-mannitol solution. Fig. 2 shows the unidirectional

water transport rates in the jejunum (left panel) and in the ileum (right panel) plotted as Fig. 1. The observed reductions in net water transport rates in the jejunum and the ileum (Fig. 1) were to be due largely to a reduction in the water transport rates from lumen to tissue (Table 1).

Sodium transport Fig. 3 summarizes the results on net sodium transport rates plotted in a way similar to net water transport (Fig. 1). Table 2 presents net and unidirectional sodium fluxes during control and after 180 min cholera toxin exposure. Statistical significance is indicated in the Table.

Both in the jejunum and in the ileum cholera toxin led to statistically significant decline in net sodium absorption. In fact, in many experiments a net secretion of sodium was recorded. Sodium secretion

Table 2 Rates of net sodium transport and unidirectional sodium fluxes before and 180 min after a 30 min intestinal incubation with cholera toxin

The intestinal segments were perfused with a krebs-glucose or a krebs-mannitol solution. Mean value \pm S.E. * asterisk denotes statistical significance.

	Net sodium movement (mmol/min \times 100 cm ²)		Sodium flux from lumen to tissue (mmol/min \times 100 m ²)	
	Control	Cholera	Control	Cholera
Jejunum				
krebs-glucose	41.9 \pm 17.1 (7)	9.8 \pm 9.1 (7)	81.1 \pm 17.0 (6)	63.5 \pm 11.7 (6)*
krebs-mannitol	39.3 \pm 9.1 (5)	69.9 \pm 1.6 (9)	100 \pm 14 (5)	25.7 \pm 8.5 (10)*
Ileum				
krebs-glucose	93.4 \pm 39.1 (6)	22.5 \pm 0.1 (6)	119.8 \pm 23.3 (5)	40.7 \pm 17.5 (6)
krebs-mannitol	60.2 \pm 6.5 (5)	77.5 \pm 1.3 (7)	107.5 \pm 13.7 (4)	34.7 \pm 9.8 (1)

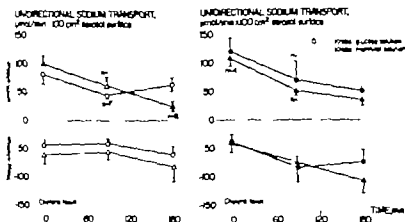


Fig. 4. Unidirectional sodium transport rates in jejunum and ileum from lumen to tissue (upper panels) and from tissue to lumen (lower panels) before and after a 30 min exposure to cholera toxin. Bars denote ± 5 S.E.

is particularly prominent when the perfusate contained mannitol but not glucose. The study of unidirectional fluxes (Table 2 and Fig. 4) revealed that a decrease of net sodium absorption could be ascribed to both a reduction of the lumen to tissue sodium flux and an augmentation of tissue to lumen flux.

Chloride transport. Fig. 5 illustrates net chloride transport before and after exposing intestinal segments to cholera toxin. Table 3 summarizes the results obtained before and 180 min after cholera toxin incubation.

It is clear that cholera toxin caused significant reductions in net chloride transport in both the jejunum and ileum, particularly when using a Krebs-mannitol solution. With no glucose in the

perfusate a marked net loss into lumen of chloride ions was observed.

Potassium transport. The results on potassium transport are presented in Fig. 6 and Table 3. In both intestinal segments, a small rate of potassium absorption during the control period was changed into a small secretion of potassium 180 min after the start of the cholera toxin exposure.

Tissue osmolality. Fig. 7 illustrates the osmotic gradient along the villi in intestinal segments extirpated 180 min after the beginning of the cholera toxin incubation. Results obtained with glucose containing solutions are indicated with circles while those obtained with Krebs-mannitol solutions are denoted with triangles in the jejunum (left panel) and in the ileum (right panel). Tip and mean osmolality in the upper 5 to 30, 5 to 50 and 5 to 100% of villous length are given in Table 4. In this table is also indicated osmolality data obtained during control; previous investigation (Hallback et al. 1979). Exposure to cholera toxin decreased the various villous tissue osmolalities measured in this study. The reduction was, however, statistically significant only in the upper parts of segments exposed to Krebs-glucose solution, and at the villous tip of a jejunal segment perfused with a Krebs-mannitol solution.

Blood flow. Total blood flow in the two intestinal segments including their lymph nodes during control conditions and after cholera toxin incubation are shown in Table 3. Cholera toxin caused statistically significant increases in total blood flow in all

Jejunum		Ileum	
Control		Cholera	
Net flux from tissue to lumen ($\mu\text{mol}/\text{min}/100\text{ cm}^2$)			
Krebs	17.8 (4)	60.6 \pm 15.4 (7)	81.5 \pm 16.2 (8)
Krebs-glucose	14.7 (5)		
Krebs-mannitol			
Tip	1.1 (5)	73	1.0 (6)
Mean	16.2 (4)	107.3 \pm 21.6 (7)	

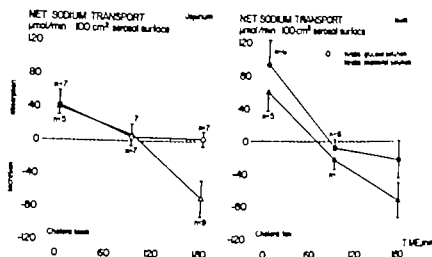


Fig. 3 Net sodium transport in the small intestine before and following a 30 min exposure to cholera toxin. Bars denote \pm S.E.

RESULTS

Water transport Fig. 1 illustrates the net water transport rate in the jejunum (left panel) and in the ileum (right panel) before 90 and 180 min after cholera toxin exposure. Table 1 summarizes net and unidirectional water transport in the jejunum and the ileum during control and after 180 min cholera toxin incubation. A positive value denotes a net water transport from lumen to tissue (absorption) and a negative value a net transport in the opposite direction (secretion). Statistically significant differences are indicated in the Table.

It is evident from Table 1 and Fig. 1 that cholera toxin caused a marked and statistically significant reduction in net water transport particularly when the intestinal segments were perfused with a Krebs-mannitol solution. Fig. 2 shows the unidirectional

water transport rates in the jejunum (left panel) and in the ileum (right panel), plotted as in Fig. 1. The observed reductions in net water transport rates in the jejunum and the ileum (Fig. 1) were to be due largely to a reduction in the water transport rates from lumen to tissue (Table 1).

Sodium transport Fig. 3 summarizes the results on net sodium transport rates plotted in a similar way as for net water transport (Fig. 1). Table 2 presents net and unidirectional sodium fluxes during control and after 180 min cholera toxin exposure. Statistical significance is indicated in the Table.

Both in the jejunum and in the ileum cholera toxin led to statistically significant decline in net sodium absorption. In fact in many experiments a net secretion of sodium was recorded. Sodium secretion

Table 1 Rates of net sodium transport and unidirectional sodium fluxes before and 180 min after small intestine incubation with cholera toxin

The intestinal segments were perfused with a Krebs-glucose or Krebs-mannitol solution. Mean values \pm S.E. Asterisks denote statistical significance.

	Net sodium movement (mmol/min/100 cm ²)		Sodium flux from lumen to tissue (mmol/min/100 cm ²)	
	Control	Cholera	Control	Cholera
Jejunum				
Krebs-glucose	41.9 \pm 17.1 (7)	9 \pm 8.9 (7)	81.1 \pm 17.0 (6)	63.4 \pm 11.7 (1)*
Krebs-mannitol	39.3 \pm 9 (5)	69.9 \pm 1.6 (9)	100 \pm 14 (5)	25.7 \pm 8.5 (10)*
Ileum				
Krebs-glucose	93.4 \pm 29.1 (6)	— 9 \pm 0 (6)	119.8 \pm 23.3 (5)	50.7 \pm 17.5 (10)*
Krebs-mannitol	60 \pm 6 (5)	— 77.5 \pm 1.3 (7)	107.5 \pm 13.7 (4)	14.7 \pm 9.8 (7)

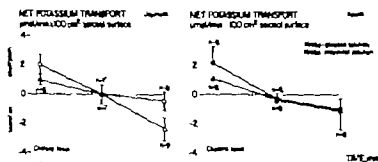


Fig. 4. Net potassium transport in jejunum and ileum before and following a 30 min exposure to cholera toxin. Bars denote $\pm 5 E$.

be majority of studies in vitro as well as in vivo show that glucose absorption and glucose associated sodium transport are unaltered by cholera toxin exposure (Serebro et al 1968 Iber et al 1969 Field 1971). On the other hand it has been suggested that cholera toxin abolishes the electrolyte transport in the neutral NaCl carrier (for references, see Field 1974).

The reduction of the unidirectional sodium transport rate from lumen to tissue after cholera toxin exposure, seen in the present study (Fig. 4) supports the view that cholera toxin caused a depression of solute uptake in agreement with some earlier reports (Phillips 1968, Swallow et al 1968, de Jonge 1973, Krejs et al 1978). The transport mechanism affected by the toxin is however difficult to ascertain from our 'black box' results, but they are consistent with the view expressed above that the cholera toxin mainly decreased the NaCl-coupled absorption at the luminal surface.

The view that cholera toxin initiates or augments an active unidirectional solute secretion from tissue to lumen can be traced back to Snow (1855) and Cohnheim (1890). Based on physiologic studies at least two secretory mechanisms in the jejunum and ileum have been proposed, i.e. an active transport of bicarbonate and by some authors, of sodium chloride. The effect of cholera toxin on these transport processes is not quite clear. According to Powell (1974) the rate of transport of both HCO_3^- and NaCl are increased, while Field (1971) favours the view that cholera toxin initiates a chloride secretion not present during physiologic circumstances. An increased outflux of sodium was observed in this study in agreement with earlier reports (Banwell et al 1968 and 1972, Phillips 1968, Swallow et al 1968, Iber et al 1969, Love 1969 and 1971, Grayner et al 1970, Love et al 1972, Krejs et al 1978, Wald et al 1977). However the present data do not allow any conclusions to be drawn with regard to the cellular actions involved in the observed increase of tissue to lumen flux of sodium.

In our experiments no consistent differences between the jejunal and ileal responses to cholera toxin exposure could be demonstrated, as far as net or unidirectional fluid and solute secretion rates are concerned. This is at variance with the observations by Carpenter et al (1968) who reported that the cholera secretion in vivo in the jejunum was rich in chloride ions while that in the ileum had a high concentration of bicarbonate ions. The latter solute was not measured in the present study but no difference in net chloride transport was observed between jejunum and ileum (Fig. 5).

In the present experiments the intestinal segments were perfused with solutions containing either mannitol or glucose. Adding glucose to the

Net blood flow ml/min (100 g tissue)	
Control	Cholera
24 (2)	41 \pm 5 (17)
	36 \pm 6 (17)
34 (2)	38 \pm 6 (6)
	33 \pm 3 (17)

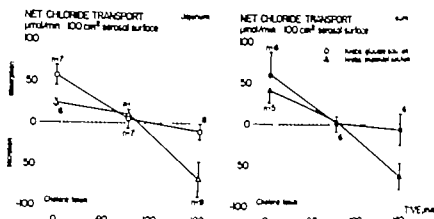


Fig. 5 Net chloride transport in the small intestine before and following a 30 min incubation with cholera toxin. Bars denote \pm S.E.

intestinal segments except in the ileum during Krebs-glucose perfusion.

DISCUSSION

The present study has shown that exposing the cat small intestine to cholera toxin *in vivo* turned a net fluid absorption into a net secretion within 1 to 2 h as earlier reported from this laboratory (Cedgård et al. 1978). Concomitant with this fluid loss a net secretion of Na, Cl and K into the lumen was observed as also reported in a large number of *in vivo* studies on other species including man (Benayati 1966; Banwell et al. 1970), dog (Carpenter et al. 1968; Swallow et al. 1968; Moore et al. 1971; Krejs et al. 1978) and rabbit (Leitch et al. 1966; Love 1969; Norris et al. 1969).

It is generally agreed that water transport across the intestinal epithelium is a passive process, sec-

ondary to the active transport of electrolytes, mainly sodium chloride. In accordance with this view cholera net secretion of fluid and electrolytes may be produced in 3 ways: (1) By a decrease of the normally occurring salt flux from lumen to tissue; (2) by an increase in oppositely directed transport; (3) by a combination of 1 and 2. During physiological circumstances at least 3 major transport mechanisms are responsible for the active transport of sodium across the intestinal epithelium (Scheele et al. 1974). A theogenic glucose-facilitated transport system and a chloride-coupled electrogenic neutral transport mechanism are located at the apical membrane of the enterocyte while a NaK-dependent ATPase carrier is situated at the basolateral membrane. The last mentioned transport system is generally believed not to be influenced by the cholera toxin (Schultz et al. 1974). Furthermore

Table 3 Net chloride transport rate, net potassium transport rate and total intestinal blood flow before and 180 min after a 30 min intestinal incubation with cholera toxin

The intestinal segment were perfused with Krebs-glucose or Krebs-mannitol solution. Mean values \pm S.E. asterisk denotes statistical significance.

	Net chloride movement ($\mu\text{mol/min } 100 \text{ cm}^2$)		Net potassium movement ($\mu\text{mol/min } 100 \text{ cm}^2$)	
	Control	Cholera	Control	Cholera
Jejunum				
Krebs-glucose	57 ± 1 (7)	10 ± 9 (8)	0.1 ± 0.06 (8)	0.46 ± 0.6 (8)
Krebs-mannitol	4 ± 4 (6)	68 ± 1 (9)	0.97 ± 0.36 (6)	37 ± 0.78 (9)*
Ileum				
Krebs-glucose	60 ± 7 (6)	7 ± 19 (6)	1.3 ± 1.10 (6)	0.99 ± 0.69 (6)*
Krebs-mannitol	41 ± 15 (5)	65 ± 16 (8)	1.08 ± 0.19 (8)	-1.16 ± 1.4 (8)

permeability especially at the villous tip. This permeability has been proposed to be the main driving force for passive water and solute absorption (Haljamäe et al. 1973; Jodal 1973; Jodal et al. 1978; Hallböök et al. 1978) and in a recent paper by Hallböök et al. (1979) a correlation between tissue hyperosmolality and net water uptake is demonstrated. One major aim of the present study was to elucidate to what extent cholera toxin decreases the villous hyperosmolality created by a countercurrent multiplier. The results demonstrate that cholera toxin caused only moderate reduction of villous tissue hyperosmolality (Fig. 7 and Table 4), which can be ascribed to at least two possible mechanisms.

First, an intestinal hyperemia occurred after cholera toxin exposure mainly localized to the mucosal part of the intestinal wall, where blood flow doubled as compared to control (Cedergård et al. 1978). This observation probably implies that also villous blood flow is increased during cholera and if so, the efficiency of the countercurrent exchanger becomes decreased (Lundgren 1967; Wane 1975). Such an effect of vasodilatation was demonstrated by Jodal et al. (1978) showing that villous tissue osmolality was lowered to approximately the same level as observed in the present study when pronounced intestinal hyperemia was induced (blood flow 150 ml/min/100 g). The fact that intestinal blood flow during cholera toxin exposure was increased only to 40–60 ml/min/100 g suggests that the flow factor is of fairly subordinate importance in explaining the decrease of villous tissue osmolality.

Second, the multiplying effect of the intestinal countercurrent exchanger is influenced by the rate of net solute transport across the villous epithelium. It was, for example, demonstrated by Haljamäe et al. (1973) that the administration of ouabain markedly reduced the sodium gradient along the villous tip, most probably reflecting a decreased efficiency of the countercurrent multiplier. In analogy with this, it seems reasonable to assume that the decreased tissue osmolality along the villi during cholera toxin exposure observed in the present study was mainly due to depressed transport capacity of sodium across the villous enterocytes as discussed in detail above.

The reduction of villous hyperosmolality induced by cholera toxin incubation in the small bowel was far too small to account for the observed secretion rate of fluid and solutes (Hallböök et al. 1979). In the normal small intestine a net loss of fluid occurs when the mean tissue osmolality in the upper third of the villi was below 400 mOsm/kg H_2O (Hallböök et al. 1979) while in the present study secretion was apparent already when tissue osmolality in the same villous parts was around 600 mOsm/kg H_2O . Part of this difference may be explained by a decrease in epithelial hydraulic conductivity demonstrated in experiments *in vitro* during cholera toxin exposure (Nellans et al. 1974; Powell 1974), lowering lumen to tissue flux of water particularly in the segments perfused with a Krebs-mannitol solution (Table 1). However, the most likely explanation seems to be an increased fluid and solute transport from tissue to lumen, as discussed above. Such an increase in water transport into the lumen was not seen in the present study. This difficulty in finding a correlation between the sodium and water transport rates from tissue to lumen was also seen in other studies that measured unidirectional water fluxes *in vivo* during cholera (Swallow et al. 1968; Barwell et al. 1972). The explanation may be found in the measurements of unidirectional fluxes *in vivo* as mentioned above and possibly also in the fairly short observation time of the present study (cf. Krejs et al. 1978).

The tissue osmolality recorded at the villous tip in the present study is equivalent to a driving force for water around 5 000 mmHg (667 kPa) assuming a reflection coefficient of 0.6 for sodium chloride (Fordtran et al. 1965). With such forces involved it seems less likely that the villi represent the main site for electrolyte and fluid secretion in cholera.

100% of
own length
D₅₀ (g H_2O)

Control	Cholera
1 (13 (9))	447 ± 34 (6)
2 (15 (4))	439 ± 13 (7)
3 (15 (4))	447 ± 31 (6)
4 (19 (4))	439 ± 14 (8)

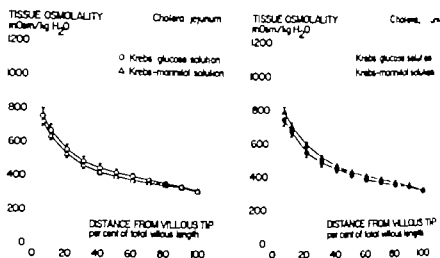


Fig. 7. Tissue osmolality in the villi of the jejunum (left panel) and ileum (right panel) 180 min after a 30 min incubation with cholera toxin. Data were obtained from intestinal segments either perfused with krebs-glucose solutions (circles) or with krebs-mannitol solution (triangles). Bars denote \pm S.E. At many points of the Figs. the S.E. is so small that it falls within the area of the symbols. For number of observations see Table 4.

perfusate markedly reduced the net secretion rates of fluid and electrolytes caused by cholera toxin exposure. Our data thus support findings by Carpenter et al. (1968), Serebro et al. (1968) and Iber et al. (1968) indicating that glucose facilitated electrolyte absorption was unaffected by the cholera toxin. Glucose has proved to be most useful in the treatment of Asian cholera (Phillips 1964; Lancet 1975).

The effects of cholera toxin on the cellular mechanisms of electrolyte transport have been studied mostly in *in vitro* preparations, which offer the possibility for more detailed cellular studies than *in vivo* investigations (cf. Schultz et al. 1974).

The difficulty of standardizing *in vivo* studies is reflected in the present study by the comparatively large scatter of results. An even more striking example of this is the fact that the literature contains reports which demonstrate that the luminal tissue flux of sodium is decreased (Swallow et al. 1968; de Jonge 1975; Krejs et al. 1978), unchanged (Iber et al. 1969; Love 1969) or increased (Blum et al. 1977; Love et al. 1977; Wald et al. 1977) after exposing the small intestine to cholera toxin.

In numerous reports from this laboratory it has been demonstrated that the vascular arrangement of the small intestinal villi can function as a counter-current multiplier and thereby create a marked

Table 4. Tip and mean osmolality in various portions of intestinal villi 180 min after a 30 min *in vivo* exposure to cholera toxin

Control values were recorded in a pre-treatment study (Hallback et al. 1979). The intestinal segments were perfused krebs-glucose or with a krebs-mannitol solution. Mean values \pm S.E. (n). An asterisk denotes statistical significance.

	Villous tip osmolality (mOsm/kg H ₂ O)		5 to 30% of villous length (mOsm/kg H ₂ O)		5 to 90% of villous length (mOsm/kg H ₂ O)	
	Control	Cholera	Control	Cholera	Control	Cholera
Jejunum						
krebs-glucose	1000 \pm 30 (9)	640 \pm 68 (6)	689 \pm 3 (9)	598 \pm 55 (6)	590 \pm 23 (9)	513 \pm 48 (4)
krebs-mannitol	901 \pm 50 (8)	751 \pm 10 (7)	655 \pm 34 (8)	588 \pm 23 (7)	580 \pm 28 (8)	523 \pm 70 (7)
Ileum						
krebs-glucose	940 \pm 33 (8)	740 \pm 63 (6)	679 \pm 22 (8)	584 \pm 54 (6)	591 \pm 19 (8)	557 \pm 47 (4)
krebs-mannitol	895 \pm 57 (8)	789 \pm 44 (8)	680 \pm 43 (8)	624 \pm 4 (8)	601 \pm 34 (8)	553 \pm 19 (3)

1. FORDTRAN, J. S. 1978. Intestinal secretion induced by vasoactive intestinal polypeptide. *J Clin Invest* 61, 1337-1343.
2. VET Editorial. 1975. Oral glucose/electrolyte therapy for acute diarrhoea. *Lancet* i 79-80.
3. ITOH, G. I., THWART, M. E. & BURROWS, W. 1966. Experimental cholera: the rabbit ligated ileal loop.
4. ITOH, G. I. 1967. Isotonic water and ion movement. *J Infect Dis* 116, 308-312.
5. JAE, A. H. G. 1969. Water and sodium absorption by the intestine in cholera. *Gut* 10, 63-67.
6. JAE, A. H. G. 1971. Studies on cholera. *Proc Roy Soc Med* 64, 1028-1029.
7. JAE, A. H. G., PHILLIPS, R. A., ROHDE, J. E. & VALL, N. 1972. Sodium-ion movement across intestinal mucosa in cholera patients. *Lancet* 2, 151-153.
8. LINDGREN, O. 1967. Studies on blood flow distribution and countercurrent exchange in the small intestine. *Acta Physiol Scand*, Suppl. 303.
9. MORAWSKI, S. G., FINKELSTEIN, R. A. & FORDTRAN, J. S. 1971. Ion transport during cholera-induced ileal secretion in the dog. *J Clin Invest* 50, 312-318.
10. JELLANS, H. N., FRIZZELL, R. A. & SCHULTZ, S. G. 1974. Brush-border processes and transapical Na and Cl transport by rabbit ileum. *Amer J Physiol* 226, 1101-1111.
11. FORBES, H. T., CURRAN, P. F. & SCHULTZ, S. G. 1969. Modification of intestinal secretion in experimental cholera. *J Infect Dis* 119, 117-125.
12. PHILLIPS, R. A. 1964. Water and electrolyte losses in cholera. *Fed Proc* 23, 705-712.
13. PHILLIPS, R. A. 1968. Asiatic cholera (With emphasis on pathophysiological effects of the disease). *Ann Rev Med* 19, 69-80.
14. POWELL, D. W. 1974. Intestinal conductance and permselectivity changes with theophylline and cholera toxin. *Amer J Physiol* 227, 1436-1443.
15. SCHULTZ, S. G., FRIZZELL, R. A. & NELLANS, H. N. 1974. Ion transport by mammalian small intestine. *Ann Rev Physiol* 36, 51-91.
16. SEREBRO, H. A., BAYLESS, T. M., HENDRIX, T. R., IBER, P. L. & MCGONAGLE, T. 1968. Absorption of D-glucose by the rabbit jejunum during cholera toxin-induced diarrhoea. *Nature (Lond.)* 217, 1272-1273.
17. STEGEL, S. 1956. Nonparametric statistics for the behavioral sciences. McGraw Hill Kogakusha, Ltd., Tokyo.
18. SNOW, J. 1855. On the mode of communication of cholera. And of Chirchill London.
19. SWALLOW, J. H., CODE, C. F. & FRETER, R. 1968. Effect of cholera toxin on water and ion fluxes in the canine bowel. *Gastroenterology* 54, 35-40.
20. WALD, A., GOTTERER, G. S., RAJENDRA, G. R., TURJMAN, N. & HENDRIX, T. R. 1977. Effect of indomethacin on cholera-induced fluid movement, unidirectional sodium fluxes, and intestinal cAMP. *Gastroenterology* 72, 106-110.
21. WINNE, D. 1975. The influence of villous counter current exchange on intestinal absorption. *J Theor Biol* 53, 145-176.

Thus the present study supports the theory of an intestinal secretion mechanism initiated by cholera toxin the site being anatomically separated from the absorptive area of the villus and probably located to the crypt regions in the small intestine (Hendrix 1971, 1972). The evidence for and against such an intestinal secretion in the crypts obtained in *in vitro* and *in vivo* expts. was recently reviewed by Hendrix & Paulk (1977). A further observation that may be of importance in this connection is the nervous mechanism proposed by Cassuto et al (1979) to be involved in the pathogenesis of cholera.

The cholera toxin was kindly supplied to us by Dr Jan Holmgren, Department of Medical Microbiology, University of Göteborg. The present research was supported by grants from the Swedish Medical Research Council (14X-855), from the Swedish Society for Medical Sciences, from Harald and Grete Jeansson's Fund from Magnus Bergvall's Stiftelse and from the Faculty of Medicine, University of Göteborg.

REFERENCES

- BANWELL, J G, PIERCE, N F, MITRA, R C, CARANASOS, G J, KEIMOWITZ, R I, MONDAL, A & MANJI, P M 1968 Preliminary results of a study of small intestinal water and solute movement in acute and convalescent human cholera. *Ind Jour Med Res* 56: 633-639.
- BANWELL, J G, PIERCE, N F, MITRA, R C, BRIGHAM, K L, CARANASOS, G J, KEIMOWITZ, R I, FEDSON, D S, THOMAS, J, GORBACK, S L, SACK, B & MONDAL, A 1970 Intestinal fluid and electrolyte transport in human cholera. *J Clin Invest* 49: 183-193.
- BANWELL, J G, SHEPHERD, R, THOMAS, J, PIERCE, N F, MITRA, R C, GORBACK, S L, BRIGHAM, K L, FEDSON, D S & MONDAL, A 1972 Net and unidirectional transmucosal flux of sodium and water in acute human diarrheal disease. *J Lab Clin Med* 80: 686-697.
- BENYAJATI, C 1966. Experimental cholera in humans. *Brit Med J* 1: 140-141.
- CARPENTER, C C J, SACK, R B, FEELEY, J C & STEENBERG, R W 1968 Site and characteristics of electrolyte loss and effect of intraluminal glucose in experimental canine cholera. *J Clin Invest* 47: 10-120.
- CASSUTO, J, JODAL, M, TUTTLE, R & LUNDGREN, O 1979 The effect of indomethacin on the secretion induced by cholera toxin in the cat small intestine. *Experientia (Basel)* In press.
- CEDGÅRD, S, HALLBÄCK, D-A, JODAL, M, LUNDGREN, O & REDFORS, S 1978 The effect of cholera toxin on intramural blood flow distribution and capillary hydraulic conductivity in the cat small intestine. *Acta Physiol Scand* 101: 144-158.
- COHNHEIM, J F 1890 Lectures on general physiology. In: A handbook for practitioners and students. Series III. The pathology of the digestive system (A B McKee translator) pp. 949-960.
- CURRAN, P F & MACINTOSH, J R 1961 A model system for biological water transport. *Nature (Lond)* 193: 347-348.
- DE JONGE, H R 1975 The response of small intestinal villous and crypt epithelium to cholera toxin in the guinea pig. Evidence against a specific role of the crypt cells in cholera toxin-induced secretion. *Biochim Biophys Acta (Amst)* 381: 128-143.
- FIELD, M 1971 Intestinal secretion: effect of cAMP and its role in cholera. *New England J Med* 284: 1137-1144.
- FIELD, M 1974 Intestinal secretion. *Gastroenterology* 66: 1063-1084.
- FORDTRAN, J S, RECTOR, F C, LUTON, M F, SOTER, N & KINNEY, J 1965 Permeability characteristics of the human small intestine. *J Clin Invest* 44: 1935-1944.
- GRAYER, D T, SEREBRO, H A, IBER, F L & HENDRIX, T R 1970 Effect of cycloheximide on unidirectional sodium fluxes in the jejunum after cholera exotoxin exposure. *Gastroenterology* 58: 1154-1159.
- HALLMÄE, H, JODAL, M & LUNDGREN, O 1971 Countercurrent multiplication of sodium in intestinal villi during absorption of sodium chloride. *Acta Physiol Scand* 89: 580-593.
- HALLBÄCK, D A, HULTÉN, L, JODAL, M, LUNDGREN, O & LUNDGREN, O 1978 Evidence for the existence of a countercurrent exchanger in the small intestine in man. *Gastroenterology* 74: 683-688.
- HALLBÄCK, D A, JODAL, M, SJÖQVIST, A & LUNDGREN, O 1979 Villous tissue osmolality in intestinal transport of water and electrolytes. *Acta Physiol Scand* 107: 115-125.
- HENDRIX, T R 1971 The pathophysiology of cholera. *Bull NY Acad Med* 47: 1169-1180.
- HENDRIX, T R 1972 Studies in the pathogenesis of cholera. *Trans Am Clin Climatol Assoc* 83: 63-9.
- HENDRIX, T R & PAULK, H T 1977 Intestinal secretion. *Gastrointestinal Physiology* 11: 237-254.
- IBER, F L, MCGONAGLE, T, SEREBRO, H A, LUEBBERS, E, BAYLESS, T M & HENDRIX, T R 1969 Unidirectional sodium flux in small intestine in experimental canine cholera. *Amer J Med Sci* 258: 340-348.
- JODAL, M 1973 The significance of the intestinal countercurrent exchanger for the absorption of water and fatty acids. Thesis. Göteborg AB, Göteborg.
- JODAL, M, HALLBÄCK, D A, SVANVİK, J & LUNDGREN, O 1975 A method for the *in vivo* study of net water transport in the feline small bowel. *Acta Physiol Scand* 95: 441-447.
- JODAL, M, HALLBÄCK, D A & LUNDGREN, O 1978 Tissue osmolality in intestinal villi during *in situ* perfusion with isotonic electrolyte solutions. *Acta Physiol Scand* 102: 94-107.
- KREIS, G J, BARRELEY, R M, READ, N W &

Aggression-provoked renin release from extrarenal and extrasubmaxillary sources in mice

BING and KNUD POULSEN

Institute for Experimental Medicine, Copenhagen and Institute for Biochemistry
Royal Dental College, Copenhagen, Denmark

BING J & POULSEN K. Aggression-provoked renin release from extrarenal and extrasubmaxillary sources in mice. *Acta Physiol Scand* 1979; 107: 51-56. Received 9 April 1979. ISSN 0001-6772. University Institute for Experimental Medicine, and Institute for Biochemistry, Royal Dental College, Copenhagen, Denmark.

In submaxillary salivary glandectomized and nephrectomized mice aggressive behaviour provoked 5 to 40-fold increases in plasma renin concentration. The changes in renin concentration with time were different in different groups of confronted mice with only partial correlation between the pattern and the observable degree of fight. The changes were similar in salivary glandectomized mice with untouched kidneys as in salivary glandectomized and nephrectomized, indicating that aggression causes no measurable, if any renal renin release. Repeated aggression with 2 hourly intervals provoked repeated renin release from extrarenal and extrasubmaxillary sources. The renin concentrations of different organs showed the same mutual relationship as in other mammals, but were about 10-fold higher. Splenectomy was without effect on the aggression-provoked renin release. Antibodies against pure mouse renin neutralized the renin in plasma and organs, which contained only insignificant, if any, peptidase activatable inactive renin. Adrenaline, apomorphine, carbachol and dibyridazine were as isoprenaline and noradrenaline without effect on renin release in salivary glandectomized and nephrectomized mice.

Key words: Splenectomy, hypertension, neurotransmitters, renin-aggression.

Aggressive behaviour provokes vast increase in plasma renin concentration, which reaches about 100 to 600-fold the normal in normal and in nephrectomized mice. Smaller but still marked increases are found in submaxillary glandectomized mice (Bing & Poulsen 1979b). Thus, most of the increase in plasma renin found after aggression in normal and nephrectomized mice is due to release of submaxillary renin. In salivary glandectomized mice the renin release was thought to originate from the kidneys, but an extrarenal release could not be excluded. The aim of the present investigation was to study if aggression provokes an increase in plasma renin concentration in mice which have been salivary glandectomized and nephrectomized, and if so, if this increase can account for the renin release in salivary glandectomized mice with untouched kidneys. Further studies aimed at elucidating differences in the effect of various degrees of aggression, the origin of the released renin and the mechanism of renin release.

MATERIAL AND METHODS

Animals. Male albino mice of the Danish State Serum Institute strain, most of which weighed 40-65 g, but some weighing 25 to 40 g, were individually housed for at least 30 days. Submaxillary glandectomy was performed at least 10 days and nephrectomy 2 h before the start of the experiments. In some mice the spleen was removed together with the kidneys. The operations were performed during short-term ether anaesthesia after pretreatment with pentobarbital. No mouse was used for more than one experiment.

Aggression was provoked by grouping for 20 mice of 3 to 4 previously isolated mice in small cages as described by Valzelli (1969). In most cases aggression was provoked and intensified by addition of one or two previously isolated non-operated mice.

Blood was sampled from tail vein during light ether anaesthesia. Tissues were removed after decapitation in order to draw as much blood as possible. Extraction of the tissue samples after addition of 1% Triton 100 and decantation of renal supernatant in plasma and extracts as performed as described by Poulsen & Jørgensen (1974), using their trapping radioimmunoassay for angiotensin I. Extracts of mesenteric, striated muscle and lung tissue were performed after pooling of pieces from 2

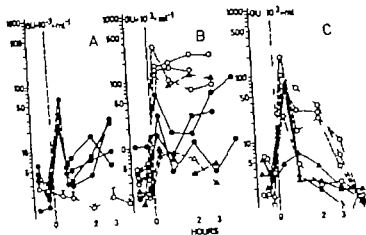


Fig. 1 (A) The time course of the plasma renin concentrations in 4 adrenalectomized and nephrectomized mice in which grouping caused vigorous fighting (marked \bullet), and the mean values and SEM of that of 9 mice which were kept isolated (\circ). (B) Values from three groups of mice (marked \circ , \bullet and Δ) which fought after addition of non-operated mice to intensify fighting. (C) Values from 2 groups of mice (marked \circ and \bullet) both after grouping only reacted with startle. In B and C the individuals of different groups are marked by different symbols. The ordinates indicate the concentration in $\text{GU} \times 10^{-3} \text{ ml}^{-1}$ on a logarithmic scale. The abscissa show the time in hours before and after the start of confrontation, which is marked by dashed line.

hours after the start of the aggression including 4 ears, 4 spleens and 3 hearts, containing 68 to 95 72 ± 90 and about $5 \text{ GU} \times 10^{-6}$ per g, respectively

Pepsin activation of renin in plasma and organ extracts from adrenalectomized and nephrectomized mice

The procedure for pepsin activation showed that plasma and extracts contained little, if any, active renin. It was performed on 11 plasma samples. Six of these were taken 2 ($n=3$) or 4 ($n=3$) hours after nephrectomy of previously adrenalectomized mice, which were kept isolated without any confrontation. Their renin concentration was 0.6 to 2.5 $\text{GU} \times 10^{-6} \text{ ml}^{-1}$ before the pepsin treatment. Each resulted in only small increases, less than 15% in 3 samples and 19–31 and 67% in the 3 other samples. Five plasma samples obtained from similarly pretreated mice 20 to 60 min after the start of an aggressive fighting of 20 min duration contained from 4.8 to 140 $\text{GU} \times 10^{-6} \text{ ml}^{-1}$. All of these the pepsin activation was without significant effect. After pepsin treatment of extracts of 5 spleens, 4 livers and 1 heart, containing 8 to 120 $\text{GU} \times 10^{-6} \text{ g}^{-1}$, 2 extracts showed small (20 and 47%) increase, while

the renin concentration was less than 15% increased in 2 and quite unchanged in the other 6 samples.

Renin concentration and activity in some organs of adrenalectomized and nephrectomized mice

The mean renin concentration in extracts of 28 livers removed from 0 to 8 hours after nephrectomy was $75 \text{ GU} \times 10^{-6} \text{ g}^{-1}$ (range 30–130), the values in this and the following groups not changing significantly with time during the 8 hours. There was no significant difference between the concentration in livers taken from the group of mice in which aggression had been provoked ($n=15$) and those taken from the group in which the mice had not been confronted ($n=13$), the mean values being 82 and 67 respectively. In 19 extracts of livers removed 4 hours after nephrectomy the mean renin concentration was significantly lower, being about $15 \text{ GU} \times 10^{-6}$ per g (range 0.3–36). In both aggressive and non-aggressive mice ($p=0.001$). As 50 g mouse has a liver weight of about 1 g, the total renin content in the liver is about $150 \text{ GU} \times 10^{-6}$ during the first 8 hours and about $3 \text{ GU} \times 10^{-6}$ 4 hours after bilophrectomy.

to 4 mice. Antibody against pure submaxillary mouse renin prepared as described by Malling & Poulsen (1977) was used for antirenin neutralisation of enzymatic activity of some of the samples, which for this purpose were mixed with antibody at 7.4. Pepsin activation was performed as previously described (Nielsen, Malling & Poulsen 1978).

The effect of different neurotransmitters and other pharmacological agents on renin release in sialoadenectomized and nephrectomized mice was determined using conscious mice in these as in all other experiments. In cases where the substances were given by intra-arterial injection a catheter was placed in the femoral artery at least 2 hours before the experiments. Blood pressure determination was in some experiments performed using a Tybjaerg-Hansen transducer and a Servo-gor 511 recorder. The agents used were adrenaline given as a 1 min lasting intra-arterial infusion of 1 µg/g b.w. ($n=7$) after pretreatment with 0.5 µg/g dihydralazine. The dopaminergic agonist apomorphine was given subcutaneously in doses of 0.1 or 0.3 mg/kg ($n=5$) or 1 to 5 mg/kg ($n=4$) of apomorphine chloride. Carbachol was given subcutaneously in doses of 3 ($n=4$) or 12 ($n=3$) µg/kg and in 3 mice in doses from 200 to 800 µg/kg. The use of the agents was based on the well documented effect of some neurotransmitters and of hypertension on renal and (or) submaxillary renin release (see Bling & Poulsen 1979a). Significance of changes in renin concentration were estimated by Student's t test.

RESULTS

I Change in plasma renin concentration with time after different degrees of aggression of sialoadenectomized and nephrectomized mice

In 4 mice which fought vigorously and looked exhausted after the 70 min lasting fight the plasma renin concentration rose markedly at the end of the fight. The control values from 9 sialoadenectomized and nephrectomized mice which were kept isolated during the experiment are marked \bar{O} (Fig. 1A). To 3 groups each of 3 sialoadenectomized and nephrectomized mice 2 non-operated mice were added in order to initiate and intensify the aggression. The results are seen in Fig. 1B. The results from groups of 3 and 4 mice respectively in which the confrontation did not result in any fight but only in nosing and small starts with small sudden movements are seen in Fig. 1C. Independent of the degree of fighting a marked increase in renin was seen immediately after the confrontation ($p<0.01$, $n=70$). The renin concentration varied considerably in the following hours but stayed elevated for several hours in most animals. Only in the 7 animals (Fig. 1C) involved in the lowest degree of reaction

the renin concentration had reached basal values at the end of the experiments.

II Comparison between the effect of aggressive behaviour on plasma renin concentration in sialoadenectomized mice which were either nephrectomized or sham operated before the confrontation

Nine isolated previously sialoadenectomized mice were divided into 3 groups. In 1 of these mice were nephrectomized and 1 sham-operated, and the third group 1 was nephrectomized and 1 sham-operated. Two hours after the operations blood was taken for renin assay whereafter the mice belonging to a group were confronted provoking aggressive behaviour. After the end of the 70 min fight the changes in plasma renin concentration were followed for about 6 h. As shown in Fig. 2 there was no significant difference between the mean values of the nephrectomized (\bar{O}) and the sham-operated (\bullet) for the first 3 hours after the confrontation, but at the end of the experiments the values of the sham-operated were somewhat higher ($p<0.05$) than those of the nephrectomized.

III Effect on the plasma renin concentrations of 3 consecutive confrontations causing aggressive behaviour with about 2 hourly intervals

The effect of repeated fightings was studied in 3 sialoadenectomized mice with untouched kidneys (not shown) and in 3 previously sialoadenectomized mice which had been nephrectomized before the first fighting (Fig. 3). The three consecutive fightings resulted in a 3-fold (range 2.4-4.0 fold) (range 1.5-5.0) and 14-fold (range 10-20) increase in renin concentration respectively ($n=6$).

IV Antirenin neutralisation of renin in plasma and organs from sialoadenectomized and nephrectomized mice

In 8 plasma samples taken at the end of a 20 min lasting aggression ($n=6$ with a renin concentration from 63 to 195 G.U. $\times 10^{-3}$ ml) or 4 and 6 hours later ($n=$ containing about 30 G.U. $\times 10^{-3}$ ml) addition of antirenin completely neutralized the enzymatic effect of the renin. A total neutralization was also obtained in 11 extracts of organ removed

III. Effect of adrenaline, apomorphine, atchachol and dihydralazine on the renin in sialadenectomized and nephrectomized mice

Mice, which after previous sialadenectomy at least nephrectomized about 2 h in advance adrenaline, the dopaminergic agonist apomorphine and atchachol did not provoke any change in plasma renin concentration. The doses, way of administration and number of mice are given in Materials and Method. Also injection of 0.5 µg/kg dihydralazine (such in 5 mice) provoked a prolonged decrease in blood pressure from a mean of 130 mmHg (range 120-140) to a mean of 60 mmHg (range 40-75) was without effect on the plasma renin concentration.

DISCUSSION

In previously submaxillary sialadenectomized and about 2 hours nephrectomized mice aggression was found to provoke a marked increase in plasma renin concentration. The concentration rose from $2-7 \times 10^{-4} \text{ ml}^{-1}$ to values about 5 to 40-fold higher. The pattern was different in different groups about an evident relation to the observable degree of fighting (Fig. 1A and B). There was a similarly marked increase in plasma renin concentration in mice, which after grouping did not fight but only reacted with startle. In these mice the plasma renin returned faster to normal values (Fig. 1C).

In sialadenectomized and nephrectomized mice aggression provoked similar changes in renin concentration previously found in sialadenectomized mice with untouched kidney (Berg & Paulsen 1979a). A direct comparison of the values in groups of these types of differently pretreated mice showed that the changes with time were not significantly different during the first 3 hours after the confrontation. The values were however somewhat higher in the mice with untouched kidneys 6 hours after the confrontation. This difference can be due to a loss of renal renin caused by the repeated bleedings, the total loss of blood being about 400 µl.

When sialadenectomized and nephrectomized mice were fighting repeatedly each new fight provoked a new increase in plasma renin concentration. Such in this way could reach higher values than after single fight (Fig. 3). But even after

single fight the increase is unexpectedly high, when compared with the total renin content in the organs studied. The liver and spleen, which had the highest concentrations had a total content of about $160 \text{ GU} \times 10^{-4}$ and the concentrations of heart, lung and mesentery were much lower. The relation between the concentration in the different organs was about the same as previously found in other mammals (Eskoldsen 1973; Ganten et al. 1977), but both in the organs and in plasma the concentration was about 10-fold higher in mice than in the other animals. Both in plasma and in organ extracts the renin was totally neutralized with antibodies against pure submaxillary renin. The marked renin release can probably not be due to transformation of inactive renin, as both plasma and organ extracts contained only small, if any, pepsin activatable renin.

The source of the renin released in sialadenectomized and nephrectomized mice is unknown. The pronounced decrease in the renin content of the liver about 24 hours after the nephrectomy was found in non-aggressive as well as in mice which had been aggressive. And the unchanged renin concentration in the liver during the first hours after the aggression makes it improbable that the liver is the main source. As splenectomized and sham-splenectomized mice reacted in the same way, the spleen cannot play a major role as source. The mesentery vessels were in a previous study found to release renin when dogs were subjected to hypotension (Ganten et al. 1970). This was, however, not confirmed in experiment on rats (Wernze & Sekl 1972) and dogs (Fingard et al. 1974), and the present study shows that in mice dihydralazine provoked marked hypotension without causing any increase in plasma renin. So far the source of the renin released by aggression in sialadenectomized and nephrectomized mice has not been determined. The evidence for persistent vascular renin activity in nephrectomized rats (Swales & Thurston 1973, 1977) makes it possible that the vessels found throughout the body are the source from where the renin is released.

It is unknown how the aggressive behaviour provokes the renin release. In the previous experiment (1) isoprenaline and noradrenaline were found to be unable to provoke renin release in sialadenectomized and nephrectomized mice. The present study shows the same lack of effect after injection of adrenaline, the dopaminergic apomorphine and atchachol.

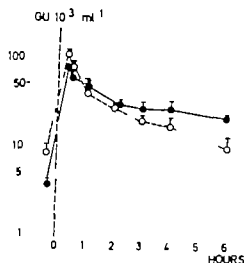


Fig. 1 The mean values of aggression-provoked changes in plasma renin concentration with time in 4 shamadenectomized mice with untouched kidneys (marked ●) and 5 shamadenectomized and nephrectomized mice (○). Vertical lines indicate SEM. Ordinate and abscissa as in Fig. 1.

In extracts of spleens removed from 0 to 8 hours after nephrectomy the renin concentration was not significantly lower in 13 isolated mice than that of the 15 mice in which aggression had been provoked with mean values 127 (range 40–400) and 218 (range 25–500) $\text{GU} \times 10^{-3}$ per g respectively. In 19 spleens removed 4 h after nephrectomy the renin concentration was the same as in those removed after 0–8 h in 9 mice which were kept isolated the concentration being 176 $\text{GU} \times 10^{-3}$ per g (range 30–220). However the mean concentration of renin in spleens removed 74 h after nephrectomy in 10 mice in which aggression had been provoked was markedly lower than in spleens removed 0–8 h after nephrectomy the mean value being 77 (range 10–180) ($p < 0.05$). The mean total renin content of the spleen of a 50 g isolated mouse was about 10 $\text{GU} \times 10^{-3}$.

In the other organs studied the renin concentrations were markedly lower than in the liver and spleen. In the heart the concentration was about 3 $\text{GU} \times 10^{-3}$ per g both in the first 8 h ($n=9$) after nephrectomy and after 74 h ($n=1$) in mice which had not been confronted. After aggression the values were similar 8 h ($n=1$) and 4 h after nephrectomy ($n=9$). The mean total renin content of a heart was 0.6 $\text{GU} \times 10^{-3}$. In mesenteric striated muscle- and lung tissue of 16 mice in which no aggression had been provoked the mean renin concentrations in $\text{GU} \times 10^{-3}$ per g were 1.7 (range 0.9–2.7), 0.6 (range 0.3–1.4) and 1.8 (range 0.8–

3.6) respectively with no difference between the concentration in tissue taken 0 to 8 and 4 h after nephrectomy.

VIII Effect of splenectomy on the aggression-provoked increase in plasma renin concentration

In 3 groups of each 7 splenectomized and sham-splenectomized mice all of which were shamadenectomized and nephrectomized a 20 min aggression was provoked 7 h after the operation. Immediately after the fight the renin concentration was unusually high being 960 $\text{GU} \times 10^{-3}$ ml⁻¹ in one of the splenectomized mice. In the other 6 splenectomized mice the mean concentration was 165 $\text{GU} \times 10^{-3}$ ml⁻¹ (range 47–420) which was the same as in the sham-splenectomized in which the mean was 165 (range 47–405). Also in the following 4 hours the values of the splenectomized and sham-operated followed each other. In one group of 2+7 mice the renin concentration stayed high as in the group marked 0 in Fig. 1B the mean concentrations being 168 and 163 milli GU per ml 4 h after the confrontation. Of the other 4+4 mice 1 sham-operated died after about 1½ h. In the other 7 mice the renin concentrations were falling throughout the experiments the mean value 4 h after the confrontation being 22 $\text{GU} \times 10^{-3}$ ml⁻¹ (range 8–38) in the splenectomized and 17 (range 6–35) milli GU per ml in the sham-splenectomized.

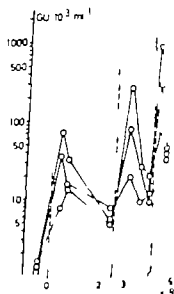


Fig. 3 The time course of the plasma renin concentration in 3 shamadenectomized and nephrectomized mice in which aggression was provoked 3 times (marked by vertical dashed lines). Ordinate as in Fig. 1.

Changes in lipoprotein-lipase activity and lipid stores in human skeletal muscle with prolonged heavy exercise

LARS LITHELL, JAN ORLANDER, RICKARD SCHÉLE, CRISTIL SJÖDIN and JAN KARLSSON

Department of Geriatrics, University of Uppsala, the Department of Animal Nutrition, Swedish University of Agricultural Sciences, Uppsala, and the Laboratory for Human Performance (FOA 57), Stockholm, Sweden

LITHELL, L., ORLANDER, J., SCHÉLE, R., SJÖDIN, C. & KARLSSON, J. Changes in lipoprotein-lipase activity and lipid stores in human skeletal muscle with prolonged heavy exercise. *Acta Physiol Scand* 1979, 107: 257-261. Received 19 April 1979. ISSN 0001-6772. Department of Geriatrics, University of Uppsala, the Department of Animal Nutrition, Swedish University of Agricultural Sciences, Uppsala, and the Laboratory for Human Performance (FOA 57), Stockholm, Sweden.

Lipoprotein-lipase (LPL) activity and intracellularly stored triglycerides were determined in muscle biopsies taken before and after an 85 km sking race from 7 volunteers. The triglyceride stores were larger in slow twitch than in fast twitch fibres (proportions 5:1 before the race). The LPL activity increased and the triglyceride stores in slow twitch fibres decreased during the race. The best trained subjects had the largest TG stores before the race and their TG stores also decreased most during the race. These subjects also had very small increases of LPL activity. The least trained subject on the other hand showed a 6-fold increase of LPL activity. The high post-race LPL activity in less trained subjects indicates a higher capacity for uptake of fatty acids from serum TG as compared to the more trained subjects.

Key words: Intermyofibrillar fat, lipoprotein-lipase activity, muscle fibre types, prolonged exercise.

During normal dietary conditions the relative exercise intensity (i.e. actual \dot{V}_{O_2} /maximal \dot{V}_{O_2}) determines to what extent energy is supplied from carbohydrates or fat (Christensen & Hansen 1939a). Christensen & Hansen (1939b) found that increasingly more energy was derived from fat metabolism during prolonged exercise at a relative intensity of about 65% but no fat adaptation was seen at intensities above 75% (Hermansen et al. 1967). Fat combustion during exercise was higher after a fat-rich diet than after a carbohydrate-rich diet (Christensen & Hansen 1939) or normal diet (Bergstrom et al. 1967). During exercise the uptake of free fatty acids (FFA) from plasma into muscle is related to its concentration in the plasma (for review Gollnick 1977). The increase in fat combustion during prolonged exercise, however, can only partly be explained by an increased uptake of plasma free fatty acids (for review Frøberg 1977). Fatty acids might also be supplied from plasma triglycerides (TG) which are hydrolysed by the en-

zyme lipoprotein-lipase (LPL) localized at the endothelium in the muscle capillaries (Robinson 1970). A work-induced increase of the enzyme activity should mean that an increased amount of fatty acids were made available to the muscles (Robinson 1970). In addition an increased utilization of intramuscular TG stores that are hydrolyzed by the intracellularly located so-called hormone-sensitive lipase (Bjorntorp & Furman 1962) has been demonstrated both in animals (Bakthwin et al. 1973; Reisman et al. 1973) and humans (Howald 1975; Eysén et al. 1977).

The objects of the present investigation has been to evaluate the changes in both LPL activity and intracellular lipid stores in muscle tissue during extremely prolonged, heavy exercise.

SUBJECTS AND METHODS

Seven male physical education students who participated in an 85 km cross-country sking race (the Vasa race 1977)

CONCLUSION

Aggression provokes a marked release of renin in sialoadenectomized and nephrectomized mice. The source of this extrasubmaxillary and extrarenal renin could not be located to any single organ and is possibly located to vessels throughout the body. A similar renin release was not provoked by injection of several catecholamines or carbachol and was not provoked by prolonged marked hypotension. Aggression causes only insignificant if any release of renal renin in sialoadenectomized mice.

This study was supported by grants from King Christian X Foundation and the Foundation of Insurance Companies of 1952. The excellent technical assistance of Vibeke Meyland-Smith is gratefully acknowledged.

REFERENCES

- BING J & POULSEN K 1979 Differences in renal and submaxillary renin release after stimulation with isoprenaline and noradrenaline. *Acta Physiol Scand* 105: 58-63.
- BING J & POULSEN K 1979 In mice aggressive behaviour provokes vast increase in plasma renin concentration causing only slight if any increase in blood pressure. *Acta Physiol Scand* 105: 64-72.
- ESKILDSEN P C 1973 Renin in different tissues, amniotic fluid and plasma of pregnant and non-pregnant rabbits. *Acta Pathol Microbiol Scand* 81: 263-68.
- FAGARD R, FOSSION E, CAMPFORTS M DE RUYCK M & AMERY A 1974 Extraction and production of renin and angiotensin II across several vascular bed in dogs. *Experientia (Basel)* 30: 598-600.
- GANTEN D, HAYDUK A, BRECHT H W, BOUCHER R & GENEST J 1970 Evidence of renin release or production in splanchnic territory. *Nature (Lond)* 226: 531-532.
- GANTEN D, SCHELLING P & GANTEN U 1971 Tissue isorenins. In: *Hypertension* (ed. J. Genest, L. Kolw & O. Kuchel) pp. 40-56. McGraw-Hill, New York.
- MALLING C. & POULSEN K 1977 A direct radioimmunoassay for plasma renin in mice and its evaluation. *Biochem Biophys Acta (Amst)* 491: 541-541.
- NIELSEN A H, MALLING C. & POULSEN K 1978 Characteristics and conversion of high molecular weight forms of renin in plasma and their receptor activation by the current acid treatment. *Biochem Biophys Acta (Amst)* 534: 46-57.
- POULSEN K. & JØRGENSEN J 1974 An enzyme radioimmunochemical microassay of renin activity in concentration and substrate in human and animal plasma and tissues based on angiotensin I trapping by antibody. *J Clin Endocrin Metab* 39: 816-825.
- SWALES J D & THURSTON H 1973 Generation of angiotensin II at peripheral vascular level: studies using angiotensin II antisera. *Clin Science and Mol Med* 45: 691-700.
- THURSTON H & SWALES J D 1977 Blood pressure response of nephrectomized hypertensive rats to converting enzyme inhibition: evidence for peripheral renin activity. *Clin Science and Mol Med* 57: 299-304.
- VALZELLI L 1969 Aggressive behaviour induced by isolation. In: *Aggressive behaviour* (ed. S. Garzanti & E. B. Sigg) pp. 167-171. Amsterdam.
- WERNZE H & SEKI A 1972 Absence of renin secretion in the portal venous system in rats. *Experientia (Basel)* 28: 649-650.

Table 2. Skeletal muscle lipoprotein-lipase (LPL) activity and volume fraction of subcellular components in muscle (ST) and fast twitch (FT) muscle fibres before and after the race
 mean values \pm S.D. Ranges are given within parentheses, $n=7$

	Before	After	Change	P
L (nmol \times min ⁻¹ g ⁻¹)	18.4 \pm 7.0 (11.9–31.4)	58.9 \pm 33.2 (16.1–116.5)	+40.5 \pm 32.2 (3.2–100.7)	<0.02
lipid droplets				
ST (%)	0.95 \pm 0.32	0.33 \pm 0.39	-0.60 \pm 0.30	<0.01
FT (%)	0.19 \pm 0.13	0.12 \pm 0.10	-0.07 \pm 0.24	>0.40
P_{rel} ST-FT	<0.001	<0.10	<0.02	
sarcomeres				
ST (%)	10.4 \pm 1.7	5.5 \pm 2.6	-4.9 \pm 2.7	<0.01
FT (%)	8.9 \pm 1.1	9.6 \pm 3.1	0.7 \pm 3.5	>0.60
P_{rel} ST-FT	<0.05	<0.05	<0.01	
mitochondria				
ST (%)	4.80 \pm 0.75	5.86 \pm 1.43	+1.06 \pm 1.34	<0.10
FT (%)	2.74 \pm 0.23	2.77 \pm 0.83	+0.03 \pm 0.84	>0.90
P_{rel} ST-FT	<0.001	<0.001	<0.10	
myofibrils				
ST (%)	83.9 \pm 2.0	88.3 \pm 2.2	+4.4 \pm 2.9	<0.01
FT (%)	88.1 \pm 1.4	87.5 \pm 2.8	-0.6 \pm 3.6	>0.60
P_{rel} ST-FT	<0.001	>0.40	<0.01	

me and that the increase was negatively correlated to the amount of ski-training before the race. As the amount of ski-training was closely correlated to the performance time ($r = -0.86$, $P < 0.05$) and \dot{V}_{O_2} ($r = 0.73$, $P < 0.10$) it is not possible to state which of the three factors—if any—that was the primary determinant for how much the LPL activity increased.

No significant relation was seen between LPL activity and the percentage of ST fibres. This could be due to the small sample size but the finding is supported by a later study with a larger sample (Lubell et al. to be published). In rats, however, all muscles have 10-fold higher LPL activity than white muscles (Lindler et al. 1976; Borenstafin et al. 1975).

Before the race more lipid was stored in ST than in FT fibres and well-trained subjects had on an average larger lipid stores. This finding is in accordance with the observations of Morgan et al. (1964) and Hoppeler et al. (1973) of 2.5 times higher lipid content in trained than in untrained human muscles.

During the race lipid stores decreased significantly only in ST fibres. Well-trained subjects used on an average more of the total stores (= ST + FT) than the less trained subjects did.

Others have reported decreased content of TG in

human muscle after prolonged heavy exercise, i.e. after a previous Vasa race (Froberg & Mossfeldt 1971) and after a 100 km race (Howald 1975) but not for ST and FT fibres separately. However, Reitman et al. (1973) found that muscle TG decreased by 70% in red, 25% in intermediate and not at all in the white portion of rats quadriceps muscles. This is in agreement with Paul's statement (1975) that intramuscular (and even more so extramuscular) fat depots of trained animals and subjects supply more fatty acids as energy substrate during exercise of long as well as of short duration as compared to the fat depots of untrained animals.

The decrease in the volume fraction of sarcomeres in ST fibres indicates a dehydration of this fibre type. This dehydration is probably connected with the glycogen depletion which Froberg et al. (1978) found to be more frequent in ST fibres (85%) than in FT fibres (5%) after a previous Vasa race as water is released when glycogen is oxidized (Sjöter 1963; Kozłowski & Saltin 1964).

There was a relationship between the change in LPL activity and the amount of lipid droplets before the race, so that the well-trained subjects who had the largest amount of lipid droplets had the smallest increase of LPL activity. There might be several reasons for this. One possibility is that in the well-trained subjects fatty acids released from the in-

Table 1 Characteristics of the 7 subjects

	Mean	S D	Range
Age (yrs)	26.7	3.7	23-32
Height (cm)	175.7	4.3	169.7-180.8
Weight (kg)	76.4	6.8	66.6-83.1
\dot{V}_{O_2} max ($l \times min^{-1}$)	4.76	0.37	4.16-5.40
\dot{V}_{O_2} max ($ml \times kg^{-1} \times min^{-1}$)	67.7	6.6	57.3-78.0
Muscle composition (%ST)	46.4	14.6	21-64
Amount of ski training (km)	429	291	100-1 000
Performance time (h)	8.07	1.39	5.3-9.6

volunteered for the study. The subjects were of normal body weight and height but varied considerably in capacity (within the upper part of the normal range) and training level as indicated in Table 1. Mean performance time was 8.07 h (range 5.32-9.6).

Biopsies were taken from the vastus lateralis the day before the race and immediately after the race with a needle technique (Bergstrom 1964). The biopsies were divided into three portions. One was embedded in a plastic medium for histochemical analysis by staining sections for myosin ATPase and identification of slow twitch (ST) and fast twitch (FT) fibres (Gomori 1941; Padykula & Herman 1955). The second portion was used for electron microscopy. Small pieces of muscle tissue were fixed in 4% phosphate-buffered glutaraldehyde, pH 7.4 (at least 2 h at 0°C), washed, post-fixed in 1% veronal-buffered osmium tetroxide, washed in Tyrode's solution and dehydrated in ethanol. After treatment with propylene oxide the muscle pieces were embedded in Epon. Approximately 60-70 nm thick longitudinal sections were cut with a LKB Ultratome I, stained with uranyl acetate and lead citrate and examined in a Siemens Elmiskop 101. About 25 micrographs (final magnification about 25 000) were taken at random from two tissue blocks per biopsy. Volume fractions of myofibrils, mitochondria, lipid droplets and sarcoplasm (including sarcoplasmic reticulum and transverse tubules) were estimated stereologically according to Weibel (1969). The study was restricted to the fibrillar space of the muscle fibres. The fibres were classified as ST or FT according to Z-line width (Payne et al. 1975; Wroblewski & Jun von 1975; Eisenberg & Kudva 1976; Tomarek 1976; Bylund et al. 1977) measured to the nearest 0.1 μm with a measuring magnifier. Only clearly demarcated Z-lines were chosen for measurement, excluding the fuzzy matrix present at the Z-line border.

Muscle LPL activity was determined in the third portion of the biopsy as described by Lithell & Buhner (1978). The biopsies were incubated in a reaction medium containing 3H -trioleate labelled intralipid (Vitrum, Stockholm, Sweden). The release of 3H -oleic acid was used as a measure of LPL activity. The activity was expressed as nmol fatty acids (FA) released per minute and per gram wet weight of muscle tissue ($nmol \times g^{-1} \times min^{-1}$). This method determines the activity of the heparin-releasable LPL located at the capillary endothelium

(Robinson 1970). Specificity tests have excluded that any of the determined enzyme activity is due to hormone sensitive lipase.

Maximal oxygen uptake (\dot{V}_{O_2} max) was determined during treadmill exercise one week before the competition according to the Douglas bag procedure (Saltin & Linnarsson 1967).

Statistical methods. Student's *t*-distribution was used when testing the means of individual changes (before-after) and differences (ST-FT) and when testing correlation coefficients.

RESULTS

Skeletal muscle LPL activity averaged $18.4 \text{ mol FA} \times g^{-1} \times min^{-1}$ (range 11.9-31.4) before the race and the average increase during the race was 29% (range 8-637%) (Table 2). The increase in LPL activity was negatively related to \dot{V}_{O_2} max ($r = -0.85$, $P < 0.05$), amount of ski training before the race ($r = -0.97$, $P < 0.01$) and fitness level, i.e. \dot{V}_{O_2} max divided by body weight ($r = 0.71$, $P < 0.05$) and positively related to performance time ($r = 0.83$, $P < 0.05$).

Before the race the volume fraction of lipid droplets was higher in ST than in FT fibres (0.95% vs. 0.19%, $P < 0.001$). The total volume fraction of lipid droplets (i.e. in ST and FT fibres) before the race was positively correlated to the amount of training ($r = 0.90$, $P < 0.05$). (The correlations for volume fraction in ST and FT separately, $r = 0.46$ and 0.72 , were not statistically significant.) During the race the volume fraction of lipid droplets decreased in ST fibres (from 0.95% to 0.35%, $P < 0.01$) but not significantly in FT fibres (Table 2).

The decrease in volume fraction of lipid droplets in the combined muscle fibre population (ST + FT) correlated positively to \dot{V}_{O_2} max ($r = 0.86$, $P < 0.05$) and amount of training ($r = 0.79$, $P < 0.05$), i.e. well-trained subjects used more of the intramuscular lipid stores than the less trained subjects did.

A 46% decrease in the volume fraction of sarcoplasm (from 10.4 to 5.5%, $P < 0.01$) was found in the ST fibres.

A negative relationship ($r = -0.81$, $P < 0.05$) was present between the increase in LPL activity and the pre-race volume fraction of fat droplets in the muscle fibres (ST + FT).

DISCUSSION

One major finding in this study was a marked increase in skeletal muscle LPL activity during exercise.

Table 2. Skeletal muscle lipoprotein-lipase (LPL) activity and volume fraction of subcellular components in muscle (ST) and fast twitch (FT) muscle fibres before and after the race
 mean values \pm S.D. Ranges are given within parentheses, $n=7$

	Before	After	Change	P
Lipid (nmol/min/g)	18.4 \pm 7.0 (11.9–31.4)	58.9 \pm 33.2 (16.1–116.5)	+40.5 \pm 32.2 (1.2–100.7)	<0.02
Lipid droplets				
ST (%)	0.91 \pm 0.32	0.35 \pm 0.39	-0.60 \pm 0.30	<0.01
FT (%)	0.19 \pm 0.15	0.12 \pm 0.10	-0.07 \pm 0.34	>0.40
P_{diff} ST-FT	<0.001	<0.10	<0.02	
Sarcoplasm				
ST (%)	10.4 \pm 1.7	5.5 \pm 2.6	-4.9 \pm 2.7	<0.01
FT (%)	8.9 \pm 1.1	9.6 \pm 3.1	+0.7 \pm 3.5	>0.60
P_{diff} ST-FT	<0.05	<0.05	<0.01	
Sarcomeres				
ST (%)	4.80 \pm 0.75	5.86 \pm 1.43	+1.06 \pm 1.34	<0.10
FT (%)	2.74 \pm 0.23	2.77 \pm 0.83	+0.03 \pm 0.84	>0.90
P_{diff} ST-FT	<0.001	<0.001	<0.10	
Mitochondria				
ST (%)	83.9 \pm 2.0	88.3 \pm 2.2	+4.4 \pm 2.9	<0.01
FT (%)	88.1 \pm 1.4	87.5 \pm 2.8	-0.6 \pm 3.6	>0.60
P_{diff} ST-FT	<0.001	>0.40	<0.01	

we found that the increase was negatively correlated with the amount of ski-training before the race. As the amount of ski-training was closely correlated to ski performance time ($r=-0.86$, $P<0.05$) and \dot{V}_{O_2} ($r=0.73$, $P<0.10$) it is not possible to state which of the three factors—if any—that was the primary determinant for how much the LPL activity increased.

No significant relation was seen between LPL activity and the percentage of ST fibres. This could be due to the small sample size but the finding is supported by a later study with a larger sample (Lindell et al. to be published). In rats, however, all muscles have 10-fold higher LPL activity than white muscles (Lindell et al. 1976; Borenstajin et al. 1975).

Before the race more lipid was stored in ST than in FT fibres and well-trained subjects had on an average larger lipid stores. This finding is in accordance with the observations of Morgan et al. (1969) and Hoppeler et al. (1973) of 2.5 times higher lipid content in trained than in untrained human muscles.

During the race lipid stores decreased significantly only in ST fibres. Well-trained subjects used on an average more of the total stores (= ST + FT) than the less trained subjects did. Others have reported decreased content of TG in

human muscle after prolonged heavy exercise i.e. after a previous Vasa race (Froberg & Mossfeldt 1971) and after a 100 km race (Howald 1975) but not for ST and FT fibres separately. However, Rentman et al. (1973) found that muscle TG decreased by 70% in red, 25% in intermediate and not at all in the white portion of rats quadriceps muscles. This is in agreement with Paul's statement (1975) that intramuscular (and even more so extramuscular) fat depots of trained animals and subjects supply more fatty acids as energy substrate during exercise of long as well as of short duration as compared to the fat depots of untrained animals.

The decrease in the volume fraction of sarcoplasm in ST fibres indicates a dehydration of this fibre type. This dehydration is probably connected with the glycogen depletion which Forsberg et al. (1978) found to be more frequent in ST fibres (85%) than in FT fibres (5%) after a previous Vasa race as water is released when glycogen is oxidized (Sreter 1963; Kozlowski & Saltin 1964).

There was a relationship between the change in LPL activity and the amount of lipid droplets before the race, so that the well-trained subjects who had the largest amount of lipid droplets had the smallest increase of LPL activity. There might be several reasons for this. One possibility is that in the well-trained subjects fatty acids released from the in-

tramuscular lipid droplets might repress the synthesis of LPL (Pykälistö 1970). Another possibility is that there is a time lag from the time when the synthesis rate increases before increased LPL activity can be detected at the endothelial level. During feeding experiments it was found that the heparin releasable LPL activity in adipose tissue was not significantly increased until 6 h after the feeding started (Pykälistö et al 1975). Furthermore very heavy work leading to exhaustion after one hour did not significantly affect the LPL activity in muscle tissue in man (Lithell et al 1979). However during heavy work for 8-9 h the LPL activity in muscle increased also in well trained subjects (Cedermarck et al. to be published).

The results of the present study confirmed earlier findings that the energy supply to the muscles during heavy physical work is partly derived from intracellularly stored lipid and that well-trained individuals both have larger stores and more readily use them. However a selective decrease of lipid droplets in human ST fibres has to the best of our knowledge not been reported earlier. Hermansen et al (1967) found lower respiratory quotients in trained as compared to untrained subjects indicating a relatively larger fat combustion in trained subjects. Those subjects who performed the race fastest also had the best capability for fat combustion in terms of larger stores of lipid and a greater readiness to use it. If the time lag before LPL activity increases at the endothelial level is about 6 h training does not seem to shorten this period but to result in larger lipid stores that can be used before increased amounts of fatty acids derived from serum triglycerides can be available.

We are indebted to Miss Kristina Stensjö for skilful technical assistance.

The study has been supported by grants from the Swedish Medical Research Council (Project No. 4251 and 5446) and the Research Council of the Swedish Sport Federation.

REFERENCES

- BALDWIN K M, REITMAN J S, TERJUNG R L, WINDER W W & HOLLOSZY J O 1973 Substrate depletion in different types of muscle and in liver during prolonged running. *Amer J Physiol* **225** 1045-1050.
- BERGSTRÖM J 1966. Muscle electrolyte in man. *Scand J Clin Lab Invest. Suppl* 68.
- BERGSTRÖM J, HERMANSEN L, HULTMAN E & SALTIN B 1967 Diet, muscle glycogen and physical performance. *Acta Physiol Scand* **71** 140-150.
- BJÖRNTORP P & FURMAN R H 1966. Lipid activity in rat heart. *Amer J Physiol* **203** 323-326.
- BORENSZTAJN J, RONE M, S. BABIRAK, S P, McGARR, J A. & OSCAI L B 1971 Effect of exercise on lipoprotein lipase activity in rat heart and skeletal muscle. *Amer J Physiol* **229** (1) 394-397.
- BYLUND A-C, BJURÖ T, CEDERBLAD G, HOLM J, LUNDHOLM K, SÖSTRÖM, V, ÅNGQUIST K A & SCHERSTEN T 1977 Physical training in man. Skeletal muscle metabolism in relation to muscle morphology and running ability. *Int J Appl Physiol* **36** 151-170.
- CEDERMARK M, FRÖBERG J, LITHELL H & TESCH P 1979 Effect of long-term (10 days) heavy exercise on skeletal muscle metabolism in man. To be published.
- CHRISTENSEN E H & HANSEN O 1939a. Respiratorischer Quotient und O₂-Aufnahme. *Skand Arch Physiol* **81** 180-189.
- CHRISTENSEN E H & HANSEN O 1939b. Untersuchungen über die Verbrennungsvorgänge bei Langdauernder schwerer Muskelarbeit. *Skand Arch Physiol* **81** 15-159.
- CHRISTENSEN E H & HANSEN O 1939c. Arbeitsfähigkeit und Ernährung. *Skand Arch Physiol* **81** 161-171.
- EISENBERG B R. & KUDA A. M 1976 Discrimination between fiber populations in mammalian skeletal muscle by using ultrastructural parameters. *J Cell Biol* **9** Res **54** 76-88.
- ESSÉN B, HAGENFELDT L. & KAUSER, L 1971 Utilization of blood-borne and intramuscular substrates during continuous and intermittent exercise in man. *J Physiol (Lond)* **265** 489-506.
- FORSBERG A, TESCH P & KARLSSON J 1977 Effect of prolonged exercise on muscle strength performance. In: *Biomechanics VI A* (ed. E. Asmussen and K. Jørgensen) pp. 6-67. University Park Press Baltimore.
- FRÖBERG S O 1977 Metabolism of skeletal muscle lipids. (Thesis.) Acta Universitatis Upsalienensis, Uppsala Sweden.
- FRÖBERG S O & MOSSFELDT F 1971 Effect of prolonged strenuous exercise on the concentration of triglycerides, phospholipids and glycogen in muscle of man. *Acta Physiol Scand* **82** 167-171.
- GOLLNICK P D 1977 Free fatty acids turnover and the availability of substrate as a limiting factor in prolonged exercise. In: *The Marathon* (Physiological, medical, epidemiological and psychological studies) (ed. P. Mälvik) of 301 pp. 64-71. The New York Academy of Sciences New York.
- GOMORI G 1941 The distribution of phosphate in normal organs and tissues. *J Cell Comp Physiol* **17** 71-83.
- HERMANSEN L, HULTMAN E & SALTIN, B 1967 Muscle glycogen during prolonged severe exercise. *Acta Physiol Scand* **71** 179-139.
- HOPPELER H, LUTHI P, CLAASSEN H, WEIBEL, E R & HOWARD H 1973 The

- the ultrastructure of the normal human skeletal muscle. A morphometric analysis on untrained men, women and well-trained orienteers. *Pflügers Arch* 344: 217-232.
- OWALD, H. 1973. Ultrastructural adaptation of skeletal muscle to prolonged physical exercise. In: *Metabolic adaptation to prolonged physical exercise* (ed. H. Howald and J. R. Poortmans), pp. 372-383. Birkhäuser Verlag, Basel.
- OWALD, H. & SALTIN, B. 1964. Effect of exercise on body fluids. *J Appl Physiol* 19: 1119-1124.
- POEL, D., CHERNIK, S. S., FLECK, T. R. & SCOW, R. O. 1976. Lipoprotein lipase and uptake of dehydronon triglyceride by skeletal muscle of rats. *Amer J Physiol* 231 (3): 860-864.
- STHELL, H. & BOBERG, J. 1978. Determination of lipoprotein-lipase activity in human skeletal muscle tissue. *Biochim Biophys Acta (Amst.)* 528: 58-68.
- STHELL, H., HELLSING, K., LUNDQVIST, G. & MALMBERG, P. 1979. Lipoprotein-lipase activity of human skeletal muscle and adipose tissue after intense physical exercise. *Acta Physiol Scand* 105: 312-315.
- YORGAN, T. E., SHORT, F. A. & COBB, L. A. 1969. Alterations in human skeletal muscle lipid composition and metabolism induced by physical conditioning. *Biochemistry of Exercise, Medicine and Sport* 3: 116-121.
- JEIKILÄ, E., TORSTI, P. & PENTTILÄ, O. 1963. The effect of exercise on lipoprotein lipase activity of rat liver, adipose tissue and skeletal muscle. *Metabolism* 12 (9): 863-865.
- PADYKULA, H. A. & HERMAN, E. 1955. The specificity of the histochemical method for adenosine triphosphatase. *J Histochem Cytochem* 3: 170-195.
- PALL, P. 1975. Effects of long lasting physical exercise and training on lipid metabolism. In: *Metabolic adaptation to prolonged physical exercise* (ed. H. Howald and J. R. Poortmans), pp. 156-193. Birkhäuser Verlag, Basel.
- PAYNE, C. M., STERN, L. Z., CURLESS, R. G. & HANNAPPEL, L. K. 1975. Ultrastructural fiber typing in normal and diseased human muscle. *J Neurol Sci* 25: 99-108.
- PYKÄLISTÖ, O. 1970. Regulation of the adipose tissue lipoprotein lipase by free fatty acid. (Thesis.) Helsinki.
- PYKÄLISTÖ, O. J., SMITH, P. H. & BRUNZELL, J. D. 1975. Determinants of human adipose tissue lipoprotein lipase. Effect of diabetes and obesity on basal and diet-induced activity. *J Clin Invest* 56: 1108-1117.
- REITMAN, J., BALDWIN, K. M. & HOLLOSZY, J. O. 1973. Intramuscular triglyceride utilization by red, white and intermediate muscle and heart during an exhausting exercise. *Proc Soc Exp Biol (N Y)* 142: 628-631.
- ROBINSON, D. S. 1970. The function of the plasma triglycerides in fatty acid transport. In: *Comprehensive biochemistry lipid metabolism* (ed. M. Florkin and E. H. Stoltz), vol. 18, pp. 51-116. Elsevier, Amsterdam.
- SALTIN, B. & ÅSTRAND, P.-O. 1967. Maximal oxygen uptake in athletes. *J Appl Physiol* 23: 353-358.
- SUETER, F. A. 1963. Distribution of water sodium and potassium in resting and stimulated mammalian muscle. *Canad J Biochem* 41: 1035-1045.
- TOMANEK, R. J. 1976. Ultrastructural differentiation of skeletal muscle fibers and their diversity. *J Ultrastr Res* 55: 21-27.
- WEIBEL, E. R. 1969. Stereological principles for morphometry in electron microscopic cytology. *Int Rev Cytol* 26: 235-302.
- WROBLEWSKI, R. & JANSSON, E. 1975. Fine structure of single fibers of human skeletal muscle. *Cell Tiss Res* 161: 471-476.

The effect of ingestion of amino acids, glucose and fat on circulating neurotensin-like immunoreactivity (NTLI) in man

UNE ROSELL and ÅKE ROKAEUS

Department of Pharmacology, Karolinska Institutet, Stockholm, Sweden

ROSELL, U. & ROKAEUS, Å. The effect of ingestion of amino acids, glucose and fat on circulating neurotensin-like immunoreactivity (NTLI) in man. *Acta Physiol Scand* 1979, 107: 263-267. Received 19 April 1979. ISSN 0001-6772. Department of Pharmacology, Karolinska Institutet, Stockholm, Sweden.

The effect of ingestion of amino acids (Vasom N), glucose, and fat (Introlipid) on the concentration of neurotensin-like immunoreactivity (NTLI) in plasma was determined in 6 healthy male volunteers. After ingestion of Introlipid (55 ml, 200 mg ml⁻¹) there was significant increase in the plasma concentration of NTLI. The calculated integrated total NTLI response (6.7 ± 2.5 nM over 180 min) was statistically significant. Although isocaloric amounts of Vasom and glucose also increased the plasma concentration of NTLI, these increases were not statistically significant. The data indicate that fat is an important stimulus for the release of NTLI from the small intestine. It is suggested that neurotensin, or metabolite in blood may be a hormone involved in the postprandial inhibition of gastric motility and gastric acid secretion elicited from the small intestine.

Key words: Enterogastrone, gastrointestinal hormone, neurotensin

In several species, including man, immunocytochemical investigations have shown that neurotensin, a tridecapeptide (Carraway & Leeman 1973, 1975), is stored in a specific type of cell (the N cell) which is present in the mucosa of the ileum and, to a lesser extent, in the colon and duodenum (Carraway & Leeman 1976, Orei et al 1974, Seidler et al 1977, Helmsaedter et al 1977, Polak et al 1977, Frigetto et al 1977). In anesthetized dogs higher concentrations of neurotensin-like immunoreactivity (NTLI) were found in blood draining from the ileum than in the arterial blood (Marshford et al 1978a), which indicates that neurotensin is released into the blood from the ileum. It has been shown in man that ingestion of mixed meal causes a marked rise in the concentration of NTLI in blood (Besterman et al 1978, Marshford et al 1978a) and food appears to exert a major influence on the blood concentration of NTLI (Marshford et al 1978a). Neurotensin administered by intravenous infusion in low doses in dogs elicits inhibition of gastric motility (Andersson et al 1977), suppression of gastric acid secretion

(Andersson et al 1976), vasodilatation in the gastrointestinal region and a delayed vasoconstriction in subcutaneous adipose tissue (Rosell et al 1976). Taken together these data suggest that neurotensin, or metabolite thereof in the blood, may be a hormone serving some physiological function in relation to the digestion of food (Marshford et al 1978a).

The present experiments were designed to find out if one or more of the principal constituents of a mixed meal has a dominant effect on the venous concentration of NTLI in humans.

METHODS

Venous plasma NTLI was examined in 6 healthy male volunteers, aged 22-47 years after an overnight fast; the experiments being started between 8 and 10 a.m. On separate days, the subjects were given amino acids (430 ml as Vasom N, Vitrum), glucose (30 g as 300 ml Glucose, ACO 100 mg ml⁻¹) or fat (11 g as 55 ml Introlipid, Vitrum, 200 mg ml⁻¹) orally in isocaloric amounts (about 460 \pm 105 kcal). After having ingested Vasom, glucose or Introlipid, sufficient water was given to make the final volume of fluid administered 500 ml. One subject was given 500 ml of

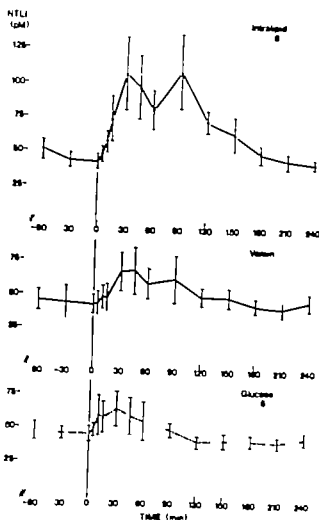


Fig. 1 Concentrations of NTLI in plasma after oral administration of Intralipid, Vitamin or glucose. Number of subjects = 6. The vertical bars indicate the standard error of the means. $p < 0.05$, $p < 0.01$.

water orally on a separate day. Each volunteer stood or sat in an upright position while ingesting the nutrients. Heparin (Vitrum 50 unit \times ml blood) and aprotinin (Trasykol 100 k.U. \times ml blood) were added to the venous blood samples. The samples were kept in ice until centrifugation at $+4^{\circ}\text{C}$. The plasma was stored at -20°C until subjected to radioimmunoassay.

The method used in the radioimmunoassay of neurotensin will be presented in detail elsewhere (to be published) and only a brief description of the method is given here. The antiserum (0-7701) was raised in rabbits by injection of neurotensin (Beckman) coupled to bovine serum albumin using 1-ethyl-3-(3-dimethyl-1-amino-propyl)-carbodiimide HCl (Goodfriend, Leese & Fasman 1964). The antigen was injected together with Freund's complete adjuvant at 3-8-week intervals. This antiserum reacts with neurotensin (NT) NT (1-11) (Gln) NT and (Gln) NT (1-11) but not with NT (4-13) or smaller C-terminal fragments of NT. It shows no cross-reactivity with the gastric inhibitory polypeptide (GIP), the vasoactive intestinal

peptide (VIP), secretin, cholecystokinin-33, cholecystokinin-39, pancreatic glucagon, substance P, neuropeptide Y, bombesin, gastrin-17, gastrin-34 or with tyrosyl-pantidecapeptide. Synthetic neurotensin (Beckman) was labelled with ^{125}I using the chloramine T method (Hart & Greenwood 1964). The assay can measure levels down to 5 pM. Work is under way to determine whether the actions of neurotensin (vasoconstriction in adipose tissue) may be caused by substances derived from neurotensin (Rosell et al. 1978).

In order to estimate the integrated NTLI response to area under the plasma concentration-time curve from the time of ingestion of the nutrients to 180 min thereafter when the NTLI concentration had returned to control, (AUC_{0-180}) was calculated using the trapezoidal rule. The control value was estimated graphically by drawing a straight line between the control sampling points before the ingestion of the nutrients and the sampling point 180-240 min post ingestion. To calculate the integrated response, the area under the straight line over 180 min was subtracted from the total AUC_{0-180} .

Statistical evaluation of the data was performed with the Wilcoxon signed rank test and Student's *t*-test for correlated means. The results are reported as mean \pm standard error of the mean ($M \pm \text{S.E.}$).

RESULTS

After an overnight fast, the mean concentration of neurotensin-like immunoreactivity (NTLI) in plasma was 51 ± 6.7 pM ($n=6$). Following ingestion of Intralipid, the concentration of NTLI increased in all the subjects. Two peaks of elevated NTLI in plasma were seen, one at 30 min and the other at 60 min (109 ± 77 pM), with return of the plasma level of NTLI to control levels by 180 min (Fig. 1). The calculated integrated NTLI response was 6.7 ± 1.0 pM \times 180 min.

Table 1 Integrated responses of NTLI after administration of nutrients (nM \times 180 min)

Subject	Intralipid	Vitamin	Glucose
AB	18	6.9	4.3
SR	8.1	0.9	0
AJ	7.6		0
AR	5	1.4	0
JL	3	0.5	0
GO	1.6		0.3
Mean \pm S.E.	6.7 ± 1.0	4 ± 1.5	1.1 ± 0.8
	$p < 0.05$	n.s.	n.s.

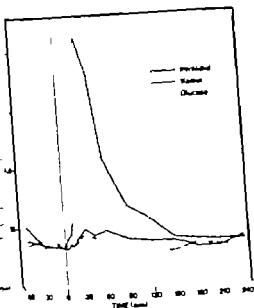


Fig. 2. Concentration of NTLI in plasma in one subject after oral administration of Intralipid, Vamin or glucose.



Fig. 3. Concentration of NTLI in plasma in one subject after oral administration of Intralipid, Vamin or glucose.

nounced interindividual variations, the lowest value being 1.6 nM over 180 min and the highest 18 nM over 180 min. The subject with the most pronounced NTLI response after Intralipid also responded with an increased release of NTLI after ingestion of Vamin, glucose and the same volume of water (500 ml) (Fig. 4).

DISCUSSION

The present results indicate that fat is a strong stimulus for the production of increased levels of

NTLI over 180 min (Table 1). After ingestion of Vamin, the NTLI in blood rose in all 4 subjects but there was an appreciable increase in only 2 subjects and the mean peak concentration did not differ significantly from the mean resting concentrations. Similarly the calculated integrated NTLI response was not significant (Table 1). After ingestion of glucose the NTLI level in blood increased in only 1 of 5 subjects. The mean concentration of NTLI in blood and the integrated response were not significantly different from resting values (Fig. 1 and Table 1).

Although all subjects responded with an increased concentration of plasma NTLI after ingestion of Intralipid, there was a pronounced interindividual variability particularly as regards time-response relationships. In some subjects there was a clearcut increase of NTLI in plasma already at 10 min with a maximum at 30 min (Fig. 2) whereas in another an increase in plasma concentration was found at 90 min (Fig. 3). These interindividual differences partly explain the finding that the mean plasma concentration curve of NTLI after Intralipid ingestion show peak values (Fig. 1). However in two subjects the plasma NTLI concentration curves did show two peaks at 30 min and 90 min respectively (Fig. 4). The integrated NTLI response after Intralipid ingestion also showed pro-

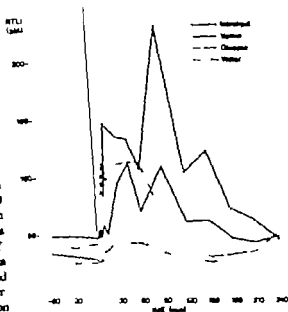


Fig. 4. Concentration of NTLI in plasma in one subject after oral administration of Intralipid, Vamin, glucose or water.

NTRI in blood. Although ingestion of amino acids and glucose caused an increase in NTRI in some subjects, fat was clearly the most active nutrient in this respect. In one subject responding with an increased NTRI to all 3 nutrients, 500 ml of water also caused a slight increase of NTRI. This may indicate that the distension of parts of the gastrointestinal tract may be of significance for the release of NTRI. However, distension is not of importance in all individuals, since ingestion of 500 ml of Vamin or glucose did not change the concentration of NTRI in blood in all subjects. We have reported earlier that there was no response of NTRI to alcohol, coffee or heavy exercise (Mashford et al. 1978a). Our new data further support and extend the hypothesis that food, and particularly fat, exerts a major effect on the plasma concentration of NTRI in humans.

The rise in NTRI is probably caused by release of neurotensin from the glandular neurotensin-containing cells in the small intestine, presumably due to a direct exposure of the gastrointestinal tract to nutrients. Evidently, the fat does not have to be absorbed, since intravenous administration of Intralipid in the same dosage as was ingested orally did not influence the concentration of NTRI (to be published). The segment of the gut from which nutrients elicit release of neurotensin is not known. One possibility is of course that neurotensin is released from the jejunum-ileum, where most of the neurotensin-containing cells are located (cf. Bloom & Polak 1978). In some of the subjects, an increased NTRI level was noticed 10 min after the ingestion of fat. This may seem a short period for the fluid to pass into the small intestine and there cause a release of neurotensin, which is detected as increased NTRI in blood. However, it has been shown in fasting normal subjects that chyme appears in the small intestine 100 cm distal to the Treitz ligament from 10 to 30 min after administration of a homogenized standard meal (Clain, Liang & Malagelada 1978). There is also the possibility that some neurotensin is released from its storage sites by the action of releasing hormones or a nervous reflex originating from the proximal part of the gastrointestinal tract. Further studies are needed to identify the site from which neurotensin is released following food intake and to elucidate the release mechanisms.

Since the end of the nineteenth century it has been known that gastric secretion and gastric

motility are inhibited when ingested fat reaches the small intestine (Ewald & Boas 1886; Babkin 1940). In man, several studies have been made in recent years to elucidate the action of fat in the small intestine on gastric secretion and gastric motility. Windsor, Cockell & Lee (1969) found that ingestion of fat into the duodenum and small intestine depressed a near maximal gastric acid output to approximately 50%. Similarly, Christensen & coworkers (1976) have demonstrated a pronounced inhibition of gastric acid secretion in the human small intestine following infusion of Intralipid 40–50 cm distal to the ligament of Treitz. Clain, Liang & Malagelada (1978) diverted the chyme from the intestine at a site 100 cm distal to the ligament of Treitz, which resulted in an increased gastric secretory response to a meal. They suggested that the distal small intestine plays an inhibitory role in postprandial gastric secretion. Thus, several groups have demonstrated in man the existence of a potent postprandial gastric acid inhibitory mechanism in the distal part of the small intestine, which is activated by fat. Experimental evidence has been obtained that this inhibition elicited by fat (and also by acid and hypertonic glucose, Gregory 1967) is caused by a hormone from the intestinal mucosa, and Kosaka & Lim (1930) named it enterogastrone. Several gastrointestinal hormones have been suggested to have enterogastrone activity (e.g. secretin, cholecystokinin and gastric inhibitory peptide, GIP), although none of these has been established as the enterogastrone (cf. Babkin 1940; Gregory 1967; Brown et al. 1975 and Cataland 1974). Our finding that ingestion of fat causes a pronounced increase in the plasma concentration of NTRI during 2 h or more suggest that neurotensin or a metabolite thereof may be involved in the postprandial inhibition of the gastric motility and gastric acid secretion elicited from the small intestine. The localization of most of the glandular neurotensin-containing cells to the small intestine, where fat seems to elicit the inhibition of gastric acid secretion and gastric motility, supports such a hypothesis. In addition, iv infusion of neurotensin in anesthetized dogs in low doses (4×10^{-8} pmol \times kg \times min $^{-1}$) inhibits motor activity in the antral part of the stomach (Andersson et al. 1977) and gastric acid secretion (Andersson et al. 1976). However, before neurotensin or some metabolite thereof can be ascribed a physiological role as an enterogastrone it remains to be shown that NTRI

secretions in blood after ingestion of fat are in a range found after the administration of doses of apomorphine capable of inhibiting gastric acidity or gastric secretion in humans.

This study was supported by the Swedish Medical Research Council (grant no. 3318) and by the Astra Research Foundation. We thank Drs R. Carraway (Harvard Univ. med. sch., Mass.), R. Chance (Lilly Res. Lab. Indianapolis, Ind.), K. Folkers (Univ. of Texas, Austin, Texas) and V. Nil (Karolinska Institute, Stockholm) for the generous supply of various peptides.

REFERENCES

- ANDERSSON S., CHANG, D., FOLKERS, K. & ROSELL, S. 1976. Inhibition of gastric acid secretion by neurotensin. *Life Sci* 19: 367-370.
- ANDERSSON S., ROSELL, S., HJELMQVIST U., CHANG, D. & FOLKERS, K. 1977. Inhibition of gastric and intestinal motor activity in dogs by (Gln)²⁷-neurotensin. *Acta Physiol Scand* 100: 231-235.
- WILKIN, B. P. 1990. Secretory mechanisms of the digestive glands. 2nd ed. Paul B. Hoeber, New York.
- FEJERMAN, H. S., SARSON D. L., JOHNSTON D. I., STEWART J. S., GUERIN S., BLOOM, S. R., BLACKBURN A. M., PATEL, H. R., MODI-GIANI, R. & MALLISON C. N. 1978. Gut hormone profile in coeliac disease. *Lancet* i: 785-788.
- ROON, S. R. & POLAK, J. M. 1978. Gut hormones review. In: Gut hormones (ed. S. R. Bloom). Churchill Livingstone, Edinburgh.
- ORR, J. C., DRYBURGH, J. R., ROSS, S. A. & DUFFLE, J. 1975. Identification and actions of gastric inhibitory polypeptide. *Rec Prog Horm Res* 31: 457-522.
- ITALAND S. 1978. Physiology of GIP in man. Gut hormones (ed. S. R. Bloom), pp. 288-293. Churchill Livingstone, Edinburgh.
- URAWAY R. & LEEMAN S. E. 1973. The isolation of a new hypotensive peptide. Neurotensin from bovine hypothalamus. *J Biol Chem* 248: 6854-6861.
- URAWAY R. & LEEMAN S. E. 1975a. The amino acid sequence of hypotensive peptide. Neurotensin. *J Biol Chem* 250: 1907-1911.
- URAWAY R. & LEEMAN S. E. 1976. Characterization of radioimmunoassayable neurotensin in the rat: its differential distribution in the central nervous system, small intestine and stomach. *J Biol Chem* 251: 7045-7052.
- KRISTIANSEN J., REHFELD, J. F. & STADIL, F. 1978. Effect of intragastric fat on meal-stimulated acid and gastric secretion in man. *Scand J Gastroint* 11: 473-476.
- LIN I. E., LIANG, V. & MALAGELADA, J. R. 1978. Inhibitory role of the distal small intestine on the gastric secretory response to meals in man. *Gastroenterology* 74: 704-707.
- WALD, C. A. & BOAS J. 1986. Beiträge zur Physiologie und Pathologie der Verdauung. *Virchows Arch* 104: 771-305.
- FRIGERIO B., RAVAZOLA, M., ITO S., BUFFA, R., CAPELLA C., SOLCIA, E. & ORCI L. 1977. Histochemical and ultrastructural identification of neurotensin cells in the dog ileum. *Histochemistry* 54: 123-131.
- GOODFRIEND T. L., LEVINE, L. & FASMAN G. D. 1964. Antibodies to bradykinin and angiotensin: A use of carbodiimides in immunology. *Science* 144: 1344-1346.
- GREGORY R. A. 1967. Enteropneustose—a reappraisal of the problem. In: Gastric secretion. Mechanisms and control (ed. Shantia, Gilbert and Harrison). Pergamon Press, pp. 469-477.
- HELMSTAEDTER, V., TAUGNER, CH., FEURLE, G. E. & FORSMANN W. G. 1977. Localization of neurotensin immunoreactive cells in the small intestine of man and various mammals. *Histochemistry* 53: 35-41.
- HUNTER, W. M. & GREENWOOD F. C. 1962. Preparation of iodine 131 labelled human growth hormone of high specific activity. *Nature* 194: 495-496.
- KOSAKA, T. & LIM, R. K. S. 1930. Demonstration of the humoral agent in fat inhibition of gastric secretion. *Proc Soc Exp Biol NY* 27: 890-891.
- MASHFORD M. L., NILSSON G., RÖKAEUS, Å. & ROSELL, S. 1978a. The effect of food ingestion on circulating neurotensin-like immunoreactivity (NTLI) in the human. *Acta Physiol Scand* 104: 244-246.
- MASHFORD M. L., NILSSON G., RÖKAEUS, Å. & ROSELL, S. 1978b. Release of neurotensin-like immunoreactivity (NTLI) from the gut in anaesthetized dogs. *Acta Physiol Scand* 104: 375-376.
- ORCI L., BAETENS O., RUFENER, C., BROWN M., VALE, W. & GUILLEMIN R. 1976. Evidence for immunoreactive neurotensin in dog intestinal mucosa. *Life Sci* 19: 559-566.
- POLAK, J. M., SULLIVAN S. N., BLOOM S. R., BUCHAN A. M. J., FACER, P., BEOWN M. R. & PEARSE, A. G. E. 1977. Specific localization of neurotensin to the N cell in human intestine by radioimmunoassay and immunocytochemistry. *Nature* 270: 183-184.
- ROSELL, S., BURCHER, E., CHANG D. & FOLKERS, K. 1978. Indirect vascular actions of neurotensin and (Gln)²⁷-neurotensin. *Acta Physiol Scand* 98: 484-491.
- ROSELL, S., RÖKAEUS, Å., CHANG, D. & FOLKERS, K. 1978. Indirect vascular actions of (Gln)²⁷-neurotensin in canine adipose tissue. *Acta Physiol Scand* 102: 143-147.
- SUNDLER, F., HÅKANSSON R., HAMMER, R. A., ALUMETS, J., CARRAWAY R., LEEMAN S. E. & ZIMMERMAN E. A. 1977. Immunohistochemical localization of neurotensin in endocrine cells of the gut. *Cell Tissue Res* 178: 313-321.
- WINDSOR, C. W. O., COCKEL, R. & LEE, M. J. R. 1969. Inhibition of gastric secretion in man by intraduodenal fat infusion. *Gut* 10: 135-142.

Increased hepatic glycogen synthetase and decreased phosphorylase in trained rats

GALBO, P. SAUGMANN and E. A. RICHTER

Institute of Medical Physiology B, University of Copenhagen, and Department of Medicine, Martsborg Hospital, Aarhus, Denmark

GALBO, H. SAUGMANN, P. & RICHTER, E. A.: Increased hepatic glycogen synthetase and decreased phosphorylase in trained rats. *Acta Physiol Scand* 1979; 107: 269-272. Received 23 April 1979. ISSN 0001-6772. Institute of Medical Physiology B, University of Copenhagen and Department of Medicine, Martsborg Hospital, Aarhus, Denmark.

Rats were either physically trained by a 12-wk swimming program or were freely eating or weight-matched, sedentary controls. Trained rats had a higher relative liver weight and total hepatic glycogen synthetase (EC 2.4.1.11) activity and lower phosphorylase (EC 2.4.1.1) activity than the other groups of rats. These changes may partly explain the demonstrated training-induced increase in glucose tolerance. None of the findings could be ascribed to differences in food intake or body weight.

Key words. Liver enzymes, glycogen, glucose tolerance test, exercise, metabolism

In a few studies of the effect of physical training on hepatic metabolic functions have been presented. It has been reported that training increases hepatic malic dehydrogenase activity (Sangster & Jones 1966) as well as the concentrations of the triphosphates and the activities of glycerol-P dehydrogenase and succinate dehydrogenase (Knaus & Knaus) whereas hepatic glycogen synthesis does not change (Askew, Huston & Dohm 1973). Furthermore the hepatic glycogen concentration has been found to be markedly increased after training (Baldin et al. 1975; Galbo et al. 1977). A few pronounced training-induced increases in muscle glycogen concentration (Holloszy & Booth 1976; Galbo et al. 1977) led to investigation of the effects of training on enzymes involved in muscle glycogen metabolism. An increased total glycogen synthetase activity in skeletal muscles of humans and rodents was found (Holloszy & Booth 1976).

In the present study we have measured hepatic glycogen synthetase and phosphorylase in order to determine if also the training-induced increase in hepatic glycogen concentration is associated with changes in total activities of these enzymes, which are involved in the control of glycogen metabolism (Hers 1976).

METHODS AND MATERIALS

Male Wistar rats weighing 90-110 g were randomly divided into 3 groups. One group was subjected to previously described (Galbo et al. 1977) 12-wk physical training program consisting of swimming 5 days a week at 33-34°C. The duration of swimming was gradually increased until after 8 wk the rats were continuously 6 h daily. Sedentary control rats were either freely eating or weight-matched with trained rats by restricted access to food up to 50 h before tissue sampling.

All rats were anesthetized with pentothal sodium intraperitoneally in the morning after 4 h without access to food. Trained rats were used 67 h after the last swim. Liver samples were, within 1 s, removed and frozen in isopentane precooled in liquid nitrogen. The samples were stored at -80°C and analyzed within 1 wk. Homogenates were prepared by homogenizing in Potter Elvehjem type homogenizer approximately 10 mg of frozen tissue (weighed at -20°C) suspended in 500 µl of ice-cold medium. The medium contained 50 mM Tris-HCl (pH 7.4 at 23°C), 0.15% (g/100 ml) bovine serum albumin (KABI) and 0.6 mM dithiothreitol. Total activities (a, b forms) of glycogen synthetase and of glycogen phosphorylase in the crude homogenate were determined; the latter after 40 min incubation with 2.5 mM ATP, 10 mM MgCl₂ and 1 U ml⁻¹ purified rabbit muscle phosphorylase kinase (Sigma). Phosphorylase was assayed in the direction of glycogen (Wang & Eummen 1972) using final concentration of 66 mM uniformly labeled (¹⁴C)-glucose 1-phosphate (3.8 · 10⁶ cpm µmol⁻¹) in 100 mM PIPES (pH 6.4 at 23°C) containing in addition 7.5

Table 1 The effect of physical training on hepatic glycogen regulating enzymes and anthropometric measures

Values are mean \pm S.E. The number of determinations is given in parentheses. * denotes value significantly different ($P < 0.05$) from the corresponding value in trained rats. # denotes that every single value was higher than the value in the weight matched trained rat. Apart from body weight ($P < 0.001$) the variables in freely eating and weight matched rats did not differ significantly ($P > 0.05$).

	Synthetase (units g ⁻¹)	Phosphorylase (units g ⁻¹)	Body weight (BW) (g)	Heart weight (% of BW)	Liver weight (% of BW)
Trained rats	3.368 \pm 0.181 (11)	10.151 \pm 0.772 (10)	364 \pm 9 (11)	0.37 \pm 0.01 (11)	3.81 \pm 0.08 (13)
Weight matched controls	2.101 \pm 0.257 [#] (4)	10.172 \pm 0.31 [*] (3)	360 \pm 10 (4)	0.39 \pm 0.01 (4)	3.42 \pm 0.15 [*] (7)
Freely eating controls	2.349 \pm 0.285 (6)	12.711 \pm 0.763 (5)	468 \pm 11 (6)	0.31 \pm 0.01 (6)	3.15 \pm 0.15 (10)

mg/ml rabbit liver glycogen. 100 mM NaF and 1.5 mM AMP. Synthetase was assayed using 4 mM UDP-¹⁴C-glucose (7.5 $\times 10^4$ cpm μ mol⁻¹) in 50 mM Tris-HCl (pH 7.4 at 37°C) containing in addition 10 mM glucose-6-phosphate and 7 mg/ml glycogen (Thomas et al 1968). The assays were performed at 30°C for 10 min. One unit of activity is the amount of enzyme that incorporates 1 μ mol of substrate into glycogen per min under the conditions of the assay. The glycogen content was determined after hydrolysis by a hexokinase method (Karlson, Darnant & Saltin 1971). Hepatic concentrations are expressed per kg wet weight. (Hepatic protein concentrations were identical in the different groups of rats.)

For glucose tolerance test (cf. Table 3) a polyethylene catheter was inserted into a carotid artery 30 min before blood sampling. Blood glucose concentrations were determined by a hexokinase method (Schmidt 1961). Data were analyzed by *t* test and the test for paired comparisons was used when applicable.

RESULTS

Physically trained rats increased their body weight less than sedentary rats but developed higher relative heart weights (Table 1). The total hepatic phosphorylase activity was low and the total synthetase activity as well as the relative liver weight were higher in trained rats than in both freely eating and weight matched control (Table 1). A higher hepatic synthetase activity was accompanied by a higher glycogen concentration (Table 1). During glucose tolerance test blood glucose concentrations were lower in trained rats than in the other groups of rats (Table 3).

DISCUSSION

The present study has shown that physically trained rats have a higher relative liver weight and total

hepatic glycogen synthetase activity and a lower phosphorylase activity than sedentary rats. In sedentary rats the measured enzyme activities agreed with previously reported values (Newman & Armstrong 1978). At the end of the experiment the training rats ate 47% more than the freely eating controls but the mentioned differences can hardly be ascribed to differences in food intake. This is since the measured hepatic parameters did not differ significantly in freely eating, sedentary rats.

Table 2 Correlation between hepatic glycogen and synthetase concentrations

Two physically trained and two freely eating, sedentary control rats were randomly selected for determination of both hepatic glycogen (expressed as mmol of glucose \times kg wet weight⁻¹) and synthetase concentrations. Trained rats were used 67 h after they had been trained for the last time. Two sedentary rats had been caged matched with the trained rats by restricted access to food up to 48 h before sampling. Liver samples were removed in the morning after 4 h without access to food. Body weights are shown in parentheses. Correlation coefficient = 0.90 ($P < 0.05$).

	Synthetase (unit g ⁻¹)	Glycogen (mmol kg ⁻¹)
Physically trained rat 1 (363 g)	3.626	633
Physically trained rat (378 g)	3.56	479
Weight matched control (368 g)	3.90	410
Freely eating control (51 g)	3.80	198
Freely eating control (490 g)	2.93	764
Weight matched control (371 g)	2.16	54

Table 3. The effect of physical training on the intravascular glucose tolerance test

Glucose concentrations \pm S.E. (mean \pm S.E.) are shown. 125 mg glucose per 100 g body weight was injected as an intra-arterial bolus through cannulated carotid artery immediately after the 0-min blood sample had been drawn from the artery. Values are significantly different from 0-min value ($P < 0.05$). * denotes value significantly different from values in sedentary controls ($P < 0.05$). Values in freely eating controls did not differ significantly from values in fasted controls ($P > 0.05$).

	10 min	0 min	5 min	10 min	30 min	60 min
3-week rats (n=6)						
right matched controls (n=5)	7.56 \pm 0.35	7.64 \pm 0.31	27.71 \pm 0.37*	21.41 \pm 0.45*	7.41 \pm 0.34	9.54 \pm 0.45*
freely eating controls (n=6)	7.42 \pm 0.77	7.77 \pm 0.32	30.85 \pm 1.09*	4.53 \pm 1.20*	15.89 \pm 1.76*	14.56 \pm 0.10*
sedentary controls (n=6)	8.38 \pm 0.38	8.45 \pm 0.40	30.81 \pm 1.09*	25.21 \pm 0.92*	13.89 \pm 1.74*	15.20 \pm 1.91

compared to sedentary rats with restricted access to food, although the former group ate 89% more than the latter. Neither can the differences in hepatic glycogen be ascribed to differences in body weight since no differences were present in comparisons between trained and sedentary rats of similar body weight, and since differences in body weight between the two sedentary groups were not accompanied by significant differences in hepatic glycogen.

The observed training-induced hepatic changes may have several consequences. The enzyme changes, the correlation between hepatic glycogen and glycogen concentrations and the higher relative liver weight in trained rats indicate an increased hepatic capacity for glycogen synthesis and storage. Probably these changes contributed to the markedly improved glucose tolerance which was found in the trained rats and which may protect against the development of diabetes mellitus (Björntorp & Sjöström 1978). However, changes in muscular capacity to metabolize glucose may also influence glucose assimilation after training (Björntorp et al. 1972). The elevation of the liver glycogen concentration in trained animals has the beneficial effect of protecting the animals against liver glycogen depletion and development of hypoglycaemia, for instance during prolonged exercise (Baldwin et al. 1975; Galbo et al. 1977). In the rat, during submaximal exercise a higher concentration of fat in trained than in untrained individuals shows a slower depletion of glycogen stores in the liver (Baldwin et al. 1975; Holloszy & Booth 1976). The lower hepatic glycogen phosphorylase and the higher glycogen synthetase activity found in trained rats may together with the previously observed diminished hormonal response to exercise after training (Galbo

et al. 1977) account for the slower depletion of liver glycogen in trained than in untrained exercising animals. The present finding of hepatic adaptive changes should encourage to further studies of metabolic adaptations to training in extramuscular tissues.

REFERENCES

- ASKEW E. W., HUSTON R. L. & DOHM G. L. 1973. Effect of physical training on esterification of glycerol-3-phosphate by homogenates of liver, skeletal muscle, heart and adipose tissue of rats. *Metabolism* 22: 473-480.
- BALDWIN R. M., FITTS R. H., BOOTH F. W. W. & HOLLOSZY J. O. 1975. Depletion of muscle and liver glycogen during exercise. *Physiology* 35: 203-212.
- BJÖRNTORP P. & SJÖSTRÖM L. 1978. Carbohydrate storage in man: Speculations and some quantitative considerations. *Metabolism* 27: Suppl. 2, 1853-1865.
- BJÖRNTORP P., FAHLÉN M., GRIMBY G., GUSTAFSSON A., HOLM J., RENSTRÖM P. & SCHERSTÉN T. 1972. Carbohydrate and lipid metabolism in middle-aged, physically well-trained men. *Metabolism* 21: 1037-1044.
- GALBO H., RICHTER E. A., HOLST J. J. & CHRISTENSEN N. J. 1977. Diminished hormonal responses to exercise in trained rats. *J. Appl. Physiol.* 43: 953-958.
- HERS H. G. 1976. The control of glycogen metabolism in the liver. *Ann. Rev. Biochem.* 45: 167-189.
- HOLLOSZY J. O. & BOOTH F. W. 1976. Biochemical adaptations to endurance exercise in muscle. *Ann. Rev. Physiol.* 38: 273-291.
- KARLSSON J., DIAMANT B. & SALTIN B. 1971. Muscle metabolism during submaximal and maximal exercise in man. *Scand. J. Clin. Lab. Invest.* 26: 383-394.
- KRAUS H. & KIRSTEN R. 1970. Die Wirkung von körperlicher Training auf die mitochondriale Energieproduktion im Herzmuskel und in der Leber. *Physiology* 32: 334-347.
- NEWMAN J. D. & ARMSTRONG J. M. D. 1978. On

- the activities of glycogen phosphorylase and glycogen synthase in the liver of the rat. *Biochim Biophys Acta* 544: 225-233.
- SANGSTER J. F. & BEATON J. R. 1966. Alterations in enzyme activities as a consequence of exercise in the rat. *Proc Soc Exp Biol* 1: 2, 543-544.
- SCHMIDT F. H. 1961. Die enzymatische Bestimmung von Glucose und Fructose nebeneinander. *Klin Wochenschr* 39: 1244-1247.
- THOMAS J. A., SCHLENDER, K. K. & LARNER, J. 1968. A rapid filter paper assay for UDP-glucose: glycogen glucosyltransferase, including an assay for biosynthesis of UDP-¹⁴C-glucose. *Anal Biochem* 25: 486-499.
- WANG P. & ESMANN V. 1972. A rapid assay of α -phosphorylase based on the filter paper technique. *Anal Biochem* 47: 495-500.

Tachycardia during egg hypothermia in incubating ptarmigan (*Lagopus lagopus*)

GABRIELSEN and JOHAN B. STEEN

Department of Physiology, Institute of Medical Biology, University of Tromsø, Norway

GABRIELSEN G. & STEEN J. B. Tachycardia during egg-hypothermia in incubating ptarmigan (*Lagopus lagopus*). Acta Physiol Scand 1979, 107: 273-277. Received 13 March 1979. ISSN 0001-6772. Department of Physiology, Institute of Medical Biology, University of Tromsø, Norway.

Incubating birds regulate the egg temperature by varying their posture and the distance between eggs and brood patch. In the present study we show that this homeostatic process is further assisted by varying the brood patch blood flow according to the temperature of the eggs. When female ptarmigan resume incubation of cooled eggs (e.g. after a period of foraging) they immediately develop pronounced tachycardia (4 times normal in wild, 2-3 times in captive birds). Tachycardia is maintained, although at decreasing intensity until the eggs have obtained normal temperature. The eggs are heated 30 to 50% slower in females where tachycardia is inhibited by β -receptor blocking agent.

Key words: Tachycardia, incubation, ptarmigan, brood patch.

Several studies have revealed behavioural techniques by which incubating birds attempt to maintain their eggs at a constant temperature during varying ambient conditions (Frith 1964, Nelson 1964, Drost 1970, White 1974). During a recent electroc study on the heart rate of incubating willow ptarmigan (Gabrielsen et al. 1977) data were obtained which indicated a physiological technique whereby the bird can vary the amount of heat transferred to the eggs. It was observed that when a female ptarmigan returned to incubate after foraging, their heart rates increased 4-5 fold above the resting level. The data further indicated that the length of the tachycardia period increased with increasing periods away from the nest and lower ambient temperatures.

In the present investigation we have tested whether this tachycardia influences the rate of egg warming. Our study involved observations of both wild and captive incubating ptarmigan in an attempt to determine the causal relationship between egg temperature and heart rate.

MATERIAL AND METHODS

The field investigation was conducted during the summers of 1976-77 and 78 on Kaituma, Troms County, Norway (Fig. 1).

A total of 8 wild willow ptarmigan hens were caught on the nest using dip nets. They were then equipped with telemetry transmitter consisting of an ECG preamplifier modulator and crystal controlled transmitter of 102.36 and 96.26 MHz. With batteries for 400 h operation and transmission range of up to 200 m, the total weight of the apparatus was 23 g. The transmitter was taped to rucksack type harness. One gold-tipped wire from the ECG amplifier was positioned close to the heart by means of a stiff plastic tubing which had been introduced through a small incision behind the sternum. The other electrode was placed under skin overlying the abdomen. Attaching the entire apparatus required about 15 min. Hens usually returned to the nest to incubate within 20 min after release, but sometimes stayed away considerably longer.

Observations were made through a telescope from an observation hut situated at least 40 m from the nest. The signals from the transmitter were received through a directional Yagi antenna and a commercial FM-radio and recorded on cassette tape for later analysis. Direct recording of ECG signals were made and heart rates were later derived by means of an on-line micro-computer.

Experiments on captive hens were carried out at the Wildlife Research Station at the University of Tromsø. Two pairs of ptarmigan were exposed to long day/short night light regime on January 1, 1978. Five weeks later the birds had started to moult into breeding plumage. Each pair was placed in a 4 x 4 m indoor room arranged in natural manner with birch branches. Food and water were

Present address: Institute of Zoophysiology, University of Oslo, Oslo, Norway.

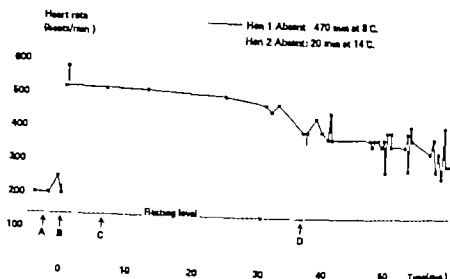


Fig. 1 Heart rate of two wild incubating willow ptarmigan hens upon returning to their clutches after different periods of absence (A) Just prior to sitting on the clutch. (B) Immediately after start of incubation (C) Turning the eggs. (D) Disturbance.

given *ad lib*. Both pairs laid a normal clutch of eggs. After a week of incubation the hens were equipped with the same telemetry equipment as was used in the field. The birds were placed under TV surveillance and could be observed directly as well.

For each hen an artificial clutch was assembled. This consisted of 9 unfertilized ptarmigan eggs plus a temperature-measuring eggs. The latter was a blown-out ptarmigan egg shell filled with paraffin wax and fastened in a fixed position in the middle of the nest. Two thermocouples were fixed inside this egg, one touching the inner surface of the shell on the uppermost part of the egg (surface egg temperature) and the other in the center of the egg (inner egg temperature).

Two series of experiments were conducted. The first series consisted of exchanging the hen's own clutch with the artificial clutch which had previously been heated or cooled to a predetermined temperature. When the hen returned to incubate the artificial clutch simultaneous measurements were made of the hen's heartbeat and change in egg temperature. The ambient temperature was always 20–1°C.

In the second series of experiments each hen was given 0.5–0.50 mg fentanyl propranolol a β -receptor blocking agent which effectively inhibits acceleration of the heart before presenting her with clutches of different temperature. 4 pairs of expts. were conducted on different hens.

Both hens eventually hatched their clutches.

RESULTS

The field experiments revealed the following pattern of heart activity. As each hen carefully approached the nest after a period of absence the heart rates varied between 200–250 b/min. Within 10 s after settling on the eggs the heart rates rose to

between 500 and 600 b/min. The duration of this tachycardia seemed to be associated with the length of time spent away from the nest and with the ambient temperatures. This is illustrated by the following examples. Hen 1 (Fig. 1) stayed away for 1

Table 1 Duration of heart rate above 500 beats/min among eight wild hens returning to eggs after varying times away from the nest and varying ambient temperature

Hen no	Ambient temp (°C)	Absence from eggs (min)	Duration of tachycardia above 500 beats/min (min)
8	17	5	1
8	15	5	1
6	15	15	1
6	15	20	1
6	16	25	3
1	14	20	3
8	15	15	3
7	9	10	2.1
1	10	15	4.1
1	10	20	4.5
4	10	20	4.5
1	10	20	5.6
1	9	20	5.6
8	10	20	5.6
1	6	20	5.6
1	7	20	5.6
3	4	20	6.7
1	7	145	10.1
6	8	40	20.5

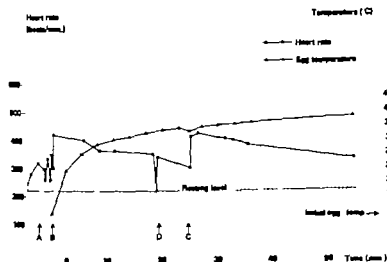


Fig. 2. Heart rate of captive hen returning to clutch of eggs cooled to 10°C and the egg temperature following incubation. A, B, C and D as in Fig. 1.

and 50 min at an ambient temperature of 8°C and upon returning maintained a heart rate above 500 for 25 min. Seven hours passed before the heart rate returned to normal. Hen 2 stayed away for 70 min at an ambient temperature of 14°C. Upon returning, the heart rate increased to 575 but dropped below 300 after 5 min. After 30 min she had resumed

normal heart rate (Fig. 1). During this decline period a temporary increase in heart rate occurred each time the hen had turned her eggs and a decrease occurred when she was disturbed. This latter response was described by Gabrielsen et al. (1977). Eighteen similar observations support the conclusion that this is a normal pattern of cardiac response among wild prairie-gull hens returning to their eggs (Table 1).

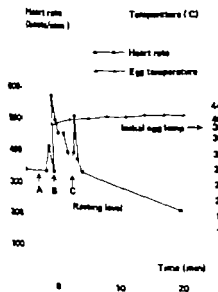


Fig. 3. Heart rate of captive hen returning to clutch of eggs at temperature of 39°C, and the egg temperature following incubation. A, B and C, as in Fig. 1.

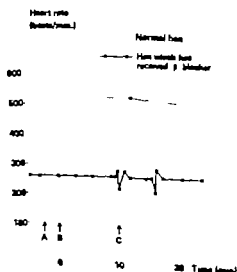


Fig. 4. Cardiac response of an indolent treated and an untreated control wild hen both incubating eggs with initial temperature of 10°C. A, B and C, as in Fig. 1.

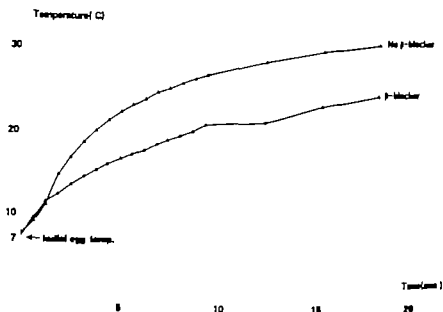


Fig. 5 Sub-surface egg temperature after onset of incubation by a captive hen before and after injection of β -blocker. Initial egg temperature in both cases 7–8°C

Captive hens have a higher resting heart rate (200–260 b/min) and a lower maximum heart rate (420–580 b/min) than their wild relatives (120–140 and 550–600 b/min respectively) probably due to lack of physical training.

Fig. 2 shows an example of the cardiac response of a captive hen returning to incubate a clutch which is previously cooled to 10°C. The same figure also gives the surface egg temperature during the subsequent period of incubation. The heart rate increased immediately and stayed high until the inner egg temperature returned to normal.

Fig. 3 illustrates the response of the same hen returning to eggs with a temperature of 39°C. There was an initial period lasting about 5 min when the heart rate was increased but very irregular. After this period it returned to normal.

Fig. 4 shows that a hen which has previously received β -blocker does not display tachycardial cardiac response upon returning to 8°C eggs. Her heart rate is remarkably stable at a rate 20–30 f above the resting level found in captive hens. The same pattern was found in all the other experiments.

Fig. 5 shows that a hen which cannot accelerate her heart rate due to β -blocker will heat her eggs slower than a hen with a normal heart function. Both hens began to incubate eggs cooled to 7–8°C. After 5 min the normal hen had heated her eggs to 22.5°C while the other hen had heated hers to

16.5°C. The results of the other experiments are compiled in Table 2.

DISCUSSION

Most bird species form a brood patch, a portion of the skin covering the pectoral muscles which becomes free from feathers and richly vascularized during incubation (Lange 1928; Allen, Stokholm & Stalsberg 1978). The incubating bird can regulate the egg temperature by varying its posture and

Table 2 Comparison of temperature increase in eggs incubated by 2 ptarmigan hens before and after they have received an intramuscular injection of the β -receptor blocking agent (propranolol)

Hen no.	Propranolol	Egg temperature (°C)		
		Initially	After 5 min incubation	Increase
1	+	7.5	22.5	15.0
1		7.0	16.5	9.5
1		14.0	30.5	16.5
1		14.0	26.0	12.0
		10.0	26.0	16.0
		10.5	21.5	11.0
2	+	20.5	37.0	16.5
		20.0	33.0	13.0

the distance to the eggs (White & Kinney 1974). In the present study we found evidence which indicates that the heat transfer to the eggs is also regulated by variations in brood-patch blood flow. Thus we showed that partridge hens increase their heart-rate 2-4 fold when they return to cold eggs. This tachycardia is maintained until the eggs have attained normal brooding temperature.

Since the temperature of the eggs increased faster in hens with tachycardia, than in those where heart acceleration was inhibited by a β -blocking agent, conclude that the blood flow to the brood patch is increased substantially during tachycardia. It is unlikely that propranolol should cause local vasodilation since arteriolar relaxation if existent, is mediated through β -receptors (Nickerson 1967). Whether the heat production of the bird is also elevated under these conditions is presently under study.

The observation that heart rate increases after contact between the brood patch and eggs at a sub-normal incubation temperature strongly supports the suggestion by White & Kinney (1974) that the bird senses egg temperature in the skin of the brood patch. This is further attested to by the cardiac response following the hen's turning of eggs. This behaviour inevitably exposes a cold egg surface to the brood patch and it always elicited acceleration of the heart. Signals from the receptors of the brood patch presumably activate the brood

patch-thermostat in the hypothalamus which maintains tachycardia and increases egg heating as long as the eggs are below the desired brooding temperature.

REFERENCES

- ALLEN H. M., STOKKAN K.-A. & STALSBERG, H. 1978. Egg incubation by willow grouse cock. *Astur* 11: 1-5.
- BENT A. C. 1965. *Laf histories of north American songbirds*. Wren, thrashers and their allies, p. 166. Dover, New York.
- DRENT R. H. 1970. Functional aspect of incubation in the Herring Gull. *Behaviour Suppl.* 17: 1-132.
- DRENT R. H., POSTUMA, K. & LOUSTRA, T. 1970. The effect of egg temperature on incubation behaviour in the Herring Gull. *Behaviour Suppl.* 17: 237-261.
- FRITH, H. J. 1962. *The Mallard-fowl: The bird that builds an incubator*. Angus & Robertson, Sydney.
- GABRIELSEN G. KANWISHER, J. & J. B. 1977. "Emotional" Bradycardia: A telemetry study on incubating willow grouse (*Lagopus lagopus*). *Acta Physiol Scand* 100: 255-257.
- LANGE, B. 1928. Die Brutflecks der Vögel und die für sie wichtigen Hauptgefühlsrichtungen. *Gegenbaurs Jahrb* 59: 601-712.
- NELSON J. B. 1966. The breeding biology of the Goshawk, *Sula bassana* on the Bass Rock, Scotland. *Ibis* 108: 584-626.
- NICKERSON M. 1967. New developments in adrenergic blocking agents. *Ann N Y Acad Sci* 139: 571-579.
- WHITE, F. N. & KINNEY J. L. 1974. Avian incubation. *Science* 10: 107.

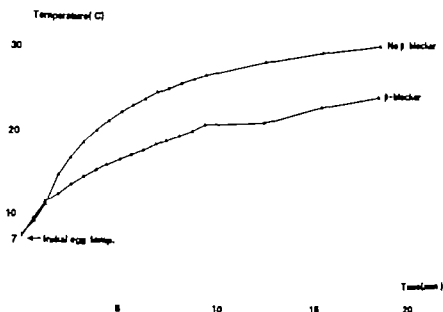


Fig. 5 Sub-surface egg temperature after onset of incubation by a captive hen before and after injection of β -blocker. Initial egg-temperature in both cases 7–8°C

Captive hens have a higher resting heart rate (200–260 b/min) and a lower maximum heart rate (470–580 b/min) than their wild relatives (170–140 and 550–600 b/min respectively) probably due to lack of physical training.

Fig. 2 shows an example of the cardiac response of a captive hen returning to incubate a clutch which is previously cooled to 10°C. The same figure also gives the surface egg temperature during the subsequent period of incubation. The heart rate increased immediately and stayed high until the inner egg temperature returned to normal.

Fig. 3 illustrates the response of the same hen returning to eggs with a temperature of 39°C. There was an initial period lasting about 5 min when the heart rate was increased but very irregular. After this period it returned to normal.

Fig. 4 shows that a hen which has previously received β -blocker does not display tachycardial cardiac response upon returning to 8°C eggs. Her heart rate is remarkably stable at a rate 20–30% above the resting level found in captive hens. The same pattern was found in all the other experiments.

Fig. 5 shows that a hen which cannot accelerate her heart rate due to β -blocker will heat her eggs slower than a hen with a normal heart function. Both hens began to incubate eggs cooled to 7–8°C. After 5 min the normal hen had heated her eggs to 22.5°C while the other hen had heated hers to

16.5°C. The results of the other experiments are compiled in Table 2.

DISCUSSION

Most bird species form a brood patch, a portion of the skin covering the pectoral muscles which becomes free from feathers and richly vascularized during incubation (Lange 1928; Allen, Stokkan & Stalsberg 1978). The incubating bird can regulate the egg temperature by varying its posture and

Table 2 Comparison of temperature increase in eggs incubated by 2 ptarmigan hens before and after they have received an intramuscular injection of the β -receptor blocking agent (propranolol)

Hen no.	Propranolol	Egg temperature (°C)			Increase
		Initially	After 5 min incubation	Incubated	
1		7.5	22.5	15.0	
1		7.0	16.5	9.5	
1		14.0	30.5	16.5	
1		14.0	6.0	1.0	
		10.0	26.0	16.0	
		10.5	1.5	11.0	
	–	20.5	37.0	16.5	
	+	20.0	3.0	1.0	

Peptides in the cat carotid body (glomus caroticum) VIP, enkephalin and substance P like immunoreactivity

AN M. LUNDBERG, TOMAS HÖKFELT, JAN FAHRENKRUG,
ÖRAN NILSSON and LARS TERENIUS

Department of Histology, Karolinska Institute, Stockholm, Sweden, Department of Clinical Chemistry,
Skejberg Hospital, Copenhagen, Denmark, Department of Physiology, Swedish University
of Agricultural Sciences, and Department of Pharmacology, Uppsala University, Sweden.

Recently an enkephalin-like peptide has been observed in the glomus cells of the adrenal medulla, in VIP cells and in some sympathetic noradrenergic neurons (Schultzberg et al. 1978, 1979). In the present paper we report preliminary results on the occurrence of an enkephalin-like peptide as well as some other peptides in the carotid body (glomus caroticum), an organ closely related to other chemoreceptive systems and belonging to the so called APUD system (see Pearse 1969).

Four male or female cats (b.wt. 2-4 kg) were anaesthetized with Nembutal (30 mg/kg, i.p.) and perfused in the ascending aorta with ice cold 10% formalin (Pfafe 1964) for 20 min. The carotid bifurcation was rapidly dissected out and immersed in the same fixative for 90 min. Serial cryostat sections were made and processed for immunohistochemistry according to the indirect technique of Coons and collaborators (see Coons 1958) as described previously (Hökfelt et al. 1977). The sections, or incubated at 4°C over night with antisera to met- or leu-enkephalin (dilution 1:160), VIP (1:160) or substance P (1:80) raised, incubated with FITC conjugated sheep anti-rabbit antiserum (SBL, Stockholm, Sweden), mounted and examined in Zeiss fluorescence microscope. The sections were pretreated with an excess of the respective peptide served as control sera. For further detail and preparation and characteristics of the antisera, see Schultzberg et al. (1978) (enkephalin antisera), Fahrenkrug et al. (1977, 1978) (VIP antiserum) and Löfdahl et al. (1978) (substance P antiserum).

After incubation with both types of enkephalin antisera, strong immunofluorescence was observed in the majority of the glomus cells (Type I

cells) (Fig. 1A). Often strongly fluorescent processes could be seen from the enkephalin immunoreactive glomus cells. No immunoreactive cells but many VIP immunoreactive strongly fluorescent varicose nerve fibres with a patchy distribution pattern were seen (Fig. 1B). They were found with the highest density around blood vessels, but some thin single fibres seemingly penetrated between the glomus cells. After incubation with substance P antiserum, some thin weakly fluorescent fibres were seen. None of the fluorescent structures described above were seen after incubation with control sera.

The present findings indicate that peptides are present in different structures of the carotid body. Whereas an enkephalin-like peptide is present in the type I glomus cells and their processes, the VIP- and substance P-like peptides are found in nerves. These results are in agreement with the previous demonstration of an enkephalin-like peptide in other chromaffin cells (DeGaulle et al. 1978, Schultzberg et al. 1978, 1979). The present study does not allow an exact identification of the peptides visualized, but it is interesting that both met- and leu-enkephalin as well as a larger (precursor?) molecule have been identified in sympathetic tissues (Hughes et al. 1977, DeGaulle et al. 1978).

The origin of the two types of peptide nerves in carotid body is uncertain. Since numerous substance P immunoreactive cells have been seen in the petrosal ganglion (Lundberg et al. 1979a), this peptide may be confined to peripheral sensory branches. VIP immunoreactive cell bodies have been observed in the superior cervical ganglion and may give rise to the blood vessel innervation observed (Lundberg et al. 1979b).

Peptides in the cat carotid body (glomus caroticum) VIP, enkephalin and substance P like immunoreactivity

AN M. LUNDBERG, TOMAS HOKFELT, JAN FAHRENKRUG,
ÖRAN NILSSON and LARS TERENIUS

Department of Histology, Karolinska Institute, Stockholm, Sweden, Department of Clinical Chemistry
Hvidovre Hospital, Copenhagen, Denmark, Department of Physiology, Swedish University
of Agricultural Sciences, and Department of Pharmacology, Uppsala University, Sweden

Recently an enkephalin-like peptide has been observed in the glomus cells of the adrenal medulla, in VIP cells and in some sympathetic noradrenergic neurones (Schultzberg et al. 1978, 1979). In the present paper we report preliminary results on the occurrence of an enkephalin-like peptide as well as other peptides in the carotid body (glomus caroticum), an organ closely related to other chromaffin systems and belonging to the so called APLD system (see Pearse 1969).

Four male or female cats (b.wt. 4-5 kg) were anesthetized with Nembutal (30 mg/kg, i.p.) and perfused via the ascending aorta with ice cold 10% formalin (Pearse 1962) for 20 min. The carotid bifurcation was rapidly dissected out and immersed in the same fixative for 90 min. Serial cryostat sections were made and processed for immunohistochemistry according to the indirect technique of Coons and collaborators (see Coons 1958) as described previously (Hokfelt et al. 1973). The sections were incubated at 4°C over night with antisera to met- or leu-enkephalin (dilution 1:160), VIP (1:160) or substance P (1:80), rinsed, incubated with FITC conjugated sheep anti-rabbit antiserum (SIL, Stockholm, Sweden), mounted and rinsed in a Zen fluorescence microscope. The camera pretreated with an excess of the respective peptide served as control sera. For further details see Schultzberg et al. (1978) (enkephalin antisera), Fahrenkrug et al. (1977, 1978) (VIP antiserum) and Larsson et al. (1978) (substance P antiserum).

After incubation with both types of enkephalin antisera, a strong immunofluorescence was observed in the majority of the glomus cells (Type I

cells) (Fig. 1A). Often strongly fluorescent processes could be seen from the enkephalin immunoreactive glomus cells. No immunoreactive cells but many VIP immunoreactive strongly fluorescent varicose nerve fibres with a patchy distribution pattern were seen (Fig. 1B). They were found with the highest density around blood vessels, but some thin single fibres seemingly penetrated between the glomus cells. After incubation with substance P antiserum some thin, weakly fluorescent fibres were seen. None of the fluorescent structures described above were seen after incubation with control sera.

The present findings indicate that peptides are present in different structures of the carotid body. Whereas an enkephalin-like peptide is present in the type I glomus cells and their processes, the VIP and substance P-like peptides are found in nerves. These results are in agreement with the previous demonstration of an enkephalin-like peptide in other chromaffin cells (DiGiulio et al. 1978, Schultzberg et al. 1978, 1979). The present study does not allow an exact identification of the peptides visualized, but it is interesting that both leu- and met-enkephalin as well as a larger (precursor?) molecule have been identified in sympathetic tissues (Hughes et al. 1977, DiGiulio et al. 1978).

The origin of the two types of peptide nerves in carotid body is uncertain. Since numerous substance P immunoreactive cells have been seen in the petrosal ganglion (Lundberg et al. 1979a), this peptide may be confined to peripheral sensory branches. VIP immunoreactive cell bodies have been observed in the superior cervical ganglion and may give rise to the blood vessel innervation observed (Lundberg et al. 1979b).

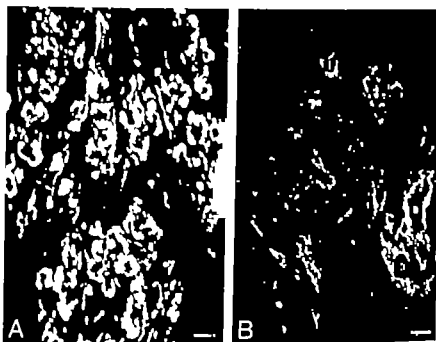


Fig. 1. Immunofluorescence micrographs of the carotid body after incubation with antiserum to met-enkephalin (A) and VIP (B). (A) Numerous enkephalin immunoreactive glomus cells of type I and short processes (arrows) are seen. (B) The VIP-like immunoreactivity is present in nerve fibres, especially around blood vessels (b). Some fibres (arrows) seem, however, to run without any obvious relation to vessels. Bars indicate 50 μ m.

The functional significance of peptides in the carotid body remains to be elucidated. The glomus cells have been ascribed several functions (see McDonald & Mitchell 1975). Our findings agree with Pearse's (1969) APUD-concept that the glomus cells are endocrine cells secreting polypeptides. According to Biscoe et al. (1970) the glomus cells release catecholamines to regulate the sensitivity of adjacent chemoreceptive nerve endings. Perhaps the enkephalin-like peptide is involved in similar regulatory mechanisms. Furthermore, the relation of the presence of an opioid peptide in the glomus cells to the well-known respiratory depressant action of morphine remains to be elucidated.

With regard to VIP immunoreactive fibres, it has been shown that intracarotid injection of VIP stimulates chemoreceptor afferents (Sand & Mutt 1970) either by a direct action or possibly due to local circulatory effects. The latter view is supported by the present demonstration of VIP immunoreactive nerves around blood vessels. On the other hand, only a very weak effect on respiration was observed after peripheral administration of substance P by the same route (McQueen 1978). It is, however, interesting to note that intraventricular

or intracisternal administration of SP caused hyperventilation (von Euler & Pernow 1956) and that medullary respiratory centres contain a dense network of SP nerve terminals (Ljungdahl et al. 1971).

The present study was supported by grants from the Swedish Medical Research Council (04X 2387, 04X 4441, 04X 3511, 05X 3766). Knut and Alice Wallenberg Stiftelse, Magnus Bergvall Stiftelse and Clas Grönroos Stiftelse. The skilful technical assistance of Mrs W. Hjert and Mrs Ulla Lundfeldt is gratefully acknowledged.

REFERENCES

- BISCOE J. H., LALL A. & SAMPSON S. R. 1970. Electron microscopic and electrophysiological studies on the carotid body following intracarotid section of the glossopharyngeal nerve. *J. Physiol.* (Lond.) **208**, 131-151.
- COONS A. H. 1958. Fluorescent antibody methods. In: *General cytochemical methods* (ed. J. F. Danielli), pp. 199-241. Academic Press, New York.
- DIGUILIO A. M., YANG H. Y. T., LUTJOLD, B., FRATTA W., HONG J. & COSTA F. 1973. Characterization of enkephalin-like material extracted from sympathetic ganglia. *Neuropharmacology* **17**, 969-977.
- EULER U. S. von & PERNOW B. 1956. Neurophysiological effect of substance P. *Acta Physiol. Scand.* **26**, 75-78.

- FÄRREKRUG, J. & SCHAFFALITZKY DE MUCKADELL, O. B. 1977. Radioimmunoassay of vasoactive intestinal polypeptide (VIP) in plasma. *J Lab Clin Med* 89: 1379-1386.
- FÄRREKRUG, J. & SCHAFFALITZKY DE MUCKADELL, O. B. 1978. Distribution of vasoactive intestinal polypeptide (VIP) in the porcine central nervous system. *J Neurochem* 31: 1445-1451.
- HÖKFELT T. FUXE, K. & GOLDSTEIN M. & JOH. T. H. 1973. Immunohistochemical localization of three catecholamine synthesizing enzymes: aspects on methodology. *Histochemistry* 33: 231-254.
- HUGHES, J. KOSTERLITZ, H. W. & SMITH T. W. 1977. The distribution of methionine-enkephalin and leucine-enkephalin in the brain and peripheral tissues. *Br J Pharmacol* 61: 639-647.
- LUNDAHL, Å. HÖKFELT T. & NILSSON G. 1978. Distribution of substance P-like immunoreactivity in the central nervous system of the rat. I. Cell bodies and nerve terminals. *Neuroscience* 3: 961-943.
- LUNDBERG, J. M. HÖKFELT T., NILSSON G. TERENIUS, L., REHFELD J. ELDE, R. P. GOLDSTEIN, M. & SAID S. 1979. Peripheral peptide and catecholamine containing neurons in the vagus, splanchnic, hypogastric and pelvic nerves. Occurrence and distribution of substance P, acetylcholinesterase (AChE) and enkephalin-like immunoreactive (EIR) pattern (EIR) and catecholamine synthesizing enzymes in trunks and ganglia. *Neuroscience*. Submitted.
- LUNDBERG, J. M. HÖKFELT T. SCHULTZBERG M. UYNÄS-WALLÉN, K. KÖHLER, C. & SAID, S. 1979b. Occurrence of vasoactive intestinal polypeptide (VIP)-like immunoreactivity in certain cholinergic neurons of the cat: evidence from combined immunohistochemistry and acetylcholinesterase staining. *Neuroscience*. In press.
- MCDONALD D. M. & MITCHELL, R. 1975. The innervation of glomus cells, ganglion cells and blood vessels in the cat carotid body: quantitative ultrastructural analysis. *J Neurocytol* 4: 177-230.
- McQUEEN, D. S. 1978. Effects of substance P on carotid chemoreceptor and vasoreceptor activity in the cat. *J Physiol (Lond.)* 284: 164P.
- PEARSE, A. C. E. 1969. The cytochemistry and ultrastructure of polypeptide hormone producing cells of the APUD series and the embryologic, physiologic and pathologic implication of the concept. *J Histochem Cytochem* 17: 303-313.
- PEASE, D. C. 1962. Buffered formaldehyde as a killing agent and primary fixative for electron microscopy. *Anal Rec* 142: 342.
- SAID S. I. & MUTT V. 1970. Polypeptide with broad biological activity. Isolation from small intestine. *Science* 192: 907-908.
- SCHULTZBERG, M., LUNDBERG, J. M. HÖKFELT T. TERENIUS, L. BRANDT J. ELDE, R. & GOLDSTEIN M. 1978. Enkephalin-like immunoreactivity in gland cells and nerve terminals of the adrenal medulla. *Neuroscience* 3: 1169-1186.
- SCHULTZBERG M. HÖKFELT T. TERENIUS L., ELFVIN L.-G. LUNDBERG, J. M. BRANDT J. ELDE, R. & GOLDSTEIN M. 1979. Enkephalin immunoreactive nerve terminals and cell bodies in sympathetic ganglia of the guinea pig and rat. *Neuroscience* 4: 249-270.

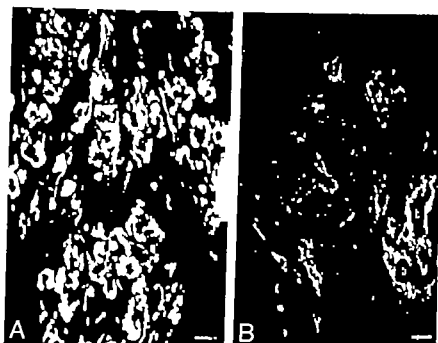


Fig. 1. Immunofluorescence micrographs of the carotid body after incubation with antiserum to met-enkephalin (A) and VIP (B). (A) Numerous enkephalin immunoreactive glomus cells of type I and short processes (arrow) are seen. (B) The VIP-like immunoreactivity is present in nerve fibres, especially around blood vessels (h). Some fibres (arrows) seem however to run without any obvious relation to vessels. Bars indicate 50 μ m.

The functional significance of peptides in the carotid body remains to be elucidated. The glomus cells have been ascribed several functions (see McDonald & Mitchell 1975). Our findings agree with Pearse's (1969) APUD-concept that the glomus cells are endocrine cells secreting polypeptides. According to Bischoff et al. (1970) the glomus cells release catecholamines to regulate the sensitivity of adjacent chemoreceptive nerve endings. Perhaps the enkephalin-like peptide is involved in similar regulatory mechanism. Furthermore, the relation of the presence of an opioid peptide in the glomus cells to the well-known respiratory depressant action of morphine remains to be elucidated.

With regard to VIP immunoreactive fibres, it has been shown that intracarotid injections of VIP stimulates chemoreceptor afferents (Said & Mutt 1970) either by a direct action or possibly due to local circulatory effects. The latter view is supported by the present demonstration of VIP immunoreactive nerves around blood vessel. On the other hand, only a very weak effect on respiration was observed after peripheral administration of substance P by the same route (McQueen 1978). It is, however, interesting to note that intraventricular

or intracisternal administration of SP caused hyperventilation (von Euler & Pernow 1956) and that medullary respiratory centres contain a dense network of SP nerve terminals (Ljungdahl et al. 1973).

The present study was supported by grant from the Swedish Medical Research Council (04X 2087, 04X 444, 04X 351, 05X 3766). Knut and Alice Wallenberg's Stiftelse, Magnus Bergvall Stiftelse and Clas Groschardt Stiftelse. The skilful technical assistance of Mrs W. Hult and Mrs. Ulla Landefeldt is gratefully acknowledged.

REFERENCES

- BISCOE J. H., LALL A. & SAMPSON S. R. 1970. Electron microscopic and electrophysiological studies on the carotid body following intra- and systemic administration of the glossopharyngeal nerve. *J. Physiol. (Lond.)* 208, 133-15.
- COONS A. H. 1958. Fluorescent antibody method. In: *General cytotechnical methods* (ed. J. F. Danielli), pp. 199-244. Academic Press, New York.
- DIGUILLIO A. M., YANG H. Y. T., LUTOLF B., FRATTA W., HONG J. & COSTA E. 1978. Characterization of enkephalin-like material extracted from sympathetic ganglia. *Neuropharmacology* 17, 997-99.
- EULER U. S. von & PERNOW B. 1956. Neurotrophic effect of substance P. *Acta Physiol. Scand.* 16, 76-77.

The effect of indomethacin on the blood flow-metabolism couple in the brain under normal hypercapnic and hypoxic conditions

AKEFUMI SAKABE and BO K. STESJO

Laboratory of Experimental Brain Research, University Hospital, Lund, Sweden

Although previous interest in the regulation of cerebral blood flow (CBF), and in the coupling of flow and cerebral metabolic rate for oxygen (CMR_{O_2}), has mainly focused on such coupling factors as intracellular H^+ and K^+ , recent results have established the influence of neurotransmitters and neurostimulators. For example, it has been demonstrated that the catecholamines noradrenaline, dopamine, and adrenaline, when gaining access to intracellular receptors, induce increases in CMR_{O_2} and CBF (MacKenzie et al. 1976a and b; McCulloch & Harper 1977; Bertman et al. 1978) and that serotonin has the opposite effects (Harper & MacKenzie 1977). It now seems that also prostaglandins exert a significant influence on CBF. Thus Polard & MacKenzie (1973), working on phenocyclobutyl anesthetized baboons, found that indomethacin (10 mg kg⁻¹) reduced normal CBF by about 40% and considerably curtailed the circulatory response to induced hypercapnia.

In the present study we repeated the experiments of Polard & MacKenzie (1973) in another species under different anesthetic circumstances, and extended them to include arterial hypoxia as well. Since the results give novel information on the blood flow-metabolism couple in the brain they are reported in preliminary form.

After the completion of operative procedures, halothane supply was discontinued and the animals were paralyzed (30 I.U. kg⁻¹) and maintained on 30% O_2 and 70% N_2O (or N_2 , see below) for 30 min steady state period, rectal temperature being maintained close to 37°C.

Control animals maintained on 70% N_2O were compared to 3 series of animals: normocapnic-normoxic, hypercapnic and hypoxic. In the first series, one group of N_2O -anesthetized animals was maintained normocapnic (P_{aCO_2} 35-40 mmHg) and normoxic (P_{aO_2} > 100 mmHg) for 30 min following the injection of indomethacin in dose of 10 mg kg⁻¹, before CBF and CMR_{O_2} were measured. Since indomethacin markedly reduced CBF an interaction with N_2O had to be excluded. Therefore, indomethacin was also given to animals in which the nitrous oxide supply was discontinued for 15 min. In this group, the adrenal glands were removed and in order to minimize pain and discomfort, the animals were given local anesthesia and protected from external stimuli. In the hypercapnic series, indomethacin (10 mg kg⁻¹) was given 15 min before the induction of hypercapnia (P_{aCO_2} = 80 mmHg) and CBF and CMR_{O_2} were measured after 30 min of hypercapnia. Separate hypercapnic animals were studied without indomethacin. In the hypoxic series, animals were treated similarly except for the fact that hypoxia (P_{aO_2} = 25 mmHg) was induced instead of hypercapnia.

Methods for measuring CBF and blood oxygen content (Ca_{O_2}), as well as for calculating CMR_{O_2} , have been described previously (Bertman et al. 1979a and b). These references should be consulted also for general physiological techniques. Statistical differences between groups were calculated using the unpaired Student's *t*-test.

The experiments were performed on fed male Wistar rats, weighing 320-415 g. Anesthesia was induced with 3% halothane and 70% N_2O and continued during operative preparations on 1% halothane and 70% N_2O . The animals were tracheotomized, intubated with tubocurarine 1 mg kg⁻¹, paralyzed with gallamine triethiodide (1.5 mg kg⁻¹) and cannulated artificially by Surling type respirator. Both femoral arteries were cannulated to allow continuous blood pressure recording and sampling of arterial blood. One femoral vein was cannulated for administration of drugs. The caudal portion of the upper lumbar spine was exposed by means of a small burr hole to obtain cerebral caudal blood. In one group of animals (see below) the adrenal glands were removed.

In all experimental groups mean body temperature was close to 37°C. Changes in arterial blood pressure and pH during hypercapnia and hypoxia were similar to those previously observed under the same experimental conditions (Bertman et al. 1979a and b) and physiological parameters were similar in unoperated and indomethacin-treated animals. In

On leave of absence from the Department of Anesthesiology, Yamaguchi University School of Medicine, 1144 Kogoshita, Ube, Yamaguchi, Japan.

Vasoactive Intestinal polypeptide (VIP) inhibits oxytocin induced activity of the rabbit myometrium

LENT OTTENSEN, HELLE ULRICHSEN, GORM WAGNER and JÁN FAHRENKRUG

From the Department of Medical Physiology B, University of Copenhagen, the Department of Obstetrics and Gynecology YA, Rigshospitalet, Copenhagen, and the Department of Clinical Chemistry, Bispebjerg Hospital, Copenhagen, Denmark

Vasoactive intestinal polypeptide (VIP), a highly active octacosapeptide, was isolated from porcine small intestine by Said and Mutt (1970). VIP was originally considered to be a gastrointestinal hormone but recent studies have demonstrated that VIP has an almost ubiquitous occurrence in the body localized in neurons and evidence is accumulating that the peptide represents a neurotransmitter (Fahrenkrug 1977). In the female genitourinary tract VIP-containing nerve fibres seem to innervate small vessels and smooth muscle cells (Larsson, Fahrenkrug & Schaffalitzky de Muckadell 1977). This finding in connection with the potent vasodilatory and smooth muscle relaxatory effects of VIP (Said 1973) suggest that the peptide plays a role in the nervous regulation of smooth muscle contractility and the blood flow in the genitourinary tract. Here we report that VIP inhibits the contractility and the myoelectrical activity of the myometrium in rabbits.

Five female rabbits of Danish Land race (age 140-170 days, weight 4-3.0 kg) had myometrial autografts placed in preinserted bilateral transparent ear-chambers by the technique of Wagner (Wagner 1975; Wagner, Hrynjuk & Nielsen 1977). Grafting was done 4-6 weeks after the ear-chamber insertion. The activity was recorded as electrical potentials by means of three platinum electrodes mounted on the base of the ear-chamber and contractions were simultaneously observed in a microscope 110-20 \times magnification stereomicroscope (Leitz). The experiments were performed not earlier than 10 days after grafting and the viability of the preparation was tested by its ability to respond to oxytocin intra-earously which should provoke potentials of magnitude of 0.5-3 mV peak to peak (Fig. 1A). Before the experiments the animals were treated for 6 days with estradiol, 25 μ g \cdot day⁻¹.

On the day of experiment the rabbit was anesthetized with mebolonal (Nembutal[®]), 30 mg/kg i.v. and a continuous infusion of oxytocin 0.3-1 mU \cdot min⁻¹ kg⁻¹ was given into an ear vein. When a stable myoelectrical response was obtained VIP was infused into the superior caval vein in the following doses in randomized order: 6 pmol \cdot min⁻¹ kg⁻¹, 25 pmol \cdot min⁻¹ kg⁻¹, 100 pmol \cdot min⁻¹ kg⁻¹ for 10-min periods. The VIP infusion periods were separated by 10 min intervals with control infusions of isotonic saline containing human serum albumin (Behringwerke, Marburg am Main, GFR), the vehicle used for dissolving VIP.

In order to estimate the concentration of VIP in the arterial blood supplying the myometrial graft VIP infusions using the protocol as above were performed on 5 additional female rabbits of identical weight and age. Blood samples were collected from the left carotid artery and the concentration of VIP measured radioimmunochemically (Fahrenkrug & Schaffalitzky de Muckadell 1977). The results are given in Table 1.

The highest dose of VIP used (100 pmol \cdot min⁻¹ kg⁻¹) completely abolished the electrical activity in the myometrial graft induced by oxytocin (Fig. 1C) while VIP had no effect on the non-oxytocin stimulated myometrium (not shown). A lag of 0.5 to 1.0 min was observed after discontinuation of the VIP infusion before the response to the continuous administration of oxytocin was regained. During infusion of VIP in a dose of 25 pmol \cdot min⁻¹ kg⁻¹ the myoelectrical response to oxytocin was modified and only a few spikes were recorded (Fig. 1D) while the oxytocin response was unaffected by the lowest VIP dose (6 pmol \cdot min⁻¹ kg⁻¹) (Fig. 1E). During the period of oxytocin induced activity blanching of the graft (contraction) occurred simultaneously with the electrical potentials.

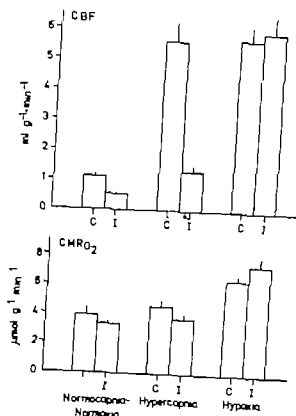


Fig 1 The influence of indomethacin on cerebral blood flow (CBF) and cerebral metabolic rate for oxygen (CMR_{O2}) under control conditions as well as in hypercapnia and in hypoxia. Values given are mean \pm SE for indomethacin injected animals (I) as compared to the corresponding control situation (C). $P < 0.001$. Statistical symbols within bars indicate differences from normocapnic-normoxic controls, while those below bars indicate differences between indomethacin-injected and control groups.

all non-hypoxic groups mean P_{aO_2} exceeded 108 mmHg and in all non hypercapnic groups mean P_{aCO_2} varied between 35 and 39 mmHg.

Results on CBF and CMR_{O2} are illustrated in Fig 1. In normocapnic-normoxic animals indomethacin reduced CBF to 50% of control with no influence on CMR_{O2}. The results confirm those of Pickard & MacKenzie (1973). Similar results were obtained in animals maintained on 70% N₂ excluding an interaction between indomethacin and nitrous oxide.

In uninjected hypercapnic animals CBF increased 5-fold and there was a suggested (but not significant) increase in CMR_{O2} (cf Bertman et al 1979a). In indomethacin-treated animals CBF during hypercapnia was only 25% of that observed in uninjected animals, and CMR_{O2} was close to control. Also these results are in close agreement with those reported by Pickard & MacKenzie (1973).

During hypoxia in uninjected animals there is the expected marked rise in CBF and an increase in CMR_{O2} (cf Bertman et al 1979b). As observed, none of these changes were influenced by indomethacin. In fact CMR_{O2} in the indomethacin treated animals approached 200% of normoxic controls. We are at present studying whether or not circulating catecholamines contribute to this high oxygen consumption rate (cf Bertman et al 1979).

The present results allow two important conclusions. First, indomethacin, known to inhibit prostaglandin synthesis, significantly influences normocerebrovascular tone and interferes with the coupling of metabolism and blood flow. Second, the drug curtails vascular dilatation during hypercapnia but not during hypoxia. This suggests that the mechanisms mediating vasodilatation in hypercapnia and hypoxia are at least partly dissimilar.

This study was supported by grants from the Swedish Medical Research Council (project No. 14X-263) and from US PHS (No. 5 R01 NS07838). The authors are grateful to Gunilla Giddo for skilful technical assistance.

REFERENCES

- BERTMAN L, DAHLGREN N & SIESJÖ B K 1978. Influence of intravenously administered catecholamines on cerebral oxygen consumption and blood flow in the rat. *Acta Physiol Scand* 104: 101-108.
- BERTMAN L, DAHLGREN N & SIESJÖ B K 1979a. Cerebral blood flow and oxygen consumption in the rat brain during extreme hypercapnia. *Neurobiology* 50: 799-805.
- BERTMAN L, CARLSSON C & SIESJÖ B K 1979b. Cerebral oxygen consumption and blood flow in hypoxia. Influence of sympathoadrenal activation. *Stroke* 10 (1): 207-215.
- HARPER A M & MACKENZIE E T 1977. Cerebral circulatory and metabolic effects of 5-hydroxytryptamine in anaesthetized baboons. *J Physiol* 271: 771-781.
- MACKENZIE E T, McCULLOCH J & O'KEAN M 1973. PICKARD J D & HARPER A M 1976a. Cerebral circulation and norepinephrine: Role of the blood-brain barrier. *Am J Physiol* 221 (2): 483-488.
- MACKENZIE E T, McCULLOCH J & HARPER A M 1976b. Influence of endogenous norepinephrine on cerebral blood flow and metabolism. *Am J Physiol* 221 (7): 489-494.
- McCULLOCH J & HARPER A M 1977. Cerebral circulation: Effect of stimulation and blockade of dopamine receptors. *Am J Physiol* 233 (2): H111-H117.
- PICKARD J D & MACKENZIE E T 1973. Inhibition of prostaglandin synthesis and the release of human cerebral circulation to carbon dioxide. *Nature (New Biology)* 245: 187-188.

- Casper studies. In: Gastrointestinal hormones (ed. James C. Thompson), pp. 591-597. Uni. of Texas Press.
- MUD, S. & MUTT, V. 1970. Polypeptide with broad biological activity isolated from small intestine. *Science* **169**: 1217-1218.
- WAGNER, G. 1973. Auto-transplantation of rabbit myometrium into ear-chamber and recording of its activity. *Acta Endocr (Kbh)* **79**: 767-777.
- WAGNER, G., HRYNZUK, J. R. & NIELSEN, J. F. 1972. EMG (from smooth muscle) by telemetry. In: *Biotelemetry* (ed. H. P. Krumholz and J. A. Vos), pp. 294-306. Elsevier NV, Leiden.

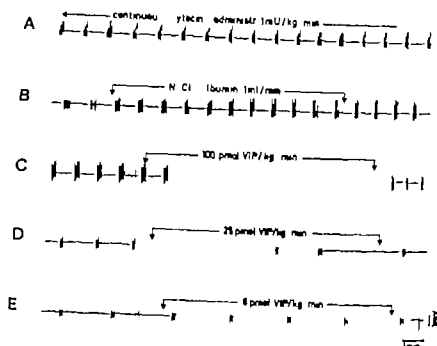


Fig. 1A-E. The myoelectrical activity recorded from ear-chambers in different rabbits. All registrations (A-E) were preceded and followed by a 10 min long period of regular potentials similar to those illustrated at the beginning and end of each trace in the figure. (A) Response to continuous oxytocin infusion. (B) Control infusion of 0.5 human serum albumin (HSA) in isotonic saline. (C) Response to 100 pmol VIP min⁻¹ kg⁻¹. (D) Response to 25 pmol VIP min⁻¹ kg⁻¹. (E) Response to 6 pmol VIP min⁻¹ kg⁻¹.

After initiation of the VIP infusion (100 pmol min⁻¹ kg⁻¹) no blanching was observed and no alteration in the blood flow was visually detectable.

Our results have demonstrated that VIP has a dose-dependent inhibitory action on the oxytocin activated myoelectrical and mechanical activity of the uterus. The present findings and the occurrence of VIPergic nerve fibres and terminals in the myometrium which seem to innervate the smooth muscle cells suggest that VIP plays a physiological role as neurotransmitter in the local control of the activity of the myometrium.

This work was supported by grant from the Danish Hospital Foundation for Medical Research Region of Copenhagen, the Farø Island and Greenland (Nr. 87/13).

and Thomas Bartholin's Fund, Denmark. The skilful technical assistance of Birgit Knudsen, Lene Poulsen and Anita Hansen is gratefully acknowledged.

REFERENCES

- FAHRENKRUG J. 1979. Vasoactive intestinal polypeptide: Measurement, distribution and putative neurotransmitter function. *Digestion* 19: 149-169.
- FAHRENKRUG J. & SCHIAFFALITZKY DE MUCKADELL, O. B. 1977. Radioimmunoassay of vasoactive intestinal polypeptide (VIP) in plasma. *J. Lab. Clin. Med.* 89: 1379-1388.
- LARSSON L. I., FAHRENKRUG J. & SCHIAFFALITZKY DE MUCKADELL, O. B. 1977. Vasoactive intestinal polypeptide occurs in nerves of the female genitourinary tract. *Science* 197: 1374-1375.

Table 1. Plasma concentration of VIP (pmol/l) in the arterial blood supplying the myometrial graft of 5 female rabbits during infusion of VIP in graded doses.

Infusion dose of VIP pmol min ⁻¹ kg ⁻¹	0	6	25	100
Concentration of VIP Median	18.0	59.8	45	66.5
Interquartile range	8.0-18.5	47.0-81.5	17.5-55	55.0-81.5

Quantitative changes in regional cerebral blood flow of rats induced by alpha- and beta-adrenergic stimulants

L. EDVINSSON, P. LACOMBE, CH. OWMAN, A. M. REYNIER REBUFFEL and J. SEYLAZ

Department of Histology, University of Lund, Sweden

EDVINSSON L., LACOMBE P., OWMAN CH., REYNIER REBUFFEL A. M. & SEYLAZ J. Quantitative changes in regional cerebral blood flow of rats induced by alpha- and beta-adrenergic stimulants. *Acta Physiol Scand* 1979, 107, 289-296. Received 30 April 1978. ISSN 0001-6772. Department of Histology, University of Lund, Sweden.

Cerebral blood flow was measured with the ^{14}C -ethanol technique in 8 regions (frontal, parieto-temporal and occipital cortex, caudate nucleus, thalamus, cerebellum, mesencephalon and pons) of rats. The highest flow values (83-89.5 ml/100 g/min) were found in cortical areas, whereas pons had the lowest flow (48 ml/100 g/min). Intravenous infusion of noradrenaline or adrenaline markedly reduced rCBF (by 2-48% of control levels) in all regions except thalamus, mesencephalon, and pons. The noradrenaline-induced reduction was blocked, and the effect of adrenaline reversed, after pretreatment with the alpha-receptor antagonist, phentolamine. Isoprenaline infusion markedly augmented rCBF in thalamus, mesencephalon, pons and also in the caudate nucleus. The response was reduced by the beta-receptor antagonist, propranolol. The experiments show the presence and heterogeneous distribution in the cerebrovascular bed of alpha- and beta-adrenoceptors that can be activated by sympathomimetics given systemically. If noradrenaline was allowed to pass the blood-brain barrier after osmotic opening with urea, an increased regional flow was obtained, probably due to a mechanism where the vasodilator effect secondary to activation of cerebral metabolism predominated over the direct vasoconstrictor effect of the amine.

Increased emphasis has been laid on a neural contribution to the regulation of cerebral blood flow (CBF) (Edvinsson & MacKenzie 1976; Owman & Edvinsson 1977) since it could be established by modern histochemical and electron microscopic studies that the brain vascular bed receives a well-developed sympathetic innervation (see Owman, Edvinsson & Nalvén 1974). The direct net effect of the noradrenaline transmitter on the cerebrovascular smooth muscle is a constriction, as has been demonstrated *in vitro* (Edvinsson & Owman 1974) and by microapplication *in vivo* (Wahl et al 1977).

Several studies have been undertaken to illustrate the influence of various sympathomimetic drugs on the cerebral circulation. The effect obtained have been contradictory both with regard to the direction and the amplitude of the response. Thus, the injection of noradrenaline or adrenaline has by some been found to decrease the flow (Klug, Schickel & Wechsler 1955; Semschbach, Madson &

Ochs 1953; Krog 1964; Haggendal 1965; von Essen 1973; Aubineau et al 1973a; Mitchell, Scriven & Rosendorff 1975) to have no effects (Gottstein 1962; Greenfield & Tindall 1968; Olsson 1977) or by others even to induce an increase in the cerebral blood flow (Meyer et al 1964; Birmmüller & Belz 1970; Mitchell et al 1975). However, when considering all available data, together with a critical evaluation of the techniques involved, noradrenaline administration or cervical sympathetic stimulation reduce total resting cerebral blood flow, but only by about 10 to 15% (see review by Edvinsson & MacKenzie 1976). There are several possible reasons for the weak response. It may be the result of a mixture of effects in regions with prominent and with little or no flow changes (Sercombe

Present address: Physiologie et Physiopathologie Cérébrovasculaire, CHU Lariboisière-Saint-Louis, 10 A, de Venkès, 75010 Paris, France.

Quantitative changes in regional cerebral blood flow of rats induced by alpha- and beta-adrenergic stimulants

L. EDVINSSON, P. LACOMBE, CH. OWMAN, A. M. REYNIER-REBUFFEL and J. SEYLAZ

Department of Histology, University of Lund, Sweden

EDVINSSON L., LACOMBE P., OWMAN CH., REYNIER-REBUFFEL A. M. & SEYLAZ J. Quantitative changes in regional cerebral blood flow of rats induced by alpha- and beta-adrenergic stimulants. *Acta Physiol Scand* 1979, 107: 289-296. Received 20 April 1978. ISSN 0001-6772. Department of Histology, University of Lund, Sweden.

Cerebral blood flow was measured with the ^{14}C -ethanol technique in 8 regions (frontal, parieto-temporal and occipital cortex, caudate nucleus, thalamus, cerebellum, mesencephalon, and pons) of rats. The highest flow values (83-89.5 ml/100 g/min) were found in cortical areas, whereas pons had the lowest flow (48 ml/100 g/min). Intravenous infusion of noradrenaline or adrenaline markedly reduced rCBF (by 22-48% of control levels) in all regions except thalamus, mesencephalon, and pons. The noradrenaline-induced reduction was blocked, and the effect of adrenaline reversed, after pretreatment with the alpha-receptor antagonist, phentolamine. Isoprenaline infusion markedly augmented rCBF in thalamus, mesencephalon, pons, and also in the caudate nucleus. The response was reduced by the beta-receptor antagonist, propranolol. The experiments show the presence and heterogeneous distribution in the cerebrovascular bed of alpha- and beta-adrenergic receptors that can be activated by sympathomimetics given systematically. If noradrenaline was allowed to pass the blood-brain barrier after osmotic opening with urea, an increased regional flow was obtained, probably due to a mechanism where the vasodilator effect secondary to activation of cerebral metabolism predominated over the direct vasoconstrictor effect of the amine.

It has been found on a neural contribution to the regulation of cerebral blood flow (CBF) (Edvinsson & MacKenzie 1976, Owman & Edvinsson 1977) since it could be established by modern histochemical and electron microscopic studies that the brain vascular bed receives a well-developed sympathetic innervation (see Owman, Edvinsson & Nefsen 1974). The direct net effect of the noradrenaline transmitter on the cerebrovascular smooth muscle is a constriction, as has been demonstrated *in vitro* (Edvinsson & Owman 1974) and by microapplication *in vivo* (Wahl et al. 1972).

Several studies have been undertaken to illustrate the influence of various sympathomimetic drugs on the cerebral circulation. The effects obtained have been contradictory both with regard to the direction and the amplitude of the response. Thus, the injection of noradrenaline or adrenaline has by some authors been found to decrease the flow (Kung, Lohoff & MacIsaac 1954, Sassenbach, Madison &

Ochs 1953, Krog 1964, Haggendal 1965, von Essen 1973, Aubureau et al. 1975, Mitchell, Scriven & Rosendorff 1974), to have no effects (Gottstein 1964, Greenfield & Tindall 1968, Olesen 1977) or by others even to induce an increase in the cerebral blood flow (Meyer et al. 1964, Bismuth & Betz 1970, Mitchell et al. 1975). However, when considering all available data, together with a critical evaluation of the techniques in which noradrenaline administration or cervical sympathetic stimulation reduce total resting cerebral blood flow but only by about 10 to 15% (see review by Edvinsson & MacKenzie 1976). There are several possible reasons for the weak response: It may be the resultant of a mixture of effects in regions with prominent and with little or no flow change (Sercombe

Present address: Physiologie et Pathophysiologie Cérébrovasculaire, CHU Lariboisière-Saint-Louis 10 A, de Verdun 75010 Paris, France.

Quantitative changes in regional cerebral blood flow of rats induced by alpha- and beta-adrenergic stimulants

L. EDVINSSON, P. LACOMBE, CH. OWMAN, A. M. REYNIER-REBUFFEL and L. SEYLAZ

Department of Histology, University of Lund, S-223 62, Sweden

EDVINSSON L., LACOMBE P., OWMAN CH., REYNIER-REBUFFEL A. M. & SEYLAZ L. Quantitative changes in regional cerebral blood flow of rats induced by alpha- and beta-adrenergic stimulants. *Acta Physiol Scand* 1979, 107, 289-296. Received 20 April 1978. ISSN 0001-6772. Department of Histology, University of Lund, Sweden.

Cerebral blood flow was measured with the ^{14}C -ethanol technique in 8 regions (frontal, parieto-temporal and occipital cortex, caudate nucleus, thalamus, cerebellum, mesencephalon, and pons) of rats. The highest flow values (83-89.5 ml/100 g/min) were found in cortical areas, whereas pons had the lowest flow (48 ml/100 g/min). Intravenous infusion of noradrenaline or adrenaline markedly reduced rCBF (by 22-48% of control levels) in all regions except thalamus, mesencephalon, and pons. The noradrenaline-induced reduction was blocked, and the effect of adrenaline reversed, after pretreatment with the alpha-receptor antagonist, phentolamine. Isoprenaline infusion markedly augmented rCBF in thalamus, mesencephalon, pons and also in the caudate nucleus. The response reduced by the beta-receptor antagonist, propranolol. The experiment shows the presence and heterogeneous distribution in the cerebrovascular bed of alpha- and beta-adrenergic receptors that can be activated by sympathomimetics given systemically. If noradrenaline was allowed to pass the blood-brain barrier after osmotic opening with urea, an increased regional flow was obtained, probably due to a mechanism where the vasodilator effect secondary to activation of cerebral metabolism predominated over the direct vasoconstrictor effect of the amine.

Increased emphasis has been laid on a neural contribution to the regulation of cerebral blood flow (CBF) (Edvinsson & MacKenzie 1976, Owman & Edvinsson 1977) since it could be established by modern histochemical and electron microscopic studies that the brain vascular bed receives well-developed sympathetic innervation (see Owman, Edvinsson & Nielsen 1974). The direct net effect of the noradrenergic transmitter on the cerebrovascular smooth muscle is constriction, as has been demonstrated *in vitro* (Edvinsson & Owman 1974) and by microapplications *in vivo* (Wahl et al. 1972).

Several studies have been undertaken to illustrate the influence of various sympathomimetic drugs on the cerebral circulation. The effects obtained have been contradictory both with regard to the direction and the amplitude of the response. Thus, the injection of noradrenaline or adrenaline has by some authors been found to decrease the flow (King, Sokoloff & Wechsler 1952, Sensenbach, Madison &

Ochs 1953, Krog 1964, Haggendal 1965, on Eassen 1973, Aubineau et al. 1973a, Mitchell, Scriven & Rosendorff 1975) to have no effects (Gottstein 1964, Greenfield & Tindall 1968, Olesen 1977) or by others even to induce an increase in the cerebral blood flow (Meyer et al. 1964, Bjemmüller & Betz 1970, Mitchell et al. 1975). However, when considering all available data, together with a critical evaluation of the techniques involved, noradrenaline administration or cervical sympathetic stimulation reduce total resting cerebral blood flow but only by about 10 to 15% (see review by Edvinsson & MacKenzie 1976). There are several possible reasons for the weak response. It may be the resultant of a mixture of effects in regions with prominent and with little or no flow changes (Sercombe

Present address: Physiologie et Pathophysiologie Cérébrovasculaire, CHU Lariboisière-Saint-Louis, 10 A, rue de Verdon 75010 Paris, France.

et al 1975) in the case of nerve stimulation probably related to the degree of sympathetic innervation (Edvinsson & Owman 1977a). The poor response to some drugs may also be related to the limited passage of such substances through the blood-brain barrier (Rapaport 1976; Edvinsson et al 1978). The effect of noradrenaline might be limited by neuronal and extraneuronal uptake mechanisms preventing it from reaching the vascular adrenergic receptors (cf McCalden & Eidelman 1976).

Studies involving the beta-receptor agonist isoprenaline have given more consistent results. This agent is only slightly affected by neuronal and extraneuronal uptake and degradation processes (Iversen 1967). The common response to systemically administered isoprenaline is vasodilation and increase in the cerebral perfusion (Laubie & Drouilhat 1867; Xanoulatos & James 1977; Aubineau et al 1973a and b).

The adrenoceptors in cerebral blood vessels and their pharmacological characteristics have been extensively analyzed (Edvinsson & Owman 1977b; Wahl & Kuschinsky 1977). Based on the recent findings of local differences in the perivascular sympathetic innervation (Edvinsson & Owman 1977a) and in the reactivity to vasoactive amines and to sympathetic nerve stimulation (Sercombe et al 1975) the present series of experiments were performed to analyze in detail the changes in regional cerebral blood flow of rats induced by alpha and beta adrenergic receptor agonists alone or in combination with specific competitive antagonists.

METHODS

Animals. The experiments were performed on adult male Sprague-Dawley rats (250–300 g b wt) having free access to tap water and commercial pellet food until operation. Anaesthesia was induced with halothane (Fluothane Hoechst, 3%) delivered via a Dräger vaporizer. When asleep the animals were tracheotomized and paralyzed (0.5 mg/kg tubocurarine chloride). Thereafter they were ventilated with a small animal respirator (Braun) on 70% N₂O and 30% O₂ without halothane. Body temperature was measured rectally and adjusted to 37°C by a heating lamp. The femoral arteries and veins were cannulated bilaterally. One of the arterial catheters was used for continuous recording of arterial blood pressure via pressure transducer (Elema, Sweden) and the other for anaerobic sampling of blood both for blood gas measurements (BMS Mk II Radiometer, Copenhagen) and for sampling of radioactive tracer. One of the femoral veins was cannulated for infusion of the radioactive tracer ¹⁴C-ethanol (specific activity 60 mCi/mmol Radiochemical

Centre, Amsterdam) 20 µCi dissolved in physiological saline and the other femoral vein for administration of the drugs to be tested and of saturated potassium chloride to stop the heart at the end of the experiments.

CBF measurements. The flow determinations were not performed until the p_aCO₂ had stabilized between 35 and 40 mmHg for at least 30 min. The regional blood flow was determined according to Renwick et al. (1966) as modified by Eklöf et al. (1973). The ¹⁴C-ethanol solution was injected into the circulatory bed via a femoral vein during 30 s using a constant rate infusion pump. Arterial blood samples were taken into 10 µl glass capillaries from a femoral artery every 3 s during the isovolumetric infusion.

Immediately after the last sample had been taken, 1 ml of saturated potassium chloride was rapidly injected to stop the heart. The animal was instantaneously decapitated, the head frozen in toto in liquid nitrogen, and stored at -55°C in a cryostat for later preparation (1–4 days). The brain was removed and various regions dissected out in a cryostat at a temperature of -15°C where also the tissue pieces were weighed on a microbalance (Mettler). The encephalic samples taken for analysis consisted mainly of grey matter. These pieces of brain tissue as well as the previously withdrawn blood samples were added to scintillation vials and counted in a Nuclear Chicago liquid scintillation counter. The blood samples were mixed directly with scintillation fluid (Instagel, Radiochemical Centre, Amsterdam) while the tissue pieces were dissolved in Soluene (Packard) before the scintillation fluid was added. Quenching was corrected according to standard procedures (see Eklöf et al. 1973).

The partition coefficient for ¹⁴C-ethanol has been determined by Eklöf et al. (1977) and found to be 1.14 for brain tissue. Calculations of the flow values were performed as described by Renwick et al. (1966). The flow values were computed on a Wang desk computer according to the protocol used by Eklöf et al. (1972), and the results are expressed on the basis of tissue wet weight: ml/100 g/min. The CO₂ response was tested by adding small quantities of CO₂ to the gas mixture delivered by the ventilator until the desired level of arterial CO₂ concentration was reached.

The results are expressed as mean ± SE and the differences between mean values were analyzed statistically with the Student's *t* test using a Packard desk computer.

Drugs. The agonists (*l*-arterenolol hydrochloride, *Sigmac*, *l*-epinephrine bitartrate, *Sigma*, *l*-isoprenaline hydrochloride, *Sigma*) were infused i.v. during a 10 min period with a LKB roller pump at a speed of 0.1 ml/min. The inhibitors phenolamine (Regitin, Ciba) and propranolol (Inderal, Scandinavia) were administered 1 min before infusion of the agonist was started. All drugs were dissolved in 0.9% NaCl and prepared fresh. The catecholamine solutions contained 0.2 mg/ml ascorbic acid to minimize oxidation of the amine.

RESULTS

Physiological parameters. The mean values of the physiological variables during the infusion experiments

Table 1 Mean arterial blood pressure and arterial blood gases and pH in anesthetized rats in which CBF was affected by infusion of noradrenaline, adrenaline or isoprenaline

Experimental groups	Mean values \pm S.E.	number of animals	MABP (mmHg)	$p_a\text{CO}_2$ (mmHg)	$p_a\text{O}_2$ (mmHg)	pH (mmHg)
Control animals	17		141 \pm 4	39.3 \pm 1.6	138 \pm 6	7.36 \pm 0.016
Noradrenaline	6		174 \pm 7	37.6 \pm 0.6	151 \pm 7	7.394 \pm 0.008
Adrenaline	6		117 \pm 14	36.8 \pm 1.5	158 \pm 7	7.388 \pm 0.006
Isoprenaline	6		160 \pm 7	42.0 \pm 1.3	135 \pm 11	7.255 \pm 0.016
Phenylephrine + noradrenaline	5		152 \pm 4	42.1 \pm 1.0	148 \pm 11	7.346 \pm 0.030
Phenylephrine + adrenaline	5		150 \pm 4	39.2 \pm 0.4	156 \pm 1	7.397 \pm 0.004
Phenylephrine + isoprenaline	4		140 \pm 5	39.8 \pm 0.8	149 \pm 6	7.335 \pm 0.014

as shown in Table 1. No major differences in pH or arterial blood gases ($p_a\text{O}_2$ and $p_a\text{CO}_2$) were found in comparison with the untreated control animals. There was a statistically insignificant reduction in MABP during the adrenaline infusion, whereas noradrenaline increased the blood pressure by about 30% ($P < 0.01$).

Cerebral blood flow: The mean CBF values (ml/100 g/min) varied according to the region studied: the cerebrocortical grey substance usually had higher flow (frontal cortex 84, parieto-temporal cortex 89.5, occipital cortex 83) than those preparations containing less grey matter (pons 48, cerebellar cortex 62.5). Deep grey regions, such as the caudate nucleus (75.5) and the thalamus (74) had intermediary flow levels, all in good agreement with other studies (Renssch et al. 1968, Ejlof et al. 1973).

Reactivity to hypercapnia. The cerebrovascular reactivity to increased arterial CO_2 tension was examined in the cerebrocortical areas and in the

caudate nucleus. A modest hypercapnia ($p_a\text{CO}_2$ approximately 53 mmHg) was induced by adding CO_2 gas to the inspired anesthetic gas mixture of N_2O and O_2 . Hypercapnia markedly increased the blood flow (Table 2) in the pooled cortical areas ($P < 0.01$) and in the caudate nucleus ($P < 0.001$). The CO_2 reactivity (expressed as flow increment per unit increase in $p_a\text{CO}_2$ above control) varied between -6 and 5.5 ml/100 g/min for each mmHg in these expts. Whether the reactivity really is higher in the caudate nucleus than in the cortex is difficult to establish on the basis of the present figures, since neither the difference between control flows nor that between the hypercapnic flow values in the two areas was statistically significant.

Infusion of noradrenaline. Continuous i.v. infusion for 10 min of noradrenaline (1 $\mu\text{g/kg/min}$) before measuring the regional CBF resulted in a variety of flow responses (Fig. 1). Thus, the anastomosis produced no significant effect in thalamus, mesence-

Table 2. Flow in cortex (mean from frontal, parieto-temporal and occipital) and caudate nucleus together with values for $p_a\text{CO}_2$ during hypercapnia as compared with the effect of noradrenaline infusion before and after opening of the blood-brain barrier in urea

Flow values corrected to control levels of $p_a\text{CO}_2$ are also given. Figures show mean values \pm S.E., number of animals per preparation. Comparison of mean values (control group vs. experimental groups) according to Student's *t*-test: * $P < 0.05$, ** $0.01 < P < 0.01$, *** $P < 0.001$.

Treatment	Cortex blood flow (ml/100 g/min)	Caudate nucleus blood flow (ml/100 g/min)	$p_a\text{CO}_2$ (mmHg)
Control animals	83 \pm 6.7 (18)	75 \pm 5 (6)	39.3 \pm 1.6
Hypercapnia	122 \pm 8 (15)	154 \pm 10*** (6)	53.3 \pm 2.5
Noradrenaline infusion	66 \pm 5.3* (18)	55 \pm 5.5 (6)	37.6 \pm 0.6
Corrected to control $p_a\text{CO}_2$	62 \pm 5.3	46 \pm 5.5**	
2 M urea followed by noradrenaline*	117 \pm 9.7* (23)	124 \pm 11** (8)	36.2 \pm 1.0
Corrected to control $p_a\text{CO}_2$	109 \pm 9.7*	107 \pm 11**	

Data calculated from material presented by Edvinsson et al. (1978).

et al 1975) in the case of nerve stimulation probably related to the degree of sympathetic innervation (Edvinsson & Owman 1977a). The poor response to some drugs may also be related to the limited passage of such substances through the blood brain barrier (Rapoport 1976, Edvinsson et al 1978). The effect of noradrenaline might be limited by neuronal and extraneuronal uptake mechanisms preventing it from reaching the vascular adrenergic receptors (cf McCaiken & Edelmann 1976).

Studies involving the beta receptor agonist isoprenaline have given more consistent results. This agent is only slightly affected by neuronal and extraneuronal uptake and degradation processes (Iversen 1967). The common response to systemically administered isoprenaline is vasodilation and increase in the cerebral perfusion (Laubie & Drouilhat 1867, Xanatos & James 1972, Aubineau et al 1973a and b).

The adrenoceptors in cerebral blood vessels and their pharmacological characteristics have been extensively analyzed (Edvinsson & Owman 1977b, Wahl & Kuschinsky 1977). Based on the recent findings of local differences in the perivascular sympathetic innervation (Edvinsson & Owman 1977a) and in the reactivity to vasoactive amines and to sympathetic nerve stimulation (Sercombe et al 1975) the present series of experiments were performed to analyze in detail the changes in regional cerebral blood flow of rats induced by α - and β -adrenergic receptor agonists alone or in combination with specific competitive antagonists.

METHODS

Animals. The experiments were performed on adult male Sprague Dawley rats (250–300 g b.wt.) having free access to tap water and commercial pellet food until operation. Anesthesia was induced with halothane (Fluothane Hoechst –3%) delivered via Dräger pump. When asleep the animals were tracheotomized and paralyzed (0.5 mg/kg tubocurarine chloride). Thereafter they were intubated with a small animal respirator (Braun) on 70% N_2O and 30% O_2 without halothane. Body temperature was measured rectally and adjusted to 37°C by heating lamp. The femoral artery and vein were cannulated bilaterally. One of the arterial catheters was used for continuous recording of arterial blood pressure in pressure transducer (Elema, Sweden) and the other for anaerobic sampling of blood both for blood gas measurements (BMS Mk II Radiometer Copenhagen) and for sampling of radioactive tracer. One of the femoral veins was cannulated for infusion of the radioactive tracer 3H -ethanol (specific activity 60 mCi/mmol Radiochemical

Centre Amersham) 20 μ Ci dissolved in physiological saline and the other femoral vein for administration of the drugs to be tested and of saturated potassium chloride to stop the heart at the end of the experiments.

CBF measurements. The flow determinations were not performed until the pCO_2 had stabilized between 40 and 42 mmHg for at least 30 min. The regional blood flow was determined according to Reivich et al. (1969) as modified by Eklof et al. (1973). The 3H -ethanol solution was injected into the circulatory bed via a femoral vein during 30 s using a constant rate infusion pump. Arterial blood samples were taken into 10 μ l glass capillaries from a femoral artery every 3 s during the radioisotope infusion.

Immediately after the last sample had been taken, 1 ml of saturated potassium chloride was rapidly injected to stop the heart. The animal was instantaneously decapitated, the head frozen in toto in liquid nitrogen, and stored at -25°C in a cryostat for later preparation (1–4 days). The brain was removed and various regions dissected out in a cryostat at a temperature of -15°C , where also the tissue pieces were weighed on a microbalance (Mettler). The tissue samples taken for analysis consisted of grey matter. These pieces of brain tissue as well as the previously withdrawn blood samples were added to scintillation vials and counted in a Nuclear Chicago liquid scintillation counter. The blood samples were mixed directly with scintillation fluid (Instagel Radiochemical Centre Amersham) while the tissue pieces were dissolved in Soluene (Packard) before the scintillation fluid was added. Quenching was corrected according to standard procedures (see Eklof et al. 1973).

The partition coefficient for 3H -ethanol has been determined by Eklof et al. (1972) and found to be 1.14 in brain tissue. Calculations of the flow values were performed as described by Reivich et al. (1969). The flow values were computed on a Wang desk computer according to the protocol used by Eklof et al. (1973), and the results are expressed on the basis of tissue wet weight as ml/100 g/min. The CO_2 responsiveness was tested by adding small quantities of CO_2 to the gas mixture delivered by the ventilator until the desired level of arterial CO_2 concentration was reached.

The results are expressed as mean \pm SE, and the difference between mean values were analyzed statistically with the Student's *t* test using a Packard desk computer.

Drugs. The agonists (L-arterenol hydrochloride Sigma), α -phenylephrine bitartrate (Sigma), isoproterenol hydrochloride (Sigma) were infused i.v. during a 10 min period with a LKB roller pump at a speed of 0.1 ml/min. The inhibitors phenolamine (Regitin Ciba) and propranolol (Inderal Scammedia) were administered i.v. before infusion of the agonists was started. All drugs were dissolved in 0.9% NaCl and prepared fresh. The catecholamine solutions contained 0.2 mg/ml ascorbic acid to minimize oxidation of the amine.

RESULTS

Physiological parameters. The mean values of the physiological variables during the infusion experiments

increase in the cortical flow was found ($P < 0.01$) in contrast to the reduction obtained with noradrenaline alone (Table 2). The flow increment was even more pronounced in the caudate nucleus ($P < 0.01$). The increase was somewhat less pronounced in both regions after correction to control values for $p_a\text{CO}_2$.

Infusion of adrenaline The pattern of response to adrenaline infusion ($1 \mu\text{g/kg/min}$) was similar to the changes in CBF found with noradrenaline (Fig. 1). Thus, no statistically significant effect was obtained in pons, thalamus, mesencephalon. The mean reduction in the caudate was the same as with noradrenaline, but due to a greater individual variability in the response the adrenaline effect was not statistically significant. In the other regions studied the vasoconstrictor response to this amine was more pronounced than for noradrenaline giving a 44–63% reduction of flow compared with untreated controls.

Administration of the alpha-receptor blocking agent, phentolamine (1 mg/kg i.v.) 30 min before the start of the adrenaline infusion totally inhibited the vasoconstrictor effect the vascular response was instead markedly reversed (Fig. 1). A highly significant increase ($P < 0.001$) in flow compared to controls occurred in pons and thalamus (92 and 42% flow increment, respectively) as well as in the caudate nucleus and mesencephalon (45–46%).

Infusion of isoprenaline In order to obtain more direct information about the vascular response to beta-receptor activation, isoprenaline ($0.5 \mu\text{g/kg/min}$) was tested during steady-state conditions (Fig. 1). Clearcut increases in regional blood flow was found in pons, mesencephalon, thalamus and caudate nucleus. The cortical regions and cerebellum only showed a tendency to flow increase which was not statistically significant.

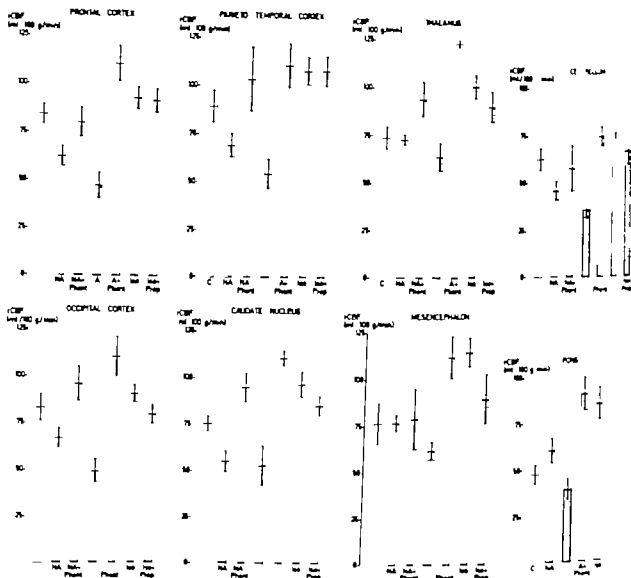
The values for $p_a\text{CO}_2$ in this group of animals was higher than in the controls. Correction of the $p_a\text{CO}_2$ levels to control values tended to reduce the figures for the flow increment. I.v. injection of 1 mg/kg of the beta-receptor blocking agent, propranolol, antagonized the response to isoprenaline in cases where this had produced a clearcut flow increase (Fig. 1).

DISCUSSION

Methodological considerations In order to obtain information on the effects of various amines on the cerebral blood flow in small animals, regional

method should be used which is atraumatic with regard to the head region and, ideally it should neither require exposure of the brain tissue by means of a craniotomy nor should it disturb the local circulation of the tissue by direct injections. A technique fulfilling these criteria has been devised by Reivich et al. (1969). This method is based on the mathematical calculations once derived by Kety (1951) using the diffusible tracer ^{14}C -antipyrine. It has later been applied to the rat and modified since it did not give adequate quantitative information in rapid flow situations (Eklöf et al. 1973). Provided the more freely diffusible tracer ^{14}C -ethanol is used and the infusion is carried out during 30 s, the method gives accurate values within the range of flow studied in the present experiments (Eklöf et al. 1973).

As with all clearance methods the animal must be in a steady state during at least the period when the clearance is recorded. Therefore, continuous infusion of the test substance was used beginning 10 min before the start of the injection of ^{14}C -ethanol. Although the method is regional it can be assumed that the pieces, weighing about 25 mg for practical reasons, are composed of several areas with different flow characteristics under normal and experimental conditions. It is an advantage, though, that the regions measured can be exactly defined (in contrast to situations when radioactivity is measured externally) and that any extracranial contamination is entirely eliminated. The control blood flow levels obtained in the present study on 250–300 g male Sprague-Dawley rats were somewhat lower than those reported for 300–400 g male Wistar rats (Eklöf et al. 1973) indicating hemodynamic variations between the two strains of highly inbred rats. The mean arterial blood pressure was affected to a varying but small extent by the different infused drugs. It has, however, been shown in numerous studies (e.g. Haggendal & Johansson 1965; Harper 1966) that the autoregulation of the cerebral circulation efficiently compensates for this. Therefore, the effects noted after the amine infusions cannot be secondary to the blood pressure changes. Attempts were made to maintain blood gases ($p_a\text{CO}_2$ and $p_a\text{O}_2$) and pH within normal limits in the various experimental groups. Despite this effort, slight variations were noted in the mean $p_a\text{CO}_2$ (as well as $p_a\text{O}_2$ and pH) values in some of the groups. For this reason, flow levels were also given corrected to control $p_a\text{CO}_2$. The same tendency in the flow



Regional cerebral blood flow (rCBF) in untreated control rats (C) and after infusion of catecholamines (NA: noradrenaline; A: adrenaline; ISO: isoprenaline) alone or after pretreatment of the animals with competitive antagonists (Phent: phentolamine; Prop: propranolol). Mean values \pm S.E. For information about the number of animals and the associated physiological parameters see Table 1.

phalon and pons. In all the other regions the flow was reduced by approximately 10 to 27%. The over all reduction in (uncorrected) cortical blood flow amounted 22% ($P < 0.05$). As shown in Tables 1 and 2 there was a slight (though statistically insignificant) fall in $p\text{CO}_2$ in conjunction with the noradrenaline infusions. Assuming a linear relationship between the flow and arterial CO_2 pressure increments in the interval tested (39 to 53 mmHg) the CBF levels could be corrected to the same (control) $p\text{CO}_2$ value. This slightly augmented the noradrenaline induced reduction in both cortical and caudate blood flow.

The reduction in local cerebral blood flow to α_1 adrenalinergic could be prevented by the injection of the α_1 receptor antagonist phentolamine (1 mg/kg i.v.) prior to the infusion of the amine (Fig. 1). There was even an increase in the flow under these conditions. The reversal was statistically significant ($P < 0.05$ and $P < 0.001$) in all regions except the parieto-temporal cortex and the cerebellum. If noradrenaline was administered after the structural blood-brain barrier had been opened through a hyperosmotic shock (see Edvinsson et al. 1978) by injection of M urea (which in itself did not significantly affect CBF) into the internal carotid and

crease in the cortical flow was found ($P < 0.01$) in contrast to the reduction obtained with noradrenaline alone (Table 2). The flow increment was even more pronounced in the caudate nucleus ($P < 0.01$). The increase was somewhat less prominent in both regions after correction to control values for $p\text{CO}_2$.

Infusion of adrenaline The pattern of response to adrenaline infusion ($1 \mu\text{g/kg/min}$) was similar to the changes in CBF found with noradrenaline (Fig. 1). Thus, no statistically significant effect was obtained in pons, thalamus, mesencephalon. The flow reduction in the caudate was the same as with noradrenaline, but due to a greater individual variability in the response, the adrenaline effect was not statistically significant. In the other regions studied the vasoconstrictor response to this amine was more pronounced than for noradrenaline giving a 41–61% reduction of flow compared with untreated controls.

Administration of the alpha-receptor blocking agent, phentolamine (1 mg/kg i.v.) 30 min before the start of the adrenaline infusion totally inhibited the vasoconstrictor effect, the vascular response to the amine markedly reversed (Fig. 1). A highly significant increase ($P < 0.001$) in flow compared to controls thus occurred in pons and thalamus (92 and 41% flow increment, respectively) as well as in the caudate nucleus and mesencephalon (45–46%).

Infusion of Isoprenaline In order to obtain more direct information about the vascular response to beta-receptor activation, isoprenaline ($0.5 \mu\text{g/kg/min}$) was tested during steady-state conditions (Fig. 1). Clearcut increases in regional blood flow was found in pons, mesencephalon, thalamus and caudate nucleus. The cortical regions and cerebellum only showed a tendency to flow increase which was not statistically significant.

The alveolar $p\text{CO}_2$ in this group of animals was higher than in the controls. Correction of the $p\text{CO}_2$ levels to control values tended to reduce the figures for the flow increment. In addition of 1 mg/kg of the beta-receptor blocking agent, propranolol antagonized the response to isoprenaline in cases where this had produced a clearcut flow increase (Fig. 1).

DISCUSSION

Methodological considerations In order to obtain information on the effects of various amines on the cerebral blood flow in small animals, a regional

method should be used which is atraumatic with regard to the head region and, ideally it should neither require exposure of the brain tissue by means of a craniotomy nor should it disturb the local circulation of the tissue by direct injections. A technique fulfilling these criteria has been devised by Renwick et al. (1969). This method is based on the mathematical calculations once derived by Kety (1951) using the diffusible tracer ^{14}C -antipyrine. It has later been applied to the rat and modified since it did not give adequate quantitative information in rapid flow situations (Eklöf et al. 1973). Provided the more freely diffusible tracer ^{14}C -ethanol is used and the infusion is carried out during 30 s the method gives accurate values within the range of flow studied in the present experiments (Eklöf et al. 1973).

As with all clearance methods, the animal must be in a steady state during at least the period when the clearance is recorded. Therefore continuous infusion of the test substance was used, beginning 10 min before the start of the injection of ^{14}C -ethanol. Although the method is regional it can be assumed that the pieces, weighing about 25 mg for practical reasons, are composed of several areas with different flow characteristics under normal and experimental conditions. It is an advantage though, that the regions measured can be exactly defined (in contrast to situations when radioactivity is measured externally) and that any extracranial contamination is entirely eliminated. The control blood flow levels obtained in the present study on 250–300 g male Sprague Dawley rats were somewhat lower than those reported for 300–400 g male Wistar rats (Eklöf et al. 1973), indicating hemodynamic variations between the two strains of highly inbred rats. The mean arterial blood pressure was affected to varying but small extent by the different infused drugs. It has, however been shown in numerous studies (e.g. Häggendal & Johansson 1965; Harper 1966) that the autoregulation of the cerebral circulation efficiently compensates for this. Therefore, the effects noted after the amine infusions cannot be secondary to the blood pressure changes. Attempts were made to maintain blood gases ($p\text{CO}_2$ and $p\text{O}_2$) and pH within normal limits in the various experimental groups. Despite this effort, slight variations were noted in the mean $p\text{CO}_2$ (as well as $p\text{O}_2$ and pH) values in some of the groups. For this reason, flow levels were also given corrected to control $p\text{CO}_2$. The same tendency in the flow

changes during the various treatments was found after this correction. No corresponding correction was made for variations in pO_2 values since it is known that as long as pO_2 is kept above 100 mmHg there is no significant influence on CBF (Borgström Johansson & Siegfö 1975).

Infusion of sympathomimetic amines. In order to achieve steady state conditions continuous infusion of the agonists was utilized. Both noradrenaline and adrenaline reduced the regional flow in cerebral and cerebellar cortical structures to a varying degree and a reduction was also observed in the caudate nucleus. A similar pattern of decrease in regional CBF has been reported during cranial sympathetic nerve stimulation in rabbits (Lacombe et al 1977).

The finding on the caudate nucleus confirms results from local measurements with the thermoclearance technique in rabbits where these amines as well as sympathetic nerve stimulation clearly reduced the caudate blood flow (Sercombe et al 1975). During those experiments another brain region, the lateral geniculate body, showed little or no response. The difference in the response could be related to the degree of vascular innervation; the caudate has a density of sympathetic nerve supply which is twice as high as that found in the vascular bed of the lateral geniculate body (Sercombe et al 1975). This regional heterogeneity in the extent of sympathetic nerve supply of intracerebral arterioles has been studied in more detail in baboons (Edvinsson & Owman 1977a). It may be that this kind of variability to some extent explains the different regional flow reactions seen also in rats (see further below).

The CBF reduction obtained after administration of the catecholamines was mediated by α -receptors in the sense that it could be prevented by previous injection of the competitive α -antagonist phentolamine. It is notable that the reduction in CBF is a net effect including a vasodilatory component as shown by the reversal, particularly of the adrenaline induced flow reduction upon administration of phentolamine. This supports previous evidence (Edvinsson & Owman 1974; Sercombe et al 1977) that direct cerebral vasodilatation is mediated by the β_2 subtype of receptors in the vessel wall (whereas peripheral vasodilatation is known to be mediated by β_1 -receptors). Regions which previously had not responded significantly to noradrenaline or adrenaline (i.e. thalamus,

mesencephalon and pons) now showed a marked flow increase. This shows that vasoconstrictor and dilator responses to catecholamines had outbalanced each other in the absence of phentolamine. This might reflect a regional heterogeneity in the relative proportion of constrictory and dilatory α -receptors, perhaps related to a local variation in the degree of sympathetic innervation as discussed above. A similar large increase in flow was observed after administration of the beta-agonist isoprenaline. The effect was antagonized by the competitive beta-receptor blocking agent, propranolol.

There is reason to believe that the above mentioned effects of the sympathomimetic amines on CBF primarily represent direct vasomotor action in this vascular bed. Amines are known to penetrate the blood-brain barrier poorly (see Rapoport 1976) but can be made to reach into the brain by transient opening of the barrier with hypertonic solutions, as shown in the rat by Edvinsson et al (1978). Under these conditions, however, noradrenaline increases local CBF by an effect that was not inhibited by phentolamine. This effect was therefore due to activation of intracerebral neurons (Mackenzie et al 1976a) mediated by beta-receptors (Edvinsson et al 1978) causing an increase in brain metabolism and secondarily an enhancement of local blood flow.

It has been claimed by Rosendorff & colleagues (1976) on the basis of intracerebral and systemic administration of amines that the effects on intracerebral vessels are mediated through beta-adrenergic receptors in the vascular wall, whereas the sympathomimetic effects on extracerebral (pial) vessels are mediated by vascular α -receptors. In our opinion both vascular beds are supplied with α as well as beta-adrenergic receptors; the effect of an exogenous amine or of noradrenaline released from perivascular sympathetic nerves represents the net effect of simultaneous α -receptor mediated constriction and beta-receptor mediated dilation in the region studied. Moreover regional variation in the sympathomimetic response may also be associated with the different degree of sympathetic perivascular innervation in the brain (Edvinsson & Owman 1977a; Sercombe et al 1975). When noradrenaline is liberated from the intracerebral neuron system or when it is administered directly into the brain (comparable to situations where the blood-brain barrier

lymphed or circumvented during systemic administration, it increases blood flow through an indirect action, i.e. a beta-receptor mediated increase in the metabolism of those cerebral neurons that are innervated by the catecholaminergic nerve endings (MacKenzie et al. 1976a and b; Edvinsson et al. 1978).

Financial support from the Swedish Medical Research Council (grant No. 04X 733), the Swedish Natural Science Research Council, and from Centre National de la Recherche.

The skilful technical assistance of Ulla-Britt Andersson and Gun Holmström is gratefully acknowledged.

REFERENCES

- ANDREAU P, SEYLAZ, J, MAMO H, SERCOMBE, R, LUFT A., PINARD E., NIELSEN K, C OWMAN CH & EDVINSSON L. 1973a. Données expérimentales sur les mécanismes de la régulation du débit sanguin cérébral. *Rev Neurol* 129 349-358.
- ANDREAU P-F, SEYLAZ, J, SERCOMBE, R & MAMO, H. 1973b. Evidence for regional differences in the effect of beta-adrenergic stimulation on cerebral blood flow. *Brain Res* 61 153-161.
- DARVILLE, H & BETZ, E. 1970. Die Regulation der isolierten kortikalen Gehirndurchblutung bei Injektion von Noradrenalin, Prostobutanol und Adrenalina. *Acta Fysiologica* 34 97-111.
- ÖRGSTRÖM, L, JOHANSSON H & SIESJÖ B. K. 1975. The relationship between arterial P_a and cerebral blood flow in hypoxic hypoxia. *Acta Physiol Scand* 93 423-432.
- EDVINSSON L, HARDEBO J, E MACKENZIE, E, T & OWMAN CH. 1978. Effect of exogenous noradrenaline on local cerebral blood flow after osmotic opening of the blood-brain barrier in the rat. *J Physiol* 284 149-156.
- EDVINSSON L & MACKENZIE, E T. 1976. Amino mechanisms in the cerebral circulation. *Pharmacol Rev* 28 275-308.
- EDVINSSON, L & OWMAN CH. 1974. Pharmacological characterization of adrenergic alpha and beta receptors mediating vasoconstrictor response of cerebral arteries *in vitro*. *Circ Res* 35 835-849.
- EDVINSSON L & OWMAN CH. 1977. Sympathetic innervation and adrenergic receptors in extracranial cerebral arterioles of baboon. *Acta Neurol Scand*, Suppl. 64 304-305.
- EDVINSSON L & OWMAN CH. 1977b. Pharmacological characterization of vasoconstrictor postsynaptic receptors in brain vessels. In: *Neurogenic control of the brain circulation* (ed. CH OWMAN and L EDVINSSON), pp. 167-183. Pergamon Press, Oxford.
- EDVINSSON, L, LARSEN N, A NILSSON L, NORBERG K, SIESJÖ B K & TORLÖF P. 1974. Regional cerebral blood flow in the rat measured by the tissue sampling technique. Critical evaluation using four indicators: C^{14} -aspirine, C^{14} -ethanol, H_2 water and Xenon¹³³. *Acta Physiol Scand* 91 1-10.
- VON ESSEN C. 1973. Effects of monoamines on cerebral blood flow in dogs. M. D. Thesis, Göteborg.
- GOTTSTEIN U. 1966. *Der Hirnkreislauf unter dem Einfluss strahlender Substanzen*. A. Huthig Verlag, Heidelberg.
- GREENFIELD J C & TINDALL, G. T. 1968. Effect of norepinephrine, epinephrine and angiotensin on blood flow in the internal carotid artery of man. *J Clin Invest* 47 1677-1684.
- HAGGENDAL, E. 1965. Effects of some vasoactive drugs on the vessels of cerebral grey matter in the dog. *Acta Physiol Scand* 66, Suppl. 258 53-79.
- HAGGENDAL, E & JOHANSSON B. 1965. Effect of arterial carbon dioxide tension and oxygen saturation on cerebral blood flow autoregulation in dogs. *Acta Physiol Scand* 66, Suppl. 258 77-83.
- HARPER, A M. 1966. Autoregulation of cerebral blood flow. Influence of arterial pressure on blood flow through the cerebral cortex. *J Neurol Neurosurg Psychiatr* 29 398-403.
- IVERSEN L. L. 1967. The uptake and storage of noradrenaline in sympathetic nerves. Cambridge University Press, Cambridge.
- KETY S S. 1951. Theory and applications of exchange of inert gas at lungs and tissues. *Pharmacol Rev* 3 1-41.
- KING B D, SOKOLOFF L & WECHSLER, R L. 1952. The effects of 1-epinephrine and 1-norepinephrine upon cerebral circulation and metabolism in man. *J Clin Invest* 31 773-779.
- KROG J. 1964. A comparative study of the effect of cervical sympathetic stimulation on cerebral blood flow. M. D. Thesis, Oslo.
- LACOMBE, P, REYNIER REBUFFEL, A M, MAMO H & SEYLAZ, J. 1977. Quantitative measurement of regional blood flow measurements during cervical sympathetic stimulation. *Brain Res* 129 129-140.
- LAUBIE, M & DROUILLAT M. 1967. Action de l'isoproterenol sur l'hémodynamique et le métabolisme cérébral du chien. *Arch Int Pharmacodyn* 170 93-98.
- MACKENZIE, E T, MCCULLOCH J, O'KEANE, M, PICKARD J D & HARPER, A M. 1976a. Cerebral circulation and norepinephrine: relevance of the blood-brain barrier. *Am J Physiol* 231 483-488.
- MACKENZIE, E T, MCCULLOCH J & HARPER, A M. 1976b. Influence of endogenous norepinephrine on cerebral blood flow and metabolism. *Am J Physiol* 231 489-494.
- MCCALDEN T A & EIDELMAN B. H. 1976. Cerebrovascular response to infused noradrenaline and its modification by catecholamine metabolism blocker. *Neurology* 26 987-991.
- MEYER, J S, LAVY S, ISHIKAWA, S & SYMON L. 1964. Effects of drugs and brain metabolism on internal carotid arterial flow. *Am J Med Electronics* 3 169-180.
- MITCHELL, G, SCRIVEN D R L & ROSEN-DORFF C. 1975. Adrenoceptors in intracerebral resistance vessels. *Br J Pharmacol* 34 11-15.

changes during the various treatments was found after this correction. No corresponding correction was made for variations in pO_2 values since it is known that as long as pO_2 is kept above 100 mmHg there is no significant influence on CBF (Borgström Johansson & Siegb 1975).

Infusion of sympathomimetic amines. In order to achieve steady state conditions continuous infusion of the agonists was utilized. Both noradrenaline and adrenaline reduced the regional flow in cerebral and cerebellar cortical structures to a varying degree and a reduction was also observed in the caudate nucleus. A similar pattern of decrease in regional CBF has been reported during cranial sympathetic nerve stimulation in rabbits (Lacombe et al 1977).

The finding on the caudate nucleus confirms results from local measurements with the thermoclearance technique in rabbits where these amines as well as sympathetic nerve stimulation clearly reduced the caudate blood flow (Sercombe et al 1975). During those experiments another brain region, the lateral geniculate body, showed little or no response. The difference in the response could be related to the degree of vascular innervation: the caudate has a density of sympathetic nerve supply which is twice as high as that found in the vascular bed of the lateral geniculate body (Sercombe et al 1975). This regional heterogeneity in the extent of sympathetic nerve supply of intracerebral arterioles has been studied in more detail in baboons (Edvinsson & Owman 1977a). It may be that this kind of variability to some extent explains the different regional flow reactions seen also in rats (see further below).

The CBF reduction obtained after administration of the catecholamines was mediated by alpha receptors in the sense that it could be prevented by previous injection of the competitive alpha antagonist phentolamine. It is notable that the reduction in CBF is a net effect including a vasodilatory component as shown by the reversal particularly of the adrenaline induced flow reduction upon administration of phentolamine. This supports previous evidence (Edvinsson & Owman 1974; Sercombe et al 1977) that direct cerebral vasodilatation is mediated by the beta subtype of receptors in the vessel wall (whereas peripheral vasodilatation is known to be mediated by beta₂-receptor). Regions which previously had not responded significantly to noradrenaline or adrenaline (i.e. thalamus

mesencephalon and pons) now showed a marked flow increase. This shows that vasoconstrictor and dilator responses to catecholamines had outbalanced each other in the absence of phentolamine. This might reflect a regional heterogeneity in the relative proportion of constrictory and dilatory adrenoceptors, perhaps related to a local variation in the degree of sympathetic innervation as discussed above. A similar large increase in flow was observed after administration of the beta-agonist isoprenaline. The effect was antagonized by the competitive beta-receptor blocking agent, propranolol.

There is reason to believe that the above-mentioned effects of the sympathomimetic amines on CBF primarily represent direct vasomotor actions in this vascular bed. Amines are known to penetrate the blood-brain barrier poorly (see Rapoport 1976), but can be made to reach into the brain by transient opening of the barrier with hypertonic solutions as shown in the rat by Edvinsson et al (1978). Under these conditions however noradrenaline increased local CBF by an effect that was not inhibited by phentolamine. This effect was therefore due to activation of intracerebral neurons (Mackenzie et al 1976a) mediated by beta-receptors (Edvinsson et al 1978) causing an increase in brain metabolism and secondarily an enhancement of local blood flow.

It has been claimed by Rovendorff & collaborators (1976) on the basis of intracerebral and systemic administration of amines that the effects on intracerebral vessels are mediated through beta-adrenergic receptors in the vascular walls, whereas the sympathomimetic effects on extracerebral (placental) vessels are mediated by vascular alpha receptors. In our opinion both vascular beds are supplied with alpha as well as beta adrenergic receptors; the effect of an exogenous amine or of noradrenaline released from perivascular sympathetic nerves represents the net effect of simultaneous alpha receptor mediated constriction and beta receptor mediated dilation in the region studied. Moreover regional variation in the sympathomimetic response may also be associated with the different degree of sympathetic perivascular innervation in the brain (Edvinsson & Owman 1977a; Sercombe et al 1975). When noradrenaline is liberated from the intracerebral neuron systems or when it is administered directly into the brain (comparable to situations where the blood-brain barrier

sympared or circumvented during systemic administration, it increases blood flow through an indirect action, via a beta-receptor mediated increase in the metabolism of those cerebral neurons that are innervated by the catecholaminergic nerve endings (Mackenzie et al. 1976a and b; Edvinsson et al. 1976).

Financial support from the Swedish Medical Research Council (grant No. 840/732), the Swedish Natural Science Research Council, and from Centre National de la Recherche Scientifique.

The skilful technical assistance of Ulla-Britt Andersson and Cecilia Eriksson is gratefully acknowledged.

REFERENCES

- BEAU P. SEYLAZ, J. MAMO H. SERCOMBE, R., LUFT A. PINARD E., NIELSEN K. C. OWMAN, CH. & EDVINSSON L. 1973a. Données expérimentales sur les mécanismes de la régulation du débit sanguin cérébral. *Rev. Neurol.* 129: 349-358.
- BEAU P.-P. SEYLAZ, J. SERCOMBE, R. & MAMO, H. 1973b. Evidences for regional differences in the effect of beta-adrenergic stimulation on cerebral blood flow. *Brain Res.* 61: 155-161.
- EXELLER, H. & BETZ, E. 1970. Die Regulation der lokalen corticalen Gehirndurchblutung bei Läsion von Noradrethalen, Histamin und Adrenalin. *Arch. Forsch.* 34: 97-111.
- EDVINSSON, L., JOHANSSON, H. & SIESJÖ, B. K. 1975. The relationship between arterial P_{O_2} and cerebral blood flow in hypoxic hypoxia. *Acta Physiol. Scand.* 93: 423-432.
- EDVINSSON, L., HARDEBO, J. E., MACKENZIE, E. T. & OWMAN, CH. 1970. Effect of exogenous noradrenaline on local cerebral blood flow after osmotic opening of the blood-brain barrier in the rat. *J. Physiol.* 214: 149-156.
- EDVINSSON, L. & MACKENZIE, E. T. 1976. Amino mechanisms in the cerebral circulation. *Pharmacol. Rev.* 21: 275-348.
- EDVINSSON, L. & OWMAN, CH. 1974. Pharmacological characterization of adrenergic α and β receptors mediating vasomotor response of cerebral arteries *in vivo*. *Circ. Res.* 35: 835-849.
- EDVINSSON, L. & OWMAN, CH. 1977. Sympathetic innervation and adrenergic receptors in intraparenchymal cerebral arterioles of baboon. *Acta Neurol. Scand. Suppl.* 64: 304-305.
- EDVINSSON, L. & OWMAN, CH. 1977b. Pharmacological characterization of exogenous postsynaptic receptors in brain vessels. In: *Neurogenic control of the brain circulation* (ed. CH. OWMAN and L. EDVINSSON), pp. 147-183. Pergamon Press, Oxford.
- ELFÖ, B., LASSEN, N. A., NILSSON, L., NORRBERG, K., SIESJÖ, B. K. & TORLÖF, P. 1974. Regional cerebral blood flow in the rat measured by the tissue sampling technique: a critical evaluation using four indicators: C^{14} antipyrine, C^{14} -ethanol, H_2 water and Xenon¹³³. *Acta Physiol. Scand.* 91: 1-10.
- VON ESSEN, C. 1973. Effects of monamines on cerebral blood flow in dogs. M.D. Thesis, Göteborg.
- GOTTSTEIN, U. 1962. Der Hirndurchlauf unter dem Einfluss inaktiver Substanzen. A. Huthig Verlag, Heidelberg.
- GREENFIELD, J. C. & TINDALL, G. T. 1968. Effect of norepinephrine, epinephrine and angiotensin on blood flow in the internal carotid artery of man. *J. Clin. Invest.* 47: 1677-1684.
- HÄGGENDAL, E. 1963. Effects of some anesthetic drugs on the level of cerebral grey matter in the dog. *Acta Physiol. Scand.* 66, Suppl. 258: 55-79.
- HÄGGENDAL, E. & JOHANSSON, B. 1965. Effect of arterial carbon dioxide tension and oxygen saturation on cerebral blood flow autoregulation in dogs. *Acta Physiol. Scand.* 66, Suppl. 258: 77-83.
- HARPER, A. M. 1966. Autoregulation of cerebral blood flow. Influence of arterial pressure on blood flow through the cerebral cortex. *J. Neurol. Neurosurg. Psychiat.* 29: 396-403.
- IVERSEN, L. L. 1967. The uptake and storage of noradrenaline in sympathetic nerves. Cambridge University Press, Cambridge.
- KETY, S. S. 1951. Theory and application of exchange of inert gas at lungs and tissues. *Pharmacol. Rev.* 3: 1-41.
- KING, B. D., SOKOLOFF, L. & WECHSLER, R. L. 1952. The effects of 1-epinephrine and 1-norepinephrine upon cerebral circulation and metabolism in man. *J. Clin. Invest.* 31: 273-279.
- KROO, J. 1964. A comparative study of the effect of cervical sympathetic stimulation on cerebral blood flow. M.D. Thesis, Oslo.
- LACOMBE, P., REYNIER-REBUFFEL, A. M., MAMO H. & SEYLAZ, J. 1977. Quantitative multi-regional blood flow measurements during cervical sympathetic stimulation. *Brain Res.* 129: 129-140.
- LAUBIE, M. & DROCILLAT, M. 1967. Action de l'isoproterenol sur l'hémodynamique et métabolisme cérébral du chien. *Arch. Int. Pharmacodyn.* 170: 93-98.
- MACKENZIE, E. T., MCCULLOCH, J., O'KEANE, M., RICHARD, J. D. & HARPER, A. M. 1976a. Cerebral circulation and norepinephrine: relevance of the blood-brain barrier. *Am. J. Physiol.* 231: 483-488.
- MACKENZIE, E. T., MCCULLOCH, J. & HARPER, A. M. 1976b. Influence of exogenous norepinephrine on cerebral blood flow and metabolism. *Am. J. Physiol.* 231: 489-494.
- MCCALDEN, T. A. & EIDELMAN, B. H. 1976. Cerebrovascular response to infused noradrenaline and its modification by catecholamine metabolism blocker. *Neurology* 26: 987-991.
- MEYER, J. S., LAVY, S., ISHIKAWA, S. & SYMON, L. 1964. Effects of drugs and brain metabolism on internal carotid arterial flow. *Am. J. Med. Electronics* 3: 169-180.
- MITCHELL, G., SCRIVEN, D. R. L. & ROSEN-DORFF, C. 1975. Adrenoceptors in intracerebral resistance vessels. *Br. J. Pharmacol.* 54: 11-15.

- OLESEN J 1977 The effect of intracarotid epinephrine, norepinephrine and angiotensin on the regional cerebral blood flow in man. *Neurology* 22: 978-987.
- OWMAN CH & EDVINSSON L 1977 Neurogenic control of the brain circulation. Wenner-Gren Center International Symposium Series. Pergamon Press, Oxford.
- OWMAN CH, EDVINSSON L & NIELSEN K C 1974 Autonomic neuroreceptor mechanisms in brain vessels. *Blood Vessels* 11: 1-31.
- RAPOPORT S I 1976. Blood-brain barrier in physiology and medicine. Raven Press, New York.
- REIVICH M, JEHLE J, SOKOLOFF L & KETY S S 1969 Measurement of regional cerebral blood flow with antipyrine- ^{14}C in awake cats. *J Appl Physiol* 27: 296-300.
- ROSENDORFF C, MITCHELL G, SCRIVEN D R L & SHAPIRO C 1976 Evidence for a dual innervation affecting local blood flow in the hypothalamus of the conscious rabbit. *Circ Res* 38: 140-145.
- SENSENBACH W, MADISON L & OCHS L 1953 A comparison of the effects of 1-norepinephrine, synthetic 1-epinephrine and USP epinephrine upon cerebral blood flow and metabolism in man. *J Clin Invest* 32: 26-32.
- SERCOMBE, R, AUBINEAU P, EDVINSSON L, MAMO H, OWMAN CH, PINARD E & SEYLAZ, J 1975 Neurogenic influence on local cerebral blood flow. Effect of catecholamines or sympathetic stimulation as correlated with the sympathetic innervation. *Neurology* 25: 944-963.
- SERCOMBE, R, AUBINEAU P, EDVINSSON L, MAMO H, OWMAN CH & SEYLAZ, J 1977 Pharmacological evidence for α_1 and α_2 adrenergic functional beta receptors in the cerebral circulation. *Pharmacol Arch* 368: 41-44.
- WAHL, M, KUSCHINSKY W, BOSSE, O, OLSEN J, LASSEN N A, INGVAR, D H, MICHAELIS J & THURAU K 1972 Effect of 1-norepinephrine on the diameter of pul arteries and arteries in the cat. *Circ Res* 31: 48-56.
- WAHL, M & KUSCHINSKY W 1977 Autonomic receptors as studied in pul vessels—microapplication in situ. In: Neurogenic control of the brain circulation (ed. CH OWMAN and L EDVINSSON), pp. 125-195. Pergamon Press, Oxford.
- XANALATOS C & JAMES I M 1972 Effect of arterial CO₂ pressure on the response of cerebral and hind-limb blood flow and metabolism to hyperventilation in the dog. *Clin Sci* 42: 63-68.

Inhibitory actions from low and high threshold cutaneous afferents on groups II and III muscle afferent pathways in the spinal cat

TORNGY JENESKOG

Department of Physiology, University of Umeå, Sweden

JENESKOG, T. Inhibitory actions from low and high threshold cutaneous afferents on groups II and III muscle afferent pathways in the spinal cat. *Acta Physiol Scand* 1979 107 297-308. Received 16 Oct 1978. ISSN 0001-6772. Department of Physiology, University of Umeå, Sweden.

The inhibitory effects caused by volley in cutaneous afferents on the transmission through some polysynaptic segmental pathways activated by high threshold muscle afferents were studied in chloralose anesthetized, spinal cats. Pathways studied were groups II and III to motoneurons as well as group II to primary afferents. The results suggested that two different mechanisms were involved. One mechanism, with a very slow time course (duration not less than 400 ms) is suggested to be an example of presynaptic inhibition between different primary afferent systems. This mechanism required high threshold ($\approx 1.6T$) conditioning shocks, and appeared simultaneously with the component II dorsal root potential being evoked by the cutaneous afferent volley. The other mechanism, with a faster time course (duration always below 300 ms), was dependent upon low threshold ($\approx 1.5T$) cutaneous conditioning volleys. This inhibitory interaction could not be ascribed to the same presynaptic mechanism, but is suggested to be an example of postsynaptic inhibition at an interneuronal level. The presumed disynaptic excitatory pathway from group II muscle afferents to flexor motoneurons was not inhibited by cutaneous conditioning shocks, but could on the contrary be facilitated by activity in low threshold cutaneous afferents, probably at the only interneurone involved in this group II pathway.

Key words: Cutaneous afferents, reflex path transmission, presynaptic inhibition, postsynaptic inhibition, spinal cat.

Inhibition of transmission through segmental polysynaptic reflex pathway to alpha-motoneurons and to primary afferent terminals may be achieved in several ways. Four main types may be considered: inhibitory interaction between afferents, such can be postsynaptic or presynaptic, and inhibition by descending systems, which can be postsynaptic or presynaptic (see Eccles 1964, Lundberg 1966, 1969, 1973, Schmidt 1973 for reviews). There is also the possibility of spatial facilitation between descending and segmental systems for postsynaptic interaction (Lundberg 1975) as well as for presynaptic interaction (e.g. Carpenter et al. 1963b, Hongo et al. 1972). One particular descending path, the dorsal root system, which gives longlasting postsynaptic inhibition to first order interneurons in a

number of polysynaptic pathways (to alpha-motoneurons to primary afferent terminals and to certain ascending systems) has been particularly well analyzed (Engberg et al. 1968a, b). This descending system was recently identified as the rubro-bulbospondinal path (RBSP) by Jeneskog & Johansson (1977). These authors found furthermore that low intensity stimulation of distal cutaneous nerves also inhibited the segmental reflex transmission in a very similar way and it was even suggested that the RBSP and the distal, low threshold cutaneous afferents may act through a common group of interneurons which postsynaptically inhibit interneurons in the segmental polysynaptic reflex pathways.

The inhibition from cutaneous afferents of polysynaptic reflex pathways has now been further

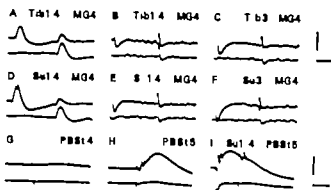


Fig. 1 A-F Low and high threshold cutaneous inhibition of Group II EPSP in a PBSt motoneurone. Each pair of traces (4 averaged) show test EPSP alone (lower) and conditioned EPSP (upper). (A) Low threshold conditioning stimulation of Tib nerve. 50 ms interval. (B) Same as A but 260 ms interval. (C) High threshold conditioning stimulation of Tib nerve. 760 ms interval. (D-F) Same as A-C but conditioning stimulations to Su nerve. (G-I) Low threshold cutaneous inhibition of Group II DRP evoked by stimulation of PBSt nerve. Each pair of traces (8 averaged) show DRP in an S1 filament (upper) and incoming volley in L7 (lower). (G-H) Stimulation of PBSt nerve at 4T and 5T respectively. (I) Suppression of Group II DRP by preceding stimulation of low threshold afferents in Su nerve. 30 ms interval. Calibrations at C horizontal bar 20 ms to A and D 100 ms to B-C and E-F vertical bar (positivity upwards) 4 mV to A-F. Calibrations at I horizontal bar 20 ms to G-I vertical bar (negativity upwards only for upper traces) 0.4 mV.

investigated. The results suggest that a pathway from low threshold cutaneous afferents may inhibit polysynaptic segmental reflex pathways from muscle afferents (groups II and III) to alpha-motoneurons and to primary afferent terminals. It is suggested that this inhibition is exerted at an interneuronal level but there are also results suggesting inhibition by a presynaptic mechanism in agreement with earlier studies (Eccles et al. 1962b). This mechanism works however only when also high threshold cutaneous afferents are activated by the conditioning volley.

METHODS

The results to be described were collected from 10 cat weighing 4-4.0 kg. The initial procedures and the care of the animals during the experiments were similar to those described previously (Jeneskog & Johanson 1977). During recording the animals were paralyzed with Flaxedil (Pharma Rhodia) and artificially ventilated.

Operation. Two laminectomies were performed exposing the lower thoracic cord (Th1-Th13) where the dura was opened and the spinal cord transected, the other exposing the lumbar enlargement. In some experiments thin dorsal rootlets from caudal L6 and/or rostral S1 were

dissected for about 15 mm and cut distally for later recording of dorsal root potentials.

Some or all of the following nerves in the left half were dissected and cut peripherally (abbreviations: *ad.* = parenthetical; *an.* = anterior; *b.* = biceps; *br.* = brachioradialis; *ABSn.* = posterior biceps and semitendinosus (PBSt); *g.* = gastrocnemius; *so.* = soleus; *GS.* = nerve to pretibial flexor (DP); *su.* = sural; *Su.* = cutaneous division of superficial peroneal (SP); and *tib.* = tibial after giving off branches to flexor digitorum and hallucis longus, tibialis posterior and popliteus (Tib). In a few experiments the nerves to the medial head of gastrocnemius (MG) and to soleus (Sol) were used separately while the one to the lateral head was omitted.

Recording. The incoming volleys evoked by stimulation of peripheral nerves were recorded at the dorsal root entry zone usually in L7. Intracellular recordings from motoneurons (mostly PBSt and triceps) are made with glass capillary micro-electrodes (tip size 10 μ m, impedance 2.5-6 M Ω m) filled with 4 M potassium citrate. Motoneurons were identified by their antiodromic invasion from the muscle nerves. Dorsal root potentials are recorded with bipolar electrodes, one of the poles close to the cord and the other at the cut end of the filament (inter-electrode distance about 15 mm).

All signals were amplified (filtered LF filter 1 Hz for intracellular and dorsal root recordings, 1 Hz for dorsal root filament recordings) and displayed on a storage oscilloscope for visual inspection and simultaneously stored on a FM tape recorder (Sabre VI, Sangamo) for later processing. The time course of long duration dorsal root potentials (DRPs) was distorted by the 1 Hz LF filter used, and appear shorter than they really were. For example as tested separately with DC recordings, a DRP with a duration of the negative wave of about 100 ms (1 Hz filter) corresponds to a real duration of some 200-50 ms (DC), and a duration of the negative wave of 1.5-1.50 ms (1 Hz filter) corresponds to a real duration of about 500 ms. We recorded a DC mode. Signals were usually computer averaged and then photographed from the oscilloscope screen.

Stimulation. Peripheral nerves were stimulated with bipolar hook electrodes. The stimuli shocks were 0.1 ms square wave pulses. The strength of stimulation is given in multiples of the threshold (T) for the most excitable fibres in the nerves, as determined from the incoming volleys at the appropriate dorsal root entry zone. All conditioning test series were performed with a low repetition frequency, usually around 1 Hz, with long conditioning-test interval down to 0.5 Hz.

Abbreviations. DRP dorsal root potential; EPSP excitatory postsynaptic potential; FRA flexor reflex afferent (cf. Eccles & Lundberg 1959); IPSP inhibitory postsynaptic potential; PSP postsynaptic potential; RBSF rubro-bulbo-spinal path (cf. Jeneskog & Johanson 1977).

RESULTS

1. Cutaneous inhibition action on Group II muscle afferent pathways

The interaction between cutaneous afferent and Group II muscle afferent path to motoneurons

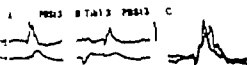


Fig. 1A-C. Low threshold cutaneous inhibition of Group II-EPSPs in GS motoneurons. Each record consists of 8 averaged sweeps, as A-B EPSPs in upper traces and incoming volley in lower traces. (A) Group II-EPSP elicited by ST stimulation of PBSt nerve. (B) Same as A, but EPSP preceded by low threshold stimulation of Su nerve, 35 ms interval. (C) Central parts of A and B superimposed and enlarged to show suppression of late EPSP components (stippled area). Calibrations in B, horizontal bar 20 ms to A-B, vertical bar (positivity upwards, in upper traces) 3 mV to A-B.

to primary afferent terminals was studied in conditioning-test experiments, using the PSPs and EPSPs elicited by single shock stimulation of muscle nerves as tests. The results that emerged were both complex and suggested that several channels were involved in the interaction.

Fig. 1A-F is from a PBSt motoneurone and shows that a Group II-EPSP from the MG nerve appearing at around 2.5T latency from end of compound incoming volley (3.6 ms) was suppressed by compound incoming volley in low threshold afferent in the mixed Tib nerve (A) or in the sensory cutaneous Su nerve (D). At longer intervals, illustrated in B and E with 260 ms, there was no effect of low threshold inhibition of this Group II-EPSP. However when the strength of the conditioning stimulation was raised to 3T the suppressive effect re-appeared (C and F). The low threshold cutaneous suppressive effect did not seem to be a nonspecific one, e.g. due to conductance changes in the motoneurone membrane, since in other cells, in the motoneurone, EPSPs evoked from muscle afferents was suppressed by a preceding low threshold volley in cutaneous afferents even though this volley gave no appreciable PSP itself in the motoneurone under study as illustrated in Fig. 1A-C for a GS motoneurone. As detailed in Fig. 2C (stippled area), only the late PSP components were suppressed (see further Results section III). Hence the inhibitory effect on muscle afferent Group II-PSPs evoked by activity in low threshold cutaneous afferents is considered to affect the reflex path transmission rather than to be an effect on the motoneurons themselves.

A similar low threshold cutaneous suppression of

transmission to primary afferent terminals is illustrated in Fig. 1G-I. In this case a supramaximal Group I stimulation (4T) of the PBSt nerve did not evoke any appreciable DRP in the ST filament recorded from (G) but when the strength was raised to 5T (H) a considerable DRP developed. This Group II-DRP was heavily suppressed by a preceding conditioning volley in low threshold afferents of the Su nerve (I). Parallel to the recordings in Fig. 1C-I a MG motoneurone was investigated (not illustrated). In this cell a Group II EPSP appeared at slightly above 4T stimulation of the PBSt nerve and further increased on raising the strength from 4T to 5T. This EPSP was likewise suppressed by a conditioning volley in the Su nerve (1 4T 30 ms interval).

The time course of low and high threshold cutaneous inhibitory actions on a Group II-EPSP is shown in greater detail in Fig. 3 for a Sol motoneurone. A and B show specimen records with different conditioning-test intervals of unconditioned Group II-EPSPs from the DP nerve (threshold for the EPSP in this cell was about 2.5T) in the lower traces and conditioned Group II-EPSPs in the upper traces. The full test series is illustrated in the diagram of Fig. 3C and demonstrates that with low threshold conditioning stimulation (SP 1 4T) the suppressive effect was maximal around 30 ms interval and then gradually faded off at 200-300 ms. With stronger conditioning stimulation (SP 3T) the suppression was more effective at all intervals where SP 1 4T also had an effect, but the inhibition was now longer lasting. A similar effect on the DRP simultaneously recorded in a caudal L6 dorsal root filament (most likely Group II-evoked since it appeared with single shock stimulation only well above 2T) is shown in Fig. 4. For the transmission to primary afferent terminals as well the high threshold conditioning stimulation (SP 3T) had a suppressive effect that was greater than and also outlasted the one obtained with the low threshold conditioning stimulation (SP 1 4T).

The more efficient and longer lasting inhibitory effect of high threshold conditioning stimulation was most probably not only a quantitative difference as indicated by the results presented in Fig. 5 with data from the same cell and from the same dorsal root filament as in Figs 3 and 4. In the diagram of Fig. 5 the transmission through the Group II pathways to the motoneurone (circles) and to the primary afferent terminals (triangles) has

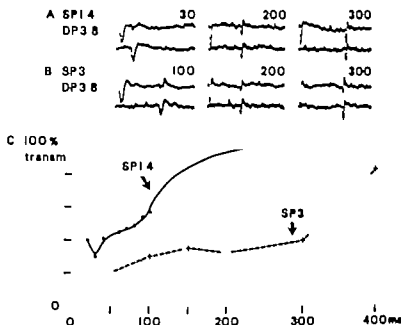


Fig. 3. Time course of inhibition of Group II IPSP in a Sol motoneurone by low and high threshold conditioning stimulation of SP nerve. (A) Specimen records (4 averaged) of unconditioned IPSPs (lower) and conditioned IPSPs (upper) at indicated conditioning-test intervals (ms) with low threshold cutaneous stimulation. (B) Same as A but with high threshold cutaneous stimulation. (C) Time course of suppression of transmission through Group II pathway to motoneurone. Abscissa is interval between arrival of conditioning and test volleys at the spinal cord. Ordinate is transmission in percent of unconditioned value. Filled circles and full line SP 1.4T; crosses and interrupted line SP 3T. Positivity upwards in PSP traces.

been plotted against the strength of the conditioning stimulation of the SP nerve. Two intervals were chosen: one short (30 ms; filled symbols) where low threshold conditioning was effective, and one long (300 ms; open symbols) where low threshold conditioning was no longer effective (cf. Jenesko & Johansson 1977 and Figs 1-3-4). As seen from the diagram, the transmission of Group II effects was suppressed already at 1.1T conditioning stimulation of the SP nerve at the short interval, and the suppression was more efficient at 1.7-1.4T. At 300 ms interval, on the other hand, there was no inhibitory effect by the conditioning cutaneous volley until the strength of stimulation was raised to 1.6-1.8T. Then the effectiveness of the conditioning stimulation grew with increased strength at least up to 3T, the strongest conditioning stimulation used.

These data should be correlated with those of Fig. 6, where some features of the dorsal root potentials evoked by these same conditioning SP volleys themselves are shown. Specimen records of the DRPs evoked in a rostral SI dorsal root filament at different stimulation strengths are shown in A. In B is illustrated the DRPs at 1.6T and 1.4T stimu-

lation, and in the lowermost trace the difference between the two, indicating that a new late component had appeared (component II DRP of Carpenter et al. 1963a). This component II had a latency of 15-20 ms from the incoming volley, in contrast to the component I DRP, which had a segmental latency of only 2-5 ms and a threshold of less than 1.1T. In the diagram of Fig. 6C the two curves show the amplitudes of the DRPs plotted against the stimulation strength. Two intervals from the arrival of the incoming volley were chosen: Firstly 15 ms, i.e. when the component II DRP (at higher strengths) had not yet started, and secondly 35 ms, i.e. approximately at the maximal amplitude of the component II DRP. As seen in the diagram, there was no appreciable difference in amplitude between the curves at stimulation strengths up to 1.4T. However, from 1.6T and upwards, the amplitude of the DRP at 35 ms interval suddenly was consistently greater than that at 15 ms interval, thus indicating the presence at those strengths of the component II DRP.

The appearance of the component II DRP at 1.6T stimulation correlates well with the appearance of

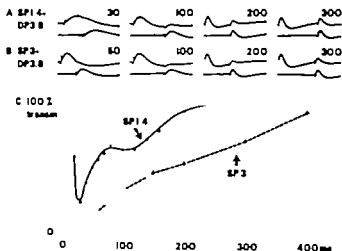


Fig. 4 Time course of inhibition of Group II-DRP in caudal L6 dorsal root filament by low and high threshold conditioning stimulation of SP nerve. (A) Specimen records (4 averaged) of unconditioned DRPs (lower) and conditioned DRPs (upper) at indicated conditioning-test intervals (ms) with low threshold cutaneous stimulation. (B) Same as A, but with high threshold cutaneous stimulation. (C) Time course of suppression of transmission through Group II pathway to primary afferent terminals. Abscissa is interval between arrival of conditioning and test volley at the spinal cord. Ordinate is transmission as percent of unconditioned value. Filled circles and full line SP 1.4 T; crosses and interrupted line SP 3 T. Negativity upwards in DRP traces.

the high threshold cutaneous inhibition of transmission through muscle afferent pathways at long intervals, as described in Fig. 5. These results indicate that more than one mechanism of inhibitory interaction between cutaneous afferent and muscle afferent pathways may be involved.

The inhibitory interaction patterns produced in other cases by conditioning stimulations applied to low and/or high threshold afferents in the Su or Tib nerves on Group II-evoked EPSPs, IPSPs or DRPs were similar to those presented in Figs 3 and 4.

It should be stressed that the inhibitory interaction described was effective irrespective of whether or not the cutaneous conditioning volley evoked a PSP by itself in the motoneurons investigated, cf. Fig. 2. The low threshold cutaneous inhibition of Group II-PSPs was studied in 23 tests in 14 flexor and extensor motoneurons. The latencies of those Group II-PSPs were 3.2–5.5 ms, as measured in seven cells from the end of the Group I incoming volley to the start of the PSP. 4 of these 14 cells in addition showed Group II-PSPs with a shorter latency. Such PSPs were, however, not inhibited by cutaneous conditioning stimulation at the conditioning test intervals tested (see section III). The term

low threshold cutaneous stimulation as used here was 1–1.5 T for either nerve, except in one single case where the Su nerve was stimulated with 1.6 T. This stimulation did not, however, evoke a component II-DRP in the caudal L6 dorsal root filament recorded from.

II Cutaneous inhibitory action on a Group III muscle afferent pathway

Group III PSPs (appearing around 10 T stimulation, or above cf. Eccles & Lundberg, 1959) were also inhibited by conditioning stimulation of cutaneous afferents with a time course similar to the one for Group II PSPs. Low threshold (up to 1.5 T) cutaneous shocks were effective as conditioning stimuli in 13 tests in 10 flexor and extensor motoneurons. In two of these cells the conditioning cutaneous volley did not evoke a PSP by itself with the strength of stimulation effective for suppression of transmission through the Group III pathway in accordance with the observations for the Group II pathways. Examples of inhibition of Group III PSPs are shown in Fig. 7. The test Group III IPSP (22 T) in a GS motoneuron (A) was suppressed by a preceding (35 ms) volley in low threshold afferents of the

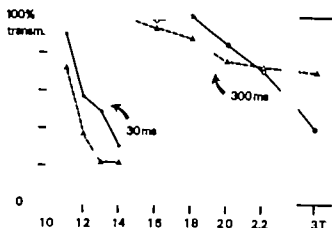


Fig. 5. Transmission through Group II muscle afferent (DP 3.8T) pathways to a Sol motoneurone (circles and full lines) and to primary afferent terminals recorded as the DRP in a caudal L6 dorsal root filament (triangles and interrupted lines) plotted against the strength of conditioning cutaneous stimulation (SP nerve). Intervals between arrival of conditioning and test volleys at the spinal cord were 30 ms (filled symbols) and 300 ms (open symbols). Note that the abscissa is broken.

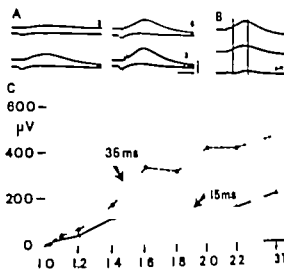


Fig. 6. Amplitudes of rostral S1 dorsal root potentials evoked by graded stimulation of SP nerve. (A) Superimposed records (4 averaged) of DRPs evoked by stimulation of S1 nerve at indicated strengths (times T) in upper traces. Incoming volleys at the L7 dorsal root entry zone in lower traces. (B) Uppermost and middle traces DRPs by SP 1.61 and 1.4T stimulation, respectively. Lowermost trace: the computed difference between the two. Observe the long latency for appearance of the high threshold component. Vertical lines indicate 15 ms and 35 ms interval from arrival of incoming volleys, respectively. (C) Amplitude of DRP at two different intervals from arrival of incoming volley at the spinal cord plotted against the strength of SP stimulation. Note that the abscissa is broken. Filled triangles and full line: 15 ms; filled circles and interrupted line: 35 ms. Calibrations in lower right A: horizontal bar 70 ms; to A-B: vertical bar (negativity upwards, only for DRPs) 0.5 mV; to A-B.

Tib nerve (B). Fig. 7C-D are from a MG motoneurone and show that the Group III IPSP (30T late component) was inhibited by a preceding (30 ms) volley in low threshold afferents also of the purely cutaneous Su nerve.

In other cases (23 tests in 14 flexor and extensor motoneurons) a low threshold cutaneous conditioning stimulation (below 1.7T) did not affect the transmission through the Group III pathway to motoneurons. Only when the strength of the conditioning stimulation was raised to or above 1.8T a suppressive effect could be demonstrated as exemplified in Fig. 7E-H from another GS motoneurone. The Group III IPSP evoked by a 50T ABSm volley (late component) was uninfluenced by a preceding (30 ms) conditioning Su volley with strengths up to 1.8T (not illustrated). However, when the strength of the Su volley was raised to 2.0T the suppressive effect appeared as seen in some of the superimposed sweeps of Fig. 7F. With stronger conditioning shocks (G-H) the inhibition of the Group III IPSP became more efficient. The results described indicate that with inhibition of transmission through Group III muscle afferent pathways too more than one mechanism is involved.

In cells where long latency Group II as well as Group III PSPs were evoked by the test stimulation a low threshold cutaneous conditioning stimu-

lation (up to 1.5T) either affected both muscle afferent PSP-components or none of them. Likewise, when the conditioning stimulation was in the high threshold range (at or above 1.8T for either cutaneous nerve used) the muscle afferent PSP components were either suppressed together or occasionally neither of them was influenced. There was thus a parallelism in the sense that no matter the low or the high threshold cutaneous pathway was operating, long latency Group II and Group III muscle afferent pathways were affected together.

III. Further interactions between cutaneous and muscle afferent pathways to motoneurons

As described above (section I) only Group II PSPs with rather long latencies (3.2–5.5 ms) were suppressed by conditioning volleys in low and/or high threshold cutaneous afferents. In addition there

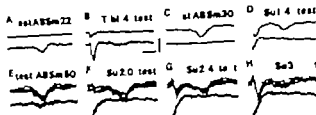


Fig. 7. Low and high threshold cutaneous inhibition of Group III-PSPs in motoneurons. (A–B) GS motoneuron with test IPSP from ABScn, and suppression of test IPSP by preceding (33 ms) volley in low threshold afferents of the Tib nerve (C–D) MG motoneuron with test IPSP from ABScn, and suppression of test IPSP by preceding (30 ms) volley in low threshold afferents of the Su nerve (E–H) GS motoneuron with test IPSP from ABScn, and suppression of test IPSP by preceding (30 ms) volley in high threshold afferents of the Su nerve. Observe lateral effect in F. Averaged (B) superimposed traces at E–H. PSPs in lower traces of A–B in upper traces of C–H. Other traces are recording volleys at L7 dorsal root entry zone. Calibration: B horizontal bar 20 ms. A–H vertical bar (positivity upwards, only for PSPs) 4 mV to A–B and E–H. 2 mV to C–D.

were in some ($n=9$) motoneurons also shorter latency EPSPs (latencies 2.0–3.1 ms, as measured in time from the end of the Group I conditioning volley to the start of the EPSP), which were not suppressed by cutaneous conditioning volleys in the range of intervals tested.

The short and long latency Group II PSPs could be evoked in the same cell as shown for a PBSt motoneuron in Fig. 8A–F. The EPSP appeared at a strength slightly above 2T stimulation of the GS nerve, and was of considerable size at 5T (A). The short latency component (2.0 ms) had the lowest threshold, but the long latency component (5.2 ms) was also evident at 5T. This component grew with stronger shocks to the GS nerve and was as pronounced with 6–7T (not illustrated) as with 10T stimulation (B) while the short latency component was probably maximal already at 5T (B) compared to A). Hence the second component is considered also as a Group II muscle afferent EPSP. In this cell the long latency Group II EPSP was unaffected by the conditioning low threshold shocks to the cutaneous nerves tested (C–E). However the short latency Group II-EPSP was instead facilitated by the same conditioning shocks, whether (C) or not (D, E) these evoked PSPs by themselves in the motoneuron. If the conditioning-test sequence was reversed, as in Fig. 8F the cutaneous low threshold EPSP (lower trace) was facilitated (upper trace) by a conditioning volley in Group II (5T) afferents of the GS nerve. Such results further indicate that short and long latency Group II muscle

afferent PSPs are evoked through different inter-neuronal pathways.

All the three PSP components dealt with in the present investigation could occasionally be demonstrated in the same cell, as illustrated in Fig. 8G–H from another PBSt motoneuron. With 10T stimulation of the homonymous PBSt nerve, the cell showed (G) the antidromic spike, the short latency Group II-EPSP (at first arrow: 3.0 ms), the long latency Group II-EPSP (at second arrow: 4.1 ms) and the Group III-EPSP (at third arrow). The two Group II-PSPs both had a threshold around 2.5T. Below this strength only the antidromic spike was elicited. The third component did not appear until the strength was raised to 8–10T and was thus considered as a Group III-EPSP. This last component (but not the two first ones) was also even more pronounced with 15T stimulation. When, as in Fig. 8H (upper trace) the 10T PBSt shock was preceded (30 ms) by a low threshold volley in the Tib nerve, the long latency Group II and the Group III EPSPs were suppressed simultaneously but the conditioning shock left the short latency Group II EPSP unaffected (compare Fig. 8H lower trace). It was even occasionally observed in other cells that, when both Group II PSP components were evoked by the test volley, the long latency PSP was suppressed, while the short latency PSP was instead simultaneously facilitated.

Fig. 8I–K are from a MG motoneuron with a test Group II-EPSP evoked by stimulation of the PBSt nerve. When this test EPSP was preceded (30

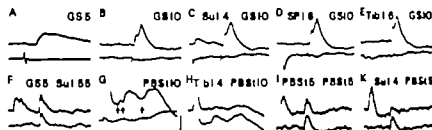


Fig. 8. Further interactions between cutaneous and muscle afferent pathways to motoneurons. (A-F) Spatial facilitation between low threshold cutaneous afferent and short latency Group II muscle afferent path to a PBSt motoneuron. (A, B) Group II EPSPs (see text) evoked by stimulation of GS nerve. (C-E) Facilitation of short latency component of Group II EPSP by preceding (35 ms) volleys in low threshold afferents of Su, SP and Tib nerves, respectively. (F) Reversed sequence: lower trace test EPSP by stimulation of Su nerve (1.55T), upper trace test EPSP conditioned by preceding (30 ms) volley in Group II afferents of the GS nerve. (G-H) From a PBSt motoneuron. (G) Antinociceptive spike and PSPs evoked by stimulation of PBSt nerve at 10T. Observe 3 components marked by arrows. (H) Lower trace, same as G, but lower amplification; upper trace, same PSPs conditioned by preceding (30 ms) volley in Tib nerve at 1.4T. Note that only second and third components are suppressed. (I-K) From a MG motoneuron. Lower traces show test Group II EPSPs by PBSt 5T stimulation. Upper trace in (I) shows absence of interaction by preceding (30 ms) volley in the same afferents. Upper trace in (K) shows low threshold cutaneous suppression of test Group II EPSP. Lower traces in A, E and G are incoming volleys at the L7 dorsal root entry zone. Other traces are PSPs. All traces are averaged sweeps. 4 in A, F, I and K, 8 in B-E and G-H. Calibrations in G: horizontal bar 4 ms to A, G-H; 70 ms to B-F and I-K. Vertical bar (positivity upward) only for PSPs) 4 mV to A-G, I-K; 8 mV to H.

ms) by a conditioning volley in the Su nerve (1.4T) there was the usual suppressive effect (k), but when the conditioning volley was in the same afferents as the test volley (l) there was no interaction at the same interval. Such results were observed for a number of tests in different cells and indicate that the inhibition of transmission through the long latency Group II pathway (and also the Group III pathway) by low threshold cutaneous conditioning volleys did not depend upon a mechanism of post excitatory depression through the test pathway to the motoneuron, which might have been the case if these low threshold cutaneous afferents somewhere shared interneurons with the test muscle afferent pathways.

DISCUSSION

The primary aim of the present investigation was to gain further insight into the mechanisms responsible for the suppression of transmission through Groups II and III muscle afferent segmental pathways by activity in cutaneous afferents which was described by Jenesko & Johansson (1977). Similar interactions between cutaneous and muscle afferent pathways to motoneurons were early studied by Kuno & Perl (1960). They showed a suppression of

Groups II and III effects on the excitability in motor nuclei by "near maximal sural volley (for myelinated fibres)" (Kuno & Perl 1960, p. 11) and thus it is not possible to decide whether the effective afferents were low or high threshold ones, as these terms are used here. Later Eccles et al. (1962b) studied inhibitory interactions between cutaneous and muscle afferent pathways in a number of test situations. They found, i.e., that the reflex discharge in flexor muscle nerves, as well as the dorsal root potentials evoked by the same type of test volleys were inhibited following single conditioning volleys in cutaneous afferents. The standard stimulation strength they used for cutaneous shocks was 4T (cf. Eccles et al. 1962a) thus again including both low and high threshold afferents. They concluded that the inhibitory interaction was due to a presynaptic mechanism working between different FRA systems (flexor reflex afferents; Eccles & Lundberg 1959) at the segmental level of the spinal cord. They also suggested (Eccles et al. 1962b, p. 77) that the interaction described by Kuno & Perl (1960) was another example of presynaptic inhibition within the FRA systems, challenging the original interpretation. Contralateral cutaneous volleys have also been shown to inhibit the transmission in

spinal FIA pathways (Eccles et al. 1964) by a presumed presynaptic mechanism. These authors also used strong conditioning shocks, but an appreciable part of the inhibition was produced by rather low threshold afferents (up to 1.7–1.8 T; Eccles et al. 1964, their Fig. 5). Some evidence also exists to the effect that identified Group II muscle afferents are recipients of presynaptic inhibition from cutaneous afferents (Eccles et al. 1963). Unilaterally only strong (4T) stimulation of cutaneous nerves was used to produce the primary afferent depolarization in Group II muscle afferents too.

Taken together the inhibition of transmission in high threshold cutaneous and muscle afferent (FIA) pathways to motoneurons and to primary afferent terminals has been attributed in whole or in part (Schmidt 1973) to a presynaptic mechanism.

The present experiments were performed on some spinal cats, in order to exclude possible long spinal or supraspinal reflex loops (e.g. Shumatsura et al. 1976). As low threshold cutaneous afferents only with distal receptive fields are effective in suppressing the transmission through high threshold muscle afferent pathways (Jensberg & Johansson 1977), the spinal, the cutaneous part of the superficial peroneal and the tibial nerves were used for conditioning stimulation. Concerning the tibial nerve, which also contains joint and muscle afferents, cutaneous afferents were assumed to be responsible for the suppressive effects, because the threshold range and the time course of effects were the same as for conditioning with afferents in the purely cutaneous nerves. Furthermore, the effects by tibial nerve stimulation appeared in parallel to the cutaneous cord dorsum potential as recorded by the surface electrode at the dorsal root entry zone. A contribution to the inhibitory effects from tibial nerve stimulation by Renshaw cell activation elicited via antidromic stimulation of motor axons seems unlikely since a recent anatomical investigation has shown that tibial motoneurons do not give off presumed collaterals at all (Cullheim & Kellerth 1977). Finally similar suppressive effects have been obtained with electrical stimulation within the spinal cord (Jensberg & Johansson 1977), clearly suggesting that cutaneous afferents in the tibial nerve may produce this kind of inhibitory interaction.

The latencies presented for Group II-PSPs were measured from the end of the Group I incoming volley at the dorsal root entry zone to the foot of the

PSP and are thus not true "central latencies". They were, however, only used to differentiate between Group II PSPs which were suppressed by cutaneous conditioning stimulation ("long latency"—presumed polysynaptic) and those which were not suppressed, but might instead be facilitated ("short latency"—presumed disynaptic for EPSPs).

The present investigation demonstrated that the inhibitory interaction between cutaneous and Groups II and III muscle afferent pathways seems to involve more than one mechanism. As far as the transmission to motoneurons is concerned, the inhibitory interactions were evident whether or not the cutaneous volley evoked a PSP by itself in the motoneurone under study. Hence it is unlikely that the suppressive effects were dependent upon action on the motoneurone membrane. It is concluded that the inhibitory actions were exerted at stages in the reflex path prior to the motoneurone itself. This conclusion is supported by the fact that the short latency excitatory Group II pathway to flexor and extensor motoneurons was never observed to be suppressed by the cutaneous conditioning volleys. Furthermore, excitatory and inhibitory polysynaptic pathways to motoneurons were similarly affected, and an involvement of Renshaw cells is thus considered unlikely, as they seem to influence only the transmission through pathways involving the reciprocal Ia inhibitory interneurons (Hallborn et al. 1971).

The transmission through high threshold muscle afferent polysynaptic pathways was suppressed by one path activated from low threshold cutaneous afferents. Pathways affected were Group II polysynaptic to alpha-motoneurons and to primary afferent terminals as well as Group III paths to alpha-motoneurons. The inhibitory effect was produced by cutaneous afferents also in the very low threshold (<1 T) range. It was not possible to determine the highest threshold cutaneous afferents involved, because with conditioning shocks of 1.6–1.8 T or greater another inhibitory path was also put into action. This high threshold cutaneous path also affected all reflex paths studied, but its characteristics were different, e.g. the time course of its action was slower than that of the low threshold path.

For a number of reasons it is suggested that the difference in time course of the inhibition of transmission through the polysynaptic muscle afferent pathways by low and high threshold cutaneous afferents is not merely due to a quantitative differ-

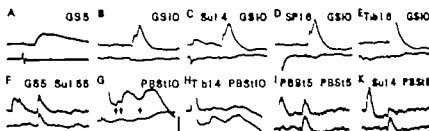


Fig. 8 Further interactions between cutaneous and muscle afferent pathways to motoneurons. (A–F) Spatial facilitation between low threshold cutaneous afferents and short latency Group II muscle afferent path to a PBSt motoneurone. (A–B) Group II EPSPs (see text) evoked by stimulation of GS nerve. (C–E) Facilitation of short latency component of Group II EPSP by preceding (35 ms) volleys in low threshold afferents of Su, SP and Tib nerves respectively. (F) Reversed sequence: lower trace test EPSP by stimulation of Su nerve (1.55T), upper trace test EPSP conditioned by preceding (30 ms) volley in Group II afferents of the GS nerve. (G–H) From a PBSt motoneurone. (G) Antadromic spike and PSPs evoked by stimulation of PBSt nerve at 10T. Observe 3 components marked by arrows. (H) Lower trace same as G but lower amplification; upper trace same PSPs conditioned by preceding (30 ms) volley in Tib nerve at 1.4T. Note that only second and third components are suppressed. (I–K) From a MG motoneurone. Lower traces show test Group II-EPSPs by PBSt 5T stimulation. Upper trace in (I) shows absence of interaction by preceding (30 ms) volley in the same afferents. Upper trace in (K) shows low threshold cutaneous suppression of test Group II EPSP. Lower traces in A–E and G are incoming volleys at the L7 dorsal root entry zone. Other traces are PSPs. All traces are averaged sweeps. 4 mV A–F, I and K, 8 mV B–E and G–H. Calibrations in G: horizontal bar 4 ms to A–G, 10 ms to B–F and I–K. Vertical bar (positivity upwards) only for PSPs 4 mV to A–G, 1–K, 8 mV to H.

ms) by a conditioning volley in the Su nerve (1.4T) there was the usual suppressive effect (K) but when the conditioning volley was in the same afferents as the test volley (I) there was no interaction at the same interval. Such results were observed for a number of tests in different cells and indicate that the inhibition of transmission through the long latency Group II pathway (and also the Group III pathway) by low threshold cutaneous conditioning volleys did not depend upon a mechanism of post excitatory depression through the test pathway to the motoneurone which might have been the case if these low threshold cutaneous afferents somewhere shared interneurons with the test muscle afferent pathways.

DISCUSSION

The primary aim of the present investigation was to gain further insight into the mechanisms responsible for the suppression of transmission through Groups II and III muscle afferent segmental pathways by activity in cutaneous afferents which was described by Jeneskog & Johansson (1977). Similar interactions between cutaneous and muscle afferent pathways to motoneurons were early studied by Kuno & Perl (1960). They showed a suppression of

Groups II and III effects on the excitability in motor nuclei by near maximal sural volley (for myelinated fibres) (Kuno & Perl 1960 p. 117) and thus it is not possible to decide whether the effective afferents were low or high threshold ones, as these terms are used here. Later Eccles et al. (1962b) studied inhibitory interactions between cutaneous and muscle afferent pathways in a number of test situations. They found (a) that the reflex discharge in flexor muscle nerves, as well as the dorsal root potentials evoked by the same type of test volleys were inhibited following single conditioning volleys in cutaneous afferents. The standard stimulation strength they used for cutaneous shocks was 4T (cf Eccles et al. 1962a) thus again including both low and high threshold afferents. They concluded that the inhibitory interaction was due to a presynaptic mechanism working between different FRA systems (flexor reflex afferent; Eccles & Lundberg 1959) at the segmental level of the spinal cord. They also suggested (Eccles et al. 1962b p. 777) that the interaction described by Kuno & Perl (1960) was another example of presynaptic inhibition within the FRA systems, challenging the original interpretation. Contralateral cutaneous volleys have also been shown to inhibit the transmission in

paternal FRA pathways (Eccles et al. 1964), by a presynaptic mechanism. These authors also used strong conditioning shocks, but an appreciable part of the inhibition was produced by other low threshold afferents (up to 1.7–1.8T; Eccles et al. 1964, their Fig. 5). Some evidence also exists to the effect that identified Group II muscle afferents are recipients of presynaptic inhibition from cutaneous afferents (Eccles et al. 1963). Unfortunately only strong (4T) stimulation of cutaneous nerves as used to produce the primary afferent depolarization in Group II muscle afferents too.

Taken together the inhibition of transmission in high threshold cutaneous and muscle afferent (FRA) pathways to motoneurons and to primary afferent terminals has been attributed in whole or in part (Schmidt 1973) to a presynaptic mechanism.

The present experiments were performed on some special cats, in order to exclude possible long spinal or supraspinal reflex loops (e.g. Shimamura et al. 1976). As low threshold cutaneous afferents only with distal receptive fields are effective in suppressing the transmission through high threshold muscle afferent pathways (Jenkinson & Johansson 1977), the spinal, the cutaneous part of the superficial peroneal and the tibial nerves were used for conditioning stimulation. Concerning the tibial nerve, which also contains joint and muscle afferents, cutaneous afferents were assumed to be responsible for the suppressive effects because the threshold range and the time course of effects were the same as for conditioning with afferents in the purely cutaneous nerves. Furthermore the effects by tibial nerve stimulation appeared in parallel to the cutaneous cord dorsum potential as recorded by the surface electrode at the dorsal root entry zone. A contribution to the inhibitory effects from tibial nerve stimulation by Renshaw cell activation elicited via antidromic stimulation of motor axons seems unlikely since a recent anatomical investigation has shown that tibial motoneurons do not give off proximal collaterals at all (Cullheim & Kellerth 1978). Finally similar suppressive effects have been obtained with electrical stimulation within the pad (Jenkinson & Johansson 1977) clearly suggesting that cutaneous afferents in the tibial nerve may produce this kind of inhibitory interaction.

The latencies presented for Group II-PSPs were measured from the end of the Group I incoming volley at the dorsal root entry zone to the foot of the

PSP and are thus not true 'central latencies'. They were however only used to differentiate between Group II-PSPs which were suppressed by cutaneous conditioning stimulation ('long latency'—presumed polysynaptic) and those which were not suppressed, but might instead be facilitated ('short latency'—presumed disynaptic for EPSPs).

The present investigation demonstrated that the inhibitory interaction between cutaneous and Groups II and III muscle afferent pathways seems to involve more than one mechanism. As far as the transmission to motoneurons is concerned the inhibitory interactions were evident whether or not the cutaneous volley evoked a PSP by itself in the motoneurone under study. Hence it is unlikely that the suppressive effects were dependent upon action on the motoneurone membrane. It is concluded that the inhibitory actions were exerted at stages in the reflex path prior to the motoneurone itself. This conclusion is supported by the fact that the short latency excitatory Group II pathway to flexor and extensor motoneurons was never observed to be suppressed by the cutaneous conditioning volleys. Furthermore, excitatory and inhibitory polysynaptic pathways to motoneurons were similarly affected, and an involvement of Renshaw cells is thus considered unlikely as they seem to influence only the transmission through pathways involving the reciprocal Ia inhibitory interneurons (Hultborn et al. 1971).

The transmission through high threshold muscle afferent polysynaptic pathways was suppressed by one pathway initiated from low threshold cutaneous afferents. Pathways affected were Group II polysynaptic to alpha-motoneurons and to primary afferent terminals as well as Group III paths to alpha-motoneurons. The inhibitory effect was produced by cutaneous afferents also in the very low threshold (<1.1T) range. It was not possible to delineate the highest threshold cutaneous afferents involved, because with conditioning shocks of 1.6–1.8T or greater another inhibitory path was also put into action. This high threshold cutaneous path also affected all reflex paths studied, but its characteristics were different, e.g. the time course of its action was slower than that of the low threshold path.

For a number of reasons it is suggested that the difference in time course of the inhibition of transmission through the polysynaptic muscle afferent pathways by low and high threshold cutaneous afferents is not merely due to a quantitative differ-

once. Firstly the low threshold path was rather labile and in a few experiments only the high threshold path could be studied because suppression of transmission was not evident until the strength of the conditioning cutaneous stimulation was raised above 1.6–2 OT. In other experiments the transmission to some motoneurons was affected by the low as well as the high threshold cutaneous path while for the transmission to other motoneurons only the high threshold path was operating. Secondly when investigating the inhibitory interaction at long conditioning test intervals (e.g. 300 ms as in Fig. 5) it was found that the lowest threshold for a suppressive effect was 1.6–1.8 T. Thirdly with high threshold stimulation all three cutaneous nerves were effective in suppressing the reflex transmission while with low threshold conditioning shocks commonly only one or two of the cutaneous nerves were effective.

Regarding the mechanisms of inhibition of transmission through the muscle afferent reflex pathways the two cutaneous paths will be discussed separately. Concerning the high threshold path the threshold for its activation was the same as that for evoking a component II DRI. The component II DRP evoked by stimulation of cutaneous nerves is considered to be an "FRA effect" from cutaneous afferents (Carpenter et al 1963a) and is presumed to represent primary afferent depolarization in FRA terminals. Taking into account also the large peripheral receptive field for activation of this cutaneous path (all three cutaneous nerves equally effective) it is thus suggested in agreement with earlier studies (see Schmidt 1973) that the inhibition of transmission through polysynaptic Groups II and III muscle afferent pathways by activity in high threshold (above 1.5 T) cutaneous afferents is due to presynaptic inhibition between these primary afferent systems. The apparent disagreement between the duration of the DRPs presented in the figures and the duration of inhibition of reflex path transmission attributed to the same mechanism is explained in Methods section. It is however not excluded that postsynaptic interneuronal inhibition may also contribute to this interaction.

The low threshold cutaneous inhibition of transmission through the reflex pathways cannot however be explained by the same mechanism although the time course of this inhibitory interaction is also rather long. It is produced by cutaneous afferents which do not evoke a component II DRP

but only a component I DRP. This DRP (evoked by the low threshold cutaneous afferents, and known to give primary afferent depolarization in other cutaneous afferents) cannot be considered as part of the FRA effect from cutaneous afferents (cf. Carpenter et al 1963 i). This is further indicated by the fact that in the decerebrate cat the inhibition of reflex paths (from Groups Ib, II and III muscle afferents) by the dorsal reticulospinal system does not include the path evoking the component I DRI (Carpenter et al 1963a; Engberg et al 1968a). There are furthermore a number of ascending paths that are activated from the FRA (Oscarsson 1973). With regard to the contribution from cutaneous afferents to the activation of ventral spinocervicobulbar paths the stimulation strength must be 1.5–3 OT or above (Oscarsson & Sjolund 1977), excluding the low threshold ones from the FRA concept at least in this respect.

Altogether and taking into account also the restricted peripheral receptive field for the low threshold cutaneous afferents responsible (only nerves with distal fields, and commonly only one of them) for the inhibition of transmission through the high threshold muscle afferent pathways, it is unlikely that this cutaneous path belongs to the FRA as originally defined (Lecles & Lundberg 1959).

There is still the possibility that the low threshold cutaneous path might inhibit the reflex transmission by another presynaptic mechanism separated from the FRA mechanism. There is however no available evidence suggesting that the component I DRP represents primary afferent depolarization in terminals other than those of cutaneous afferents (Carpenter et al 1963a). In fact, only the rather long time course of the low threshold cutaneous inhibitory action reminds of a presynaptic action. It is however well known that postsynaptic interneuronal inhibition may have a rather long time course in some systems. The dorsal reticulospinal system (Engberg et al 1968a, b) or the RBSI (Jeneskog & Johansson 1977) is one example where postsynaptic inhibition of transmission through reflex pathways has a long time course. The latter authors described furthermore a similar inhibitory action from low threshold cutaneous afferents with distal receptive fields on the same reflex pathways. The effect was suggested to be a postsynaptic inhibition at an interneuronal level because facilitatory interaction between descending and segmental actions was revealed.

There are several reasons to believe that the low threshold cutaneous inhibition studied by Jørgensen & Johansson (1977) and the one studied in the present investigation is the same mechanism. The time course of effects is similar: the peripheral receptive field for the cutaneous afferents in question is similarly restricted and the range of thresholds for their activation is the same. The most likely explanation is, in fact, for the mechanism is therefore that low threshold (less than 1 ST) cutaneous afferents may inhibit the transmission through polysynaptic Groups II and III muscle afferent pathways at an interneuronal level.

Alternatively the low threshold cutaneous inhibition could be an "experimental artifact" due to postsynaptic depression in Groups II and III muscle afferent pathways, provided that the low threshold cutaneous afferents also activated interneurons in these paths. This explanation is however not likely because when conditioning and test stimuli were applied to the same afferents and thus should have affected the same interneuronal system, there was no inhibitory effect on the transmission through the test reflex pathway but with low threshold cutaneous conditioning the suppression was readily apparent (cf. Fig. 8I-K).

It should finally be recalled that regarding Group II muscle afferent pathways, only the polysynaptic ones were affected by the two mechanisms described above. The short latency Group II path to flexor motoneurons which is considered to be monosynaptic (Lundberg et al. 1975), was never inhibited by preceding activity in cutaneous afferents. On the other hand, it was sometimes possible to demonstrate a facilitatory interaction between low threshold cutaneous afferents and (low threshold) Group II muscle afferents in the transmission to motoneurons, regardless of whether the cutaneous or the muscle afferent volley was used to elicit the test response. If this Group II muscle afferent pathway is disynaptic, the facilitatory effect from low threshold cutaneous afferents would be exerted at the only interneurone involved as the facilitation could be produced by cutaneous nerve stimulation that did not evoke PSP in the motoneurone by itself. The influence from cutaneous afferents is thus assumed to be disynaptic on the Group II interneurone, as the shortest path to motoneurons from low threshold cutaneous afferents is presumably trisynaptic (Lundberg 1973). Lundberg et al. (1977) has recently reported a similar convergence

from cutaneous joint and Group II muscle afferents in inhibitory reflex pathways to extensor motoneurons. Such a convergence between low threshold cutaneous and Group II muscle afferents (most likely from spindle secondary endings) in reflex paths is of great interest, as also recently pointed out by Appelberg et al. (1977). These authors reported dynamic fusimotor neurones to be strongly influenced by activity in such afferents. From the point of view of load compensation in motor control, a co-operation of the afferents in question on skeletomotor as well as on dynamic fusimotor neurones would seem to be of a particular value.

The author wishes to thank Doc. B. Appelberg for helpful discussions and valuable criticism throughout this work and Mrs G. Kristrom for skilful technical assistance. This work was supported by the Swedish Medical Research Council (Project No. B71-04X-04957-01).

REFERENCES

- APPELBERG B, JOHANSSON H & KALISTRATOV G 1977 The influence of group II muscle afferents and low threshold skin afferents on dynamic fusimotor neurones to triceps surae of the cat. *Brain Research* 132, 153-158.
- CARPENTER D, LUNDBERG A & NORSELL U 1963 A primary afferent depolarization evoked from the sensorimotor cortex. *Acta Physiol Scand* 39, 126-142.
- CARPENTER D, ENGBERG I, FUNKENSTEIN H & LUNDBERG A 1963 Decerebrate control of reflexes to primary afferents. *Acta Physiol Scand* 59, 424-437.
- CULLHEIM S & KELLERTH J-O 1978 A morphological study of the axons and recurrent axon collaterals of cat α -motoneurons supplying hand-forearm muscles. *J Physiol (Lond)* 281, 285-299.
- ECCLES J C 1964 Presynaptic inhibition in the spinal cord. In *Physiology of Spinal Neurons*, pp. 65-89. Progress in Brain Research 12. Elsevier Publ. C, Amsterdam.
- ECCLES J C, KOSTYUK P G & SCHMIDT R F 1962 Central pathways for depolarization of primary afferent fibres. *J Physiol (Lond)* 161, 237-257.
- ECCLES J C, KOSTYUK P G & SCHMIDT R F 1962b Presynaptic inhibition of central actions of flexor reflex afferents. *J Physiol (Lond)* 161, 258-281.
- ECCLES J C, SCHMIDT R F & WILLIS W D 1963 Depolarization of central terminals of group Ib afferents of muscle. *J Neurophysiol* 26, 1-27.
- ECCLES R M & LUNDBERG A 1959 Synaptic actions in motoneurons by afferents which may evoke the flexion reflex. *Arch ital Biol* 97, 199-221.
- ECCLES R M, HOLMQUIST B & VOORHOFVE P E 1964 Presynaptic inhibition from contralateral

- cutaneous afferent fibres. *Acta physiol scand* 62, 464-473.
- ENGBERG I, LUNDBERG A & RYALL, R. W. 1968a Reticulospinal inhibition of transmission in reflex pathways. *J Physiol (Lond)* 194, 201-23.
- ENGBERG I, LUNDBERG A & RYALL, R. W. 1968b Reticulospinal inhibition of interneurons. *J Physiol (Lond)* 194, 25-36.
- HONGO T, JANKOWSKA E. & LUNDBERG A. 1972 The rubrospinal tract. III. Effects on primary afferent terminals. *Exp Brain Res* 15, 39-53.
- HULTBORN H, JANKOWSKA E. & LINDSTRÖM S. 1971 Recurrent inhibition from motor axon collaterals of transmission in the Ia inhibitory pathway to motoneurons. *J Physiol (Lond)* 215, 591-61.
- JENESIK T & JOHANSSON H. 1977 The rubro-bulbospinal path: A descending system known to influence dynamic fusimotor neurones and its interaction with distal cutaneous afferents in the control of flexor reflex afferent pathways. *Exp Brain Res* 7, 161-179.
- KUNO M & PERL, E. R. 1960. Alteration of spinal reflexes by interaction with suprasegmental and dorsal root activity. *J Physiol (Lond)* 151, 103-122.
- LUNDBERG A. 1966. Integration in the reflex pathway. In: *Muscular Afferents and Motor Control* pp. 275-305. Ed. R. Granit. Almqvist & Wiksell, Stockholm.
- LUNDBERG A. 1969. Convergence of excitatory and inhibitory action on interneurons in the spinal cord. In: *The Interneuron* pp. 231-265. Ed. M. A. B. Brazier. Univ. of California Press, Los Angeles.
- LUNDBERG A. 1975. Control of spinal mechanisms from the brain. In: *The Nervous System, Vol. 1 The Basic Neurosciences* pp. 253-265. Ed. R. O. Brady. Raven Press, New York.
- LUNDBERG A, MALMGREN K. & SCHOMBURG E. D. 1975. Characteristics of the excitatory pathway from group II muscle afferents to alpha-motoneurons. *Brain Research* 88, 538-542.
- LUNDBERG A, MALMGREN K. & SCHOMBURG E. D. 1977. Convergence from cutaneous, joint and group II muscle afferents in inhibitory reflex pathways to alpha-motoneurons. *Pflügers Arch* 368 Suppl. R36.
- OSCARSSON O. 1973. Functional organization of spinocerebellar paths. In: *Handbook of Sensory Physiology, Vol. II, Somatosensory System*, pp. 339-380. Ed. A. Iggo. Springer, Berlin-Heidelberg-New York.
- OSCARSSON O & SJÖLUND B. 1977. The ventral spino-olivocerebellar system in the cat. III. Functional characteristics of the five paths. *Exp Brain Res* 28, 505-570.
- SCHMIDT R. F. 1973. Control of the access of afferent activity to somatosensory pathways. In: *Handbook of Sensory Physiology, Vol. II, Somatosensory System*, pp. 151-206. Ed. A. Iggo. Springer, Berlin-Heidelberg-New York.
- SHIMAMURA, M., KOGURE I. & IGUSA, Y. 1971. Ascending spinal tracts of the spino-bulbo-spinal reflex in cats. *Jap J Physiol* 26, 577-589.

Morphological and mechanical properties of small mesenteric arteries and veins in spontaneously hypertensive rats

C. AALKJÆR and M. J. MULVANY

From the Institute of Biophysics, University of Aarhus, Denmark

AALKJÆR, C. & MULVANY, M. J. Morphological and mechanical properties of small mesenteric arteries and veins in spontaneously hypertensive rats. *Acta Physiol Scand* 1979; 107: 309-312. Received 2 Feb. 1979. ISSN 0001-6772. Institute of Biophysics, University of Aarhus, Denmark.

Segments of small mesenteric arteries (~150 µm lumen diameter) and of corresponding veins are taken from 5-month-old spontaneously hypertensive rats (SHR) and from age-matched Wistar Kyoto (WKY) controls. The segments were mounted on a myograph which enabled their mechanical and morphological parameters to be investigated simultaneously. Compared with the WKY arteries the lumen diameter of the SHR arteries was smaller, while the media thickness and active wall tension response were greater. On the other hand there were no differences between the corresponding veins from SHR and WKY animals although, compared with the arteries, the veins had a greater lumen diameter, a smaller media thickness and a smaller tension response. The findings suggest that the morphological and mechanical differences seen in arteries from SHR are not found on the venous side.

Key words. Morphology, arteries, veins, spontaneously hypertensive rats.

Essential hypertension in man is accompanied by an increase in the wall thickness of resistance vessels, in particular those having lumen diameters of about 100 µm (Furuyama 1962; Suwa & Takahashi 1971). In the spontaneously hypertensive rat (SHR), widely used as a model for human essential hypertension (Udenfriend et al. 1975), we have demonstrated previously a greater wall thickness of arteries of diameter ~150 µm (Mulvany, Hansen & Aalkjær 1978). In smaller arteries and arterioles the media thickness is reported to be reduced (Göteborg & Lobach 1978; Hanzon, Hertel & Aasman 1978), while in the portal vein wall hypertrophy has been observed (Greenberg & Bohr 1975). This has therefore raised the possibility that in the SHR wall (and media) hypertrophy is a general characteristic of the larger vessels, rather than being associated with the greater pressure to which the vessels are exposed as suggested by the indirect perfusion experiments of Folkow et al. (1974). To test this possibility we have therefore in the present study sought to determine whether the differences we have found in 150 µm arterial

resistance vessels are also present in the corresponding veins.

MATERIAL AND METHODS

Segments of third generation vessels of a. or mesenterica sup. about 0.7 mm long, were taken from 5-month-old spontaneously hypertensive rats (SHR) and from age-matched normotensive Wistar Kyoto (WKY) controls, all supplied by Møllegaards A. H. Laboratorium, L.1 Skovsvej, Denmark. In every second experiment it was the arterial vessel which was first dissected out and tested, and then later during the same day the corresponding venous vessel was tested through the same procedure. In the other experiments it was the venous vessel which was tested first.

The myograph used for testing the vessels has been described in detail earlier (Mulvany & Halpern 1977; Mulvany et al. 1978). With this arrangement we were able to measure simultaneously the internal circumference of the vessel, the wall and media thickness, as well as the vessel's isometric wall tension.

Nomenclature

The force developed by the vessel is expressed as circumferential wall tension, T , defined by:

$$T = F/2a$$

where F is the force measured by the force transducer and a is the segment length. The active wall tension

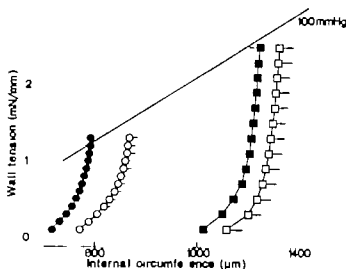


Fig. 1 Relation of passive wall tension and internal circumference of arteries (circles) and veins (squares) from SHRs (filled symbols) and WKYs (open symbols). Each point shows the mean internal circumference for each wall tension level obtained from 9 expts (where necessary by interpolation). Horizontal bars show S.E. The line marked 100 mmHg joins points which are equivalent (see text) to an effective pressure of 100 mmHg (13.3 mN/mm²).

is the total wall tension following activation less the wall tension immediately before activation.

To estimate the characteristics which the vessels would have had *in situ* we have calculated (Mulvany & Halpern 1977) the effective internal diameter d and (using Laplace equation) the effective pressure p according to the following equations.

$$d = L/\pi$$

$$p = T/(d/r)$$

where L is the internal circumference

Solutions

The physiological salt solution (PSS) used had the following composition in mM (Murphy, Herby & Mergeman 1974): NaCl 119, NaHCO₃ 14.9, KCl 4.7, KH₂PO₄ 1.18, MgSO₄ 1.17, CaCl₂ 1.6, ethylenediaminetetraacetic

acid (EDTA) 0.026, glucose, 5.5. Vessels were activated by a potassium solution (K PSS) which was as for PSS but with an equimolar substitution of KCl for NaCl as with 2.5 mM CaCl₂. Solutions were bubbled with 5% CO₂ in O₂ adjusted to pH 7.4 and held at 37°C.

Protocol

The protocol used was in general similar to that described previously (Mulvany et al. 1978). First with the vessel in PSS the internal circumference was increased in steps of about 20 μm at 1 min intervals until the effective pressure (see above) equalled 100 mmHg (13.3 mN/mm²) the internal circumference being defined as L_{100} . Vessels were then released through a similar sequence and the passive characteristic was then taken as the curve defined by the points obtained in this sequence.

Vessels were then set to an internal circumference $L = 0.9L_{100}$ and mean wall and media thicknesses estimated in two ways. First as described previously, the microscope was focussed on the outer edge of the mounting wires so that the wall (and the media within it) could be seen in longitudinal section and measured using an ocular micrometer. Second as a new method, the microscope was focussed on the portion of the upper wall between the wires and the preparation was optically sectioned, that is we measured the vertical movement of the microscope stage required to move the plane of focus through the successive layers of the wall. The advantage of the second method was that we could make measurements on those portions of the wall which were not in contact with the mounting wires. Measurements were made in 12 positions with each method and the reported values are the means of these measurements.

The active characteristics of vessels were then determined by activating them at L_{100} with the high potassium solution (K PSS) and measuring the active wall tension after 3 min. Finally vessels were fixed on the myograph at L_{100} in 5% glutaraldehyde post-fixed in osmium tetroxide and embedded in Epon for later histological examination.

RESULTS

The passive wall tension—internal circumference relations of the SHR and WKY arterial and venous

Table 1 Morphological and mechanical parameters of the vessels used in this investigation

Values show mean \pm S.E. of parameters measured with vessel held at normalized internal circumference L_{100}

	Artery		Vein	
	SHR	WKY	SHR	WKY
Number of vessels	9	9	9	9
Effective lumen μ m	162.0 \pm 5.7	214.0 \pm 5.4	366.0 \pm 12.7	377.0 \pm 18.7
Wall thickness μ m	17.7 \pm 1.1	13.3 \pm 0.9	1.7 \pm 0.2	6.8 \pm 0.4
Media thickness μ m	12.6 \pm 0.5	8.5 \pm 0.5	4.2 \pm 0.1	4.6 \pm 0.1
Active wall tension mN/mm	3.0 \pm 0.1	3.0 \pm 0.1	0.5 \pm 0.1	0.5 \pm 0.1

Indicate significant difference between the SHR parameter concerned and the corresponding WKY parameter at the 5% and 0.1% levels respectively as determined by the two-tail Student t test.

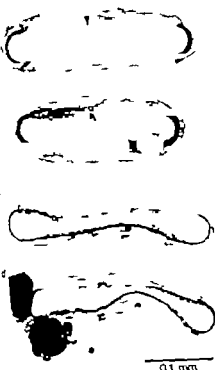


Fig. 2 Cross-sections of vessels fixed on the cryograph at L_4 : (a) WKY artery, (b) SHR artery, (c) WKY vein, (d) SHR vein. Sections stained with toluidine blue.

vessels are shown in Fig. 1. For any given wall tension the SHR arteries had a smaller internal circumference ($L_{i0}/r=16.4 \mu\text{m}$) than the WKY arteries ($L_{i0}/r=21.4 \mu\text{m}$). There was however no significant difference between the corresponding internal circumference of the SHR and WKY veins ($L_{i0}/r=366 \mu\text{m}$ and $377 \mu\text{m}$ respectively) both being about twice as large as those of the arteries. By contrast, with the vessels set to internal circumference L_0 , media thicknesses of the SHR arteries ($12.6 \mu\text{m}$) were greater than those of the WKY arteries ($8.5 \mu\text{m}$) while there was no significant difference between media thicknesses of the SHR and WKY veins ($5.7 \mu\text{m}$ and $6.8 \mu\text{m}$ respectively). Similar findings were made as regards the wall thicknesses. These results are summarised in Table 1. Light micrographs of cross-sections of vessels fixed at L_0 (Fig. 2) indicated that while there were about 4 layers of smooth muscle cells in the

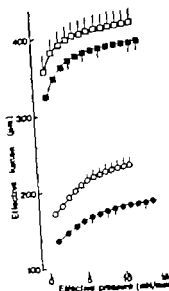


Fig. 3 Relation between effective pressure and effective tension calculated as described in Methods from data used for Fig. 1. Symbol as in Fig. 1.

SHR arteries or about 3 layers of cells in the WKY arteries, the veins contained less than one layer. That is the media of the veins was irregular and did not fully cover the internal elastic lamina.

The active response of the vessels to K PSS is shown in Table 1. The active wall tension produced was greater in the SHR arteries (3.0 mN/mm) than in the WKY arteries (2.3 mN/mm). By contrast there was no difference between the active wall tensions produced by the SHR and WKY veins. The active wall tension of the veins (0.5 mN/mm) was however substantially lower than the active wall tension developed by the arteries.

DISCUSSION

The results of this investigation show that the thickened media and decreased lumen which I seen in $150 \mu\text{m}$ arterial resistance vessels in the SHR mesenteric bed (Malvady et al. 1978) are structural differences which are not present in the corresponding veins. Bohlen, Gore & Hutchins (1977) have shown that the absolute blood pressure differences of SHR and WKY animals are confined almost entirely to the precapillary vessels. Therefore our finding that the structural differences are also confined to precapillary vessels suggests that there is a connection between these vascular differences

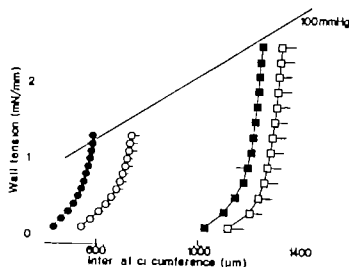


Fig. 1. Relation of passive wall tension and internal circumference of arteries (circles) and vein (squares) from SHR (filled symbols) and WKY (open symbols). Each point shows the mean internal circumference for each wall tension level obtained from 9 expts. (where necessary by interpolation). Horizontal bars show S.E. The line marked 100 mmHg joins points which are equivalent (see text) to an effective pressure of 100 mmHg (13.3 mN/mm²).

is the total wall tension following activation less the wall tension immediately before activation.

To estimate the characteristic which the vessel would have had *in situ* we have calculated (Mulvany & Halpern 1977) the effective lumen diameter d and (using Laplace equation) the effective pressure p according to the following equations:

$$d = L/\pi$$

$$p = T/(d/2)$$

where L is the internal circumference.

Solutions

The physiological salt solution (PSS) used had the following composition in mM (Murphy, Herikhy & Mergerman 1974): NaCl 119, NaHCO₃ 14.9, KCl 4.7, KH₂PO₄ 1.18, MgSO₄ 1.17, CaCl₂ 1.6, ethylenediaminetetraacetic

acid (EDTA) 0.026, glucose, 5.5. Vessels were activated by a potassium solution (K-PSS) which, as for PSS, but with an equimolar substitution of KCl for NaCl at 5 mM CaCl₂. Solutions were bubbled with 5% O₂ in O₂ adjusted to pH 7.4 and held at 37°C.

Protocol

The protocol used was in general similar to that described previously (Mulvany et al. 1978). First with the endothelial PSS the internal circumference was increased in steps of about 20 μm at 1 min intervals until the effective pressure (see above) equalled 100 mmHg (13.3 mN/mm²), the internal circumference being defined as L_{100} . Vessel were then released through a similar sequence and the passive characteristic was then taken as the curve defined by the points obtained in this sequence.

Vessels were then set to an internal circumference $L_0 = 0.9L_{100}$ and mean wall and media thicknesses estimated in two ways. First as described previously the microscope was focussed on the outer edge of the mounting wires so that the wall (and the media when it could be seen in longitudinal section) and measured using an ocular micrometer. Second as a new method, the microscope was focussed on the portion of the upper wall between the wires and the preparation was optically sectioned; that is we measured the vertical movement of the microscope stage required to move the plane of focus through the successive layers of the wall. The advantage of the second method was that we could make measurements on those portions of the wall which were not in contact with the mounting wires. Measurements were made in 10 positions with each method and the reported value are the means of these measurements.

The active characteristics of vessels were then determined by activating them at L_0 with the high potassium solution (K-PSS) and measuring the active wall tension after 3 min. Finally vessels were fixed on the myograph at L_0 in 5% glutaraldehyde, post-fixed in osmium tetroxide and embedded in Epon for later histological examination.

RESULTS

The passive wall tension—internal circumference relations of the SHR and WKY arterial and venous

Table 1. Morphological and mechanical parameters of the vessel used in this investigation. Values show mean \pm S.E. of parameters measured with vessel held at normalized internal circumference L_0 .

	Artery		Vein	
	SHR	WKY	SHR	WKY
Number of vessels	9	9	9	9
Effective lumen μ m	162.0 \pm 5.7	140.0 \pm 14	166.0 \pm 1.7	377.0 \pm 18.7
Wall thickness μ m	17.7 \pm 1.1	13.3 \pm 0.9	5.7 \pm 0	6.8 \pm 0.4
Media thickness μ m	1.6 \pm 0.5	1.4 \pm 0.5	4 \pm 0.1	4.6 \pm 0
Active wall tension, mN/mm	3.0 \pm 0.2	3.0 \pm 0.1	0.5 \pm 0.1	0.5 \pm 0.1

Indicate significant difference between the SHR parameter concerned and the corresponding WKY parameter at the 5% and 0.1% levels respectively as determined by the two-tail Student t test.

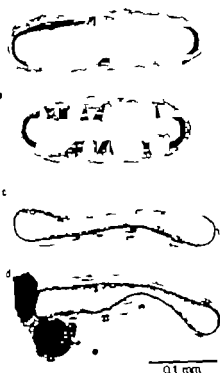


Fig. 2. Cross-sections of vessels fixed on the cryograph. (a) WKY artery, (b) SHR artery, (c) WKY vein, (d) SHR vein. Sections stained with toluidine blue.

vessels are shown in Fig. 1. For any given wall tension the SHR arteries had a smaller internal circumference ($L_0/r=162 \mu\text{m}$) than the WKY arteries ($L_0/r=14 \mu\text{m}$). There was however no significant difference between the corresponding internal circumference of the SHR and WKY veins ($L_0/r=366 \mu\text{m}$ and $377 \mu\text{m}$, respectively), both being about twice as large as those of the arteries. In contrast, with the vessels set to internal circumference L_0 , media thicknesses of the SHR arteries ($12.6 \mu\text{m}$) are greater than those of the WKY arteries ($8.5 \mu\text{m}$) while there was no significant difference between media thicknesses in the SHR and WKY veins ($5.7 \mu\text{m}$ and $6.8 \mu\text{m}$, respectively). Similar findings were made as regards the Δ thicknesses. These results are summarised in Table 1. Light micrographs of cross-sections of vessels fixed at L_0 (Fig. 2) indicated that while there were about 4 layers of smooth muscle cells in the

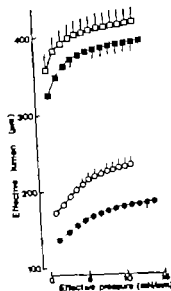


Fig. 3. Relation between effective pressure and effective lumen calculated as described in Methods from data used for Fig. 1. Symbols as in Fig. 1.

SHR arteries, or about 3 layers of cells in the WKY arteries the veins contained less than one layer. That is the media of the veins was irregular and did not fully cover the internal elastic lamina.

The active response of the vessels to K PSS is shown in Table 1. The active wall tension produced was greater in the SHR arteries (3.0 mN/mm) than in the WKY arteries (2.3 mN/mm). By contrast there was no difference between the active wall tensions produced by the SHR and WKY veins. The active wall tension of the veins (0.5 mN/mm) was however substantially lower than the active wall tension developed by the arteries.

DISCUSSION

The results of this investigation show that the thickened media and decreased lumen which is seen in $150 \mu\text{m}$ arterial resistance vessels in the SHR mesenteric bed (Mullvany et al. 1978) are structural differences which are not present in the corresponding veins. Bohlen, Gore & Hutchins (1977) have shown that the absolute blood pressure differences of SHR and WKY animals are confined almost entirely to the precapillary vessels. Therefore our finding that the structural differences are also confined to precapillary vessels suggests that there is a connection between these vascular differences

and the loading to which they have been subjected. Whether the structural differences are a result or a cause of the increased pressure cannot at present be determined. We have however shown in a recent age study (Warsaw, Mulvany & Halpern 1979) that the media hypertrophy occurs concurrently with the increase in blood pressure of the SHR from the age of 6 weeks. Thus in vessels of this size it seems at least that media thickness and transmural blood pressure are closely associated and that the structural differences seen are not general properties of the vasculature. This conclusion is therefore in contrast to Greenberg & Bohr's (1975) finding that there is hypertrophy of the SHR portal vein in which there is little elevation of blood pressure. One possible reason for the discrepancy is that Greenberg & Bohr's control animals were stock Wistar rats whereas ours were Wistar Kyoto rats.

Hallböck, Lundgren & Weiss (1974) have from measurements of the perfusion pressure and flow rate in an isolated vascular bed determined the relation between the radius of an average vessel and its transmural pressure under relaxed conditions. Fig. 3 shows the calculated effective pressure—effective lumen relations of our vessels based (as described in Methods) on the internal circumference—wall tension relations of the relaxed vessels (Fig. 1). The results suggest that the distensibility of the SHR arteries is lower than that of the WKY arteries and also that the veins have a smaller distensibility than the arteries for transmural pressures above about 10 mmHg (75 mmHg). These findings are remarkably similar to those presented by Hallböck et al. (1974). The decreased distensibility of the arteries could be due either to a thicker media or to altered elastic properties of the wall components. Our morphological measurements indicate that the decreased distensibility of the arteries is at least in part due to the increased media thickness. By contrast this cannot explain the lower distensibility of the veins for here the wall is much thinner. Therefore in the veins it must be the elastic properties of the wall components which differ from those of the arteries.

In conclusion our results support the indirect evidence of Folkow et al. (1974) based on perfusion studies that the structural changes within the SHR vasculature are confined to the precapillary vessels

with little change in the structure of the postcapillary vessels.

REFERENCES

- BOHLEN H G, GORE R W & HUTCHINS, P M 1977 Comparison of microvascular pressures in normal and spontaneously hypertensive rats. *Microvasc Res* 13: 125–130.
- FOLKOW B, HALLBÖCK M, LUNDGREN Y, WEISS L, ALBRECHT I & JULIUS S. 1974 Analysis of design and reactivity of series coupled sections in spontaneously hypertensive rats (SHR). *Acta Physiol Scand* 90: 654–656.
- FURUYAMA M 1966 Histometrical investigations of arteries in reference to arterial hypertension. *Tohoku J Exper Med* 76: 388–414.
- GREENBERG S & BOHR D F 1975 Venous smooth muscle in hypertension. *Circ Res* 36 and 37 (Suppl. 1): 1208–1215.
- HALLBÖCK M, LUNDGREN Y & WEISS, L 1974 The distensibility of the resistance vessels in spontaneously hypertensive rats (SHR) as compared with normotensive control rats (NCR). *Acta Physiol Scand* 90: 57–68.
- HENRICH H, HERTEL R & ASSMANN R 1971 Structural differences in the mesentery microcirculation between normotensive and spontaneously hypertensive rats. *Pflügers Arch* 375: 153–160.
- MULVANY M J & HALPERN W 1977 Contractile properties of small arterial resistance vessels in spontaneously hypertensive and normotensive rats. *Circ Res* 41: 19–26.
- MULVANY M J, HANSEN P K & AALKJÆR C 1978 Direct evidence that the greater contractility of resistance vessels in spontaneously hypertensive rats is associated with a narrower lumen, a thicker media and a greater number of smooth muscle cell layers. *Circ Res* 43: 854–864.
- MURPHY R A, HERLIHY J T & MERGERMAN J 1974 Force-generating capacity and contractile protein content of arterial smooth muscle. *J Gen Physiol* 64: 691–705.
- SUWA N & TAKAHASHI T 1971 Morphological and morphometrical analysis of circulation in hypertension and ischemic kidney. Urban & Schwarzenberg, München, Berlin, Wien.
- UDENFRIEND S, BUMPUS F M, POSTER, H L, FREIS E D, HANSEN C T, LOVENBERG W M & YAMORI Y 1975 Guide for the care and use of spontaneously hypertensive (SHR) rats in biomedical research. Ed. by the Committee on care and use of spontaneously hypertensive (SHR) rats. Institute of Laboratory Animal Resources, National Academy of Sciences, Washington D C.
- WARSHAW D M, MULVANY M J & HALPERN W 1979 Mechanical and morphological properties of arterial resistance vessels in young and old spontaneously hypertensive rats. *Circ Res* 45: 550–559.

Relationship between serum IgE levels and anaphylactic histamine release from isolated rat mast cells

SYDBOM and T. KARLSSON

of Pharmacology, Karolinska Institute, Stockholm, Sweden,

Department of Medical and Physiological Chemistry

Centre, Uppsala, Sweden

SYDBOM A. & KARLSSON T. Relationship between serum IgE levels and anaphylactic histamine release from isolated rat mast cells. *Acta Physiol Scand* 1979; 107: 313-318. Received 11 April 1979. ISSN 0001-6772. Department of Pharmacology, Karolinska Institute, Stockholm, Sweden, and Department of Medical and Physiological Chemistry Biomedical Centre, Uppsala, Sweden.

Inbred Hooded Lister rats were immunized with egg albumin with B. pertussis vaccine used as an adjuvant. The serum levels of total IgE and IgE antibody (egg albumin specific) were determined by radioimmunoassay techniques before and after immunization. The basic level of total IgE in serum was 560 ± 110 ng/ml. After immunization a maximal peak at day 11 of 1940 ± 160 ng/ml was registered. Anti-egg albumin IgE antibody showed a maximum around day 13 of 75 ± 11 units/ml. Pleural mast cells were isolated on Ficol between day 14 and 20 after immunization. A significant negative correlation between the basic total IgE level and histamine release by antigen (egg albumin) was found and also a significant positive correlation of specific IgE antibody (determined at day 11) and histamine release. The correlation between IgE level and histamine release was slightly improved if instead the ratio of specific IgE antibody over total IgE was used.

Key words: inbred Hooded Lister rats, immunization, pertussis vaccine, rat IgE-radioimmunoassay.

IgE antibody is considered to be responsible for the anaphylactic reactions of antigen exposed sensitized mast cells of many species among them the rat (Steckschulte et al. 1970). There have been a number of reports attempting to correlate the serum IgE levels with the clinical symptoms (see e.g. Elgefors et al. 1974). The results are diverging and the significance of the level of circulating IgE for the development of atopic reactions has been disputed (Henderson et al. 1971).

By the use of animal models for immunization studies it has been possible to follow the IgE antibody response by passive cutaneous anaphylaxis (PCA) or the histamine release from mast cells from immunized animals. With PCA it is however often difficult to get well reproducible results. Jarrett & Stewart (1973) reported that in the rat there was no direct relationship between the size of skin test reactions and the level of specific circulating IgE antibody tested by PCA. Neither did Yamamoto et al. (1974) register any correlation be-

tween the reagent titre and histamine release from different *in vitro* systems in the rat. However Stahl Skov et al. (1977) have measured histamine release from human basophils and found a significant correlation between specific but not total IgE and cell sensitivity when IgE had been determined by a radioimmunoassay technique (RAST). After the discovery of IgE myelomas in LOU rats (Bazin et al. 1973, 1974) new techniques to measure total IgE and specific IgE antibody in rats have been developed. Radioimmunoassay techniques used for measurement of human IgE can be used also for rat IgE. Assays based on paper disc coupled anti IgE antibodies (PRIST: paper radio immunosorbent test) for total IgE (Karlsson et al. 1979) and antigens (allergens) (PRAST: paper radio allerge sorbent test) for specific IgE antibody have been described (Karlsson et al. 1979b). These techniques have made it possible to detect low levels as well as small differences in total IgE and specific IgE antibody levels down to ng amounts.

and the loading to which they have been subjected. Whether the structural differences are a result or a cause of the increased pressure cannot at present be determined. We have however shown in a recent age study (Warsaw, Mulvany & Halpern 1979) that the media hypertrophy occurs concurrently with the increase in blood pressure of the SHR from the age of 6 weeks. Thus in vessels of this size it seems at least that media thickness and transmural blood pressure are closely associated and that the structural differences seen are not general properties of the vasculature. This conclusion is therefore in contrast to Greenberg & Bohr's (1975) finding that there is hypertrophy of the SHR portal vein in which there is little elevation of blood pressure. One possible reason for the discrepancy is that Greenberg & Bohr's control animals were stock Wistar rats, whereas ours were Wistar Kyoto rats.

Hallböck, Lundgren & Weiss (1974) have from measurements of the perfusion pressure and flow rate in an isolated vascular bed determined the relation between the radius of an average vessel and its transmural pressure under relaxed conditions. Fig. 3 shows the calculated effective pressure—effective lumen relations of our vessels based (as described in Methods) on the internal circumference—wall tension relations of the relaxed vessels (Fig. 1). The results suggest that the distensibility of the SHR arteries is lower than that of the WKY arteries and also that the veins have a smaller distensibility than the arteries for transmural pressures above about 10 mmHg (75 mmHg). These findings are remarkably similar to those presented by Hallböck et al. (1974). The decreased distensibility of the arteries could be due either to a thicker media or to altered elastic properties of the wall components. Our morphological measurements indicate that the decreased distensibility of the arteries is at least in part due to the increased media thickness. By contrast this cannot explain the lower distensibility of the veins, for here the wall is much thinner. Therefore in the veins it must be the elastic properties of the wall components which differ from those of the arteries.

In conclusion, our results support the indirect evidence of Folkow et al. (1974) based on perfusion studies that the structural changes within the SHR vasculature are confined to the precapillary vessels

with little change in the structure of the postcapillary vessels.

REFERENCES

- BOHLEN H G, GORE R W & HUTCHINS P M 1977 Comparison of microvascular pressures in normal and spontaneously hypertensive rats. *Microvasc Res* 13 125–130.
- FOLKOW B, HALLBÄCK M, LUNDGREN Y, WEISS L, ALBRECHT I & JULIUS S 1974 Analysis of design and reactivity of series coupled sections in spontaneously hypertensive rats (SHR). *Acta Physiol Scand* 90: 654–656.
- FURUYAMA M 1962 Histometrical investigations of arteries in reference to arterial hypertension. *Tohoku J Exper Med* 76 388–414.
- GREENBERG S & BOHR D F 1975 Venous smooth muscle in hypertension. *Circ Res* 36 and 37 (Suppl. 1): 1208–1215.
- HALLBÄCK M, LUNDGREN Y & WEISS L 1974 The distensibility of the resistance vessels in spontaneously hypertensive rats (SHR) as compared with normotensive control rats (NCR). *Acta Physiol Scand* 90: 57–68.
- HENRICH H, HERTEL R & ASSMANN R 1978 Structural differences in the mesentery microcirculation between normotensive and spontaneously hypertensive rats. *Pflügers Arch* 375 153–160.
- MULVANY M J & HALPERN W 1977 Contractile properties of small arterial resistance vessels in spontaneously hypertensive and normotensive rats. *Circ Res* 41 19–26.
- MULVANY M J, HANSEN P K & AALKJÆR C 1978 Direct evidence that the greater contractility of resistance vessels in spontaneously hypertensive rats is associated with a narrower lumen, a thicker media and a greater number of smooth muscle cell layers. *Circ Res* 43 854–864.
- MURPHY R A, HERLIHY J T & MERGERMAN J 1974 Force-generating capacity and contractile protein content of arterial smooth muscle. *J Gen Physiol* 64 691–705.
- SUWA N & TAKAHASHI T 1971 Morphological and morphometrical analysis of circulation in hypertension and ischemic kidney. Urban & Schwarzenberg, München, Berlin, Wien.
- UDENFRIEND S, BUMPUS F M, FOSTER H L, FREIS E D, HANSEN C T, LOVENBERG W M & YAMORI Y 1975 Guide for the care and use of spontaneously hypertensive (SHR) rats in biomedical research. Edited by the Committee on care and use of spontaneously hypertensive (SHR) rats. Institute of Laboratory Animal Resources, National Academy of Sciences, Washington, D.C.
- WARSHAW D M, MULVANY M J & HALPERN W 1979 Mechanical and morphological properties of arterial resistance vessels in young and old spontaneously hypertensive rats. *Circ Res* 45 250–259.

Table 1. Concentration of IgE in rat serum

Total IgE and specific IgE antibody was determined in serum samples taken from Hooded Lister rats just prior to and at different days after immunization with 20 µg egg albumin in pertussis vaccine

Days after immunization	Specific IgE antibody (units/ml)			Total IgE (ng/ml)	
	\bar{x}	S.E.		$\bar{x} \pm$ S.E.	
Basic				560 ± 110	13
5	6 ± 2	1	NS	630 ± 70	26
11	59 ± 5	32		1 940 ± 160	37
13	80 ± 12	5		1 250 ± 140	4
14	NS 70 ± 19	5		680 ± 130	3
19	NS 65 ± 9	10		630 ± 140	10
23	NS 63 ± 7	7		1 000 ± 130	7
27	49 ± 5	6		910 ± 140	6
27	47 ± 7	5	NS	790 ± 90	7

Student's *t*-test between specific IgE antibody on day 13 and subsequent day

Student's *t*-test between basic total IgE and total IgE on day 5 and day 27 resp

Student's *t*-test between total IgE on day 11 and subsequent day

NS not significant 0.01 < *p* < 0.05 ** 0.001 < 0.01 *** *p* < 0.001

RESULTS

The serum IgE pattern after immunization

Blood samples for IgE determinations were taken maximally 4 times from one single rat before immunization, at day 5, day 11 and finally when the rat was killed between day 12 and day 27. The basic total IgE level for these Hooded Lister rats were 560 ± 110 ng/ml (*n* = 13). Before day 5 no changes could be seen but between day 5 and 11 both the total IgE and the IgE antibody levels were increased. Between day 13 and 14 there was a maximum of IgE antibody of about 74 ± 11 units/ml (*n* = 10) (Fig. 1, Table 1). The specific IgE antibody level does not decrease significantly until day 21. The total IgE shows a maximum around day 11 of about 1 940 ± 160 ng/ml (*n* = 37). The total serum IgE declines faster than the specific IgE antibody. There is an apparent increase in total IgE at day 23. However, when examining the data more carefully we could see that those rats with high levels on day 20 also showed extremely high IgE levels on day 11.

Correlation between IgE levels and histamine levels

Of totally 48 rats used only 22 rats were used for histamine release studies and tested for all parameters mentioned, namely basic total IgE and total IgE and specific IgE antibody on day 11 as well as on

the day of death. The results from these 22 rats were used for correlation calculations.

Basic total IgE. Histamine release was measured after challenge of isolated sensitized mast cells with antigen. The antigen concentration 10 µg/ml was the lowest concentration that gave maximal response and released 18.4 ± 1.2% (*n* = 51) of histamine from mast cells isolated from unimmunized Hooded Lister rats. A significant negative correlation could be seen between the per cent histamine released and the basic total IgE level (Fig. 1a). High basic total IgE level mast cells reacted less (weaker) upon antigen challenge with decreased histamine release.

Total IgE. The total serum IgE level measured either at the optimal day (day 11) or at the time of death, shows no significant correlation with the amount of histamine released with antigen from isolated mast cells (Table 2).

Specific IgE antibody. The anti-egg albumin IgE antibody level at day 11 shows a significant positive correlation with the histamine release with a correlation coefficient of 0.61 (*p* = 0.003) (Fig. 2b). However, there was no correlation between specific IgE antibody levels at the time of death and the histamine release (Table 2).

Specific IgE antibody/total IgE ratio. The correlation of the ratio of specific IgE antibody over total IgE with histamine release is highly significant (*r* = 0.67, *p* = 0.0007) (Fig. 2c) and slightly improved



Fig. 1 Changes of IgE in rat serum after immunization. Total IgE (ng/ml) and anti-egg albumin IgE antibody (units/ml) measured in rat serum at different days after and just prior to immunization with $70 \mu\text{g}$ of egg albumin in pertussis vaccine.

It is a well known fact that rats from some strains are difficult to sensitize to obtain specific IgE antibodies (Jarrett 1978; Karlsson et al. 1979b) as well as good histamine release from isolated mast cells after challenge with purified antigen without serum factors (e.g. phosphatidylserine) (Norm 1968; Sydöhm & Uvnäs 1976). We have also seen a rather great variation in the response within a group of animals and it is therefore advantageous to be able to select out the poor or non responders. By the use of these techniques (PRIST, PRAST) we have tried to find a correlation between IgE levels (total or specific) and anaphylactic histamine release that eventually would enable us to predict the degree of sensitization in one single rat. The histamine release studies were performed in an *in vitro* system using isolated rat mast cells and histamine was measured by a fluorescent technique (Shore et al. 1959). The mast cells were isolated from Hooded Lister rats as this strain has been found to give good IgE antibody responses (Bennlich et al. 1978) which enables the study of anaphylactic histamine release without the addition of exogenous factors like phosphatidylserine (Sydöhm et al. 1979).

MATERIALS AND METHODS

Egg albumin was purchased from Difco Laboratories, Detroit, Michigan, USA. Ficoll from Pharmacia Fine Chemicals AB, Uppsala, Sweden, and pertussis vaccine (lot no. 120 274) from Statens Serum Institut, Copenhagen, Denmark. Inbred Hooded Lister rats originating from rats purchased from Møllegaard A/Laboratorium ApS, L. Skensved, Denmark, were used. All other materials were obtained from the usual commercial sources. Due to refined purification methods by many manufacturers, the B. pertussis vaccine has lost its adjuvant activity on the IgE

production in rats, presumably because of loss of the lymphocytosis promoting factor as reported by Tada et al. (1972). However, we have found that the Danish purified B. pertussis still possesses high adjuvant activity.

Immunization of rats. Male rats were injected s.c. with 1 ml of pertussis vaccine together with $70 \mu\text{g}$ egg albumin per animal. Mast cells were usually taken from the rats from the rats before immunization and at day 5 and 11 after immunization and finally when the rats were killed for isolation of mast cells. About 1 ml of blood was collected by cutting the tail and allowed to clot for 15 min at RT before centrifugation, 15 000–20 000 $\times g$ for 15 min at 4°C . The serum was kept at -20°C before testing.

Determination of IgE in rat serum. Total IgE and IgE antibody (egg albumin specific) were determined by solid phase radioimmunoassay techniques earlier described for human IgE (Ceska & Lundkvist 1971; Wide et al. 1967; Wide et al. 1977) and modified for rat IgE. Total IgE, as measured by PRIST (paper radioimmunoassay) based on paper disc coupled anti rat IgE antibodies of rabbit origin, an IgE myeloma standard (IR2) and immunosorbent purified ^{125}I -anti Fc- ϵ (rat) antibodies as expressed in ng per ml (Karlsson et al. 1979a). IgE antibody against egg albumin as determined by PRAST (paper radioallergy sorbent test) based on paper disc coupled antigen (egg albumin), egg albumin positive rat standard serum and immunosorbent purified ^{125}I -anti Fc- ϵ (rat) antibodies was expressed as units per ml where 1 unit of specific IgE antibody corresponded to less than 1 ng of total IgE (Karlsson et al. 1979b).

Isolation of mast cells. Mast cells were collected from the pleural cavities (Sydöhm & Uvnäs 1976) of immunized rats and isolated by density gradient centrifugation on Ficoll according to the method of Thon & Uvnäs (1967). The mast cells were washed three times at 20°C with an isotonic saline solution containing 10^{-4} M (Na_2HPO_4 + K_2HPO_4 , 67 mM) pH 6.3 and human serum albumin (1 mg/ml).

Incubation procedure. The isolated mast cells were incubated with antigen (10 $\mu\text{g}/\text{ml}$) for 10 min at 37°C in incubation medium and the mast cell concentration was usually about 5000 cells/ml.

The standard incubation medium was an isotonic saline solution (NaCl 137 mM, KCl 2.7 mM, CaCl_2 1.8 mM, MgCl_2 1 mM) containing 10^{-4} M (Na_2HPO_4 + K_2HPO_4) phosphate buffer (67 mM) pH 6.7 and human serum albumin (0.5 mg/ml). The incubation was terminated by placing the tubes in ice water and centrifuged (350 $\times g$) for 10 min at 4°C . The supernatants were decanted into new tubes and 0.1 ml of 0.1 M HCl was added to the cell residues. The supernatants and the cell residues were heated in a boiling water bath for 5 min. 1.8 ml of incubation medium was added to the cell residue to readjust the volume to 1 ml. Histamine was determined both in the supernatant and the cell residues by the method of Shore et al. (1959) omitting the extraction procedure (Bergendorff & Uvnäs 1977). Histamine release was expressed as percentage of total histamine. The spontaneous histamine release has been subtracted from the values presented. The spontaneous histamine release from mast cells of immunized Hooded Lister rats averaged $8.8 \pm 0.7\%$ ($n=11$).

Table 2. Correlation between histamine release and serum IgE

Total and basic total IgE (ng/ml) and specific IgE antibody (units/ml) determined in Hooded Lister rat serum prior to immunization, at day 11 after immunization or at the death-day is correlated to the histamine release (%) after addition of 10 µg/ml of egg albumin (10 min incubation at 37°C) to isolated mast cells. Partial correlation was calculated as described by Spear (1961). The variables are histamine release (1), specific IgE antibody day 11 (2) and basic total IgE (3). The partial correlation coefficient r_{12} is then the correlation between histamine release and basic total IgE keeping the specific IgE antibody constant

Correlation between histamine release (1) and	Correlation coefficient	Significance level	Partial correlation coefficient
Basic IgE (3)	0.55		-0.65 (r_{12} , IgE antibody constant)
Total IgE (at 11)	-0.36	N.S.	
Total IgE (death-day)	-0.19	N.S.	
IgE antibody (at 11) (2)	0.61		0.68 (r_{12} , basic IgE constant)
IgE antibody (death-day)	-0.05	N.S.	
IgE antibody/basic IgE (at 11)	0.67		
IgE antibody/basic IgE (death-day)	0.37	N.S.	

N.S. not significant $\rightarrow 0.001 < p < 0.01$ $p < 0.001$

Sydbom et al. 1979). Our original rationale for using Hooded Lister rats was their high basic levels of serum IgE (Karlsson et al. 1979) and the subsequent finding of good responsiveness to antigen challenge with good histamine release from isolated mast cells (Sydbom et al. 1979; Pauwels et al. 1979).

It was therefore near at hand to assume that high basic total IgE levels would correspond to high histamine releasing capacity. However we found that very high basic levels of serum IgE counteracted the histamine release. This could be due to a competition for the mast cell receptors between the basic total IgE present in serum and specific IgE antibody synthesized as a result of the immunization. Basic total IgE may fluctuate in both immunized and nonimmunized animals due to environmental factors (Karlsson et al. 1979a).

As expected the level of specific IgE antibody is significantly correlated to the histamine releasing capacity of the mast cells (Fig. 2b). This significant correlation is restricted to the specific IgE antibody on day 11 and cannot be seen for specific IgE antibody on the day of death. This might be due to the different half-lives of IgE in serum and on mast cells. Tada et al. (1975) have calculated the half-life to be 12 hours in rat serum and 7.4 days on the mast cell surface. This means that the serum levels of specific IgE antibody can be very low even at a time when the mast cells may be loaded and therefore show high histamine releasing capacity. The correlation between histamine release and the

specific IgE antibody should therefore be more significant when using the maximal specific IgE antibody levels, here on day 11, i.e. the highest specific IgE antibody concentration that the mast cells have been exposed to. In view of the competition situation the finding that the ratio of specific IgE antibody over total IgE is somewhat better correlated with the histamine release than specific IgE antibody itself is not unexpected. So in spite of a correlation coefficient not being very impressive it can be concluded that if a rat shows a low basic total IgE level prior to immunization and a high specific IgE antibody level on day 11 after immunization, there is a very high probability for high antigen induced histamine release from isolated mast cells from that rat.

In conclusion we found no correlation between specific IgE antibody on the day of death and histamine release but a significant negative correlation between basic total IgE and histamine release and a significant positive correlation between specific IgE antibody on day 11 and histamine release from isolated sensitized mast cells challenged with antigen. The correlation coefficients are however not very impressive and there could be a number of explanations for this. We have not measured the IgG antibody levels and must take into account the influence they can have on the histamine release situation. Also local cellular differences can be of importance as Yamamoto et al. (1974) have reported that the antigen induced histamine release

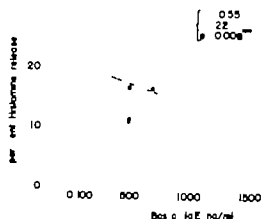


Fig. 2a. Correlation between basic total IgE and histamine release. Basic total IgE (ng/ml) was measured in rat serum collected just prior to immunization with 20 μ g of egg albumin in pertussis. Histamine release (%) was measured after addition of 10 μ g/ml of egg albumin (10 min incubation at 37°C) to isolated rat mast cells taken between day 1 and 27 after immunization. (Basic total IgE was defined as total serum IgE when measured on day 0 or at the latest on day 5 after immunization. There were no significant difference between IgE levels on day 0 and day 5 (Table 1).

than when comparing the specific IgE antibody alone with histamine release. This is true for day 11 but there is no significant correlation when using the values from the time of death (Table 2). When three or more variables affect each other and cooperate this can be evaluated either by partial correlation or by forming a ratio between two of the variables. Both ways were tested and gave a better

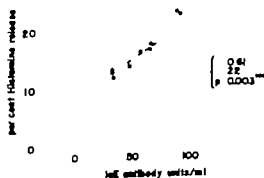


Fig. 2b. Correlation between specific IgE antibody (day 11) and histamine release. Specific IgE antibody (units/ml) was measured in rat serum collected at day 11 after immunization with 20 μ g of egg albumin in pertussis. Histamine release (%) was measured after addition of 10 μ g/ml of egg albumin (10 min incubation at 37°C) to isolated rat mast cells taken between day 12 and 27 after immunization.

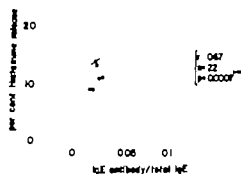


Fig. 2c. Correlation between specific IgE antibody/total IgE (day 11) and histamine release. The ratio of specific IgE antibody (units/ml) over total IgE (ng/ml) both measured in rat serum collected at day 11 after immunization with 20 μ g/ml of egg albumin (10 min incubation at 37°C) to isolated rat mast cells taken between day 12 and 27 after immunization.

correlation of about the same magnitude. The correlation coefficient between specific IgE antibody (day 11) and histamine release was 0.61 and increased to 0.68 when calculated with partial correlation (Spiegel 1961) and to 0.67 when using a ratio (Table 2).

DISCUSSION

The specific IgE antibody in serum from immunized Hooded Lister rats show a maximum between day 11 and 14 (Fig. 1) in agreement with earlier studies (Karlsson 1978). The total IgE time course pattern is under the experimental conditions used rather similar to the specific IgE antibody but declines faster, possibly because the increase in total IgE is an effect of adjuvant stimulation of already existing IgE producing cells as after reimmunization and therefore of a different nature than the expression of IgE antibody after primary immunization.

The finding that there is a significant negative correlation between the basic total IgE before immunization and the histamine release from isolated rat mast cells challenged with antigen was somewhat unexpected (Fig. 2a). Using a pure system for histamine release studies, that is isolated mast cells instead of mixed peritoneal cells, a pure antigen and not horse serum and without the addition of phosphatidylserine will result in very low histamine release (4-9%) from mast cells originating from Sprague Dawley rats (Stechschulte & Austen 1974).

Fibre types in human abdominal muscles

T. HÄGGMARK and A. THORSTENSSON

Department of Physiology III, Karolinska Institute, and the Department of Surgery, Karolinska Späkhuset, Stockholm, Sweden

HÄGGMARK T & THORSTENSSON A. Fibre types in human abdominal muscles. *Acta Physiol Scand* 1979; 107: 319-325. Received 23 April 1979. ISSN 0001-6772. Department of Physiology III, Karolinska Institute and the Department of Surgery, Karolinska Späkhuset, Stockholm, Sweden.

Histochemical muscle fibre composition was studied in biopsies from the four different muscles of the abdominal wall (rectus abdominis, RA, obliquus externus, OE, obliquus internus, OI and transversus abdominis, Tr) in 13 normal human subjects (9 females and 4 males, age 24-55 years) undergoing gall-bladder surgery. Muscle fibres were classified as Type I (IA, IB or IC) on the basis of their myofibrillar ATPases pH lability. There were large inter-individual variations in fibre composition, however, in general the differences between the different muscles were minor or non-existent. Mean fibre distribution ranges were 35-54% I, 15-23% II A, 21-28% II B and 0-1% II C fibres. The least fibre diameters were similar for all types and muscles (range of means 50-54 μ m) except for Tr, in which the Type II fibres were smaller (mean 45 μ m). There was a high correlation in the size of Type I vs. II fibres and Type II A vs. II B fibres in all layers. The oxidase potential (NADH-diphosphorase staining intensity) appeared high in Type I fibres and low in Type II fibres, irrespective of subgroups. Thus, based on histochemical fibre composition, the different abdominal muscles appear to have similar functional capacity. However, functional differences between individuals were indicated by the large inter-individual variation in muscle fibre distribution.

Key words: Muscle fibre composition, muscle fibre size, human abdominal muscles.

Human skeletal muscles contain a varying distribution of muscle fibre types, most commonly distinguished with the histochemical staining for myofibrillar ATPase and classified as Type I (ST) or Type II (FT), with subgroups II A, II B and II C (see e.g. Sjölin et al. 1977). The fibre types differ in metabolic profile (Essen et al. 1975; Thorstensson et al. 1977), contractile properties and fatigability although the direct evidence for these latter aspects is thus far relatively incomplete in humans (see however Eberstein & Goodgold 1968; Buchthal & Schmalbruch 1970, cf. also Thorstensson 1976). Thus, the distribution of histochemical fibre types in a muscle gives an indication of its functional capacity, e.g. the predominance of Type I fibres in the slow soleus muscle (Gollnick et al. 1974; see also Burke & Edgerton 1975).

The information about fibre distribution in the trunk muscles is scarce. Of the four muscles in the abdominal wall the rectus abdominis (RA) has been reported to consist of an approximately even dis-

tribution of Type I and Type II fibres but with large individual differences (range 32-65% Johnson et al. 1973; Colling-Sahlén 1979). No corresponding data is available on the obliquus externus (OE), obliquus internus (OI) or transversus abdominis (Tr) muscles.

The muscles of the abdominal wall control the movements of the trunk and regulate the pressure within the abdominal cavity. One important function of this pressure, which may exceed the intrathoracic pressure, may be to transform the abdominal cavity into a shock-absorber that helps the spinal column to support part of the static and dynamic load of the upper part of the trunk (e.g. Bartelink 1957; Morris et al. 1961; Grillner et al. 1978). In both trunk control and pressure regulation there appear to be differences between the individual abdominal muscles. RA, OE and OI perform ventroflexion whereas OE and OI are mainly responsible for lateral flexion and rotation (Floyd & Silver 1950; Partridge & Walters 1959). The differences in

was different in different target organs tested. The response of a single mast cell is therefore probably the result of the histamine releasing capacity of the single cell as well as the IgE situation on the mast cell surface, local differences and dependence of other factors and other cells.

This study was supported by grants from the Swedish Medical Research Council (B77-04X 39-13A, B78-04X 39-14B and project No. 13X 3556).

REFERENCES

- BAZIN H, BECKERS A, DECKERS C & MORI AMÉ M 1973 Transplantable immunoglobulin-secreting tumours in rats. V. Monoclonal immunoglobulins secreted by 250 ileocecal immunocytomas in LOU/Wistar rats. *J Natl Cancer Inst* 51: 1359-1361.
- BAZIN H, QUERINJEAN P, BECKERS A, HEREMANS J F & DESSY F 1974 Transplantable immunoglobulin secreting tumours in rats. IV. Sixty-three IgE secreting immunocytoma tumours. *Immunol* 76: 713-723.
- BENNICH H, ELLERSON J R & KARLSSON T 1978 Evaluation of basic serum IgE levels and the IgE antibody response in the rat by radioimmunoassays. *Immunol Rev* 41: 261-287.
- BERGENDORFF A & UYNAS B 1972 Storage of 5-hydroxytryptamine in rat mast cells: Evidence for an ionic binding to carboxyl groups in a granule heparin-protein complex. *Acta Physiol Scand* 84: 320-331.
- CESKA M & LUNDKVIST U 1972. A new and simple radioimmunoassay method for the determination of IgE. *Immunochimistry* 9: 1021-1030.
- ELGEFORS B, JULIN A & JOHANSSON S G O 1974 Immunoglobulin E in bronchial asthma. *Acta Allergologica* 29: 327-336.
- HENDERSON L L, SWEDLUND H A, van DELLEN R G, MARCOUX J P, CARRIER H M, PETERS G A & GLEICH G J 1971 Evaluation of IgE tests in an allergy practice. *J Allergy Clin Immunol* 48: 361-365.
- JARRETT E E. E. 1978 Stimuli for the production and control of IgE in rats. *Immunological Rev* 41: 5-76.
- JARRETT E E. E. & STEWART D C 1973 The significance of circulating IgE: Correlation of amount of circulating reaginic antibody with cutaneous sensitivity in the rat. *Immunology* 4: 37-45.
- KARLSSON T 1978. Immunoglobulin E and the mast cell. The rat as an animal model in allergy research. Doctoral thesis from the faculty of medicine, Uppsala University, Uppsala, Sweden. ISBN 91 506-0148.
- KARLSSON T, ELLERSON J R, DAHLBOM I & BENNICHI H 1979 Analysis of the serum IgE levels in non-immunized rats of various strains by a radioimmunoassay. *Scand J Immunol* 9: 217-228.
- KARLSSON T, ELLERSON J R, HAIG D M, JARRETT E E. E. & BENNICHI H 1979 A radioimmunoassay for evaluation of the IgE and IgG antibody responses in the rat. *Scand J Immunol* 9: 229-238.
- NORN S 1968. Antigenic histamine release from fractionated and unfractionated peritoneal cells from sensitized rats. *Acta Pharmacol Toxicol* 76: 373-383.
- PAUWELS R, BAZIN H, PLATTEAU B & van der STRAETEN M 1979 Relation between total serum IgE levels and IgE antibody production in rats. *Int Archs Allergy Appl Immunol* 58: 351-357.
- SHORE P A, BURKHALTER A & COHN V H JR 1959 A method for the fluorimetric assay of histamine in tissue. *J Pharm Exp Ther* 177: 182-186.
- SPIEGEL M R 1961 Theory and problems of statistics, p. 772. Schaum Publ. Co., New York.
- STAHL SKOV P, NORN S & WEEKE, B 1977 Basophil histamine release in patients with hay fever. Results compared with specific IgE and total IgE during immunotherapy. *Clin Exp Immunol* 77: 43-49.
- STECHSCHULTE D J & AUSTEN K F 1974 Phosphatidylserine enhancement of antigen-induced mediator release from rat mast cells. *J Immunol* 111: 970-978.
- STECHSCHULTE D J, ORANGE, R. P & AUSTIN K F 1970 Immunohistochemical and biologic properties of rat IgE. I. Immunohistochemical identification of rat IgE. *J Immunol* 105: 108L-1086.
- SYDBOM A & UYNAS B 1976. Potentiation of anaphylactic histamine release from isolated rat peritoneal mast cells by rat serum phospholipids. *Acta Physiol Scand* 97: 2-32.
- SYDBOM A, FREDHOLM B B & UYNAS B 1979 Effect of sensitization on spontaneous and phosphatidylserine-induced histamine release and cyclic AMP and GMP levels in isolated rat mast cell. *Acta Physiol Scand* 106: 473-480.
- TADA T, OKUMURA K, OCHIAI T & IWASA, S 1972 Effect of lymphocytosis-promoting factor of *Bordetella pertussis* on the immune response. II. Adjuvant effect for the production of reaginic antibody in the rat. *Int Arch Allergy* 43: 207-216.
- TADA T, OKUMURA K, PLATTEAU B, BECKERS A & BAZIN H 1975 Half-lives of two types of rat homocytotropic antibodies in circulation and in the km. *Int Arch Allergy* 48: 116-131.
- THON I L & UYNAS B 1967 Degranulation and histamine release: two consecutive steps in the response of rat mast cell to compound 48/80. *Acta Physiol Scand* 71: 301-315.
- WIDE L, BENNICHI H & JOHANSSON S G O 1967 Diagnosis of allergy by an *in vitro* test for allergen antibodies. *Lancet* i: 1105-1107.
- WIDE L, ARONSSON T, FAGERBERG E & ZETTERSTRÖM O 1972 Radioimmunoassay of allergen specific IgE. In *Allergy: Proceedings of the Eight European Congress of Allergy* (Mancini, ed J Chaurin) pp 85-91. Excerpta Medica, Amsterdam.
- YAMAMOTO S, SLO K, FUJIWARA Y, MALDA M & YAMAMURA T 1974 Correlation between *in vitro* anaphylactic histamine release from tissue and reagent titer in rat. *Int Arch Allergy* 47: 329-338.

Table 1 Mean values (\pm S.D.) and ranges for the different muscle fibre characteristics studied in *m. rectus abdominis* (RA), *m. obliquus externus* (OE), *m. obliquus internus* (OI) and *m. transversus abdominis* (Tr)

	RA	OE	OI	Tr
% Type I fibres	55 \pm 8 39-68	58 \pm 11 40-77	56 \pm 13 36-74	46 \pm 4 51-64
% Type II A fibres	22 \pm 9 9-36	21 \pm 13 7-45	23 \pm 11 13-45	15 \pm 8 6-29
% Type II B fibres	24 \pm 5 17-33	21 \pm 8 9-42	21 \pm 9 5-37	28 \pm 8 1-37
Mean Type I fibres, μ m	50 \pm 10 35-67	50 \pm 8 36-63	50 \pm 14 32-71	49 \pm 10 31-61
Mean Type II A fibres, μ m	52 \pm 14 34-83	52 \pm 14 37-71	51 \pm 15 34-82	47 \pm 9 31-62
Mean Type II B fibres, μ m	52 \pm 15 34-84	54 \pm 12 33-73	52 \pm 15 31-75	43 \pm 8 29-55
rect index	0.99 \pm 0.34	0.88 \pm 0.22	0.96 \pm 0.26	1.23 \pm 0.25
% Type II fibres	0.45-1.60	0.55-1.28	0.64-1.38	0.97-1.71
di area	54 \pm 14	54 \pm 14	55 \pm 18	60 \pm 7
% I fibres, %	29-73	33-72	28-85	52-75

thoroughly evaluate the occurrence of fibre grouping (cf. Johanson et al. 1973). No difference was observed between males and females.

The distribution of the two main types of muscle fibres, Type I and II, was similar in all four muscle layers (mean range 55-58% Type I fibres, Table 1). However, within each muscle layer the variation in fibre composition was large between individuals (Fig. 2) especially for the RA, OE and OI muscles (total range 36-77% Type I fibres, Table 1). There was a significant correlation between % Type I fibres in the RA, OE and OI muscles ($r=0.6-0.8$, $P<0.01$). Three persons showed a predominance of Type II fibres in these muscles (Fig. 2). In the Tr muscle, on the other hand, a smaller range of fibre distribution was observed and none of the eight cases showed a predominance of Type II fibres (Fig. 2). The distribution of Type I fibres in Tr was not correlated to that of the other abdominal muscles.

Also, with respect to the distribution of subgroups of the Type II fibres (II A and B), no significant differences were seen between the different muscle layers. Large variations between individuals were observed in each layer (Table 1). There was no difference between % Type II A and II B fibres for RA, OE and OI muscles. In Tr, however, the % II B fibres was higher than the % II A fibres in 7 of

the 8 subjects (the difference was significant at the 5% level) and a high % II B fibres also corresponded to a low % II A fibres in the Tr muscle ($r=-0.86$, $P<0.01$). Relating percentage distribution of Type II subgroups to % Type I fibres, significant positive correlation coefficients ($r=0.70-0.87$, $P<0.01$) were found between % II A and % I fibres within the RA, OE and OI muscles.

There were no differences between the different abdominal muscles with respect to Type I fibre size

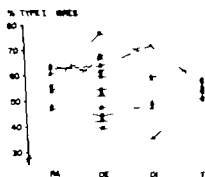


Fig. 2. Individual values for the relative distribution of Type I fibres in *m. rectus abdominis* (RA), *m. obliquus externus* (OE), *m. obliquus internus* (OI) and *m. transversus abdominis* (Tr). The values for each individual are connected with thin lines.

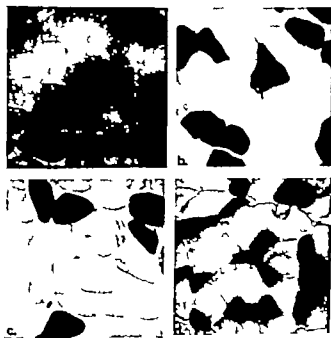


Fig. 1 Cross-sections of muscle biopsy specimens stained for myofibrillar ATPase after preincubation at pH 10.3. The biopsies were taken from (a) m. rectus abdominis, (b) m. obliquus externus, (c) m. obliquus internus, and (d) m. transversus abdominis in the same person. (Type I fibres stain light and Type II fibres dark with this procedure.)

anatomical arrangement between the muscles also influence their involvement in the production of intraabdominal pressure (IAP) where the electromyographic activity of RA for example appears to be less closely related to changes in IAP (Bar telink 1957, Morris et al 1961, Grillner et al 1978). In addition it has been shown that the abdominal muscles are active to maintain postural stability (e.g. Klausen 1965) and during a variety of natural movements including locomotion (Grillner et al 1978 and unpubl.).

The present study was undertaken to investigate the intra- and interindividual differences in muscle fibre composition in the four muscles of the abdominal wall to obtain a basis for evaluation of their specific functional capacities.

MATERIAL AND METHODS

Muscle specimens were obtained during surgery from 13 subjects: 9 females and 4 males. Their age and weight ranged between 4–55 years (median 44 years) and 57–76 kg (median 60 kg) respectively. The patients were well informed before the operation and gave their consent to participate.

The subjects were of normal body constitution and do not suffer from any neuromuscular disorder. They were all undergoing gall-bladder surgery. All were operated with an oblique incision 10–15 cm long, beneath the costal margin on the right side. The different muscle layers were identified as they were cut and the biopsies (approx. 0.5 g) were taken surgically from the different muscles: m. rectus abdominis (RA), m. obliquus externus abdominis (OE), m. obliquus internus abdominis (OI) and m. transversus abdominis (Tr). Due to technical difficulties, biopsies from Tr were obtained in only 8 cases (5 females and 3 males).

The biopsies were directly prepared for histochemical analysis and frozen in isopentane, cooled with liquid nitrogen. Until further analysis was performed, the muscle samples were kept at -80°C in a freezer.

The histochemical analyses were carried out on 19 μm thick serial cross-sections cut in a cryostat at -23°C . Muscle fibre types were classified on the basis of the pH-lability of their myofibrillar ATPases (Brooke & Kaiser 1970a and b). Serial sections were preincubated at pH 10.3 and 4.3 to differentiate the two main fibre types Type I (acid stable ATPase) and Type II (alkaline stable ATPase) and at pH 4.6 to differentiate the subgroups of Type II fibres. Type II A and Type II B fibres, Type II A having a more acid labile myofibrillar ATPase and thus staining lighter than the Type II B fibres at pH 4.6 (cf. Fig. 4). Undifferentiated fibres, i.e. fibres showing an even dark staining intensity at all pH-levels, were called Type IIC according to Brooke & Kaiser (1970a). No muscle sample contained less than 700 fibres. The average number of fibres counted from each biopsy was 763 (s.d. 47). The oxidative potential of the fibres was estimated on serial sections with the histochemical staining method for NADH-diaphorase (Novikoff et al 1961). The staining intensity of the fibres was arbitrarily and subjectively classified as dark, medium or light and the sections were then matched with the ATPase stain (pH 4.6) for fibre type identification. Comparison of staining intensity as done on each muscle sample separately, no evaluation of absolute staining intensity was performed between layers or subjects.

Fibre sizes were estimated with the method of least diameter (Dubowitz & Brooke 1973). A minimum of 30 fibres was included in the calculation of mean least diameter for each fibre type. Assuming circular shaped fibres the area ratio between Type I and Type II fibres was calculated as well as the relative area occupied by Type I fibres (see Gollnick et al 1977 and Thorstensson 1978).

Differences were tested for significance with Student's *t*-test.

RESULTS

All four of the abdominal muscles demonstrated a mosaic pattern of Type I IIA and IIB fibres (IIC fibres comprised only 0–3% of the total number of fibres). The fibre types appeared evenly distributed throughout the muscle sample cross sections (cf. Figs. 1 and 4). No attempt was, however, made to



Fig. 4. Serial sections of muscle biopsy from the obliquus internus muscle stained for (a) myofibrillar ATPase after preincubation at pH 4.6 (Type I and IIB fibres stain dark and Type IIA fibres stain light) and (b) NADH diaphorase. Some corresponding fibres are identified and marked in the two pictures.

ing-Saltin (1979) reported that RA contained about twice as many Type IIA fibres as Type IIB fibres, which is similar to what has earlier been found for the vastus lateralis muscle (see Saltin et al 1977). In the present study nearly equal proportions of IIA and IIB fibres were seen in RA as well as OE and OF, whereas Tr demonstrated an even higher percentage Type IIB fibres. Tr also differed from the other layers with respect to fibre size (least diameter), showing smaller Type II fibres. In general, however, the fibre sizes in the abdominal muscles (range 43–54 μm) were in good agreement with those earlier reported for other normal human skeletal muscles (for refs see Saltin et al 1977) including RA, for which muscle Polgar et al

(1973) found average least diameters of 43 μm (Type I fibres) and 55 μm (Type II fibres) in 6 subjects investigated post mortem.

Thus, the abdominal muscles appear to have similar characteristics to the majority of the other human skeletal muscles with respect to fibre type distribution. The deviations seen in Type II subgroup composition and fibre size particularly in Tr might be related to the activity pattern of the muscles (and of the subjects in general). All the subjects in the study had a relatively low level of daily physical activity although none of them was extremely inactive. Increases in the relative number of Type IIA fibres and in the size of a specific fibre type have been reported in connexion with physical

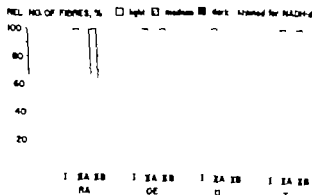


Fig. 5. Mean relative number of muscle fibres of each type and within each individual muscle that were independently rated as having dark, medium or light staining intensity for NADH-diaphorase. Abbreviations are the same as in Fig. 2.

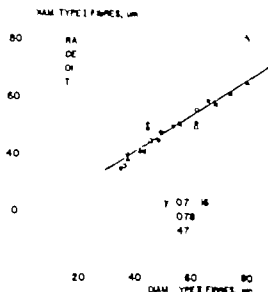


Fig. 3. The relationship between the mean values for least fibre diameter of Type I and Type II fibres in the four abdominal muscles in the different subjects. Abbreviation and symbols are the same as in Fig. 1. Line of identity is given along with the linear regression line for all points ($r = 0.78$, $P < 0.01$).

(least diameter Table 1) whereas the Type II fibres (both II A and B) were smaller in Tr than in the other layers ($P < 0.05$ cf. Fig. 1). Mean values and ranges are shown in Table 1. A comparison of the least diameters of the different fibre types within the different layers showed significant ($P < 0.05$) differences only for OE in which Type II fibres were larger than Type I fibres and for Tr which showed the opposite pattern and in which muscle also the II A fibres were larger than the II B fibres. Within all layers there were highly significant correlations in fibre sizes between Type I and II fibres ($r = 0.86$ – 0.97 , $P < 0.01$, Fig. 3) as well as between Type II A and II B fibres ($r = 0.76$ – 0.87 , $P < 0.01$).

The calculated ratio between Type I and II fibre area demonstrated large differences between individuals (Table 1). However, there were no significant differences between the RA, OE and OI muscles. The Tr muscle had a higher Type I/Type II area ratio than the other muscles (see above). Consequently, the relative distribution of Type I fibres (% Type I area, Table 1) was higher for the Tr muscle than shown by just the percentage value. However, there were still no significant differences (or correlations) in fibre distribution (% Type I area) between Tr and the other abdominal muscle layers.

The majority of the Type I fibres (86–100) stained dark for NADH-diaphorase compared to the other fibre types in all layers (Figs. 4 and 5). Type I fibres were found with a light staining intensity. Relatively small differences were present between II A and II B fibres, the majority of both subgroups stained light for NADH-diaphorase in all layers (Figs. 4 and 5). Not more than a third of the II A fibres had a medium staining intensity in any of the samples tested. Type II B fibres with a medium staining intensity were found only occasionally (Fig. 5).

DISCUSSION

All four muscle layers of the anterior abdominal wall contained a mosaic of Type I and Type II fibres without obvious signs of fibre grouping. The proportion of Type I and Type II fibres was about equal in all muscle layers, the mean range was 55–58% Type I fibres. No differences were observed between males and females, but large inter-individual differences in fibre composition were present. These observations on the abdominal muscles are similar to what has earlier been reported for the majority of skeletal muscles studied in normal man (e.g. Johnson et al. 1973). Some exceptions exist, however, e.g. the soleus muscle, which shows a consistent predominance of Type I fibres (Gottlieb et al. 1974; see also Saltin et al. 1977).

The fibre compositions of RA, OE and OI were shown to be correlated with one another. Individuals could be found with either a predominance of Type I (slow) or Type II (fast) fibres in these muscles. It is not known if, for example, slow abdominal muscles correspond also to slow characteristics of other muscles in the same individual. Tendencies towards such intraindividual correlations in fibre composition between different muscles have been reported for some extremity muscles (see Saltin et al. 1977). However, these studies were limited to a small number of subjects in autopsied post mortem.

Up to now, fibre composition of the abdominal muscles has only been studied in the RA muscle. The present finding of a mean of 55% Type I fibres in RA is in good agreement with the values earlier obtained by Johnson et al. (1973, 46%) and Colling & Saltin (1979, 51%). Both authors also report large differences between individuals (3–76% Col-

- twitch fibres in human skeletal muscle. *Am J Physiol* 235: 505-541.
- ESSEN, B. JANSSON E., HENRIKSSON J. TAYLOR, A. W. & SALTIN B. 1975 Metabolic characteristics of fibre types in human skeletal muscles. *Acta Physiol Scand* 95: 153-165.
- FLOYD, W. F. & SILVER, P. H. S. 1951 Electromyographic study of patterns of activity of the anterior abdominal wall muscles in man. *J Anat* 84: 132-145.
- GOLLNICK, P. D. ARMSTRONG, R. B. SAUBERT IV C. W. MEHL, K. & SALTIN B. 1972 Enzyme activity and fibre composition in skeletal muscle of untrained and trained men. *J Appl Physiol* 33, 31L: 319.
- GOLLNICK, P. D. SJÖDIN B. KARLSSON J. JANSSON, E. & SALTIN B. 1974 Human soleus muscle. A comparison of fiber composition and enzyme activities with other leg muscles. *Pflügers Arch* 348: 247-255.
- GRIFFNER, S. NILSSON J. & THORSTENSSON A. 1978 Intra-abdominal pressure changes during natural movements in man. *Acta Physiol Scand* 103: 275-281.
- HENRIKSSON J. 1976 Human skeletal muscle adaptation to physical activity. Thesis, Karolinska Institute, Stockholm.
- JOHNSON, M. A. POLGAR, J. WEIGHTMAN D. & APPLETON D. 1973 Data on distribution of fibre types in thirty-six human muscles. An autopsy study. *J Neurol Sci* 18: 111-129.
- KLAUSEN, K. 1965 The force and function of the loaded lumbar spine. *Acta Physiol Scand* 65: 176-190.
- MORRIS, J. M. LUCAS, D. B. & BRESLER, M. S. 1961 Role of the trunk in stability of the spine. *J Bone Jt Surg (Amer)* 43: 327-351.
- NACHEMSON A. L. 1971 Low back pain, its etiology and treatment. *Clin Med* 71: 18-24.
- NOVIKOFF A. B. SHIN W. & DRUCKER, J. 1961 Mitochondrial localization of oxidation enzymes: staining results with tetrazolium salts. *J Biochem Biophys Cytol* 9: 47-61.
- PARTRIDGE M. J. & WALTERS, E. 1959 Participation of the abdominal muscles in various movements of the trunk in man. *Phys Ther Rev* 39: 791-800.
- POLGAR, J. JOHNSON M. A., WEIGHTMAN D. & APPLETON D. 1973 Data on fibre size in thirty six human muscles. An autopsy study. *J Neurol Sci* 19: 307-318.
- SALTIN B., HENRIKSSON J. NYGAARD E., ANDERSEN P. & JANSSON E. 1977 Fiber types and metabolic potentials of skeletal muscles in sedentary man and endurance runners. *Ann NY Acad Sci* 301: 3-29.
- THORSTENSSON A. 1976. Muscle strength, fiber types and enzyme activities in man. *Acta Physiol Scand*, Suppl. 443.
- THORSTENSSON A., TESCH P. SJÖDIN B. & KARLSSON J. 1977 Actomyosin ATPase myokinase CPK and LDH in human fast and slow twitch muscle fibres. *Acta Physiol Scand* 99: 225-229.

training (Henriksson 1976, Thorstensson 1976). A relatively low level of utilization of the abdominal muscles, particularly the Type II fibres, might also be the explanation for the low oxidative potential seen in the Type II A fibres as compared to what is normally found in extremity muscles (cf. Essén et al. 1975, Henriksson 1976).

The abdominal muscles function to control the trunk both during posture (e.g. Klausen 1965) and natural movements including locomotion (Grillner et al. 1978 and unpubl.). This includes the regulation of the intraabdominal pressure (IAP). This pressure can act to support the upper part of the body and thereby take up part of the load on the spine (for discussion and refs. see Grillner et al. 1978). The differentiation of the abdominal wall into different individual muscles with varying main fibre directions makes possible a refined control of the movements of the trunk. The coordination of the different muscles varies in different movements as evidenced by the electromyographic activity (EMG) (Floyd & Silver 1950, Partridge & Walters 1959, Carlson et al. unpubl.). The differences in anatomical arrangement seem to have an effect also on the involvement of the individual muscle layers in regulating the IAP. From an anatomical point of view the Tr appears to have a mechanical advantage in the production of IAP since it is forming a girdle around the abdominal cavity. EMG recordings with surface electrodes placed over the OE muscles (probably also picking up signals from the OI and Tr) have shown close relations with changes in IAP (Bartelink 1957, Morris et al. 1961, Grillner et al. 1978) whereas the RA activity appeared less consistent in this respect. Thus functional differentiation exists between the different abdominal muscles. However, this does not appear to correspond to a differentiation between the layers in terms of fibre distribution. The even distribution of fibre types indicates a functional capacity for both fast contractions and endurance in each muscle layer. This arrangement appears appropriate in light of the wide spectrum of demands that are put on the abdominal muscles during natural movements. These functional demands may include maximal isometric contraction as in lifting (e.g. Bartelink 1957, Morris et al. 1961), fast compensatory contractions as in walking down from steps or repeated submaximal contractions in association with the IAP changes occurring with each step during normal locomotion (Grillner et al. 1978).

The large differences in fibre type distribution between individuals indicate differences in performance capacities. It is conceivable that all else being equal, a person with a high proportion of Type II (particularly Type IIB) fibres in the abdominal muscles will be more affected by fatigue and thus be less capable of producing any appropriate fast corrective movements of the trunk or accomplish an adequate intraabdominal pressure. On the other hand, a low proportion of Type II fibres in the abdominal muscles could also under non-fatigued conditions decrease the capacity to produce a fast rise in tension (and IAP) in response to sudden loads on the body, e.g. walking down the stairs or jumping down from a height. In both situations this inadequacy in the functional capacity of the abdominal muscles, due to an extreme muscle fibre composition, would lead to an increased mechanical load on the spine, which may in turn be a detrimental factor in the etiology of back pain (cf. Nachemson 1971).

The authors are indebted to Å. Arvidsson, M. Lindqvist and M. Wilén for skilful technical assistance and to Drs H. Carlsson, S. Grillner and M. Zomlefer for valuable comments on the manuscript.

The study was supported by grants from the Swedish Defense Research Organization (Project No. H657) and the Research Council of the Swedish Sport Federation.

REFERENCES

- BARTELINK, D. L. 1957. The role of abdominal pressure in relieving the pressure of the lumbar vertebral discs. *J. Bone Jt. Surg. (Brit.)* 39: 718-725.
- BROOKE, M. H. & KAISER, K. K. 1970a. Muscle fibre types: how many and what kind. *Arch. Neurol. (Chicago)* 3: 369-379.
- BROOKE, M. H. & KAISER, K. K. 1970b. Three myosin-ATPase systems: the nature of their pH lability and sulphydryl dependence. *J. Histochem. Cytochem.* 18: 670-672.
- BUCHTHAL, F. & SCHMALBRUCH, H. 1970. Contraction times and fibre types in intact human muscle. *Acta Physiol. Scand.* 79: 435-45.
- BURKE, R. E. & EDGERTON, V. R. 1975. Motor unit properties and selective recruitment in movement. *Exercise and Sport Sciences*, vol. 1, pp. 31-81. Academic Press, New York.
- COLLING-SAL, T. A. S. 1979. Enzyme histochemistry on skeletal muscle of the human foetus. *J. Neurol. Sci.* (accept. for publ.).
- DUBOWITZ, V. & BROOKE, M. H. 1973. Muscle biopsy: a modern approach. In: *Major problems in Neurology*, vol. 2. W. B. Saunders, London.
- EBERSTEIN, A. & GOODGOLD, J. 1968. Slow and fast

The effect of propranolol on the serotonin concentration in the portal plasma after vagal nerve stimulation in the cat

GÖSTA PETTERSSON, HÅKAN AHLMAN, HEMENDRA N. BHARGAVA,
ANNICA DAHLSTRÖM, JAN KEWENTER, INGER LARSSON
and JOHN K. SIEPLER

Department of Surgery III and the Institute of Neurobiology, University of Göteborg,
and Department of Pharmacology and Pharmacognosy, College of Pharmacy,
University of Illinois, Chicago, USA

PETTERSSON, G., AHLMAN, H., BHARGAVA, H. N., DAHLSTRÖM, A., KEWENTER, J., LARSSON, I. & SIEPLER, J. K. The effect of propranolol on the serotonin concentration in the portal plasma after vagal nerve stimulation in the cat. *Acta Physiol. Scand.* 1979, 107, 327-331. Received 26 April 1979. ISSN 0001-6772. Department of Surgery III and Institute of Neurobiology, University of Göteborg, and Department of Pharmacology and Pharmacognosy, College of Pharmacy, University of Illinois, Chicago, USA.

Efferent cervical vagal nerve stimulation in the cat caused a marked increase of the portal plasma 5-HT concentration. This increase was more than two-fold within 15 min of stimulation. After cessation of stimulation portal plasma 5-HT returned to basal levels within 10 min. Treatment with the β -adrenoceptor antagonist propranolol, in various doses (0.3–2 mg/kg b.w.t.), did not abolish but significantly reduced the response to vagal stimulation, particularly during the final part of the stimulation period. The results confirm the existence of β -adrenoceptor-mediated release of 5-HT but also suggest that other mechanisms for 5-HT release may be involved in the response on vagal nerve stimulation.

Key words: Portal plasma, serotonin (fluorimetric assay), propranolol, vagal nerve stimulation, cat.

The serotonin (5-HT) in the gut is mainly stored in the enterochromaffin cells (EC) of the mucosa (Omont & Wong 1957; Penttilä 1966). The EC is a local-translated entero-endocrine cell with unique handling properties according to the APUD concept (Pearse 1969). Different populations of EC have been demonstrated to contain a polypeptide, e.g. motilin, substance P or enkephalin in addition to the main 5-HT (Pearse et al. 1974; Pearse & Polak 1975; Aluwet et al. 1978).

EC may release their content of 5-HT after humoral stimuli, such as mechanical stimulation, low pH or hypertonic glucose. However, evidences for a neural release mechanism have also been presented (Burks & Long 1966; Hohenleitner et al. 1971; Tansy et al. 1971; Ahlman et al. 1976). This release appears to be mainly adrenergic in nature, and it is likely that β -adrenoceptor mechanism is involved

(Ahlman et al. 1976b; Pettersson et al. 1978, 1979). These previous studies were made using a cyto-fluorimetric method where the 5-HT content in individual EC was studied after *in vivo* vagal nerve stimulation (Ahlman et al. 1976a, b), after *in vitro* incubations with adrenergic drugs (Pettersson et al. 1978) or transmural field stimulation (Pettersson et al. 1979).

The present investigation was performed to further study the importance of the postulated β -adrenoceptor mechanism for the release of 5-HT from EC into the portal circulation upon vagal nerve stimulation *in vivo* using various doses of the β -adrenoceptor antagonist, propranolol.

MATERIAL AND METHODS

Animals and blood sampling. 23 adult cats of both sexes were used. Prior to the experiments the animals were

Table 1. The 5-HT concentrations ($\mu\text{g/ml}$) in portal plasma of untreated cats, cats with ligated adrenals and cats treated with propranolol (various doses) before, during and after efferent vagal nerve stimulation. Data are S.E.M. Difference from control calculated from the changes in 5-HT levels indicated by * ($P < 0.05$)

	Initial levels 0'	During vagal stimulation			After vagal stimulation		
		5'	10'	15'	20'	25'	30'
Control (n 7)	197 \pm 17	326 \pm 38	443 \pm 49	487 \pm 56	309 \pm 19	208 \pm 29	181 \pm 10
Adrenals ligated (n 4)	202 \pm 19	275 \pm 19*	361 \pm 2*	483 \pm 8	325 \pm 20	272 \pm 15	223 \pm 10
Propranolol, 2 mg/kg (n 6)	267 \pm 24	364 \pm 19	501 \pm 35	257 \pm 15	237 \pm 19*	318 \pm 29	328 \pm 31
Propranolol, 1.05 mg/kg (n 3)	191 \pm 38	256 \pm 61	318 \pm 14	220 \pm 31	232 \pm 24	265 \pm 20	259 \pm 35
Propranolol, 0.105 mg/kg (n 3)	240 \pm 48	332 \pm 37	402 \pm 41	285 \pm 48	281 \pm 48	265 \pm 52	341 \pm 34

the delay in onset of the supramaximal 5-HT response was slower in onset but reached the same maximum level at 15 min stimulation as in the control group (Table 1).

Propranolol did not completely block but reduced and altered the response to vagal stimulation in all three doses tested (Fig. 1 and Table 1). The peak 5-HT levels was now seen after 10 min stimulation (instead of at 15 min as in the control group) followed by a return of plasma 5-HT to basal levels at 15 min stimulation. The difference from control stimulation without propranolol treatment) was statistically significant ($P < 0.05$) for propranolol 0.105 mg/kg already at 5 min stimulation and for all lower propranolol groups at 15 min (end of stimulation) (Table 1). During the first 10 min of stimulation the blockade after the highest dose of propranolol seemed to be less effective although no significant difference between the various doses of propranolol could be demonstrated. The reduction from control of the 5-HT levels after propranolol groups taken together, calculated by difference in one series (Fig. 1) was about 50%. In the propranolol groups there was a minor but constant secondary increase of the portal plasma 5-HT after the end of stimulation at 25 and 30 min.

DISCUSSION

The present study demonstrates a rise of the 5-HT concentration in portal plasma after vagal nerve stimulation. This effect cannot be explained by changes in blood flow since splanchnic blood flow was not reduced but rather increased after vagal stimulation (Hansen 1965, Mattsson 1965). The increase in 5-HT concentration on vagal stimulation is antagonized by propranolol, most obviously

during the final part of the stimulation period. Since even the lowest dose of propranolol tested (0.1 mg/kg) was effective in this respect a specific β -adrenoceptor mechanism seems probable.

As shown in Fig. 1 the 5-HT concentrations in portal plasma during the first 10 min of vagal nerve stimulation in propranolol pretreated cats were still very high. This may be due to a propranolol resistant release of 5-HT to an initially reduced blood flow or a combination of the two alternatives. A reduction of blood flow is likely to occur after propranolol. Furthermore, through its membrane stabilizing effect propranolol inhibits the uptake of 5-HT into platelets. Oral administration of propranolol (3 mg/kg) reduced the 5-HT uptake into platelets by 50% in human expts. (Grobeck et al. 1973). Similar concentrations of propranolol are probably reached after 2 mg i.v. in the present expts. Under normal conditions more than 50% of the 5-HT released from the gut is taken up into platelets before reaching the liver (Jaffe et al. 1977) indicating that inhibition of this mechanism by propranolol may contribute to an increase of the measured portal plasma 5-HT levels. Thus even if the high dose of propranolol further decreased the 5-HT release from EC, this effect may have been masked by the inhibition of the platelet 5-HT uptake resulting in high plasma 5-HT levels.

The present results are in accordance with the previous cytofluorimetric findings that the decrease in intracellular levels of 5-HT in EC after efferent stimulation of the vagal nerves was blocked by propranolol pretreatment. Removal of the superior cervical sympathetic ganglia one week prior to the experiments also blocked the vagally induced 5-HT decrease in EC indicating that adrenergic nerve fibres from these neck ganglia were modulating this

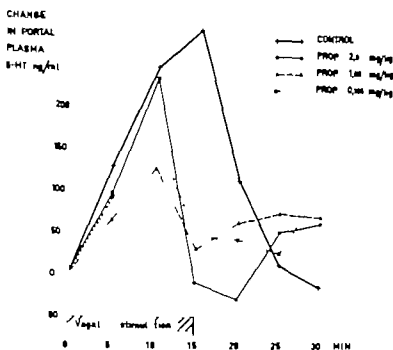


Fig. 1 Diagram illustrating the changes in portal plasma 5-HT concentrations (mean values) on efficient vagal nerve stimulation in untreated cats and cats treated with various doses of propranolol based on the values given in Table 1

fasted for 24 h but had free access to water. Anaesthesia was induced with ether and maintained with chloralose (50 mg/kg of b wt). Blood samples (7 ml each) for assays of 5-HT were drawn before, during and after nerve stimulation (according to the time schedule in Fig. 1) through a heparinized catheter inserted into the portal vein with the tip in the liver hilus region. For volume replacement all animals were given 10 ml of physiological saline through the femoral vein before the initiation of electrical stimulation and additional 10 ml was given during stimulation. Blood samples were stored on ice during the experiments and then centrifuged. The plasma was kept frozen until the assays.

Nerve stimulation. The vagal nerves were dissected free at the cervical level and cut. The distal ends were placed in circular electrodes insulated on the outside. A square wave impulse generator (Grass Instruments Co Model S4) was used for the electrical stimulation. Both vagal nerves were stimulated simultaneously for 15 min with supramaximal parameters: 20 V, 2 ms, 8 Hz. The efficiency of the nerve stimulation was judged by the presence of bradycardia, fall in blood pressure and small bowel contractions.

Experimental groups. 7 cats served as controls. In 4 cats the adrenals were bilaterally ligated. 12 cats were given propranolol (d,l propranolol Isotalol® ICI) in 3 different doses: 2 mg/kg b wt as a bolus dose 20 min before the stimulation (6 cats), 0.75 mg/kg b wt as a bolus dose 70 min before the stimulation and in addition 0.3 mg/kg b wt/15 min as a constant infusion during the stimulation (3 cats), 0.075 mg/kg b wt as a bolus dose 20 min before the stimulation and in addition 0.03 mg/kg b wt/15 min as a constant infusion during the stimulation (3 cats).

Assay of 5-HT in plasma. The plasma concentration of 5-HT was determined by the modified fluorimetric method of Cox & Perbach (1973) for brain tissue. Briefly the method consisted of vortexing 250 µl of plasma with 3 ml n-butanol for 1 min followed by shaking for 5 min on a mechanical shaker at 160 oscillations per minute. The mixture was then centrifuged at 3000 rpm for 5 min at 4°C. A 2.2 ml aliquot of butanol phase was transferred to a tube containing 5 ml of n-heptane and 1.2 ml of 0.1 N HCl containing 0.1% cysteine. The mixture was shaken for 5 min at 160 oscillations per min and then centrifuged at 3000 rpm for 5 min. One ml of aqueous phase was withdrawn and mixed with 0.4 ml of 0.012% o-phthalaldehyde in 10 N HCl. The mixture was heated in boiling water for 10 min. After cooling, the fluorescence of the sample was read at 470 nm after being excited at 360 nm on an Aminco-Bowman spectrofluorometer. The recovery of 5-HT ranged from 72–81% and the assays were reproducible within 5%.

Statistics. Wilcoxon's tests for paired and unpaired data were used.

RESULTS

In the control cats ($n=7$) the vagal nerve stimulation caused a prompt and steady increase in the portal plasma 5-HT levels up to a maximum of 250% of initial levels after 15 min stimulation (Table 1 and Fig. 1). The increase was significant already after 5 min ($P<0.05$). After cessation of stimulation the 5-HT values were normal within 10 min. In the 4

Table 1 The 5-HT concentrations (ng/ml) in portal plasma of untreated cat cats with ligated adrenals and cats treated with propranolol (various doses) before during and after efferent vagal nerve stimulation. Mean values and S.E.M. Difference from control calculated from the changes in 5-HT levels indicated by * ($P < 0.05$)

	Initial levels 0'	During vagal n. stimulation			After vagal n. stimulation		
		5'	10'	15'	20'	25'	30'
Control (n = 7)	197 ± 17	326 ± 38	443 ± 49	487 ± 56	309 ± 19	708 ± 29	181 ± 10
Adrenals ligated (n = 4)	202 ± 19	775 ± 19*	361 ± 22	483 ± 8	325 ± 20	272 ± 15	223 ± 10
Propranolol, 0.5 mg/kg (n = 6)	267 ± 24	364 ± 19	501 ± 35	257 ± 15	237 ± 19*	318 ± 29	328 ± 31
Propranolol, 1.05 mg/kg (n = 3)	191 ± 38	236 ± 61	318 ± 14	220 ± 31	252 ± 24	265 ± 20	259 ± 35
Propranolol, 0.105 mg/kg (n = 3)	240 ± 48	332 ± 37	402 ± 41	285 ± 48*	281 ± 48	765 ± 52	341 ± 34

cats with ligation of the suprarenals the 5-HT response was slower in onset but reached the same maximum level at 15 min stimulation as in the control group (Table 1).

Propranolol did not completely block but reduced and altered the response to vagal stimulation at all three doses tested (Fig. 1 and Table 1). The peak 5-HT levels was now seen after 10 min stimulation (instead of at 15 min as in the control group) followed by a return of plasma 5-HT to basal levels at 15 min stimulation. The difference from control (stimulation without propranolol treatment) was statistically significant ($P < 0.05$) for propranolol 0.5 mg/kg already at 5 min stimulation and for all three propranolol groups at 15 min (end of stimulation) (Table 1). During the first 10 min of stimulation the blockade after the highest dose of propranolol seemed to be less effective although no significant difference between the various doses of propranolol could be demonstrated. The reduction from control of the 5-HT levels after propranolol (groups taken together), calculated by difference in curve areas (Fig. 1) was about 50%. In the propranolol groups there was a minor but constant secondary increase of the portal plasma 5-HT after the end of stimulation at 25 and 30 min.

DISCUSSION

The present study demonstrates a rise of the 5-HT concentration in portal plasma after vagal nerve stimulation. This effect cannot be explained by changes in blood flow since splanchnic blood flow is not reduced but rather increased after vagal stimulation (Kewenter 1965; Martensson 1965). The increase in 5-HT concentration on vagal stimulation was antagonized by propranolol, most obviously

during the final part of the stimulation period. Since even the lowest dose of propranolol tested (0.1 mg/kg) was effective in this respect, a specific β -adrenoceptor mechanism seems probable.

As shown in Fig. 1 the 5-HT concentrations in portal plasma during the first 10 min of vagal nerve stimulation in propranolol pretreated cats were still very high. This may be due to a propranolol resistant release of 5-HT to an initially reduced blood flow or a combination of the two alternatives. A reduction of blood flow is likely to occur after propranolol. Furthermore, through its membrane stabilizing effect propranolol inhibits the uptake of 5-HT into platelets. Oral administration of propranolol (3 mg/kg) reduced the 5-HT uptake into platelets by 50% in human expts. (Grobecker et al. 1973). Similar concentrations of propranolol are probably reached after 2 mg i.v. in the present expts. Under normal conditions more than 50% of the 5-HT released from the gut is taken up into platelets before reaching the liver (Jaffe et al. 1977) indicating that inhibition of this mechanism by propranolol may contribute to an increase of the measured portal plasma 5-HT levels. Thus, even if the high dose of propranolol further decreased the 5-HT release from EC this effect may have been masked by the inhibition of the platelet 5-HT uptake resulting in high plasma 5-HT levels.

The present results are in accordance with the previous cytofluorimetric findings that the decrease in intracellular levels of 5-HT in EC after efferent stimulation of the vagal nerves was blocked by propranolol pretreatment. Removal of the superior cervical sympathetic ganglia one week prior to the experiments also blocked the vagally induced 5-HT decrease in EC indicating that adrenergic nerve fibres from these neck ganglia were mediating this

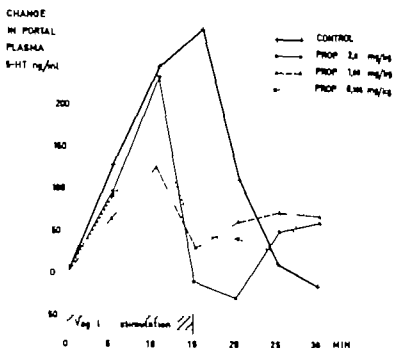


Fig 1 Diagram illustrating the changes in portal plasma 5-HT concentrations (mean values) on efferent vagal nerve stimulation in untreated cats and cats treated with various doses of propranolol based on the values given in Table 1

fasted for 24 h but had free access to water. Anesthesia was induced with ether and maintained with chloralose (50 mg/kg of b wt). Blood samples (2 ml each) for assays of 5-HT were drawn before, during and after nerve stimulation (according to the time schedule in Fig. 1) through a heparinized catheter inserted into the portal vein with the tip in the liver hilus region. For volume replacement all animals were given 10 ml of physiological saline through the femoral vein before the initiation of electrical stimulation and additional 10 ml was given during stimulation. Blood samples were stored on ice during the experiments and then centrifuged. The plasma was kept frozen until the assays.

Nerve stimulation. The vagal nerves were dissected free at the cervical level and cut. The distal ends were placed in circular electrodes insulated on the outside. A square wave impulse generator (Grass Instruments Co Model S4) was used for the electrical stimulation. Both vagal nerves were stimulated simultaneously for 15 min with supramaximal parameters: 20 V, 2 ms, 8 Hz. The efficiency of the nerve stimulation was judged by the presence of bradycardia, fall in blood pressure and small bowel contractions.

Experimental groups. 7 cats served as controls. In 4 cats the adrenals were bilaterally ligated. 12 cats were given propranolol (d-1-propranolol, Inderal® ICI) in 3 different doses: 2 mg/kg b wt as a bolus dose 70 min before the stimulation (6 cats), 0.75 mg/kg b wt as a bolus dose 20 min before the stimulation and in addition 0.3 mg/kg b wt/15 min as a constant infusion during the stimulation (3 cats), 0.075 mg/kg b wt as a bolus dose 20 min before the stimulation and in addition 0.03 mg/kg b wt/15 min as a constant infusion during the stimulation (3 cats).

Assay of 5-HT in plasma. The plasma concentration of 5-HT was determined by the modified fluorimetric method of Cox & Perhach (1973) for brain tissue. Briefly the method consisted of vortexing 50 µl of plasma with 50 µl n-butanol for 1 min followed by shaking for 5 min on a mechanical shaker at 160 oscillations per minute. The mixture was then centrifuged at 3000 rpm for 5 min at 4°C. A 0.1 ml aliquot of butanol phase was transferred to a tube containing 5 ml of n-heptane and 1.2 ml of 0.1 N HCl containing 0.1% cysteine. The mixture was shaken for 5 min at 160 oscillations per min and then centrifuged at 3000 rpm for 5 min. One ml of aqueous phase was withdrawn and mixed with 0.4 ml of 0.012% o-phthalaldehyde in 10 N HCl. The mixture was heated in boiling water for 10 min. After cooling the fluorescence of the sample was read at 470 nm after being excited at 360 nm on an Aminco-Bowman spectrofluorimeter. The recovery of 5-HT ranged from 72–81% and the assays were reproducible within 5%.

Statistics. Wilcoxon's tests for paired and unpaired data were used.

RESULTS

In the control cats ($n=7$) the vagal nerve stimulation caused a prompt and steady increase in the portal plasma 5-HT levels up to a maximum of 50% of initial levels after 15 min stimulation (Table 1 and Fig. 1). The increase was significant already after 5 min ($P<0.05$). After cessation of stimulation the 5-HT values were normal within 10 min. In the 4

Table 1. The 5-HT concentrations (ng/ml) in portal plasma of unanesthetized cats with ligated adrenals and cats pretreated with propranolol (various doses) before, during and after efferent vagal nerve stimulation. Mean values and S.E.M. Difference from control calculated from the changes in 5-HT levels indicated by $(P < 0.05)$

	Initial levels 0'	During vagal n. stimulation			After vagal stimulation		
		5'	10'	15'	20'	25'	30'
Control (n = 7)	197 ± 17	326 ± 38	443 ± 49	487 ± 56	309 ± 19	298 ± 79	181 ± 10
Adrenals ligated (n = 4)	202 ± 19	273 ± 19*	361 ± 22*	483 ± 8	325 ± 20	272 ± 15	223 ± 10
Propranolol, 2 mg/kg (n = 6)	267 ± 4	364 ± 19	501 ± 35	257 ± 13	237 ± 19*	318 ± 29	328 ± 31
Propranolol, 1.05 mg/kg (n = 3)	191 ± 38	256 ± 61	318 ± 14	220 ± 31	25 ± 4	265 ± 20	259 ± 33
Propranolol, 0.105 mg/kg (n = 3)	40 ± 48	332 ± 37	402 ± 41	285 ± 48*	281 ± 48	265 ± 52	341 ± 34

cats with ligation of the suprarenals the 5-HT response was slower in onset but reached the same maximum level at 15 min stimulation as in the control group (Table 1).

Propranolol did not completely block, but reduced and altered the response to vagal stimulation in all three doses tested (Fig. 1 and Table 1). The peak 5-HT levels were now seen after 10 min stimulation (instead of at 15 min as in the control group) followed by a return of plasma 5-HT to basal levels at 15 min stimulation. The difference from control stimulation without propranolol treatment) was less significant ($P < 0.05$) for propranolol 1.05 mg/kg already at 5 min stimulation and for all three propranolol groups at 15 min (end of stimulation) (Table 1). During the first 10 min of stimulation the blockade after the highest dose of propranolol seemed to be less effective although no significant difference between the various doses of propranolol could be demonstrated. The reduction from control of the 5-HT levels after propranolol (groups taken together) calculated by difference in curve areas (Fig. 1) was about 50%. In the propranolol group there was a minor but constant secondary increase of the portal plasma 5-HT after the end of stimulation at 25 and 30 min.

DISCUSSION

The present study demonstrates a rise of the 5-HT concentration in portal plasma after vagal nerve stimulation. This effect cannot be explained by changes in blood flow since splanchnic blood flow was not reduced but rather increased after vagal stimulation (Kewenter 1963; Martinsson 1965). The increase in 5-HT concentration on vagal stimulation is antagonized by propranolol most obviously

during the final part of the stimulation period. Since even the lowest dose of propranolol tested (0.1 mg/kg) was effective in this respect, a specific β -adrenoceptor mechanism seems probable.

As shown in Fig. 1 the 5-HT concentrations in portal plasma during the first 10 min of vagal nerve stimulation in propranolol pretreated cats were still very high. This may be due to a propranolol resistant release of 5-HT to an initially reduced blood flow or a combination of the two alternatives. A reduction of blood flow is likely to occur after propranolol. Furthermore, through its membrane stabilizing effect propranolol inhibits the uptake of 5-HT into platelets. Oral administration of propranolol (3 mg/kg) reduced the 5-HT uptake into platelets by 50% in human expts. (Grobeck et al 1973). Similar concentrations of propranolol are probably reached after 2 mg s.c. in the present expts. Under normal conditions more than 50% of the 5-HT released from the gut is taken up into platelets before reaching the liver (Jaffe et al 1977) indicating that inhibition of this mechanism by propranolol may contribute to an increase of the measured portal plasma 5-HT levels. Thus even if the high dose of propranolol further decreased the 5-HT release from EC, this effect may have been masked by the inhibition of the platelet 5-HT uptake resulting in high plasma 5-HT levels.

The present results are in accordance with the previous cytofluorimetric findings that the decrease in intracellular levels of 5-HT in EC after efferent stimulation of the vagal nerves was blocked by propranolol pretreatment. Removal of the superior cervical sympathetic ganglia one week prior to the experiments also blocked the vagally induced 5-HT decrease in EC, indicating that adrenergic nerve fibres from these neck ganglia were mediating this

response (Ahlman et al 1976b). The previous cytofluorimetric and the present studies together indicate that vagal nerve stimulation causes a release of 5-HT from EC into the portal blood and that this effect is at least partly mediated via a β -adrenoceptor mechanism. Other neural mechanisms may also release 5-HT from EC as studied in the rat (Tobe et al 1976). In vitro studies of the rat duodenum by cytofluorimetry after drug incubations not only supported the probable existence of a β -adrenergic release mechanism for 5-HT from EC but also suggested a cholinergic mechanism (Pettersson et al 1978). However in the cat atropine could not block the decrease of 5-HT in EC after vagal stimulation (Ahlman et al 1976b), indicating that in this species the cholinergic mechanism is of less importance.

Using fluorescence microscopy catecholamine containing nerve fibres have been demonstrated in the cervical vagal nerve (Muryobayashi et al 1968). Adrenergic nerve terminals have also been observed near EC in the intestinal crypts (Ahlman et al 1976a). Part of these terminals probably emanate from the cervical sympathetic ganglia via the vagal nerve as indicated by studies using the retrograde HRP tracing technique (Lundberg et al 1978). Ultrastructural studies have demonstrated autonomic nerve endings of cholinergic, adrenergic and peptidergic types near the base of most EC in the crypts of the guinea pig duodenum (Lundberg et al 1978). Furthermore a true synapse between a probable adrenergic terminal and a basal-granulated gut endocrine cell was recently demonstrated in the rat (Newson et al 1979). Thus a morphological basis for an adrenergic neural control of the EC via the vagal nerves has been established. In addition circulating catecholamines released from the adrenals at the fall in blood pressure may also contribute to release of 5-HT from EC at vagal nerve stimulation. However in the four cats with bilateral ligation of the adrenals the 5-HT level after 15 min of stimulation was the same as in controls although the initial rise was slower (Table 1). This clearly indicates the importance of the direct neural influence on the 5-HT release.

A propranolol resistant release of 5-HT on vagal nerve stimulation may have several explanations. (a) It may be mediated via nonadrenergic neural mechanisms (see above). (b) A 5-HT release from serotonergic nerves in the gut is less probable since Ahlman & Enerbäck (1974) could find no ob-

jective evidence for the presence of 5-HT in the myenteric plexus of the guinea pig. (c) The possibility of an indirect stimulation of the EC by increased intraluminal pressure or acid pH in the duodenum (Bulbring & Crema 1959; Resnick & Gray 1967) after vagal nerve stimulation cannot be ruled out.

The results of the present study confirm the existence of a β -adrenoceptor mediated release of 5-HT. However the results also suggest that other mechanisms for 5-HT release may be involved in the total response on vagal nerve stimulation.

Supported by the Swedish Medical Research Council (Grants nos 17X-05220, 04X-207, 04P-4173); the Göteborg Medical Society; the Swedish Society of Medical Sciences; the Medical Faculty, University of Göteborg; the M. Bergvall's Foundation and H. and G. Jeansson's Foundation. The technical assistance of Mrs H. Andersson is gratefully acknowledged.

REFERENCES

- AHLMAN H & ENERBÄCK L 1974 A cytofluorimetric study of the myenteric plexus in the guinea pig. *Cell Tiss Res* 453: 419-434.
- AHLMAN H, DAHLSTRÖM A, KEWENTER J & LUNDBERG J M 1976 Vagal influence on serotonin concentration in enterochromaffin cells in the cat. *Acta Physiol Scand* 97: 362-368.
- AHLMAN H, LUNDBERG J M, DAHLSTRÖM A & KEWENTER J 1976b A possible vagal adrenergic release of serotonin from enterochromaffin cells in the cat. *Acta Physiol Scand* 98: 366-375.
- ALUMETS J, HÄKANSSON R, SUNDLER F & CHANG K S 1978 Leu-enkephalin-like material in nerves and enterochromaffin cells in the gut. *Histochemistry* 56: 187-196.
- BENDITT E P & WONG R L 1957 On the concentration of 5-hydroxytryptamine in mammalian enterochromaffin cells and its release by reserpine. *J Exp Med* 105: 509-520.
- BURKS T F & LONG J P 1966 Catecholamine-induced release of 5-hydroxytryptamine from perfused vasculature of isolated dog intestine. *J Pharm Sci* 55: 1381-1386.
- BULBRING E & CREMA A 1959 The release of 5-hydroxytryptamine in relation to pressure exerted on the intestinal mucosa. *J Physiol (Lond)* 146: 18-28.
- COX R H Jr & PERHACH J L Jr 1973 A sensitive, rapid and simple method for the simultaneous spectrophotofluorimetric determinations of norepinephrine, dopamine, 5-hydroxytryptamine and 5-hydroxyindolacetic acid in discrete areas of the brain. *J Neurochem* 20: 1777-1780.
- GROBECKER H, LEMMER D, HELLENBRECHT D & WEITHOLD G 1973 Inhibition by atropine

- alysins and beta-sympatholytic drugs of serotonin uptake by human platelets; Experiments *in vitro* and *in vivo* *Europ J Clin Pharmacol* 5: 145-150.
- HOHENLEITNER, F. J. TANSY M. F. & GOLDER, R. 1971 Effect of vagal stimulation on duodenal serotonin in the guinea pig. *J Pharm Sci* 60: 471-472.
- LUFE, B. M. KOPEN D. F. & LAZAN D. W. 1977 Endogenous serotonin in the control of gastric acid secretion. *Surgery* 82: 136-140.
- KEWENTER, J. 1965. The vagal control of the jejunal and ileal motility and blood flow. *Acta Physiol Scand* Suppl. 251.
- LUNDBERG, J. M. DAHLSTRÖM A., BYLÖCK, A., AHLMAN, H. PETTERSSON G. LARSSON I. HANSSON H. A. & KEWENTER, J. 1978. Ultrastructural evidence for an innervation of epithelial enterochromaffin cells in the guinea pig duodenum. *Acta Physiol Scand* 104: 3-12.
- LUNDBERG, J. M., DAHLSTRÖM, A., LARSSON I. PETTERSSON G. AHLMAN H. & KEWENTER, J. 1978. Efferent innervation of the small intestine by serergic neurons from the cervical sympathetic and pelvic ganglia, studied by retrograde transport of peroxidase. *Acta Physiol Scand* 104: 33-42.
- MINTHUSON, J. 1965 Studies on the efferent vagal control of the stomach. *Acta Physiol Scand*, Suppl. 25.
- KIKUYABAYASHI, T. MORI I. FUJIWARA M. & SHIMAMOTO K. 1968 Fluorescence histochemical demonstration of adrenergic nerve fibres in the vagus nerve of cats and dogs. *Jap J Pharmacol* 18: 285-293.
- ERSON, B. AHLMAN H. DAHLSTRÖM A. DES GUPTA, T. K. & NYHUS, L. 1979 On the innervation of the ileal mucosa in the rat—a synapse. *Acta Physiol Scand* 105: 387-389.
- PEARSE, A. O. E. 1969 The cytochemistry and ultrastructure of polypeptide hormone producing cells of the APUD series and the embryologic physiologic and pathologic implications of the concept. *J Histochem Cytochem* 17: 303-313.
- PEARSE, A. O. E. & POLAK, J. M. 1975 Immunocytochemical localization of substance P in mammalian intestine. *Histochemistry* 41: 373-375.
- PEARSE, A. O. E. POLAK J. M. BLOOM, S. R., ADAMS, C. DRYBURGH J. R. & BROWN C. 1974 Enterochromaffin cells of the mammalian small intestine as the source of motilin. *Virchows Arch B Cell Pathol* 16: 111-120.
- PENTTILÄ, A. 1966. Histochemical reactions of the enterochromaffin cells and the 5-hydroxytryptamine content of the mammalian duodenum. *Acta Physiol Scand*, Suppl. 281.
- PETTERSSON G. DAHLSTRÖM A. LARSSON I. LUNDBERG, J. M. AHLMAN H. & KEWENTER, J. 1978. The release of serotonin from rat duodenal enterochromaffin cells by adrenoceptor agonists studied *in vitro*. *Acta Physiol Scand* 103: 219-224.
- PETTERSSON G. AHLMAN H. DAHLSTRÖM A. KEWENTER, J. LARSSON I. & LARSSON P. A. 1979 The effect of transoral field stimulation on the serotonin content in rat duodenal enterochromaffin cells—in vitro. *Acta Physiol Scand*. In press.
- RESNICK, R. M. & GRAY S. J. 1962. Chemical and histological demonstration of hydrochloric acid-induced release of serotonin from intestinal mucosa. *Gastroenterology* 42: 48-55.
- TANSY M. F. ROTHMAN G. BARTLETT J. FARBER, P. & HOHENLEITNER, F. S. 1971 Vagal adrenergic degeneration of enterochromaffin cell system in guinea pig duodenum. *J Pharm Sci* 60: 81-84.
- TOBE, T. IZUMIKAWA, F. SANO M. & TANAKA, C. 1976. Release mechanisms of 5-HT in mammalian gastrointestinal tract—especially vagal release of 5-HT. In: *Endocrine gut and pancreas* (ed. T. Fujita), pp. 371-380. Elsevier Scientific, Amsterdam.

Adenosine 3' 5' cyclic monophosphate calcium and magnesium excretion in ethanol intoxication and hangover

RAIKO LINKOLA, FREJ FYHRQUIST and REINO YLIKAHRI

Neuro Institute for Medical Research, Helsinki, and Third Department of Medicine, University of Helsinki, Finland

LINKOLA, R., FYHRQUIST, F. & YLIKAHRI, R. Adenosine 3' 5' cyclic monophosphate, calcium and magnesium excretion in ethanol intoxication and hangover. *Acta Physiol Scand* 1979 107 333-337. Received 27 April 1979. ISSN 0001-6772. Neuro Institute for Medical Research, Helsinki, and Third Department of Medicine, University of Helsinki, Finland.

Effect of ethanol on adenosine 3' 5' cyclic monophosphate (cAMP), calcium (Ca) and magnesium (Mg) excretion was studied in controlled clinical conditions in man. Seven male volunteers served as their own controls. In 5 subjects cAMP excretion was primarily suppressed by ethanol. Ethanol appeared to have a biphasic effect on Ca excretion, an initial stimulation followed by a conservation phase. Mg excretion was stimulated by ethanol in 5 subjects. Subjects having nausea and vomiting and the most severe hangover symptoms had the lowest urinary Ca excretion and the lowest initial cAMP excretion. Ca and Mg metabolism and the susceptibility of the body to the toxic effects of ethanol appeared to be interrelated.

Key words. Cyclic AMP, calcium, magnesium, ethanol

Adenosine 3' 5' cyclic monophosphate (cAMP) acts as a renal cellular messenger for parathormone (PTH), which regulates phosphate and calcium (Ca) metabolism (Chase & Aurbach 1967; Massary & Cohen 1973). In addition, renal tubular transport of Ca appears to share common reabsorptive mechanism with magnesium (Mg) (Samly et al 1968; Cohen et al 1970).

Ethanol may acutely decrease serum Ca and renal phosphate concentration, but also urinary excretion of these ions in man (Kalbfleisch et al 1963; Mäkkilä & Nanto 1966). On the other hand, chronic human alcoholics frequently display abnormal serum Ca values (Martin et al 1969; Finkelshtam et al 1964). Furthermore, ethanol has been shown to induce hypomagnesaemia (Fluck et al 1964; Henton et al 1962), which reportedly is a consequence of urinary Mg loss (Henton et al 1964; Kalbfleisch et al 1963). Because recent observations (Linkola et al 1978; Linkola et al 1979) indicated biphasic effects of ethanol on water and elec-

trolyte balance, we measured stepwise urinary excretion of cAMP, Ca and Mg during ethanol intoxication and hangover in controlled clinical conditions.

MATERIALS AND METHODS

The experiments were carried out in metabolic ward as described in previous paper (Linkola et al 1978; Linkola et al 1979). Seven healthy men, age 25-35, volunteered for the experiments. Isocaloric diet (about 30 kcal day⁻¹ kg⁻¹) containing 100 mmol sodium (Na) and 90 mmol potassium (K) per day was eaten for 5 days. In the morning of the 5th day the subjects received 4/3 the calories of that day and all Na as NaCl. Then, beginning at noon, they fasted to 6 p.m. and were asleep for 22 h. From 6 p.m. to 9 p.m. they received deionized water 10 ml/kg. At 8 a.m. next morning they received water 5 ml/kg. At 10 a.m. they assumed standing position walking slowly around. They had nothing to eat until noon. After that they had meal (about 30 kcal/kg, 100 mmol Na and 90 mmol K).

Beginning in the morning of the 7th day the same procedure as two days earlier was repeated, except that water in

Table 1 Urinary cAMP excretion in subjects I-VII in $\mu\text{mol/g}$ creatinine during control (C) and ethanol (E) experiment

Subject	C				E				C Total	E Total
	p.m		a.m		p.m		a.m			
	6-9	9-12	0-6	6-12	6-9	9-1	0-6	6-1		
I		1.65								
II	2.09	1.26	.48	2.57	1.66	1.42	.44	.81	6.50	8.33
III	1.33	2.53	.65	2.33	1.33	3.11	.16	1.92	8.33	9.57
IV	1.88	1.50	.48	1.18	0.47	1.04	1.90	1.47	8.52	4.88
V	3.18	9.40	1.48	1.35	1.48	0.93	1.50	.35	6.1	6.26
VI			6.09		1.67	3.75		4.78	18.67	10.20
VII	3.42	3.86	3.81	2.05	3.15	2.97	3.32	3.78	13.14	13.2
	1.65	1.69	1.29	1.63	1.85	0.30		1.68	6.26	3.83

the evening was replaced by 15% w/v ethanol (10 ml/kg). Urine was collected 6-9 p.m. 9-1 p.m. 0-6 a.m. and 6-12 a.m. Urine cAMP was determined by competitive protein binding assay (Linkola & Fyhrquist 1978). Ca and Mg concentrations were measured as described (Ylikahri et al. 1974). Hewlett Packard 9810 A calculator was used in paired *t* test analyses.

RESULTS

Urinary excretion of cAMP was primarily suppressed by ethanol in 5 subjects (all but I and VII) (Table 1). In 4 subjects (I, II, IV and VI) cAMP excretion was stimulated during hangover (6-12 a.m.). In one subject (I) ethanol only enhanced cAMP excretion. Statistically significant effects of ethanol on cAMP excretion were not observed.

There was an initial stimulated phase in Ca excretion due to ethanol in most subjects (Table 2) but in some subjects (II and V) Ca excretion was amplified also in later phases of ethanol intoxication. Totally ethanol appeared to increase Ca output in 3 subjects

(I, III and VI) but decrease it in the other four subjects. The suppression of urinary Ca output during hangover (0-12 a.m.) was almost significant ($t=2.176$, $P=0.05$). Thus effects of ethanol on Ca excretion appeared to be biphasic.

In Mg excretion there was an ethanol-induced stimulated phase in 6 subjects (all but V) (Table 3). Enhanced Mg output appeared to be more widely distributed through the whole measured period in ethanol experiment than enhanced Ca output. Totally in 5 subjects (all but IV and V) ethanol increased Mg excretion. No statistically significant effect of ethanol was observed.

Amplified cAMP excretion was in some cases (II, VI and VII) clearly simultaneous with attenuated Ca and Mg excretion and conversely in one subject (III). The symptoms of intoxication and hangover are represented in Table 4. Subjects II, III and IV having the lowest urinary Ca excretion and the lowest initial cAMP excretion after ethanol also had nausea and vomitus and the most serious subjective

Table 2 Urinary Ca excretion in subjects I-VII in mmol during control (C) and ethanol (E) experiment

Subject	C				E				C Total	E Total
	p.m.		a.m.		p.m.		a.m.			
	6-9	9-12	0-6	6-1	6-9	9-12	0-6	6-1		
I		0.47	0.81	0.86	0.43	0.79	0.61	0.57	14	2.40
II	0.54	0.35	0.41	0.80	0.59	0.30	0.55	0.62	10	0.6
III	0.3	0.15	0.1	0.43	0.47	0.79	0.13	0.13	1.02	1
IV	0.38	0.33	0.5	0.48	0.37	0.48	0.4	0.11	1.44	1.38
V	1.24	0.52	1.48		1.1	0.3	1.1		3.4	2.96
VI	0.5	0.29	0.55	0.43	1.15	0.98	0.15	0.5	1.49	2.6
VII	0.86	0.49	0.77	1.76	0.38	1.03		1.68	3.83	3.09

Table 3. Urinary Mg excretion in subjects I-VII in mmol during control (C) and ethanol (E) experiment

Subject	C				E				C Total	E Total
	p.m.		a.m.		p.m.		a.m.			
	6-9	9-12	0-6	6-12	6-9	9-12	0-6	6-12		
I		0.8	0.5	0.5	0.5	0.6	0.7	0.6	1.8	2.4
II	1.1	0.7	1.2	1.5	1.1	0.6	1.5	1.4	4.5	4.6
III	0.8	0.7	0.8	0.9	1.3	1.1	0.4	1.1	3.2	3.9
IV	0.7	0.6	0.9	1.0	0.7	0.7	0.5	0.7	3.2	2.6
V	0.9	0.3		1.4	0.8	0.3		1.1	1.6	2.2
VI	0.7	0.4	0.6	0.7	1.2	1.4	0.7	0.5	2.4	3.8
VII	0.8	0.9	1.1	1.3	0.4	1.3		3.0	4.2	4.7

pa of hangover. Results on blood ethanol, vasopressin, renin, aldosterone, cortisol, urine output, sodium and potassium were described previously in the same journal (Linkola et al. 1978, Linkola et al. 1979). Subject III having in those previous studies the highest endocrine responses to ethanol also had the highest renal Ca conservation during the control experiment.

DISCUSSION

During the first 2 h of ethanol intoxication cAMP excretion was lower than during the corresponding control time in most subjects (Table 1). This may be due to the suppressed PTH response as has been suggested in rats (Peng & Gitelman 1974). It has recently been reported that during two or six hours ethanol increases serum PTH concentration in rats (Glab et al. 1978), but the corresponding data on man is lacking.

In 2 subjects (I and VII) ethanol primarily enhanced cAMP excretion. This may be partly attributed to the stimulating effect of ethanol on adenylyl cyclase activity observed in many tissues (Volter & Gold 1971) or to increased extrarenal cAMP release. Interestingly these subjects also had the best endocrine responses to ethanol and no apparent decrease of plasma vasopressin after ethanol ingestion (Linkola et al. 1978, Linkola et al. 1979). Ethanol reportedly increases serum C (Kalbfleisch et al. 1963, Markkunen & Nanto 1966). This may lead to suppression of PTH response in kidneys (Beck et al. 1974). Thus, high Ca output in subject VII may reflect high renal Ca supply and suppression of cAMP excretion by this ion after 9 p.m. In a control experiment urinary excretion of Ca

and Mg varied considerably. The lowest Ca output was in the subject III having the most pronounced endocrine responses after ethanol, and the highest Ca output was in the subject VII with low endocrine responses to ethanol (Linkola et al. 1978, Linkola et al. 1979). After ethanol ingestion, all subjects had a phase during which Ca excretion was enhanced when compared to the control experiment (Table 1). However only in 3 subjects (I, III and VI) the total effect of ethanol was stimulative. Thus ethanol obviously had a biphasic effect on Ca excretion.

Increased urinary output of Ca has been described in man during ethanol intoxication (Markkunen & Nanto 1966). The present results suggest that this mainly occurs during the early phase of intoxication. Subjects II, III and IV having nausea and vomiting and the most serious subjective signs of hangover (Table 4) had the lowest urinary Ca output during ethanol experiment (Table 2). These subjects also had the lowest cAMP excretion in the

Table 4. Subjects' feeling of hangover and vomiting during ethanol experiment

Subject	Subjective feeling of hangover	Vomiting during	
		Intoxication	Hangover
I	-	-	-
II	+	-	-
III	+	-	+
IV	+	-	+
V	-	+	-
VI	-	-	-
VII	-	-	-

early phase of intoxication. The cause or effect relationships of this phenomenon remained unclear. However, the finding that subject III, having the most pronounced endocrine responses to ethanol (Linkola et al 1978; Linkola et al 1979), also during the control experiment had the highest renal Ca conservation, may suggest an association between individual responses to ethanol and Ca metabolism. Results in subject IV support this assumption. Interestingly, it has been previously reported that Ca metabolism is associated with ethanol tolerance in rodents, because intraventricular CaCl_2 enhanced ethanol-induced sleeping-time and behavioral intoxication in rats and mice (Erickson et al 1978). Blood ethanol curves (Linkola et al 1978) indicate that responses to ethanol are hardly due to differences in blood ethanol concentration. Moreover, subjects II, III and IV had blood ethanol peak concentrations later than other subjects, which may indicate their slower ethanol absorption rate from the stomach.

Similar two phases as in Ca excretion were not seen in Mg excretion after ethanol ingestion. In many subjects (all but IV and V) stimulated Mg excretion continued still during hangover. Urinary output of Mg and Ca appeared to be, at least partly, conversely related to cAMP excretion, because of the concomitance of low cAMP excretion and stimulated Mg and Ca output. This is in agreement with the generally accepted idea that parathormone and cAMP decrease Ca and Mg excretion (Massry & Coburn 1973; Kuntzinger et al 1974). In subject V, with the highest cAMP output, ethanol was not able to increase Mg output at all. On the other hand, before the beginning of the experiment, this subject exhibited a surprisingly low serum $[\text{Mg}]$ (0.70 mmol/l) which may have limited the increase in Mg excretion caused by ethanol (Sullivan et al 1966). In other subjects, serum $[\text{Mg}]$ was within normal limits, and no correlation was observed between serum $[\text{Mg}]$ and Mg excretion. If the excretion values of Ca regarding this exceptional subject V are not taken into account, Ca excretion was stimulated (subjects I, III, IV, VI and VII) or unaffected (subject II) by ethanol during 6–12 p.m. (paired *t*-test values was 2.170). Also the conservation phase in Ca excretion is more obvious after this manipulation (paired *t*-test value was increased from 2.176 to 2.421, which means significant Ca conservation during 0–12 a.m., $P < 0.05$).

Hypomagnesaemia is reportedly a more frequent

and long-lasting consequence of ethanol drinks than other electrolyte changes (Martin et al 1955). It has been suggested causative to ethanol withdrawal syndrome (Victor & Wolfe 1971). Hypomagnesaemia may also cause tremor, hyperirritability (Flink et al 1954; Fankushen et al 1966) and decreased response of target organs to PTH (Rude et al 1976). Furthermore, low Mg levels have also been suggested to predispose subjects to have severe hangover (Ylikahri et al 1974). Thus, the symptoms in subjects II, III and IV (Table 4), the low cAMP output and high Mg output in subject V may reflect Mg depletion. This might also explain why ethanol did not significantly increase K excretion in the present experiment (Sullivan et al 1966). Previously it was already suggested that subjects II, III and IV had lost K (Linkola et al 1978). Thus, excessive leakage of intracellular cations Na and K may be associated with the symptoms in subjects II, III and IV. The study provides evidence that Ca and Mg metabolism and the susceptibility of the body to the toxic effects of ethanol are interrelated.

We thank Mrs Eira Meskanen and Mrs Yrsa Österberg for technical assistance and Mrs Kirsti Alanne for typing. Support was given by the Finnish Foundation for Alcohol Studies, the Sigrid Jusélius Foundation, the Märsi Foundation, Helsinki and the Nordisk Foundation, Copenhagen.

REFERENCES

- BECK, N., SINGH, H., REED, S. W. & DAVIS, B. B. 1974. Direct inhibitory effect of hypercalcaemia on renal actions of parathyroid hormone. *J. Clin. Invest.* 53, 717–725.
- CHASE, L. R. & AURBACH, G. D. 1967. Parathyroid function and the renal excretion of 3, 5-adenylic acid. *Proc. Natl. Acad. Sci. (US)* 58, 518–525.
- COBURN, J. W., MASSRY, S. G. & KLEEMAN, C. R. 1970. The effect of calcium infusion on renal handling of magnesium with normal and reduced glomerular filtration rate. *Nephron* 7, 131–143.
- ERICKSON, C. K., TYLER, T. D. & HARRIS, R. A. 1978. Ethanol: Modification of acute intoxication by divalent cations. *Science* 199, 119–121.
- FANKUSHEN, D., RASKIN, D., DIMICH, A. J. & WALLACH, S. 1964. The significance of hypomagnesaemia in alcoholic patients. *Amer. J. Med.* 27, 402–412.
- FLINK, E. B., STUTZMAN, F. L., ANDERSON, A. R., KONIG, T. & FRASER, R. 1954. Magnesium deficiency after prolonged parenteral fluid administration and after chronic alcoholism complicated by delirium tremens. *J. Lab. Clin. Med.* 43, 169–183.
- HEATON, F. W., PYRAH, L. N. & BERESFORD, C. C.

- KRYSON, R. W. & MARTIN, D. F. 1962. Hypomagnesemia in chronic alcoholism. *Lancet* 2: 802-803.
- KALFLEISCH, J. M., LINDEMAN, R. D., GINN, R. E. & SMITH, W. O. 1963. Effects of ethanol administration on urinary excretion of magnesium and other electrolytes in alcoholic and normal subjects. *J Clin Invest* 42: 1471-1475.
- KATZIGER, H., AMIEL, C., ROINEL, N. & MOREL, F. 1974. Effects of parathyroidectomy and cyclic AMP on renal transport of phosphate, calcium, and magnesium. *Amer J Physiol* 227: 905-911.
- LINEOLA, J., FYHRQUIST, P. & YLIKAHRI, R. 1978. Renin, aldosterone and cortisol during ethanol intoxication and hangover. *Acta Physiol Scand* 106: 75-82.
- LINEOLA, J., YLIKAHRI, R., FYHRQUIST, P. & VALLENIUS, M. 1978. Plasma vasopressin in ethanol intoxication and hangover. *Acta Physiol Scand* 104: 180-187.
- MAKKANEN, T. & NÄNTÖ, V. 1966. The effect of ethanol infusion on the calcium-phosphorus balance in man. *Experientia* 22: 753-754.
- MARTIN, H. E., McCUSKEY, C. JR. & TUPIKOVA, M. 1959. Electrolyte disturbance in acute alcoholism with particular reference to magnesium. *Am J Clin Nutr* 7: 191-196.
- MASSRY, S. G. & COBURN, J. W. 1973. The hormonal and non-hormonal control of renal excretion of calcium and magnesium. *Nephron* 10: 66-112.
- PENG, T.-C. & GITELMAN, H. J. 1974. Ethanol-induced hypocalcemia, hypomagnesemia and inhibition of the serum calcium-raising effect of parathyroid hormone in rats. *Endocrinology* 94: 608-611.
- RUDE, R. K., OLDHAM, S. B. & SINGER, F. R. 1976. Functional hypoparathyroidism and parathyroid hormone end-organ resistance in human magnesium deficiency. *Clin Endocr* 5: 209-224.
- SAMIY, A. H. E., BROWN, J. L., GLOBUS, D. L., KESSLER, R. H. & THOMPSON, D. D. 1960. Interrelation between the renal transport systems of magnesium and calcium. *Amer J Physiol* 198: 599-602.
- SHAH, J. H., BOWSER, E. N., HARGIS, G. K., WONGSUKAWAT, N., BANERJEE, P., HENDERSON, W. J. & WILLIAMS, G. A. 1978. Effect of ethanol on parathyroid hormone secretion in the rat. *Metabolism* 27: 257-260.
- SULLIVAN, J. F., LANKFORD, H. G. & ROBERTSON, P. 1966. Renal excretion of lactate and magnesium in alcoholism. *Am J Clin Nutr* 18: 231-236.
- VICTOR, M. & WOLFE, S. M. 1973. In: *Alcoholism, progress in research and treatment* (eds. P. Q. Bowne & R. Fox) pp. 137-169. Academic Press, New York.
- VOLICER, L. & GOLD, B. I. 1975. Interactions of ethanol with cyclic AMP. *Adv Exp Med Biol* 56: 11-237.
- YLIKAHRI, R. H., POSO, R., HUTTUNEN, M. O. & HILLBOM, M. E. 1974. Alcohol intoxication and hangover. Effects on plasma electrolyte concentrations and acid-base balance. *Scand J Clin Lab Invest* 34: 327-336.

Modification of human pain threshold by specific tactile receptors

ANTTI PERTOVAARA

Department of Physiology, University of Helsinki, Finland

PERTOVARA, A. Modification of human pain threshold by specific tactile receptors. *Acta Physiol Scand* 1979; 107: 339-341. Received 28 April 1979. ISSN 0001-6772. Department of Physiology, University of Helsinki, Finland.

The effects of conditioning vibrotactile stimulation of particular tactile receptor groups on thresholds to painful electric stimuli were studied in seven healthy adults. Preferentially Pacinian afferents were activated with conditioning sinusoidal vibration of 40 Hz at 20 and 200 μ m amplitudes and preferentially non-Pacinian tactile fibers were activated with conditioning sinusoidal vibration of 20 Hz at 200 and 400 μ m amplitudes. None of the subjects showed pain threshold elevation during activation of non-Pacinian tactile fibers. However 6 of the 7 subjects showed significant pain threshold elevation with conditioning vibratory stimulus of 240 Hz at 200 μ m amplitude, and 4 subjects showed significantly elevated pain thresholds with conditioning stimulus of 40 Hz at 20 μ m amplitude. It is concluded that the activation of Pacinian afferents causes inhibition of pain conducting pathways.

Key words: tactile fibers, pain conducting pathways, cross-modal inhibition, cutaneous stimulation.

Wall & Cronley-Dillon (1960) observed an elevation in subjective thresholds for detecting pain in the presence of vibratory stimulus of 60 Hz at an amplitude of 4 mm peak-to-peak. Later it has been shown that the amplitude used at 60 Hz by Wall & Cronley-Dillon activates both Pacinian and intradermal, rapidly adapting receptors (Talbot et al. 1968, Merzenich & Harrington 1969). Talbot et al. and Merzenich & Harrington showed that high frequency mechanical vibration at low amplitudes activated preferentially Pacinian receptors, whereas low frequency and low amplitude activated preferentially non-Pacinian intradermal receptors.

Fernstrom et al. (1977) examined human detection thresholds for vibratory stimuli when different tactile receptor groups were simultaneously activated by mechanical vibration of 30 and 300 Hz at low amplitudes. They observed elevations in detection thresholds when preferentially Pacinian receptors were activated by conditioning stimulation. No elevation in detection threshold was observed when selectively non-Pacinian intradermal mechanoreceptors were activated.

The purpose of the present work was to find out

whether subjective pain threshold to electric stimuli could be elevated with stimulation of particular tactile receptor groups.

METHODS

Experiments were performed on 7 healthy adults, females and 5 males aged 25 to 40 years. All of them were experienced subjects in physiological testing. During the experiments the subject, who was seated comfortably had his right hand on a table, palm downwards.

The sinusoidal mechanical vibration was delivered by an electromechanical vibrator (Bruel & Kjaer Mini-Shaker 4810) driven by a function generator (Hewlett-Packard 202C) the signal of which was amplified by conventional power amplifier. Before starting the experiments of this investigation the amplitude calibration of the vibrator was done with miniature piezoelectric accelerometer (Bruel & Kjaer 4339) fixed between the moving coil of the vibrator and the stimulus probe. The diameter of the stimulus probe was 1 cm and it was made of perspex. The dorsal surface of the right hand was stimulated. This area is innervated by the superficial sensory branch of the radial nerve. The stimulus probe was positioned about 1 mm into the skin to ensure constant contact between the stimulus probe and the skin.

The conditioning vibratory stimuli were of 2 frequencies. Firstly 20 Hz sinusoidal at 200 and 400 μ m (peak-

Table 1 The thresholds of one subject to painful electric stimuli without and with each conditioning vibrotactile stimulus and the percentual threshold elevations with simultaneous conditioning vibrotactile stimuli and the statistical significances of the threshold elevations

The number of measurements was 10 without vibration and 5 with vibration in each condition. Na means nonsignificant

Conditioning stimulus	Pain threshold in mA		Percentual elevation	Significance of elevation $P <$
	Without vibration	With vibration		
70 Hz, 200 μ m	0.10 \pm 0.00	0.10 \pm 0.00	0.0	Na
20 Hz, 400 μ m	0.11 \pm 0.02	0.12 \pm 0.03	9.1	Na
40 Hz, 70 μ m	0.10 \pm 0.00	0.14 \pm 0.02	40.0	0.001
240 Hz, 700 μ m	0.12 \pm 0.02	0.21 \pm 0.06	75.0	0.001

to-peak) amplitudes was used to activate preferentially non-Pacinian tactile receptors (anatomically Meissner-Merkel and Ruffini receptors). Secondly a sinusoidal vibration of 740 Hz at 20 and 700 μ m amplitudes was used to activate Pacinian receptors (Talbot et al. 1968, Merzenich & Harrington 1969).

According to threshold estimations on human hairy skin vibratory stimuli of 20 Hz at 200 μ m amplitude and of 240 Hz at 70 μ m amplitude are roughly of equal subjective magnitude (about 2-3x threshold) and 400 μ m at 20 Hz is about 4x threshold whereas 200 μ m at 240 Hz is about 20x threshold (Merzenich & Harrington 1969).

Electric pulses of 1 ms duration (with one subject of 8 ms duration) were used as painful stimuli. Pulses were applied from Nihon Kohden MSE 3R function generator via Nihon Kohden MSE JM isolation unit to a Grass CCU 1 A constant current unit. From the constant current unit the electric pulses were applied to the skin by two closely spaced Pb-Zn cup-electrodes of 8 mm diameter. The skin was cleaned with alcohol and the electrodes were smeared with electrode paste. The electrodes were placed about 2-4 cm distally from the stimulus probe of the mechanical vibrator. Subjects were instructed to report when they first felt a pain that could be described as 'prick'. The magnitude of the electric current given to the subject could be varied and during a single trial the intensity of current was increased until the subject reported pain. It was not possible to begin the trial with suprathreshold intensities and then decrease the current because the subjects felt extreme pain only slightly above the pain threshold. The pain threshold was determined in 5-10 trials during each conditioning stimulus. Prior to the experimental control pain thresholds in mA were determined separately for each subject as an average of 5-10 measurements. During each pain stimulus the threshold in mA was determined three times, once before the vibratory stimulus was started once during vibratory stimulation and once after it. For each vibration frequency-amplitude combination 15-25 measurements were made. The mean and standard deviation values of each series of trials were calculated and expressed as per cent of the control pain threshold for each individual. Student's *t* test (two tailed) was used in statistical calculations.

The duration of the whole experiment was about 15-20 min for each individual and the duration of the thresh-

old determination in each condition was usually about 1 min. The order of the conditioning vibrotactile stimuli was in every experiment: 20 μ m, 240 Hz, 200 μ m, 20 Hz, 200 μ m, 240 Hz, (400 μ m, 20 Hz was used only with three subjects).

RESULTS

The pain thresholds without conditioning stimuli varied between 0.1 and 1.2 mA and the mean for all subjects was 0.40 mA. The range of the standard deviations of the pain thresholds varied between 0.00 and 0.32 mA and the mean of the standard deviations was 0.07 mA.

Table 1 gives the results of one subject in different experimental situations and statistical significances of the results.

None of the 7 subjects showed significantly elevated pain thresholds during conditioning stimuli of 700 μ m and 400 μ m at the frequency of 20 Hz. 4 subjects showed significantly elevated pain thresholds during conditioning stimuli of 70 μ m at the frequency of 240 Hz and 6 subjects showed significantly elevated pain thresholds with conditioning stimuli of 200 μ m at 240 Hz.

The mean threshold elevation caused by 20 μ m, 240 Hz stimulation was 19% and that caused by 700 μ m, 240 Hz was 40% (Table 2). The statistical significances of the mean percentual threshold elevations with each conditioning vibrotactile stimulus for all the subjects are also given in Table 2. The mean threshold elevation of all the subjects was significant with conditioning stimuli of 20 and 200 μ m at the frequency of 240 Hz.

No after effects were observed: the pain thresholds decreased immediately at the termination of the vibration.

Pain threshold during simultaneous auditory

Table 1. Percentual elevations of pain thresholds and their statistical significances for all the subjects
in whom non-significant

Containing stimulus	The mean threshold elevation, %	Statistical significance, $P <$
20 Hz, 200 μ m	9.4 ± 11.0 ($N=7$)	N
20 Hz, 400 μ m	1.3 ± 2.3 ($N=3$)	N
20 Hz, 20 μ m	19.0 ± 16.4 ($N=7$)	0.05
20 Hz, 200 μ m	40.1 ± 29.8 ($N=7$)	0.02

level of 40 Hz was determined for two subjects and no significant elevation of thresholds was observed.

DISCUSSION

According to previous studies (Talbot et al. 1968; Merzenich & Harrington 1969) 240 Hz vibration activated preferentially Pacinian receptors. And of the 70 amplitudes used the smaller one (20 μ m) probably activated only Pacinian receptors. In the results of Merzenich & Harrington 20 Hz vibration at 200 μ m amplitude activated preferentially non-Pacinian tactile fibers, most of which were activated at these amplitudes.

In the present study none of the subjects showed raised pain thresholds when non-Pacinian tactile afferents were activated. However 6 of the 7 subjects showed threshold elevation when Pacinian afferents are preferentially activated and 4 subjects had higher pain thresholds with high frequency small amplitude vibration which most probably activated only Pacinian corpuscles. Therefore the elevation in pain thresholds with 240 Hz continuous vibratile stimuli was most probably caused by activation of Pacinian afferents. Since activation of non-Pacinian tactile fibers did not elevate pain thresholds it appears that these receptors do not contribute to the pain threshold elevation. However since each sine wave causes one nerve impulse (Talbot et al. 1968) the low frequency vibration used to activate non-Pacinian mechanoreceptive afferents most probably generated less nerve im-

pulses per time unit than the high frequency vibration used to activate Pacinian afferents. Thus it is also possible that the total number of impulses generated in mechanoreceptive afferents contributes to the pain threshold elevation.

In the light of the present experiment the pain threshold elevations caused by 60 Hz vibrotactile stimulus in the experiments of Wall & Cronley Dillon (1960) can be explained as a result of activation of Pacinian afferents. There appears to be similar inhibitory effect from Pacinian afferents to pain-conducting pathways as was assumed to exist from Pacinian afferents to non-Pacinian mechanosensitive pathways by Bystrzycka et al. (1977) and Ferrington et al. (1977).

On the basis of the present experiments it is not possible to exclude the non-Pacinian mechanoreceptive fibers as a source of inhibition to pain-conducting pathways in certain situations e.g. if high amplitude stimulation is used and consequently the number of nerve impulses generated in non-Pacinian afferents is comparable to the number of nerve impulses generated in Pacinian afferents.

I wish to thank Professor J. Hyvärinen for comments on the manuscript.

REFERENCES

- BYSTRZYCKA, E., NAIL, B. S. & ROWE, M. 1977. Inhibition of cutaneous neurons: Its afferent source and influence on dynamically sensitive 'tactile' neurons. *J. Physiol. (Lond.)* 268: 251-270.
- FERRINGTON, D. G., NAIL, B. S. & ROWE, M. 1977. Human tactile detection thresholds: Modification by inputs from specific tactile receptor classes. *J. Physiol. (Lond.)* 272: 415-433.
- MERZENICH, M. M. & HARRINGTON T. 1969. The sense of flutter-vibration evoked by stimulation of the hairy skin of primates: Comparison of human sensory capacity with the responses of mechanoreceptive afferents innervating the hairy skin of monkeys. *Exp. Brain Res.* 9: 36-260.
- TALBOT, W. H., DARIAN-SMITH, I., KORNHUBER, H. H. & MOUNTCASTLE, V. B. 1968. The sense of flutter-vibration: Comparison of the human capacity with response patterns of mechanoreceptive afferents from the monkey hand. *J. Neurophysiol.* 31: 301-334.
- WALL, P. D. & CRONLEY DILLON, J. R. 1960. Pain, itch and vibration. *Arch. Neurol. (Chic.)* 2: 365-375.

Firing behaviour in a stochastic nerve membrane model based upon the Hodgkin-Huxley equations

ERIK SKAUGEN and LARS WALLØE

Institute of Physiology and Informatics, University of Oslo, Norway

SKAUGEN E. & WALLØE, L. Firing behaviour in a stochastic nerve membrane model based upon the Hodgkin-Huxley equations. *Acta Physiol Scand* 1979, 107, 343-363. Received 3 May 1979. ISSN 0001-6772. Institutes of Physiology and Informatics, University of Oslo, Norway.

A nerve membrane model with a two-state pore system was investigated by computer simulation in the uniform (space-clamped) case. Both sodium and potassium conducting pores were modelled, each pore having four independent gates which switched randomly between the open and the closed position, governed by the assumed rate constants. Each pore conducted only when all the gates were open. The model was based upon the Hodgkin-Huxley equations for the giant axon in squid, and in the limit of an infinite number of pores it was identical to these. The firing behaviour of this model as a function of the number of pores and the injected current were investigated. The mean firing frequency and the distribution of interspike intervals were mainly used in the presentation of the results. It was found that for pore numbers less than about 20 000 the main effects due to a finite number of pores were: lowering of the current threshold for firing and a more linear frequency-current relationship relative to that of the original H-H equations. For higher pore numbers an increase in the current threshold and a pronounced burst firing close to the threshold were found.

This is the first of two papers discussing the firing behaviour of a nerve membrane model with a two-state pore system. The model is based upon the Hodgkin-Huxley equations for the squid giant axon membrane (Hodgkin & Huxley 1952).

When Hodgkin and Huxley formulated their equations they discussed a possible physical basis for these. The interpretation they gave as the simplest was that the different ions could only cross a particular region of the membrane when four particles were all in a certain position in that region (the open position). Even if only one particle was in the shut position, that region was closed. The total conductance of the membrane at a certain time was then the sum of all the conductances of the open regions of the membrane. The potential dependent parameters α and β in the Hodgkin-Huxley equations then determined the rate of transfer for one type of particle from the shut to the open and from the open to the shut position, respectively. This physical interpretation has been strengthened by the discovery that ions cross the

membrane mainly through channels or pores and that there is a different pore system for each type of ion (Hille 1970, 1972, 1973). The simplest assumption for the Hodgkin-Huxley equations is then that each pore has 4 gates and that an ion can only pass through the pore if it is of the type admitted by the pore, and if all gates are open. The word 'gate' is used instead of 'particle' in order to make it easier to picture the process.

Very little is known about the processes that open and close the pores. Some experiments on membrane noise seem to indicate that the pores can be partially conducting (Verveen & Derksen 1969, Fishman 1973), but as later results can be well fitted by assuming only an open and a closed state for each pore (Cotté et al. 1975, Cotté et al. 1976) the former possibility will not be considered here. Other sources of membrane electrical noise are not taken into account here, only the effects of conductance fluctuations are studied.

If we now assume that the gates are independent of each other, the α and β parameters in the Hodg-

kin-Huxley equations must determine the probability of transfer for one gate from the shut to the "open" and from the open to the shut position respectively. It is then a matter of chance if at a given time a particular pore is open or shut and since the pores are independent the total number of open pores and hence the total membrane conductance will fluctuate around a mean value.

The statistical nature of the suggested physical basis of Hodgkin & Huxley's equations was not taken into account when these equations were originally solved: the mean values of the different ionic conductances were then used. For all practical purposes this is accurate enough when the number of pores is very large as it probably is in the squid giant axon. But what happens when the number of pores is small? And how small must the number be for these effects to be important? In order to answer these questions we have simulated a model of the nerve membrane where the statistical properties of the pores were taken into account.

This statistical model is meant to represent an isolated patch of nerve membrane for instance a certain length of an axon which is electrically insulated at both ends. The patch is so small that there is no need to consider the spatial extension of the nerve membrane and the Hodgkin-Huxley equations can thus be used in their simplest form as a basis for the calculation.

The only independent parameters introduced in addition to the parameters in the Hodgkin-Huxley equations are the numbers of sodium and potassium pores in the patch of nerve membrane considered. The results are not directly dependent upon the actual area of the membrane but the area will of course determine the total numbers of pores. In order to use the results presented here to find the predicted firing behaviour of a space-clamped nerve cell or part thereof one should estimate the number of pores in the membrane and then use this number as the pore number in the figures. In most actual cases the membrane will not be described very well by the Hodgkin-Huxley equations and the results presented here must then be taken as indications of the expected effects of a finite pore number. This is discussed at the end of the next paper (Skaugen 1979).

Under the assumptions made here the spectra of the membrane conductance fluctuations in the voltage-clamped membrane model will be as derived by

Hill et al. (1977) and Stevens (1977) for the two-state pore.

One of the most important properties of a nerve cell as an information carrying and processing element in the nervous system is the firing frequency as a function of the input current. For the model presented here we have obtained the mean firing frequency and the interspike interval distribution as functions of the injected current and for different values of the number of pores.

Stein has made corresponding calculations for a much simpler model of a pore system in the Hodgkin-Huxley nerve membrane model (Stein 1965, 1967a).

In later papers we shall give corresponding results for a model where the spatial extension of the nerve cell is taken into account. Preliminary reports of the results obtained here in the later papers have been given at meetings of the Scandinavian Physiological Society (Skaugen 1974, 1976), and the results have been used in a Ph.D. thesis (Skaugen 1978).

THEORY

Conventions

The membrane potential is here defined as the potential inside the nerve membrane relative to the potassium equilibrium potential which is accordingly set equal to zero. The membrane potential is then always positive, except possibly in the case of an externally induced hyperpolarization. This definition makes the computation a little simpler. Note that the membrane potential increases if the cell is depolarized, decreases if it is hyperpolarized.

The equations found by Hodgkin and Huxley for the potential of the squid giant axon (Hodgkin & Huxley 1952) will here be termed the "H-H" equations.

Na-conducting pores are termed Na-pores and K-conducting pores are termed K-pores.

Assumptions

The model presented here is based upon the following assumptions.

1. There are no potential differences along the nerve membrane.

2. The nerve membrane conducts ions through pores. In addition there is a leakage conductance which is constant.

3. A particular pore conducts only a certain type of ion, either sodium or potassium ions.

4. All pores which conduct the same type of ion have the same conductance when in the open state.

5. There is no coupling between neighbouring pairs of pores.

6. Each pore has four gates. The pore is open only if all four gates are open.

7. The transition probabilities of a gate from one state to another either from shut to open or from open to shut, are only potential dependent and given by the α and β parameters of the H-H equations.

8. The transition times of the gates are so short that they can be ignored. (The transition time is the time used by the gate to go from the shut to the open position, or vice versa.)

The rest of the assumptions necessary to completely specify the model are stated in the paper by Hodgkin & Huxley (1952). We will restate the necessary equations here.

For a patch of membrane with area A the membrane potential E is governed by the differential equation

$$C \frac{dE}{dt} = -\frac{1}{C} (g_{Na}(E - E_{Na}) + g_K(E - E_K) + g_L(E - E_L) - I) \quad (1)$$

where E_{Na} and E_K are the equilibrium potential and the specific membrane conductance for the sodium ion; g_L is the specific potassium conductance (E_L is defined to be zero), and E_L is the equilibrium potential for the specific membrane leakage conductance g_L . C is the specific capacitance of the membrane and I is the specific injected current. With specific values of the parameters we have given their values per square centimeter of the membrane. Note that the area A does not appear in this equation. The parameters g_{Na} and g_K depend on the total numbers N_{Na} and N_K of open Na-pores and K-pores

$$g_{Na} = \frac{N_{Na}}{N_{Na0}} g_{Na0} \quad g_K = \frac{N_K}{N_K0} g_{K0} \quad (2)$$

where N_{Na0} and N_K0 are the total numbers of Na-pores and K-pores in the patch of membrane with area A . Instead of total numbers of pores it would perhaps have been more natural to use the specific values of these parameters, that is the pore densities. But the total numbers are used because we must know these in order to simulate this model

with a computer. The parameters g_{Na0} and g_{K0} are the specific Na- and K-conductances of the membrane when all the pores are open. In all of the calculations and figures in this paper g_{Na0} and g_{K0} are taken to be constants equal to their values in squid axon membrane.

As in the H-H equations the firing behaviour is not directly dependent upon the membrane area A (for the space-clamped case considered here) but it depends upon the numbers N_{Na} and N_K of pores, and it is thus indirectly coupled to this area. Note that the densities (q_{Na} and q_K) of Na- and K-pores, and the conductances (g_{Na} and g_K) of single pores now do not enter into these calculations. This means that we are free to choose any combination of pore densities and conductances of single pores such that $g_{Na0} = q_{Na} g_{Na}$ and $g_{K0} = q_K g_K$ have the values found in the squid giant axon. We are also free to choose any area of the nerve membrane investigated. The total numbers of pores are then given by $N_{Na} = q_{Na} A$ and $N_K = q_K A$. These numbers are the pore numbers used in the figures.

As an example, let us assume that a space-clamped axon with membrane area $A = 300 \mu m^2$ is investigated. The sodium pore density q_{Na} is taken to be 400 pores per μm^2 so that, as g_{Na0} is as in squid, g_{Na} is taken to be $g_{Na0}/q_{Na} = 3 \times 10^{-12}$ MHO per pore. The injected current is 0.018 nA. The total number of Na-pores is now $N_{Na} = q_{Na} A = 12000$, and the specific injected current is $i = 0.018 \text{ nA}/300 \mu m^2 = 6 \text{ pA}/\mu m^2$. These values must then be used in order to obtain the predicted firing behaviour from the results presented here.

For the majority of unmyelinated nerve cells the pore densities are generally smaller than assumed in this example where a realistic value for the squid giant axon was used (Jack 1975). As shown above these smaller pore densities are accounted for by the model presented here, if the conductances of single pores can be assumed to be correspondingly larger. But the conductances of single pores are probably more or less constant, independent of the pore densities. That is the maximal specific conductances g_{Na0} and g_{K0} are smaller than in squid if the pore densities are smaller. The results presented here cannot therefore be applied directly to cases where the pore densities are much smaller than in the giant axon of squid. This is discussed in a following paper where it is shown that the results presented here still can be indirectly used as a reasonable approximation (Skagen 1979).

For the squid giant axon the values of the membrane parameters at 6.3°C are

$$\bar{g}_{Na} = 120 \text{ mMHO/cm}^2$$

$$\bar{g}_h = 35 \text{ mMHO/cm}^2$$

$$\bar{g}_L = 0.3 \text{ mMHO/cm}^2$$

$$E_h = 127.0 \text{ mV}$$

$$E_L = 22.6 \text{ mV}$$

$$E_K = 0$$

$$C = 1.0 \text{ } \mu\text{F/cm}^2$$

$$g_{Na} = \bar{g}_{Na} \bar{g}_h$$

$$g_h = n \bar{g}_h$$

(3)

According to the H-H equations we must assume that in the Na pores there is one gate of a certain type which we term the *h*-gate and three gates of another type which we term the *m*-gate. In the K-pores there are four gates of the same type which we term the *n*-gate. For the *h*, *m* and *n* gates the probabilities that a shut gate will open in a time interval Δt are $\alpha_h \Delta t$, $\alpha_m \Delta t$ and $\alpha_n \Delta t$ respectively. The probabilities that an open gate will close in a time interval Δt are $\beta_h \Delta t$, $\beta_m \Delta t$ and $\beta_n \Delta t$ respectively. These α and β parameters are functions of the potential only

$$\alpha_h = 0.07 e^{-0.05E + 0.6} \text{ ms}^{-1}$$

$$\beta_h = (e^{-0.1E - 4.2} + 1) \text{ ms}^{-1}$$

$$\alpha_m = 0.1 (-E + 37) / (e^{-0.1E - 3.7} - 1) \text{ ms}^{-1}$$

$$\beta_m = 4 e^{E/10 - 2.7} \text{ ms}^{-1}$$

$$\alpha_n = 0.01 (-E + 22) / (e^{-0.1E - 2.2} - 1) \text{ ms}^{-1}$$

$$\beta_n = 0.125 e^{-E/70 + 0.15} \text{ ms}^{-1}$$

(4)

where E is given in mV relative to E

The assumptions stated above together with the values of the parameters given here completely determine the model when the total numbers N_{Na} and N_K of pores are chosen. It is for instance found that the membrane potential fluctuates around the value $E = 12 \text{ mV}$ when the injected current is set equal to zero.

The model in the limit of an infinite large number of pores

When the number of pores becomes very large the relative fluctuations of the membrane conductances become insignificant. If at a given time the numbers of open *h*, *m* and *n* gates relative to the total numbers of these gates are h , m and n respectively the expected numbers n_{Na} and n_K of open Na and K pores are close to $h m^3 N_{Na}$ and n . Equation (2) then becomes

since we assume that in this case the actual parameters are equal to their expected values. Note that h , m and n must have values in the range 0 to 1.

In a short time interval Δt the change Δh of h is equal to the relative number of closed gates ($1-h$) which open minus the relative number of open gates (h) which close in this time interval

$$\Delta h = (1-h)\alpha_h \Delta t - h\beta_h \Delta t \quad (6)$$

Corresponding equations are obtained for m and n . If we divide through with Δt letting Δt go to zero we obtain

$$\frac{dh}{dt} = \alpha_h(1-h) - \beta_h h$$

$$\frac{dm}{dt} = \alpha_m(1-m) - \beta_m m$$

$$\frac{dn}{dt} = \alpha_n(1-n) - \beta_n n \quad (7)$$

These rates of changes are expected values and must be equal to the actual rates of changes of h , m and n in the limit of an infinite number of pores. Equations (5) and (7) together with Eqs. (1), (3) and (4) are the equations for the giant squid axon membrane found by Hodgkin & Huxley (1952). The model thus reduces to the H-H equations in the limit of an infinite number of pores.

The model for a finite number of pores: a simple method of computation

In the case of a finite number of pores a simple method of computation suggests itself. While the computer keeps track of the states of all gates in all the pores the model time t is increased in small steps Δt . At each step the potential is computed and the α and β parameters are calculated. For each gate which is closed the probability of opening during the next time step is $\alpha \Delta t$ and for each open gate the probability of closing is $\beta \Delta t$ ($\alpha = h$, m or n as required). For each gate the probability is drawn from an appropriate binary probability distribution. The result of the drawing determines if the state of the gate is changed. The total numbers n_{Na} and n_K of

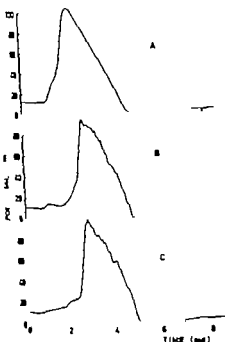


Fig. 1. An action potential calculated by the H-H equations (A), and spontaneously generated (B and C). $\lambda = 400$, and $N = 100$ for B and C, and $=0$ for all cases. In case A the action potential was started by a short current pulse of 0.5 ms duration.

open pores (where all four gates are open) are then counted and new values of g_{Na} and g_K are calculated from Eq. (2). To obtain a reasonably accurate calculation Δt must be kept small. The error due to a finite value of Δt can in this and the later methods be evaluated by calculating the mean firing frequency f for different values of Δt taking as the true value the value approached when Δt approaches zero. We will here assume Δt to be sufficiently small if f is less than 2.5 s⁻¹ from the extrapolated true value. This error of ~ 5 s⁻¹ is also approximately equal to the standard error of the mean (S.E.) resulting from taking the mean firing frequency f over a model time of 5 s.

Fig. 1B and C shows the potential as a function of time calculated by this method for two cases. In both cases the injected current was zero, and the numbers of Na- and K-pores were 400 and 100, respectively. The only difference between the two cases is that they represent different runs on the computer.

The resting potential fluctuates and in both cases

it becomes so large at a certain time that an action potential is generated. The membrane thus fires even if the injected current is zero and the H-H equations give a constant potential equal to the resting potential $E = -1$ mV. We note also that the forms of the action potentials thus generated closely follow the form of the action potential calculated by the original H-H equations, which is also shown in Fig. 1.

It is, however, quite impractical to calculate firing frequencies by this method because the computer time used becomes prohibitively large for relatively small pore numbers (larger than 10). And in this case the computer time relative to the model time is proportional to the number of pores, and to the reciprocal of the time step length. In the next section two faster methods for computation are presented.

METHODS

Computation method 2

This method has been used for membranes with total number of pores up to 10 000. The computation time relative to the model time is approximately proportional to the total number of pores, and the accuracy of the method increases as the number of pores increases.

At certain time t_n , the potential E and the state of all the pores are known. It is not necessary to consider the order of open and closed gates of the same type in one pore, the state of a pore is therefore here defined by the number of open gates of each type. A Na-pore has 8 possible states and a K-pore has 3. These states are for the Na-pore: all gates closed, all m -gates closed and the k -gate open, one m -gate open and the k -gate closed, and so on until the state where all gates are open. For the K-pore the states are: all gates closed, one gate open, and so on until all four gates are open. (Here all gates are n -gates.)

The state where k k -gates and j m -gates are open is termed the state SN_{kj} , while the state where j j -gates are open is termed the state SK_j . The numbers N_{Na} and N_K are the numbers of pores in the states SN_{Na} and SK_K , respectively. The expected values of these numbers are close to

$$N_{Na} = (1)k^4(1-k)^{4-k}m^4(1-m)^{4-m}N_{Na} \\ N_K = (1)j^3(1-j)^{3-j}N_K \quad (8)$$

where k , m and j can be calculated from Eq. (7). Since k and m are functions of E only this calculation is straightforward because the previous values of E are known. In the model, the numbers N_{Na} and N_K are integers which fluctuate around their expected values.

The probability that a certain pore in the state SN_{Na} or SK_K , will change to the state SN_{Na} or SK_K , in the infinitesimally small time interval dt is given by

$$\begin{aligned}
P(SN_{k,j} \rightarrow SN_{k,j-1}) dt &= \alpha_k dt \\
P(SN_{k,j} \rightarrow SN_{k,j+1}) dt &= \beta_k dt \\
P(SN_{k,j} \rightarrow SN_{k,j}) dt &= (3-j) \alpha_k dt \\
P(SN_{k,j} \rightarrow SN_{k,j-1}) dt &= j \beta_k dt \\
P(SK_j \rightarrow SK_{j-1}) dt &= (4-j) \alpha_k dt \\
P(SK_j \rightarrow SK_{j+1}) dt &= j \beta_k dt
\end{aligned} \quad (9)$$

The time Δt to this change is given by a negative exponential distribution with an expected value $E(\Delta t)$ given by

$$\begin{aligned}
E(\Delta t) &= [P(SN_{k,j} \rightarrow SN_{k,j+1})]^{-1} \\
\text{or } E(\Delta t) &= [P(SK_j \rightarrow SK_{j+1})]^{-1}
\end{aligned} \quad (10)$$

The drawing procedure consists in first drawing the time Δt to the first time one of all the pores changes its state. According to the properties of the negative exponential distribution this time Δt is also given by a negative exponential distribution with an expected value $E(\Delta t)$ given by

$$\begin{aligned}
E(\Delta t) &= \left[\sum_{k=0}^1 \sum_{j=0}^3 \sum_{p,q \neq \pm 1}^1 P(SN_{k,j} \rightarrow SN_{k,j+p}) NN_{k,j} \right. \\
&\quad \left. + \sum_{j=0}^4 \sum_{q \neq \pm 1} P(SK_j \rightarrow SK_{j+q}) NK_j \right]^{-1}
\end{aligned} \quad (11)$$

By a new drawing it is then determined which of the 28 different possible transitions is actualized and the numbers $NN_{k,j}$ or NK_j are changed accordingly. This is done by a drawing between each of these 28 possibilities. The probability that just the transition $SN_{k,j} \rightarrow SN_{k,j+1}$ will occur for one of the pores in the state $SN_{k,j}$ is

$$P(SN_{k,j} \rightarrow SN_{k,j+1}) NN_{k,j} E(\Delta t) \quad (12)$$

with a corresponding expression for the transition $SK_j \rightarrow SK_{j+1}$. Note that if Eq. (12) is divided by $E(\Delta t)$ we obtain one of the terms in the sum shown by Eq. (11). If for instance the transition $SN_{k,j} \rightarrow SN_{k,j+1}$ is drawn the number $NN_{k,j}$ is reduced by one and the number $NN_{k,j+1}$ is increased by one.

The state of the membrane at time $t + \Delta t$ is now known, and the membrane conductances can be calculated from Eq. (2). Note that by definition $\pi_{k+1} = NN_{k+1,1}$ and $\pi_k = NK_k$. The conductances will thus change only if the states SN or SK are involved in the transition. In the time interval Δt from t to $t + \Delta t$ the conductances are always constants and equal to their values calculated at t .

The potential at time $t + \Delta t$ can now be calculated from Eq. (1) because g_{Na} and g are constants in the time interval from t to $t + \Delta t$.

$$\begin{aligned}
E &= E_m + (E - E_m) e^{-\Delta t/\tau} \\
\text{where } \tau &= C/(g_{Na} + g + g_i) \\
E_m &= (g_{Na} E_{Na} + g E_i) / (g_{Na} + g + g_i) \\
E &= \text{value of } E \text{ at time } t
\end{aligned} \quad (13)$$

g_{Na} and g are the values of the conductances for $t < t < t + \Delta t$. In a corresponding way new values of h , m

and n are calculated by integrating Eq. (7) where α and β are known functions of time since E now is a known function of time. This is not necessary here, but it is used in some later methods.

At the new time $t + \Delta t$ thus arrived at, the potential and the number of pores in the different states are known and the process described here can be repeated over and over again, generating E as a function of time.

The only error introduced by this procedure is the underlying simplification that $E(\Delta t)$ is not dependent upon the change of the potential E and hence the parameters α and β in the time interval after t . This is seen by noting that the transition probabilities as given by Eq. (9) are used in Eq. (11) to calculate $E(\Delta t)$ are calculated at the time t . For large numbers of pores this error is small because the average time step then is small. This error can be reduced by several methods: all of them making use of a special property of the negative exponential distribution which is that the probability of an event occurring within small time interval dt is independent of what has happened before. From this it follows that if a time interval Δt drawn which is so long that the potential changes "too much" any point within this time interval can be chosen as a starting point for a new drawing.

The simplest method of correcting the error discussed here is to set an upper limit Δt_{max} to the time step of Δt . If the time step Δt drawn at the time t is larger than Δt_{max} , a new value of E is calculated at the time $t + \Delta t_{max}$ and the drawing procedure is repeated. The maximum time step Δt of the calculation of E is thus Δt_{max} . By choosing Δt_{max} sufficiently small, the error in the calculation can be made as small as we want.

An extra safeguard against too large changes of E in one step of the calculation can be obtained by choosing an upper limit ΔE_{max} to the change of E in one step Δt . By using Eq. (13) an upper limit for Δt can in this case be obtained for each new time step

$$\Delta t_{max} = \begin{cases} \Delta t & \text{if } \Delta t \ll \Delta t_E \\ \Delta t_E & \text{if } \Delta t > \Delta t_E \end{cases} \quad (14)$$

$$\Delta t_E = \begin{cases} \alpha \text{ if } |E_m - E| \leq \Delta E_{max} \\ -\tau \ln \left(1 - \frac{\Delta E_{max}}{|E_m - E|} \right) \text{ if } |E_m - E| > \Delta E_{max} \end{cases}$$

where Δt is the largest allowed value of Δt_{max} and τ is defined in Eq. (13). If Δt is found to be larger than Δt_{max} the drawing procedure is repeated at the time $t + \Delta t_{max}$ in the simpler method. In the later calculations $\Delta t = 0.01$ ms and $\Delta E_{max} = 1$ mV was used in most cases as this was found to give an error in the mean firing frequency f of less than 2.5%.

Comparison method 2 b

The method described in the preceding section can be greatly simplified by taking into account only the fluctuations of the numbers of pores with all m -gates or all n -gates open, that is the numbers $NN_{m,1}$, $NN_{n,1}$ and NK_1 . The numbers which are connected to these through the transition probabilities shown in Eq. (9) are $NN_{m,1}$, NK_1

and N_{ij} , and these are then at all times set equal to their expected values given by Eq. (5). In general these numbers are then not integers, but this does not matter because their values are now used only to calculate probabilities. All the other numbers are now of no interest as they can only "influence" the numbers important for the calculation (NN_{ij} and NK_{ij}) through the numbers NN_{ij} , NV_{ij} , and NK_{ij} . This reduces the number of possible transitions from 28 to 8, but the reduction in computer time is not greater. Around the resting potential only about 0.022 and 0.032 of the transitions in the sodium and potassium pore systems, respectively, occur between the states now taken into account.

In order to use Eq. (5) the values of k , m and n must be known at all times when drawing procedures is started. These parameters must be found by numerical integration of Eq. (7). It is then practical to use the time step length Δt and the calculation of E . The errors introduced by this numerical integration are then also reduced when the maximum value of Δt is reduced. As the number of pores is increased, the accuracy increases rapidly and it was found that method 2b could be used for rather low pore numbers, down to 10 pores approximately.

Different combinations of these two methods can now easily be constructed. Here all states with 4, 3 and down to 1 gates open are included in the drawing procedure while the number of states with fewer gates open are set equal to their mean values. This has been done in order to use these methods, but only methods 2a and 2b were used in order to calculate the results presented here. Method 2a was used for $N < 10$ and $N_{ij} < 10$, and method 2b was used for the other cases.

When E becomes much larger than $E = 12$ mV there is a rapid increase of the number of pores in the states where nearly all gates are open, and for method 2b the average length of the time steps Δt decreases correspondingly. The computer therefore uses a disproportionately long time to go through an action potential. To avoid these difficulties this method of computation can be abandoned when E increases over a certain threshold value E_c which has to be followed by an action potential. ($E_c = 40$ mV used here.) The expected value of E is then computed from the original H-H equations until the action potential has ended. The numbers of pores in the different states are then set equal to their expected values according to Eq. (5), and the computation method described here is again used. This is a good approximation because the fluctuations of E during and some time after an action potential are small compared to the fluctuations between the action potentials, and the mean firing frequency f is mainly determined by the latter fluctuations. Appendix I shows how the accuracy of method 2b depends upon the number of pores, i.e. the action potentials are computed by a stochastic method. In the later calculations a threshold of $E_c = 40$ mV was used for $N_{ij} > 100$ and $N > 100$. For smaller pore numbers, method 2b was used during the action potentials also. This gave a negligible error in the mean firing frequency.

The main virtue of method 2b is that it of all the changes of states only considers those changes which are important for the number of open pores. This makes it quick. These events are, however, placed accurately, not jumped

at certain evenly spaced times as in the simple method described before. This makes it accurate.

This method was found useful for a number of pores up to 10000. For still larger numbers a faster but more inaccurate method had to be devised.

Computation method 3

This method has been used for membranes with total number of pores from 10000 and upwards. The computation time is independent of the number of pores, and the accuracy of the method increases as the number of pores increases.

The computation is done in time steps Δt of constant length. As in method 2b the fluctuations of NN_{ij} , NN_{ij} and NK_{ij} are neglected and these numbers are set equal to their expected values as shown by Eq. (5). The values of k , m and n are obtained by integration of Eq. (7).

It is convenient for the computation to change the notation, as it is necessary to consider only a small part of the symbols used in method 2a

$$\begin{aligned} S &= SN_{ij} & V &= NV_{ij} \\ S &= SN_{ij} & V &= NN_{ij} \\ S &= SN_{ij} & V &= NN_{ij} \\ S &= SN_{ij} & V &= NN_{ij} \\ S &= SK_{ij} & V &= NK_{ij} \\ S &= SK_{ij} & V &= NK_{ij} \end{aligned} \quad (15)$$

The probabilities p_{ij} that pores in certain state S , will go to another state V during the time interval Δt are given approximately by Eq. (9) if Δt is sufficiently small

$$\begin{aligned} p_{10} &= A_1 \Delta t \\ p_{11} &= a_1 \Delta t \\ p_{12} &= p_{10} + p_{11} \Delta t \\ p_{13} &= a_1 \Delta t \\ p_{14} &= a_1 \Delta t \\ p_{15} &= 4a_1 \Delta t \end{aligned} \quad (16)$$

and where all other p_{ij} ($j = 1, 2, \dots, 6$) are zero.

In Eq. (16) the parameters a_1 and A_1 are functions of the potential E . This equation therefore holds true only when E does not change noticeably during the time interval Δt .

The actual number of pores ΔV which goes from certain state S , to another state V is then given by a binomial distribution, where the probability $p(i, j, k)$ that certain number k of pores is transferred is

$$p(i, j, k) = \binom{V}{k} p^k (1-p)^{V-k} \quad (17)$$

When the expected value of the number k is large, but small compared to V , this distribution can be approximated by a Gaussian distribution. The net number of pores transferred from state S to V , is described by corresponding distribution where i and j are interchanged. The net number V of pores transferred is then described by the difference of two Gaussian distributions, which is a new Gaussian distribution.

$$\Pr(\Delta V_0 \in [k, k + dk]) =$$

$$\exp \left\{ \frac{(V_1 p_L - V_1 p_R - k)^2}{2[V_1 p_0(1-p_0) + V_1 p_R(1-p_R)]} \right\} dk \quad (18)$$

Note that $\Delta_0 = -\Delta V_0$.

At each step the numbers ΔV_{11} , ΔV_{12} , ΔV_{21} and ΔV_{22} are drawn from their respective distributions (ΔV_{11} is set equal to the integer closest to the result of the drawing). The numbers of pores in the states S_1 , S_2 and S_3 are in the time interval Δt changed to

$$\begin{aligned} V + \Delta V \quad \text{where } \Delta V &= \Delta V_{11} + \Delta V \\ V + \Delta V_2 \quad \text{where } \Delta V_2 &= \Delta V_{12} - \Delta V \\ V + \Delta V \quad \text{where } \Delta V &= -\Delta V_{21} \end{aligned} \quad (19)$$

The changes occurring in the time interval Δt have thus been calculated, but we do not know when these changes occur. If we as an approximation assume that all the changes occur at the same time in the interval, the calculation becomes particularly simple. It is then reasonable to assume that the changes occur in the midst of the time interval Δt . Between the times $t - \frac{1}{2}\Delta t$ and $t + \frac{1}{2}\Delta t$ all the conductances are then constants, and in this time interval Eq. (1) is easily integrated. Since we need to know the value of the potential at time t in order to calculate the changes of the conductances at $t + \frac{1}{2}\Delta t$, the integration is done in two steps:

$$\begin{aligned} E &= E_m + (E - E_m)e^{-\Delta t/\tau} \\ E &= E_m + (E - E_m)e^{-\Delta t/\tau} \end{aligned} \quad (20)$$

where τ and E_m are given by Eq. (13). Note that the conductances in Eq. (13) have been calculated at the earlier time $t - \Delta t$. E and E and the values of the potential at $t - \frac{1}{2}\Delta t$ and $t + \frac{1}{2}\Delta t$ respectively.

We have now arrived at the time $t + \frac{1}{2}\Delta t$ with the potential E and the conductances known. The process described here can then be repeated over and over again, generating E as a function of time. The values of \bar{m} and \bar{n} can then be integrated from Eqs. (4) and (7).

This method of computation was also used during the action potentials, since the speed of calculation is, in contrast to method 2b, independent of the number of open pores.

When Δt is decreased, there is a decrease of the inaccuracies introduced by the lumping of the conductance changes and the probabilities p_{ij} used. At the same time, however, the expected number of pores transferred from one state to another decreases, which decreases the accuracy of Eq. (18), and Eq. (17) may have to be used. In addition, the accuracy of this method will decrease when the number of pores decreases, because the fluctuations of the potential then increase and Eq. (13) becomes more inaccurate. At the same time the accuracy of Eq. (18) also decreases.

Testing the different methods with different step lengths and different pore numbers showed that an error of less than 2.5% in the mean firing frequency f was obtained for the following restrictions:

Method 1	$\Delta t \leq 0.05$ ms
Method 2a	$\Delta t_{\max} \leq 0.2$ ms
Method 2b	$\Delta t_{\max} \leq 0.1$ ms and $N \geq 5$ $N_{Na} \geq 1$
Method 2b with a non-stochastic calculation of the action potentials,	$\Delta t_{\max} \leq 0.1$ ms and $N \geq 10$ $N_{Na} \geq 1$
Method 3	$\Delta t \leq 0.05$ ms and $N_{Na} \geq 500$ $N_{K} \geq 5000$

RESULTS

The internal parameters of the model are determined by the H-H equations, except for the two independent variables N_{Na} and N_K which are the numbers of Na-pores and K-pores. When both of these parameters are infinite the model reduces to the H-H equations. We will first study the effects upon the firing behaviour of each of these parameters separately. This is done by assuming the other parameter infinite. In Figs. 2 and 3 it is shown for different values of the injected current how the mean firing frequency over 5 seconds of model time changes as either N_{Na} or N_K is increased from zero towards large values, while the other number (N_K or N_{Na}) is infinite. The Appendix shows how the statistical parameters used here are calculated. The values of N_{Na} and N_K are presented on a logarithmic scale. Note that the maximal specific conductances \bar{g}_{Na} and \bar{g}_K of the pore systems are constants equal to their values in squid axon membrane (Eq. (3)). When the numbers of pores are increased, one can interpret this as a corresponding increase of the area of the patch of nerve membrane under consideration.

Fig. 2 shows that for all values of the injected current used here the mean firing frequency is rather small for low values of N_{Na} , especially when N_K is less than about 10. For low values of N_{Na} ($N_{Na} < 200$) the normal state of the membrane is zero Na-conductance or no Na-pores open. This corresponds to the case where $N_{Na} = 0$ which gives a potential E of 11.1 mV above E_K . The probability of finding a single Na-pore open at a given time is approximately $N_{Na} / (N_{Na} + N_K) = 7.5 \times 10^{-4}$. A single Na-pore will occasionally open, however. This gives an ionic current into the cell of magnitude $(E - E_K) \approx (13800/N_{Na}) \mu A/cm^2$ which has the same effect as a sudden increase of the injected current by the same amount. According to Hodgkin and Huxley a shock strength of approximately 6 nA/cm² is barely sufficient to start an action poten-

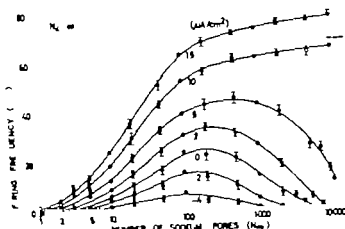


Fig. 2. Mean firing frequency as function of N_{Na} for different values of the injected current. I is infinite. Numbers show value of I in $\mu A/cm^2$. S.E. is shown by vertical bars.

from the resting potential of 1 mV (Hodgkin and Huxley 1952). Using this we find that at $E = 2$ mV, here the mean open time is 0.083 ms, the opening of a single Na-pore gives a mean shock strength of $6 \mu A/cm^2$ if $N = 190$. For lower values of I the occasional opening of a single Na-pore will in most cases start an action potential. The rapid increase of the mean firing frequency f when N increases towards 190 therefore reflects the increasing rate of openings of single Na-pores. At the same time the probability that two or more Na-pores open at about the same time begins to become significant. Even if the opening of a single pore fails to start a spike, the potential is increased somewhat, and this increases the probability that a second pore will open. The increasing rate of multipore openings also contributes to the increase of the mean firing frequency f which reaches a maximum at about 200 Na-pores for $I=0$. As N increases above 190, however, the opening of a single Na-pore more and more often fails to start an action potential. Moreover the fluctuations of the Na-conductance due to the random opening and shutting of Na-pores eventually start to decrease and f decreases to zero as N is increased further.

When the injected current I is increased, the mean value of the potential is also increased and this increases the probability that a Na-pore will open. The event is now also more likely to start an action potential. The mean firing frequency f is thus increased at all values of N_{Na} . The local maximum of f at $N_{Na} \approx 200$ for $I=0$ is shifted towards higher

values of N_{Na} when I is increased, due to the smaller current shock necessary to start a spike. At the same time multipore openings begin to become important at lower values of N_{Na} , due to the increased probability of pore opening.

When the injected current I is smaller than the threshold current $I_{th} = 6.3 \mu A/cm^2$ in the H-H equations the mean firing frequency f decreases to zero as N_{Na} is increased. When I is larger than I_{th} the asymptotic value of f for $N_{Na} = \infty$ is indicated by broken lines to the extreme right in the figure.

The effects of a finite number of K-pores are shown in Fig. 3. When there are no K-pores ($N_K = 0$) the K-conductance is zero and there is a stable value of the potential E for $E > E_{th} = 22.6$ mV when the injected current I is larger than zero. Repetitive firing is not found due to the lack of the K-conductance. With a single K-pore the situation is different. During the peak of an action potential the probability that the single K-pore will open is very high and this must eventually happen. The potential is then rapidly reduced towards zero and the probability that the open K-pore will close increases.

When this happens the potential first increases towards the equilibrium potential E_K of the K-conductance which is then dominating. This increases the Na-conductance and a new action potential is generated. When there are several K-pores the same process is repeated when the last K-pore closes after an action potential a new spike is triggered off. The mean firing frequency is reduced towards zero when the injected current is decreased

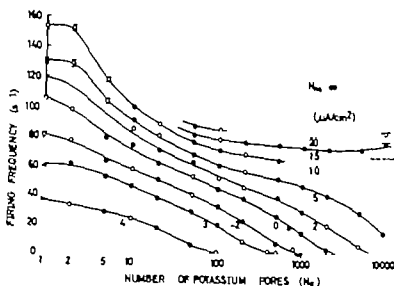


Fig. 3 Mean firing frequency as a function of N_k for different values of the injected current i when N_{Na} is infinite. Numbers show value of i in $\mu\text{A}/\text{cm}^2$. S.E. is shown by vertical bars.

from zero towards $-4.7 \mu\text{A}/\text{cm}^2$. At this value the closing of all K pores simultaneously will not be sufficient to start an action potential. Note that there is no corresponding lower limit of the injected current for firing when we have a small number of Na-pores.

When N_k is increased multi-pore closing and opening become more important, but the mean firing frequency decreases. If the injected current i is smaller than the current threshold i_T , the mean firing frequency f eventually falls to zero. When i is

larger than i_T , the asymptotic value of f when N increases is larger than zero and is indicated by the broken lines to the extreme right in the figure. In this case the examples used in the figure when $i = 10, 15$ and $20 \mu\text{A}/\text{cm}^2$ show that a minimum value of f is obtained for $N \approx 1000$. When N_k is increased above this value, there is a slight increase of the firing frequency.

The data used in Figs. 2 and 3 can also be presented as the mean firing frequency as a function of the injected current for different values of N_{Na} and

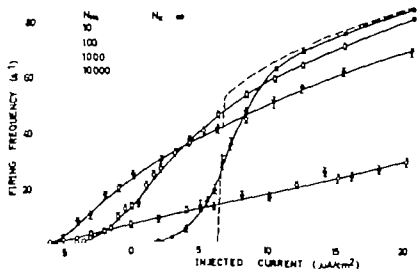


Fig. 4 Mean firing frequency as a function of the injected current for different values of N_{Na} when N_k is infinite. Broken line shows the case where also V_{Na} is infinite. S.E. is shown by vertical bars.

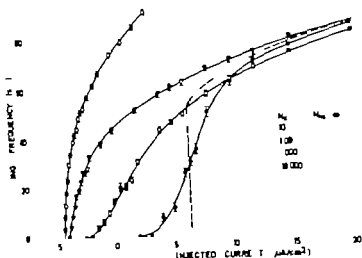


Fig. 5. Mean firing frequency as a function of the injected current for different values of N when N_{Na} is infinite. Broken lines show the case where also N is infinite. S.E. is shown by vertical bars.

is shown by Figs. 4 and 5. The corresponding curve for an infinite number of both Na- and K-pores is shown by the broken line (Stein 1967*b*). The most noticeable effects on this current-frequency relationship introduced by a finite number of either Na- or K-pores are a change of the current threshold for firing, and a much more linear relationship. This is similar to the results obtained by Stein in his calculations (Stein 1967). But in his model the behaviour of the pores was assumed independent of the membrane potential and the pores were assumed to carry all of the current.

Twenty open pores were assumed to give the threshold current and their mean open time was taken to be 1 msec. The pores were also assumed to give positive currents inwards, and would thus correspond to sodium pores. As each of the "pores" in Stein's model would have about 12 times as large an effect upon the membrane potential as the sodium pores assumed here due to the longer mean open time, 1 msec against 0.083 msec, his model would correspond roughly to our model with $N_{Na} = (E_{Na} - E_m) / (0.1/20 \text{ pores (1 msec/0.083 msec)}) \approx 3600$ pores. The results presented in his

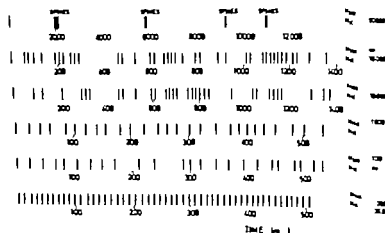


Fig. 6. Traces of action potentials for different values of N_{Na}/N and the injected current ($\mu\text{A}/\text{cm}^2$). The values are shown in the figure. Note changes of time scale.

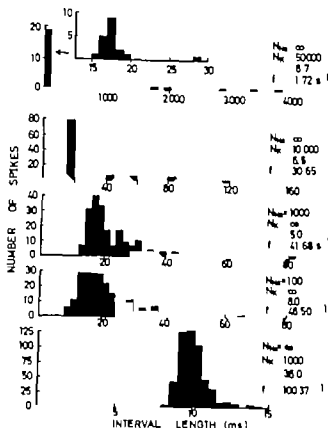


Fig. 7. Interspike interval histograms for different values of N , N and the injected current i (in $\mu A/cm^2$). The values are shown in the figure. These examples are also used in Fig. 6. Note changes of interval length scale.

Fig. 7 then agree well with the results obtained here as shown in our Fig. 4.

The minimum of f around $N = 1000$ which was seen in Fig. 3 is more clearly shown in Fig. 5 where we see that for $i > 9 \mu A/cm^2$, $N_h = 1000$ gives a lower firing frequency than both higher and lower values of N_h .

At pore numbers of 10, 100, 1000 and 10000 the results of Figs. 4 and 3 and 5 can be cross-checked. This gives the smaller uncertainties in Figs. 2 and 3 at these numbers.

When the number of pores is increased above 5000 pores the distribution of spikes in a train of action potentials changes markedly. Fig. 6 shows typical spike trains for pore numbers from 100 to 50000. For pore number below 5000 the spikes in the train seem to be randomly distributed but as the pore numbers are increased above this value there is an increasing tendency of the spikes to occur in bursts. For large numbers the typical burst behaviour is fairly long trains of action potentials with a regular firing frequency of approximately

55–60 s⁻¹ separated by long periods with no firings.

The length of these silent periods fluctuates greatly.

This burst activity is due to a larger probability for firing about 20 ms after the peak of an action potential. This is connected with the slight overshoot of the membrane potential over its final value about 20 ms after an action potential which is seen in the H-H equations (Hodgkin & Huxley 1952), in the case of a single firing. For small pore numbers when the fluctuations are large compared to this overshoot it has almost no effect. But for large pore numbers when the fluctuations are small compared to the overshoot there is a greatly increased probability for firing at this time. If the membrane fails to fire then however it can take very long time before the fluctuations by chance build up sufficiently to trigger off an action potential. In the original H-H equations it is seen that for an injected current i close to the threshold for firing the spikes occur just at this overshoot. If the membrane fails to fire then (because i is too small) it cannot fire at a later time unless i is increased. This explains the minimum firing frequency $f_T = 55 s^{-1}$ of the H-H equations (Hodgkin & Huxley 1952; Stein 1967b). The time from a spike to this overshoot is just equal to $1/f_T$. Accordingly the mean firing frequency during bursts of spikes should be approximately equal to f_T which fits well with the results from the stochastic models.

The minimum firing frequency $f_T = 55 s^{-1}$ in the H-H equations is important in the following discussion of the results obtained and is termed the threshold frequency. It is the point of division between quite different modes of behaviour in the stochastic models.

Fig. 7 shows examples of the interspike interval histograms for finite numbers of either the Na- or the K-pores and for different values of the injected current i . These histograms show the effects of the stochastic fluctuations of the nerve membrane conductances upon the distribution of the interspike intervals. These effects are quite similar for the two cases of either a finite number of Na-pores or a finite number of K-pores. No systematic differences between these two cases could be seen by inspection of the histograms which were obtained during the computations.

When there is typical burst firing the peak of the histogram is narrowed and shifted to the left relative to the base because most of the interspike intervals are now of approximately the same short length $1/f_T$.

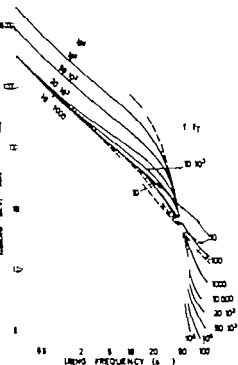


Fig. 8. Standard deviation ΔT of the interspike intervals as a function of the mean firing frequency f for different values of N_{∞} and N . The numbers shown are the values of N_{∞} when N is infinite (continuous lines), and of N when N_{∞} is infinite (broken lines, shown only if different from the other case). Dotted line shows the relationship $\Delta T = 0.5/f$ and $f = f$.

burst intervals), but some intervals are much longer than these (the intervals during bursts). In order to get a quantitative expression for the degree of burst firing, a burst factor BF is defined as

$$BF = \frac{\text{Median of the interval}}{\text{Mean of the intervals}} \quad (21)$$

With a symmetrical distribution the median is equal to the mean and the burst factor $BF = 0$. When there is typical burst activity with almost all intervals equal and short, and a few intervals very long, the mean will be much larger than the median, and BF approaches one. Note that BF is a measure of the skewness of the interspike interval distribution.

Fig. 7 shows that the width of the histograms changes a lot when the injected current and the pore numbers are changed. The standard deviation ΔT of

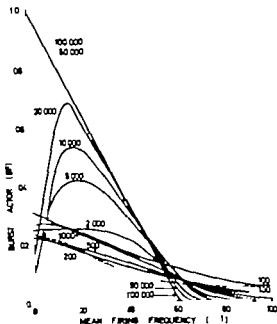


Fig. 9. Burst factor BF as a function of the mean firing frequency for different values of N_{∞} when N is infinite (continuous lines), and of N when N_{∞} is infinite (broken lines, shown only if different from continuous lines). Dotted line shows simplified relationship given by Eq. (1.4) with $f = 60$ s.

the intervals from their mean, as calculated in the Appendix is here used as a measure of this width. Figs. 8 and 9 show the parameters ΔT and BF respectively as functions of the mean firing frequency f for different pore numbers. Note that for BF linear axes are used, while logarithmic axes are used for ΔT . It was found much more useful to present ΔT and BF as functions of f than as functions of the injected current. Among other things this made it easier to compare the firing behaviour for different pore numbers. When N_{∞} , N and f are specified, I is given and cannot be chosen independently. Its value can be obtained from Figs. 2, 3, 4 and 5.

Each of the curves shown in Figs. 8 and 9 is drawn as the best fit to the results obtained. The different symbols shown are used only to distinguish the different curves. An example of the data obtained in the actual simulations is shown in Fig. 10, where the curves used in Figs. 8 and 9 are also shown. For pore numbers above 200 the results were almost independent of the types of pores considered, and in these cases only one curve is used to

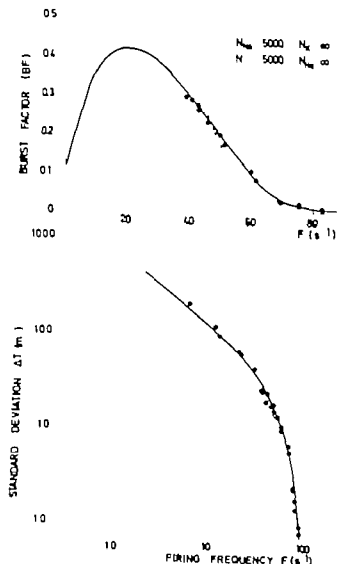


Fig. 10. Results from simulation which were used to obtain curves similar to those shown in Figs. 8 and 9 for $N_a = 5000$ and N_e infinite (filled circles) and for $N_e = 5000$ and N_a infinite (open circles).

show the results for N_a infinite and N_e equal to the number indicated and for N_e infinite and N_a equal to the same number.

When the mean firing frequency f was less than f_T and for pore numbers larger than about 100 000 the burst firing became so pronounced that it was not possible to obtain reliable estimates of ΔT (or BF) because the burst periods and the intervals between them often became longer than the maximum model time which could be simulated. (This time was set equal to 70 s for economical reasons.) But a minimum value of ΔT could be obtained. The model was then "sampled" several times and minimum values of the mean number of spikes in a burst were estimated at different values of the in-

jected current. Minimum values of ΔT were then calculated according to the simple model in the Appendix.

It should be noted that for small values of f there is a large uncertainty in the results shown by Figs. 8 and 9 because the data are then based upon a few interspike intervals. This is seen as a spreading of the results as f is decreased.

Fig. 8 shows that for firing frequencies below f_T all the curves for pore numbers less than 50 000 are close to each other independent of the number and types of pores. For mean firing frequencies f below about 70 s⁻¹ these curves can be approximately described by a straight line given by $\Delta T = 0.8/f$. For all pore numbers the curves are well approximated by straight lines described by $\Delta T = \text{constant}/f$ for $f < 70$ s⁻¹ (except for 50 000 pores). In the Appendix it is shown that for burst firing ΔT will for $f < 60$ s⁻¹ be given by $\Delta T = \sqrt{N_a + 1}/f$. Eq. (19). Fig. 8 indicates that N , the mean number of intervals in one burst, is a function of the pore number only independent of f for $f < 70$ s⁻¹. The constant $\sqrt{N_a + 1}$ can be read directly from the figure as the value of ΔT in seconds for $f = 1$ s⁻¹. This gives that N is 4, 17 and 70 for pore numbers of 50 000, 10⁵ and 10⁶ respectively. For pore numbers smaller than 20 000 $\Delta T/f = 0.8$ which indicates that the variability is not mainly due to burst activity (since from Eq. (19) N then is negative). These results agree well with the burst behaviour of the spike trains, see Fig. 6 for some examples.

For mean firing frequencies f above f_T the standard deviation ΔT continues to decrease when f is increased. But here this decrease is much more rapid for large pore numbers than for small pore numbers. As the pore numbers are increased the case of a regular firing is approached and in the limit of infinite values of both N_a and N_e the interspike intervals are all equal which gives $\Delta T = 0$, as in the non-stochastic H-H equations.

The results shown here are similar to the results obtained by Stein with his pore model (Stein 1967a) which corresponds to our model with 3600 Na pores. The data presented in his Fig. 9 where he shows $\Delta T/f$ as a function of $1/f$ closely matches the results obtained here for 1000 $< N_a < 10$ 000.

When f is smaller than f_T however there is no underlying regular firing and the durations of the interspike interval fluctuate even if N_a and N_e approach infinite values. Fig. 8 shows that ΔT even increases when the number of pores is increased.

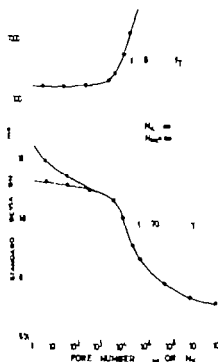


Fig. 11. Standard deviation ΔT as a function of N_m when $f = 60$ s (continuous lines), and of N when N_m is infinite (broken lines), shown only when different from continuous lines and for $f = 25$ and $f = 70$ s.

above 20 000 in this case. This increase is due to the increasing burst activity when the pore numbers are increased, in particular the increasing number of spikes in one burst. The results shown by Fig. 8 are presented in a more condensed form in Fig. 11 which shows ΔT as a function of the pore numbers for $f = 25$ and $f = 70$ s.

It should be noted that there do not exist any firing frequencies below f for the H-H equations (Stern 1967b). The behaviour of these equations cannot therefore be properly approached by increasing the pore numbers if f is kept in the region between 0 and f . For any finite pore numbers it is possible to keep f in this region by a sufficiently small adjustment of the injected current. As we see from Figs 4 and 5 the current region which permits non-zero firing frequencies less than f decreases when the number of pores is increased, but for finite pore numbers it will not become zero.

The burst factor BF shown in Fig. 9 as a function of the mean firing frequency f is seen to approach the relationship given by Eq. (14) when the number of pores is increased. This relationship is shown by

the dotted line in the figure where a burst frequency $f = 60$ s has been chosen. The mean firing frequency during the bursts actually changes slightly when the mean firing frequency f is changed but for large pore numbers this change is almost unnoticeable in the figure. For pore numbers larger than 50 000 the relationship given by Eq. (14) is closely followed. If the pore numbers are decreased from this value a large deviation is first seen at small values of f . For pore numbers of 20 000 for instance there was no clear burst activity when f was smaller than 10 s. The increase of BF above the theoretical relationship (dotted line) when the pore number is decreased is due to the increasing fluctuations of the length of the interspike intervals during bursts ($f < f_0$) or during continued firing ($f > f_0$).

The results shown here are presented in a more condensed form in Fig. 12, which shows BF as a function of the pore numbers for $f = 25$ s and $f = 70$ s.

Fig. 13 shows the current threshold i for firing as a function of the pore numbers N_m and N . In the stochastic model investigated here, there is no sharply defined threshold for firing as in the H-H equations, where the threshold current is $i_{T0} = 6.3 \mu A/cm^2$ (shown by the dotted line in the figure). For pore numbers less than 50 000, i is here defined as the value of the injected current i which gives a mean firing frequency of $f = 1$ s. This value is found from figures similar to Figs. 4 and 5. The vertical bars shown in the figure indicate the variation of i obtained by drawing the curves in Figs. 4 and 5 at the extremes of the vertical bars shown there.

For large pore numbers, i could not be reliably estimated by this method due to the pronounced burst firing. At small values of f the intervals between bursts often became longer than the maximum model time which could be simulated and a reliable estimate of f could not be obtained. Instead i was defined as the value of i which, with a probability of 0.5 gave firing up to one second after the onset of the current. At the onset the membrane almost always responded with at least one action potential which often was the start of a typical burst of spikes. If the burst ended and no new burst was initiated before the second period ended, the injected current used was defined as below threshold. If the firing continued out the one second period, or if a new burst, or even a single spike, was

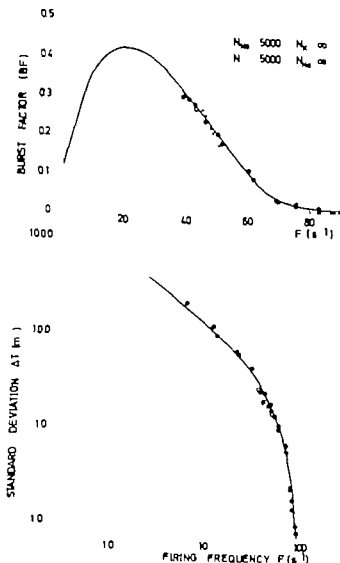


Fig. 10. Results from simulations which were used to obtain curves similar to those shown in Figs. 8 and 9 for $N_m = 5000$ and N infinite (filled circles) and for $N = 5000$ and N_m infinite (open circles).

show the results for N_m infinite and N equal to the number indicated, and for N_m infinite and N_m equal to the same number.

When the mean firing frequency f was less than f_T and for pore numbers larger than about 100 000 the burst firing became so pronounced that it was not possible to obtain reliable estimates of ΔT (or BF) because the burst periods and the intervals between them often became longer than the maximum model time which could be simulated (This time was set equal to 70 s for economical reasons). But a minimum value of ΔT could be obtained. The model was then "sampled" several times and minimum values of the mean number of spikes in a burst were estimated at different values of the in-

jected current. Minimum values of ΔT were then calculated according to the simple model in the Appendix.

It should be noted that for small values of f there is a large uncertainty in the results shown by Figs. 8 and 9 because the data are then based upon a few interspike intervals. This is seen as a spreading of the results as f is decreased.

Fig. 8 shows that for firing frequencies below f_T all the curves for pore numbers less than 40 000 are close to each other, independent of the number and types of pores. For mean firing frequencies f below about 70 s⁻¹ these curves can be approximately described by a straight line given by $\Delta T = 0.8/f$. For all pore numbers the curves are well approximated by straight lines described by $\Delta T = \text{constant}/f$ for $f < 20$ s⁻¹ (except for 70 000 pores). In the Appendix it is shown that for burst firing ΔT will for $f = f_m = 60$ s⁻¹ be given by $\Delta T = \sqrt{2N + 1}/f$. Eq. (19). Fig. 8 indicates that N_m , the mean number of intervals in one burst, is a function of the pore number only, independent of f for $f < 20$ s⁻¹. The constant $\sqrt{2N_m + 1}$ can be read directly from the figure as the value of ΔT in seconds for $f = 1$ s⁻¹. This gives that N_m is 4, 17 and 70 for pore numbers of 50 000, 10⁵ and 10⁶ respectively. For pore numbers smaller than 20 000 $\Delta T = 0.8$ which indicates that the variability is not mainly due to burst activity (since from Eq. (19) N_m then is negative). These results agree well with the burst behaviour of the spike trains, see Fig. 6 for some examples.

For mean firing frequencies f above f_T the standard deviation ΔT continues to decrease when f is increased. But here this decrease is much more rapid for large pore numbers than for small pore numbers. As the pore numbers are increased the case of a regular firing is approached and in the limit of infinite values of both N_m and N the interspike intervals are all equal, which gives $\Delta T = 0$, as in the non-stochastic H-H equations.

The results shown here are similar to the results obtained by Stein with his pore model (Stein 1967a) which corresponds to our model with 3600 Na pores. The data presented in his Fig. 9 where he shows $\Delta T/f$ as a function of $1/f$ closely matches the result obtained here for $1000 < N_m < 10000$.

When f is smaller than f_T however there is no underlying regular firing and the durations of the interspike intervals fluctuate even if N_m and N approach infinite values. Fig. 8 shows that ΔT even increases when the number of pores is increased.

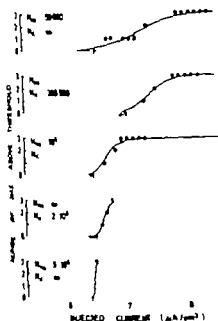


Fig. 14. Number of cases above threshold as a function of the injected current for different values of N_{Na} and N . These values are shown in the figure. Examples of results not shown for pore numbers larger than 10 000. See text for explanation.

For pore number is increased. A correspondingly larger value of i is then needed to give these fluctuations a probability to start an action potential. The value i_{70} is reached by i at N_{Na} or $N = 40 000$ and a maximum value of $7.6 \mu A/cm^2$ is reached at about 100 000 pores. As the pore number is further increased, i_{70} decreases towards i_{70} . The reason for the increase of i above i_{70} is closely connected to the mechanisms which give burst firing. For large pore numbers ($> 20 000$) the conductance fluctuations are very small and do not affect the generation of an action potential much. If the injected current is slightly above i_{70} , the model therefore fires quite regularly with firing frequency approximately equal to that of the H-H equations (f/f_0). This is the behaviour during a burst of spikes. The conductance fluctuations may however delay a spike so much that the period for greatest probability for firing is passed, and the firing then stops. The model is now in a situation which corresponds to the one studied in the H-H equations by slowly increasing i to its present value. Due to accommodation the firing will not then start even if i is somewhat

higher than i_{70} . When the firing in the model stops, a relatively large fluctuation is therefore needed to start the firing again and this may take a long time to happen. This silent period is the period between bursts. When the current i is increased the probability that the firing will start again increases while the probability that it will stop decreases. For small pore numbers it is the probability that the firing starts which is important while for large pore numbers ($> 100 000$) it is the probability that the firing stops which determines the threshold.

We will now consider the case where both N_{Na} and N are finite. Figs 15 and 16 show the mean firing frequency f as functions of N_{Na}/N when the total number $N_{Na} + N$ of pores is 500 and 2000, respectively. The numbers N_{Na} and N must then change between zero and the sum $N_{Na} + N$ when N_{Na}/N is increased from zero to infinity. The dotted line shows f as a function of N_{Na} when N is infinite and the broken line shows f as a function of N when N_{Na} is infinite. These curves are taken directly from Figs 3 and 4. In most cases the fluctuations of the numbers of open Na- and K-pores combine to give a firing frequency which is higher than at least one of the values of f obtained from each of these pore systems separately. We cannot expect a linear addition of these effects, because the stochastic processes described by the model are highly nonlinear. For small values of N_{Na} ($N_{Na} < 45$ in Fig. 10), the combined effects of the finite Na- and K-pores even give a smaller value of f than the effect of either the system of Na-pores or the K-pores alone. At these low values of N_{Na} the probability that a Na-pore will open is very small even if all K-pores close and the potential increases to $E = 22.6$ mV. And when the Na-pore system in this way does not respond to sudden increases of the potential, no action potentials will be generated.

The firing behaviour was further investigated for a constant value of the quotient N_{Na}/N equal to 4. This is a rather arbitrary choice; the only reason it was preferred being that it gives approximately equal conductances for single Na- and K-pores. Fig. 17 shows the mean firing frequency f as a function of the injected current for different values of the total number $N_{Na} + N_K$ of pores. It is seen that the general form of the frequency-current relationship lies between those of the two cases considered before, that is, either N_{Na} infinite or N infinite.

The other phenomena seen: burst firing and the

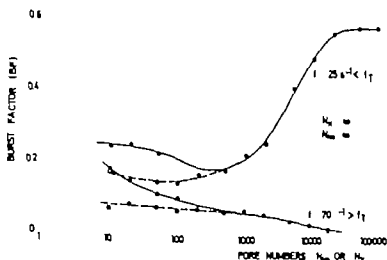


Fig. 12 Burst factor BF as a function of N_m when N is infinite (continuous lines), and of N when N_m is infinite (broken lines, shown only when different from continuous lines) and for $f=25\text{ s}^{-1}$ and $f=70\text{ s}^{-1}$.

initiated during the one second period i was defined as above threshold. Note that one spike generated per second gives $f=1\text{ s}^{-1}$ the threshold value used for small pore numbers.

Around the value of i where the current threshold was believed to be found three simulations were performed for each value of i which were changed in steps of $0.1\text{ }\mu\text{A}/\text{cm}^2$. Fig. 14 shows some typical results obtained. The number of times a result was obtained which indicated "above threshold" is plotted for each value of i . If normalized the curve fitted to these results gives the probability of obtain-

ing firing up to one second after the onset of the current as defined above. The threshold current i_T is now found as the value of i where this curve gives a probability of 0.5 and this value of i is plotted in Fig. 13. (For N_m or $N_e \geq 10,000$.) The vertical bars in Fig. 13 show the current range where the probability for firing lies between 0.1 and 0.9.

Fig. 13 shows that the threshold current i_T increases towards the threshold current i_{T0} in the H-H equations when the pore number is increased from small values. This is due to the decreasing amplitude of the conductance fluctuations when the

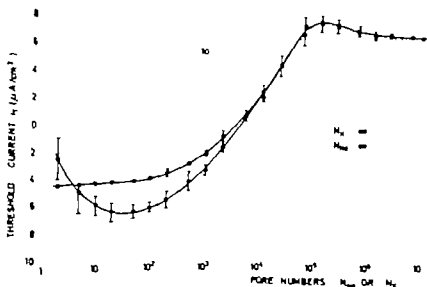


Fig. 13 Threshold current i_T for firing as a function of N_m when N is infinite (filled circles) and of N when N_m is infinite (open circles). Uncertainty shown by vertical bars. See text for explanation.

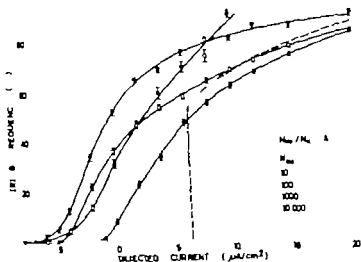


Fig. 17. Mean firing frequency as a function of the injected current for different values of N_{∞}/N when $N_{\infty}/N = 4$. Broken line shows the case where N_{∞}/N is infinite. S.E. is shown by critical burst.

(1) a different current threshold for firing, smaller for small pore numbers and larger for large pore numbers (>40000).

(2) a more linear relationship between the mean firing frequency and the injected current.

(3) fluctuations of the length of the time intervals between two action potentials (the interspike interval).

(4) burst firing for large pore numbers (>20000).

These differences become unnoticeable when the number of pores approaches infinity but they were clearly seen for surprisingly large pore numbers up to several hundred thousand for case (1).

It is worth noting that for large pore numbers (N_{∞} and $N \geq 50000$) the firing behaviour for a certain number of Na-pores ($N = \infty$), is almost identical to that of the same number of K-pores ($N_{\infty} = \infty$) even if the gating mechanisms are quite different in the two cases.

The change of the threshold could easily have been obtained in the original H-H equations by for instance a change of the leakage conductance g . The more linear relationship is, however, much more functionally important for the cell. It may for instance mean larger capacity to transmit information. This result is made even more interesting by the fact that it is difficult to obtain an approximately linear current-frequency relationship by equations of the same type as the H-H equations. It can be done, however, by fine tuning of the α and β

parameters and by including some additional membrane conductances (Staugen 1975 Connor & Stevens 1971).

DISCUSSION

The calculations presented here were made in order to find how the firing behaviour of a well-known, space-clamped nerve membrane depends upon the number of sodium and potassium conducting pores. The Hodgkin-Huxley equations were chosen as an example, but corresponding results would be expected if another set of equations had been chosen, for instance the equations describing a node of a myelinated nerve fibre as used (Frankenhaeuser & Huxley 1964). That is, one would expect a lowering of the firing threshold, a more linear frequency-current relationship, etc. as the total number of pores was decreased (by decreasing the total membrane area for instance). The phenomenon of burst firing is, however, closely connected with the maximum probability for firing at a certain time after the action potential (~ 20 ms for the H-H equations) but occurs only very close to the threshold current for firing. In the H-H equations the virtual discontinuity of the frequency-current relationship around the threshold is also due to this phenomenon. In nerve cell models where the non-stochastic equations do not show this discontinuity (as the model for the isolated Gastropod neurone soma (Connor &

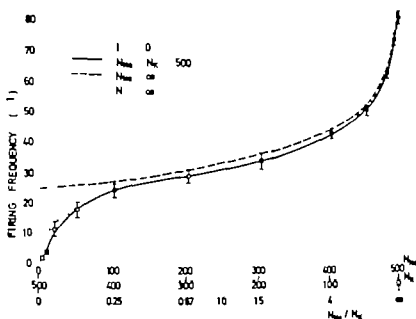


Fig. 15. Mean firing frequency f as a function of N_{∞}/N when $N_{\infty} + N = 500$ (continuous line). Dotted line shows f as a function of N_{∞} when N is infinite and broken line shows f as a function of N when N_{∞} is infinite. S.E. is shown by vertical bars.

change of threshold were quite similar to the results obtained for the two cases considered before that is N_{∞} finite and N infinite and vice versa. This is as expected since these two cases gave approximately the same results when the standard deviation ΔT , the burst factor BF and the current threshold for firing i_T were considered.

Conclusion

The results presented here show that when the effects of a finite number of pores are introduced into the H-H equations the firing behaviour of the nerve membrane can be quite different from that predicted by the original H-H equations. These differences are mainly

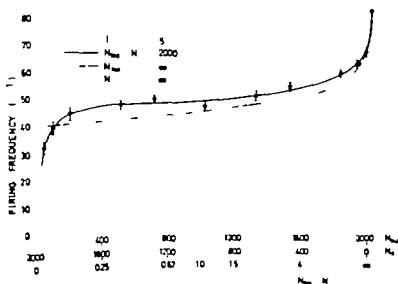


Fig. 16. Mean firing frequency f as a function of N_{∞}/N when $N_{\infty} + N = 1000$ (continuous line). Dotted line shows f as a function of N_{∞} when N is infinite and broken line shows f as a function of N when N_{∞} is infinite. S.E. is shown by vertical bars.

REFERENCES

- CONWAY, J. A. & STEVENS, C. F. 1971 Prediction of repetitive firing behaviour from voltage clamp data on an isolated axon. *J Physiol (Lond)* 213: 31-53.
- CONIL, F. & FELICE, L. J. & WANKER, E. 1975 Potassium and sodium ion current noise in the membrane of the squid axon. *J Physiol (Lond)* 248: 45-62.
- CONIL, F., HILLE, B., NEUMACKE, B., NONNER, W. & STÄMPFLI, R. 1976 Measurement of the conductance of the sodium channel from current fluctuations at the node of ranvier. *J Physiol (Lond)* 262: 699-727.
- FRANKMAN, H. M. 1973 Relaxation spectra of potassium channel noise from squid axon membranes. *Proc Natl Acad Sci USA* 70: 876-879.
- FRANKENHAUSER, B. & HUXLEY, A. F. 1964 The action potential in the myelinated nerve fibre of *Xenopus laevis* as computed on the basis of voltage clamp data. *J Physiol (Lond)* 171: 302-315.
- GILL, T. L. & CHEN, Y. 1972 On the theory of ion transport across the nerve membrane. *Biophys J* 12: 948-959.
- HILLE, B. 1976 Ionic channels in nerve membrane. *Prog Biophys Mol Biol* 21: 1-32.
- HILLE, B. 1972 The permeability of the sodium channel to metal cations in myelinated nerve. *J Gen Physiol* 59: 637-658.
- HILLE, B. 1973. Potassium channels in myelinated nerve: selective permeability to small cations. *J Gen Physiol* 61: 668-686.
- HODGKIN, A. L. & HUXLEY, A. F. 1952 A quantitative description of membrane current and its application to conduction and excitation in nerve. *J Physiol (Lond)* 117: 500-544.
- JACK, J. J. B. 1975 Physiology of peripheral nerve fibres in relation to their size. *Br J Anaesth* 47: 173-182.
- KEYNES, R. D. & ROJAS, E. 1974 Kinetics and steady-state properties of the charged system controlling sodium conductance in the squid giant axon. *J Physiol (Lond)* 239: 393-434.
- SKAUGEN, E. 1974 Possible functional significance of the geometry of the initial segment in nerve cells. *Acta Physiol Scand Suppl.* 396: 111.
- SKAUGEN, E. 1975 Repetitive firing behaviour in nerve cell models based upon a simplified form of the Hodgkin-Huxley equations. *Mathem Biosci* 26: 119-155.
- SKAUGEN, E. 1976 Firing behaviour in a nerve cell model with a two-state pore system. *Acta Physiol Scand* 96: 19A-20A.
- SKAUGEN, E. 1978 The effects of finite number of sodium and potassium conducting pores upon firing behaviour in nerve models. Ph.D. thesis, University of Oslo, Oslo.
- SKAUGEN, E. 1980 Firing behaviour in stochastic nerve membrane models with different pore densities. *Acta Physiol Scand* in press.
- STEIN, R. B. 1963 A theoretical analysis of neuronal variability. *Biophys J* 3: 173-194.
- STEIN, R. B. 1967 Some models of neuronal variability. *Biophys J* 7: 37-68.
- STEIN, R. B. 1967b The frequency of nerve action potentials generated by applied currents. *Proc Roy Soc* 167: 64-86.
- STEVENS, C. F. 1972 Interferences about membrane properties from electrical noise measurements. *Biophys J* 12: 1028-1047.
- VERVEEN, A. A. & DERKSEN, H. H. 1969 Amplitude distribution of axon membrane noise voltage. *Acta Physiol Pharmacol Neerl* 15: 353-379.

Stevens 1971) we would therefore not expect so pronounced burst firing for large pore numbers as in the H-H equations.

A general discussion is presented at the end of the following paper where effects of gating currents, multistate pore systems and other sources of electrical noise in the nerve membrane are considered (Skaugen *in press*). It is also shown that from simple space-clamped membrane models like the one discussed here it may be possible to obtain some general indications of the effects of finite pore numbers upon the firing behaviour of physiological ly operating nerve cells.

We would like to thank Daniel Kernell, David Attwell, Julian J. B. Jack, Jan K. S. Jansen, Knut Læstøl, Arild Njå and Sveinung Rekaa for stimulating discussions and comments on the manuscript, and Torhild Iachsen for drawing the figures. The work was supported by The Norwegian Research Council for Science and the Humanities.

APPENDIX. CALCULATIONS OF SOME STATISTICAL PARAMETERS

Results of the simulations are presented for the case where the injected current is zero up to time zero and then is increased suddenly to a constant value. This is the value of the current shown in the figures. The mean firing frequency is calculated by

$$f = N / \sum_{j=1}^N T_j \quad (1.1)$$

where the T_j are the interspike time intervals and N is the number of these.

An estimate of the standard deviation ΔT of the interspike intervals from their mean value was obtained by the following expression

$$\Delta T = \left(\frac{1}{N-1} \sum_{j=1}^N (T_j - 1/f)^2 \right)^{1/2} \quad (1.2)$$

where $T_N + 1 = T + 1/f$ —time at last spike.

From Eq. (1.2) an estimate of the standard error of the mean of f can be obtained

$$\Delta f = \left[\left(\frac{1}{f} - \frac{\Delta T}{fN} \right)^2 - \left(\frac{1}{f} + \frac{\Delta T}{fN} \right)^2 \right]^{1/2} \quad (1.3)$$

In the figures the interval $f - \Delta f$ to $f + \Delta f$ is shown by vertical bar.

In the typical burst activity a burst of $N + 1$ spikes (N intervals) is followed by a silent period of duration T . For

different bursts both N and T change a lot, but the firing frequency f during a burst is approximately constant, and the fluctuations of the interspike intervals during a burst can be neglected. If the mean value of N is larger than one, the median of the interspike interval distribution is then $1/f$, while the mean of this distribution is $1/f$, where f is the mean firing frequency. According to Eq. (1) the burst factor BF is then given by

$$BF = \begin{cases} 1 - 1/f & \text{for } f < f_m \\ 0 & \text{for } f \geq f_m \end{cases} \quad (1.4)$$

In general f is a function of f , f increases somewhat when f is increased, but f_m will always be close to the threshold frequency f when $f \ll f_m$. The simulations showed that f was nearly constant in this case, with a value $f \approx 60$ s. The burst factor BF will then be described by two straight lines.

Assume now that in the period of observation a number of N bursts and N silent periods of length T occur. If N is the mean value of N , the standard deviation ΔT from the mean of the interspike intervals can be determined from Eq. (1.2)

$$\Delta T^2 = \frac{N}{N(N+1)} \left((1/f - 1/f_m)^2 + \sum_{i=1}^N (1/f - T_i)^2 \right) \quad (1.5)$$

The mean value T of T can be expressed by the other parameters used here

$$T_m = \frac{1}{N} \sum_{i=1}^N T_i = \frac{1}{f} + (N+1) \left(\frac{1}{f} - \frac{1}{f_m} \right) \quad (1.6)$$

By using Eqs. (1.5) and (1.6) ΔT can then be written as

$$\Delta T = \left(N_m \left(\frac{1}{f} - \frac{1}{f_m} \right)^2 + \frac{T^2}{N+1} \right)^{1/2} \quad (1.7)$$

$$\text{where } T^2 = \frac{1}{N} \sum_{i=1}^N (T_i - T)^2$$

The long interburst intervals T may be assumed exponentially distributed for $t > 1/f$ if the $1/f$ are large compared to the correlation time for correlations in the membrane potential [13]. T is then equal to $T = 1/f_m$, since all T are larger than $1/f$ and Eq. (1.7) becomes

$$\Delta T = \left(\frac{1}{f} - \frac{1}{f_m} \right) \sqrt{N_m + 1} \quad (1.8)$$

For the case where f is small this simplifies to

$$\Delta T = f \sqrt{2N_m + 1} \quad f \ll f_m \quad (1.9)$$

REFERENCES

- CONNOR, J. A. & STEVENS, C. F. 1971. Prediction of repetitive firing behaviour from voltage clamp data on an isolated neurone soma. *J Physiol (Lond)* 213: 31-53.
- CONTE, F. de FELICE, L. J. & WANKER, E. 1975. Potassium and sodium ion current noise in the membrane of the squid axon. *J Physiol (Lond)* 248: 45-82.
- CONTE, F., HILLE, B., NEUMCKE, B., NONNER, W. & STÄMPFLI, R. 1976. Measurement of the conductance of the sodium channel from current fluctuations at the node of ranvier. *J Physiol (Lond)* 262: 699-727.
- FISHMAN, H. M. 1973. Relaxation spectra of potassium channel noise from squid axon membranes. *Proc Natl Acad Sci USA* 70: 876-879.
- FRANKENHAEUSER, B. & HUXLEY, A. F. 1964. The action potential in the myelinated nerve fibre of *Xenopus laevis* as computed on the basis of voltage clamp data. *J Physiol (Lond)* 171: 303-315.
- HILL, T. L. & CHEN, Y. 1972. On the theory of ion transport across the nerve membrane. *Biophys J* 12: 943-959.
- HILLE, B. 1970. Ionic channels in nerve membrane. *Prog Biophys Mol Biol* 21: 1-52.
- HILLE, B. 1972. The permeability of the sodium channel to metal cations in myelinated nerve. *J Gen Physiol* 59: 637-658.
- HILLE, B. 1973. Potassium channels in myelinated nerve: selective permeability to small cations. *J Gen Physiol* 61: 649-686.
- HODGKIN, A. L. & HUXLEY, A. F. 1952. A quantitative description of membrane current and its application to conduction and excitation in nerve. *J Physiol (Lond)* 117: 500-544.
- JACK, J. J. B. 1975. Physiology of peripheral nerve fibres: relation to their size. *Br J Anaesth* 47: 173-182.
- KEYNES, R. D. & ROJAS, E. 1974. Kinetics and steady-state properties of the charged system controlling sodium conductance in the squid giant axon. *J Physiol (Lond)* 239: 393-434.
- SKAUGEN, E. 1974. Possible functional significance of the geometry of the initial segment in nerve cells. *Acta Physiol Scand, Suppl.* 396: 111.
- SKAUGEN, E. 1975. Repetitive firing behaviour in nerve cell models based upon simplified forms of the Hodgkin-Huxley equations. *Mathem Biosci* 26: 119-155.
- SKAUGEN, E. 1976. Firing behaviour in nerve cell model with two-state pore system. *Acta Physiol Scand* 96: 19A-20A.
- SKAUGEN, E. 1978. The effects of finite number of sodium and potassium conducting pores upon firing behaviour in nerve models. Ph.D. thesis, University of Oslo, Oslo.
- SKAUGEN, E., 1980. Firing behavior in stochastic nerve membrane models with different pore densities. *Acta Physiol Scand* in press.
- STEIN, R. B. 1965. A theoretical analysis of neuronal variability. *Biophys J* 5: 173-194.
- STEIN, R. B. 1967. Some models of neuronal variability. *Biophys J* 7: 37-68.
- STEIN, R. B. 1967b. The frequency of nerve action potentials generated by applied currents. *Proc Roy Soc* 167: 64-86.
- STEVENS, C. F. 1972. Inferences about membrane properties from electrical noise measurements. *Biophys J* 12: 1028-1047.
- VERVEEN, A. A. & DERKSEN, H. H. 1969. Amplitude distribution of axon membrane noise voltage. *Acta Physiol Pharmacol Neerl* 15: 353-379.

On the nature of basal vascular tone in cat skeletal muscle and its dependence on transmural pressure stimuli

PER-OLOF GRÄNDE, PER BORGSTRÖM and STEFAN MELLANDER

Department of Physiology and Biophysics, University of Lund, Sweden

GRÄNDE, P.-O., BORGSTRÖM, P. & MELLANDER, S. On the nature of basal vascular tone in cat skeletal muscle and its dependence on transmural pressure stimuli. *Acta Physiol Scand* 1979, 107, 365-376. Received 17 May 1979. ISSN 0001-6772. Department of Physiology and Biophysics, University of Lund, Sweden.

The aim of the present study was to elucidate in some detail the characteristics of the intrinsic basal vascular tone in the adrenergically blocked skeletal muscle with regard to its extent and site along the vascular bed, its dependence on arterial pressure, its static and dynamic transmural pressure stimuli and its sensitivity to local metabolic influence. Basal tone, which apparently is of myogenic nature, was pronounced in proximal arterial vessels ($>25 \mu\text{m}$ i.d.) and in the 'microvessels' ($<25 \mu\text{m}$), but low in large veins. Its functional characteristics, however, were different in the 'proximal arterial vessels' and the 'microvessels'. Normal basal tone in the microvessels thus seemed to be extremely dependent on the arterial blood pressure level and, at least partly, masked by its static acute pressure distension effect as well as by its dynamic pulse pressure oscillations. It could be virtually abolished by 'transmural pressure decrease applied at fast rate' (strong laboratory dynamic transmural pressure stimulus). Basal tone in the proximal arterial vessels, on the other hand, was little affected by arterial pressure and almost insensitive to transmural pressure stimuli. Basal tone in the 'microvessels' was much more sensitive to metabolic stimuli than that in the 'proximal arterial vessels'. The present results, viewed in the light of some recent electrophysiological studies on vascular smooth muscle, suggest that smooth muscle in the microvessel is mainly of the spike-generating type, whereas that in the proximal arterial vessels seems to be of different nature, possibly of the non-spike-generating type.

Key words: Basal vascular tone; myogenic mechanisms; transmural pressure stimuli; pulse pressure autoregulation; metabolic control; spike-generated tone.

In 1902, Bayliss put forward his classical hypothesis that the intra-arterial pressure via distension caused a direct stimulating action on the vascular smooth muscle contributing to existing vascular tone and its regulation. The term myogenic reactivity has since then by convention been used to denote the ability of the vascular smooth muscle to respond to the mechanical force exerted by blood pressure. Terminology which is adopted in the present paper. Although the myogenic hypothesis of Bayliss was questioned for considerable length of time (e.g. by Auer 1912, and others) it received quite conclusive experimental support from more recent hemodynamic and vital microscopy studies (e.g. Folkow 1949, Folkow & Öberg 1961, Mel-

lander Öberg & Odehlin 1964, Johnson 1968, Baez, Lundberg & Orkin 1974).

The myogenic mechanism is thus now quite widely appreciated as an important factor in the development of active responses to changes in arterial blood pressure, for instance in autoregulation of blood flow (for ref. see Johnson 1964) implying that it acts by increasing or decreasing the normal basal vascular tone. Basal vascular tone in this context refers to the marked intrinsic tone which at normal pressure remains on the arterial side of most vascular beds after elimination of known nervous and humoral excitatory influences. There is much to indicate that this basal tone is mainly of myogenic origin (e.g. Folkow 1962) but

its initiating mechanisms are not yet experimentally defined. Basal tone might possibly result from spontaneous myogenic automaticity in the vascular smooth muscle but it might also require some specific continuing stimulus for its development and maintenance for instance initiated by the arterial blood pressure distension as apparently envisaged by Bayliss. It is possible that basal tone might be established by somewhat different mechanisms in the various sections of the vascular bed in view of the documented heterogeneity of vascular smooth muscle in different parts of the circulatory system (e.g. Bohr 1965, Vanhoutte 1978).

In the present investigation an attempt was made to elucidate some characteristics of the basal tone in consecutive sections of the vascular bed of skeletal muscle, special attention being paid to its dependence on vascular transmural pressure stimuli. The fact that the myogenic response to decreased transmural pressure is effected by inhibitory interference with basal tone might imply that myogenic reactions and myogenic basal tone are mediated via some common cellular mechanism(s). Further insight into this problem might be gained from more detailed studies about such myogenic inhibitory interaction, particularly in view of a recent description of the cellular mechanisms behind myogenic reactivity in single unit vascular smooth muscle *in vitro* (Johansson & Mellander 1975).

Since similar mechanisms might be operating *in vivo* as well, it would be of interest to determine the maximal extent to which basal vascular tone in different sections of the vascular bed can be inhibited by a true myogenic reaction evoked by decrease in transmural pressure. Recent experiments (Grände et al 1977, 1978) have demonstrated the existence of a small static and a much more prominent dynamic or rate sensitive component in myogenic vascular control in skeletal muscle: the former component related to the amplitude of the steady state constant increase or decrease in vascular transmural pressure (P_T) and the latter to the rate of the transmural pressure change (dP_T/dt). Observations of the active dynamic myogenic dilator response to a strong inhibitory (negative) dP_T/dt stimulus in terms of a rapid transmural pressure decline were therefore made when applied at normal basal tone. Comparison of this active dilator response with that evoked by a supramaximal dose of papaverine (which abolishes vascular tone whatever its cause) provided a rough estimate

of the maximal extent to which basal tone could be inhibited by myogenic mechanisms evoked via transmural pressure stimuli.

In a second series of experiments various attempts were made to determine to what extent basal tone in different sections of the vascular bed could be dependent upon the normal arterial blood pressure level. Special attention was paid to the possibility that the arterial pressure via static and/or dynamic transmural pressure stimuli could contribute to the initiation and maintenance of basal myogenic tone.

The results indicate that the basal tone is of somewhat different nature in the microvessels compared to that in the more proximal arterial vessels. This difference will be tentatively discussed in the light of some recent electrophysiological studies on vascular smooth muscle.

METHODS

The study was performed on 25 cats b.w.t. 3.0–4.3 kg, anesthetized with α -chloralose (50 mg/kg b.w.t.) and urethane (100 mg/kg b.w.t.). The cats were breathing spontaneously through a tracheal cannula. Body temperature was kept at $38 \pm 0.5^\circ\text{C}$. A few preparations which were technically unsuccessful were excluded from the study.

Experimental preparation. The observations were made on the α - and β -adrennergically blocked vascular bed in the acutely denervated lower leg muscles of the right hindlimb. The muscle region was prepared so that the popliteal artery and vein formed the sole vascular connections with the body. Surgical procedures and the experimental set up were basically the same as described previously (see Grände, Lundvall & Mellander 1977) and will be only briefly summarized. The muscle region was auto-perfused via a shunt circuit placed between the femoral and the popliteal artery, except for one series of experiments where the muscle region was perfused with a pressure servo-controlled roller pump (see below). Mean arterial blood flow (Q) to the region was continuously recorded with a reliable pressure gradient flowmeter (Grände & Borgström 1978). Venous blood flow from the region was diverted via a catheter to the right jugular vein. Mean arterial inflow pressure (AP) and venous outflow pressure (VP) were measured from T-tubes close to the cannulated popliteal artery and vein. By means of a screw clamp placed around the shunt tube, arterial pressure could be adjusted to desired level. Pressures from arterial microvessel (small artery pressure: SAP) and from venous microvessels (small vein pressure: SVP) were continuously monitored using a technique modified from that originally described by Haddy et al (1954) (for detail about the technique and its validity see Grände 1979). For this purpose the sural artery and vein on the posterior surface of the gastrocnemius muscle were ligated at a site just distal to the adjacent fat pad and flexible nylon tubings (i.d. of tip ≈ 0.3 mm) were inserted just below

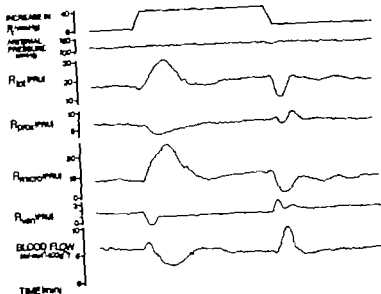


Fig. 1 Effects of strong dynamic transmural pressure (P) stimuli ($dP/dt = \pm 5$ mmHg/s) on basal vascular tone in cat skeletal muscle. Note the marked reinforcement of microvascular basal tone (R_{micro}) evoked by the positive dynamic stimulus, and, especially, the almost complete abolition of this tone evoked by the negative dynamic stimulus.

line ligatures. Pressures were recorded with Statham transducers. All parameters were registered on a Grass Polygraph.

The muscle preparation with the intact vascular connective was placed in a hermetically closed temperature-controlled plethysmograph (31°C) filled with Tyrode's solution. The fluid in the plethysmograph was connected via tubing with an external, open reservoir (isolated in the vertical direction to prevent variation of the hydrostatic fluid pressure in the plethysmograph to desired levels in the atmosphere) (Grande, Ilkovic & Malenka (1974)). In the control situation (i.e. at atmospheric plethysmographic pressure), venous pressure was adjusted to level (≈ 5 mmHg) which established an isovolumetric state of the preparation and kept it thus level throughout the exp't. By lowering the reservoir all parts of the muscle vascular bed could be exposed to increased vascular transmural pressure (P) and this could be applied at any desired rate dP/dt .

In one series of exp'ts, somatosensor-motor nerve stimulation was initiated and accompanied by electrical stimulation (1 V, 1 ms) of the distal end of the cat sciatic nerve for adrenergic and cholinergic blockade.

The following substances were used: Heparin (1000 U/kg b.wt.), phenoxylbenzamine (10 mg/kg i.v.), aprindol chloride (1 mg/kg i.v.), and atropine sulfate (1 mg/kg i.v.). The latter substances were given and caused effective autonomic blockade of the vascular bed.

Data are presented as mean values \pm S.E. Recordings of vascular resistance. With the use of Statham pressure transducers (National Series LX

1601 D) and electronic divider circuits, as described by Grande & Borgström (1978), the present technique permitted continuous recordings of total and segmental resistances in the muscle vascular bed according to the following definitions. Total vascular resistance = $(AP - VPMQ) / \text{proximal arterial resistance} = (AP - SAP) / \text{microvascular resistance} = (SAP - SVP) / \text{large vein resistance} = (SVP - VPMQ)$. This approach, according to previous evaluations (see Orskov et al. 1977, 1978, Grande 1979), permits reliable recordings of the mentioned vascular resistances. This holds true also during phasic change of vascular transmural pressure, except for 'large vein resistance' which then is somewhat unreliable due to the induced transcapillary fluid loss.

Pump perfusion exp'ts. In one series of exp'ts, shifts are made from normal pulsatile to non-pulsatile pressure perfusion. For this purpose, pressure servo-controlled roller pump was inserted in the arterial shunt circuit. This pump could simulate normal cardiac pulsations by feeding into the servo-control system reference input signal of normal undamped arterial pressure obtained from pressure transducer connected to the brachial artery. The pump permitted shift to non-pulsatile perfusion at unchanged mean arterial inflow pressure.

RESULTS

The exp'ts were performed on the sympathetotomized and adrenergically blocked vascular bed of skeletal muscle with well preserved basal vascular

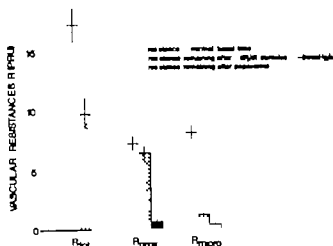


Fig 2 Average effects ($n=8$) of a strong inhibitory dynamic transmural pressure stimulus ($dP_T/dt = -5$ mmHg/s) and of a supramaximal dose of papaverine on basal tone in the whole vascular bed (R_{tot}) in the proximal arterial vessels (R_{prox}) and in the microvessels (R_{micro}). Note the pronounced inhibition of basal tone by the dynamic transmural pressure stimulus effected by an almost selective relaxation in the microvessels

tone within the normal range (cf Mellander & Johansson 1968). Total and segmental vascular resistances in the muscle region were followed continuously throughout the expt from blood flow and differential pressure measurements (see Methods). The average value for small artery pressure in the present material was 70 ± 3 mmHg at an arterial inflow pressure of about 125 mmHg indicating that small artery pressure was monitored from arterial microvessels smaller than about $25 \mu\text{m}$ (i.d.) (cf Fronek & Zweifach 1975, Grände 1979). The site for separation along the vascular tree between the proximal arterial vessels and microvessels therefore roughly refers to this vessel dimension.

Effects of a strong inhibitory transmural pressure stimulus on basal vascular tone. As mentioned in introduction the myogenically reactive vascular smooth muscle is especially sensitive to dynamic transmural pressure stimuli dP_T/dt . Previous studies (Grände & Mellander 1978) have indicated that such a stimulus with regard to inhibitory responses approaches its effector maximum (dilation) at a dP_T/dt value of -5 mmHg/s which was applied in this study and accomplished by a P_T decrease of 40 mmHg in 8 s. To minimize the inevitable (and disturbing) passive vascular collapse effect especially in the venous section of such a P_T decline the expts. were performed as illustrated in Fig. 1. The vascular bed was first exposed to a

P_T increase of 40 mmHg above normal control, in this case at the rate of 5 mmHg/s accomplished by a decrease of extravascular (plethysmographic) pressure P_T was then maintained at this constant increased level until the pronounced dynamic constrictor response had vanished and the small static constrictor response had reached a steady state. After this the test inhibitory transmural pressure stimulus was applied by decreasing P_T back to the control level at the specified rate of -5 mmHg/s. The initial P_T increase thus served the dual purpose to minimize passive vascular collapse and to prevent vascular transmural pressure from falling below the normal control level during the subsequent P_T decline.

The figure shows recordings of the resistance responses evoked in the whole vascular bed (R_{tot}) in the proximal arterial vessels (R_{prox}) in the microvessels (R_{micro}) and in the large veins (R_{vein}) to such transmural pressure stimuli. The responses to the mentioned P_T increase confirm in essential respects our previous observations (Grände et al 1977). It evoked a strong dynamic myogenic constriction in the microvessels in response to phasic increase in P_T i.e. to the positive dP_T/dt stimulus which was reflected in total vascular resistance also whereas the proximal arterial vessels and especially the veins were almost irresponsive to the dynamic stimulus merely showing passive distension. The static myogenic constrictor responses to constant increased P_T were small in the microvessels comprising about 0.5 PRU and in the proximal arterial vessels about 0.8 PRU above the control values. Large vein resistance was simultaneously decreased passively slightly below control. The net effect on overall vascular resistance to constant increased P_T was moderate as depicted in the R_{tot} -curve.

The vascular responses to the inhibitory dP_T/dt stimulus of -5 mmHg/s are shown in the latter part of Fig. 1. Note the marked active dilation in the microvessels which lowered microvascular resistance from about 10.5 PRU to 1.5 PRU thus far below the initial control value of about 8.5 PRU at normal basal tone (see initial part of the curve). The proximal arterial vessels showed a bi-phasic response: an initial active dilation which lowered resistance somewhat below the initial control level followed by moderately raised resistance. A small resistance increase also was noted in the large vein section. Increased resistance in the latter sec

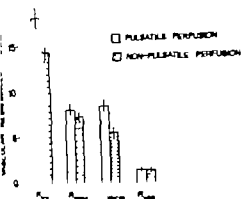


Fig. 2. Effects of shift from pulsatile to non-pulsatile perfusion at constant mean perfusion pressure on total and segmental vascular resistances in skeletal muscle. Note the marked decline in total vascular resistance (R_T) during non-pulsatile perfusion, an effect mainly caused by inhibition of basal tone in the microvessels. Resistance in the proximal arterial vessels (R_{micro}) was much less, and in large veins (R_{large}) hardly at all affected.

tion during the P_T decline most likely can be ascribed to passive elastic recoil (which thus could not be prevented entirely). The described active dilator responses, however, dominated the behaviour with regard to overall vascular resistance resulting in a net decrease in R_{tot} from the control value of about 18 down to 10 PRU.

The described pattern of response to the strong inhibitory transmural pressure stimulus was similar in all expts (8 cats). For the whole material (see Fig. 1), this stimulus decreased microvascular resistance from an average control value at normal basal tone of 8.0 ± 0.6 PRU down to an average of 1.3 ± 0.2 PRU and proximal arterial resistance during the initial dilator phase) from 7.3 ± 0.5 to 6.5 ± 0.4 . Total vascular resistance decreased from an average of 17.4 ± 1.4 to 9.9 ± 0.8 PRU. These dilator effects should be compared to those ($n=8$) evoked by a supramaximal dose of papaverine (100 mg/kg muscle tissue) which caused complete elimination of the vascular smooth muscle tone. Microvascular resistance during such papaverine infusion averaged 0.4 ± 0.1 PRU, proximal arterial resistance 0.7 ± 0.1 PRU, large vein resistance 0.5 ± 0.1 PRU and total vascular resistance 1.7 ± 0.2 PRU at normal perfusion pressure.

The data in Fig. 2 show that a pronounced basal tone existed in the vascular bed under control conditions which could be abolished by papaverine and

that this basal tone mainly resided in the proximal arterial vessels and the microvessels whereas the large veins had low tone. The applied transmural pressure stimulus (negative dP_T/dt) was capable to very effectively inhibit basal tone in the microvessels where resistance decreased by almost 90% of that evoked by papaverine but was less effective in the more proximal arterial vessels where resistance during the initial dilator phase decreased by only some 10% of the papaverine effect. Data for this inhibitory effect in the large vein section are not included in the figure since they are less reliable due to hazards in determining resistance in these vessels during phasic shift in P_T where also a passive elastic recoil effect was quite significant. Mention should be made that some passive elastic recoil might have been present in the other vascular sections as well especially in the proximal arterial vessels being quite distensible (cf. Caro et al. 1978), which implies that the inhibitory effects of the dP_T/dt stimulus might have been somewhat underestimated by the data given in Fig. 2. A rough estimate of this effect was obtained by determining it on the papaverine-treated vascular bed in response to the negative dP_T/dt stimulus. Such analysis suggested that the mentioned effect was relatively small.

The fact that the applied dynamic inhibitory transmural pressure stimulus via a myogenic mechanism was capable to effectively interfere with basal tone only in the microvessels suggests that basal tone in the microvessels and in the larger arterial vessels is of somewhat different nature.

Effects of normal arterial pressure pulsations on basal vascular tone. Some previous studies (Mellander & Arvidsson 1974; LaLone et al. 1975) have shown that shift from normal pulsatile to non-pulsatile arterial pressure perfusion leads to decreased overall vascular resistance in a skeletal muscle preparation, suggesting that the arterial pulsations might contribute to the establishment of normal basal vascular tone, perhaps via repetitive dynamic transmural pressure stimulation. The aim of this series of expts. was to investigate if such an effect is mainly confined to the microvessels, a possibility suggested by the results in the previous section showing that basal tone in these vessels was especially sensitive to the experimentally applied external dynamic transmural pressure stimulus.

For this purpose total and segmental vascular

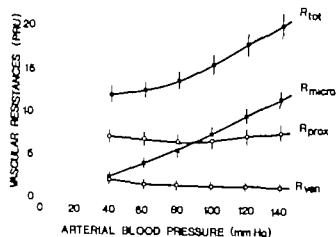


Fig. 4 Effects of short term (<60 s) reductions of arterial blood pressure on total and segmental vascular resistances in skeletal muscle. Note that the evoked decline in total vascular resistance could be almost entirely explained by dilation in the microvessels.

resistances in the adrenergically blocked muscle region were analysed at normal basal tone upon shift from pulsatile to non-pulsatile perfusion accomplished with the use of a servo-controlled roller pump (see Methods) under maintenance of a normal and constant mean arterial venous pressure difference.

Fig. 3 summarizes the average result of 8 observations on 5 cats. It can be seen that shift from pulsatile to non-pulsatile perfusion caused a pronounced inhibition of basal tone in terms of a decrease by almost 70% in total vascular resistance in the muscle region. Note that the major part of this dilator response was localized to the microvessels (smaller than about $25 \mu\text{m}$ i.d.) the resistance of which decreased by almost 35% below control (or about 35% of the maximal papaverine induced inhibitory response). Some inhibition of tone occurred also in the more proximal arterial vessels in which resistance decreased by some 10%. A special test expt. on the papaverine-relaxed vascular bed demonstrated that total and segmental vascular resistances if anything were somewhat smaller during pulsatile than non-pulsatile perfusion. This indicates that the resistance decline during non-pulsatile perfusion as depicted in Fig. 3 was caused by active smooth muscle responses and not by passive effects for instance related to rheological or other physical phenomena (cf. Mellander & Arvidsson 1974).

The demonstrated clear inhibition of normal basal tone upon elimination of the arterial pulsa-

tions at maintained normal mean distending pressure thus seems to be an effect mainly localized to the microcirculation. Such oscillations thus appear to be essential for the development of normal microvascular basal tone and the effect might result from repetitive positive dynamic transmural pressure stimuli on the vascular smooth muscle evoked during the rising phase of the pulse pressure curve.

Effects of arterial pressure reduction on basal vascular tone and possible underlying mechanisms. Observations of total and segmental vascular resistances in the adrenergically blocked muscle region were performed on 5 cats during graded reductions of arterial inflow pressure which was accomplished by adjustments of a screw-clamp placed around the arterial shunt tubing (see Methods) proximal to the site of the arterial pressure measurement. Such compression of the tubing produced not only a decrease of mean arterial blood pressure from its control value of about 140 mmHg in these expts. but also a simultaneous gradual attenuation of the arterial pulse pressure oscillations which were virtually abolished at a mean pressure of 40 mmHg. Mean arterial pressure was reduced to the various levels depicted on the abscissa in Fig. 4 and this was done for short periods of time (<60 s) to minimize possible metabolic vasodilator influence. The resistance data on the ordinate in Fig. 4 refer to the steady state after such a short-lasting pressure reduction. Complete recovery of vascular tone was instituted between successive pressure reductions.

It can be seen from the figure that total vascular resistance in the muscle region (R_{tot}) decreased with decreasing arterial inflow pressure. This resistance decline was steepest in the pressure range down to about 80 mmHg and implied a fairly well developed autoregulation of blood flow in this pressure range. Note that the decline in total vascular resistance could be almost entirely explained by dilation in the microvessels the basal tone of which was almost completely abolished (inhibited by almost 80% of maximum) at the arterial pressure of 40 mmHg. Resistance in the proximal arterial vessels and the large veins remained fairly constant or at the low arterial pressure levels even tended to increase with decreasing arterial pressure. The latter effect might mainly be ascribed to passive elastic recoil in these quite distensible vessels (cf. Caro et al. 1978) during the reduced arterial pressure which thus possibly could have obscured some minor concomitant inhibition of their basal tone.

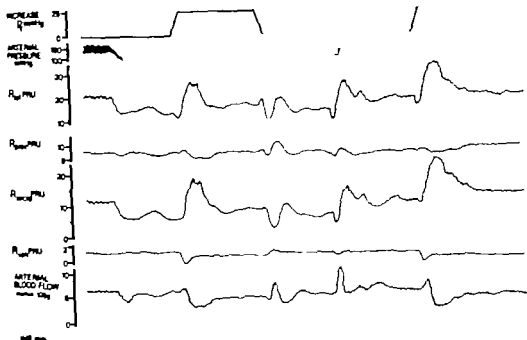


Fig. 5 Experiment serving to illustrate that basal tone in the microvessels (R_{MV}), which is markedly decreased by reduction of arterial pressure, can be partially restituted by experimental restoration of mean distending pressure to normal accomplished by superimposed increase of transmural pressure (P) in decrease of extravascular pressure. The experiment also demonstrates that dynamic and static myogenic reactivity is quite well preserved during the induced arterial hypotension. For further details see text.

It is concluded that basal vascular tone in the microvessels is distinctly dependent upon the arterial pressure level and an attempt will be made to elucidate the underlying mechanisms. It can be deduced from the data in Fig. 3 that a significant part of the described inhibitory effect on microvascular tone of arterial pressure reduction can be attributed to the concomitant experimental attenuation of the arterial pulsations. Some 35% of the inhibitory effect could be ascribed to the latter factor at the lowest arterial pressure level (40 mmHg), where the pulsations were virtually eliminated. The remaining inhibitory effect might be attributed to several factors, for instance to decreased static transmural pressure distension caused by fall of mean arterial pressure to decreased dynamic transmural pressure stimuli (see Discussion) to possible metabolic inhibitory influence on basal tone and/or on myogenic reactivity etc.

The expt. depicted in Fig. 5 provides some information about the importance of static transmural pressure distension for vascular tone and about static and dynamic myogenic reactivity during

arterial pressure reduction. In this expt. arterial pressure was reduced from about 150 to 100 mmHg i.e. in the range where blood flow was reasonably well autoregulated to minimize possible metabolic dilator influence. Flow (mean value) was thus reduced by only some 1 % in this case. Total vascular resistance (R_{TV}) decreased by about 5.5 PRU during the pressure reduction, almost entirely explained by inhibition of basal tone in the microvessels.

This arterial pressure reduction led to a fall of mean distending pressure in the whole vascular bed by about .5 mmHg, calculated as $(AP+VP)/2$ and to attenuation of the pulse pressure oscillations. The low mean distending pressure could now under maintained arterial hypotension be roughly restored to normal by increasing overall vascular transmural pressure in decrease of plethysmographic (extravascular) pressure by the same amount, a procedure shown in Fig. 5. This compensatory increase of transmural pressure was applied at the rate of .5 mmHg/s and led to an initial pronounced dynamic myogenic constrictor response in the microvessels which raised vascular

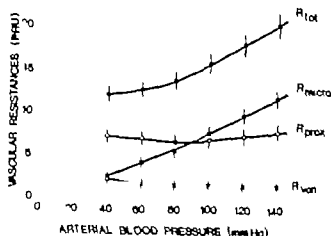


Fig. 4 Effects of short term (<60 s) reductions of arterial blood pressure on total and segmental vascular resistances in skeletal muscle. Note that the evolved decline in total vascular resistance could be almost entirely explained by dilation in the microvessel.

resistances in the adrenergically blocked muscle region were analysed at normal basal tone upon shift from pulsatile to non-pulsatile perfusion as accomplished with the use of a servo-controlled roller pump (see Methods) under maintenance of a normal and constant mean arterio-venous pressure difference.

Fig. 3 summarizes the average result of 8 observations on 5 cats. It can be seen that shift from pulsatile to non pulsatile perfusion caused a pronounced inhibition of basal tone in terms of a decrease by almost 50% in total vascular resistance in the muscle region. Note that the major part of this dilator response was localized to the microvessels (smaller than about $25 \mu\text{m}$ i.d.) the resistance of which decreased by almost 35% below control (or about 35% of the maximal papaverine-induced inhibitory response). Some inhibition of tone occurred also in the more proximal arterial vessels in which resistance decreased by some 10%. A special test experiment on the papaverine-relaxed vascular bed demonstrated that total and segmental vascular resistances if anything were somewhat smaller during pulsatile than non pulsatile perfusion. This indicates that the resistance decline during non-pulsatile perfusion as depicted in Fig. 3 was caused by active smooth muscle responses and not by passive effects (for instance related to rheological or other physical phenomena (cf. Mellander & Arvidsson 1974)).

The demonstrated clear inhibition of normal basal tone upon elimination of the arterial pulsa-

tions at maintained normal mean distending pressure thus seems to be an effect mainly localized to the microcirculation. Such oscillations thus appear to be essential for the development of normal microvascular basal tone and the effect might result from repetitive positive dynamic transmural pressure stimuli on the vascular smooth muscle evoked during the rising phase of the pulse pressure curve.

Effects of arterial pressure reduction on basal vascular tone and possible underlying mechanisms. Observations of total and segmental vascular resistances in the adrenergically blocked muscle region were performed on 5 cats during graded reductions of arterial inflow pressure which was accomplished by adjustments of a screw-clamp placed around the arterial shunt tubing (see Methods) proximal to the site of the arterial pressure measurement. Such compression of the tubing produced not only a decrease of mean arterial blood pressure from its control value of about 140 mmHg in these experiments but also a simultaneous gradual attenuation of the arterial pulse pressure oscillations which were virtually abolished at a mean pressure of 40 mmHg. Mean arterial pressure was reduced to the various levels depicted on the abscissa in Fig. 4 and this was done for short periods of time (<60 s) to minimize possible metabolic vasodilator influence. The resistance data on the ordinate in Fig. 4 refer to the steady state after such a short-lasting pressure reduction. Complete recovery of vascular tone was instituted between successive pressure reductions.

It can be seen from the figure that total vascular resistance in the muscle region (R_{tot}) decreased with decreasing arterial inflow pressure. This resistance decline was steepest in the pressure range down to about 80 mmHg and implied a fairly well developed autoregulation of blood flow in this pressure range. Note that the decline in total vascular resistance could be almost entirely explained by dilation in the microvessels, the basal tone of which was almost completely abolished (inhibited by almost 80% of maximum) at the arterial pressure of 40 mmHg. Resistance in the proximal arterial vessel and the large veins remained fairly constant or at the low arterial pressure levels even tended to increase with decreasing arterial pressure. The latter effect might mainly be ascribed to passive elastic recoil in these quite distensible vessels (cf. Caro et al. 1978) during the reduced arterial pressure which thus possibly could have obscured some minor concomitant inhibition of their basal tone.

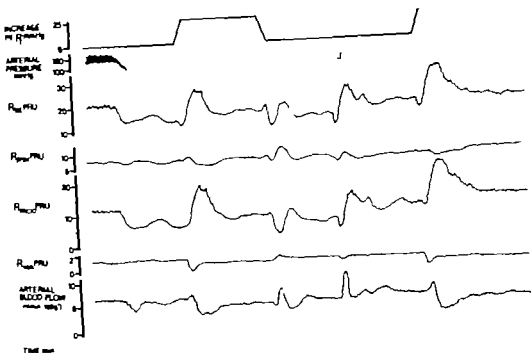


Fig. 5. Experiment serving to illustrate that basal tone in the microvessels (R_{stat}), which is markedly decreased by reduction of arterial pressure, can be partially restored by experimental restoration of mean distending pressure to normal accomplished by superimposed increase of transmural pressure (P_t) is decrease of extravascular pressure. The experiment also demonstrates that dynamic and static myogenic reactivity is quite well preserved during the induced arterial hypotension. For further details see text.

It is concluded that basal vascular tone in the microvessels is distinctly dependent upon the arterial pressure level and an attempt will be made to elucidate the underlying mechanisms. It can be deduced from the data in Fig. 3 that a significant part of the described inhibitory effect on microvascular tone of arterial pressure reduction can be attributed to the concomitant experimental attenuation of the arterial pulsations. Some 35% of the inhibitory effect could be ascribed to the latter factor at the lowest arterial pressure level (40 mmHg), where the pulsations were virtually eliminated. The remaining inhibitory effect might be attributed to several factors, for instance to decreased static transmural pressure distension caused by fall of mean arterial pressure to decreased dynamic transmural pressure stretch (see Discussion) to possible metabolic inhibitory influence on basal tone and/or on myogenic reactivity etc.

The apt depicted in Fig. 5 provides some information about the importance of static transmural pressure distension for vascular tone and about static and dynamic myogenic reactivity during

arterial pressure reduction. In this expt. arterial pressure was reduced from about 140 to 100 mmHg, i.e. in the range where blood flow was reasonably well autoregulated to minimize possible metabolic dilator influence. Flow (mean value) was thus reduced by only some 12% in this case. Total vascular resistance (R_w) decreased by about 5.5 PRU during the pressure reduction, almost entirely explained by inhibition of basal tone in the microvessels.

This arterial pressure reduction led to a fall of mean distending pressure in the whole vascular bed by about 25 mmHg, calculated as $(AP + VP)/2$ and to attenuation of the pulse pressure oscillations. The low mean distending pressure could now under maintained arterial hypotension, be roughly restored to normal by increasing overall vascular transmural pressure, i.e. decrease of plethysmographic (extravascular) pressure by the same amount, a procedure shown in Fig. 5. This compensatory increase of transmural pressure was applied at the rate of ~ 3 mmHg/s and led to an almost pronounced dynamic myogenic constrictor response in the microvessels which raised vascular

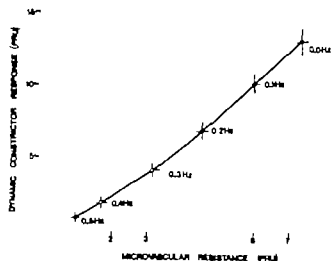


Fig. 6 Effects of simulated light muscle exercise (low frequency somatomotor fibre stimulation) on microvascular tone (abscissa) and on the superimposed dynamic myogenic constrictor response (ordinate) to a standardized test transmural pressure stimulus (pressure increase by 40 mmHg applied at the rate of 2.5 mmHg/s). Note the parallel decrease in microvascular tone and in the dynamic constrictor response with increasing rates of somatomotor fibre excitation.

tone also in the whole vascular bed above the control level at normal arterial pressure. The evoked dynamic constrictor response was of almost the same magnitude as that observed at normal arterial pressure (see latter part of Fig. 5) demonstrating that dynamic myogenic microvascular reactivity was quite well preserved during the arterial pressure reduction (cf. Grände 1979).

When static mean distending pressure was restored, i.e. in the period of constant increased vascular transmural pressure (Fig. 5) small though clearcut static myogenic constrictions developed in the microvessels as well as in the proximal arterial vessels which raised tone in the whole vascular bed by about 1.8 PRU. Such experimental restoration of static vascular transmural pressure distension (but not of the pulse pressure oscillations) during lowered arterial pressure thus led to a partial but not complete recovery of basal vascular tone. The average of 5 such expts. indicated that basal tone in this way could be restored to almost 35% in the whole vascular bed and to about 35% in the microvessels of what was lost during the initial arterial pressure reduction. The static myogenic response during lowered arterial pressure was of almost the same order of magnitude as during normal arterial pressure (see latter

part of Fig. 5) indicating that static myogenic reactivity was quite well preserved during the arterial hypotension.

Return of plethysmographic pressure to zero (Fig. 5) caused an initial marked dynamic microvascular dilator response after which tone returned to the previous low level instituted by the arterial pressure decline. Release of arterial pressure to the control level finally evoked an initial quite pronounced dynamic microvascular constriction after which tone via an oscillatory behaviour returned to the control level in all sections of the vascular bed.

In some additional expts. similar to that depicted in Fig. 5 overall vascular transmural pressure was raised from an AP level of about 80 mmHg by 65 mmHg corresponding to the normal mean distending pressure at an AP of 125 mmHg. This resulted in an average static constrictor response in the microvessels of about 2.8 PRU and in the proximal arterial vessels of about 0.8 PRU. The latter data might serve as rough estimates of the extent to which the static distension effect of normal mean arterial pressure contributes to the establishment of normal basal vascular tone.

These data and those presented in Figs. 7 and 8 provide strong circumstantial evidence for the opinion that basal vascular tone, especially in the microvessels, during normal arterial blood pressure to a significant extent is dependent both on its static distension effect related to mean arterial pressure and on its pulse pressure oscillations. Yet these two factors do not seem to be the only ones responsible for the initiation of basal vascular tone (see Discussion).

The decline in microvascular tone during arterial pressure reduction as illustrated in Fig. 5 might in part be explained by the action of metabolic dilator factors accumulating during the resulting flow reduction, even if it was small in this case. The fact that static and especially dynamic myogenic reactivity was shown to be quite well preserved during the arterial pressure reduction suggests that such an influence was small unless the metabolic control system interferes with basal tone via some mechanism completely unrelated to myogenic reactivity. The latter possibility was examined in a special series of expts. by determining myogenic reactivity in terms of its prominent dynamic component under more defined activation of the metabolic control system of skeletal



Fig. 7 Histogram summarizing in approximate figures the extent of normal basal tone in proximal arterial vessels ($>25 \mu\text{m}$) and microvessels ($<25 \mu\text{m}$) in skeletal muscle (total height of columns) and its dependence on transmural pressure (see key). Note that a considerable fraction of the normal basal tone in the microvessels depends on arterial pressure, both via its static distension effect related to mean arterial pressure and its dynamic pulse pressure distension. Note further that a strong inhibitory dynamic transmural pressure (P^*) stimulus ($dP/dt = 5 \text{ mmHg/s}$) could virtually abolish basal tone in these vessels. Basal tone in the proximal arterial vessels was much less affected by such transmural pressure stimuli.

made, viz. by graded somato-motor fibre excitation.

Fig. 6 summarizes the results of 7 experiments in which observations of microvascular tone and of the dynamic myogenic constrictor response to a standardized transmural pressure increase at a rate of 2.5 mmHg/s were performed under simultaneous somato-motor fibre stimulation in the low frequency range up to 0.5 Hz , simulating light exercise (cf. Lundvall 1972). It can be seen that such metabolic influence in fact decreased microvascular tone and the dynamic myogenic constrictor response in parallel, and that these effects were graded in relation to the excitation rate with close to maximal inhibitory effects evoked at 0.5 Hz .

It is concluded that the metabolic control system distinctly interacts with the mechanism(s) responsible for dynamic myogenic reactivity at least when activated by skeletal muscle contraction. It therefore appears that metabolic influence did not significantly contribute to the inhibition of basal microvascular tone during the moderate arterial pressure reduction produced in Fig. 5 since myogenic reactivity was then well preserved (cf. Grande 1979). This does not refine the possibility that metabolic influence can be of significant importance during more pronounced and longlasting arterial hypotension.

Mention should finally be made that the proximal arterial vessels were shown to be much less sensitive than the microvessels to the metabolic influence of muscle contraction (cf. Folkow et al. 1971), basal tone in the former vessels being virtually unaffected by somato-motor fibre stimulation in the range up to 0.5 Hz . Stronger metabolic stimuli, however, caused gradual inhibition of this tone also maximal relaxation in these vessels being observed at excitation rates around 4 Hz , corresponding to the metabolic influence of heavy exercise (cf. Lundvall 1972).

DISCUSSION

The aim of the present study was to elucidate in some detail the characteristics of the intrinsic basal vascular tone in skeletal muscle with regard to its extent and site along the vascular bed, its dependence on static and dynamic transmural pressure stimuli and its sensitivity to local metabolic influence. A method was used which according to previous evaluation (see Grande et al. 1977, Grande 1979) seems to provide quite reliable determinations of total vascular resistance as well as segmental resistances in what is denoted proximal arterial vessels, microvessels and large veins. The data indicated that the site for separation between proximal arterial vessels and microvessels referred to an approximate vessel diameter as small as $25 \mu\text{m}$ implying that the former vessels extended somewhat into the domain of the microcirculation. The described active resistance reactions in the microvessels of this study can be considered to refer to the terminal arterial vessels mainly even if the capillaries and minute venous vessels were also included in these resistance measurements (Grande et al. 1977).

The results first confirmed previous observations (see Mellander & Johansson 1968) that basal tone in the adrenergically blocked vascular bed under control conditions was high on the arterial side and low in the large veins, as evidenced by comparison of segmental vascular resistances at normal tone and after complete smooth muscle relaxation with papaverine. The main results of the present study therefore deal with the characteristics of basal tone in the proximal arterial vessels and the microvessels and they may be summarized schematically and in rough figures, as illustrated in Fig. 7. The extent of smooth muscle tone is here expressed in

terms of its active vascular resistance corollary (PRU) i.e. the resistance at the normal level of basal tone minus the small physical resistance remaining after complete smooth muscle relaxation.

The following main conclusions may be drawn. Under control conditions basal tone corresponded to an average of 6.6 PRU in the proximal arterial vessels and 7.8 PRU in the microvessels. The normal arterial blood pressure seemed to be partially responsible for the initiation and maintenance of this basal tone both via its pulse pressure oscillations and its mean pressure level, the former quite likely creating a repetitive dynamic and the latter a static transmural pressure stimulation of the smooth muscle. Note however that the fraction of basal tone which could be attributed to these two stimuli was much greater in the microvessels than in the proximal arterial vessels (Fig. 7). Experimental application of a strong (probably maximal) inhibitory dynamic transmural pressure stimulus ($dP_T/dt = -5$ mmHg/s) caused a very effective though not complete inhibition of the normal basal tone in the microvessels but such a stimulus had only a slight effect on tone in the more proximal vessels (Fig. 7).

Mention should be made in this context that dynamic transmural pressure stimulation of the vascular bed might not solely be affected by pulse pressure oscillations but perhaps also by segmental pressure oscillations in the longitudinal direction created for instance by the intermittent local constrictions and dilations denoted vasomotion.

The demonstration that normal microvascular basal tone to such a significant extent is depending upon static and dynamic transmural pressure stimuli created by the normal arterial blood pressure might offer a very simple explanation of myogenic autoregulatory phenomena in the microcirculation. Fall of arterial blood pressure within a certain range would lead to a graded inhibition of basal tone simply due to partial elimination of its initiating static and dynamic pressure stimuli. Conversely raised arterial pressure might lead to reinforced vascular tone due to increased static mean pressure distension and to the usually associated increase in the amplitude and/or frequency of the pulse pressure oscillations or other possible mechanisms facilitating the dynamic transmural pressure stimuli. The fact that basal tone in the proximal arterial vessels was largely independent of arterial blood pressure per se might then possibly

explain why autoregulation of flow occurs only within a limited range of arterial pressures.

The described results which demonstrate that basal tone is much more dependent upon and sensitive to transmural pressure stimuli in the microvessels than in the proximal arterial vessels suggest that basal tone is of somewhat different nature in these two sections. The site for such a possible functional differentiation of the smooth muscle along the arterial vascular tree is probably not precisely at the vessel dimension of $25 \mu\text{m}$ (Ld) but perhaps at a more proximal level the small fraction of basal tone sensitive to transmural pressure stimuli in what was here called proximal arterial vessels (Fig. 7) thus might reflect the behaviour in their smallest ramifications which should be denoted microvessels rather than proximal vessels. Whatever the case the fact remains that the by far largest fraction of basal tone in the microvessels ($< \text{about } 25 \mu\text{m}$ l.d.) was sensitive to transmural pressure stimuli while the by far largest fraction of basal tone in the more proximal vessels seemed to be irresponsive to such stimuli. Another difference between the proximal arterial vessels and the microvessels was that basal tone in the latter (Fig. 6) was much more sensitive to metabolic stimuli than that in the former (cf. Folkow et al. 1971). Even if basal tone in both sections might be considered to be of myogenic origin (see Introduction) the described functional discrepancies might suggest somewhat different cellular mechanisms behind the basal tone in the proximal and distal arterial vessels, a possibility which will be discussed in the light of some recent electrophysiological studies on vascular smooth muscle.

The cellular mechanisms responsible for basal vascular tone and myogenic reactions are not yet experimentally defined in the arterial microvessels specifically but a recent *in vitro* study (Johansson & Mellander 1975) has clarified the electrophysiological events behind myogenic reactivity to mechanical stimuli in the single unit spike generating vascular smooth muscle of the rat portal vein which seems to have several characteristics in common with arterial microvascular smooth muscle. The myogenic contractile response pattern is thus quite similar in both these types of vascular smooth muscle (Johansson & Mellander 1975; Grände et al. 1977, 1978). Both exhibit a static as well as a dynamic component in their myogenic responses of which the latter component is the

much more prominent one: a maximal excitatory dynamic stimulus was thus some 15 times more effective in causing constriction *in vitro* and microvascular constriction *in vivo* than a maximal static stimulus. A strong inhibitory dynamic stimulus was furthermore capable of abolishing contractile activity in the portal vein and, as shown in this study, also could effectively inhibit basal microvascular tone *in vivo*. Such close resemblance between the portal vein and the arterial microvessels with regard to their myogenic contractile patterns of response and stimulus-effector characteristics makes it quite likely that the myogenic responses in both types of muscle are mediated via some common cellular mechanism.

The portal vein shows a characteristic spontaneous regular rhythmic contractile activity in the control state at low preload which is caused by bursts of action potentials primarily generated from a pacemaker cell (Johansson & Mellander 1975). When it was exposed to excitatory static or dynamic stimuli (passive stretch at graded rates) spike discharge and myogenic mechanical activity increased in parallel. The dynamic electrical and mechanical responses were graded in relation to the rate of length (L) change, dL/dt . Similarly there are graded decreases in electrical and mechanical activity in response to the rate of passive shortening (negative dL/dt). A strong inhibitory dynamic stimulus caused complete abolition of electrical (and mechanical) activity: a finding which deserves special attention in the interpretation below. Excitatory and inhibitory myogenic effector reactions in the spike-generating type of vascular smooth muscle are thus mediated via facilitation and inhibition of normal pacemaker generated spontaneous spike discharge.

It follows from the considerations above that the myogenic reactions to transmural pressure stimuli in the arterial microvessels quite likely could be mediated in variations in pacemaker spike discharge as well (even if the size of their length units must be much smaller than in the portal vein). If this conclusion is valid it would imply that at least a major fraction of the basal tone in the microvessels is dependent upon action potentials, viz. that fraction (see Fig. 7) which was abolished by the inhibitory dynamic transmural pressure stimulus ($dP/dt = -5$ mmHg/s). Part of the normal basal tone in these vessels might then be due to a spontaneous pacemaker discharge (like

in the portal vein) and parts initiated by the normal arterial pressure via its static and dynamic transmural pressure stimuli (Fig. 7), leading to continuous reinforcement of electrical activity in the control situation.

Basal tone in the proximal arterial vessels was little affected by transmural pressure stimuli (Fig. 7) and its major fraction might therefore be virtually independent of action potentials. Smooth muscle in these vessels might then be mainly of the same non-spike-generating type as demonstrated in large arterial vessels *in vitro* (Su Bevan & Ursillo 1964; Hermansmeyer 1971; Sonhø Vinall & Sonhø 1971; von Lob & Bohr 1973; Casteels et al. 1977; Johansson 1978) where tone is considered to be caused by contracture and established by graded membrane depolarization. The small fraction of basal tone in the microvessels which remained upon exposure to the strong inhibitory transmural pressure stimulus (see Fig. 7) might possibly be explained by a similar mechanism. The suggested differentiation of smooth muscle along the arterial vascular bed in skeletal muscle might therefore not be very distinct characteristic (cf. *in vitro* studies by Roddie 1960; Steedman 1966; Biamino & Kruckenberg 1969) but include an element where the difference is mainly of quantitative nature. Intrinsic basal tone in the large *cirs* was low and normal resting tone might here be established by action potentials initiated by extrinsic especially adrenergic stimuli to their smooth muscles which seem to be more of the multi-unit type (cf. Mellander & Johansson 1968).

This study was supported by grant B79-04X/2210-138 from the Swedish Medical Research Council and by grants from the Medical Faculty, University of Lund, Sweden.

REFERENCES

- ANREP G. 1912 On local vascular reactions and their interpretation. *J Physiol (Lond)* 45: 318-327.
- BAEZ S., LAIDLAW Z. & ORKIN L. R. 1974 Localization and measurement of microvascular and macrocirculatory responses to venous pressure elevation in the rat. *Blood Vessels* 11: 260-276.
- BAYLISS W. M. 1902 On the local reactions of the arterial wall to changes in internal pressure. *J Physiol (Lond)* 26: 220-231.
- BIAMINO G. & KRUCKENBERG P. 1969 Synchrotronization and conduction of excitation in the rat aorta. *Amer J Physiol* 217: 376-382.
- BOHR, D. P. 1965 Ion channels among vascular smooth muscles. In: *Electrolytes and cardiovascular diseases*

terms of its active vascular resistance corollary (PRU) i.e. the resistance at the normal level of basal tone minus the small physical resistance remaining after complete smooth muscle relaxation.

The following main conclusions may be drawn. Under control conditions basal tone corresponded to an average of 6.6 PRU in the proximal arterial vessels and 7.8 PRU in the microvessels. The normal arterial blood pressure seemed to be partially responsible for the initiation and maintenance of this basal tone both via its pulse pressure oscillations and its mean pressure level: the former quite likely creating a repetitive dynamic and the latter a static transmural pressure stimulation of the smooth muscle. Note, however, that the fraction of basal tone which could be attributed to these two stimuli was much greater in the microvessels than in the proximal arterial vessels (Fig. 7). Experimental application of a strong (probably maximal) inhibitory dynamic transmural pressure stimulus ($dp_1/dt = -5$ mmHg/s) caused a very effective though not complete inhibition of the normal basal tone in the microvessels, but such a stimulus had only a slight effect on tone in the more proximal vessels (Fig. 7).

Mention should be made in this context that dynamic transmural pressure stimulation of the vascular bed might not solely be affected by pulse pressure oscillations but perhaps also by segmental pressure oscillations in the longitudinal direction created for instance by the intermittent local contractions and dilations denoted vasomotion.

The demonstration that normal microvascular basal tone to such a significant extent is depending upon static and dynamic transmural pressure stimuli created by the normal arterial blood pressure might offer a very simple explanation of myogenic autoregulatory phenomena in the microcirculation. Fall of arterial blood pressure within a certain range would lead to a graded inhibition of basal tone simply due to partial elimination of its initiating static and dynamic pressure stimuli. Conversely raised arterial pressure might lead to reinforced vascular tone due to increased static mean pressure distension and to the usually associated increase in the amplitude and/or frequency of the pulse pressure oscillations or other possible mechanisms facilitating the dynamic transmural pressure stimuli. The fact that basal tone in the proximal arterial vessels was largely independent of arterial blood pressure per se might then possibly

explain why autoregulation of flow occurs only within a limited range of arterial pressures.

The described results which demonstrate that basal tone is much more dependent upon and sensitive to transmural pressure stimuli in the microvessels than in the proximal arterial vessels suggest that basal tone is of somewhat different nature in these two sections. The site for such a possible functional differentiation of the smooth muscle along the arterial vascular tree is probably not precisely at the vessel dimension of 25 μ m (i.d.) but perhaps at a more proximal level the small fraction of basal tone sensitive to transmural pressure stimuli in what was here called proximal arterial vessels (Fig. 7) thus might reflect the behaviour in their smallest ramifications which should be denoted microvessels rather than proximal vessels. Whatever the case the fact remains that the by far largest fraction of basal tone in the microvessels (< about 25 μ m i.d.) was sensitive to transmural pressure stimuli while the by far largest fraction of basal tone in the more proximal vessels seemed to be irresponsive to such stimuli. Another difference between the proximal arterial vessels and the microvessels was that basal tone in the latter (Fig. 6) was much more sensitive to metabolic stimuli than that in the former (cf Folkow et al. 1971). Even if basal tone in both sections might be considered to be of myogenic origin (see Introduction) the described functional discrepancies might suggest somewhat different cellular mechanisms behind the basal tone in the proximal and distal arterial vessels, a possibility which will be discussed in the light of some recent electrophysiological studies on vascular smooth muscle.

The cellular mechanisms responsible for basal vascular tone and myogenic reactions are not yet experimentally defined in the arterial microvessels specifically but a recent *in vitro* study (Johansson & Mellander 1975) has clarified the electrophysiological events behind myogenic reactivity to mechanical stimuli in the single unit spike-generating vascular smooth muscle of the rat portal vein which seems to have several characteristics in common with arterial microvascular smooth muscle. The myogenic contractile response pattern is thus quite similar in both these types of vascular smooth muscle (Johansson & Mellander 1975; Grande et al. 1977, 1978). Both exhibit a static as well as a dynamic component in their myogenic responses of which the latter component is the

each more prominent one: a maximal excitatory dynamic stimulus was thus some 15 times more effective in causing contraction *in vitro* and microvascular constriction *in vivo* than a maximal static stimulus. A strong inhibitory dynamic stimulus was furthermore capable to abolish contractile activity in the portal vein and, as shown in this study, also could effectively inhibit basal microvascular tone *in vivo*. Such close resemblance between the portal vein and the arterial microvessels with regard to their myogenic contractile patterns of response and stimulus-effector characteristics makes it quite likely that the myogenic responses in both types of vessels are mediated via some common cellular mechanism.

The portal vein shows a characteristic spontaneous regular rhythmic contractile activity in the control state at low preload which is caused by bursts of action potentials primarily generated from a pacemaker cell (Johansson & Mellander 1975). When it was exposed to excitatory static or dynamic stimuli (passive stretch at graded rates) spike discharge and myogenic mechanical activity increased in parallel. The dynamic electrical and mechanical responses were graded in relation to the rate of length (L) change, dL/dt . Similarly there were graded decreases in electrical and mechanical activity in response to the rate of passive shortening (negative dL/dt). A strong inhibitory dynamic stimulus caused complete abolition of electrical (and mechanical) activity, a finding which deserves special attention in the interpretation below. Excitatory and inhibitory myogenic effector reactions in the spike-generating type of vascular smooth muscle are thus mediated via facilitation and inhibition of normal pacemaker generated spontaneous spike discharge.

It follows from the considerations above that the myogenic reactions to transmural pressure stimuli in the arterial microvessels quite likely might be mediated via variations in pacemaker spike discharge as well (even if the size of their single units must be much smaller than in the portal vein). If this conclusion is valid it would imply that at least a major fraction of the basal tone in the microvessels is dependent upon action potentials, viz. that fraction (see Fig. 7) which was abolished by the inhibitory dynamic transmural pressure stimulus ($dP/dt = -5 \text{ mmHg/s}$). Part of the normal basal tone in these vessels might then be due to a spontaneous pacemaker discharge (like

in the portal vein) and parts initiated by the normal arterial pressure via its static and dynamic transmural pressure stimuli (Fig. 7) leading to continuous reinforcement of electrical activity in the control situation.

Basal tone in the proximal arterial vessels was little affected by transmural pressure stimuli (Fig. 7) and its major fraction might therefore be initially independent of action potentials. Smooth muscle in these vessels might then be mainly of the same non-spike-generating type as demonstrated in large arterial vessels *in vitro* (Su, Bevan & Ursillo 1964; Hermansmeyer 1971; Somlyo, Vinall & Somlyo 1971; von Lob & Bohr 1973; Casteels et al. 1977; Johansson 1978) where tone is considered to be caused by contracture and established by graded membrane depolarization. The small fraction of basal tone in the microvessels which remained upon exposure to the strong inhibitory transmural pressure stimulus (see Fig. 7) might possibly be explained by a similar mechanism. The suggested differentiation of smooth muscle along the arterial vascular bed in skeletal muscle might therefore not be a very distinct characteristic (cf. *in vitro* studies by Roddie 1960; Steedman 1966; Biamino & Kruckenberg 1969) but include an element where the difference is mainly of quantitative nature. Intrinsic basal tone in the large veins was low and normal resting tone might here be established by action potentials initiated by extrinsic, especially adrenergic, stimuli to their smooth muscles which seem to be more of the multi-unit type (cf. Mellander & Johansson 1968).

This study was supported by grant B79-04X 2210-138 from the Swedish Medical Research Council and by grants from the Medical Faculty, University of Lund, Sweden.

REFERENCES

- ANREP G. 1912. On local vascular reactions and their interpretation. *J Physiol (Lond.)* 45: 318-327.
- BAEZ, S., LAIDLAW, Z. & ORKIN, L. R. 1974. Localization and measurement of microvascular and macrocirculatory responses to venous pressure elevation in the rat. *Blood Vessels* 11: 260-276.
- BAYLISS, W. M. 1902. On the local reactions of the arterial wall to changes in internal pressure. *J Physiol (Lond.)* 28: 220-231.
- BIAMINO G. and KRUCKENBERG P. 1969. Synchronization and conduction of excitation in the rat aorta. *Amer J Physiol* 17: 376-382.
- BOHR, D. F. 1965. Individualities among vascular smooth muscles. In: *Electrolytes and cardiovascular diseases*

- (ed E. Bajusz) pp 34-355 S Karger Basel New York
- CARO C G PEDLEY T J SCHROTER R C & SEED W A 1978 The mechanics of the circulation Oxford University Press.
- CASTEELS R KITAMURA K KURIYAMA H & SUZUKI H 1977 The membrane properties of the smooth muscle cells of the rabbit main pulmonary artery *J Physiol (Lond)* 271 41-61
- FOLKOW B 1949 Intravascular pressure as a factor regulating the tone of the small vessels *Acta Physiol Scand* 17 289-310
- FOLKOW B 1962 Transmural pressure and vascular tone—some aspects of an old controversy *Arch Int Pharmacodyn* 139: 455-469
- FOLKOW B & ÖBERG B 1961 Autoregulation and basal tone in consecutive vascular sections of the skeletal muscles in reserpine treated cats. *Acta Physiol Scand* 53 105-113
- FOLKOW B SONNENSCHNEIN R R. & WRIGHT D L 1971 Loci of neurogenic and metabolic effects on precapillary vessels of skeletal muscle *Acta Physiol Scand* 81 459-471
- FRONEK K & ZWEIFACH B W 1975 Microvascular pressure distribution in skeletal muscle and the effect vasodilation *Amer J Physiol* 228 791-796.
- GRANDE, P-O 1979 Influence of neural and humoral β -adrenoceptor stimulation on dynamic myogenic microvascular reactivity in cat skeletal muscle *Acta Physiol Scand* 106: 457-465
- GRANDE P-O & BORGSTRÖM P 1978 An electronic differential pressure flowmeter and a resistance meter for continuous measurement of vascular resistance *Acta Physiol Scand* 102: 224-230
- GRANDE P-O JARHULT J & MELLANDER S. 1974 Method for gravimetric registration of changes in tissue volume *Acta Physiol Scand* 91 211 215
- GRANDE P-O LUNDVALL J & MELLANDER S 1977 Evidence for a rate sensitive regulatory mechanism in myogenic microvascular control *Acta Physiol Scand* 99: 43-47
- GRANDE, P-O & MELLANDER S 1978 Characteristics of static and dynamic regulatory mechanisms in myogenic microvascular control *Acta Physiol Scand* 102: 231- 45
- HADDY F J RICHARDS, A G ALDEN J L & VISSCHER M B 1954 Small vein and artery pressures in normal and edematous extremities of dogs under local and general anaesthesia. *Amer J Physiol* 176: 355-360.
- HERMSMEYER, K. 1971 Contraction and membrane activation in several mammalian vascular muscles. *Life Sci* 10: 23-34.
- JOHANSSON B 1971 Electromechanical and mechano-electrical coupling in vascular smooth muscle *Angiologia* 8: 129-143
- JOHANSSON B 1978. Vascular smooth muscle biophysics. In: *Microcirculation II* (ed. O. Hakey and B. M. Altura) pp. 83-117 University Park Press, Baltimore.
- JOHANSSON B & MELLANDER S. 1975 Static and dynamic components in the vascular myogenic response to passive changes in length as revealed by electrical and mechanical recordings from the rat portal vein *Circulat Res* 36: 76-83
- JOHNSON P C 1964 (ed) Symposium on autoregulation of blood flow *Circulat Res* 15 Suppl 1 1-91
- JOHNSON P C. 1968 Autoregulatory responses of cat mesenteric arterioles measured in vivo. *Circulat Res* 22: 199-212.
- LALONE B SCHWINGHAMER, J & MAJOR T 1975 Autoregulation of skeletal muscle blood flow during pulsatile and non-pulsatile perfusion *Fed Proc* 34 369
- VON LOH D & BOHR D F 1973 Membrane potentials of smooth muscle cells of isolated resistance vessels. *Proc Soc Exp Biol (N Y)* 144 513-516.
- LUNDVALL, J 1972 Tissue hyperosmolality as a mediator of vasodilatation and transcapillary fluid flux in exercising skeletal muscle *Acta Physiol Scand Suppl* 379: 1-14..
- MELLANDER, S & ARVIDSSON S 1974 Possible dynamic component in the myogenic vascular response related to pulse pressure distension. *Acta Physiol Scand* 90: 283-85
- MELLANDER, S & JOHANSSON B 1968 Control of resistance exchange and capacitance functions in the peripheral circulation. *Pharmacol Rev* 20: 117 196.
- MELLANDER S ÖBERG B & ODELRAM H 1964. Vascular adjustments to increased transmural pressure in cat and man with special reference to shift in capillary fluid transfer *Acta Physiol Scand* 61 34-48
- RODDIE I C 1962 The transmembrane potential changes associated with smooth muscle activity in turtle arteries and veins. *J Physiol (Lond)* 163 138-140
- SOMLYO A V VINALL, P & SOMLYO A P 1971 Excitation-contraction coupling and electrical events in two types of vascular smooth muscle *Microvasc Res* 1 354-373
- STEEDMAN W M 1966. Micro-electrode studies on mammalian vascular muscle *J Physiol (Lond)* 186: 38-400
- SU C BEVAN J A & URSILLO R C 1964 Electrical quiescence of pulmonary artery smooth muscle during sympathomimetic stimulation. *Circ Res* 15 20-27
- VANHOUTTE P M 1978 Heterogeneity in vascular smooth muscle. In: *Microcirculation II* (ed. O. Hakey and B. M. Altura) pp 181 309 University Park Press, Baltimore

Efflux of cyclic AMP, prostaglandin E_2 and $F_{2\alpha}$ and thromboxane B_2 in leg lymph of rabbits after scalding injury

CARL-EVERT JONSSON, YASUYUKI SHIMIZU, BERTIL B. FREDHOLM, ELISABETH GRANSTRÖM and ERNST OLIW

Department of Plastic and Reconstructive Surgery and Surgical Research Laboratory Karolinska sjukhuset, Stockholm, and Departments of Pharmacology and Chemistry Karolinska institutet, Stockholm, Sweden

JONSSON C-E, SHIMIZU Y, FREDHOLM B B, GRANSTRÖM E & OLIW E. Efflux of cyclic AMP, prostaglandin E_2 and $F_{2\alpha}$ and thromboxane B_2 in leg lymph of rabbits after scalding injury. *Acta Physiol Scand* 1979; 107: 377-384. Received 2 July 1979. ISSN 0001-6772. Department of Plastic and Reconstructive Surgery and Surgical Research Laboratory Karolinska sjukhuset, Stockholm, and Departments of Pharmacology and Chemistry Karolinska institutet, Stockholm, Sweden.

Leg lymph was collected from pentobarbital anaesthetized rabbits before and after scalding injury of the paw (73°C for 20 s), and the contents of cyclic AMP (cAMP), prostaglandin E_2 (PGE₂) and PGE₂ and thromboxane B_2 (TXB₂) in lymph were determined. After injury lymph flow increased about four times. The maximal rate of flow was found between 30 and 60 min after scalding. The efflux of cAMP and immunoreactive PGE₂, PGE₂ and TXB₂ also increased. The maximum values were detected at approximately 0-30, 30-60, 30-60 and 180-240 min, respectively, after the injury. The output of cAMP, PGE₂ and PGE₂ and TXB₂ in lymph of the contralateral non-scalded paw remained low throughout the experiments. When rabbits were injected with indomethacin (2.5 mg/kg) or diclofenac sodium (2.5 mg/kg) immediately after the scalding injury, the efflux of cAMP, PGE₂ and PGE₂ were low. Lymph flow was markedly reduced after treatment with diclofenac sodium; treatment with indomethacin did not significantly affect lymph flow. The results suggest prostaglandin-dependent formation of cAMP following scalding injury which may be related to the local responses to scalding.

Key words: Scalding injury, lymph flow, cAMP, thromboxanes, prostaglandins.

Scalding injury is followed by vascular reactions, i.e. erythema and edema formation, the extent of which depends on the duration and magnitude of the increased temperature (Arturson 1961). In the acute phase of burn there is a rapid loss of intravascular fluid to the injured tissue, mainly due to modulation, increased microvascular permeability and increased extravascular osmotic pressure (Arturson & Mellander 1964). Once edema is formed, blood flow seems to be reduced in the injured tissue (Hassan et al. 1979). For a long time it has been assumed that the effects of scalding are mediated by vasoactive compounds formed or released in the tissues. For example, there is evi-

dence to suggest that histamine (Edery & Lewis 1963) and prostaglandins, mainly prostaglandin E_2 (PGE₂) (Wålin 1970, Jonason 1971, Williams 1979) mediate the initial vascular response.

Recently intermediates in the biosynthesis of prostaglandins, the prostaglandin endoperoxides (PGG₂ and PGH₂) were isolated (Hamberg & Samuelsson 1973, Nugteren & Hazelhof 1973). The availability of the prostaglandin endoperoxides led to the discovery of two unstable and very potent products, thromboxane A₂ (TXA₂, Hamberg et al.

Present address: Dept. of Dermatology, Tohoku University, Yagoto, Japan.

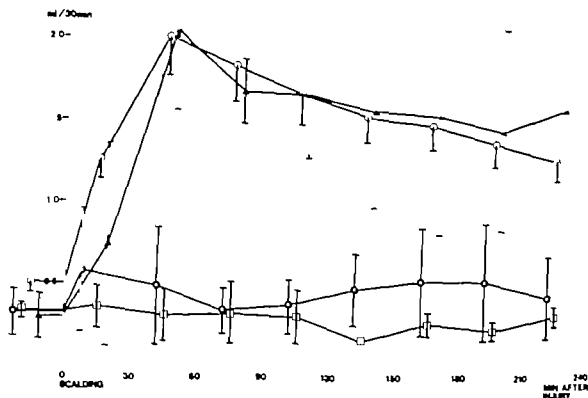


Fig. 1 Leg lymph flow before and after scalding injury. At 0-time the paw was injured by immersion in water of 75°C for 20 s. Lymph was collected in 30 min periods in every experiment. However for purposes of clarity of presentation the points in the graph have not all been plotted at the mid point of each collection interval. Non-treated rabbits $n=12$. \square — \square $n=12$ mean value and range. Rabbits treated immediately after scalding with indomethacin (2.5 mg/kg, $n=2$, \blacktriangle — \blacktriangle) or diclofenac sodium (2.5 mg/kg, $n=2$, \bullet — \bullet) mean values and ranges are given.

1975) and prostacyclin PGI (Moncada et al 1976). Although the prostaglandin endoperoxides are precursors of prostaglandins as well as of the thromboxanes and PGI₂, the conversion of the prostaglandin endoperoxides to their different products varies between tissues (Pace-Asciak 1977; Vane 1978). For example vessel walls and heart may convert the endoperoxides mainly to PGI (Moncada & Vane 1979) while platelets and lung tissue convert them mainly to TXA₂ (Hamberg et al 1977). In other tissues "primary" prostaglandins PGD₂, PGE₂ and PGF_{2 α} are the dominating products (e.g. Fredholm & Hamberg 1976; Oliw et al 1979). The different products of endoperoxide metabolism display a wide variety of biological effects. Thromboxane is for example a potent vasoconstrictor, PGI₂ is a potent vasodilator and of the "primary" prostaglandins, PGE₂ is a vasodilator while PGF_{2 α} may cause vasoconstriction (Svensson & Fred-

holm 1977; Samuelsson et al 1978a). There is considerable evidence that cyclic AMP (cAMP) mediates several effects of prostaglandins (Samuelsson et al 1978b). In particular it is an interesting possibility that vasodilatation induced by PGI₂ and PGE₂ is due to stimulation of cyclic AMP production in vascular smooth muscle since cyclic AMP is known to mediate vasodilatation due to several agents (see Bar 1974 for review).

In this communication we report studies on the efflux of cAMP, prostaglandins and thromboxanes in leg lymph of rabbit after scalding injury of the paw. Thromboxane B (TXB₂), a degradation product of the very unstable thromboxane A (TXA₂) was determined as an indicator of TXA₂ synthesis.

MATERIALS AND METHODS

Rabbits weighing between 2.0 and 3.0 kg were anaesthetized with sodium pentobarbital (18 mg/kg). Additional

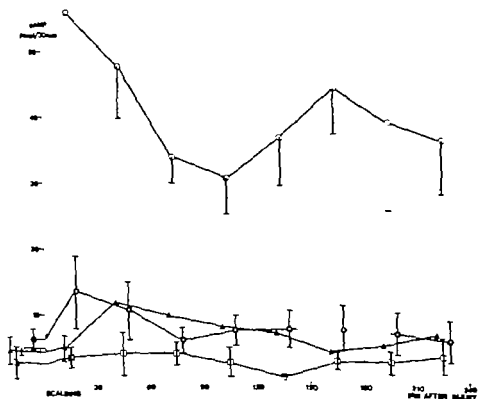


Fig. 2 cAMP in lymph before and after scalding injury expressed as pmol per 30 min periods in every experiment. However, for purposes of clarity of presentation the points in the graph have not all been plotted at the mid point of each collection interval. Lymph from non-treated rabbits, \circ — \circ mean and S.E. given. Lymph from control (2 \square — \square) rabbits treated with indomethacin (\triangle — \triangle) or diclofenac sodium (\square — \square). Mean values and S.E. are given in these experiments.

does were given when required. For visualization of the lymph vessels, Fluorescein Dextran (FITC-Dextran 150, Pharmacia, Sweden) 25 mg in 0.5 ml saline, was injected into the subcutaneous tissue of the paw. A leg lymph vessel was cannulated as described (Jocsson & Skarvén 1979). Lymph flow was facilitated by gentle massage or sucking of the paw every 5 s. Blood from the carotid artery as used for assay of cAMP in plasma. Ice-chilled control tubes (containing EDTA) were filled with blood (2 ml). After centrifugation plasma was pipetted off and frozen.

Lymph was collected in 30 min periods in ice-chilled glass tubes (1 ml). For assay of cAMP the tubes contained 50 μ l 0.3 M EDTA (final concentration about 25 mM). The tubes were kept at -20°C before assay which was usually performed within two weeks. Lymph volume was estimated by weighing the tubes before and after collection of lymph. The scalding injury was effected by immersion of the paw in water of 75°C for 20 s.

Indomethacin (2.5 mg/kg, Merck Sharp & Dohme, Rahway USA) and diclofenac sodium (2.5 mg/kg, o-(2,6-dichlorophenyl)-methyl-phenylacetate sodium, Ciba-

Geigy, Basel, Switzerland), were freshly prepared in 0.1 M potassium phosphate buffer pH 8.0, immediately before use. The drugs were injected intravenously immediately after the scalding injury.

Cyclic AMP Assays Assays of cAMP were conducted in duplicate according to the method of Brown et al. (1972) using (8- ^3H)-cyclic AMP (26 Ci/mmol, The Radiochemical Centre, Amersham). Binding protein was prepared from bovine adrenal cortex, and North G SX (N.V. Algemene Noort, Amsterdam) was used to separate free and bound cyclic nucleotide. In order to validate the assay some samples were assayed also by radioimmunoassay (using reagent kit from New England Nuclear Boston), after delipidation and acetylation as described by Harper & Brooker (1975).

Results were virtually identical in samples of intact lymph and in lymph deproteinized with trichloroacetic acid followed by 5 times extraction with ether (13.6 ± 0.4 pmol/l vs. 14.8 ± 1.4 pmol/l, $n=16$). The lymph bound less than 1.5% of the cAMP in the absence of exogenous binding protein. Deproteinization was therefore not routinely carried out. Secondary purification of cAMP on

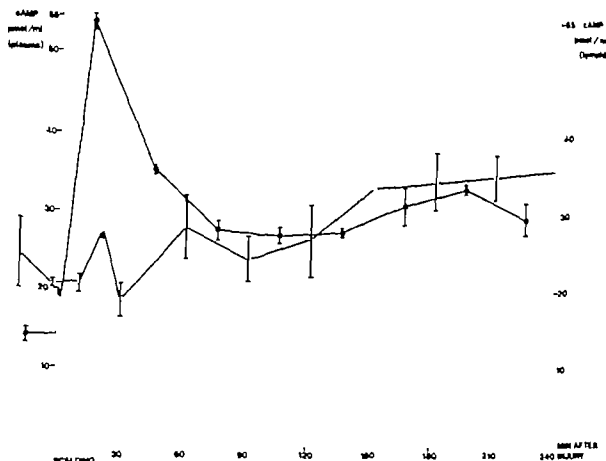


Fig 3 cAMP (pmol/ml) in lymph (●—●) and plasma (○—○) before and after scalding. Mean values ($n=5$) and range (bars) are given.

Dowex 50 columns did not alter the values. Finally treatment with phosphodiesterase removed 90% or more of the binding activity.

On the other hand it was found to be necessary to treat the lymph samples immediately with EDTA (5–20 mM) in order to preserve the cAMP. Samples obtained and stored in the absence of EDTA contained substantially less cAMP (3.7 ± 0.6 pmol/ml vs. 15.4 ± 1.4 pmol/ml). In order to further study the breakdown of cAMP 32 P cyclic AMP (2 pmol/ml) (New England Nuclear, Boston 327 Ci/mmol) was incubated with lymph in the presence or in the absence of EDTA for varying lengths of time at 0°C, 20°C or 37°C. In the presence of EDTA (5 mM) less than 5% of the cAMP was hydrolyzed in 20 min. In the absence of EDTA 8–10% was broken down in 20 min at 20°C or 37°C. These findings indicate that less than 10% of the cAMP content of lymph is likely to be broken down during collection of samples and that provided that EDTA is present, very little breakdown will occur during further processing of the samples.

Prostaglandins and thromboxanes PGE_2 , $\text{PGF}_{2\alpha}$ and TXB₂ were measured in duplicate in unextracted lymph by radioimmunoassay. $\text{PGF}_{2\alpha}$ was measured using a $\text{PGF}_{2\alpha}$ -antiserum while PGE_2 was reduced to $\text{PGF}_{2\alpha}$ and $\text{PGF}_{2\alpha}$ with NaBH₄ and measured using an antiserum raised against $\text{PGF}_{2\alpha}$ (Oliw et al. 1978; Oliw 1979). TXB₂ was determined by radioimmunoassay as previously de-

scribed (Granström et al. 1976). Due to the very low amount of lymph no conclusive identification of the compounds could be performed and the values obtained by radioimmunoassay are referred to as IPGE_2 , $\text{IPGF}_{2\alpha}$ and ITXB_2 , i.e. immunoreactive PGE_2 , $\text{PGF}_{2\alpha}$ and TXB₂, respectively in the text.

RESULTS

Lymph flow. Before scalding injury lymph flow was approximately 0.5 ml/30 min and increased to a peak of about 7.0 ml/30 min 30–60 min after the injury (Fig. 1). The lymph flow decreased somewhat after 1 h. However, at 4 h after the injury the flow was still above control values. Lymph flow in the control leg did not show any significant change during the experiments.

Cyclic AMP. The rate of cyclic AMP appearance in lymph was initially low (approximately 5 pmol/30 min) but increased ten fold immediately following scalding and stayed elevated for the rest of the experiment (Fig. 2).

Before scalding injury the lymph cyclic AMP

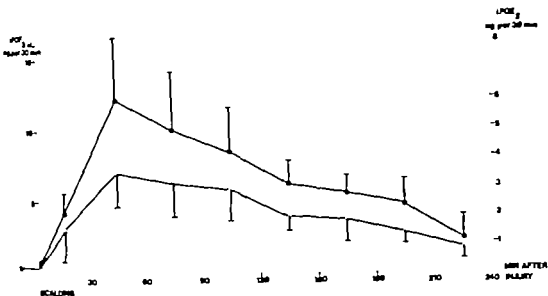


Fig. 4 Effect of iPGE₄ (O—O) and iPGF_{2α} (●—●) in lymph before and after scalding. Mean values ($n=5$) and S.E. (bars) are given.

levels were lower than those in plasma (14.1 ± 4.5 pmol/l (mean, range, $n=2$) vs. 25.6 ± 4.4 pmol/l, $n=4$). Already in the first sample after scalding, the lymph cyclic AMP level was increased more than three-fold, whereas the plasma cyclic AMP concentration was essentially unchanged. Thereafter the lymph cyclic AMP concentration decreased progressively and after one hour the lymph levels were close to those found in plasma, which instead progressively increased after the scalding injury (Fig. 3).

Prostaglandins The levels of PGE₂ and IPGF_{2α} were below the detection limit before scalding injury (Fig. 4). After the injury both iPGE₄ and iPGF_{2α} were detected. Maximum levels were found 30–60 min after scalding and corresponded to an efflux of 8 and 12 ng/30 min into lymph for iPGE₄ and iPGF_{2α} respectively. After that time the rate decreased, but 4 h after the injury immunoreactive material was still detectable.

Thromboxane Before and 0–30 min after scalding the output of TXB₂ in lymph was low (0.4 ng/30

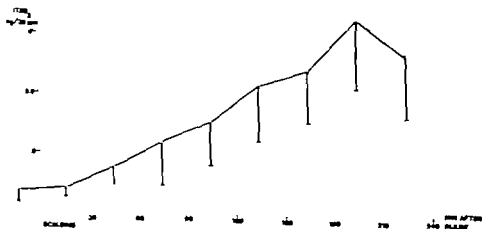


Fig. 5 Effect of iTXB₂ in lymph before and after scalding. Mean values ($n=4$) and S.E. (bars) are given.

min) (Fig. 5). The rate gradually increased and the highest levels were found 180–240 min after the injury or even later in a few animals.

Effect of Indomethacin and diclofenac sodium
After treatment with diclofenac sodium (2.5 mg/kg, $n=2$) directly after the scalding injury the lymph flow was very low (Fig. 1). On the other hand in two rabbits treated with indomethacin (2.5 mg/kg) lymph flow still increased after the injury. In an earlier study in dogs indomethacin caused a marked suppression of lymph flow (Arturson & Jonsson 1973). The failure to observe a significant effect in the present experiments may have been fortuitous and caused by the small number of experiments in which paired controls were unobtainable. The rate of cAMP release into lymph was markedly reduced by both drugs (Fig. 2). However, even after pre-treatment with these drugs a significant two-fold increase in cyclic AMP overflow in lymph was detected. $i\text{PGE}_2$ and $i\text{PGF}_{2\alpha}$ were below levels of detection after treatment with either drug.

DISCUSSION

The results demonstrate increased efflux of cAMP, $i\text{PGE}_2$, $i\text{PGF}_{2\alpha}$ and $i\text{TXB}_2$ in leg lymph after scalding injury of the paw. The compounds appeared in lymph in a characteristic sequence. Maximum secretion of cAMP appeared during the first 30 min period followed by $i\text{PGE}_2$, $i\text{PGF}_{2\alpha}$ (maximum 30–60 min) and $i\text{TXB}_2$ (maximum 180–240 min after injury or later). Lymph flow also increased and reached its level between 30 and 60 min following injury.

The very small levels of the compounds found in control lymph (Fig. 2) indicate that the compounds were formed in the injured tissue and were not filtered out from the blood circulation. As for cAMP this assumption was strengthened by the finding that lymph levels of cAMP increased above the plasma levels. On the other hand the late increase in lymph cAMP co-incided with a rise in the plasma level (Fig. 3) and may have been caused by filtration from plasma. The increased efflux of $i\text{PGE}_2$ and $i\text{PGF}_{2\alpha}$ reflects an increased prostaglandin biosynthesis in the injured tissues (Hamberg & Jonsson 1973). The efflux of TXB_2 indicates that the same is most probably true for TXA_2 as capacity for TXA_2 biosynthesis has been described in many tissues (Samuelsson et al. 1978b).

Before discussing the significance of these results it must be pointed out that the values are based on radioimmunoassay. Because of the small amounts of lymph recovered conclusive identification of the compounds could not be carried out. Indomethacin and diclofenac sodium inhibit biosynthesis of prostaglandins *in vitro* (Vane 1971; Ku et al. 1975) as well as *in vivo* in the rabbit (Olaf et al. 1978). When the rabbits were treated with either of these drugs the efflux of $i\text{PGE}_2$ and $i\text{PGF}_{2\alpha}$ in lymph was markedly reduced supporting the assumption that the measured immunoreactive activity in lymph was in fact related to prostaglandin endoperoxide synthesis.

The initial vascular response to acute injury is vasodilatation (Arturson & Mellander 1964). Vasodilatation induced by several different agents may be caused by increased levels of smooth muscle cyclic AMP (Bär 1974). The markedly increased production of cAMP may thus reflect the effect of vasodilatory compounds on the arterial smooth muscle although other sources than smooth muscle are likely to contribute to lymph cAMP.

There is evidence that the vasodilatation is abolished or considerably reduced by anti-inflammatory drugs (Spector & Willoughby 1959; Arturson & Jonsson 1973). It is therefore interesting that two structurally unrelated anti-inflammatory drugs considerably reduced the efflux of cyclic AMP into lymph. As these drugs inhibit prostaglandin biosynthesis it is tempting to speculate that the vasodilatation and cyclic AMP overflow is prostaglandin mediated. However, a slight but significant elevation of cyclic AMP overflow was seen also in the presence of the PG-synthesis inhibition suggesting that also other material capable of stimulating cyclic AMP formation is formed following scalding. Since there was no increase in cyclic AMP efflux in the contralateral paw this PG-unrelated compound could not be a circulating agent or be released following a generalized nerve activation. The nature of this unknown local factor remains unknown.

However, the fact remains that most of the cyclic AMP production of the scalded paw could be abolished by PG-synthesis inhibitors.

The most pronounced cyclic AMP overflow was found during the first 30 min after scalding. On the other hand $i\text{PGE}_2$ appeared later. It is therefore possible that some other product of prostaglandin-endoperoxides was responsible for the cyclic AMP

increase (and the vasodilatation). It is known that PGI_2 is a potent vasodilator (Moncada & Vane 1979). It is also known that this unstable product is a potent stimulator of cyclic AMP production in several cell types (Gorman et al. 1977; Tateoson et al. 1977; Hyndahl et al. 1978). It is an interesting possibility that PGI_2 may be responsible for some of the effects of scalding. We are not aware of any direct evidence that PGI_2 is produced by scalded skin. However an unidentified peak of smooth muscle stimulating material was detected by Hamberg & Jonsson (1973). This material was more potent than PGE_2 and $\text{PGF}_{2\alpha}$ and may have been identical with 6-keto- $\text{PGF}_{2\alpha}$, the stable breakdown product of PGI_2 . For the above reasons and because of the potent hyperalgesic effect of PGI_2 (Higgs et al. 1978) attempts to demonstrate PGI_2 following scalding are definitely called for.

Vasodilatation in the injured tissue is followed by a state of decreased blood perfusion (Hamar et al. 1979). The simplest explanation for this may be compression of the vessels by the edema. Since TXA_2 has very potent vasoconstricting effects, and the decrease in lymph flow co-incided with increasing levels of TXB_2 , it is tempting to suggest that TXA_2 may contribute to the vasoconstriction in the edema phase. The vascular effects of TXA_2 have not been studied in vessels in the paw and thus much work must be done before definitive conclusions can be drawn. It is interesting to note, however, that a role for TXA_2 in the production of inflammatory edema has been proposed (Kuehl et al. 1977; Chang et al. 1978).

In conclusion the present results demonstrate a marked increase in cyclic AMP efflux into lymph from the scalded rabbit paw. This increase is due to local formation of the cyclic nucleotide and precedes the increase in lymph flow. The increase in cyclic AMP overflow was considerably blunted by two different inhibitors of PG-synthesis suggesting that some product(s) of the endoperoxide synthetase reaction was responsible. Immunoreactive PGE_2 and $\text{PGF}_{2\alpha}$ were released into lymph but occurred later than cyclic AMP. Thromboxane B_2 , an indicator of thromboxane A_2 , occurred even later following scalding. The possibility exists that the initial increase in cyclic AMP may have been caused by PGI_2 . At any rate the results show that different products derived from PG-endoperoxides may be formed and released by injured tissue in a specific sequence.

This study was supported by grants from The Swedish Medical Research Council (nos. 2211 and 2553), Magnus Bergvalls stiftelse and Karolinska Institutets fondar.

REFERENCES

- ARTURSON O. 1961 Pathophysiological aspects of the burn syndrome. *Acta Chir Scand*, Suppl. 274.
- ARTURSON O. & MELLANDER, G. 1964. Acute changes in capillary filtration and diffusion in experimental burn injury. *Acta Physiol Scand* 62: 457-463.
- ARTURSON O. & JONSSON C. E. 1973 Effects of indomethacin on the transcapillary leakage of macromolecules and the efflux of prostaglandins in the paw lymph following experimental scalding injury. *Ups J Med Sci* 78: 181-188.
- BÄR, H. P. 1974. Cyclic nucleotides and smooth muscle. In: *Advances in cyclic nucleotide research* vol. 4 (ed. P. Greengard and G. A. Robison) pp. 195-237. Raven Press, New York.
- BROWN B. L., EKINS, R. P. & ALBANO, J. D. L. 1972. Saturation assay for cyclic AMP using endogenous binding protein. *Adv. Cyclic Nucleic Res* 2: 25-40.
- CHANG W.-C., MURATA, S. J. & TSURUFUJI, S. 1978. Inhibition of thromboxane B_2 and 6-keto-prostaglandin $\text{F}_{2\alpha}$ formation by antiinflammatory drugs in carrageenin-induced granuloma. *Biochem Pharmacol* 27: 109-111.
- EDERY H. & LEWIS, G. P. 1963. Kinase-forming activity and histamine in lymph after thermal injury. *J Physiol* 169: 568-583.
- FREDHOLM, B. B. & HAMBERG, M. 1976. Metabolism and effect of prostaglandins and thromboxane A_2 . *Fed Proc* 11: 507-511.
- GRANSTRÖM, E., KINDAHL, H. & SAMUELSSON B. 1976. Radioimmunoassay for thromboxane B_2 . *Analytical Letters* 9: 611-617.
- HAMAR, J., JONSSON C.-E. & KOVÁCH, A. G. B. 1979. Acute effect of scalding injury on blood flow in muscle and subcutaneous tissue in the paw of the anaesthetized dog. *Scand J Plast Reconstr Surg* 13: 39-43.
- HAMBERG M. & JONSSON C. E. 1973. Increased synthesis of prostaglandins in the guinea pig following scalding injury. *Acta Physiol Scand* 87: 240-245.
- HAMBERG, M. & SAMUELSSON B. 1973. Detection and isolation of an endoperoxide intermediate in prostaglandin biosynthesis. *Proc Natl Acad Sci (USA)* 70: 899-903.
- HARPER, J. F. & BROOKER, G. 1975. Potent and sensitive radioimmunoassay for cyclic AMP and cyclic GMP after 2'-O-acetylation by acetic anhydride in aqueous solution. *J Cyclic Nucleic Res* 1: 207-218.
- HIGGS, E. A., MONCADA, S. & VANE, J. R. 1978. Inflammatory effects of prostacyclin (PGI_2) and 6-oxo- $\text{PGF}_{2\alpha}$ in the rat paw. *Prostaglandins* 16: 153-162.
- HJEMDAHL, P., FREDHOLM, B. B., MALMSTEN, C. & SAMUELSSON B. 1978. Tissue differences in the relative potency of PGI_2 and PGE_2 : Studies on human lymphocytes and rat adipocytes. Seventh Int Congress of Pharmacology, Paris, July 1978. Abstract 873.

- JONSSON C E 1971 Smooth muscle stimulating lipids in peripheral lymph after experimental burn injury. *Scand J Plast Reconstr Surg* 5: 1-5
- JONSSON C E & SHIMIZU Y 1979 Cannulation of small lymph vessels using a tissue glue. *Scand J Clin Lab Invest* 39: 283-285
- KU E C, WASVARY J M & CASH W D 1975 Diclofenac sodium (G P 45 840 Voltaren): a potent inhibitor of prostaglandin synthetase. *Biochem Pharmacol* 4: 641-643
- KUEHL, P A Jr, EGAN R W, HUMES L, BEVERIDGE E & VAN ARMAN C G 1977 Evidence for a pivotal role of the endoperoxide PGG_2 in inflammatory processes. In: *Biochemical aspects of prostaglandins and thromboxanes. Intra-science research foundation symposium 1976* (ed N Kharasch and J Fried). Academic Press, New York, 1977
- MONCADA S & VANE J R 1979 The role of prostacyclin in vascular tissue. *Fed Proc* 38: 66-71
- MONCADA S, GRYGLEWSKI R, BUNTING S & VANE J R 1976 An enzyme isolated from arteries transforms prostaglandin endoperoxides to an unstable substance that inhibits platelet aggregation. *Nature* 263: 663-665
- NUGTEREN D H & HAGELHOF E 1973 Isolation and properties of intermediates in prostaglandin biosynthesis. *Biochim Biophys Acta* 326: 448-461
- OLIW E 1979 Prostaglandins and kidney function. An experimental study in the rabbit. *Acta Physiol Scand* 105 (Suppl. 461)
- OLIW E, LUNDÉN I & ANGÅRD E 1978 In vivo inhibition of prostaglandin synthesis in rabbit kidney by non-steroidal anti-inflammatory drugs. *Acta Pharmacol Toxicol* 42: 179-184
- OLIW E, LUNDÉN I, SJÖQUIST B & ÅNGÅRD E 1979 Determination of 6-keto-prostaglandin $\text{F}_{1\alpha}$ in rabbit kidney and urine and its relation to sodium balance. *Acta Physiol Scand* 105: 359-366
- PACE ASCIAK C R 1977 Oxidative biotransformations of arachidonic acid. *Prostaglandins* 13: 811-817
- SAMUELSSON B, FOLCO G, GRANSTRÖM E, KINDAHL H & MALMSTEN C 1978a Prostaglandins and thromboxanes: biochemical and physiological considerations. *Advances Prostaglandin and thromboxane research* vol 4 (ed F Coccani and P M Olley) pp 1-5. Raven Press, New York.
- SAMUELSSON B, GOLDSBYNE M, GRANSTRÖM E, HAMBERG M, HAMMARSTRÖM S & MALMSTEN C 1978b Prostaglandins and thromboxanes. *Ann Rev Biochem* 47: 997-1029
- SPECTOR, W G & WILLOUGHBY D A 1959 Experimental suppression of the acute inflammatory changes following thermal injury. *J Pathol Bacteriol* 78: 121-132
- SVENSSON J & FREDHOLM B B 1977 Vasoconstrictor effect of thromboxane A_2 . *Acta Physiol Scand* 101: 366-368
- TATESON J E, MONCADA S & VANE J R 1977 Effect of prostacyclin (PGX) on cyclic AMP concentration in human platelets. *Prostaglandins* 13: 389-397
- VANE J R 1971 Inhibition of prostaglandin synthesis as a mechanism of action for aspirin-like drugs. *Nature New Biol* 231: 232-235
- VANE, J R 1978. Inhibition of prostaglandin biosynthesis and thromboxane synthesis. In *Advances in prostaglandin and thromboxane research* (ed F Coccani and P M Olley) pp 27-44. Raven Press, New York
- WILLIAMS T J 1979 Prostaglandin E_2 , prostaglandin I and the vascular changes of inflammation. *Br J Pharmacol* 65: 517-524
- WILLIS A L 1970 Identification of prostaglandin E_2 in rat inflammatory exudate. *Pharmacol Res* 2: 397-399

Erroneous estimates of intrarenal blood flow distribution in the dog with radiolabelled microspheres

G. CLAUSEN, A. KIRKEBØ, I. TYSSEBØ, E. S. ØFJORD and K. AUKLAND

Institute of Physiology, University of Bergen, Norway

Since the introduction of the radioisotope labelled microspheres (Ms) for measurement of regional cortical blood flow by McNay & Abe in 1970, the method has been extensively used in dogs under many experimental conditions. However several observations may suggest a skewing of 15 μ m Ms at the offspring of the afferent arterioles from the interlobular arteries, resulting in lower Ms concentration in blood feeding the deep glomeruli than that feeding more superficial glomeruli (Kaltz et al. 1971, Markind et al. 1978, Clausen et al. 1977, 1979). Such skewing would be expected to be more pronounced for 15 than for 10 μ m Ms (Phibbs & Dong 1976, Øfjord, Clausen & Aukland 1979). Failure of Ms to enter deep arterioles in proportion to blood flow due to pore steric restriction seems excluded in this diameter range (Chenutz et al. 1976, Markind et al. 1978). We therefore decided to compare the distribution of 10 and 15 μ m Ms in the dog kidney

prior to and lasting for 60 min after Ms infusion. Sampling of renal venous blood at rate of 1 or 1.4 ml/min started simultaneously and was maintained for 3-5 min. The tylos snares were then tightened simultaneously and the undrained kidneys were excised, weighed and frozen in CO₂-alcohol mixture. Dissection of renal tissue samples were made from a sagittal 5 mm thick frozen slice cut out by saw. 5-10 sections were divided in 3 cortical zones of equal thickness (C₁, C₂ and C₃) whereas the medulla was divided in 2 outer medullary zones (OM₁, OM₂) and inner medulla (IM). The tissue samples weighed between 0.05 and 0.2 g. Radioactivity in arterial and venous blood and in tissue samples was counted in 3-channel well scintillation gamma counter (Searle Analytic Inc. Mod. 1185) for 10 min. Average renal blood flow per gram tissue was calculated from local flow rates and the respective zonal volumes taken to be: C₁ 29%, C₂ 23%, C₃ 18%, OM₁ 12%, OM₂ 8% and IM 10% of total kidney volume. The relationship between the amount of Ms flowing into the kidney and the amount escaping through the renal vein was calculated directly from the arterial and venous sampling rates and blood radioactivities.

Mean arterial blood pressure averaged 125 (105-135) mmHg whereas renal venous pressure ranged from 3 to 9 mmHg. The renal extraction of Ms measured in 5 of the 9 kidneys was practically complete: 99.3 (S.D. 0.5)% and 99.9 (S.D. 0.06)% for 10 and 15 μ m Ms, respectively. As shown in Table 1, 15 μ m Ms gave higher flow in C₁ but lower flow in all deeper zones as compared to 10 μ m Ms. Since calculated total RBF was 6.5 (S.D. 3.5)% higher with 10 μ m Ms, the zonal Ms concentrations in each sector were normalized to those of C₁ in each kidney. This procedure which obviates possible errors due to different isotope counting efficiencies in blood and tissue or to different Ms concentrations in sampled arterial and renal arterial blood, confirmed the disparity of the two intrarenal Ms distribution patterns (Fig. 1). The present results demonstrate beyond doubt that under the experimental conditions used here, 15 μ m Ms are greatly

Mongrel dogs, weighing 14-20 kg, were anesthetized by Nembutal, 25 mg/kg b.wt. In 3 expts (5 kidneys), mid-line abdominal incision was made and venous cannulae placed in the abdominal aorta and inferior vena cava. A polyethylene tube of 10 mm inner diameter cannulae were placed as the closest to the kidney for blood sampling and pressure measurement. In 2 expts (4 kidneys) the kidneys were approached retroperitoneally and catheter inserted into the left renal vein via the spermatic vein for sampling of venous blood. Nylon snares were placed loosely around both renal pedicles. Blood flow in the left renal artery (electromagnetic flow probe) and arterial blood pressure were recorded. A mixture of 10.5 (S.D. 1.2) μ m and 14.9 (S.D. 1.0) μ m microspheres (hereafter referred to as 10 μ m Ms and 15 μ m Ms) labelled with ⁸⁶Sr and ¹⁴¹Ce respectively, sonicated to ensure dispersion, were infused into the left ventricle through catheter inserted via the left common carotid artery. The infused doses gave about 0.5 spheres of each type per glomerulus. Blood sampling at constant rate of 12 ml/min was made from the aorta near the renal arteries through catheter inserted via femoral artery beginning

Table 1 Average onal blood flow and onal percentage of calculated total renal blood flow (RBF) obtained in 9 dog kidneys by microspheres (M_s)

C C_1 C_2 Outer middle and inner cortex OM OM₁ Outer and inner halves of outer medulla IM Inner medulla

Flow	MS	C	C_1	C_2	OM	OM ₁	IM	C + M	RBF
ml/min g									
10 μ m	10.22	5.22	4.15	2.07	0.59	0.17	0.03	0.96	93
15 μ m	5.37	3.65	1.70*	0.4	0.04	0.02*	0.71	74	
% of RBF									
10 μ m	51.7	32.6	12.7	4.4	0.44	0.10	15.6		
15 μ m	56.9*	30.7	11.2*	1.0*	0.15	0.06*	12.4*		

$P < 0.01$ $P < 0.05$ paired *t*-test.

under represented in deep cortex relative to 10 μ m M_s . Since it is very unlikely that 10 μ m M_s should be overrepresented in blood flowing into the deep afferent arterioles as compared to blood in the interlobular arteries. It would appear that blood flow in deep cortex is underestimated and superficial cortical flow is overestimated with 15 μ m M_s . It is of interest that similar results have recently been obtained in experiments on rats (Bankir 1979; Casellas & Mimran 1978; Aperia—personal communication 1979).

The results clearly indicate transglomerular passage of some 10 μ m M_s into the medulla (Table 1). This prompted microscopic investigations as yet preliminary suggesting a postglomerular location of

5 to 30% of the cortical 10 μ m M_s as compared to only a few per cent of the 15 μ m M_s . Calculations indicate that postglomerular interzonal passage of 10 μ m M_s could not possibly account for more than a fraction of the disparate M_s distributions in the renal cortex. We must therefore conclude that a different degree of skimming of 10 and 15 μ m M_s along the interlobular arteries (Fig. 2) is the main cause of the difference in M_s distribution. Thus it seems highly dubious that 15 μ m M_s or 10 μ m M_s reflect true glomerular blood flow distribution in the dog kidney. In view of the large number of studies on intrarenal circulation made by the radiolabelled M_s technique the crucial question is: Do microspheres of 10 or 15 μ m diameter give reasonable

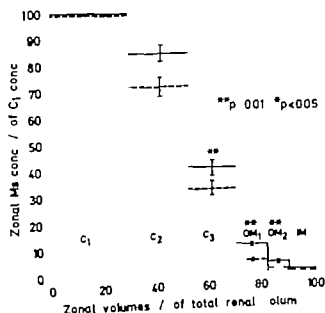


Fig. 1 Relative concentrations of 15 μ m (broken lines) and 10 μ m (solid lines) microspheres (M_s) in 3 cortical zones of equal thickness (C , C_1 , C_2), in outer and inner halves of outer medulla (OM and OM₁) and in inner medulla (IM). Mean \pm S.D. of 9 kidneys.

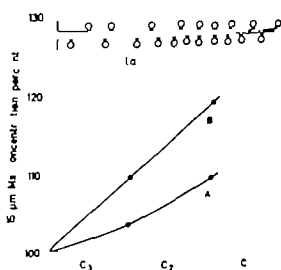


Fig. 2 Estimated concentration of 15 μ m M_s in interlobular arterial (I.I.) blood reaching midcortex (C) and outer cortex (C_1) expressed in per cent of the initial I.I. concentration in inner cortex (C_2). The calculations are made on the assumption that true zonal glomerular flow is obtained by A: 10 μ m M_s or B: 251 I-iodoantipyrine (Clausen et al. 1979).

information on changes in blood flow distribution in the kidney? The results of Mørkrid et al (1978) would suggest that vasodilation produced by lowering the renal perfusion pressure may reduce the staining of $15\text{ }\mu\text{m}$ Ms more than that of $10\text{ }\mu\text{m}$ Ms. This is compatible with results from four preliminary experiments of the present design in dog kidneys during vasodilation by acetylcholine. In conclusion, until more is known about the distribution of Ms under various experimental conditions, it seems at least highly hazardous to estimate regional cortical blood flow with this indicator.

REFERENCES

- BANKIR, L., TAN, M.-M., TRINH TRANG & GRÜN-FELD, J.-P. 1979. Measurement of glomerular blood flow in rabbits and rats. Erroneous findings with $15\text{-}\mu\text{m}$ microspheres. *Kidney International* 15: 126-133.
- CASELLAS, D. & MIMRAN, A. 1978. The influence of microsphere (MS) size on the estimation of intra-renal blood flow distribution (IRBFD) in the rat. *Europ Soc Clin Invest*, Abstract 12th annual meeting, Rotterdam 20-22 April 1978, p. 31.
- CHEWITZ, W. R., NEVINS, B. A. & HOLLENBERG, M. K. 1976. Preglomerular resistance and glomerular perfusion in the rat and dog. *Amer J Physiol* 231: 961-966.
- CLAUSEN G., HOPE, A., KIRKEBO, A., TYS-SEBOTN, I. & AUKLAND, K. 1977. Effect of vasodilation on distribution of microspheres and on zonal blood flow measured with diffusible indicators in the dog kidney. (Abstr.) *Proc Internat Union Physiol Sci* 13: 141.
- CLAUSEN G., HOPE, A., KIRKEBO, A., TYS-SEBOTN, I. & AUKLAND, K. 1979. Distribution of blood flow in the dog kidney. I. Saturation rates for inert diffusible tracers, ^{125}I -iodoantipyrine and treated water: cross uptake of microspheres under control conditions. *Acta Physiol Scand* 107: 69-81.
- KATZ, M. A., BLANTZ, R. C., RECTOR, F. C., J. & SELDIN, D. W. 1971. Measurement of intrarenal blood flow. I. Analysis of microsphere method. *Amer J Physiol* 220: 1903-1913.
- McNAY, J. L. & ABE, Y. 1970. Pressure-dependent heterogeneity of renal cortical blood flow in dogs. *Circulat Res* 27: 571-587.
- MØRKRID, L., ØFSTAD, J. & WILLASSEN, Y. 1978. Diameter of afferent arterioles during autoregulation estimated from microsphere data in the dog kidney. *Circulat Res* 42: 181-191.
- ØFJORD, E. S., CLAUSEN, G. & AUKLAND, K. 1979. Do microspheres measure correct local blood flow in the renal cortex? In vitro experiments. (Abstr.) *Upsala J Med Sci Suppl* 26: 58.
- PHIBBS, R. H. & DONG, L. 1970. Nonuniform distribution of microspheres in blood flowing through medium-size artery. *Can J Physiol Pharmacol* 48: 415-421.

Immunohistochemical evidence for substance P immunoreactive nerve fibres in the taste buds of the cat

JAN M. LUNDBERG, TOMAS HÖKFELT, ANDERS ÅNGGÅRD,
BENGT PERNOW and PIERCE EMSON

Departments of Histology and Pharmacology, Karolinska Institutet, Department of Clinical Physiology,
Karolinska Hospital, Stockholm, Sweden and MRC Neurochemical Pharmacology Unit,
Department of Pharmacology, Cambridge, England

Substance P was discovered by von Euler & Gaddum (1931). Forty years later Chang et al. (1971) isolated and structurally characterized this factor as a decapeptide. Substance P was shown to have a marked regional distribution both in the central nervous system and in peripheral tissues (Pernow 1953) and Lembeck (1953) suggested that it may be a transmitter substance in primary sensory neurons. This view was strongly supported by the elegant biochemical and electrophysiological experiments of Otsuka and colleagues (see Otsuka & Takahashi 1977). Using antibodies raised against this peptide the distribution of immunoreactive substance P was studied with the indirect immunofluorescence technique of Coons and collaborators. Extensive neuronal systems containing substance P-like peptide were found within the brain, spinal cord and periphery (see Hökfelt et al. 1977). One such substance P system is represented by primary sensory neurons with cell bodies in spinal ganglia and central branches in the dorsal horn of the spinal cord and peripheral branches in many peripheral tissues including skin (Hökfelt et al. 1977). A substance P-like peptide has also been demonstrated by immunohistochemistry in some sensory neurons of the nodose ganglion of the vagus system (Lundberg et al. 1978). In the present study further sensory system has been investigated: gustatory nerves in the cat tongue. Evidence is presented that numerous substance P immunoreactive fibres are present in the taste buds.

Four adult cats were perfused with ice-cold 10% formalin for 30 min. The tongue was dissected out and immersed in the same fixative for 90 min. After rinsing in 0.1 M phosphate buffer with 5% sucrose added for at least 4 h, pieces of the tongue including the papillae vallatae were cut on a cryostat and

the sections were incubated with substance P antiserum in a humid atmosphere at 4°C for 18-48 h. After rinsing the sections were incubated with fluorescein isothiocyanate (FITC) conjugated sheep anti-rabbit antibodies for 30 min at 37°C, rinsed, mounted and examined in a Zeiss fluorescence microscope. Substance P antiserum pretreated with an excess of substance P served as control serum.

In frontal sections of the papillae vallatae numerous substance P immunoreactive fibres could be seen within the connective tissue of the papillae (Fig. 1A, B). The highest concentrations of fluorescent fibres were seen in the peripheral parts of the papillae close to the epithelium. The fibres formed small bundles and often penetrated into the epithelium (Fig. 1B). Particularly in the basal part of the papillae numerous taste buds could be observed. In all of these buds substance P immunoreactive fibres could be seen (Fig. 1A, B). Their number as seen in a single section varied and could range from a few fibres up to a dozen ones. They were slightly varicose and were mostly running towards the pore of the taste bud. Only few substance P immunoreactive fibres were seen in regions of the tongue outside the vallate papillae. No such fibres could be seen after incubation with control serum.

The present findings indicate that a substance P-like peptide is present in nerve terminals within the taste buds in the papillae vallatae of cat tongue. The fibres are mostly numerous and seem to be present in all taste buds. They therefore presumably represent the peripheral branches of gustatory nerves. Since the circumvallate papillae mostly are innervated by the glossopharyngeal nerve, it is interesting to note that in the rat and guinea-pig substance P-like immunoreactivity is present in gan-

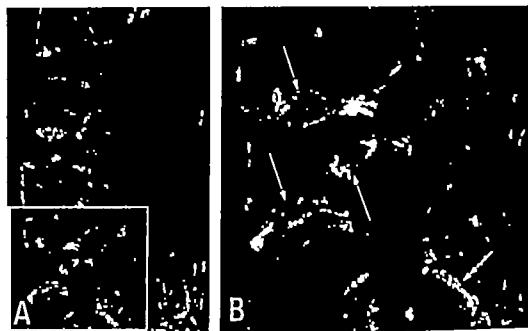


Fig. 1. A, B. Immunofluorescence micrographs of the basal part of a cat vallate papillae after incubation with substance P antiserum. B represents a higher magnification of part of A as indicated by rectangle. Numerous taste buds are seen, all of which contain substance P immunoreactive fibres (arrows). Note bundles of fluorescent fibres (double arrow) also in the connective tissue under the epithelium. Magnifications $\times 130$ (A) and $\times 350$ (B).

gion cells of the petrosal ganglion (Lundberg, unpublished data) as well as in the entire nucleus tractus solitarius (Ljungdahl et al. 1978). The latter brain area and the petrosal ganglion are now studied in the cat with regard to possible occurrence of substance P-like immunoreactivity.

The possible functional role of substance P in presumable gustatory neurons is not known. It has been suggested that substance P may act as a neurotransmitter released in the spinal cord from the central branches of primary sensory neurons (Lembeck 1953; Otsuka & Takahashi 1977) and it may have a similar function in the gustatory neurons. Of special interest is however the occurrence of the peptide in the peripheral branches within the taste buds, since evidence is now accumulating that substance P may exert an action also peripherally. Thus substance P may be the agent released to cause the vasodilation induced by antidromic stimulation (Himsey & Gasser 1931). In fact Olgarth et al. (1977) have shown that substance P can be released by nervous stimulation from presumable peripheral sensory branches in the tooth pulp. Furthermore it has recently been demonstrated that more than 90% of the substance P immunoreactive material produced in sensory ganglia (nodose ganglion) is transported into the

peripheral branches (Bilmyoin et al. 1980). A possible function of substance P in the periphery should therefore be seriously considered.

It is well known that structural integrity of the taste buds is dependent on their sensory innervation (Olmsted 1970). The taste buds disappear after transection of the gustatory nerves but reappear when reinnervated by gustatory nerve fibres (Guth 1958). The differentiation of the taste buds is under the influence of a neurotrophic substance (Torrey 1934). Also non-gustatory nerves can cause re-appearance of taste buds (Pontsky & Singer 1963). Transplantation experiments to the anterior eye chamber have shown that different types of sensory ganglia can induce taste bud formation (Zalewski 1974) and that even in vallate papillae grafted alone to the anterior eye chamber reformation of taste buds can occur (Gómez Ramo et al. 1979). It is interesting to note that sensory branches of substance P neurons are available in all models discussed above: in pinial sensory ganglia (Hokfelt et al. 1977), in the nodose ganglion (Lundberg et al. 1978) and as free nerve endings in the iris (Hokfelt et al. 1977). Could it be that substance P or a factor present in the same neuron represent the neurotrophic factor responsible for the structural integrity of taste bud? Further functions should however

be considered. Thus, substance P could e.g. modulate the threshold of excitability of its own nerve ending or of the taste cells.

In conclusion, the present and earlier findings suggest that a substance P-like peptide is present in several types of sensory systems and may be involved in different sensory modalities such as pain, visceral sensation and taste.

The present study was supported by grants from the Swedish Medical Research Council (04X-587, 04X-1495), Magnus Bergvalls Stiftelse and Kung och Alice Wallenberg Stiftelse.

We thank Professor Yngve Zotterman for many valuable suggestions and discussions on topics related to taste and sensory mechanisms.

We are grateful to to Mrs W. Hiort and Miss U. Lindstedt for skilful technical assistance and Mrs Birgit Frickson for excellent secretarial help.

REFERENCES

- BRINJOLIN S, LUNDBERG J M, BRODIN E & HÖKFELT T 1980. Axonal transport of substance P in the vagus and sciatic nerves of the guinea-pig. *Brain Res.* In press.
- CHANG, M M, LEEMAN S E & NIALL, H D 1971. Amino acid sequence of substance P. *Nature (New Biol)* 232: 86-87.
- EULER, U S von & GADDUM J H 1931. An unidentified depressor substance in certain tissue extracts. *J Physiol (Lond)* 72: 74-87.
- GÓMEZ RAMOS, P, LEON-FELIU E & RODRÍGUEZ ECHANDÍA, E L 1979. Taste buds in valve pupillae grafted to the anterior eye chamber of the eye. *Anat Embryol* 156: 217-224.
- GUTH, L 1938. Taste buds on the cat circumvallate papilla after reinnervation by glossopharyngeal vagus and hypoglossal nerves. *Anat Rec* 130: 25-37.
- HINSEY J C & GASSER, H S 1930. The component of the dorsal root mediating vasodilation and the Sherrington contraction. *Am J Physiol* 9: 679-689.
- HÖKFELT T, JOHANSSON O, KELLERTH J-O, LJUNGDAHL, Å, NILSSON G, NYGÅRDS A. & PERNOW B 1977. Immunohistochemical distribution of substance P. In: Substance P. Nobel Symposium 37 (ed U S. von Euler & B Pernow), pp. 117-145. Raven Press, New York.
- LENBECK, F 1953. Zur Frage der zentralen Übertragung afferenter Impulse. III. Mitteilung. Das Vorkommen und die Bedeutung der Substanz P in den dorsalen Wurzeln des Rückenmarks. *Naunyn-Schönbeinbergs Arch Pharmacol* 219: 197-13.
- LJUNGDAHL, Å, HÖKFELT T & NILSSON O 1978. Distribution of substance P-like immunoreactivity in the central nervous system of the rat. I. Cell bodies and nerve terminals. *Neuroscience* 3: 861-943.
- LUNDBERG J M, HÖKFELT T, NILSSON G, TERENIUS, L, REHFELD, J, ELDE, R. & SAID S 1978. Peptide neurons in the vagus splanchnic and sciatic nerves. *Acta Physiol Scand* 104: 499-501.
- OLGARTH L, GAZELIUS, B, BRODIN E. & NILSSON G 1977. Release of substance P-like immunoreactivity from the dental pulp. *Acta Physiol Scand* 101: 510-512.
- OLMSTED J M D 1920. The results of cutting the seventh cranial nerve in *Amblystoma Nebulosum*. *J Exp Zool* 31: 369-403.
- OTSUKA, M & TAKAHASHI, T 1977. Putative peptide neurotransmitters. *Ann Rev Pharmacol Toxicol* 17: 425-439.
- PERNOW B 1953. Studies on substance P. Purification, occurrence and biological actions. *Acta Physiol Scand* 105 Suppl. 79: 1-60.
- PORITSKY R L & SINGER, M 1963. The fate of taste buds in tongue transplants to the orbit in the neotoma *Triturus*. *J Exp Zool* 153: 211-218.
- TORREY W T 1934. The relation of taste buds to their nerve fibres. *J Comp Neurol* 59: 203-220.
- ZALEWSKI A A 1974. Regeneration of taste buds in tongue grafts after reinnervation by neurons in transplanted lumbar sensory ganglia. *Exp Neurol* 40: 161-169.

Evidence for a dopaminergic pathway in the rat descending from the A11 cell group to the spinal cord

TOMAS HÖKFELT, OLIVER PHILLIPSON and MENEK GOLDSTEIN

Department of Histology, Karolinska Institute, Stockholm, Sweden and Department of Psychiatry, New York University Medical Center, New York, USA

It was suggested several years ago by Magnusson (1973) that part of the dopamine in the spinal cord serves an independent, non-precursor role. The existence of dopamine nerve fibers within the spinal cord has further been corroborated by the studies of Comessou et al (1978, 1979) on the basis of biochemical experiments as well as of lesion studies. Very recently Blessing & Chalmers (1979) have demonstrated that in the rabbit hypothalamic catecholamine neurons of the A13 cell group of Fuxe (1965) project to the thoracic part of the spinal cord. Their evidence rests on a technique combining retrograde peroxidase tracing with catecholamine histochemistry. In the present preliminary paper we report with a similar combination of retrograde tracing and transmitter immunohistochemistry the projection of dopaminergic A11 cells to the spinal cord of the rat.

Male specific pathogen-free Sprague-Dawley rats were used (b.w. 150 g). The fluorescent dye primuline (Kuyper et al. 1977) dissolved in distilled water (10% w/v) was injected into the spinal cord at the lower thoracic and upper lumbar level (two bilateral injections of each 1 µl were made). After 4-10 days the rats were perfused with ice-cold formalin, and the brain and spinal cord were dissected out and immersed in the same fixative for 90 min. After rinsing in 0.1 M phosphate buffer containing 5% sucrose for at least 4 h frontal sections of the hypothalamus and the rostral mesencephalon were cut on a cryostat (section thickness 15 µm). The sections were mounted in a mixture of glycerol and phosphate buffer (3:1) and examined in a fluorescence microscope. Cells containing clear yellow fluorescent granules were photographed. The cover slip was then removed and the sections were processed for the indirect immunofluorescence technique of Coons and collaborators (see Coons 1958). Briefly the sections were incubated with an-

tiserum to tyrosine hydroxylase diluted 1:100, rinsed, incubated with fluorescein isothiocyanate (FITC) (SBL, Stockholm, Sweden) conjugated sheep anti-rabbit antibodies, rinsed, mounted in a mixture of glycerol and phosphate buffer (3:1) and examined again in the fluorescence microscope. Cells containing both the yellow fluorescent granules and tyrosine hydroxylase-like immunoreactivity were photographed again. The technique described above is based on studies on retrogradely transported fluorescent dyes carried out by Kuyper and collaborators (Kuyper et al. 1977) and has been described in detail previously (Hökfelt et al. 1979b,c). The enzyme tyrosine hydroxylase is a marker for catecholamine neurons in general. To differentiate between dopamine and noradrenaline neurons, adjacent sections were processed with antiserum against dopamine-β-hydroxylase, a marker for noradrenaline (and adrenaline) neurons. Normal rabbit serum was used as control serum.

After injection of primuline into the spinal cord numerous intensely yellow fluorescent granules were found in cells in many areas of the hypothalamus (e.g. the paraventricular nucleus) and the mesencephalon (e.g. the nucleus ruber). Of particular interest was a group of cells in the paraventricular area at the border between the mesencephalon and the hypothalamus. These cells were located in the grey matter around the third ventricle medial to the fasciculus retroflexus (Fig. 1A) and their fluorescent granules were present in the perinuclear cytoplasm but extended often also into the cell processes (Fig. 1A). After incubation with tyrosine hydroxylase antiserum, but not after incubation with dopamine-β-hydroxylase antiserum, numerous cells in the same area exhibited the characteristic green fluorescence induced by FITC (Fig. 1B). The cells were often multipolar



The present study was supported by grants from the Swedish Medical Research Council (04X 2887), Magnus Bergström Stiftelse and Konrad and Alice Wallenberg's Stiftelse.

We thank Mrs W Haert, Miss U Lindefeldt and Miss G Norrby for skilful technical assistance and Mrs Birgit Färdier for excellent secretarial help.

REFERENCES

- BLESSING W W & CHALMERS J P 1979 Direct projection of catecholamine (presumably dopamine)-containing neurones from hypothalamus to spinal cord. *Neurosci Lett* 9: 35-40.
- COMMISSONO J W, GALLI C. L. & NEFF N O 1978 Differentiation of dopaminergic and noradrenergic neurones in rat spinal cord. *J Neurochem* 30: 1095-1099.
- COMMISSONO J W, GENTLEMAN S & NEFF N O 1979 Spinal cord dopaminergic neurones: evidence for an increased nigrospinal pathway. *Neuropharmacol* 18: 565-568.
- COONS, A. H. 1958. Fluorescent antibody methods. In *General cytochemical methods* (ed J F Danielli), pp. 399-422. Academic Press, New York.
- DAHLSTRÖM A. & FUXE, K. 1964 Evidence for the existence of monoamine containing neurones in the central nervous system. I. Demonstration of monoamines in the cell bodies of brain stem neurones. *Acta Physiol Scand* 62, Suppl. 232: 1-55.
- FUXE, K. 1965 Evidence for the existence of monoamine neurones in the central nervous system. IV. Distribution of monoamine nerve terminals in the central nervous system. *Acta Physiol Scand* 64, Suppl. 247: 37-45.
- HÖKFELT T., FUXE, K. GOLDSTEIN M JOHANSSON O LJUNGDAHL Å. LUNDBERG J & SCHULTZBERG M 1979 Immunocytochemical studies on catecholamine cell systems with aspects on relations to putative peptide transmitters. In: *Catecholamines. Basic and clinical frontiers* (ed. E. Usdin & J. Koppe & J. Barchas), pp. 1007-1019. Pergamon Press, New York.
- HÖKFELT T. KUYPERS, H. G. J. M. BENTIVOGLIO M., CATSMAN-BERREVOETS, C. E., VAN DER KOOY D. DANN O PHILLIPSON O GOLDSTEIN M. STEINBUSCH H., VERHOFFSTAD A. & NILSSON O 1979 A combined method for transmitter histochemical identification of retrogradely traced neurones. Studies on the nigrostriatal dopamine system and on descending spinal systems using antisera to catecholamine synthesizing enzymes, serotonin and substance P. *J Neurosci Methods*, to be submitted.
- HÖKFELT T. PHILLIPSON O KUYPERS, H. G. J. M. BENTIVOGLIO M. CATSMAN-BERREVOETS, C. E. & DANN O 1979 Tracing of transmitter histochemically identified neuron projections. Immunocytochemistry combined with fluorescent retrograde labelling. *Neurosci Lett, Suppl.* 3: 342.
- KUYPERS, H. G. J. M. CATSMAN-BERREVOETS, C. E. & PADT R. E. 1977 Retrograde axonal transport of fluorescent substances in the rat forebrain. *Neurosci Lett* 6: 177-183.
- MAGNUSSON T. 1973 Effect of chronic transection on dopamine, noradrenaline and 5-hydroxytryptamine in the rat spinal cord. *Narabay-Schmedeberg Arch Pharmacol* 77: 13-22.
- SWANSON L. W. & HARTMAN B 1975 The central adrenergic system. An immunofluorescence study on the location of cell bodies and their efferent connections in the rat utilizing dopamine- β -hydroxylase as marker. *J Comp Neurol* 163: 467-505.

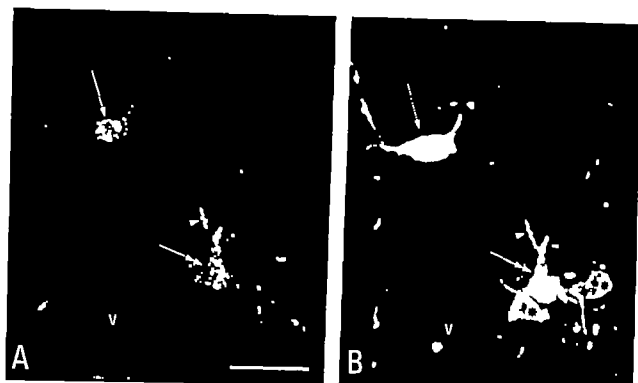


Fig. 1 A, B. Fluorescence micrographs of the periventricular grey at the border between mesencephalon and hypothalamus after injection of primuline into the spinal cord (A) and after incubation of the same section with tyrosine hydroxylase antiserum. Two cell bodies (arrows) contain both primuline (fluorescent granules in A) and tyrosine hydroxylase (B). The granules are mostly obscured by the immunofluorescence in B, but they can be seen in the process indicated by arrow heads. Two cells (asterisk) are only tyrosine hydroxylase immunoreactive. V indicates a blood vessel. Bar indicates 50 μ m.

with a size of about 30–40 μ m and their localization corresponded well to that of the so-called A11 catecholamine group described by Dahlström & Fuxe (1964). Several of these cells also contained the yellow fluorescent granules, which easily could be distinguished from the clear green FITC induced immunofluorescence, particularly after prolonged exposure to UV light, which induced a fading of the immunofluorescence. No yellow fluorescent granules could be observed in tyrosine hydroxylase immunoreactive cells located more rostrally in the zona incerta belonging to the A13 cell group (Fuxe 1965). No dopamine β -hydroxylase immunoreactive cell bodies were observed in the adjacent sections and no fluorescent cells were seen after incubation with control serum.

The present findings give evidence for a direct descending projection to the spinal cord from periventricular cells localized at the level of the posterior hypothalamus and the rostral mesencephalon and thus confirms the existence of a hypothalamo-spinal catecholamine system first described by Blessing & Chalmers (1979). The

dopaminergic nature of these cells is indicated by their content of the enzyme tyrosine hydroxylase, but the apparent lack of the noradrenaline synthesizing enzyme dopamine β -hydroxylase is in agreement with previous immunohistochemical studies (Swanson & Hartman 1974; Hökfelt et al. 1979a).

The pathway described by Blessing & Chalmers (1979) originates in the A13 cell group, i.e. in the zona incerta rostral to the A11 group. This discrepancy may be due to the fact that different species, rat and rabbit, have been studied. Furthermore, more extensive studies in our laboratory may be necessary to establish an additional projection also from the A13 group. Commissiong et al. (1979) have shown a decrease of dopamine in the spinal cord after lesion of substantia nigra. Thus, there may exist several descending dopaminergic projections to the spinal cord. On the other hand, it must be clarified whether or not the lesions made by Commissiong et al. (1979) possibly could interfere with the descending projection from the more rostrally located A11 dopamine cells.

The present study was supported by grants from the Swedish Medical Research Council (04X 2187), Magnus Bergvalls Stiftelse and Kurt och Alice Wallenbergs Stiftelse.

We thank Mrs W. Huot, Miss U. Lindefeldt and Miss G. Kozl for skilful technical assistance and Mrs Birgit Peters for excellent secretarial help.

REFERENCES

- BLESSING, W. W. & CHALMERS, J. P. 1979. Direct projection of catecholamine (presumably dopamine)-containing neurons from hypothalamus to spinal cord. *Neurosci Lett* 9: 35-40.
- COMMISSIONO, J. W., GALLI, C. L. & NEFF, N. G. 1974. Differentiation of dopaminergic and noradrenergic neurons in rat spinal cord. *J Neurochem* 30: 1095-1099.
- COMMISSIONO, J. W., GENTLEMAN, S. & NEFF, N. G. 1979. Spinal cord dopaminergic neurons: evidence for an increased nigrospinal pathway. *Neuropharmacol* 18: 965-968.
- COONS, A. H. 1958. Fluorescent antibody methods. In: *General cytochemical methods* (ed. J. F. Danielli), pp. 369-422. Academic Press, New York.
- DARLSTRÖM, A. & FUXE, K. 1964. Evidence for the existence of monoamine containing neurons in the central nervous system. I. Demonstration of monoamines in the cell bodies of brain stem neurons. *Acta Physiol Scand* 62, Suppl. 332: 1-55.
- FUXE, K. 1965. Evidence for the existence of monoamine neurons in the central nervous system. IV. Distribution of monoamine nerve terminals in the central nervous system. *Acta Physiol Scand* 64, Suppl. 347: 37-85.
- HÖKFELT, T., FUXE, K., GOLDSTEIN, M., JOHANSSON, O., LJUNGDAHL, Å., LUNDBERG, J. & SCHULTZBERG, M. 1979a. Immunocytochemical studies on catecholamine cell systems with aspects on relations to putative peptide transmitters. In: *Catecholamines: Basic and clinical frontiers* (ed. E. Usdin, L. J. Kopin & J. Barchas), pp. 1007-1019. Pergamon Press, New York.
- HÖKFELT, T., KUYPERS, H. G. J. M., BENTIVOGLIO, M., CATSMAN-BERREVOETS, C. E., VAN DER KOOP, D., DANN, O., PHILLIPSON, O., GOLDSTEIN, M., STEINBUSCH, H., VERHOFFSTAD, A. & NILSSON, G. 1979b. A combined method for transmitter histochemical identification of retrogradely traced neurons. Studies on the nigrostriatal dopamine system and on descending spinal systems using antisera to catecholamine synthesizing enzymes, serotonin and substance P. *J Neurosci Methods*, to be submitted.
- HÖKFELT, T., PHILLIPSON, O., KUYPERS, H. G. J. M., BENTIVOGLIO, M., CATSMAN-BERREVOETS, C. E. & DANN, O. 1979c. Tracing of transmitter histochemically identified neuron projections. Immunohistochemistry combined with fluorescent retrograde labelling. *Neurosci Lett*, Suppl. 3: 34.
- KUYPERS, H. G. J. M., CATSMAN-BERREVOETS, C. E. & PADT, R. E. 1977. Retrograde axonal transport of fluorescent substances in the rat forebrain. *Neurosci Lett* 6: 127-135.
- MAGNUSSON, T. 1973. Effect of chronic transection on dopamine, noradrenaline and 5-hydroxytryptamine in the rat spinal cord. *Naunyn-Schmiedeberg Arch Pharmacol* 278: 13-22.
- SWANSON, L. W. & HARTMAN, B. 1975. The central adrenergic system. An immunofluorescence study on the location of cell bodies and their efferent connections in the rat utilizing dopamine- β -hydroxylase as marker. *J Comp Neurol* 163: 467-505.

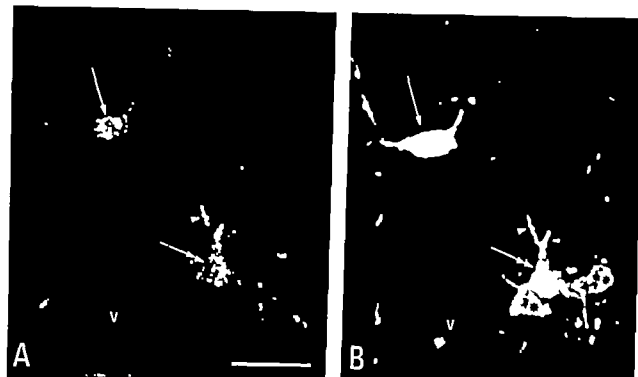


Fig. 1. A, B. Fluorescence micrographs of the periventricular grey at the border between mesencephalon and hypothalamus after injection of primuline into the spinal cord (A) and after incubation of the same section with tyrosine hydroxylase antiserum. Two cell bodies (arrows) contain both primuline (fluorescent granules in A) and tyrosine hydroxylase (B). The granules are mostly obscured by the immunofluorescence in B, but they can be seen in the process indicated by arrow heads. Two cells (asterisk) are only tyrosine hydroxylase immunoreactive. v indicates blood vessel. Bar indicates 50 μ m.

with a size of about 30–40 μ m and their localization corresponded well to that of the so-called A11 catecholamine group described by Dahlström & Fuxe (1964). Several of these cells also contained the yellow fluorescent granules which easily could be distinguished from the clear green FITC induced immunofluorescence, particularly after prolonged exposure to UV light which induced a fading of the immunofluorescence. No yellow fluorescent granules could be observed in tyrosine hydroxylase immunoreactive cells located more rostrally in the zona incerta belonging to the A13 cell group (Fuxe 1965). No dopamine β -hydroxylase immunoreactive cell bodies were observed in the adjacent sections and no fluorescent cells were seen after incubation with control serum.

The present findings give evidence for a direct descending projection to the spinal cord from periventricular cells localized at the level of the posterior hypothalamus and the rostral mesencephalon and thus confirms the existence of a hypothalamo-spinal catecholamine system first described by Blessing & Chalmers (1979). The

dopaminergic nature of these cells is indicated by their content of the enzyme tyrosine hydroxylase but the apparent lack of the noradrenaline synthesizing enzyme dopamine- β -hydroxylase is in agreement with previous immunohistochemical studies (Swanson & Hartman 1975; Hökfelt et al. 1979a).

The pathway described by Blessing & Chalmers (1979) originates in the A13 cell group, i.e. in the zona incerta rostral to the A11 group. This discrepancy may be due to the fact that different species, rat and rabbit, have been studied. Furthermore, more extensive studies in our laboratory may be necessary to establish an additional projection also from the A13 group. Commissiong et al. (1979) have shown a decrease of dopamine in the spinal cord after lesion of substantia nigra. Thus, there may exist several descending dopaminergic projections to the spinal cord. On the other hand, it must be clarified whether or not the lesions made by Commissiong et al. (1979) possibly could interfere with the descending projection from the more rostrally located A11 dopamine cells.

Evidence for a selective reduction of adrenaline turnover in the dorsal midline area of the caudal medulla oblongata of young spontaneous hypertensive rats

KJELL FUXE, DETLEV GANTEN, GÖSTA JONSSON, PER BOLME, LUIGI F. AGNATI, KURT ANDERSSON, MENEK GOLDSTEIN and TOMAS HÖKFELT

Department of Histology, Karolinska Institute, Stockholm, Department of Pediatrics, Huddinge Hospital, Stockholm, Sweden, Department of Human Physiology, University of Bologna, Bologna, Italy, Department of Biochemistry, New York University Medical Center, New York, USA and Department of Pharmacology, University of Heidelberg, Heidelberg, Germany

The adrenaline pathways innervate the cardiovascular areas of the brain (Hökfelt et al. 1973) and it has been proposed that the adrenaline neurons represent important central vasodepressor systems (Fuxe et al. 1975). Increases in PNMT activity and changes in adrenaline levels have been observed in young and adult spontaneous hypertensive animals (Savvedra et al. 1976, Sauter et al. 1977, Wijnen et al. 1978, Savvedra 1979). Recently it has been found that adrenaline turnover is reduced in the cardiovascular areas of the medulla oblongata in adult spontaneous hypertensive animals (Fuxe et al. 1979). Therefore in the present study adrenaline turnover has also been analyzed in young spontaneous hypertensive animals to evaluate if the reduction of adrenaline turnover is primary or secondary to the hypertensive process.

before killing) (Corrodi et al. 1970, Pendleton et al. 1976). The hypothalamus and the DCMO were punched out from frozen coronal sections of the diencephalon and the medulla oblongata respectively. DCMO contains later also the nuc. tractus solitarius, nuc. dorsalis motorius, nervi vagi and parts of the nuc. cuneus, nuc. cuneus, nuc. cuneus (see Fuxe et al. 1979). The catecholamine levels were determined by means of high pressure liquid chromatography in combination with electro-chemical detection, using *o*-methyl dopamine as an internal standard (Keller et al. 1976).

The arterial blood pressure in the young sp-SH rats was 117 ± 3.2 (n=13) mmHg and in the normotensive WKy rats 96.5 ± 1 (n=13) mmHg. This difference was significant ($P < 0.01$, Student's *t*-test for unpaired data).

As seen in Table 1 the hypothalamic dopamine and noradrenaline levels were significantly reduced and increased respectively in the 4-week old spontaneous hypertensive rats, and there was also a trend for an increase of the adrenaline stores in the hypothalamus. The dopamine, noradrenaline and adrenaline levels in the DCMO were however not changed in the sp-SH rats compared with normotensive WKy rats. In Table 1 it is demonstrated that a marked reduction of the FLA 63 and SK&F 64139 induced adrenaline disappearance occurs in the DCMO of 4-week old sp-SH rats compared with normotensive WKy controls. The disappearance of adrenaline stores in the hypothalamus following amine synthesis inhibition is not changed in sp-SH rats versus WKy rats. Furthermore the FLA 63 induced noradrenaline disappearance in the hypothalamus and the DCMO is not significantly different in the sp-SH rats versus the WKy controls.

Female, 4-week old SH rats of the stroke prone strain (sp-SH) are compared with normotensive Wistar Kyoto (WKy) control rats (Okamoto et al. 1974), which were originally derived from the Wistar Kyoto strain (Okamoto 1972) and bred for 4 years at the department of Pharmacology, University of Heidelberg. Tail cuff plethysmography was used to measure systolic arterial blood pressure. The rats were given food pellets and water ad libitum and were kept on regular day and night schedule (lights on at 6 a.m. and off at 6 p.m.). They were killed by decapitation between 9 and 12 a.m. Adrenaline turnover in the hypothalamus and in the dorsal midline area of the caudal medulla oblongata (DCMO) were measured by measuring the disappearance of the adrenaline stores using inhibitors of dopamine- β -hydroxylase (FLA 63 (bis-(1-methyl-1-*h*-isopropenyl)-thiocarbonyl)-disulphide, 10 mg/kg, *p* 2 h before killing) and of phenylethanolamine-N-methyltransferase, SK&F 64139 (7,8-dichloro-1,2,4-triazolo-4,5-dihydroquinoline hydrochloride 40 mg/kg, *p* 2 h

aneous hypertension but appear to increase their contents of adrenaline in agreement with previous work (Gianutsos & Moore 1978; Wjnen et al. 1978). It is likely that the differential regulation of medulla oblongata and hypothalamic adrenaline terminals is due to the fact that adrenaline terminals in the hypothalamus not only subserve cardiovascular functions but also neuroendocrine and behavioural functions (Hökfelt et al. 1973; Wjnen et al. 1978). Furthermore, the present findings do not support the view that the noradrenaline systems within the hypothalamus and the DCMO play a major role in the development of spontaneous hypertension. It seems possible that the increase of hypothalamic noradrenaline levels found in the sp-SH rats could be secondary to the marked reduction of adrenaline activity in the brain stem, especially since treatment with SK&F 64139 increased the noradrenaline levels in the normotensive Wky animals alone. The mechanism for the reduction in hypothalamic dopamine levels in young sp-SH rats remains to be elucidated. In conclusion the present results indicate that adrenaline turnover is markedly reduced in the DCMO of young female sp-SH rats versus Wky control rats which may lead to reduced activity in the central baroreceptor reflex pathway and thus contribute to the development of the hypertension.

This work was supported by grant (04X-4426) from the Swedish Medical Research Council and by grant from Magnus Bergvall Stiftelse.

REFERENCES

- CORDOGI, H., FUXE, K., HANBERGER, B. & LUNDGAHL, Å. 1970 Studies on central and peripheral noradrenaline neurons using a new dopamine- β -hydroxylase inhibitor. *Europ J Pharmacol* 12, 143-155.
- FUXE, K., GANTEN, D., JONSSON, G., AGNATI, L., F. BOLME, P., ANDERSSON, K., GOLDSTEIN, M., HALLMAN, H., UNGER, T. & RASCHER, W. 1979a. Catecholamine turnover changes in hypo-
- thalamus and dorsal midline area of the caudal medulla oblongata of spontaneously hypertensive rats. *Neurosci Lett*, in press.
- FU
- graph of central catecholamine pathway in relation to their possible role in blood pressure control. In: *Central action of drugs in blood pressure regulation* (ed. D. S. Davies & J. S. Read), pp. 8-22. Pitman Medical, London.
- GIANUTSOS, G. & MOORE, A. E. 1978. Epinephrine contents of sympathetic ganglia and brain regions of spontaneously hypertensive rats of different ages. *Proceedings of the Society for Experimental Biology and Medicine* 158, 45-49.
- HÖKFELT, T., FUXE, K., GOLDSTEIN, M. & JOHANSSON, O. 1973. Evidence for adrenergic neurons in the rat brain. *Acta Physiol Scand* 89, 266-288.
- KELLER, R., OKE, A., MIDFORD, I. & ADAMS, R. M. 1976. Liquid chromatographic analysis of catecholamines-oxidase assay for regional brain mapping. *Lif Sci* 19, 993-1004.
- OKAMOTO, K. 1972. Spontaneous hypertension, its pathogenesis and complications. Igaku Shoin Ltd, Tokyo.
- OKAMOTO, K., YAMORI, Y. & NAGAOKA, A. 1974. Establishment of the stroke-prone spontaneously hypertensive rat (SHR). *Circ Res* 34(Suppl 1), 143-153.
- PENDLETON, R. G., KAISER, C. & GESSNER, G. 1976. Studies on adrenal phenylethanolamine N-methyltransferase (PNMT) with SK&F 64139 selective inhibitor. *J Pharmacol Exp Ther* 197, 623-632.
- SAAVEDRA, J. M. 1979. Adrenaline levels in brain stem nuclei and effects of PNMT inhibitor on spontaneously hypertensive rats. *Brain Res* 166, 283-292.
- SAAVEDRA, J. M., GROBECKER, H. & AXELROD, J. 1976. Adrenaline forming enzymes in the brain stem: elevation in genetic and experimental hypertension. *Science* 191, 483-484.
- SAUTER, A., LEW, J. J., MATSUMOTO, J. & GOLDSTEIN, M. 1977. PNMT and epinephrine levels in the CNS of spontaneous hypertensive rats. *Trans Amer Soc Neurochem* 8, Abstr 65, 96.
- WJNEN, H., PALKOVITS, M., DE JONG, W. & VERSTEEG, D. 1978. Elevated adrenaline content in nuclei of the medulla oblongata and the hypothalamus during the development of spontaneous hypertension. *Brain Res* 157, 191-195.

Table 1 Catecholamine levels in the hypothalamus and the dorsal part of the caudal medulla oblongata (DCMO) of young sp-SH and Wky rats

Means \pm S.E. are shown. n = number of animals. The values are given as ng/g wet weight. The statistical comparisons have been made between the corresponding values in the Wky and sp-SH rats using Student's t -test for unpaired data. NS = not significant.

	Hypothalamus			DCMO		
	Wky		sp-SH n	Wky		sp-SH n
DA	573 \pm 34	$P < 0.05$	464 \pm 70	707 \pm 48	NS	191 \pm 1
NA	1858 \pm 91	$P < 0.025$	2146 \pm 60	2107 \pm 63	NS	1628 \pm 260
A	58 \pm 5	$P = 0.1$	75 \pm 8	48 \pm 9	NS	50 \pm 10

Table 2 Per cent depletion of NA and A stores in hypothalamus and DCMO of young sp-SH and Wky rats following treatment with FLA 63 and SK & F 64139

The CA levels are given in per cent of the CA levels of untreated Wky and sp-SH rats respectively (for absolute levels, see Table 1). Means \pm S.E. n = number of rats. Student's t test. For further details see Table 1 and text.

Treatment	CA	CA levels in % Wky	Statistical significance Wky vs. sp-SH	CA levels in % sp-SH	n
<i>Hypothalamus</i>					
No drug treatment	DA	100 \pm 6		100 \pm 4	7-9
FLA 63	DA	134 \pm 7	$P < 0.05$	178 \pm 13	8
SK & F 64139	DA	119 \pm 5	NS	113 \pm 7	8
No drug treatment	NA	100 \pm 5		100 \pm 5	7-9
FLA 63	NA	69 \pm 6	NS	57 \pm 3	8
SK & F 64139	NA	116 \pm 6	$P < 0.05$	100 \pm 7	8
No drug treatment	A	100 \pm 9		100 \pm 8	7-8
FLA 63	A	75 \pm 1	NS	56 \pm 4	8
SK & F 64139	A	66 \pm 3	NS	61 \pm 11	7
<i>DCMO</i>					
No drug treatment	DA	100 \pm 14		100 \pm 11	5-7
FLA 63	DA	704 \pm 27	NS	164 \pm 70	5-7
SK & F 64139	DA	11 \pm 2	NS	170 \pm 10	6-8
No drug treatment	NA	100 \pm 13		100 \pm 16	5-7
FLA 63	NA	50 \pm 4	NS	77 \pm 9	5-7
SK & F 64139	NA	100 \pm 5	NS	108 \pm 9	6
No drug treatment	A	100 \pm 19		100 \pm 0	5-7
FLA 63	A	31 \pm 4	$P < 0.001$	86 \pm 8	5-7
SK & F 64139	A	39 \pm 6	$P < 0.001$	100 \pm 8	5-8

However, treatment with SK & F 64139 results in an increase of the hypothalamic noradrenaline stores of the Wky control rats, an effect which is not observed in the sp-SH rats.

The present paper gives evidence for a marked reduction of adrenaline turnover in the DCMO of young female spontaneous hypertensive rats compared with appropriate normotensive Wky controls at a time when the increase in the arterial blood pressure begins to develop in the sp-SH rats. These results support the hypothesis that adrenaline nerve

terminals in the cardiovascular areas of the medulla oblongata represent an important vasodepressor mechanism (Fixe et al 1979) which can be pathologically disturbed in animals which will develop spontaneous hypertension. It seems possible that such a disturbance can be one of the factors producing spontaneous hypertension. The hypothalamic adrenaline nerve terminals seem to be independently controlled from the DCMO adrenaline terminals. Thus they do not change their turnover in relation to the development of sponte-

scious hypertension but appear to increase their contents of adrenaline in agreement with previous work (Gianutsos & Moore 1978; Wijnen et al. 1978). It is likely that the differential regulation of medulla oblongata and hypothalamic adrenaline terminals is due to the fact that adrenaline terminals in the hypothalamus not only subserve cardiovascular functions but also neuroendocrine and behavioural functions (Hökfelt et al. 1973; Wijnen et al. 1978). Furthermore, the present findings do not support the view that the noradrenaline systems within the hypothalamus and the DCMO play a major role in the development of spontaneous hypertension. It seems possible that the increase of hypothalamic noradrenaline levels found in the sp-SH rats could be secondary to the marked reduction of adrenaline activity in the brain stem, especially since treatment with SK&F 64139 increased the noradrenaline levels in the normotensive WKy animals alone. The mechanism for the reduction in hypothalamic dopamine levels in young sp-SH rats remains to be elucidated. In conclusion, the present results indicate that adrenaline turnover is markedly reduced in the DCMO of young female p-SH rats versus WKy control rats, which may lead to reduced activity in the central baroreceptor reflex pathway and thus contribute to the development of the hypertension.

This work was supported by grant (04X-4626) from the Swedish Medical Research Council and by grant from Nopan Bergvall, Södertälje.

REFERENCES

- COLLODI, H., FUXE, K., HAMBERGER, B. & LJUNGDAHL, Å. 1970 Studies on central and peripheral noradrenaline neurons using a new fluorescent- β -hydroxyamine inhibitor. *Europ. J. Pharmacol.* **12**, 145-155.
- FUXE, K., GANTEN, D., JONSSON, O., AGNATI, L., F. BOLME, P., ANDERSSON, G., GOLDSTEIN, M., HALLMAN, H., UNGER, T. & RASCHER, W. 1979 Catecholamine turnover changes in hypothalamus and dorsal midline area of the caudal medulla oblongata of spontaneously hypertensive rats. *Neurosci. Lett.*, in press.
- FUXE, K., HÖKFELT, T., BOLME, P., GOLDSTEIN, M., JOHANSSON, O., JONSSON, G., LIDBRINK, P., LJUNGDAHL, Å. & SACHS, C. 1973 The topography of central catecholamine pathways in relation to their possible role in blood pressure control. In: *Central action of drugs in blood pressure regulation* (ed. D. S. Davies & J. S. Reid), pp. 8-22. Pitman Medical, London.
- GIANUTSOS, G. & MOORE, K. E. 1978. Epinephrine contents of sympathetic ganglia and brain regions of spontaneously hypertensive rats of different ages. *Proceedings of the Society for Experimental Biology and Medicine* **158**, 45-49.
- HÖKFELT, T., FUXE, K., GOLDSTEIN, M. & JOHANSSON, O. 1973 Evidence for adrenaline neurons in the rat brain. *Acta Physiol. Scand.* **89**, 286-288.
- KELLER, R., OKE, A., MIDFORD, I. & ADAMS, R. N. 1976. Liquid chromatographic analysis of catecholamines-routine assay for regional brain mapping. *Lif. Sci.* **19**, 995-1004.
- OKAMOTO, K. 1972. Spontaneous hypertension. Its pathogenesis and complications. Igaku Shoin Ltd. Tokyo.
- OKAMOTO, K., YAMORI, Y. & NAGAOKA, A. 1974 Establishment of the stroke-prone spontaneously hypertensive rat (SHR). *Circ. Res.* **34**(3 Suppl. 1), 143-153.
- PENDLETON, R. O., KAISER, C. & GESSNER, G. 1976. Studies on adrenal phenyl-ethanolamine N-methyltransferase (PNMT) with SK&F 64139, a selective inhibitor. *J. Pharmacol. Exp. Ther.* **197**, 623-632.
- SAAVEDRA, J. M. 1979. Adrenaline levels in brain stem nuclei and effects of PNMT inhibitor on spontaneously hypertensive rats. *Brain Res.* **166**, 283-292.
- SAAVEDRA, J. M., GROBECKER, H. & AXELROD, J. 1976. Adrenaline forming enzyme in the brain stem: elevation in genetic and experimental hypertension. *Science* **191**, 483-484.
- SAUTER, A., LEW, J. J., MATSUMOTO, I. & GOLDSTEIN, M. 1977. PNMT and epinephrine levels in the CNS of spontaneous hypertensive rats. *Trans. Amer. Soc. Neurochem. & Abstr.* **65**, 96.
- WIJNEN, H., PALKOVITS, M., DE JONG, W. & VERSTEEG, D. 1978. Elevated adrenaline content in nuclei of the medulla oblongata and the hypothalamus during the development of spontaneous hypertension. *Brain Res.* **157**, 191-195.

Acta

Vol 107

Physiologica Scandinavica

Editorial Board

F. Bechtel
København

M. R. Bergström
Helsinki

J. Jänne
Oslo

Y. Zotterman
Stockholm

U. S. von Euler
(Editor) Stockholm

Contents

Vol. 107, No. 1 September 1979

- 1 NORESSON E, RICKSTEN S E, HALLBACK NORDLANDER, M. & THORÉN P. Performance of the hypertrophied left ventricle in spontaneously hypertensive rats. Effects of changes in preload and afterload
- 9 NORESSON E, RICKSTEN S E & THORÉN P. Left atrial pressure in normotensive and spontaneously hypertensive rats
- 13 THORÉN P, NORESSON E & RICKSTEN S E. Resetting of cardiac C-fiber endings in the spontaneously hypertensive rat
- 19 GALBO H, HOLST J J & CHRISTENSEN N J. The effect of different diets and of insulin on the hormonal response to prolonged exercise
- 33 BERGH U & EKBLOM, B. Influence of muscle temperature on maximal muscle strength and power output in human skeletal muscles
- 39 ÖRLANDER, J, KIESSLING K. H. & LARSSON L. Skeletal muscle metabolism, morphology and function in sedentary smokers and nonsmokers
- 47 FUGLMEYER, A. R., SJÖSTRÖM M. & WÄHLBY L. Human plantar flexion strength and structure
- 57 NÄSLUND G, LINDQVIST I, RÖNQVIST G & NILSSON B O. The effect of α -aminoisobutyric acid and 2,4-diaminobutyric acid on mouse blastocyst outgrowth in vitro
- 63 CLAUSEN G, HOPE, A. & AUKLAND K. Partition of 125 I-iodoantipyrine among erythrocytes, plasma, and renal cortex in the dog
- 69 CLAUSEN G, HOPE, A., KIRKEBØ A., TYSSEBOTN J & AUKLAND K. Distribu-

HELVE, H Metabolic properties of nerve endings isolated from rat brain

- 213 PARTANEN S., KAAKKOLA, S & KAAKIAINEN L. Tryptophylglycine dipeptide in ACTH/MSH cells of the human hypothalamus: its identification and studies on its antinociceptive effects in mice

- 219 HYVÄRINEN J, LAAKSO M, ROINE, R. & LEINONEN L. Comparison of effects of pentobarbital and ethanol on the neuronal activity in the posterior parietal association cortex

- 227 ABDUL-RAHMAN A, DAHLGREN N, JOHANSSON B B & SIESJÖ B K. Increase in local cerebral blood flow induced by circulating adrenaline: involvement of blood-brain barrier dysfunction

- 233 EDSTROM, A, HANSON M, WALLIN M & CEDERHOLM, B. Inhibition of fast axonal transport and microtubule polymerization in vitro by colchicine and colchicine

- 239 HALIBACK, D A, JODAL, M. & LUNDGREN O. Effects of cholera toxin on villous tissue osmolality and fluid and electrolyte transport in the small intestine of the cat

- 251 BING, J & POULSEN K. Aggression-provoked renin release from extrarenal and extrahepatic sources in mice

- 257 LITHELL, H, ORLANDER, J, SCHÉLE, R, SJÖDIN B & KARLSSON J. Changes in lipoprotein-lipase activity and lipid stores in human skeletal muscle with prolonged heavy exercise

- 263 ROSELL, S. & RÖKAEUS Å. The effect of ingestion of amino acids, glucose and fat on circulating neurotensin-like immunoreactivity (NTLI) in man

- 269 GALBO H, SAUGMANN P & RICHTER, E A. Increased hepatic glycogen synthetase and decreased phosphorylase in trained rats

- 273 GABRIELSEN G & STEEN J B. Tachycardia during egg-hypothermia in localizing paramegan (*Lagopus lagopus*)

Short Communications

- 279 LUNDBERG J M, HÖKFELT T, FAHRENKRUG J, NILSSON G & TERENIUS L. Peptides in the cat carotid body (glomus caroticum): VIP, enkephalin and substance P-like immunoreactivity

- 283 SAKABE, T & SIESJÖ B K. The effect of

lindomethacin on the blood flow-metabolism couple in the brain under normal hypercapnic and hypoxic conditions

- 285 OTTESEN B, ULRICHSEN H, WAGNER, G & FAHRENKRUG, J. Vasoactive intestinal polypeptide (VIP) inhibits oxytocin induced activity of the rabbit myometrium

Appendix Supplement

Supplementum 473 XVI Scandinavian Congress of Physiology and Pharmacology Oslo 1979

Vol. 107 No. 4 December 1979

- 289 EDVINSSON L, LACOMBE, P, OWMAN CH., REYNIER REBUFFEL, A. M. & SEYLAZ, J. Quantitative changes in regional cerebral blood flow of rats induced by alpha- and beta-adrenergic stimulants

- 297 JENESKOG T. Inhibitory actions from low and high threshold cutaneous afferents on groups II and III muscle afferent pathways in the spinal cat

- 309 AALJÆR, C. & MULVANY M. J. Morphological and mechanical properties of small mesenteric arteries and veins in spontaneously hypertensive rats

- 313 SYDBOM A. & KARLSSON T. Relationship between serum IgE levels and anaphylactic histamine release from isolated rat mast cells

- 319 HÄGGMARK, T & THORSTENSSON A. Fibre types in human abdominal muscles

- 327 PETTERSSON G, AHLMAN H, BHARGAVA, H N., DAHLSTROM A, KEW ENTER, J, LARSSON I & SIEPLER, J K. The effect of propranolol on the serotonergic concentration in the portal plasma after vagal nerve stimulation in the cat

- 333 LINKOLA, J., FYHRQUIST F & YLIKÄHRI R. Adenosine 3',5' cyclic monophosphate, calcium and magnesium excretion in ethanol intoxication and hangover

- 339 PERTOVAARA A. Modification of human pain threshold by specific tactile receptors

- 343 SKAUGEN E. & WALLÖE, L. Firing behaviour in a stochastic nerve membrane model based upon the Hodgkin-Huxley equations

- 365 GRÄNDE, P-O, BOROSTROM, P & MELANDER, S. On the nature of basal vascular tone in cat skeletal muscle and its dependence on transmural pressure stimuli

- 377 JONSSON C. E., SHIMIZU Y., FRED-

- tion of blood flow in the dog kidney 1 Saturation rates for inert diffusible tracers ¹²⁵I iodoantipyrine and tritiated water versus uptake of microspheres under control conditions
- 83 PETTERSSON G AHLMAN H DAHLSTRÖM A KEWENTER J LARSSON I & LARSSON P A The effect of transmural field stimulation on the serotonin content in rat duodenal enterochromaffin cells—in vitro
- 89 HALLBÄCK D A JODAL M & LUNDGREN O Importance of sodium and glucose for the establishment of a villous tissue hyperosmolality by the intestinal countercurrent multiplier
- Appended Supplements*
- Supplementum 469 ÅKERSTEDT T Altered sleep/wake patterns and circadian rhythms
- Supplementum 470 PETTERSSON G The neural control of the serotonin content in mammalian enterochromaffin cells
- Vol 107 No 2 October 1979
- 97 WIBERG T VAAGE J & SCOTT E Release of prostaglandin like substances during elevations of left atrial pressure in the cat
- 105 MANNISTÖ P T KOKKONEN J & RANTA T Effects of acute hypotension and hypertension on serum TSH concentrations in male rats
- 109 KAINULAINEN H PILSTRÖM L & VIHKO V Morphometry of myocardial apex in endurance-trained mice of different ages
- 115 HALLBACK D A JODAL M SJÖQVIST A & LUNDGREN O Villous tissue osmolality and intestinal transport of water and electrolytes
- 127 HAKUMÄKI M O K Influence of intravenous infusion on heart rate sympathetic and vagal efferentation and left atrial and aortic baroreceptor activity in dogs
- 135 ABRAHAMSSON T HOLMGREN S NILSSON S & PETTERSSON K On the chromaffin system of the African lungfish *Protopterus aethiopicus*
- 141 ABRAHAMSSON T HOLMGREN S NILSSON S & PETTERSSON K Adrenergic and cholinergic effects on the heart the lung and the spleen of the African lungfish *Protopterus aethiopicus*
- 149 ABRAHAMSSON T IÖNSSON A-C & NILSSON S Catecholamine synthesis in the chromaffin tissue of the African lungfish *Protopterus aethiopicus*
- 153 HARDEBO J E & NILSSON B Estimation of cerebral extraction of circulating compounds by the brain uptake index method Influence of circulation time volume injection and cerebral blood flow
- 161 HARDEBO J E FALCK B & ÖWMAN CH A comparative study on the uptake and subsequent decarboxylation of monoamine precursors in cerebral microvessels
- 169 EDIN R AHLMAN H & KEWENTER J The vagal control of the feline pyloric sphincter
- Short Communications*
- 175 SEJRSEN P A note on the bolus injection residue detection method for measurement of capillary permeability
- 177 FUXE K JONSSON G BOLME P AN DERSSON K AGNATI L F GOLDSTEIN M & HÖKFELT T Reduction of adrenaline turnover in cardiovascular areas of rat medulla oblongata by clonidine
- 181 TONPE N & LINDBLOM B The influence of prostaglandin synthetase inhibition on the spontaneous contractile activity and induced responses of the human oviduct
- 185 EDIN R LUNDBERG J M AHLMAN H DAHLSTRÖM A FAHRENKRUG J HÖKFELT T & KEWENTER J On the VIP-ergic innervation of the feline pylorus
- 189 NIELSEN R A 3 to 2 coupling of the Na-H pump responsible for the transepithelial Na transport in frog skin disclosed by the effect of Ba
- Appended Supplements*
- Supplementum 471 WALLEVIK K In vivo structure and stability of serum albumin in relation to its normal catabolism
- Supplementum 472 DAHLBERG B Transcapillary solute exchange in skeletal muscle after injury and during shock
- Vol 107 No. 3 November 1979
- 193 CASS A & DALMARK M Chloride transport by self-exchange and by HCl salt diffusion in gramicidin-treated human red blood cells
- 205 JANSSON S E HÄRKÖNEN M II &

- DAHLSTRÖM, A., see PETTERSSON G.
 DALMARK, M. see CASS A
- EDIN, R. AHLMAN H. & KEWENTER, J.
 The vagal control of the feline pyloric sphincter
- EDIN R., LUNDBERG J M AHLMAN
 H DAHLSTRÖM A. FAHRENKRUG J
 HÖKFELT T & KEWENTER, J VIP-ergic
 innervation of pylorus
- EDSTRÖM, A. HANSON M. WALLIN M
 & CEDERHOLM, B Axonal transport and
 colchicine
- EDVINSSON L. LACOMBE, P OWMAN
 CH REYNIER REBUFFEL, A. M & SEY
 LAZ, J Sympathomimetic effects on CBF
- EKBLOM, B. see BERGH U
- EMSON P. see LUNDBERG J M
- FAHRENKRUG J. see EDIN R.
- FAHRENKRUG J. see LUNDBERG J M
- FAHRENKRUG J. see OTTESEN B
- FALCK, B. see HARDEBO J E.
- FREDHOLM B B. see JONSSON C. E
- FUGLMEYER A. R. SJÖSTRÖM, M. &
 WÄHLBY L. Human plantar flexion strength
 and structure
- FUXE, K. GANTEN D. JONSSON G.
 BOLME P. AGNATI L. F. ANDERSSON
 K., GOLDSTEIN M. & HÖKFELT T. Ad-
 renaline turnover in medulla of hypertensive
 rats
- FUXE, K. JONSSON G. BOLME, P. AN-
 DERSSON K. AGNATI L. F. GOLD-
 STEIN M. & HÖKFELT T. Clonidine on
 adrenaline turnover
- FYHRQUIST F. see LINKOLA, J
- GABRIELSEN G. & STEEN J B. Incuba-
 tion tachycardia
- GALBO H. HOLST J J. & CHRISTEN-
 SEN N J. Hormonal regulation during pro-
 longed exercise
- GALBO H. SAUGMANN P. & RICHTER,
 E. A. Hepatic glycogen synthetase in trained
 rats
- GANTEN D. see FUXE, K.
- GOLDSTEIN M. see FUXE, K.
- GOLDSTEIN M. see FUXE, K.
- GOLDSTEIN M. see HÖKFELT T.
- GRANDE, P.-O., BORGSTRÖM P. & MEL-
 LANDER, S. Characteristics of basal vascular
 tone
- GRANSTRÖM E. see JONSSON C. E.
- HÄGGMARK, T. & THORSTENSSON A.
 Fibre types in human abdominal muscles
- HAKUMÄKI M. O. K. Vagal and sympa-
 thetic discharges
- HALLBÄCK, D. A. JODAL, M. &
 LUNDGREN O. Intestinal countercurrent
 multiplier I
- HALLBÄCK, D. A. JODAL, M. &
 LUNDGREN O. Cholera and intestinal coun-
 tercurrent multiplier
- HALLBÄCK D. A. JODAL, M. SJÖ-
 QVIST A. & LUNDGREN O. Intestinal
 countercurrent multiplier II
- HALLBÄCK-NORDLANDER, M. see
 NORESSON E.
- HANSON M. see EDSTRÖM A.
- HARDEBO J E. & NILSSON B. Cerebral
 extraction of circulating compounds
- HARDEBO J E., FALCK B. & OWMAN
 CH. Monoamine precursors and the blood-
 brain barrier
- HÄRKÖNEN M. H. see JANSSON S. E.
- HELVE H. see JANSSON S. E.
- HÖKFELT T. see EDIN R.
- HÖKFELT T., see FUXE, K.
- HÖKFELT T. see FUXE, K.
- HÖKFELT T. see LUNDBERG J M.
- HÖKFELT T. see LUNDBERG J M.
- HÖKFELT T., PHILLIPSON O. & GOLD-
 STEIN M. Dopamine projections to spinal cord
- HOLMGREN S. see ABRAHAMSSON T.
- HOLMGREN S. see ABRAHAMSSON T.
- HOLST J J. see GALBO H.
- HOPE, A. see CLAUSEN G.
- HOPE, A., see CLAUSEN G.
- HYVÄRINEN J. LAAKSO M. ROINE R.
 & LEINONEN L. Pentobarbital and ethanol
 in association cortex
- JANSSON S. E., HÄRKÖNEN M. H. &
 HELVE, H. Energy metabolism in synap-
 tosome
- JENESKÖG T. Cutaneous inhibition of high
 threshold muscle afferent pathways
- JODAL, M. see HALLBÄCK, D. A.
- JODAL, M. see HALLBÄCK, D. A.
- JODAL, M. see HALLBÄCK, D. A.

HOLM B B GRANSTRÖM E & OLIV E. Efflux of cyclic AMP prostaglandin E_2 and F_2 and thromboxane B_2 in leg lymph of rabbits after scalding injury

Short Communications

- 385 CLAUSEN G KIRKEBØ A TYSSE BOTN I ØFJORD E S & AUKLAND K Erroneous estimates of intrarenal blood flow distribution in the dog with radiolabelled microspheres
- 389 LUNDBERG J M HÖKFELT T ÅNGGÅRD A PERNOW B & EMSON P Immunohistochemical evidence for substance P containing fibres in the taste buds of the cat
- 393 HÖKFELT T PHILLIPSON O & GOLDSTEIN M Evidence for a dopaminergic pathway in the rat descending from the A11 cell group to the spinal cord

397 FUXE K GANTEN D JONSSON G BOLME P AGNATI L F ANDERSSON K GOLDSTEIN M & HÖKFELT T Evidence for a selective reduction of adrenaline turnover in the dorsal midline area of the caudal medulla oblongata of young spontaneously hypertensive rats

Appended Supplements

- Supplementum 474 FORSSBERG H On integrative motor functions in the rat's spinal cord
- Supplementum 475 OSCARSON J HÅKANSSON R LIEBERG G LUNDQVIST G SUNDLER F & THORELL J Variated sensory gastrin concentration, trophic effects on the gastrointestinal tract of the rat

Index Auctorum

- 309 AALKJÆR C & MULVANY M J Morphology of small SHR arteries and veins
- 227 ABDUL RAHMAN A DAHLGREN N JOHANSSON B B & SIESJÖ B K Adrenaline and local brain blood flow
- 149 ABRAHAMSSON T JONSSON A-C & NILSSON S Amine synthesis in a lungfish
- 135 ABRAHAMSSON T HOLMGREN S NILSSON S & PETTERSSON K Chromaffin tissue in a lungfish
- 141 ABRAHAMSSON T HOLMGREN S NILSSON S & PETTERSSON K Drug effects in a lungfish
- 177 AGNATI L F see FUXE K
- 397 AGNATI L F see FUXE K
- 169 AHLMAN H see EDIN R
- 185 AHLMAN H see EDIN R
- 83 AHLMAN H see PETTERSSON G
- 377 AHLMAN H see PETTERSSON G
- 177 ANDERSSON K see FUXE K
- 397 ANDERSSON K see FUXE K
- 389 ÅNGGÅRD A see LUNDBERG J M
- 63 AUKLAND K see CLAUSEN G
- 69 AUKLAND K see CLAUSEN G
- 385 AUKLAND K see CLAUSEN G
- 33 BERGH U & EKBLOM B Muscle temperature and strength
- 327 BHARGAVA H N see PETTERSSON C
- 251 BING J & POULSEN K Extrasubnavicular and extrarenal renin release
- 177 BOLME P see FUXE K
- 397 BOLME P see FUXE K
- 365 BORGSTRÖM P see GRÄNDE P-O
- 193 CASS A & DALMARK M Chloride transport in erythrocytes
- 233 CEDERHOLM B see EDSTRÖM A
- 19 CHRISTENSEN N J see GALBO H
- 63 CLAUSEN G HOPE A & AUKLAND K Renal cortical 125 I-iodoantipyrine space
- 69 CLAUSEN G HOPE A KIRKEBØ A TYSSEBOTN I & AUKLAND K Local blood flow in dog kidney
- 385 CLAUSEN G KIRKEBØ A TYSSEBOTN I ØFJORD E S & AUKLAND K Blood flow distribution in the dog
- 227 DAHLGREN N see ABDUL RAHMAN A
- 185 DAHLSTRÖM A see EDIN R
- 83 DAHLSTRÖM A see PETTERSSON G

DAHLSTRÖM, A., see PETTERSSON G
DALMARK M. see CASS A.

EDIN R. AHLMAN H & KEWENTER, J
The vagal control of the feline pyloric sphincter
EDIN R. LUNDBERG J M AHLMAN
H. DAHLSTRÖM A. FAHRENKRUG J
HÖKFELT T & KEWENTER, J VIP-ergic
innervation of pylorus

EDSTRÖM A. HANSON M. WALLIN M
& CEDERHOLM, B Axonal transport and
colchicine

EDVINSSON L. LACOMBE, P. OWMAN
CH., REYNIER REBUFFEL, A. M. & SEY
LAZ, J Sympathomimetic effects on CBF

EKBLÖM B., see BERGH, U
EMSON P. see LUNDBERG J M

FAHRENKRUG J. see EDIN R.
FAHRENKRUG J. see LUNDBERG, J M.
FAHRENKRUG J. see OTTESEN B.
FALCK, B. see HARDEBO J E.
FREDHOLM, B B. see JONSSON C. E.
FUGL-MEYER, A R. SJÖSTRÖM M. &
WÄHLBY L. Human plantar flexion strength
and structure

FUXE, K. GANTEN D. JONSSON O
BOLME, P. AGNATI L. F. ANDERSSON
K., GOLDSTEIN M. & HÖKFELT T Ad-
renaline turnover in medulla of hypertensive
rats

FUXE, K. JONSSON G. BOLME P. AN-
DERSSON K. AGNATI L. F. GOLD-
STEIN M. & HÖKFELT T Clonidine on
adrenaline turnover

FYHRQVIST F. see LINKOLA, J

GABRIELSEN O & STEEN J B. Incuba-
tion tachycardia

GALBO H. HOLST J J & CHRISTEN-
SEN N J Hormonal regulation during pro-
longed exercise

GALBO H. SAUGMANN P & RICHTER
E A Hepatic glycogen synthetase in trained
rats

GANTEN D. see FUXE, K

GOLDSTEIN M. see FUXE, K

GOLDSTEIN M., see FUXE, K.

GOLDSTEIN M. see HÖKFELT T

GRANDE P-O. BORGSTRÖM P & MEL-

LANDER, S Characteristics of basal vascular
tone

GRANSTRÖM E. see JONSSON C. E.

HÄGOMARK, T & THORSTENSSON A.
Fibre types in human abdominal muscles

HAKUMÄKI M. O K. Vagal and symp-
thetic discharges

HALLBÄCK, D A. JODAL, M. &
LUNDGREN O Intestinal countercurrent
multiplier I

HALLBÄCK, D A. JODAL, M. &
LUNDGREN O Cholera and intestinal coun-
tercurrent multiplier

HALLBÄCK, D A. JODAL, M., SJÖ-
QVIST A & LUNDGREN O Intestinal
countercurrent multiplier II

HALLBÄCK-NORDLANDER, M. see
NORESSON E.

HANSON M. see EDSTRÖM, A.

HARDEBO J E. & NILSSON B Cerebral
extraction of circulating compounds

HARDEBO J E., FALCK B & OWMAN
CH. Monoamine precursors and the blood-
brain barrier

HÄRKÖNEN M. H. see JANSSEN S. E.

HELVE, H., see JANSSEN S. E.

HÖKFELT T., see EDIN R.

HÖKFELT T. see FUXE, K.

HÖKFELT T. see FUXE, K.

HÖKFELT T. see LUNDBERG J M.

HÖKFELT T. see LUNDBERG J M.

HÖKFELT T., PHILLIPSON O & GOLD-
STEIN M. Dopamine projection to spinal cord

HOLMGREN S. see ABRAHAMSSON T

HOLMGREN S., see ABRAHAMSSON T

HOLST J J. see GALBO H

HOPE, A. see CLAUSEN G

HOPE, A. see CLAUSEN G

HYVÄRINEN I. LAAKSO M. ROINE, R.
& LEINONEN L. Pentobarbital and ethanol
in association cortex

JANSSEN S. E. HÄRKÖNEN M. H. &
HELVE, H. Energy metabolism in synap-
somes

JENESKOG T Cutaneous inhibition of high
threshold muscle afferent pathways

JODAL, M. see HALLBÄCK D A.

JODAL, M. see HALLBÄCK, D A.

JODAL, M. see HALLBÄCK, D A.

- 227 JOHANSSON B B see ABDUL RAHMAN A
- 149 JÖNSSON A-C see ABRAHAMSSON T
- 177 JONSSON G see FUXE K
- 397 JONSSON G see FUXE K
- 377 JONSSON C E SHIMIZU Y FREDHOLM B B GRANSTRÖM E & OLIW E Cyclic AMP prostaglandins and thromboxanes in burns
- 213 KAAKKOLA S see PARTANEN S
- 713 KÄÄRIÄINEN I see PARTANEN S
- 109 KAINULAINEN H PILSTRÖM L. & VIHKO V Apex mitochondria and training
- 257 KARLSSON J see LITHELL, H
- 313 KARLSSON T see SYDBOM A
- 169 KEWENTER J see EDIN R
- 185 KEWENTER J see EDIN R
- 83 KEWENTER J see PETTERSSON G
- 377 KEWENTER J see PETTERSSON G
- 39 KIESSLING K H see ÖRLANDER J
- 69 KIRKEBØ A see CLAUSEN G
- 385 KIRKEBØ A see CLAUSEN G
- 105 KOKKONEN J see MÄNNISTÖ P T
- 219 LAAKSO M see HYVÄRINEN J
- 289 LACOMBE P see EDVINSSON L
- 39 LARSSON L see ÖRLANDER J
- 83 LARSSON I see PETTERSSON G
- 377 LARSSON I see PETTERSSON G
- 83 LARSSON P A see PETTERSSON G
- 719 LEINONEN L. see HYVÄRINEN J
- 181 LINDBLOM B see TONPE N
- 57 LINDQVIST I see NÆSLUND G
- 333 LINKOLA J FYHRQUIST F & YLIKAHRI R cAMP and ethanol intoxication
- 257 LITHELL H ÖRLANDER J SCHÉLE R. SJÖDIN B & KARLSSON J Muscle LPL and lipid stores in heavy exercise
- 185 LUNDBERG J M see EDIN R
- 389 LUNDBERG J M HÖKFELT T ÅNGGÅRD A PERNOW B & EMSON P Immunohistochemical evidence for substance P
- 779 LUNDBERG J M HÖKFELT T FAHRENKRUG J NILSSON G & TERENIUS L. Peptides in carotid body
- 89 LUNDGREN O see HALLBÄCK D A
- 115 LUNDGREN O see HALLBÄCK D A
- 239 LUNDGREN O see HALLBÄCK D A
- 105 MÄNNISTÖ P T KOKKONEN J & RANTA T Blood pressure and TSH secretion
- 365 MELLANDER S see GRÄNDE, P-O
- 309 MULVANY M J see AALJÆR, C.
- 57 NÆSLUND G LINDQVIST I RÖNQVIST G & NILSON B O Effect of AIB and DAB on blastocyst outgrowth
- 189 NIELSEN R Coupled Na and K transport
- 135 NILSSON S see ABRAHAMSSON T
- 141 NILSSON S see ABRAHAMSSON T
- 149 NILSSON S see ABRAHAMSSON T
- 153 NILSSON B see HARDEBO J E.
- 279 NILSSON G see LUNDBERG J M
- 57 NILSSON B O see NÆSLUND G
- 1 NORESSON E. RICKSTEN S E. HALLBÄCK NORDLANDER M & THORÉN P Heart performance in hypertensive rat
- 9 NORESSON E RICKSTEN S. E. & THORÉN P Left atrial pressure in SHR hypertension
- 13 NORESSON E see THORÉN P
- 385 ØFJORD E S see CLAUSEN G
- 377 OLIW E see JONSSON C E
- 39 ÖRLANDER J KIESSLING K H & LARSSON L. Human muscle and smoking
- 257 ÖRLANDER J see LITHELL, H
- 285 OTTESSEN B ULRICHSEN H WAGNER G & FAHRENKRUG J VIP and myometrial activity
- 289 OWMAN CH see EDVINSSON L.
- 161 OWMAN CH see HARDEBO J E
- 713 PARTANEN S KAAKKOLA S. & KAARIÄINEN I Tryptophylglycine in human hypophysis
- 389 PERNOW B see LUNDBERG J M
- 339 PERTOV VARA A Pain threshold and tactile receptors
- 135 PETTERSSON K see ABRAHAMSSON T
- 141 PETTERSSON K see ABRAHAMSSON T
- 777 PETTERSSON G AHLMAN H BJAR GAVA H N DAHLSTRÖM A KEWENTER J LARSSON I & SIEPLER J K. Serotonin in portal plasma
- 83 PETTERSSON G AHLMAN H DAHLSTRÖM A KEWENTER J LARSSON,

- 1 L & LARSSON P A. Serotonin in enterochromaffin cells
- 178 PHILLIPSON O see HOKFELT T
- 110 PILSTRÖM L see KAINULAINEN H
- 21 FOULSEN K see BING J
- 165 RANTA, T see MÄNNISTÖ P T
- 29 REYNIER REBUFFEL, A.-M. see EDVINSSON L.
- 20 RICHTER, E. A., see GALBO H.
- 1 RICKSTEN S. E., see NORESSON E.
- 9 RICKSTEN S. E., see NORESSON E.
- 11 RICKSTEN S. E. see THORÉN P
- 119 ROINE R. see HYVÄRINEN J
- 21 ROKAEUS Å. see ROSELL, S
- 51 RONQUIST G see NÄSLUND G
- 33 ROSELL, S & ROKAEUS Å Nutrients and neurotensin-like immunoreactivity
- 21 SAKABE, T & SIESJÖ B K Indomethacin and brain circulation-metabolism
- 29 SAUGMANN P see GALBO H
- 27 SCHÉLE R. see LITHELL, H
- 97 SCOTT E see WIBERG T
- 175 SEJRSEN P Capillary permeability measurement
- 29 SEYLAZ, J see EDVINSSON L.
- 37 SHIMIZU Y see JONSSON C. E
- 117 SIEPLER, J K see PETTERSSON G
- 227 SIESJÖ B K see ABDUL RAHMAN A.
- 21 SIESJÖ B K. see SAKABE, T
- 257 SJÖDIN B see LITHELL, H
- 115 SJÖQVIST A see HALLBÄCK D A
- 47 SJÖSTRÖM M see FUGL-MEYER A R.
- 343 SKAUGEN E & WALLØE, L. Firing in a stochastic membrane. I
- 273 STEEN J B see GABRIELSEN G
- 313 SYDBOM, A. & KARLSSON T Correlation of IgE with histamine release
- 279 TEREINUS L. see LUNDBERG J M
- 1 THORÉN P see NORESSON E.
- 9 THORÉN P see NORESSON E.
- 13 THORÉN P NORESSON E. & RICKSTEN S E. Resetting of cardiac afferents in hypertension
- 319 THORSTENSSON A., see HÄGGMARK T
- 181 TONPE, N & LINDBLOM, B PG synthesis and tubal contractility
- 69 TYSSBOTN I., see CLAUSEN G
- 385 TYSSBOTN I see CLAUSEN G
- 285 ULRICHSEN H see OTTESEN B
- 97 VAAGE, J see WIBERG T
- 285 WAGNER, G see OTTESEN B
- 47 WÄHLBY L. see FUGL-MEYER, A. R.
- 233 WALLIN M. see EDSTRÖM, A.
- 343 WALLØE, L. see SKAUGEN E.
- 97 WIBERG T VAAGE, J & SCOTT E. Prostaglandins and pulmonary hypertension
- 109 VIHKO V see KAINULAINEN H
- 333 YLIKAHRI R. see LINKOLA, J

